Project Title:

BRIDGE CONDITION ASSESSMENT USING REMOTE SENSORS

Sponsoring Organization:

United States Department of Transportation
Research and Innovative Technology
Administration

Cooperative Agreement Number:

DT0S59-10-H-00001

Research Agency:

Michigan Technological University

in cooperation with

Center for Automotive Research
Michigan Department of Transportation

Principal Investigators:

Theresa M. Ahlborn, PhD, PE, FPCI
Civil & Environmental Engineering

Robert A. Shuchman, PhD
Michigan Tech Research Institute

Lawrence L. Sutter, PhD
Michigan Tech Transportation Institute

Devin K. Harris, PhD
Civil & Environmental Engineering

Colin N. Brooks, MEM
Michigan Tech Research Institute

Joseph W. Burns, PhD
Michigan Tech Research Institute

Date:

February 6, 2013

Volume II of II – Appendices

Michigan Tech

Table of Contents – Volume I of II: Main Body

Abstract i

Acknowledgements iii

Disclaimer v

Acronyms vii

List of Figures xvii

List of Tables xxvii

1. Introduction 1-1

2. Background 2-1
   2.1. Current Evaluation Process 2-1
      2.1.1. Visual Inspection 2-2
      2.1.2. Defects 2-3
      2.1.3. Traditional Inspection Tools 2-4
      2.1.4. Advanced Inspection Techniques 2-4
      2.1.5. Condition Rating 2-5
   2.2. Condition Monitoring 2-7
   2.3. Remote Sensing 2-8

3. Methodology 3-1
   3.1. Laboratory Study 3-1
      3.1.1. Three Dimensional Optical Bridge-evaluation System 3-1
      3.1.2. Bridge Viewer Remote Camera System 3-1
      3.1.3. Thermal Infrared Imagery 3-1
      3.1.4. Digital Image Correlation 3-2
      3.1.5. Ground Penetrating Radio Detection and Ranging 3-2
   3.2. Field Demonstration 3-2
      3.2.1. Bridge Selection 3-2
      3.2.2. Field Demonstration Design 3-12

4. Designing and Deploying the Three Dimensional Optical Bridge-evaluation System 4-1
   4.1. Methodology 4-1
   4.2. Results and Discussion 4-9
   4.3. Implementation and Next Steps 4-18

5. Deployment of the Bridge Viewer Remote Camera System 5-1
5.1. Methodology 5-1
5.1. Results and Discussion 5-2
5.2. Implementation and Next Steps 5-4

6. Image Data Collection GigaPan System 6-1
6.1. Methodology 6-1
6.2. Results and Discussion 6-3
6.3. Implementation and Next Steps 6-6

7. Evaluation of Surface Defect Detection using Light Detection and Ranging 7-1
7.1. Laboratory Testing, Proof of Concept, Software Description, and Field Deployment. 7-5
7.1.1. Point Cloud Density Decay 7-9
7.1.2. Maximum Radius of Capture 7-16
7.1.3. Mobile Light Detection and Ranging 7-20
7.2. Field Demonstration Results and Discussion and Integration into the DSS 7-24
7.2.1. 3D Optical Bridge-evaluation System Spall Detection Algorithm 7-24
7.2.2. Light Detection and Ranging Data Derived Digital Elevation Models and Processing in the 3D Optical Bridge-evaluation System Spall Algorithm 7-25
7.2.3. Ground Truth Measure for Comparison 7-29
7.2.4. International Roughness Index Using Light Detection and Ranging Digital Elevation Models 7-38
7.3. Challenges for Implementation, Costing Comments, Data Fusion With Other Technologies, and Future Plans 7-42
7.3.1. Sensing Bridge Surface Condition 7-43
7.4. Conclusions 7-43
7.5. Potential Future Work 7-44

8. Implementation of Thermal Infrared Imagery 8-1
8.1. Concepts of Application for Concrete Bridge Evaluation 8-1
8.2. Limitations of Application and Environmental Effects 8-3
8.3. Advantages for Bridge Inspections 8-4
8.4. Methodology 8-4
8.4.1. Laboratory Experiment 8-4
8.4.2. Field Deployment Methodology 8-10
8.5. Results and Discussion 8-13
8.5.1. Inspection Results for Top of the Bridge Deck 8-13
8.5.2. Ground Truth Results 8-23
8.5.3. Inspection Results for Bridge Deck Underside and Bridge Girders 8-25
8.6. Implementation and Next Steps 8-26

9. Evaluation of Digital Image Correlation Method 9-1
9.1. Background 9-2
9.1.1. Theory 9-2
9.1.2. Concept 9-4
9.1.3. Literature Review and State of Practice 9-5
9.2. Methodology 9-8
9.2.1. Computer Software Algorithms 9-8
9.2.2. Preliminary Laboratory Evaluation 9-11
9.2.3. Field Deployment 9-15
9.3. Results and Discussion 9-17
9.3.1. Field Deployment Results 9-17
9.3.2. Field Environment Considerations 9-18
9.3.3. Retested Laboratory Evaluation 9-19
9.3.4. Pros and Cons of Method 9-25
9.3.5. Integration into the Decision Support System 9-26
9.4. Implementations and Next Steps 9-27
9.4.1. Limitations 9-27
9.4.2. Re-evaluation of Software Algorithms and Noise Detection Approach 9-28
9.4.3. Data Combination 9-31
9.5. Future Plans and Final Remarks 9-32

10. Ultra Wide Band Imaging Example of Ground Penetrating Radar 10-1
10.1. Commercial Systems 10-2
10.1.1. Application to Bridge Condition Sensing 10-4
10.1.2. Examples of Available Commercial Systems 10-5
10.2. Ground Penetrating Radio Detecting and Ranging Experiments 10-6
10.2.1. Field Data Collections 10-8
10.3. Benefits, Limitations and Next Steps 10-23

11. Synthetic Aperture Radio Detection and Ranging Applications 11-1
11.1. Methodology 11-1
11.2. Results and Discussion 11-6
11.3. Next Steps and Implementation 11-7

12. Use of Multispectral Satellite Imagery 12-1
12.1. Results and Discussion 12-2
12.2. Implementation and Next Steps 12-3

13. The Bridge Condition Decision Support System 13-1
13.1. Design and Development 13-3
13.1.1. Client-server Architecture 13-4
13.1.2. Data and Database System 13-5
13.1.3. Integration of Remote Sensing Data 13-6

13.2. Outcomes and Product Delivered 13-7
13.2.1. Current Features of the Web Application 13-7
13.2.2. Alternatives and Justifications 13-14
13.3. Implementation and Next Steps 13-17
13.3.1. User Feedback 13-18
13.3.2. Potential Barriers to Adoption and Implementation 13-20
13.3.3. Needed Improvements for Implementation 13-21

14. Economic Evaluation of Promising Commercial Remote Sensors and Systems 14-1
14.1. Bridge Inspection and Maintenance in the Context of Declining Transportation Revenues 14-1
14.2. Description of Existing Bridge Inspection Practices 14-4
14.2.1. Cost Estimates of Current Bridge Inspection Techniques 14-6
14.2.2. Time Spent on Inspections 14-7
14.2.3. Findings from Interviews with Bridge Inspection and Management Experts 14-7
14.2.4. Bridge Scoping 14-8
14.3. Remote Sensing Technologies for Bridge Condition Assessment 14-9
14.4. Economic Evaluation of Bridge Inspection Using Remote Sensing Technologies 14-10
14.4.1. Economic Evaluation Methods for New Technologies 14-11
14.4.2. Quantifying Costs of Remote Sensing Technologies 14-13
14.4.3. Data collection system 14-14
14.4.4. Assumptions and Deployment Scenarios of Remote Sensing Technologies 14-15
14.4.5. Cost Analysis of Alternative Deployments 14-18
14.4.6. Benefits of Remote Sensing Technologies 14-19
14.4.7. Benefits of Decision Support System 14-21
14.5. Conclusions and Recommendations 14-22

15. Findings 15-1
15.1. Technology Evaluation 15-1
15.2. Implementation and Field Readiness 15-4
15.3. Bridge Signature 15-5
15.4. Path Forward 15-6

References Ref-1

Table of Contents – Volume II of II: Appendices

Table of Contents - Volume I of II i

Table of Contents - Volume II of II v

Appendices App-1
- Appendix A – Commercial Sensor Evaluation Report App-2
- Appendix B – State of the Practice Report App-3
- Appendix C – Technical Memorandums App-4
- Appendix D.1 – Inspection Report: Poor Selection – Mannsiding NB App-5
- Appendix D.2 – Inspection Report: Fair Selection – Willow Road App-6
- Appendix D.3 – Inspection Report: Satisfactory Selection – Freer Road App-7
- Appendix D.4 – Inspection Report: Supplemental Selection – Mannsiding SB App-8
- Appendix E – Thermal Infrared Imagery Data App-9
- Appendix F.1 – Economic Evaluation: First Interview with MDOT Stakeholders App-10
- Appendix F.2 – Economic Evaluation: Second Interview with MDOT Stakeholders App-11
- Appendix G – Economic Evaluation: Costs of Remote Sensing Technologies App-12
- Appendix H – Technical Evaluation Score Spreadsheet App-13

Appendices

A	**Commercial Sensor Evaluation Report**
B	**State of the Practice Report**
C	**Technical Memorandums**
D.1	**Bridge Inspection Report: Poor Selection – Mannsiding North Bound**
D.2	**Bridge Inspection Report: Fair Selection – Willow Road**
D.3	**Bridge Inspection Report: Satisfactory Selection – Freer Road**
D.4	**Bridge Inspection Report: Supplemental Selection – Mannsiding South Bound**
E	**Thermal Infrared Imagery Data**
F.1	**Economic Evaluation: First Interview with MDOT Stakeholders**
F.2	**Economic Evaluation: Second Interview with MDOT Stakeholders**
G	**Economic Evaluation: Costs of Remote Sensing Technologies**
H	**Technical Evaluation Score Spreadsheet**

Appendix A – Commercial Sensor Evaluation Report

An Evaluation of Commercially Available Remote Sensors for Assessing Highway Bridge Condition

T. M. Ahlborn, Ph.D., P.E.[1], R. Shuchman Ph.D[2], L. L. Sutter Ph.D.[1], C. N. Brooks[2], D. K. Harris, Ph.D.[1], J. W. Burns Ph.D[2], K. A. Endsley[2], D. C. Evans[1], K. Vaghefi[1], R. C. Oats[1]

[1]Department of Civil and Environmental Engineering
Michigan Tech Transportation Institute
Michigan Technological University
1400 Townsend Drive
Houghton, Michigan USA 49931
(906) 487-2625; fax (906) 487-1620; email: tess@mtu.edu

[2]Michigan Tech Research Institute
Michigan Technological University
3600 Green Court, Suite 100
Ann Arbor, Michigan USA 48105
(734) 913-6840; fax (734) 913-6880; email: cnbrooks@mtu.edu

October 2010

Table of Contents

Executive Summary 1
Acknowledgements 2
1.0 Introduction 3
1.1 Current Approach to Condition Assessment 3
1.2 Remote Sensing Approaches to Condition Assessment 4
2.0 Remote Sensing Techniques and Terminology for Transportation Infrastructure 5
3.0 Challenges for National Bridge Inventory Infrastructure 11
3.1 Deck Surface 13
3.1.1 Map Cracking 13
3.1.2 Delamination 14
3.1.3 Scaling 15
3.1.4 Spalling 16
3.1.5 Expansion Joints 17
3.2 Deck Subsurface 17
3.2.1 Expansion Joint 18
3.2.2 Delamination 18
3.2.3 Scaling 19
3.2.4 Spalling 19
3.2.5 Corrosion 20
3.2.6 Chloride Ingress 21
3.3 Girder Surface 21
3.3.1 Steel Structural Cracking 22
3.3.2 Concrete Structural Cracking 22
3.3.3 Steel Section Loss 23
3.3.4 Paint 25
3.3.5 Concrete Section Loss 25
3.4 Girder Subsurface 26
3.4.1 Concrete Structural Cracking 27
3.4.2 Concrete Section Loss 27

3.4.3 Prestress Strand Breakage 27
3.4.4 Corrosion 28
3.4.5 Chloride Ingress 29
3.5 Global Metrics 29
3.5.1 Bridge Length 30
3.5.2 Bridge Settlement 30
3.5.3 Bridge Movement 31
3.5.4 Surface Roughness 31
3.5.5 Vibration 31
4.0 Technology Rating Methodology 33
5.0 Performance Evaluation of Remote Sensing Technologies 39
5.1 Ground Penetrating Radar (GPR) 39
5.2 Spectral Analysis 44
5.3 3D Photogrammetry 46
5.4 EO Airborne and Satellite Imagery 46
5.5 Interferometry 51
5.6 LiDAR 52
5.7 Thermal/Infrared (IR) Imaging 53
5.8 Digital Image Correlation (DIC) 54
5.9 Radar Images, Backscatter, and Speckle 57
5.10 Interferometric Synthetic Aperture Radar (InSAR) 60
5.11 Acoustics 61
5.12 StreetView-style Photography 62
6.0 Conclusions and Recommendations 64
7.0 References 66

List of Tables

Table 1: Examples of radar bands, frequency, and their wavelength 10
Table 2: Definition for the criteria used in rating remote sensing technologies for their efficacy in detecting bridge condition indicators 34
Table 3: Performance Rating of Commercial Remote Sensing Technologies 38
Table 4: Representative list of some common commercial GPR systems available for purchase 40
Table 5: Representative list of companies that perform GPR surveys as a service 41
Table 6: Representative list of some commercially available spectroradiometers 45
Table 7: A list of some companies offering aerial photography by commission 47
Table 8: A list of some companies offering satellite imagery for sale or by commission 49
Table 9: Partial list of commercial and non-commercial SAR 61

List of Figures

Figure 1: An example of the electro-magnetic spectrum and its relationship to wavelength 6
Figure 2: An example of the trade-offs of spatial resolution in terms of accuracy needs and the size of an object or part of an area on the ground that needs to analyzed via remote sensing (Luhmann et al. 2006) 8
Figure 3: An example of the parts of the electro-magnetic spectrum captured by Digital Globe's WorldView-2 satellite and available as digital images (Digital Globe Webpage 2009) 9
Figure 4: Michigan Department of Transportation Bridge Deck Preservation Matrix (Michigan Department of Transportation 2008) 12
Figure 5: Map cracking on bridge deck surface (FHWA 2006) 14
Figure 6: Concrete deck surface scaling (FHWA 2006) 16
Figure 7: Spalling on concrete deck surface (FHWA 2006) 17
Figure 8: Material in expansion joint (FHWA 2006) 18
Figure 9: Spalling on bridge deck surface 20
Figure 10: Corroded reinforcement in bridge deck 21
Figure 11: a) Steel section loss in bridge girder viewed from the side; b) Steel section loss viewed from along the beam 24
Figure 12: Paint loss on girder surface 25
Figure 13: Concrete section loss (FHWA 2006) 26
Figure 14: Corroded reinforcing bars 29
Figure 15: Significant spalling of a bridge bay that merits full replacement 43
Figure 16: Example image from Bing Maps' "Bird's eye" imagery exhibiting Pictometry International's oblique aerial photography 50
Figure 17: Photograph of fascia beam on box-beam bridge with thin, 45-degree crack near top of pier and post-tension box 50
Figure 18: Two images of paint spots on a structural I-beam for digital image correlation. (a): the paint spots should have a wide distribution of sizes; (b): post-processing of images is used to bring the spots to a contrast threshold 56

Figure 19: Three images of road surface (pavement) condition from TARUT study (Brooks, Schaub et al. 2007). (a): road roughness as determined from SAR speckle contrast; (b): road roughness according to the International Roughness Index (IRI); (c): rough sufficiency according to the PASER standard 59
Figure 20: Example image from Google's StreetView showing the underside of a box-beam bridge in Michigan. With higher-resolution panoramas, such an interface could be extremely valuable to bridge inspectors and managers. 63

Executive Summary

The nation's bridge program faces some daunting challenges as our transportation infrastructure continues to age. Current bridge inspection techniques consist largely of labor-intensive subjective measures for quantifying deterioration of various bridge elements. Some advanced non-destructive testing techniques such as ground penetrating radar are being implemented, however little attention has been given to remote sensing technologies.

Remote sensing technologies can be used to assess and monitor the condition of bridge infrastructure and improve the efficiency of inspection, repair, and rehabilitation efforts. Most important, monitoring the condition of a bridge using remote sensors can eliminate the need for traffic disruption or total lane closure as remote sensors do not come in direct contact with the structure.

The challenges of understanding deterioration common to bridges throughout our nation have been grouped into five broad areas: deck surface, deck subsurface, girder surface, girder subsurface, and global response. Each area has specific indicators that identify condition or deterioration (e.g. map cracking, delamination, and excessive vibration). A number of remote sensing technologies have been reviewed to evaluate potential applicability for monitoring bridge condition and structural health.

This report focuses on evaluating twelve forms of remote sensing that are potentially valuable to assessing bridge condition. The techniques are: ground penetrating radar (GPR), spectra, 3-D optics (including photogrammetry), electro-optical satellite and airborne imagery, optical interferometry, LiDAR, thermal infrared, acoustics, digital image correlation (DIC), radar (including backscatter and speckle), interferometric synthetic aperture radar (InSAR), and high-resolution "StreetView-style" digital photography.

Using a rating methodology developed specifically for assessing the applicability of these remote sensing technologies, each technique was rated for accuracy, commercial availability, cost of measurement, pre-collection preparation, complexity of analysis and interpretation, ease of data collection, stand-off distance, and traffic disruption. Key findings from the evaluation are that 3-D optics and "StreetView-style" photography appear to have the greatest potential for assessing surface condition of the deck and structural elements, while radar technologies including GPR and higher frequency radar, as well as thermal/infrared imaging demonstrate promise for subsurface challenges. Global behavior can likely be best monitored through electro-optical satellite and airborne imagery, optical interferometry, and LiDAR.

Monitoring how damage or deterioration changes over time will provide state and local engineers with additional information used to prioritize critical maintenance and repair of our nation's bridges. The ability to acquire this information remotely from many bridges without the expense of a dense sensor network will provide more accurate and temporal assessments of bridge condition. Improved assessments allow for limited resources to be better allocated in

repair and maintenance efforts, thereby extending the service life and safety of bridge assets, and minimizing costs of service-life extension.

Acknowledgements

This work is supported by the Commercial Remote Sensing and Spatial Information program of the Research and Innovative Technology Administration (RITA), U.S. Department of Transportation (USDOT), Cooperative Agreement # DTOS59-10-H-00001, with additional support provided by the Michigan Department of Transportation, the Michigan Tech Transportation Institute, the Michigan Tech Research Institute, and the Center for Automotive Research. The views, opinions, findings, and conclusions reflected in this paper are the responsibility of the authors only and do not represent the official policy or position of the USDOT, RITA, or any state or other entity. Additional information regarding this project can be found at www.mtti.mtu.edu/bridgecondition.

1.0 Introduction

The condition of transportation infrastructure, specifically bridges, has received a great deal of attention in recent years as a result of catastrophic failures, deteriorating conditions, and even political pressure. However, the challenges of a deteriorating infrastructure have been at the forefront of transportation authorities' attention for many years as they attempt to establish maintenance priorities for an aging infrastructure with decreasing funds. The U.S. is home to nearly 600,000 highway bridges. Structural deficiency, which describes the condition of significant load-carrying elements and adequacy of waterway openings, typically correlates directly to the age of a bridge (AASHTO 2008). The number of bridges listed as structurally deficient as of 2009 was 71,179 (11.8% of U.S. highway bridges), clearly demonstrating the need for a uniform rating system to make sure the correct bridges receive the necessary and needed funding (FHWA 2009).

The concept of structural health monitoring (SHM) presents a broad generic framework that is well suited to help address the challenges that pertain to the deteriorating bridge infrastructure in the United States. SHM is the practice of monitoring a structure to ensure that its structural integrity and safety remain intact. In a more general sense, the objective of SHM is to observe infrastructure condition, assess in-service performance, detect deterioration, and estimate remaining service life.

1.1 Current Approach to Condition Assessment

Included within the scope of SHM for bridges is condition assessment, which serves as the basis for determining safety, remaining service life, and maintenance, repair and rehabilitation schedules for state and local transportation agencies. Current practices used for condition assessment are a function of the level of inspection which can include initial, routine, hands-on, fracture-critical, underwater, in-depth or scoping, damage, or special inspections (NCHRP 2007), with routine/hands-on type inspections serving as the primary mechanism for long-term condition assessment and performance evaluation.

A variety of methods are used when conducting the inspection of a bridge, but all inspections are completed in accordance with the National Bridge Inspection Standards (NBIS) (FHWA 2004). The Bridge Inspector's Reference Manual (BIRM) is available to help the bridge inspector with programs, procedures, and techniques for inspecting and evaluating a variety of in-service highway bridges (FHWA 2006). The BIRM is sponsored by the National Highway Institute through the Federal Highway Administration (FHWA). All inspectors must be certified through a NBI comprehensive training program and are required to keep this certification current through refresher courses.

According to NBIS, publicly-owned bridges in the U.S. must be inspected at least every two years. Some bridges with problem areas need to be inspected more frequently than the two year minimum requirement. Any structure that has a span length greater than twenty feet is required to be rated for National Bridge Inventory (NBI). The condition of a bridge can also be used in the load rating process for a bridge, which in some cases results in a reduced load rating

capacity for bridges in poor condition. From a transportation agency perspective, bridge condition affects maintenance and repair schedules, but it also influences allowable load limits for vehicle traffic, all of which significantly impact the public's experience and perception of the current state of the U.S. bridge infrastructure.

Within the scope of current practices for bridge inspection and condition assessment include: visual evaluation serves as the primary tool for used by inspectors. Other techniques for assessment can be employed such as specialized sensor technologies to evaluate specific challenges or measurement of bridge response to known loading; however, these techniques are often reserved for inspections beyond the routine and hands-on type. As a result, routine inspections are highly subjective and rely on experience-based expertise that must be developed over the years with practice. At first pass this may appear ineffective, but when considering the volume of bridges in service, available resources, and most importantly the lack of an all-encompassing solution for evaluating structural condition, few alternative approaches exist.

1.2 Remote Sensing Approaches to Condition Assessment

The use of remote sensing technologies presents a potential alternative to the above challenge and has the potential to augment current practices by providing both qualitative and quantitative measures of a bridge's condition. This report synthesizes the findings of an investigation of commercial remote sensing technologies with potential applications for bridge condition assessment. Presented herein are summaries of the challenges that may be addressed with remote sensing technologies and a description and ranking of the appropriateness of these technologies.

2.0 Remote Sensing Techniques and Terminology for Transportation Infrastructure

For the typical bridge engineer the concept of remote sensing is often associated with satellite imagery and aerial photography for applications in the earth sciences; however, additional remote sensing techniques have been used in infrastructure applications without being specifically labeled as such. A general definition of remote sensing is the collection and measurement of spatial information about an object, area, or phenomenon at a distance from the data source, without direct contact (Falkner 1995; Aronoff 2005). Classic examples that may be familiar to the bridge engineer or inspector include satellite imagery, aerial photography, laser scanning (such as LiDAR, light detection and ranging) and ground penetrating radar (GPR). Remote sensing can also be understood as a form of "stand-off" structural health monitoring (SHM), and a form of non-destructive evaluation (NDE) and non-destructive testing (NDT), where the device gathering data is not touching the object or feature being measured. Remote sensing does not include emplaced sensors such as strain gauges or temperature sensors, which are in direct contact with the feature whose characteristic is being measured, even if these data are being transmitted from the bridge to another location for remote monitoring. Those are "in situ" sensors, which can be valuable in combination with remote sensing data, but this report stems from a USDOT/RITA project that is focused on understanding the value and practicality of applying remote sensing techniques to assessing bridge condition. Being able to apply remote sensing techniques to the field of bridge inspection and monitoring has large potential value, especially considering the sheer number of bridges in the United States transportation infrastructure system and appropriate challenging funding environment for inspection, maintenance and rehabilitation (Ahlborn et al. 2010 a). The formal integration of remote sensing techniques into the bridge monitoring and condition assessment scheme has the potential to enhance inspection practices and also provide temporal assessments between inspection cycles, without traffic disruptions.

This assessment report focuses on twelve forms of remote sensing that are potentially valuable to assessing bridge condition. Those techniques are described in following sections, and are: GPR, spectra, 3-D optics (including photogrammetry), electro-optical satellite and airborne imagery, optical interferometry, LiDAR, thermal infrared, remote acoustics, digital image correlation (DIC), radar (including backscatter and speckle), interferometric synthetic aperture radar (InSAR), and high-resolution "StreetView-style" digital photography. More specific details on the remote sensing technologies are included in the project state of the practice report (Ahlborn et al. 2010 b).

Before discussing these technologies and the bridge condition challenges that can be measured and monitored, it is useful to describe the terms and principles frequently encountered when reading about or applying remote sensing methods. One such area is the use of active versus passive sensors. Active sensors emit a signal from the sensor and a reflected signal is collected off the feature of interest (such as a radar signal or actively emitted light used in

LiDAR). Passive sensors collect only the reflected ambient visible and infrared wavelengths that "bounce" (reflect) off an object. These ambient wavelengths are typically visible and infrared sunlight, which produce spectral reflectance patterns from the object. Aerial photography and Landsat satellite imagery are examples of passive sensors.

The concept of the electro-magnetic (EM) spectrum and the different wavelengths it consists of are important to understanding remote sensing. Figure 1 shows two example diagrams of the EM spectrum from short to long wavelengths. Noteworthy is that visible light is only a small part of the spectrum, between approximately 400 nanometers (nm) and 700 nm. Infrared light includes both the "near infrared" and thermal infrared that is used to record temperature. Visible and near-infrared light are often referred to as electro-optical (EO), while radar (Radio Detection and Ranging) uses radio-wavelength parts of the spectrum, typically with an active emitter and sensor. In general remote sensing can be done with wavelengths at any part of the spectrum; most common in transportation applications are visible, infrared, and radio-range wavelengths.

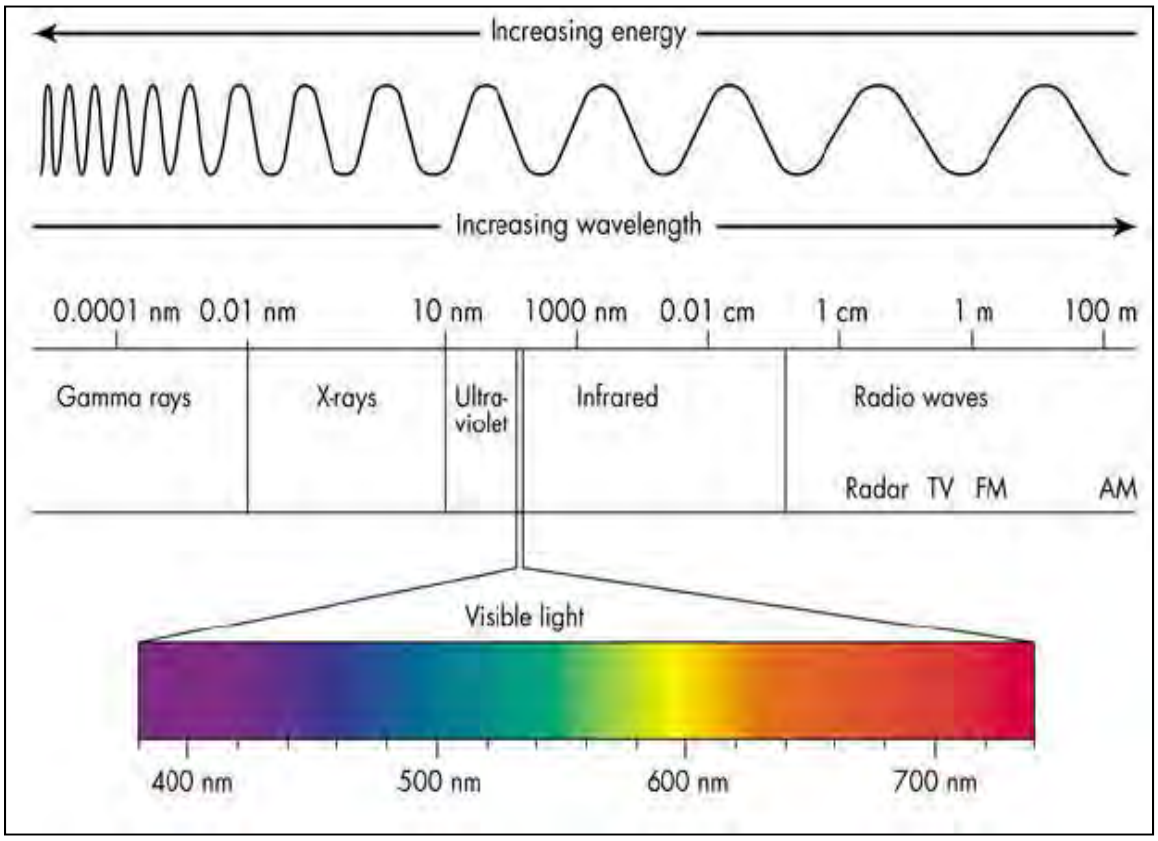

Figure 1: An example of the electro-magnetic spectrum and its relationship to wavelength

Resolution is another important concept. Resolution is most frequently used to refer to spatial resolution, which can be understood as the area on the ground that an image's pixel (picture element) covers, the smallest feature that can be resolved or identified in an image, or the "ground-sample distance" (GSD) between measurements. Spatial resolution usually affects a term known as “swath width” – this is the size of an area that is collected on the ground, usually

as a continuous strip of imagery. Higher spatial resolution satellites usually have smaller swaths, meaning smaller areas on the ground are collected. Lower spatial resolution usually means larger areas are collected.

Other types of resolution are temporal, spectral, and radiometric. Temporal resolution refers to frequency in time in which a site or feature can be sensed by an instrument. For example, the Landsat 5 Thematic Mapper satellite gathers an image of the same area on the ground once every 16 days as it circles the earth. A remote sensing technology mounted on a vehicle, such as a terrestrial LiDAR system, would have a temporal resolution of however often it was chosen to be deployed to a location depending on budget and need. Spectral resolution most typically refers to size and number of divisions of the EM spectrum that a sensor can collect. Landsat 5 collects seven spectral bands ranging from the visible (blue, green, and red) to the near infrared and thermal. Digital Globe's Quickbird satellite collects four spectral bands (blue, green, red, and one band of near infrared). A typical consumer digital camera collects the three visible bands of blue, green, and red. Radiometric resolution refers to the number of "bits" used to collect a remotely sensed piece of data. For example, 8-bit color records information on a scale of 0-255 (or 256 values); 24-bit color is recorded with 16,777,216 values, meaning that many finer gradations in a color can be recorded about a feature and displayed later on in software tools and printed products.

Resolution needs impact the type of remote sensing device or platform that should be used to measure a particular indicator of interest, such as the amount of spalling on a bridge. Figure 2 shows an example, adapted from (Luhmann et al. 2006), that MTRI researchers used to define the remote sensing platform needed for an unpaved road condition study. The smaller the object area and the smaller the feature of interest (such as rutting), the higher accuracy is needed, which defines the platform used to collect the data. In the case of this study, the requirements to evaluate unpaved road conditions helped define than an unmanned aerial vehicle (UAV) platform for photogrammetry was needed and suitable for this remote sensing study. Photogrammetry is the science of making reliable geometric measurements from photographs (such as elevation or height data), most often from aerial photographs and satellite images (Falkner 1995).

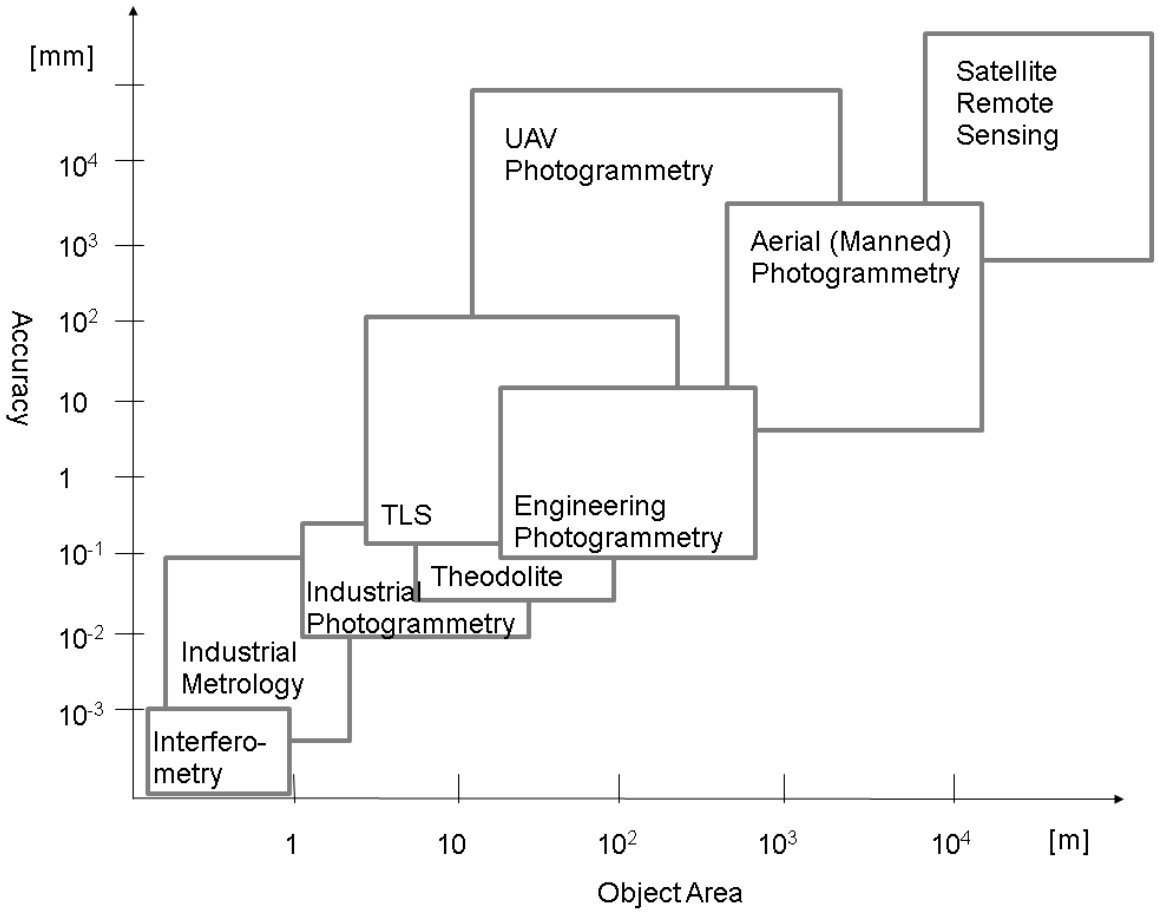

Figure 2: An example of the trade-offs of spatial resolution in terms of accuracy needs and the size of an object or part of an area on the ground that needs to analyzed via remote sensing (Luhmann et al. 2006)

When discussing remote sensing, the terms "multispectral", "hyperspectral", and panchromatic are often used when referring to remotely sensed data, especially satellite imagery and aerial photography. Multispectral and hyperspectral both mean remote sensing data that has been collected with many "bands" to capture parts of the electromagnetic spectrum. For example, the commercial WorldView-2 satellite captures data in eight parts of the EM spectrum (8 bands), which are shown in Figure 3. The importance of capturing multiple parts of the spectrum is that features can reflect parts of the EM spectrum differently depending on the type or condition of a surface being imaged by a remote sensing device. For example, this means that a bridge surface in different condition could look different in certain parts of the EM spectrum. In the case of a multispectral sensor (such as WorldView-2, or a typical aerial photography professional digital camera), only a few bands or "slices" of the EM spectrum are collected by the remote sensing platform (typically from three to approximately 30). Hyperspectral sensors are typically 100 to 200 or more bands of the EM spectrum, typically with narrow bandwidths of the spectrum being collected. Panchromatic means a single band of information of information

was collected by the remote sensing platform – this typically takes the form a black and white (or grayscale) image. Panchromatic data is limited in color information but takes up relatively little storage space, making it suitable to some transportation applications.

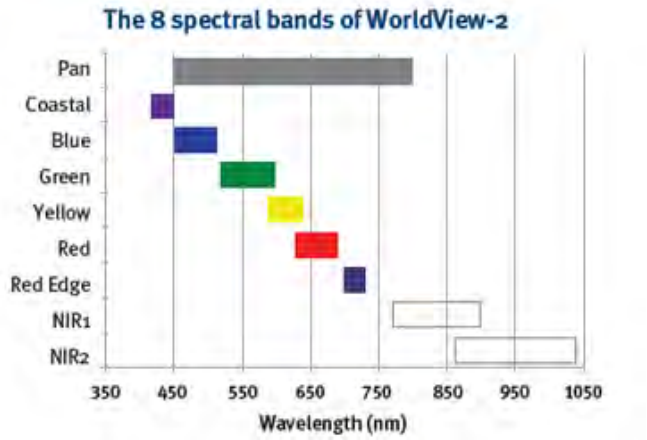

Figure 3: An example of the parts of the electro-magnetic spectrum captured by Digital Globe's WorldView-2 satellite and available as digital images (Digital Globe Webpage 2009)

Radar remote sensing technologies can contribute to transportation infrastructure assessment. Different radar platforms operate at different wavelengths of the radio spectrum. Table 1 lists some example radar bands that operate at different wavelengths and frequencies. The relationship between wavelength and frequency is define by the equation $c = \lambda v$ where c = the speed of light, λ = wavelength, and v = frequency. More important to bridge assessment is that different wavelengths have different penetrative capabilities, such as is seen in applications of GPR in bridge deck assessment. Longer wavelengths have greater penetration but with the tradeoff of lower spatial resolution (i.e., you can see further in, but smaller features are harder to discern), while shorter wavelengths typically do not penetrate as far, but small features are easier to identify (Aronoff 2005).

Table 1: Examples of radar bands, frequency, and their wavelength

Radar Band	Frequency (GHz)	Wavelength (cm)
Ka	26 - 40	0.8 – 1.1
K	18.5 – 26.5	1.1 – 1.7
Ku	12 - 18	1.67 – 2.5
X	8 - 12.5	2.4 – 3.8
C	4 - 8	3.8 – 7.5
S	2 - 4	7.5 - 15
L	1 - 2	15 – 30
P	0.3 - 1	30 - 100

Additional resources are available to understanding remote sensing. This report further defines particular technologies and their applications to bridge condition assessment in the upcoming sections.

3.0 Challenges for National Bridge Inventory Infrastructure

To maintain updated records on infrastructure within the national bridge inventory, routine bridge inspections must be completed at a minimum of every two years. Bridge inspections processes are crucial to the life cycle preservation of bridge structures as they help to maintain safe operating conditions, prioritize maintenance and repair operations, and dictate funding priorities. With these processes, bridges can be monitored and issues mitigated to help extend the service life of a structure. The primary components of a bridge can be categorized as the bridge deck, superstructure and substructure. While all three components are essential to the performance of a bridge, considerations for the deck and superstructure are presented herein. From a maintenance and condition evaluation perspective, the bridge deck and superstructure are of major interest because they have the primary role of transferring loads to the substructure. In addition, the deck serves as the driving surface while also providing protection from the environment and contaminants (salts and chemicals) to the superstructure and substructure elements below. The expectation is that remote sensing technologies have the greatest potential to address challenges associated with these components.

In the United States, the majority of the bridges constructed and in service utilize reinforced concrete decks, with the remaining population comprised of a variety of alternative materials such as: timber, steel orthotropic, steel grid, and composite or polymeric. Bridge decks can be classified, to certain extent, as a sacrificial element because it can be replaced as it degrades [Figure 4]. However, as the integrity of the deck is compromised during the degradation process, the protection afforded to the superstructure and substructure elements also diminishes, often providing a catalyst for deterioration or accelerating degradation of these elements. The use of remote sensing technologies for condition assessment of concrete bridge decks has the potential to make a significant impact on current practices from an inspection and maintenance point of view as well as from a safety perspective. From a broad perspective, the issues that most often plague concrete bridge decks can be categorized by location as either surface challenges or subsurface challenges, with one often leading to the manifestation of the other.

DECK CONDITION STATE				REPAIR OPTIONS	POTENTIAL RESULT TO DECK BSIR		NEXT ANTICIPATED EVALUATION
Top Surface		Bottom Surface			Top Surface BSIR #58a	Bottom Surface BSIR #58b	
BSIR #58a	Deficiencies % (a)	BSIR #58b	Deficiencies % (b)				
≥ 5	N/A	N/A	N/A	Hold (c) Seal Cracks/Healer Sealer (d)	No Change	No Change	1 to 8 years
	≤ 5%	> 5	≤ 2%	Epoxy Overlay	8, 9	No Change	10 to 15 years
	≤ 10%	≥ 4	≤ 25%	Deck Patch (e)	Up by 1 pt.	No Change	3 to 10 years
4 or 5	10% to 25%	5 or 6	≤ 10%	Deep Concrete Overlay (h)	8, 9	No Change	25 to 30 years
		4	10% to 25%	Shallow Concrete Overlay (h, i)	8, 9	No Change	10 to 15 years
				HMA Overlay with water-proofing membrane (f, h, i)	8, 9	No Change	8 to 10 years
		2 or 3	> 25%	HMA Cap (g, h, i)	8, 9	No Change	2 to 4 years
≤ 3	>25%	> 5	< 2%	Deep Concrete Overlay (h)	8, 9	No Change	20 to 25 years
		4 or 5	2% to 25%	Shallow Concrete Overlay (h, i)	8, 9	No Change	10 years
				HMA Overlay with water-proofing membrane (f, h, i)	8, 9	No Change	5 to 7 years
		2 or 3	>25%	HMA Cap (g, h, i)	8, 9	No Change	1 to 3 years
				Replace Deck	9	9	40+ years

(a) Percent of deck surface area that is spalled, delaminated, or patched with temporary patch material.
(b) Percent of deck underside area that is spalled, delaminated or map cracked.
(c) The "Hold" option implies that there is on-going maintenance of filling potholes with cold patch and scaling of incipient spalls.
(d) Seal cracks when cracks are easily visible and minimal map cracking. Apply healer sealer when crack density is too great to seal individually by hand. Sustains the current condition longer.
(e) Crack sealing can also be used to seal the perimeter of deck patches.
(f) Hot Mix Asphalt overlay with waterproofing membrane. Deck patching required prior to placement of waterproofing membrane.
(g) Hot Mix Asphalt cap without waterproofing membrane for ride quality improvement. Deck should be scheduled for replacement in the 5 year plan.
(h) If bridge crosses over traveled lanes and the deck contains slag aggregate, do deck replacement.
(i) When deck bottom surface is rated poor (or worse) and may have loose or delaminated concrete over traveled lanes, an in-depth inspection should be scheduled. Any loose or delaminated concrete should be scaled off and false decking should be placed over traveled lanes where there is potential for additional concrete to become loose.

Figure 4: Michigan Department of Transportation Bridge Deck Preservation Matrix (Michigan Department of Transportation 2008)

The superstructure elements of most bridges in the United States are typically constructed of either steel or concrete (pre-stressed or reinforced) girders and are frequently paired with a reinforced concrete deck. These members serve as the primary load carrying members and their importance correlates directly to safety and integrity of the structural system. Superstructure elements are not replaced as often as bridge decks in maintenance operations and they are expected to last for the duration of the bridge design life. However, the consequences of failure for superstructure elements are critical considering human life factors. These dramatic consequences are highlighting the importance of quality inspection and maintenance practices for these members. Thus, the issues related to the condition of superstructure members must be observed over time and must also consider challenges on the surface as well as those internal to the member.

Other issues related to bridge performance can only be observed at the bridge system or global level due to the couple multi-directional response and redundancy inherent to most bridges. These challenges are essential to assessing performance of a structure versus the

intended design behavior and have the potential to characterize the overall health and performance of a bridge.

In this evaluation, bridge challenges are organized into five categories including:

- Deck surface
- Deck subsurface
- Girder surface
- Girder subsurface
- Global metrics

The division into these five categories allowed for a focused investigation on certain bridge condition challenges more susceptible to that particular bridge location and the pairing of appropriate remote sensing technologies to evaluate the challenge. In the following section, those bridge categories and the identified challenges within those locations are discussed. The challenges selected were based on specific issues that were deemed critical to bridge performance and issues that manifest into poor condition ratings during inspections. Also included within each of the identified challenges are potential remote sensing technologies for each particular challenge with more detail provided in the Performance Evaluation of Remote Sensing Technologies section (section 5). General details on the appropriateness of the remote sensing technology for each challenge are presented within the Technology Rating Methodology section (section 4) with specific details provided in Table 3.

3.1 Deck Surface

The deck surface plays an important role in bridge maintenance because deterioration at this location can lead to further subsurface issues which can affect the entire bridge system. There are several different challenges associated with maintaining a bridge deck including: surface cracking, spalling and scaling along with issues with the expansion joints. When considering bridge deck inspections, some primary difficulties relate to assessing condition in a safe manner without disrupting traffic, and this becomes increasingly difficult on the underside of bridges. Assessment of the deck surface using remote sensing technologies, specifically optical (non-penetrative) approaches, appears promising especially considering that most deck surface issues are assessed visually in a routine inspection.

3.1.1 Map Cracking

Map cracking is a challenge associated with concrete decks in which the surface has a pattern of cracks caused by material failure. The magnitude of the cracks considered in this study ranged from 1/16” to 3/16” in width (FHWA 2006). An example of map cracking is presented in Figure 5. Traditional inspection techniques used for the assessment of map cracking include: visual evaluation, ultrasonic testing and impact-echo testing (FHWA 2006).

Potential remote sensing technologies for measuring map cracking:

- 3D photogrammetry
- StreetView-style photography
- Thermal IR
- LiDAR
- Optical interferometry
- EO airborne/satellite imagery
- Spectra
- Acoustics
- Radar (backscatter/speckle)

Figure 5: Map cracking on bridge deck surface (FHWA 2006)

3.1.2 Delamination

Delaminations revealed through surface cracks are similar to map cracking, but the actual locations of delaminations are beneath the concrete surface. These delaminations will typically turn into spalls over time. The magnitude of delamination cracks considered in this study was 1/16” to 3/16” in width (FHWA 2006). Similar to surface crack evaluation, traditional inspection techniques used for the assessment of surface cracks include: visual evaluation, ultrasonic testing and impact-echo testing (FHWA 2006).

Potential remote sensing technologies for measuring delamination:

- 3D photogrammetry

- StreetView-style photography
- Thermal IR
- LiDAR
- Optical interferometry
- Spectra
- Acoustics

3.1.3 Scaling

Scaling is an issue with the deck surface that covers the loss of material due to material degradation. Within this review, scaling is considered on the order of magnitude of 1/4” to 1” in depth (FHWA 2006). Figure 6 provides a representative example of moderate surface scaling of the deck surface. The current method for identifying the amount of scaling on a bridge structure is visual assessment and quantification.

Potential remote sensing technologies for measuring scaling:

- 3D photogrammetry
- StreetView-style photography
- Thermal IR
- LiDAR
- Optical interferometry
- EO airborne/satellite imagery
- Spectra
- Radar (backscatter/speckle).

Figure 6: Concrete deck surface scaling (FHWA 2006)

3.1.4 Spalling

Spalling is an issue with the deck surface that covers the loss of material due to delaminations in the concrete deck. With this review, spalling is considered on the order of magnitude of 1/4” to 1” in depth (FHWA 2006). An example of spalling in the concrete deck surface is shown in Figure 7. The current method for identifying the amount of spalling on a bridge structure is visual assessment and quantification.

Potential remote sensing technologies for measuring spalling:

- 3D photogrammetry
- StreetView-style photography
- Thermal IR
- LiDAR
- Optical interferometry
- EO airborne/satellite imagery
- Spectra
- Radar (backscatter/speckle)

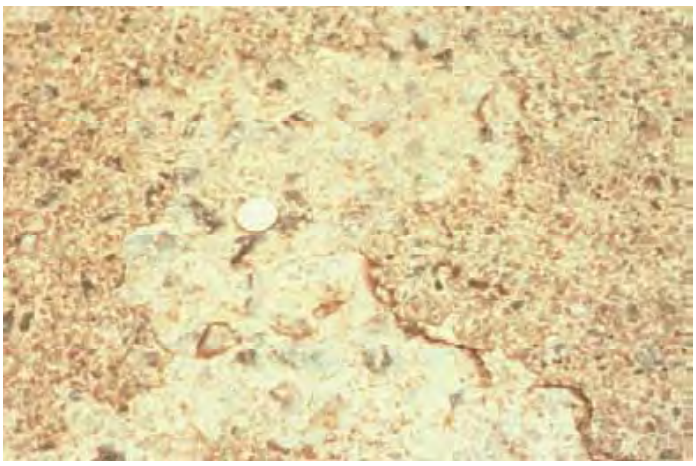

Figure 7: Spalling on concrete deck surface (FHWA 2006)

3.1.5 Expansion Joints

There are several different issues related to the expansion joints of the bridge. These include torn or missing seals, armored plate damage, chemical leaching on the bottom of joint, cracks within two feet of the joint and spalls within two feet of the joint. The indicators for the majority of these issues are represented by the titles of the different issues whereas the magnitude of the sensitivity for cracking and spalling is identical to those for surface cracking (1/16” to 3/16” in width) and spalling (1/4” to 1” in depth) (FHWA 2006). These issues are currently assessed through visual inspection by the bridge inspector. With the cracking and spalling, it is at the discretion of the inspector if they were caused by an expansion joint failure.

Potential remote sensing technologies for measuring expansion joint challenges:

- 3D photogrammetry
- StreetView-style photography
- Thermal IR
- LiDAR
- Optical interferometry
- EO airborne/satellite imagery
- Spectra
- Radar (backscatter/speckle)

3.2 Deck Subsurface

The main challenge with assessing the condition of the deck throughout its depth is that it is not visible to human eye. This can severely limit the identification of issues occurring below the deck surface. While these issues are of significant importance to bridge inspectors, traditional

subsurface evaluation techniques are extremely limited and have only had moderate success within the bridge community. Similar to deck surface evaluation, there are still issues with keeping the traffic disruption during inspections to a minimum. The primary challenges associated with a bridge deck subsurface can be categorized as: material in the expansion joint, delamination, scaling and spalling on an unobserved surface (interior or hidden), corrosion and chloride ingress.

3.2.1 Expansion Joint

Excessive material in the expansion joint causes increased stresses in the components of the bridge due to the inability to expand. The quantity of material is inconsequential, but the presence of material fill is typically noted from visual assessment. Figure 8 shows an expansion joint that was filled with material.

Potential remote sensing technologies for measuring expansion joint challenge:

- Optical interferometry

Figure 8: Material in expansion joint (FHWA 2006)

3.2.2 Delamination

Delamination in a concrete deck is the separation of material along a horizontal plane within the concrete interior. There are several indicators that can possibly show where a

delamination has occurred including: a hollow sound, internal horizontal crack, moisture in horizontal cracks and fracture planes or open spaces in the concrete. The magnitude for the internal horizontal crack considered in this evaluation was considered to be approximately on the order of 0.004" (0.1 mm) level (FHWA 2006). No quantitative measure of moisture was considered, but the extent of the horizontal crack is determined by comparing the difference of the moisture content in the crack to the moisture content of the surrounding concrete. Similarly, relative changes in the measured radar signal with the use of integrated volume are used to evaluate fracture planes or open spaces within the concrete interior. Current techniques used to location delaminations include: acoustic wave sonic/ultrasonic velocity measurements, ground-penetrating radar, infrared thermography, ultrasonic testing, chain drag and visual evaluation (FHWA 2006).

Potential remote sensing technologies for measuring delamination:

- Ground-penetrating radar
- Thermal IR
- Acoustics
- Radar (backscatter/speckle)

3.2.3 Scaling

Scaling of material in the deck subsurface is defined as any loss of material that cannot be seen from the surface. The concept is to apply the instrument from the deck surface and observe the unseen section of the deck. The magnitude of material loss considered for this review, was ¼" to 1" in depth (FHWA 2006). Current practice for detecting scaling includes visual evaluation when it is observable.

Potential remote sensing technologies for measuring scaling:

- Ground-penetrating radar
- Thermal IR

3.2.4 Spalling

The concept of spalling of the deck subsurface is analogous to the aforementioned definition for subsurface scaling. Similarly, the magnitude of material loss considered for this review was ¼" to 1" in depth (FHWA 2006). Figure 9 shows an example of subsurface spalling representing the bottom surface of a bridge deck. Current practice for detecting spalling would be visual evaluation. The current in practice techniques for detecting spalling would be visual evaluating when it is observable.

Potential remote sensing technologies for measuring spalling:

- Ground-penetrating radar
- Thermal IR

Figure 9: Spalling on bridge deck surface

3.2.5 Corrosion

Reinforcement corrosion in a bridge deck results in a volume expansion of the deck due to the growth of corrosion by-products. The consequences of this volume expansion include: delamination and crack enlargement, as well as reduction in reinforcement cross section, load capacity and stiffness of the bridge deck (Nowak et al. 2000). The presence of corrosion and evolution of corrosion rate has been identified by changes in concrete resistivity. Higher concrete resistivity measurements in the range of 5 to 20 kΩ-cm imply lower corrosion rates (ACI 2001). Other mechanisms for assessing corrosion have centered on identify size and consistency of embedded reinforcing steel. Figure 10: Corroded reinforcement in bridge deck provides a typical example of high level corrosion of reinforcing steel and the associated ramifications. Current approaches for measuring corrosion include: half-cell potential, acoustic emissions, nonlinear vibro-acoustic method, four-probe electrical resistivity test, electrical resistant method, optical fiber sensors, magnetic flux leakage, magnetostrictive sensors, and microwave based thermoreflectometry (Sekulic et al. 2001).

Potential remote sensing technologies for measuring corrosion:

- Ground-penetrating radar

- Acoustics
- Radar (backscatter/speckle)

Figure 10: Corroded reinforcement in bridge deck

3.2.6 Chloride Ingress

Chloride contamination in concrete is a contributing factor to accelerate corrosion of reinforcement embedded in concrete bridge decks. Commonly accepted threshold values of 0.4% to 1% chloride by mass of concrete in the concrete cover, have been classified for medium corrosion risk (Angst et al. 2009). A number of standard AASHTO and ASTM tests (AASHTO T-260, ASTM C 1152, ASTM C 1218, AASHTO T277-93) and the neutron probe test have been used to quantify chloride ingress (ACI 2001; FHWA 2006).

Potential remote sensing technologies for measuring chloride ingress:

- Ground-penetrating radar
- Radar (backscatter/speckle)

3.3 Girder Surface

As the primary load carrying members within a bridge, defects observed in and on a girder have the potential to result in a decrease in section capacity. Several challenges associated with the girder surface include: steel structural cracking, concrete structural cracking, steel

section loss, concrete section loss, and deterioration of protective paint. These challenges can be associated with either material distress or unexpected structural behavior issues, but in both cases the ramifications with respect to safety are paramount.

3.3.1 Steel Structural Cracking

One challenge that arises in bridges is structural (or large) cracking on the bridge girder. Structural cracking is categorized as the separation or breakage of materials. This type of structural cracking has various implications pertaining to the type of failure (flexure, shear, torsion, and fatigue). Within this evaluation, the specified resolution for steel structural cracking was selected as hairline size cracks with an approximate size of 0.004" (0.1mm) cracks or smaller (FHWA 2006). Current practices for evaluating structural cracks in steel include visual evaluation, eddy current applications, magnetic particle and imaging devices.

Potential remote sensing technologies for measuring steel structural cracking:

- 3D photogrammetry
- Optical interferometry
- Thermal IR
- Spectra

3.3.2 Concrete Structural Cracking

Concrete structural cracking can be defined as the separation of sections of concrete girder components. Similar to steel structural cracking, concrete structural cracking has various implications pertaining to the type of failure (flexure, shear and torsion). Within this evaluation, the specified resolution for concrete structural cracking was selected as hairline size cracks with an approximate size of 0.004" (0.1mm) cracks or smaller (FHWA 2006). Current techniques for evaluating structural cracking in concrete are similar to those of the steel structural cracking and include: visual evaluation, imaging devices, eddy current and magnetic particle applications (FHWA 2006; AASHTO 2008).

Potential remote sensing technologies for measuring concrete structural cracking:

- 3D photogrammetry
- Optical interferometry
- Acoustics
- Thermal IR
- Spectra

3.3.3 Steel Section Loss

Steel section loss is defined as the change (reduction) in area or volume of a structural component in which the structure's stiffness or strength is decreased. Indicators of this type of steel section loss would be a loss or change in cross sectional area or thickness of elements. Representative examples of steel section loss are shown in Figure 11a and 11b. A quantitative measure of section loss is essential to determine the appropriate reduction, relative to design values, in capacity and stiffness that must be considered for structural load rating and capacity analyses. Techniques commonly used for measuring steel section loss include: visual evaluation, dye penetration, fiber optics and imaging devices (FHWA 2006).

Potential remote sensing technologies for measuring steel section loss:

- Thermal IR
- LiDAR
- EO airborne/satellite imagery
- Radar (backscatter/speckle)
- 3D photogrammetry

(a)

(b)

Figure 11: a) Steel section loss in bridge girder viewed from the side; b) Steel section loss viewed from along the beam

3.3.4 Paint

Paint is typically used as a protective layer on steel beams (often aesthetics on concrete beams) to prevent or minimize corrosion from initiating or continuing to grow. The loss of this protective coating provides a mechanism for corrosion to initiate, but may also be indicative of underlying issues with the member such as member cracking. Figure 12 demonstrates loss of paint from the surface of the girders. Current methods used for evaluating the condition of paint include visual evaluation and imaging techniques (FHWA 2006).

Potential remote sensing technologies for measuring paint condition:

- Thermal IR
- Spectra

Figure 12: Paint loss on girder surface

3.3.5 Concrete Section Loss

Concrete section loss is defined as the loss of area or volume of the concrete along the surface where the stiffness or strength is compromised. Indicators of concrete section loss would be a loss or change in cross sectional area or thickness of elements (spalled sections of concrete

are typical). Figure 13 shows the section loss in a concrete girder component in which the reinforcement is showing. Similar to steel section loss, a quantitative measure of section loss is essential to determine the appropriate reduction, relative to design values, in capacity and stiffness that must be considered for structural load rating and capacity analyses. Current techniques used for evaluating section loss include visual evaluation, imaging devices, and fiber optics (FHWA 2006).

Potential remote sensing technologies for measuring concrete section loss:

- 3D photogrammetry
- Thermal IR
- LiDAR
- EO airborne/satellite imagery
- Acoustics
- Radar (backscatter/speckle)

Figure 13: Concrete section loss (FHWA 2006)

3.4 Girder Subsurface

Issues occurring within the cross-section of girders have the same consequences as those on the girder surface. However, the difficulty of observing these issues is significantly more as

challenge may be hidden or not easily accessible. Several challenges associated with the girder subsurface include: concrete structural cracking, concrete section loss, prestress strand breakage, reinforcement corrosion, and chloride ingress.

3.4.1 Concrete Structural Cracking

Concrete structural cracking can be defined as the separation of sections of concrete girder components (previously defined). These are distinguished from surface cracks in that they are not visible from the surface as would be the case for interior sections of side-by-side box beams. This type of concrete structural cracking has various implications pertaining to the type of failure (flexure, shear and torsion). Within this evaluation, the specified resolution for concrete structural cracking was selected as approximately 0.03125" (0.8mm). Current techniques for evaluating subsurface concrete structural cracking include: imaging devices, eddy current, and magnetic particle applications (FHWA 2006; AASHTO 2008).

Potential remote sensing technologies for measuring concrete structural cracking:

- Thermal IR
- Acoustics

3.4.2 Concrete Section Loss

Concrete section loss is defined as the loss of area or volume of the concrete along the surface where the stiffness or strength is compromised (previously defined). This section loss is distinguished from surface concrete section loss in that the area or volume would not be visible from the surface as would be the case for interior sections of side-by-side box beams. Indicators of concrete section loss would be a loss or change in cross sectional area or thickness of elements (spalled sections of concrete are typical). A quantitative measure of section loss is essential to determine the appropriate reduction, relative to design values, in capacity and stiffness that must be considered for structural load rating and capacity analyses. Current techniques for evaluating subsurface concrete section loss include: imaging devices, visual inspection (if accessible) and fiber optics (FHWA 2006).

Potential remote sensing technologies for measuring concrete section loss:

- Acoustics
- Radar (backscatter/speckle)

3.4.3 Prestress Strand Breakage

Within a prestressed concrete girder, the prestressing strand provides the tensile resistance to the girder, but also minimizes crack formation under service loads. Breakage of

these prestressing strands results in a redistribution of stresses within the member and potential failure of the structure. In this evaluation, the sensitivity of resolution would be to the size of the strand under consideration, 0.08” (2mm) for an individual wire or 0.375” (9.5 mm) for a typical strand (PCI 2004). Current practices used for investigating strand breaks include visual evaluation (sag in structure or exposed broken strand), eddy current, ground penetrating radar (GPR) and ultrasonic wave applications (FHWA 2006).

Potential remote sensing technologies for measuring prestress strand breakage:

- Ground-Penetrating Radar
- Acoustics
- Radar (backscatter/speckle)

3.4.4 Corrosion

Reinforcement corrosion within bridge girders yields by-products, causing a volume change in the surrounding concrete which causes the formation of cracks and delaminations near surfaces, similar to the case for deck subsurface corrosion (previously described). Figure 14 demonstrates the effects of corrosion on reinforcing bars in a concrete bridge girder. As with the deck subsurface scenario, the presence of corrosion and evolution of corrosion rate has been identified by changes in concrete resistivity. Higher concrete resistivity measurements in the range of 5 to 20 kΩ-cm imply lower corrosion rates (ACI 2001). Other mechanisms for assessing corrosion have centered on identify size and consistency of embedded reinforcing steel. Current approaches for measuring corrosion include: half-cell potential, acoustic emissions, nonlinear vibro-acoustic method, four-probe electrical resistivity test, electrical resistant method, optical fiber sensors, magnetic flux leakage, magnetostrictive sensors, and microwave based thermoreflectometry (Sekulic et al. 2001).

Potential remote sensing technologies for measuring corrosion:

- Ground-Penetrating Radar
- Acoustics
- Radar (backscatter/speckle)

Figure 14: Corroded reinforcing bars

3.4.5 Chloride Ingress

Similar to bridge decks (previously described), chloride contamination is a contributing factor to accelerate corrosion of reinforcement embedded in concrete bridge girders decks. Commonly accepted threshold values of 0.4% to 1% chloride by mass of concrete in concrete cover, have been classified for medium corrosion risk (Angst et al. 2009). A number of standard AASHTO and ASTM tests (AASHTO T-260, ASTM C 1152, ASTM C 1218, AASHTO T277-93) and the neutron probe test have been used to quantify chloride ingress (ACI 2001).

Potential remote sensing technologies for measuring chloride ingress:

- Ground-Penetrating Radar
- Radar (backscatter/speckle)

3.5 Global Metrics

The challenges described in the previous sections related specifically to member behavior and material degradation issues. Other challenges which related to the entire bridge system cannot be categorized within these definitions are categorized in this evaluation as global metrics. Global metric challenges include: change in bridge length, bridge settlement, bridge movement, surface roughness and vibration. These challenges may not be observable during a routine inspection of the bridge or individual elements, but their influence on the system behavior has the potential to influence the member categories.

3.5.1 Bridge Length

Change in bridge length (often a reduction) resulting from pavement shove has the potential to change the state of stress within a bridge. This change in length can also influence support restraint by altering design boundary conditions (e.g. squeezing expansion joints and rotating support rockers). This change in length is taken along the span of the bridge. According to Manual for Bridge Inspection, bridge length measurements will take place when bridge plans are not available; 0.1ft is the limit of accuracy for measuring this feature (AASHTO 2008). Current methods for measuring bridge length include: measuring wheel and electronic distance meter (EDM) (AASHTO 2008).

Potential remote sensing technologies for measuring bridge length:

- 3D photogrammetry
- EO airborne/satellite imagery
- Digital image correlation
- InSAR

3.5.2 Bridge Settlement

Bridge settlement, defined as vertical movement of the bridge (z-axis), can cause cracks to form within the bridge deck, superstructure and/or substructure. Bridge settlement can be uniform or differential, with differential settlement resulting in more severe damage within the structure due to unforeseen constraint. Soil bearing failure, consolidation of soil, scour, undermining and subsidence from mining or solution cavities are the main causes of the bridge settlement vertical movement (FHWA 2006). In this evaluation, an approximate sensitivity of ¼” to ½” was defined. Current methods for evaluating settlement have included GPS and tiltmeters (FHWA 2006).

Potential remote sensing technologies for measuring bridge settlement:

- 3D photogrammetry
- Digital image correlation
- LiDAR
- InSAR

3.5.3 Bridge Movement

Bridge movement is defined as horizontal movement of the bridge either in the longitudinal or transverse directions (X or Y axis). Horizontal movement of bridge can cause cracks on the bridge deck and substructure. In this evaluation, an approximate sensitivity of ¼" to ½" was defined. Current methods for measuring bridge movement included strain sensors and tiltmeters (FHWA 2006).

Potential remote sensing technologies for measuring bridge movement:

- 3D photogrammetry
- Digital image correlation
- LiDAR
- InSAR

3.5.4 Surface Roughness

Surface roughness correlates primarily to user comfort and ride quality, but has broader implications with respect to dynamic amplification on a bridge, with a rougher surface correlating to lager dynamic response within the structure. Current methods for assessing road surface roughness primarily rely on visual evaluation methods with subjective ratings.

Potential remote sensing technologies for measuring surface roughness:

- 3D photogrammetry
- StreetView-style photography
- LiDAR
- Optical interferometry
- EO airborne/satellite imagery
- InSAR
- Radar (Backscatter/Speckle)
- Spectra

3.5.5 Vibration

Vibration is defined as the oscillation or periodic motion of a rigid body. In bridges, vibration is considered as the oscillation of its structural members. Typically, vibrations documented out of the bridge's natural vibration range can indicate problems such as unseen cracks or fractures within the structure. Typical methods used for vibration measurements include accelerometers and GPS receivers. In this evaluation, the range of fundamental

frequencies considered ranged from 0.5-20 Hz range with relatively small amplitudes, representing a range common to routine bridges.

Potential remote sensing technologies for measuring vibration:

- Optical interferometry
- Digital image correlation
- InSAR
- Radar (backscatter/speckle)

4.0 Technology Rating Methodology

The demonstration rating given in this commercial remote sensing evaluation is an unweighted, cumulative score of points awarded to a particular technology's capability in detecting a specific indicator of bridge structural health. The criteria for each technology-indicator appraisal was developed based on the experience, and each is intended to be an objective dimension of remote sensing technology as it would be used in bridge condition assessment. The rating system is similar to the work of Gucunski, et al. (2010), where non-destructive evaluation/testing (NDE/NDT) techniques were assigned grades to assess their performance for various NDE/NDT applications. Our assessment encountered some of the same difficulties as theirs, particularly the lack of information in the literature regarding specific performance measures. The performance criteria that Gucunski, et al. (2010) used were: i) accuracy, ii) repeatability, iii) ease of data collection, analysis, and interpretation, iv) speed of data collection and analysis, and v) cost of data collection and analysis. The list of criteria used in this evaluation is listed in the left column of Table 2.

A major component in the rating of technologies for bridge condition evaluation was a growing library of references that we initially generated for the State of the Practice Synthesis Report (Ahlborn et al. 2010 b). The highest level of detail and scope applicable to bridge-related remote sensing were used wherever possible for this commercial remote sensors rating methodology. Ideal inputs for the commercial sensor evaluation were papers that demonstrated a remote sensing technology in the field, attempted to characterize a potential defect or other relevant aspect of bridge condition, reported on the resolution or sensitivity they achieved, and estimated the error. In addition, the domain expertise of the project team, particularly in the areas of radar (including GPR and InSAR), interferometry, digital image correlation, electro-optical (EO) imagery from both airborne and satellite instruments, as well as high-resolution "StreetView-style" digital panoramas were critical to the evaluation.

All performance criteria receive a score from 0 to 2 (low to high). This narrow range was chosen so as to avoid artificially inflating scores. For all performance criteria, a higher score is more satisfactory; a score of zero indicates the technology does not satisfy that criterion.

Criteria A and B: The most important criteria in the appraisal are criterion A and B, respectively: whether the technology has the capability to satisfy the spatial, spectral, or temporal resolution required and whether or not the technology is commercially available, only research-grade, or has never been used for that application before. Their importance is reflected in the total rating, for if either one of these criteria received a zero score, the total rating is zero. This reflects the fact that if the technology does not meet the requirements (i.e. it cannot sense the bridge condition indicator of interest) or is not actually available for use (i.e. only theoretical) for a given indicator, then the technology is not considered applicable for observing that specific bridge condition indicator and it is not recommended for further research and development or commercial implementation as part of this study. At this point in the assessment of remote sensing technologies' performance, the even weighting of each rating is a demonstration

methodology and will be reviewed as part of supplementary report in the future. Additional knowledge of the capabilities of the remote sensing technologies may allow for more refined rating scales and weighting.

Table 2: Definition for the criteria used in rating remote sensing technologies for their efficacy in detecting bridge condition indicators

Criteria	Score (0-2)	
A: Is the requirement met?	**2**	Resolution is specifically within the current capabilities of the technology Full range of measurements are met or better Other requirements directly measured
	1	Lower limit of resolution/requirements is not within capabilities, but upper limit is Technology can measure somewhere between the range or within 25 % of upper limit Some requirements are only indirectly measured
	0	Upper limit of resolution not met within 25 % current capabilities do not allow direct measurement at any necessary resolution
B: Availability of instrument	**2**	Technology is currently commercially available and used for similar application(s) Technologies components are immediately available for use as manufacturer intends (e.g. there is no commercial DIC or 3D Photogrammetry platform, but digital cameras are widely available for the same purpose)
	1	Technology is available only for research purposes Components are available commercially but they may have not been applied to this purpose and are not specifically designed for the application
	0	A complete system has not been demonstrated in research The technology is only theoretically available and would have to be built from very fundamental components
C: Cost of measurement	**2**	Low capital cost Moderate capital cost with reuse (low operational cost)
	1	Moderate capital cost Low capital cost with high operational cost (e.g. dedicated equipment that cannot quickly or easily be reused)
	0	High capital cost Moderate capital cost with high operational cost
D: Pre-collection preparation	**2**	Absolutely no preparation of the structure No/minimal calibration of the instrument are required
	1	The structure requires moderate preparation The instrument requires moderate calibration
	0	Both the structure and/or instrument require extensive preparation

E: Complexity of analysis	**2**	Analysis consists of either pattern recognition by user (bridge inspector can easily understand the output) Automated "turn-key" processing by a computer (software commercially available)
	1	Analysis consists of detailed measurements made by a human user from raw data Processing by an algorithm that must be tuned or trained for each dataset More than one algorithm is needed
	0	Analysis consists of very complex calculations and measurements made by a human user from raw data Processing by an algorithm that either i) requires extensive human supervision ii) a large amount of time per bridge (more than a day) iii) requires multiple algorithms chained together WITH human-in-the-loop I/O
F: Ease of data collection	**2**	Instrument is used in a straightforward manner as intended by manufacturer AND requires little more from the operator than supervision (i.e. "push the start button and start collecting") Easily accessible structure components
	1	Instrument is used in a custom fashion (may have been modified for this purpose) Requires input from operator Requires real-time verification (QA/QC) of results Environmentally dependent Considerable time window for data collection Physical challenges
	0	Instrument is used in a custom fashion AND requires EITHER input from the operator OR real-time verification (QA/QC) of results Hidden components Team needed
G: Stand-off distance rating	**2**	No part of the platform is touching the earth
	1	Part of the platform is on the earth or bridge (i.e. on a ground-based vehicle or some other grounded mount) AND the instrument is NOT in contact with the structure
	0	Instrument is in direct contact with structure; technique is not technically remote sensing
H: Traffic Disruption	**2**	Absolutely no lane closure or traffic disruption
	1	Minor/ short term traffic disruption or minor lane closure
	0	Major/ long term traffic disruption or major lane closure

Criterion C: the cost of measurement is an important consideration as the most likely customer of remote sensing technologies for bridge condition evaluation will be state and local transportation agencies (DOTs) whose budgets are modest. The cost of measurement has been

defined on a “per bridge” basis where possible. Such an estimate is extremely difficult to produce when evaluating hypothetical use cases; best judgments based on our domain expertise and experience were used.

Criterion D: the pre-collection preparation is intended to be a measure of the amount of time and work required to prepare a bridge structure, element, or remote sensing instrument (i.e. calibration) before usable data can be collected. Depending on the technology and the application, this has been deemed to include such preparation as installing corner reflectors for radar on a structure, calibrating a camera with specific shots, loading a structure or element, or artificially illuminating a target.

Criterion E: the complexity of the analysis is similar to criterion D, and is intended to represent the amount of time and work required to process the remote sensing data collected into useful information for bridge condition assessment. If the data can be interpreted immediately after acquired by the device—not including any post-processing that may be done automatically by the receiver—the highest score is given for criterion E. If the remote sensing data do require post-processing, in order to receive the highest score for criterion E that processing must be what is termed “turn-key”—it must generally consist only of “plugging in” data and having it automatically processed by an algorithm, much like inserting a key into a lock and turning it. This criterion reflects yet another condition of industry: state and local DOTs typically have neither the time nor the expertise for sophisticated post-processing of bridge condition data.

Criterion F: the ease of data collection reflects how easy it is to make measurements that characterize the condition of a bridge. The highest score is given to technologies that require little more of an operator than pushing the “start” button. Another way of measuring this ease for commercial instruments is to specify whether the instrumentation is used as the manufacturer intended or has been modified for use in an unconventional way. If the latter is true, it is assumed that the instrument’s operation is not straightforward. An additional consideration in this criterion is that the structural element intended to be scanned is easily accessible. This also reflects the industry condition that end-users may likely have no formal remote sensing instrument training or, at the very least, no special expertise in the technique as it is applied.

Criterion G: the stand-off distance rating is like a “remote sensing quotient” in that it is a measure of how far the instrument is from the target or target enclosure’s surface (for subsurface features) when making a measurement. Technologies that receive a score of zero for a particular application are those which require direct contact and are therefore not technically remote sensing technologies at all. “Near bridge,” non-contact technologies receive a one, while stand-off technologies more traditionally defined as remote sensing receive a two.

Criterion H: traffic disruption is intended to measure how much the technique interferes with traffic when collecting data. This may not be independent from criterion G because technologies with high stand-off distances present no opportunity for traffic disruption. However, it was important to capture a representational score for technologies at low stand-off that do not interfere with traffic, such as GPR or StreetView-style imagery which may both be operated from a vehicle moving with traffic. This is an important measure of a commercial

technology's practicality for bridge condition evaluation as, according to a personal estimate from Michigan DOT bridge inspectors, lane closures can cost from $2,000 to $3,000 a day. Scored results of the rating methodology are listed in Table 3.

Table 3: Performance Rating of Commercial Remote Sensing Technologies

Location	Challenges	Indicator	Desired Measurement Sensitivity	GPR	Spectra	3D Photo-grammetry	EO Airborne/ Satellite Imagery	Optical Inter-ferometry	LiDAR	Thermal IR	Acoustics	DIC	Radar (Backscatter/ Speckle)	InSAR	Streetview-Style Photography
				Rating Based, in Part, on Theoretical Sensitivity for Measurement Technologies											
Deck Surface	Expansion Joint	Torn/Missing Seal		0	8	14	12	11	13	11	0	0	9	0	13
		Armored Plated Damage		0	0	14	12	11	13	11	0	0	0	0	13
		Cracks within 2 Feet	0.8 mm to 4.8 mm (1/32" to 3/16") width	0	8	14	0	12	12	11	0	0	9	0	13
		Spalls within 2 Feet	6.0 mm to 25.0 mm (1/4" to 1") depth	0	8	14	12	12	12	11	0	0	9	0	13
		Chemical Leaching on Bottom		0	11	0	0	0	0	0	0	0	0	0	0
	Map Cracking	Surface Cracks	0.8 mm to 4.8 mm (1/32" to 3/16") width	0	8	14	12	12	12	11	8	0	9	0	13
	Scaling	Depression in Surface	6.0 mm to 25.0 mm (1/4" to 1") depth	0	8	14	12	12	12	11	0	0	9	0	13
	Spalling	Depression with Parallel Fracture	6.0 mm to 25.0 mm (1/4" to 1") depth	0	8	14	12	12	12	11	0	0	9	0	13
	Delamination	Surface Cracks	0.8 mm to 4.8 mm (1/32" to 3/16") width	0	8	14	0	12	12	11	8	0	0	0	13
Deck Subsurface	Expansion Joint	Material in Joint		0	0	0	0	11	0	0	0	0	0	0	0
	Delamination	Moisture in Cracks	Change in moisture content	11	0	0	0	0	0	11	0	0	0	0	0
		Internal Horizontal Crack	Approximately 0.1 mm (0.004") level	0	0	0	0	0	0	11	8	0	0	0	0
		Hollow Sound		0	0	0	0	0	0	0	8	0	0	0	0
		Fracture Planes / Open Spaces	Change in signal from integrated volume	12	0	0	0	0	0	0	8	0	12	0	0
	Scaling	Depression in Surface	6.0 mm to 25.0 mm (1/4" to 1") depth	12	0	0	0	0	0	11	0	0	0	0	0
	Spalling	Depression with Parallel Fracture	6.0 mm to 25.0 mm (1/4" to 1") depth	12	0	0	0	0	0	11	0	0	0	0	0
	Corrosion	Corrosion Rate (Resistivity)	5 to 20 kΩ-cm	0	0	0	0	0	0	0	0	0	0	0	0
		Change in Cross-Sectional Area	Amplitude of signal from rebar	13	0	0	0	0	0	0	8	0	13	0	0
	Choride Ingress	Choride Content through the Depth	0.4 to 1.0 % chloride by mass of cement	12	0	0	0	0	0	0	0	0	12	0	0
Girder Surface	Steel Structural Cracking	Surface Cracks	< 0.1 mm (.004"), hairline	0	8	11	0	12	0	11	0	0	0	0	0
	Concr. Structural Cracking	Surface Cracks	.1 mm (.004")	0	8	11	0	12	0	11	8	0	0	0	0
	Steel Section Loss	Change in Cross-Sectional Area	Percent thickness of web or flange	0	0	11	12	0	13	11	0	0	11	0	0
	Paint	Paint Condition	Amount of missing paint (X %)	0	9	0	0	0	0	11	0	0	0	0	0
	Concrete Section Loss	Change in Cross-Sectional Area	Percent volume per foot	0	0	11	12	0	13	11	7	0	11	0	0
Girder Subsurface	Concr. Structural Cracking	Internal Cracks (e.g. Box Beam)	Approx 0.8 mm (1/32")	0	0	0	0	0	0	11	8	0	0	0	0
	Concrete Section Loss	Change in Cross-Sectional Area	Percent volume per foot	0	0	0	0	0	0	0	7	0	11	0	0
	Prestress Strand Breakage	Change in Cross-Sectional Area	Wire 2 mm or strand 9.5 mm diameter	9	0	0	0	0	0	0	8	0	9	0	0
	Corrosion	Corrosion Rate (Resistivity)	5 to 20 kΩ-cm	0	0	0	0	0	0	0	0	0	0	0	0
		Change in Cross-Sectional Area	Amplitude of signal from rebar	8	0	0	0	0	0	0	8	0	13	0	0
	Choride Ingress	Choride Content through the Depth	0.4 to 1.0 % Chloride by mass of cement	10	0	0	0	0	0	0	0	0	11	0	0
Global Metrics	Bridge Length	Change in Bridge Length	Accuracy to 30 mm (0.1ft) (smaller)	0	0	15	13	0	0	0	0	9	0	12	0
	Bridge Settlement	Vertical Movement of Bridge	Approximately 6 mm to 12 mm	0	0	12	0	0	12	0	0	9	0	12	0
	Bridge Movement	Transverse Directions	Approximately 6 mm to 12 mm	0	0	12	0	0	12	0	0	9	0	12	0
	Surface Roughness	Surface Roughness	Change over time	0	9	14	13	12	12	0	0	0	11	13	13
	Vibration	Vibration	.5 -20 Hz, amplitude?	0	0	0	0	12	0	0	0	10	12	12	0

5.0 Performance Evaluation of Remote Sensing Technologies

Several remote sensing technologies were explored in broad, but appropriate, categories for their effectiveness and practicality in evaluating bridge condition. An emphasis on commercial availability and well-established practices was used in the literature search wherever possible to keep a focus on the potential for implementation. The commercial availability of these technologies has been represented, as detailed in the "Technology Rating Methodology" section. Included in this section is a short definition of each of the remote sensing modalities considered for review. They are defined here to better constrain the techniques that have been rated for their sufficiency in conveying information about bridges' structural health. Additionally, detailed information on these techniques is available in the State of the Practice Synthesis Report (Ahlborn et al. 2010 b).

5.1 Ground Penetrating Radar (GPR)

GPR is a type of radar acquisition characterized by relatively low electromagnetic frequencies (center frequencies as low as 100 MHz but usually no lower than 500 MHz) and a wide bandwidth, intended to maximize depth penetration and the radar's sensitivity to embedded features. In this review, both air- and ground-coupled GPRs that are either pulsed or continuous wave (CW/FM-CW) operation were considered.

The functional difference between GPR and other ground-based radar measurements, as mentioned, is based merely on collection frequencies and bandwidth. As such, in the rating of this technology and the suite of commercial GPR systems available the scope was limited to subsurface applications, specifically the bridge deck subsurface and girder subsurface. Furthermore, most commercial GPR systems intentionally "gate-out" or ignore returns from the air-ground interface. Although it would be easy to modify a commercial GPR to include surface information or modify a more generalized radar system (or network analyzer) to work as a GPR, it was decided that limiting the scope of this technology category to typical subsurface applications was appropriate. For completeness, both subsurface and surface applications are included for review in the "Radar Images, Backscatter, and Speckle" category, however, the subsurface ratings for that category are identical to those found in GPR—a consequence of the fact that GPR is just a special type of radar collection.

GPR is already commercially available and many companies offer GPR instrumentation for purchase for a wide variety of applications. A representative list of commercial GPR systems is included in Table 4. Some companies perform GPR surveys as a service and do not sell instrumentation; some of these are listed in Table 5. GPR can be performed from a moving vehicle platform (Shuchman et al. 2005), enabling rapid bridge condition characterization on an inventory scale. Analysis of GPR data can be complex, however, as signals must be "migrated" to identify subsurface features and for some applications the dielectric properties of the medium need to be estimated. While used for moisture or chloride evaluations, GPR is sensitive to

environmental factors such as rain and snow, though some users of commercial GPR systems indicate the effect is not significant (Kim et al. 2003). There is commercial software available for post-processing radar data, most notably the RADAN software suite developed by Geophysical Survey Systems Incorporated (GSSI), which automatically integrates GPS location data.

Table 4: Representative list of some common commercial GPR systems available for purchase

Instrument	Company	Bandwidth
Profiler EMP-400	GSSI*	1-16 kHz
TerraVision	GSSI	400 MHz
BallastScan	GSSI	2.0 GHz
BridgeScan	GSSI	1.6 GHz
RoadScan	GSSI	500 MHz
StructureScan Mini	GSSI	1.6 GHz
StructureScan Standard	GSSI	1.6 GHz or 2.6 GHz
StructureScan Professional	GSSI	1.6 GHz
StructureScan Optical	GSSI	1.6 GHz or 2.6 GHz
SIR-20 or SIR-3000	GSSI	Depends on choice of antenna
OKO-2	Geotech	Depends on choice of antenna
Detector DUO	IDS Australasia	250 MHz, 700 MHz
RIS-MF	IDS Australasia	200-600 MHz
Aladdin	IDS Australasia	2.0 GHz
GPR for Road	IDS Australasia	600 MHz and 1.6 or 2.0 GHz
Mira Series	Mala Geoscience	
CX Concrete Imaging System	Mala Geoscience	
ProEx System	Mala Geoscience	

***Geophysical Survey Systems Incorporated**

In general, GPR scored very high for concrete deck applications in this evaluation. With the exception of detecting moisture in cracks, however, the technology only partially or indirectly met the requirements for detecting subsurface conditions. The reason is that, as with all radar techniques, features that may be smaller than a range bin (smaller than the limit of resolution) are usually still able to be detected by their contribution to the overall signal from that range bin. In this way, the question of whether or not GPR can detect a subsurface feature should instead be framed as whether or not GPR is *sufficiently sensitive* to an embedded feature, as GPR makes no direct measurement of a target's dimensions. GPR does provide, however, a measurement of the target's position within a subsurface cross-section, and this is how the technique has been successfully employed in locating rebar as well as providing qualitative estimates of the rebar's condition. Rebar, made of metal and therefore highly conductive, causes diffractions in the GPR reflection data (Cardimona et al. 2000), which, when migrated, collapse to the point of origin. Currently, the technique is limited to deformation mapping—the gridding

of GPR reflection amplitudes. Harris, et al. (2010) demonstrated that this technique performs just as well or better than standard methods (half-cell potential and sounding) at locating areas of rebar corrosion in most cases. Barrile and Pucinotti (2005) used this technique to characterize the number and position of longitudinal rebar, detect voids, and derive stirrup spacing in structural members. Both studies used commercial radar systems; Harris et al. (2010) utilized a GSSI instrument while Barrile and Pucinotti (2005) used an RIS-series instrument built by IDS Australia.

Table 5: Representative list of companies that perform GPR surveys as a service

Company	Website
NGPRS	http://www.ngprs.com/
GPA Data LLC	http://www.gprdata.com/
Sensors & Software Inc.	http://www.sensoft.ca/index.html
Penetradar Corporation	http://www.penetradar.com/index.htm
GPR Professional Services Inc.	http://www.gprps.com/
Global GPR	http://www.global-gpr.com/
Virtual Underground	http://www.virtualug.com/Services.html
GeoView Inc.	http://www.geoviewinc.com/services/civil.htm

Radar has been shown to be sensitive to moisture content. Maierhofer and Leipold (2001), using a GSSI SIR 10 radar system operated at 500, 900, 1000, and 1500 MHz, determined that by measuring the travel time of the backside reflection, determining the permittivity, and generating calibration curves, the moisture of a mortar structure could be determined to within between 1 and 5 percent by volume. In place of calibration curves, an inversion model of moisture in concrete might be used in order to estimate the moisture content. Some bridge managers or inspectors may be interested in quantifying the amount of moisture content and, where that is the case, GPR is also an appropriate choice: it can be used in detecting relative changes in moisture content where strict environmental controls are employed (the technique is sensitive, of course, to moisture held by a bridge after a rainstorm and would be affected by snow or standing water on the bridge deck).

GPR has been frequently used to locate delaminations in concrete bridge decks. These experiments have constrained the penetration depth of GPR to between 7 and 12 cm at typical stand-off and emission frequencies (Warhus et al. 1994). Voids and areas of potential delamination are mapped with GPR, but the dimensions of these areas are not usually known due to the limitations of the technology. By combining synthetic aperture radar (SAR) with GPR, Scott et al. (2001) have demonstrated the potential to measure the dimensions of subsurface features. In the FHWA-funded project “HERMES”, the HERMES mobile road assessment system was used to locate and characterize the condition of embedded steel reinforcement, detect corrosion-related delamination, as well as locate voids and debonds. HERMES, used ultra-wideband sources emitting in the 0.5 to 5 GHz range, was developed by the Lawrence Livermore

National Laboratory. They were able to penetrate only to 12 cm below the concrete surface, and acknowledged the need for improved range resolution and signal-to-noise ratio as well, but found that synthetic aperture radar (SAR) processing enabled them to display 2D projections of 3D bridge deck features.

It is expected that GPR measurements made from the top of the deck will also be useful for characterizing conditions on the deck's bottom surface, specifically scaling and spalling [Figure 15]. However, in considering GPR for use in characterizing the condition of girders, beams, and piers, it is anticipated that the need to scan or "sweep" the surfaces of these elements with the GPR (from below the bridge) will significantly increase the time and cost of a bridge inspection with this tool. Other areas of concern which may be evaluated with GPR include: corrosion, prestress strand breakage, and internal structural cracks of the girder subsurface. It was determined that GPR does not meet the requirements for detecting corrosion, as the technique does not measure resistivity directly and it seems unlikely to be back-calculated from the dielectrics. GPR also rated insufficiently for detecting internal concrete structural cracks, as domain experience highlighted that the technology is not sensitive enough. It is believed that commercial GPR systems should however have the potential to provide information about prestress strand breakage although it may not be cost-effective or practical from a concept-of-operations perspective.

Figure 15: Significant spalling of a bridge bay that merits full replacement

Commercial GPR seems promising for characterizing chloride ingress in girders and the deck subsurface, however. The potential use of GPR for this application was first reported by Maser (1986) when it was observed that radar signal was attenuated in areas of high chloride concentration. The available literature shows that the presence of chloride in a concrete deck increases the material's conductivity and decreases its permittivity. This increase in conductivity results in signal attenuation as less electromagnetic energy is reflected back throughout the volume (Lim 2001). Kim et al. (2003) noted that areas with a high dielectric constant (low electromagnetic velocity) and high attenuation are typically zones of delamination, which are likely marked by high moisture and chloride content.

When assessing GPR as a technology for use in non-destructive evaluation, it should be noted that the technology cannot be used to resolve some embedded features directly. Delaminations are one such example; however, they are also the most common bridge condition issue GPR is used to detect. The previously noted delamination indicators—high dielectric

constant and signal attenuation—are mapped for the entire bridge deck, but the results are limited to delamination. For this approach, the processing required is not complex, and may include only noise elimination and frequency tilt removal, but more advanced processing has the potential to produce greater accuracy.

5.2 Spectral Analysis

Spectral analysis is the measurement of a target surface's spectral reflectance or absorption of light (both visible and infrared). This includes spectroscopy—any measurements based on identifying characteristic peaks or spectra corresponding to structural defects as well as infrared (IR) spectroscopy, which is distinct from IR deformation mapping or thermal mapping–techniques that are instead magnitude-based. Reflectance and/or absorption are measured using a camera with a range of color bands (termed multispectral or hyperspectral electro-optical imaging) so the response within fine wavelength bins is known. The device used to measure reflectance and/or absorption is referred to as a *spectroradiometer*. Spectral analysis is typically described as the identification of characteristic peaks—wavelengths at which a large amount of radiation is absorbed or reflected.

Though spectroscopy can convey information about a target's composition, it is really limited to surface features since that is what absorbs or reflects the light captured by a spectroradiometer. A representative list of commercial spectroradiometers currently available is provided in Table 6. For cost comparative purposes, ASD FieldSpec 3 cost approximately $60,000 (as of 2007). In the performance evaluation of this technology, it was found that spectroscopy is impractical for most deck surface applications with the exception of chemical leaching. The problem inherent in using spectral analysis for crack detection, spotting expansion joint damage, or delamination cracks is that the only indicator of these features which can be detected is the shadow of the feature or a tone difference between the damaged and undamaged concrete. It is anticipated that it would be challenging to obtain consistent detection results for that application with this technique. Other deck features such as scaling and spalling could potentially be detected by the difference in tone between intact concrete and the feature of interest, but this precludes direct measurement and there is no way to measure the dimensions of these features using this technology. Spectral analysis is then restricted to a defect detector rather than a robust technology for measuring bridge condition. It is not clear how deck features could be deconvolved from the total signal—how a defect that makes up a certain proportion of the spectroradiometer's area of integration could be quantified. According to the available literature, no attempt has been made to produce calibration curves or a model of spectral reflectance based on bridge deck defects.

In addition to these difficulties, this imaging technology requires the surfaces be clean and visible. Unfortunately, their appearance is likely to be highly variable due to dirt, water, debris, snow, or ice. To remove these obstructions, some surface preparation before data collection would be required. In general, spectroradiometers also need to be white-balanced before collection. Field collection is typically done with a backpack unit and hand-held spectroradiometer, however, a vehicle-mounted device is conceivable. A preliminary field test

performed by the project team using an ASD FieldSpec3 highlighted the difficulty in obtaining consistent spectral signatures of bridge condition—a significant obstacle for practical implementation. According to the available literature, spectroradiometers have not been demonstrated for use in evaluating bridge condition.

Table 6: Representative list of some commercially available spectroradiometers

Instrument Name	Company	Bandwidth	Spectral Resolution
PS-100	Apogee Instruments Inc.	350-1000 nm	0.5 nm
PS-200	Apogee Instruments Inc.	300-850 nm	0.5 nm
FieldSpec 3	ASD Inc.	350-2500 nm	3 nm (700 nm), 10 nm (1400/2100 nm)
FieldSpec 3 Hi-Res	ASD Inc.	350-2500 nm	8.5 nm (1000-2500 nm), 6.5 nm (1800-2500 nm)
Visible Compact	Edmund Optics	380-750 nm	4 nm
Visible Compact Near IR	Edmund Optics	350-1050 nm	6 nm
LS-100	EKO Instruments	350 - 1050 nm	
MS-701	EKO Instruments	300-400 nm	0.8 nm
GS-1290-0	Gamma Scientific	200-780 nm	0.6 nm
GS-1290-1	Gamma Scientific	260-900 nm	0.6 nm
GS-1290-2	Gamma Scientific	300-1100 nm	0.9 nm
GS-1290-3	Gamma Scientific	380-810 nm	0.4 nm
GS-1290-DMS-1	Gamma Scientific	380-930 nm	0.6 nm
GS-1290-DMS-2	Gamma Scientific	380-1100 nm	0.9 nm
GS-1290-DMS-3	Gamma Scientific	380-800 nm	0.4 nm
SPR-4001	Luzchem Research Inc.	235-850 nm	1 nm
SPR-03	Luzchem Research Inc.	235-1050 nm	1 nm
CS-2000	Konica Minolta	380-780 nm	1 nm

Though it requires some pre-collection preparation and the collection geometry might not allow for rapid assessment, spectral analysis does appear promising for objectively characterizing chemical leaching. Kanada, Ishikawa et al. (2005) investigated the use of spectral analysis as compared to traditional techniques of detecting carbonation and chloride intrusion. They found characteristic peaks in absorbance curves where an increase at 2266 nm was associated with chloride intrusion, an increase at 1750 nm with sulfate attack, and a decrease at 1410 nm associated with carbonation. Difference spectra enabled even easier distinction between unaffected concrete and damaged concrete. Paint loss has been detected through a different technique called laser-induced breakdown spectroscopy that uses highly energetic laser pulses to ablate surface material before analyzing the spectra of the emission. Stand-off distances are low

where this technique has been employed, however, ranging from 0.5 to 2.4 meters (Cremers 1987). The same can likely be expected for passive spectral analysis techniques in this area.

5.3 3D Photogrammetry

3D photogrammetry is the generation of 3D models from stereo pairs of electro-optical (EO) imagery in the visual spectrum. These models provide depth and height information that cannot otherwise be obtained from individual EO images. The instrumentation, consisting merely of high-quality digital cameras, is already commercially available. The cameras are conventionally flown aboard an aerial platform, either manned or unmanned. However, in order to achieve the resolution required for some applications, a lower stand-off distance is often necessary. In the performance rating of 3D photogrammetry it was found that the technology scored very high for deck surface applications and global metrics; less so for girder surface features. Deck surface features such as spalling, scaling, and expansion joint damage are 3D features that are likely to be measurable with 3D photogrammetry in most cases. Map cracking, cracks near expansion joints, and delaminations expressed as surface cracks are features which do not have an important depth component but are also likely to be measurable with 3D photogrammetry. The scale of features in the image plane can be known from the collection geometry; by knowing the distance from the camera to the target and camera specifications. There are no theoretical resolution limits specified in the literature as the resolution is a product of the collection geometry. Deck and girder surface features that require higher feature resolution imagery is likely best suited for a vehicle-mounted system, where as global metrics may be evaluated using an aerial platform, such as an unmanned aerial vehicle (UAV). Knowing the collection geometry for deck surface features is straightforward for a vehicle-mounted camera imaging the deck from a fixed height. Underneath the bridge, however, this is a much more difficult proposition and so 3D photogrammetry is less practical for girder surface features. Stereo photographs for use in typical commercial 3D photogrammetry cannot be oblique—girders, beams, and bays that are not directly above the instrument, fascia beams that are too high at close stand-off, and pier surfaces that are not facing the instrument will not allow for viable measurement with this technique. In order to image these surfaces with 3D photogrammetry, the operational costs will increase with the time spent and lane closure(s) required.

5.4 EO Airborne and Satellite Imagery

EO sensors collect imagery in the visual, near-IR, or thermal IR bands. In this category, imagery collected either by earth-observing satellites or aerial vehicles was considered. The aerial vehicles may be manned or unmanned, and this category excludes imagery that is used in 3D models (excluding imagery collected as stereo pairs) as such imagery as technology for review has already been captured under “3D Photogrammetry.”

EO imagery may be useful for identifying deck condition indicators. Hauser and Chen (2009) reported a lower limit of 13 mm resolution using small-format aerial photography (SFAP), which may be sufficient for spotting some features or defects of bridge decks including spalling, scaling, and map cracking. A partial list of companies providing aerial photography

services is included in Table 7. It is less likely that this imagery will be capable of resolving expansion joints and damage to them, but sub-pixel estimates of expansion joint conditions can likely be made with advanced post-processing. Sub-pixel (or "mixed pixel") detection techniques have been demonstrated in other applications where the problem domain is essentially the same. Kant and Badarinath (2002) showed that oil fires less than 2% the spatial extent of a pixel could still be identified. Mikhail, Akey et al. (1984) achieved accuracies to within 0.03-0.05 pixel in measuring the position of sub-pixel targets. This indicates that the potential exists for detecting the presence of cracks that are otherwise too small to resolve and damage to expansion joints. Of course, quantifying and rigorously characterizing these features or defects may not be possible unless the resolution is improved.

Table 7: A list of some companies offering aerial photography by commission

Company	Services	Instrument	Spectral Range
Aero-Metric, Inc.	Aerial photography		
Air Flight Services	Aerial photography, airborne video surveillance, aerial mapping and surveys		
Airborne Corporation	Aerial photography	UltraCamX (Vexcel Imaging)	
Airborne Scientific, Inc.	Aerial photography, wide area oblique imagery, orthophotography, remote sensing, videography photo aircraft rent/support		
ASL Borstad Remote Sensing Inc.	Airborne image data acquisition	CASI SFSI-2 AISA	403-914 nm 1230-2380 nm 400-2400 nm
ATLIS Geomatics	Air photo acquisition	DiMAC Digital Frame Sensor	
Cooper Aerial Surveys Co.	Aerial survey, photo, and mapping	Leica RC-30	
Digital Aerial Solutions, LLC	Digital aerial imagery	ADS 40	4 bands, 610-885 nm
HyVista Corporation Pty Ltd	Airborne hyperspectral remote sensing data		
I. F. Rooks and Associates, Inc.	Aerial photography, helicopter mapping, topographic and planimetric mapping		
Richard B. Davis Co., Inc.	Aerial photography, aerial mapping and photogrammetry		
Terresense	Airborne remote sensing services		

Much of concrete deck cracking sensitivities are below the lower limit of aerial EO resolution specified by Hauser and Chen (2009) in their report to the U.S. Department of Transportation (Report #01221). This includes cracks near expansion joints and delamination cracks. Spaceborne EO resolution is even coarser: the commercial platforms offering the highest resolution today are GeoEye-1 at 0.41 m and WorldView-2 at 0.46 m. A partial list of companies that sell and acquire on-demand satellite imagery is provided in Table 8. Structural cracks below the deck are also too fine to be resolved with current commercial capabilities [Figure 16]. In addition to the resolution requirements of defect detection on girder surfaces, in order to view these surfaces at all, highly oblique imagery is required. Such an extreme viewing angle cannot be achieved by commercial space-based platforms, and even many aerial platforms are unlikely to be able to provide a sufficient viewing angle. Pictometry International, however, is one company that specializes in oblique aerial photography. Though structural cracks are too fine to be resolved, steel and concrete section loss might be identified through aerial photography, particularly when acquired from low-altitude flights by unmanned aerial vehicles (UAVs).

It is anticipated that EO imagery will be very useful for investigating a bridge's global metrics of structural health as the medium offers a synoptic view. Identifying bridge settlement, however, cannot be done without taking stereo pairs of EO images, and this technique is categorically excluded from this discussion: instead, see "3D Photogrammetry." Transverse bridge movement also cannot be detected from this kind of imagery because it is below the limit of resolution. A change in bridge length, however, could be detected using SFAP. A pixel-to-pixel match of two images separated in time is not necessary in order to assess a change in bridge length. Rather, a comparison of the total length of the bridge, measured to a high degree of precision in both photographs, would suffice. Deck surface roughness is another area where EO imagery can provide useful information, as demonstrated in the TARUT study, which used commercial EO satellite imagery (Digital Globe's Quickbird at 2.4 m spatial resolution) as an input to generating a road sufficiency rating (Brooks et al. 2007) for a Michigan freeway. Sub-pixel techniques and the comparison of tone changes over time can also indirectly relate how surface roughness is changing.

Barriers to entry with this technology start with the costs; commercial satellite imagery on-demand costs anywhere from $800 to $3200. Archived imagery—imagery that a third party requested in the past—is significantly cheaper (with minimum orders of around $300), but may not suit the real or perceived immediacy of the application. Aerial imagery costs are generally limited to the costs of commissioning a flight, but are not insubstantial. In all cases, these costs can be offset or mitigated by encompassing a large volume of the bridge inventory with a purchase that captures multiple bridges within a single satellite scene or sequence of aerial photographs. With on-demand satellite imagery, an additional consideration must be the time it takes to acquire the imagery which could be up to 2 months if the satellite is already tasked for government work or if cloud cover obscures the scene.

Table 8: A list of some companies offering satellite imagery for sale or by commission

Satellite	Spectral Resolution	Spatial Resolution	Revisit Time	Owner
SPOT 4	4 bands, 500-890 nm, 1580-1750 nm	10 m pan, 20 m multi-spec	2-3 days	CNES (distributed by Spot Image)
SPOT 5	4 bands	2.5 m pan, 10 m multi-spec	2-3 days	CNES (distributed by Spot Image)
Quick Bird	4 bands, 450-900 nm	0.61 m pan, 2.4 m multi-spec	2-3 days	DigitalGlobe
Worldview-1	NA	0.50 m pan	2-5 days	DigitalGlobe
Worldview-2	8 bands	0.46 m pan, 1.8 m multi-spec	1-4 days	DigitalGlobe
GeoEye-1	4 bands, 450-920 nm	0.41 m pan, 1.65 m multi-spec	< 3 days	GeoEye
IKONOS	4 bands, 445-853 nm	0.82 m pan, 4 m multi-spec	3 days	GeoEye
OrbView-2	8 bands, 402-885 nm	1.1 km multi-spec	1 day	GeoEye
EROS-A		1.9 m pan		ImageSat International
EROS-B		0.7 m pan		ImageSat International
Kompsat-2	4 bands, 450-900 nm	1 m pan, 4 m multi-spec	3 days	Korean Aerospace Research Institute (distributed by Spot Image)
Formosat-2	4 bands	2 m pan, 8 m multi-spec	1 day	NSPO (distributed by Spot Image)
RapidEye				RapidEye AG
WNISAT-1				Weathernews Inc.

Figure 16: Example image from Bing Maps' "Bird's eye" imagery exhibiting Pictometry International's oblique aerial photography.

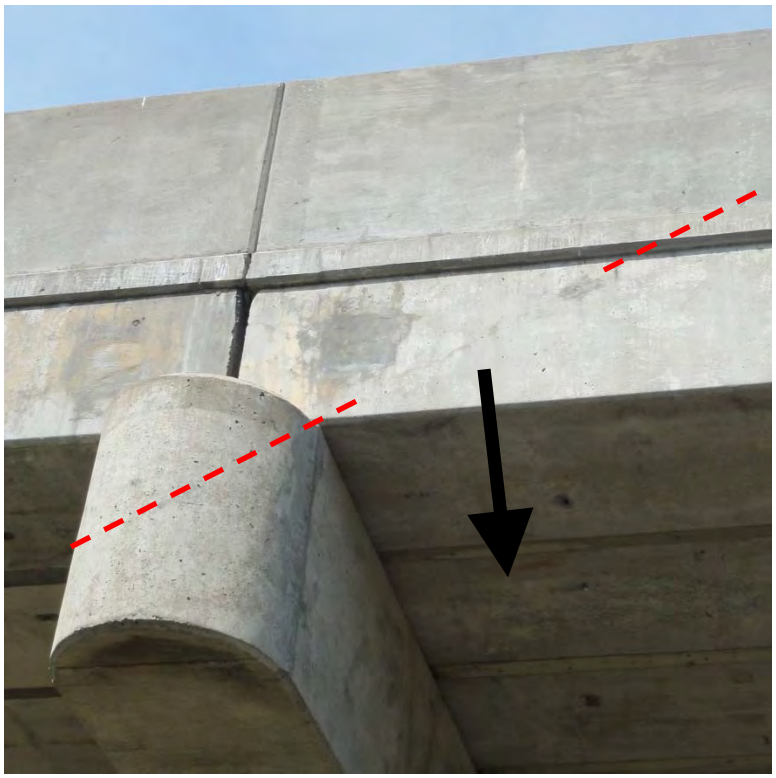

Figure 17: Photograph of fascia beam on box-beam bridge with thin, 45-degree crack near top of pier and post-tension box

5.5 Optical Interferometry

Interferometry is a broad term, but here it is limited to the use of images with visual, near-IR, or thermal IR wavelengths from which interferograms are made and interference fringes derived. Most notably, this consists of techniques to generate Young's fringes/isothetic fringes and (optical) speckle pattern interferometry (SPI). This category excludes interferometric radar techniques, which are considered under "Radar Images, Backscatter, and Speckle."

Interferometry can potentially yield information about subsurface features and internal stresses, but the depth to which it is sensitive is extremely shallow—delaminations deeper than 0.7 mm (in composite laminates) were beyond detection by holography in one study (Ambu et al. 2006). In the performance assessment, it was found that the technology, like most digital camera-based (CCD-based) techniques, was most useful for yielding information about deck surface conditions. The technology's semblance to other optical imaging techniques means that its resolution capabilities are also a product of the collection geometry; for interferometry the spatial resolution is especially high. It was determined that the resolution offered by this technology may be too fine for some applications, such as expansion joint damage including a torn or missing seal and armor plate damage on strip-seal joints. Surface cracks at millimeter and sub-millimeter scales have successfully been detected using optical interferometric techniques, namely electronic SPI or ESPI (Hatta et al. 2005). The measurement of spalls and scaling on the concrete deck should be possible as sub-millimeter depth resolution has already been achieved for other materials (Krajewski 2006).

Optical interferometric techniques are likely to also provide an indication of whether expansion joints are filled with gravel and other debris based on their resolution capabilities. The high resolution this technique promises makes it one of the few technologies reviewed that may help in measuring fine structural cracks in concrete or steel girders and beams (Figure 17). The global metrics of bridge structural health that this technology is likely to assist in characterizing include vibration and surface roughness. These are classic problem domains that optical interferometry is applied to. ESPI, SPI, and speckle photography are all virtually direct measures of surface roughness. Even though the wavelengths of light are far smaller than the grain size of a concrete deck's potential roughness, optical interferometric techniques possess the spatial resolution from which surface roughness can be derived as well. As for vibration, the frequency response of video cameras—the common collection platform for optical interferometry—is likely to be more than adequate for bridge structure and structural element vibrations.

Commercial interferometry systems are already available, most notably those of Dantec Dynamics (formerly Dantec Ettemeyer), which manufactures the Q-300 3D ESPI system, and Trilion Optical Test Systems. Commercial software such as ISTRA (from Dantec Dynamics) exists that can be used for data processing as well as control acquisition (Hatta et al. 2005). The underlying algorithms of this processing are well-understood and require no user intervention—processing is fully automated. This technology presents a moderate to high capital cost for state and local transportation agencies, but the equipment can be re-used over the entire bridge inventory for a long time

5.6 LiDAR

Light Detection and Ranging is the use of timed light pulses to measure the distance to a target. In this review, both terrestrial laser scanning (TLS) and aerial/airborne laser scanning (ALS) were considered. Simply put, this category includes any sensor that collects point elevations/positions by timed laser pulses. LiDAR was initially considered in this performance assessment for a wide variety of bridge structural health concerns. After review, it was found that the technology was most applicable for deck surface and global structural health applications.

LiDAR scanning is most often used to generate high-density 3D models of target surfaces and structures, and it is anticipated that this derivative product will retain its value for bridge structural health monitoring. A high-resolution 3D model of the bridge deck surface, with up to 1 mm^2 grid spacing (Laefer et al. 2009), can enable the extraction of information on expansion joint conditions such as seal and armor plate integrity, cracks and spalls near expansion joints, map cracking, scaling and spalling of the riding surface, and delaminations expressed as surface cracks. There are limitations to LiDAR's effectiveness for these applications, particularly in its tendency to overestimate crack widths.

In measuring the dimensions of concrete volume loss (such as spalling and loss of section), Teza, Galgaro et al. (2009) found that, at 50 m standoff with TLS, LiDAR's depth resolution is limited to 1.09 cm with an accuracy of 0.5 cm. Hauser and Chen (2009) found that resolution of LiDAR for section loss was 0.5 mm. By any estimate, commercial LiDAR capabilities only partially meet the requirements for sensing the bridge deck condition indicators highlighted in the challenges section; they do not meet the lower limit of resolution. The lower resolution limit of LiDAR does not meet the upper limit required for resolving structural cracking of steel and concrete girders (see Figure 17 for an example). The sensing requirements for steel and concrete section loss in the girder subsurface, as laid out for performance evaluation, state that a volume percent needs to be known. Based on Hauser and Chen's estimate (2009), however it is clear that LiDAR can contribute useful information for identifying and mapping steel and concrete section loss. LiDAR in combination with high-resolution digital photography of a bridge, in a "StreetView" style system (similar to Google StreetView) holds promise as a means of assisting bridge inspectors with reviewing and understanding bridge condition features, as will be discussed below.

LiDAR can also make a contribution to the understanding of a bridge's global metrics. It is anticipated that through scanning a bridge profile with TLS, bridge settlement on the order of 6 to 12 mm should be measurable. However, there is no reported margin of error in the available literature. With the appropriate scan geometry, likely from either bridge approach or an aerial platform, the long-term, transverse movement of the bridge can also be detected. No consideration was given to the application of LiDAR for measurement of bridge vibration, although such a scenario is clearly similar to laser vibrometry (laser Doppler vibrometry or LDV and continuous scan LDV), commercial LiDAR systems optimized for point cloud generation are not designed for this use.

Difficulties in implementing commercial LiDAR as part of any bridge structural health evaluation include the high capital cost of equipment with potentially high operational costs. Some acquisitions, for example, have been documented to take up to a full day to complete for a single bridge (Lubowiecka et al. 2009). These operational costs might be high with less streamlined systems, but with fully-automated, modern, commercial instrumentation the use of LiDAR for these applications should have low operational costs. More modern, sophisticated instrumentation also allows for more rapid collection, as well, potentially imaging the entire bridge deck or substructure while driving by.

LiDAR processing consists mostly of transforming the coordinates for use in the real-world coordinate system. Commercial software is available that does this automatically, but additional tasks such as the subdivision of point clouds (into structural elements) and curvature computation (for volume calculations) are additional steps that may be necessary for damage identification and 3D modeling.

5.7 Thermal/Infrared (IR) Imaging

Thermal/infrared (IR) imaging, in this case, refers to magnitude-only-based deformation mapping; the production of deformation maps by mapping thermal anomalies/contrasts. The collection of these data can be passive (solar illumination or night collection) or active (artificial illumination or cooling [e.g. liquid nitrogen]). This category excludes IR spectroscopy, which is considered under “Spectral Analysis.”

For obvious reasons, infrared imaging promises to be useful in characterizing several deck and girder surface features, but the performance rating of the technology indicates it may have the potential to convey information about some subsurface conditions as well. These include features indicative of delaminations, scaling and spalling of the deck underside, as well as structural cracking. Delaminations are the most common feature IR imaging is used to detect. DelGrande and Durbin (1999), in a paper that distinguishes itself by the adoption of “thermal inertia” mapping, describe both laboratory and field validation of a custom IR imaging system. They report being able to distinguish true delaminations in the field from surface clutter or shadow based on the size, shape, relative volume and location, as well as thermal contrast of thermal anomalies. IR imaging has been used frequently to find areas of debonding and air-filled voids in composite concrete decks, but by most accounts the data analysis has been limited to defect mapping and few, if any constraints, have been discovered and reported. Stimolo (2003), however, reported on the detection of delaminations, cavities, and air blisters at 10^{-2} to 10^{-3} m spatial resolution and 2.0 - 3.5 m standoff using passive, solar radiation and the Agema LW900 IR camera, but also reported some limitations to the technique including the lack of depth information and the technology’s sensitivity to environmental interference.

A literature review found no studies where surface defects such as expansion joint damage, cracks and spalls near expansion joints or otherwise, and map cracking were imaged using IR thermography, but it is believed that these defects will exhibit thermal anomalies. In these applications, though IR thermography may not provide sufficient resolution of the extent or dimensions of bridge condition indicators, the technology should enable the detection of these

features where they occur and provide an estimate of the surface area or volume. Hu et al. (2002) demonstrated the use of IR thermography to predict crack propagation, however, the technique was not applied to locating existing cracks. Concrete and steel structural members will store and transfer heat differently when damaged so concrete and steel section loss and structural cracking, as well, can likely be detected using IR thermography. It is also anticipated that paint condition can also be assessed with IR thermography.

5.8 Digital Image Correlation (DIC)

The term "digital image correlation" (DIC) refers to a technique consisting of the correlation, typically on a pixel-by-pixel basis, of two electro-optical images separated in space or time. This is done by automated computer algorithms which measure changes between the two photographs and calculate the displacement of features in the image plane (structural elements) or, most commonly, markers such as paint spots (Figure 18) or a pattern of dots projected on a surface. These displacements may be rigid, global displacements or local deformation.

The rating of this technique for application to bridge condition issues is based on the strict definition above. As such, four applications were identified for which DIC might be useful: detecting a change in bridge length, measuring bridge settlement, measuring transverse bridge movement, and measuring the vibration of a bridge or a structural element. These are all global metrics of a bridge and this is a consequence of the fact the technique is limited to the correlation of surface observations separated in time. It would not be appropriate to use this technique to detect bridge conditions that do manifest themselves in displacement, deflection, or deformation over time. For these applications, DIC did not score high in the performance evaluation. This is due in part to systematic qualities such as the need for a projected or painted pattern on the target surface, the required post-processing, and the short stand-off distance. This technique boasts high spatial resolution; with project experiments confirming that $1/10^{th}$ of an inch resolution (2.5 mm) can be achieved at close stand-off. There is, however, a compromise between spatial resolution and extent; in order to achieve higher spatial resolution, only a small coverage area can be imaged and thus, for larger targets, multiple images must be stitched together. The frequency response is dependent on the camera used, and may not be sufficiently high enough for measuring the vibration of some bridges. To its advantage, the camera-target geometry ensures that data collection will not interfere with bridge traffic, but the target surface preparation is a part of the measurement that demands contact with the bridge structure. Hutt and Cawley (2008) describe their collection using a two-camera system developed by Dantec Dynamics and processing using ARAMIS (software by Gesellschaft für Optische Messtechnik or GOM), which consisted of simple-windowed block matching where correlations took from a few seconds up to several minutes. Kuntz et al. (2006) used CORRELI 3D and a fast Fourier transform (FFT) algorithm to measure displacements of 1.4 microns as well as cracks.

DIC is really only practical for measuring vibration and in that application still suffers from an unknown frequency response, necessary target preparation, and small coverage area.

Where DIC might be used for measuring bridge settlement, transverse movement, or detecting a change in bridge length the required temporal resolution makes the technique impractical. To enable the correlation of images separated by 6 months, a year, or several years, the camera would have to remain in the exact same place, sheltered from environmental interference and anything else that would induce artificial displacements. These displacements are likely inevitable, and though their effect can probably be removed with sophisticated post-processing, only non-rigid displacements and deformations would be preserved. Even when the technique is applied to images separated seconds or less in time, the post-processing is not trivial. The analysis can be performed automatically using an analysis package such as MATLAB software, but requires additional post-processing and tuning for meaningful results. Image processing is often required before analysis to increase the contrast of the fiducial markers or features of interest (Figure 18b). Inversion in MATLAB 7.0+ is the most common processing technique in the available literature.

(a)

(b)

Figure 18: Two images of paint spots on a structural I-beam for digital image correlation. (a): the paint spots should have a wide distribution of sizes; (b): post-processing of images is used to bring the spots to a contrast threshold

5.9 Radar Images, Backscatter, and Speckle

Radio detection and ranging (radar) is a well-established technique for calculating the distance to, as well as the speed and direction of a target. In this case, the term “speckle” refers only to coherent, radar speckle which is a feature of any radar image (and is usually considered noise). Also considered in this category are the amplitude-only radar images or “backscatter” images. The use of Synthetic Aperture Radar (SAR) processing was considered, but did not exclude measurements performed without SAR. Interferometric SAR (InSAR) is excluded from this category and considered in the “Interferometric Synthetic Aperture Radar (InSAR)” category.

These generalized radar collection techniques, based on backscatter or coherent speckle without interferometric processing, have a wide variety of applications for monitoring bridge structural health. Of these applications, those which deal with subsurface features or defects have been scored the same as for GPR. This is because GPR is just a type of radar collection—one characterized by a wide bandwidth and low emission frequencies. This distinction is still useful, however, because GPR has become such a specialized, commercialized technique for the transportation industry. In other words, the GPR category refers specifically to the off-the-shelf GPR instruments that state and local transportation agencies are already familiar with, while this category deals with a much broader set of instruments designed for a much broader set of applications. Importantly, this more general category not only includes GPR, but also coherent speckle, synthetic aperture radar (SAR) processing, and commercial radar systems, not designed strictly for ground penetration.

The performance evaluation of radar indicates that the technology is not well-suited for resolving deck and girder surface features. This is primarily because—as previously noted in the section on GPR—radar is not capable of directly resolving features at the required scale. It is possible that a vehicle-mounted radar platform moving along a bridge deck to create a synthetic aperture can achieve sufficient cross-range resolution so as to be sensitive to cracks and spalls. These features have not been the focus of research in radar for structural health monitoring; instead, displacement, vibration, surface roughness, and subsurface features are the subjects of exploration, according to the current literature.

Fine structural cracks in steel or concrete are thought to be too small for the sensitivity of practical radar deployment. Steel and concrete section loss, however, might be measurable as a bulk effect if it is above a certain threshold and may be quantified through modeling or calibration. For the girder subsurface, radar and GPR can both make valuable contributions to the assessment of reinforcing bar condition. Barrile and Pucinotti (2005) bounded the error of rebar diameter estimation to within 3 mm at the 86% significance level for 13, 25 and 38 mm bars. These rebar diameters are still larger than the diameter of some reinforcement in concrete girders and the error may be too great for any meaningful interpretations to be made. Chloride ingress detection and moisture content characterization are also promising applications of both GPR and other radar techniques.

While commercial GPR cannot characterize global metrics of a bridge because of its collection geometry, most other radar platforms and techniques are also insufficient for these applications because they lack the required resolution or sensitivity. For global metrics such as change in bridge length, bridge settlement, and transverse bridge movement, interferometric radar techniques, such as InSAR, promise to be helpful and provide great efficiency. Several Italian reports on ground-based interferometric radar address these condition indicators with measurements down to 0.1 mm displacement resolution at up to 2 km stand-off distance (Pieraccini et al. 2008). Both interferometric radar and non-interferometric radar may shed light on surface roughness. Without resorting to interferometric processing, coherent radar speckle can provide an indirect measurement of surface roughness. As reported by Shuchman,et al. (2005), speckle contrast from SAR imagery can be correlated with road surface roughness measured in situ in order to derive a calibration curve from which surface roughness can then be remotely sensed (Figure 19a) This was done for the TARUT study and the results compared to the International Roughness Index or IRI (Figure 19b) and the PASER standard (Figure 19c). Radar can also provide a measure of vibration in bridges and other structures, using Doppler techniques or interferometric techniques (see section on InSAR). Using interferometric radar, displacements on the order of 0.1 mm (Pieraccini et al. 2009) have been measured with a frequency resolution of about 0.02 Hz (Gentile 2009).

Radar data collection might require significant preparation depending on the application. A visit to the bridge ahead of collection may be necessary to plan the collection geometry. Such a visit might reveal that reflector targets need to be installed on the structure. When collection begins, it is likely that a skilled operator will be needed. In addition, the collection geometry and required resolution indicate that the instrumentation will likely be deployed on the bridge deck close to the surface. As with GPR, more versatile radar instrumentation can likely be operated for a vehicle-mounted platform; however, it is possible that lane closure(s) will be necessary.

There are several commercial radars already available. The Olson Instruments IBIS-S system is one frequently described as part of civil engineering research in literature (Olson 2010). From experience with the commercial system built by Akela Inc., data processing can be done in a dedicated environment such as the commercial RADAN software program by GSSI or using custom algorithms developed in MATLAB. The processing likely consists of migration or coordinate transformations and will not be simple. Advanced post-processing is required to achieve the highest resolution and the best results.

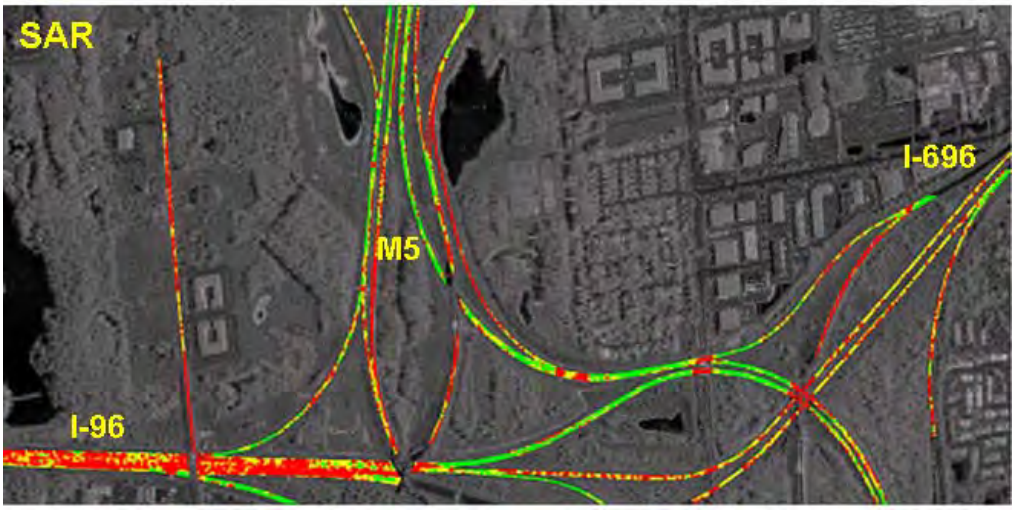

(a)

(b)

(c)

Figure 19: Three images of road surface (pavement) condition from TARUT study (Brooks, Schaub et al. 2007). (a): road roughness as determined from SAR speckle contrast; (b): road roughness according to the International Roughness Index (IRI); (c): rough sufficiency according to the PASER standard

5.10 Interferometric Synthetic Aperture Radar (InSAR)

Interferometric synthetic aperture radar (InSAR) is a type of radar collection with two antennas in which the resultant two images are made to interfere; and pixel-by-pixel differences in amplitude and phase are compared. This category includes microwave differential interferometry. SAR images are coherent radar images in three dimensions, where the first two coordinates specify the spatial location of a signal and the third coordinate contains the phase. It is the phase information from which height or depth measurements are made (Shinozuka et al. 2000). There are many commercial vendors of synthetic aperture radar (SAR) data whose products can be used to create InSAR images. Most notable among them are MDA Geospatial Services Inc., which markets data from the Canadian platforms RADARSAT-1 and RADARSAT-2. A longer list, including both commercial and non-commercial instruments is provided in Table 9.

The cost of InSAR for most bridge remote sensing applications is encapsulated by the price of commercial SAR imagery, which is not insignificant. In addition, for change detection in global metrics, multiple images of the same scene at different times would need to be purchased. Ground-based acquisitions have capital costs associated with the equipment purchase and possible operational costs depending on deployment and the expertise of the available staff. Complex processing is also required for InSAR data, as artifacts commonly need to be removed, including problematic multiple reflections from bridges over water. It is not clear that commercial vendors remove these artifacts before distributing the imagery. In addition to artifact removal, significant pre-processing is required to transform InSAR data into a world coordinate system (Soergel et al. 2008). However, aerial or space-borne InSAR offers the potential of rapid assessment of bridges from high stand-off without requiring calibration or preparation of the structure and without interfering with traffic.

In the performance evaluation, InSAR was determined to be useful in only a few applications, all of which were global metrics and in these applications, the technique scored well. Bridge settlement is one metric that may be measurable using InSAR, which is capable of detecting changes in height by the calculation of phase differences in the two signals. The changes must at least be on the order of a wavelength in size to be detected and even at X-band, 10 GHz, the wavelength is 30 mm. This means that only changes of at least 30 mm can be detected at that frequency. However, at higher frequencies and smaller wavelengths, smaller changes might be detected. Shinozuka et al. (2000) report detecting a 10 cm change in building height using this technique on simulated data.

InSAR might also be useful for detecting changes in bridge length and position (transverse bridge movement). For this application, the difference in backscatter between two images would be used rather than the phase difference. Using backscatter from range bins rather than phase information limits the resolution to that of the SAR image, which is typically on the order of 10^{-1} to 10^{0} m. Changes in surface roughness of the concrete deck can also be fully recovered from the ratios of InSAR coherence from image to image (Hajnsek and Cloude 2005).

Change in surface roughness can also be measured from coherent speckle contrast in SAR imagery, as described in the previous section "Radar Images, Backscatter, and Speckle" (see Figure 19). Whether or not InSAR can sufficiently measure bridge vibration is less clear, as there is no indication from the available literature as to how sensitive InSAR is to frequency. However, the amplitudes of vibration that need to be detected are likely within the capabilities of ground-based InSAR (Pieraccini et al. 2000). It is unlikely that vibration can be measured sufficiently from aerial or space-borne platforms.

Table 9: Partial list of commercial and non-commercial SAR

Sensor	Owner	Platform	Country	Ownership
RADARSAT-1	MacDonald, Dettwiler and Associates Ltd.	Satellite	Canada	Commercial
RADARSAT-2	MacDonald, Dettwiler and Associates Ltd.	Satellite	Canada	Commercial
AirSAR	Jet Propulsion Laboratory (JPL)	Airborne	U.S.	Government
UAVSAR	Jet Propulsion Laboratory (JPL)	Airborne	U.S.	Government
ERS	European Space Agency (ESA)	Satellite	E.U.	Government
ENVISAT	European Space Agency (ESA)	Satellite	E.U.	Government
JERS	National Space Development Agency of Japan	Satellite	Japan	Government
TerraSAR-X	InfoTerra	Satellite	Germany	Commercial

5.11 Acoustics

Acoustics is not strictly a remote sensing technique. Although the subsurface bridge condition indicators that are measured with acoustic techniques are not in contact with the equipment when a measurement is made, the bridge or structural element itself is in contact with the instrument. The technique utilizes reflected or transmitted acoustic waves (sound waves) in a medium to measure certain parameters of that medium and infer its condition or composition. Sophisticated instrumentation is used to monitor these acoustic waves and objectively measure their flight time (travel time through a medium), frequency content, and amplitude. There are different ways of measuring acoustic waves and these have given rise to different acoustic techniques. All modern, instrumented acoustic techniques are considered here, including i) acoustic emission monitoring, the measurement of ultrasonic wave velocity, ii) the impact-echo method, where the frequency content of a reflected wave is measured, iii) acoustic tomography, and iv) Lamb wave monitoring. Though these techniques are similar in spirit to the tap test and chain dragging, those traditional methods of bridge inspection are not considered in this category nor in any part of this technology performance evaluation.

As acoustics require significant traffic disruption, preparation of the structures, are in direct contact with the bridge or structural element, and are sensitive to environmental noise, they did rate well in this performance evaluation for any application. This literature review

indicated the technologies are only applicable to subsurface features or cracks and section loss of deck and girder surfaces.

5.12 StreetView-style Photography

The term "StreetView-style Photography" refers to any serial collection of photographs from the ground (from the bridge deck) with a 3D geospatial projection, especially where the photographs have been projected into a continuous 360-degree viewing environment (see Google StreetView). This instrumentation has the potential to be mounted on a vehicle platform for rapid collection and with little to no interference with traffic. As many bridges may not allow for driving underneath or along side, this category must be limited to collection from a vehicle driving along the deck surface.

The value of this technology is realized when the bridge inspector or manager uses a StreetView-style application to assess a bridge from the office. The technology enables anyone to review a bridge's structural condition, in which indicators can be detected visually, without actually traveling to the bridge (see Figure 20). Bridge inspectors might find such an application useful for reviewing a bridge they have already performed an inspection on or for looking at updated imagery of a bridge ahead of its next scheduled inspection. Such a scenario might occur where an inspector suspects that he or she should increase the inspection frequency of a bridge, but does not have the funds or time to do so. In the performance evaluation of high-resolution, panoramic photography such as StreetView, it was determined the technology would be most useful for bridge deck surface features including torn or missing expansion joint seals, damage to armored expansion joint plating, cracks and spalls near expansion joints, map cracking, scaling and spalling of the bridge deck, and delaminations expressed as surface cracks. For all of these features, StreetView-style imagery offers immediate commercial viability, automated image processing for visual inspection of results, a vehicle-based collection platform and, consequently, no traffic disruption whatsoever. The resolution requirements for these challenges can very likely be met, but there appears to be no available literature on using high-resolution panoramas to assess these or any other bridge condition indicators. It is likely that hairline cracks in steel or concrete are too fine to be resolved from this imagery, buthigh-resolution panoramas may be useful in assessing surface roughness in addition to the deck challenges previously described.

The capital cost of StreetView-style photography instrumentation could be high if a dedicated, commercial platform is used (such as the Trimble MX-8, which also offers 3D laser scanning). However, high-resolution digital cameras mounted on a vehicle could potentially provide the same results at a lower cost. Data collection consists merely of driving along or underneath a bridge and so operational costs should be very low.

Figure 20: Example image from Google's StreetView showing the underside of a box-beam bridge in Michigan. With higher-resolution panoramas, such an interface could be extremely valuable to bridge inspectors and managers.

6.0 Conclusions and Recommendations

While remote sensing technologies have been successfully implemented in a number of industries, their use within the transportation industry has been somewhat limited to date. This report presents a performance evaluation and rating of commercially available remote sensing technologies for infrastructure condition assessment, specifically bridges. In this study, a number of remote sensing technologies were reviewed to evaluate their potential to detect a series of indicators related to common challenges faced by the typical U.S. bridge. The technologies evaluated include:

1. Ground Penetrating Radar (GPR)
2. Spectral Analysis (Spectra)
3. 3D Photogrammetry
4. EO Airborne and Satellite Imagery
5. Optical Interferometry
6. LiDAR
7. Thermal/Infrared Imaging
8. Digital Image Correlation
9. Radar Imaging, Backscatter, and Speckle
10. Interferometric Synthetic Aperture Radar (InSAR)
11. Acoustics
12. StreetView-style Photography

Each remote sensing technique was rated using criteria that assessed the following:

A) Accuracy
B) Commercial availability
C) Cost of measurement
D) Pre-collection preparation
E) Complexity of analysis and interpretation
F) Ease of data collection
G) Stand-off distance
H) Traffic disruption

The challenges considered were grouped into broad fields related to their location of occurrence including the deck surface, deck subsurface, girder surface, and girder subsurface, in addition to a global metrics category describing the challenges that pertain to the bridge system level performance. Within these broad categories, specific challenges (e.g. spalling on bridge deck surface, delamination within the bridge deck, prestress strand breakage internal to a concrete girder, etc.) and pertinent indicators of these challenges were established as the threshold for assessing remote sensor viability. Using the rating criteria, sensor technologies

were scored for their applicability to the challenges within the broad categories. As a whole, the results of this evaluation demonstrated that remote sensing technologies could have a potentially significant impact in the assessment of bridge condition and that successful implementation will likely require using the sensors in a complementary manner such as: integrating the sensors in a vehicle-mounted system to minimize traffic impacts, coupling sensors with traditional assessment methodologies, and utilizing temporal sensor outputs to enhance the bridge inspection and decision making process. Some of the key findings from the evaluation include (see Table 3 - Performance Rating of Commercial Remote Sensing Technologies):

a) 3-D Photogrammetry and StreetView-Style Photography appear to have the greatest potential for evaluating deck surface conditions. These conditions primarily relate to challenges observable with the human eye, but have the added benefit of providing qualification of the challenge of interest. Other relevant challenges that may be addressed by these technologies include surface issues on the superstructure elements such as cracking and section loss and stand-off observables such as long-term structure movement.
b) EO Airborne/Satellite Imagery, Optical Interferometry, and LiDAR demonstrated applicability to deck surface challenges as well, but were not always able to satisfy the resolution requirements. These technologies demonstrated promise to global metrics related to system performance such as long-term structure movement as well as real-time measurement of vibration.
c) Radar technologies including GPR and higher frequency radar (backscatter/speckle) as well as thermal/infrared imaging provided the most promise for subsurface challenges, but can be limited in resolution (radar and thermal/infrared) or have challenges associated with collection (thermal/infrared).

While the rating results highlighted sensor technologies that have the potential to impact current practices, it also highlighted technologies that have low potential and those requiring additional research, sensor development and commercialization. Ongoing and future activities of this study will investigate the performance of some of these technologies for specific challenges related to bridge performance. The technologies to be evaluated include: digital image correlation, radar (including GPR), optical interferometry, spectral reflectance, StreetView-style photography, and 3D digital photogrammetry. These technologies were selected based on the preliminary rating with consideration of the domain expertise of the project team and other ongoing projects in these areas.

7.0 References

Ahlborn, T. M., D. K. Harris, C. N. Brooks, K. A. Endsley, D. C. Evans and R. C. Oats (2010 a). Remote Sensing Technologies for Detecting Bridge Deterioration and Condition Assessment. NDE/NDT for Highways and Bridges: Structural Materials Technology (SMT) 2010. New York, American Society for Nondestructive Testing (ASNT).

Ahlborn, T. M., R. Shuchman, L. L. Sutter, C. N. Brooks, D. K. Harris, J. W. Burns, K. A. Endsley, D. C. Evans, K. Vaghefi and R. C. Oats (2010 b). The State-of-the-Practice of Modern Structural Health Monitoring for Bridges: A Comprehensive Review.

Ambu, R., F. Aymerich, F. Ginesu and P. Priolo (2006). "Assessment of NDT interferometric techniques for impact damage detection in composite laminates." Composites Science and Technology 66(2): 199-205.

American Association of State and Highway Transportation Officials (AASHTO) (2008). "Bridging the Gap: Restoring and Rebuilding the Nation's Bridges."

American Association of State Highway and Transportation Officials (AASHTO) (2008). The Manual for Bridge Evaluation.

American Concrete Institute (ACI) Committee 222 (2001). Protection of Metals in Concrete Against Corrosion , Farmington Hills, MI.

Angst, U., B. Elsener, C. K. Larsen and O. Vennesland (2009). "Critical chloride content in reinforced concrete – a review." Cement and Concrete Research 39: 1122-1138.

Aronoff, S. (2005). Remote Sensing for GIS Managers. Redlands, CA, ESRI Press.

Barrile, V. and R. Pucinotti (2005). "Application of radar technology to reinforced concrete structures: a case study." NDT & E International 38: 596-604.

Brooks, C., D. Schaub, B. Thelen, R. Shuchman, R. Powell and E. Keefauver (2007). TARUT pilot studies technical details report. Deliverable 5.3-B. M. D. o. Transportation, Michigan Tech Research Institute.

Cardimona, S., B. Willeford, J. Wenzlick and J. Anderson (2000). Investigation of bridge decks utilizing ground penetrating radar. International Conference on the Application of Geophysical Technologies to Planning, Design, Construction, and Maintenance of Transportation Facilities. St. Louis, Missouri, U.S.A.

Cremers, D. A. (1987). The analysis of metals at a distance using laser-induced breakdown spectroscopy.

DelGrande, N. and P. F. Durbin (1999). Delamination detection in reinforced concrete using thermal inertia. Nondestructive Evaluation of Bridges and Highways III, Newport Beach, CA, USA, SPIE.

Falkner, E. (1995). Aerial Mapping: Methods and Applications. Boca Raton, FL, Lewis Publishers – CRC Press

Federal Highway Administration (FHWA). (2009). "National Bridge Inventory (NBI)." from http://www.fhwa.dot.gov/bridge/deficient.cfm.

Federal Highway Administration (FHWA). (2004). "National Bridge Inspection Standards (NBIS)." from www.fhwa.dot.gov/bridge/nbis.htm.

Federal Highway Adminstration (FHWA) (2006). Bridge Inspector's Reference Manual (BIRM). Washington, D.C.

Gentile, C. (2009). Radar-based measurement of deflections on bridges and large structures: advantages, limitations and possible applications. IV ECCOMAS Thematic Conference on Smart Structures and Materials.

Gucunski, N., S. Nazarian, P. Shokouhi and D. Kutrubes (2010). SHRP 2 validation study of performance of NDT technologies in identification and characterization of concrete bridge deck deterioration. NDE/NDT for Highways and Bridges. New York City, NY, U.S.A., American Society for Nondestructive Testing: 121-128.

Hajnsek, I. and S. Cloude (2005). "The potential of InSAR for quantitative surface parameter estimation." Canadian Journal of Remote Sensing 31(1): 85-102.

Harris, D., S. Hong and S. A. Newbolds (2010). Practical evaluation of bridge deck reinforcement corrosion using ground penetrating radar, half-cell, and sounding. TRB Annual Meeting, Transportation Research Board.

Hatta, H., M. S. Aly-Hassan, Y. Hatsukade, S. Wakayama, H. Suemasu and N. Kasai (2005). "Damage detection of C/C composites using ESPI and SQUID techniques." Composites Science and Technology 65(7-8): 1098-1106.

Hauser, E. W. and S.-E. Chen (2009). Integrated remote sensing and visualization (IRSV) system for transportation infrastructure operations and management. Charlotte, NC, U.S.A., Center for Transportation Policy Studies, University of North Carolina at Charlotte.

Hu, C. W., J. K. C. Shih, R. Delpak and D. B. Tann (2002). Detection of air blisters and crack propagation in FRP-strengthened concrete elements using infrared thermography. Inframation - The Thermographer's Conference.

Hutt, T. and P. Cawley (2008). "Feasibility of digital image correlation for detection of cracks at fastener holes." NDT & E International 42: 141-149.

Kanada, H., Y. Ishikawa and T. Uomoto (2005). Utilization of near-infrared spectral imaging system for inspection of concrete structures. New Technologies for Urban Safety of Mega Cities in Asia. Singapore.

Kant, Y. and K. V. S. Badarinath (2002). "Sub-pixel fire detection using Landsat-TM thermal data." Infrared Physics & Technology 43(6): 383-387.

Kim, W., A. Ismail, N. L. Anderson, E. A. Atekwana and A. Buccellato (2003). Non-destructive testing (NDT) for corrosion in bridge decks using GPR. The 3rd International Conference on Applied Geophysics. Orlando, Florida, U.S.A.

Krajewski, J. E. (2006). Bridge inspection and interferometry. Worcester, Massachusetts, Worcester Polytechnic Institute. Master of Science in Civil Engineering: 120.

Kuntz, M., M. Jolin, J. Bastien, F. Perez and F. Hild (2006). "Digital image correlation analysis of crack behavior in a reinforced concrete beam during a load test." Canadian Journal of Civil Engineering 33: 1418-1425.

Laefer, D. F., M. Fitzgerald, E. M. Maloney, D. Coyne, D. Lennon and S. W. Morrish (2009). "Lateral image degradation in terrestrial laser scanning." Structural Engineering International 19: 184-189.

Lim, M. K. (2001). NDE Using Impulse Radar to Evaluate Material Properties in Concrete Structures. Structural Faults and Repair 2001. P. M. Forde. London, UK, Published by Engineering Technics Press, Edinburgh.

Lubowiecka, I., J. Armesto, P. Arias and H. Lorenzo (2009). "Historic bridge modelling using laser scanning, ground penetrating radar and finite element methods in the context of structural dynamics." Engineering Structures 31(11): 2667-2676.

Luhmann, T., S. Robson, S. Kyle and I. Harley (2006). Close-range photogrammetry: principles, methods, and applications. Hoboken, NJ Caithness : Whittles.

Maierhofer, C. and S. Leipold (2001). "Radar investigation of masonry structures." NDT & E International 34(2): 139-147.

Maser, K. R. (1986). Detection of progressive deterioration in bridge decks using ground penetrating radar. ASCE/EM Division Specialty Conference. Boston, MA, U.S.A., American Society of Civil Engineers.

Michigan Department of Transportation. (2008). "Bridge Deck Preservation Matrix." from http://www.michigan.gov/documents/mdot/MDOT_BridgeDeckMatrix_182438_7.pdf.

Mikhail, E. M., M. L. Akey and O. R. Mitchell (1984). "Detection and sub-pixel location of photogrammetric targets in digital images." Photogrammetria 39(3): 63-83.

National Cooperative Highway Research Program (NCHRP) (2007). Bridge Inspection Practices - NCHRP Synthesis 375. Washington DC, Transportation Research Board.

Nowak, A. S., M. M. Szerszen and D. A. Juntunen (2000). Michigan deck evaluation guide. C. a. T. Division. Lansing, MI.

Olson, L. D. (2010). Innovations in bridge superstructure condition assessment with sonic and radar methods. NDE/NDT for Highways and Bridges. New York City, NY, U.S.A., American Society for Nondestructive Testing.

Pieraccini, M., M. Fratini, D. Dei and C. Atzeni (2009). "Structural testing of Historical Heritage Site Towers by microwave remote sensing." Journal of Cultural Heritage 10(2): 174-182.

Pieraccini, M., M. Fratini, F. Parrini, C. Atzeni and G. Bartoli (2008). "Interferometric radar vs. accelerometer for dynamic monitoring of large structures: An experimental comparison." NDT & E International 41(4): 258-264.

Pieraccini, M., D. Tarchi, H. Rudolf, D. Leva, G. Luzi, G. Bartoli and C. Atzeni (2000). "Structural static testing by interferometric synthetic radar." NDT & E International 33(8): 565-570.

Precast / Prestressed Concrete Institute (PCI) (2004). PCI Design Handbook. Chicago, IL., PCI.

Scott, M., A. Rezaizadeh and M. Moore (2001). Phenomenology study of HERMES ground-penetrating radar technology for detection and identification of common bridge deck features.

Sekulic, D., D. Bjegovic and D. Mikulic (2001). "Non-destructive methods for monitoring of reinforcing steel in concrete." Structural Faults and Repair.

Shinozuka, M., R. Ghanem, B. Houshmand and B. Mansouri (2000). "Damage detection in urban areas by SAR imagery." Journal of Engineering Mechanics 126(7): 769-777.

Shuchman, R., N. Subotic, C. Roussi, J. Ruiter, W. Buller and D. Schaub (2005). Simulated RADAR data sets for transportation applications of the restricted use technology study, Altarum.

Soergel, U., E. Cadario, A. Thiele and U. Thoennessen (2008). "Feature extraction and visualization of bridges over water from high-resolution InSAR data and one orthophoto." IEEE Journal of Selected Topics in Applied Earth Observations and Remote Sensing 1(2).

Stimolo, M. (2003). Passive infrared thermography as inspection and observation tool in bridge and road construction. Non-Destructive Testing in Civil Engineering 2003.

Teza, G., A. Galgaro and F. Moro (2009). "Contactless recognition of concrete surface damage from laser scanning and curvature computation." NDT & E International 42: 240-249.

Warhus, J. P., J. E. Mast, E. M. Johansson and S. D. Nelson (1994). Improved ground-penetrating radar, bridge decks. Structural Materials Technology Non-Destructive Technology Conference. Atlantic City, NJ, U.S.A.

Appendix B – State of the Practice Report

The State-of-the-Practice of Modern Structural Health Monitoring for Bridges: A Comprehensive Review

T. M. Ahlborn, Ph.D., P.E.[1], R. Shuchman Ph.D[2], L. L. Sutter Ph.D.[1], C. N. Brooks[2], D. K. Harris, Ph.D.[1], J. W. Burns Ph.D[2], K. A. Endsley[2], D. C. Evans[1], K. Vaghefi[1], R. C. Oats[1]

[1]Department of Civil and Environmental Engineering
Michigan Tech Transportation Institute
Michigan Technological University
1400 Townsend Drive
Houghton, Michigan USA 49931
(906) 487-2625; fax (906) 487-1620; email: tess@mtu.edu

[2]Michigan Tech Research Institute
Michigan Technological University
3600 Green Court, Suite 100
Ann Arbor, Michigan USA 48105
(734) 913-6840; fax (734) 913-6880; email: cnbrooks@mtu.edu

June 30, 2010

Michigan Tech

Table of Contents

Abstract iii
Acknowledgements iii
1.0 Overview 1
2.0 Bridge Evaluation Process 6
2.1 Inspection Basics 6
2.2 Visual Inspection 7
2.3 Defects 7
2.4 Traditional Inspection Tools 9
2.5 Advanced Inspection Techniques 9
2.6 Condition Rating 10
3.0 In-Situ Monitoring Techniques 13
3.1 Accelerometers and Velocimeters 13
3.2 Electrical Resistance 14
3.3 Electromechanical Impedance 15
3.4 Fiber Optics 16
3.5 GPS and Geodetic Measurements 19
3.6 Magnetic and Magneto-Elastic 20
3.7 Ultrasonic Emissions and Lamb Waves 22
4.0 On-Site Monitoring Techniques 25
4.1 Eddy Currents 25
4.2 Electrical Time-Domain Reflectometry (TDR) 26
4.3 Infrared Thermography and Spectroscopy 26
4.4 Laser Scanning 29
4.5 Nuclear Magnetic Resonance (NMR) Imaging 31
4.6 Microwave Radar 33
4.7 Ground-Penetrating Radar (GPR) 34
4.8 X-Ray, Gamma Ray, and Neutron Radiography 36
5.0 Remote Monitoring Techniques 39
5.1 Electro-Optical Imagery and Photogrammetry 39
5.2 Speckle Photography and Speckle Pattern Interferometry 40
5.3 Interferometric Synthetic Aperture Radar (IfSAR) 43
6.0 Exceptional Materials and Structures 45
6.1 Fiber-Reinforced Polymer Composites 45
7.0 Case Studies 49
7.1 Commodore Barry Bridge, Philadelphia, PA 49
7.2 Golden Gate Bridge, San Francisco, CA 50

7.3 Tsing Ma Bridge, Hong Kong, China 50
7.4 Vernon Avenue Bridge, Barre, Massachusetts 51
7.5 Cut River Bridge, Michigan 52
7.6 Field Monitoring of Four Integral Abutment Bridges, Pennsylvania 53
7.7 Bridge Monitoring TestBed 54
8.0 References 56

Abstract

Since the National Bridge Inventory (NBI) was first conducted, structural health monitoring (SHM) of the United States bridge infrastructure has consisted largely of labor-intensive, subjective measures like chain dragging and the tap test. Recent developments in a variety of sensor technologies and an improvement of computing and networking capabilities have allowed for the installation of in-situ sensor networks responsible for monitoring—among other parameters—the strain and deformation of structural members and concrete deck cracking. These relatively new techniques are quite costly, however, and in many cases are infeasible for SHM because they require installation in hard-to-reach places or during construction, limiting their application to the small number of bridges being built today compared to the current population of in-service bridges. Stand-off SHM techniques such as radar, electro-optical, laser scanning and other remote sensing technologies may offer an innovative, cost-effective method of monitoring the dynamic conditions of U.S. bridges in real-time. This paper investigates the state of the practice of SHM and provides summaries of existing technologies, both in-situ sensors and networks and remote techniques, as well as case studies of instrumented bridges.

Acknowledgements

This work is supported by the Commercial Remote Sensing and Spatial Information program of the Research and Innovative Technology Administration (RITA), U.S. Department of Transportation (USDOT), Cooperative Agreement # DTOS59-10-H-00001, with additional support provided by the Michigan Department of Transportation, the Michigan Tech Transportation Institute, the Michigan Tech Research Institute, and the Center for Automotive Research. The views, opinions, findings, and conclusions reflected in this paper are the responsibility of the authors only and do not represent the official policy or position of the USDOT, RITA, or any state or other entity. Additional information regarding this project can be found at www.mtti.mtu.edu/bridgecondition .

5.0 Overview

The transportation infrastructure of the United States is in need of rehabilitation and repair. According the American Society of Civil Engineers (ASCE), more than 27% of the nation‘s bridges are either structural deficient or functionally obsolete. One succinct and startling statistic is that the average American bridge is now 43 years old. The ASCE estimates that the total investment needed to bring the nation‘s bridge infrastructure up to code over 5 years is 930 billion dollars, but in that time only $549.5 billion is projected to be spent (ASCE 2009). With a finite amount of funding, the allocation of such funds may make up the difference in the long run. Rehabilitation, for instance, is far cheaper than replacement when damage is minor. Better management of funds used to inspect and maintain existing bridge infrastructure could reduce costs. A report by the Federal Highway Administration indicates that, given more time and funding to complete bridge inspections, the use of non-destructive evaluation (NDE) methods would increase by state and county transportation agencies (USDOT 2001). NDE promises a way to improve the allocation of funding by improving the information these decisions are based on, by improving the assessment of existing bridge conditions.

Currently, structural health monitoring (SHM) in the United States and most other developed nations is characterized by traditional visual inspection along with referencing of old inspection reports to maintain an accurate account of the bridges condition. The standard evaluations used by the Federal Highway Administration have been limited to auditory tests and visual inspection since the National Bridge Inventory (NBI) was first conducted (Chong et al. 2003) almost 40 years ago. The NBI has its roots in the Federal Highway Act of 1968, which was enacted following the tragic collapse of the Silver Bridge in Ohio. Krajewski (2006), an excellent reference that reads like a history of bridge inspection, describes the training and resources provided to bridge inspectors as part of the federal initiative. The program emphasizes visual inspection techniques with manuals that provide photographs of the various types and degrees of deterioration in bridge elements. Bridge inspectors are trained in identifying all the types of deterioration, but there is a subjective component when dealing with the rating of the bridges. The NBI uses a rating system of zero to nine for the rating of the condition of the bridge to system to allow for uniform characterization of bridge condition.

Traditional slow and subjective methods used in assessing deck condition, which include impact sounding, chain dragging, half-cell potential, and core analysis, are being replaced by more modern techniques. The use of remote sensing techniques and robust, permanent sensor networks on bridges are being investigated. As of 2005, about 40 long-span (100 m or longer) bridges worldwide have been equipped with sophisticated health monitoring instrumentation systems. These systems are lauded as ―array[s] of inexpensive, spatially distributed, wirelessly powered, wirelessly networked, embedded

sensing devices supporting frequent and on-demand acquisition of real-time information about the loading and environmental effects, structural characteristics, and responses" (Ko and Ni 2005). Despite these advantages, permanent, in-situ sensor networks are costly and can be difficult to install on some bridges or bridge elements, particularly when they were not considered during the construction phase.

Permanent networks of sensors are deployed on bridges with two distinct goals in mind: the generation of alerts for bridge managers and the viewing/analysis of continuous real-time structural data. These goals are achieved by networks that emphasize two discriminating factors: the time-scale of the change and the severity of the change. Traditionally, these networks have consisted of in-situ sensors coupled with structural elements and wired to both a data-acquisition system and a power source. Consequently, these networks are costly, cumbersome, and in some cases interrupt the normal operation of the structure (Kim et al. 2007).

In-situ sensor networks paved the way for modern bridge monitoring practices, including electronic data collection and distribution. Bridge inspection officials have indicated that the best way to improve the performance of bridge inspections is to allow for electronic data to be uploaded directly to a Bridge Management System; many have also cited the establishment of such a system as a major accomplishment for their team (USDOT 2001). This is a popular idea in most conceptions of modern bridge monitoring by large, disseminated networks of permanent, in-situ sensors. Ideally, SHM should incorporate remote sensing techniques that provide the same capability for the remote collection of high-resolution (both spatial and temporal), real-time structural data without the need for costly hardware and its installation, calibration, and maintenance. In this paper, modern in-situ techniques (where sensors are in direct-contact with bridge elements), on-site surveys (where instrumentation is brought to the bridge to make measurements), as well as standoff remote sensing techniques (where remote sensors are used far from the bridge) for the SHM of bridges are summarized.

In its 1998 survey, the Federal Highway Administration (FHWA) surveyed the use of NDE techniques for SHM among state and Iowa county DOTs as well as independent contractors. From the 14 (out of 42) state DOT respondents, they learned that the most common NDE techniques being employed in the field (by ASNT Level III personnel) were liquid penetrant testing, ultrasonic testing, and magnetic particle testing with a smaller number reporting expertise in radiographic and electromagnetic techniques. All of these techniques increased in reported use from 1993 to 1998 according to three different surveys. Citing a similar survey from 1994, the FHWA concluded, from an increase of 19 to 33 percent response, that use of the American Society for Non-destructive Testing (ASNT) Level III certification has increased (USDOT 2001). Visual inspection dominated among NDE techniques then being used on existing bridges of all types, followed by the aforementioned techniques for steel

bridges. On concrete bridges, mechanical sounding was second to visual inspection, followed by some innovation such as electrical potential and radar measurements. While many state DOTs reported a variety of advanced NDE techniques such as these being used, almost no county or local agencies reported using anything other than visual techniques and mechanical sounding. Of the state transportation agencies that use advanced NDE techniques, some indicated that they had ceased using techniques such as ultrasonic testing of pin/hanger connections, various pile testing, radar, and acoustic emissions due to unreliable performance or other reasons.

It is important to describe modern instrumentation in detail. For both remote and in-situ instrumentation, traditional and modern techniques can be broken down into two distinct categories of monitoring. While ―local" health monitoring methods are used to precisely determine the location and extent of damage, ―global" methods can only determine damage of the structure as a whole (Chang et al. 2003). Both are equally valuable, as global methods easily and quickly establish that damage has occurred to the structure. Local methods would not be used to initially assess whether damage has occurred, but are necessary for isolating exactly where known damage exists. In all SHM practice, the first step should be to determine what parameters need to be measured, as this will determine what methods are used. For concrete bridges the most critical parameters are strain, temperature, cracking of concrete, and corrosion of reinforcement (Casas and Cruz 2003).

Modern global health monitoring techniques rely on finding shifts in resonant frequencies or changes in structural mode shapes. The challenge with these modern techniques is to differentiate real structural damage from environmental factors such as moisture and temperature by distinguishing significant shifts from the background (Chang et al. 2003). Stress-wave propagation, for example, is a promising global, non-destructive evaluation (NDE) for concrete structures and has been employed with great success where it involves mechanical impacts (Chong et al. 2003). Ground-penetrating radar (GPR) and infrared thermography have also been cited as the most promising emerging techniques for bridge monitoring (Maser and Roddis 1990), especially in the evaluation of a bridge‘s concrete deck (traffic surface). Reinforced concrete decks have a far shorter life span than the finite elements or bridge superstructure, and as such deserve special attention.

Chang et al. (2003) also describes several innovative monitoring techniques for local SHM including micro-electromechanical system (MEMS) devices for accelerometers and velocimeters, nuclear magnetic resonance (NMR) for the detection of chloride intrusion, as well as shearography and LiDAR. Two major areas of interest with respect to the SHM of bridges are crack detection and inspection of the concrete deck (traffic surface). Visual techniques and dye penetration have historically been used for crack detection but new electromagnetic methods including the use of eddy currents and

radar (ground-penetrating, interferometric, microwave) as well as acoustic methods (ultrasonic, acoustic impedance, and acoustic attenuation) can also be employed. Electro-optical imaging techniques are also promising as cracks reflect and absorb light differently than intact regions. Piezoelectric wafers are deployed at problem areas and relied upon to produce signals which indicate when cracks and degradation take place. Other innovative techniques for SHM include X-ray and Gamma-ray imaging for steel cables and slabs. Fiber optic sensors allow for complex, distributed networks of sensors capable of detecting cracks in concrete, the presence of chloride ions, or corrosion of reinforcing steel. Chang et al. (2003) distinguishes these multifarious NDE techniques categorically: acoustic signals, electromagnetic, radiography (X-ray and Gamma ray), fiber optics, radar and radio frequency, optics (TLS and LiDAR), and piezoelectric detectors of acoustic impedance. This is how these techniques are classified in this paper, though some are given more emphasis than others based on their perceived acceptance and use in industry.

A report (USDOT 2001) by the Federal Highway Administration‘s Turner-Fairbank Highway Research Center details the state of routine bridge inspection practice as of 2001. Using the results of a survey they conducted and the results of 42 state Departments of Transportation (DOTs), 72 Iowa county DOTs, and 15 bridge inspection contractors, they profiled the activities of these agencies in the U.S. They found that more than 90% of state DOTs conducted bridge surveys with their own employees as well as contractors while half of Iowa county DOTs relied solely on contractors. The services that contractors performed included the inspection of moveable bridges, ultrasonic testing of hanger pins, scour analysis, fracture-critical inspections, and complex traffic control; two state DOT respondents also indicated they hired contractors when the agency was behind schedule. The authors provided an example of a specific bridge type (20-years old, two-span, two-lane, steel, four-girder bridge with welded flange cover plates, concrete deck and abutments, and a single three-column concrete pier with pier cap) and found that the average time for state and county DOTs to perform such a bridge inspection is 4.5 man-hours; about 2 people are usually assigned. The authors also found that while 83% of contractors who responded have a Professional Engineer (PE) on-site for 81-100% of their bridge inspections, about half of state and county DOTs rarely, if ever, have a PE on-site. When a PE is present, it is usually either because they are a routine member of the inspection team or because a follow-up inspection is being performed. Fracture-critical and closure conditions are also cases in which a PE is likely to be deployed for bridge inspection. State and county agencies listed the areas in which they would allocate additional time and money for bridge inspections were it available. The most common responses included the increased use of NDE, additional personnel and equipment, improvements to their Bridge Management System, and an increase in the amount of time allowed for inspection.

All of the respondents—county and state DOTs and contractors—indicated that previous inspection reports for a bridge were made available both before the inspector arrived and also at the bridge site. Results from the survey indicate that state DOTs inspect, on average, 6,300 bridges per year while county DOTs and contractors inspect 240 and 820 bridges per year, on average, respectively. However, bridge inspection counts from the Iowa county DOTs seem too high in light of the total number of bridges in Iowa. The most common quality assurance/quality control (QA/QC) measures taken include an office review of inspection reports, rotation of bridge inspectors, field re-inspection programs, and "ride-alongs" by a PE on bridge inspections in conjunction with a field review.

2.0 Bridge Evaluation Process

2.1 Inspection Basics

The performance evaluation of bridges starts with the inspection of the bridge to determine the present condition. This is completed in a variety of ways depending on the particular personnel and department conducting the inspection of the bridge, but all inspections are completed in accordance with the National Bridge Inspection Standards (NBIS). The Bridge Inspector‘s Reference Manual (BIRM) aids the bridge inspector with programs, procedures, and techniques for inspecting and evaluating a variety of in-service highway bridges (Ryan et al 2006). The BIRM is sponsored by the National Highway Institute for the Federal Highway Administration (FHWA). Before an inspector is qualified for the inspecting of bridges they are required to attend an inspection course that satisfies the requirement of the NBIS for a comprehensive training program. This is typically a one to two week course depending on the background of the inspector and types of inspections to be completed. To determine the overall condition of a bridge inspectors follow the guidelines provided for them, but also include personnel or experience based judgment when assigning a rating for a particular bridge. This is where concern can come into play with structural health monitoring because of the limited consistency from one inspector‘s rating to the next inspector‘s rating.

According to NBIS, bridges must be inspected at least every two years. Some bridges with problem areas at the discretion of the owner may need to be inspected more frequently than two year minimum required. Any structure that has a span length of greater than twenty feet as defined by the NBIS regulations is required to be rated for National Bridge Inventory (NBI). There are currently 603,248 bridges rated within the NBI system as of December 2009. The number of bridges listed as structurally deficient as of 2009 was 71,179 (11.8%) and 78,462 (13.0%) were classified as functionally obsolete, demonstrating the need for a uniform rating system to ensure the correct bridges receive the appropriate attention and funding (Federal Highway Administration).

A general rating system is used to classify the condition on a 9 to 0 scale with 9 being a new bridge and 0 being out of service. A structurally deficient bridge would be rated at a ~~4~~” (poor) or less for superstructure, deck and/or substructure. A structurally deficient bridge could also have waterway adequacy that is rated at a ~~2~~” or less. Structural deficient bridges cannot support the intended traffic loads which results in postings to reduce weight and/or speed on the structure. In contrast functionally obsolete bridges do not typically represent a safety threat, but typically no longer have an adequate approach alignment, geometry or clearance for the given traffic needs and are below current design standards (Amey 2009).

2.2 Visual Inspection

BIRM states the typical routine inspection performed for the bridge would be a review of the previous inspection and a visual inspection of all the different members from on top of the bridge and underneath the bridge. The second type of visual inspection would be the in-depth inspection of one or more elements at less than an arm‘s length from the inspector. With a visual inspection of the bridge, the inspector would be looking for various distress or signs of those defects in the different members of the structure. If a defect is seen or suspected the inspector will often perform other inspection techniques to determine the extent of the defect on the structure. The location of fracture critical members is important when performing an inspection because these are often non-redundant members in the structure. The inspector pays particularly close attention to ensure that any defect that could potentially affect the capacity of a member or the bridge overall is closely inspected.

2.3 Defects

Bridges are designed with a variety of materials with the three main materials being concrete, steel and timber. Each of these materials has special characteristic that determine which types of defects that the inspector must monitor to confirm the material still has adequate remaining useful life for the member being inspected. The NBI is composed of 64.3% of concrete bridges and 30.9% of steel bridges. The use of timber is limited with about 4.2% of bridges being classified as a timber bridges along with only 0.3% of bridges being masonry (Federal Highway Administration). Table 1 shows the defects according to BIRM for the different materials that compose the different structural elements of the bridge. These defects are often associated with one or more structural groupings including deck, superstructure or substructure.

Table 1: Material Defects

Material	Defects
Concrete	cracking, scaling, delamination, spalling, chloride contamination, efflorescence, ettringite formation, honeycombs, pop-outs, wear, collision damage, abrasion, overload damage, reinforcing steel corrosion, prestressed concrete deterioration.
Steel	corrosion, fatigue cracking, overloads, collision damage, heat damage, paint failures
Timber	natural defects, decay, insects, chemical contamination, delaminations, loose connections, fire damage, weathering, warping, protective coating failure
Masonry	weathering, spalling, splitting, fire damage

When inspecting the deck of the bridge the inspector will look for key defects over the entire bridge. Of primary importance are the defects that affect ride quality of the bridge deck because the public often only feels irregularities from the riding surface. BIRM states that the inspector is typically looking for unevenness, settlement and roughness when determining the condition of the deck. Spalling is one of the defects that inspectors take into account with the safety of cars being of concern with falling concrete. Cracking is also of concern with rebar being exposed to elements possibly causing corrosion. Also the condition of the expansion joint is considered with the inspection of the deck. If there is a problem with the expansion joint could lead to superstructure degradation or alert the inspector to possible other damage in the bridge deck. The evaluation of bridge deck deterioration prompts deck repair, rehabilitation and replacement decisions. Sometimes asphalt is used to overlay the deck the bridge inspector would then have to look for other signs of distress in the deck below the overlay.

The superstructure is of particular importance from a safety perspective, to ensure that the members are adequate for the loads supported by these members. The inspection of the superstructure is searching for any of the defects in structural members. Some of the main defects that an inspector is looking for are exposed reinforcement, steel section loss and frozen bearing. The inspector should also confirm that the given members match those from plans. Additionally the bearing supports should also be checked thoroughly to ensure critical members are appropriately transferring the load from the superstructure to the substructure.

The substructure also has to be inspected for several different issues to be assured that it is not approaching failure. Some of the main defects the inspector would be looking for in the substructure members would be degradation, exposed rebar, cracking and corrosion. BIRM states that the inspector should determine the dimensions of the substructure to compare to those of the plan. Additionally, settlement of the substructure should be checked. According to BIRM this can be completed by looking along the

superstructure to see if any of the vertical faces are tilting. Inspection of the substructure is typically finished with checking for scour or undermining of the structure.

2.4 Traditional Inspection Tools

BIRM suggests several tools that the inspector could use while performing the inspection to insure an accurate assessment of the structure‘s condition. The inspector should carry tools to clear debris (broom, wire brush, scraper, flat bladed screwdriver and shovel), and an inspection hammer for sounding concrete, checking for sheared or loose connections and loosening dirt and debris. The inspection hammer can be used by the trained inspector to determine the condition of member by the sound produced by tapping the hammer to the material. A chain drag apparatus is often used to determine the location of any delaminations that are located in the concrete bridge deck. The chains produce a clear ringing sound in areas where there are no delaminations and produce a dull or hollow sound where there is a delamination in the concrete (Scheff and Chen 2000); however this technique is ineffective where asphalt overlays are applied.

2.5 Advanced Inspection Techniques

When evaluation beyond the aforementioned basic techniques is required, more advanced inspections are typically performed. These advanced techniques often require specialized equipment and may require specialized personnel. The different types of inspection techniques available are numerous and are constantly evolving, but can generally be categorized into two types, destructive and nondestructive. A summary of these different techniques listed in BIRM can be seen in Table 2. The purpose of a nondestructive test is to determine characteristics such as: strength and location of abnormalities, without compromising the integrity of the structure. This is important when inspecting a bridge because the less destructive tests required the better the structure will maintain its integrity. Destructive tests can affect the integrity of the structure, so the amount of testing is typically limited. Also the time required for destructive tests is extensive, often requiring the material samples to be delivered to a lab for testing. As a result, destructive tests are often used to confirm the findings of a nondestructive test. A typical example of confirmation destructive testing would be coring of concrete to confirm location and degree of delamination observed from an IR survey. Each individual test provides different information, so the inspector should use discretion for what test to use for the given situation.

Table 2: Bridge Testing Methods

Material	Test Type	Tests
Steel	Nondestructive	acoustic emissions testing, corrosion sensors, smart paint, dye penetrant, magnetic particle, radiographic testing, computer tomography, ultrasonic testing, eddy current
Steel	Destructive	Brinell hardness test, Charpy impact test, tensile strength test
Concrete	Nondestructive	acoustic wave sonic, delamination detection machinery, ground-penetrating radar, electromagnetic methods, pulse velocity, flat jack testing, impact-echo testing, infrared thermography, laser ultrasonic testing, magnetic field disturbance, nuclear methods, pachometer, rebound and penetration methods ultrasonic testing
Concrete	Destructive	core sampling, carbonation, concrete permeability, concrete strength, endoscopes, videoscopes, moisture content, reinforcing steel strength, petrographic examination
Timber	Nondestructive	Pol-Tek, spectral analysis, ultrasonic testing, vibration
Timber	Destructive	boring, drilling, moisture content, probing, shigometer

2.6 Condition Rating

The rating of the condition of the three main components is done on a scale of zero to nine according to the Recording and Coding Guide for the Structure Inventory and Appraisal of the Nation‘s Bridges (Federal Highway Administration 1995). This guide was created to help promote uniformity in bridge structure rating. The bridge section of this guide is located between Items 58 to 62. A detailed guide of what each rating of a structure stands for with a nine standing for excellent condition and a zero being failed condition out of service. The rating of the deck members that are integral with the superstructure are to be rated as a deck only not on how it influences the superstructure. Rating the deck, superstructure and substructure separately allows for an overall view of where the structural deficiencies are occurring. These ratings are then placed into the Pontis database system which forms the annual basis of the National Bridge Inventory (NBI). This inventory/rating database allows the federal government to get an accurate account of the condition of the United States bridge system. The rating system is key to providing a high-level summary of how and where work is need on the system of bridges and prioritizing funding on a national level.

Table 3: Condition Ratings

Rating	Definition	Description
9	Excellent Condition	
8	Very Good Condition	No problems noted
7	Good Condition	Some minor problems
6	Satisfactory Condition	Structural elements show some minor deterioration
5	Fair Condition	All primary structural elements are sound but may have some minor section loss, cracking, spalling or scour
4	Poor Condition	Advanced section loss, deterioration, spalling or scour
3	Serious Condition	Loss of section, deterioration, spalling or scour have seriously affected primary structural components. Local failures are possible. Fatigue cracks in steel or shear cracks in concrete may be present.
2	Critical Condition	Advanced deterioration of primary structural elements. Fatigue cracks in steel or shear cracks in concrete may be present or scour may have removed substructure support. Unless closely monitored it may be necessary to close the bridge unless corrective action is taken.
1	"Imminent" Failure Condition	Major deterioration or section loss present in critical structural components or obvious vertical or horizontal movement affecting structural stability. Bridge closed to traffic but corrective action may put it in light service.
0	Failed Condition	Out of service – beyond corrective action

3.7 Load Rating Another important rating criteria is load rating which defines the load limit on the structure to prevent catastrophic failure. There are two different rating levels that the New Mexico Department of Transportation uses when applying load ratings to a bridge inventory and operating levels. The inventory level represents the live load that a bridge can safely sustain for an indefinite period of time, whereas the operating level defines the level of permit load allowed across the bridge (Castro et al. 2009). According to The Manuel for Bridge Evaluation (MBE, 2008) there are three distinct procedures for the load and resistance factor rating of bridges: design load rating, legal road rating and permit load rating. The design load is a measure of how the bridge in its current condition performs under current LRFD bridge design standards. If the bridge can support all the LRFD limit states the bridge would be satisfactory for legal

loads. The legal load rating considers the effect of legal loaded truck traffic on the bridge. This can be the basis for posting load limits on the bridge or a bridge strengthening project. Permit load rating would be to check the effects of an overweight vehicle would have on the bridge taking into consideration the different factors on an individual permit basis.

3.0 In-Situ Monitoring Techniques

3.1 Accelerometers and Velocimeters

Accelerometers are relatively simple devices that compare the acceleration they experience to the acceleration due to gravity and are commonly provided as microelectro-mechanical systems (MEMS)—tiny machines with computing power. Velocimeters typically work through the same principles as interferometry. In SHM, both are primarily used for measuring displacement—through the integration of acceleration or velocity measurements—of structural members they are attached to. As the second derivative of displacement, however, acceleration can never provide information about the absolute position of the structure making it useless for detecting differential settlements, leaning, or any permanent offsets (Kijewski-Correa 2005). GPS may provide absolute positioning, but even when it is used to inform accelerometer measurements, the second integral of acceleration provides larger relative displacements than those provided by GPS due to scale factor errors and sensor biases. In addition, the signal noise of an accelerometer is device-specific and all have a band-pass frequency response including significantly poor performance at vibration frequencies lower than 0.2 Hz which prohibits their application to long-span bridges (Meng et al. 2007).

Accelerometers have been used for their ability to detect higher-frequency vibrations, particularly those that cannot be monitored by GPS. These vibrations are either the result of ambient or forced bridge loading. Ambient movements are those which abound during the everyday life of the bridge; the results of traffic, wind, and water. Forced movements are specific loads applied to the bridge as tests for the purpose of measuring its response. Due to the cost of forced movement on long-span bridges and because it is virtually identical to the ambient movement of long-span bridges, it is generally not practiced (Meng et al. 2007).

Accelerometers have been used to monitor rigidly bolted joints for damage (Tanner et al. 2003) and could be used more generally to monitor the 3D displacement of large structural elements due to wind or load variance in real time. Accelerometers are also used in conjunction with innovative signal processing and time-series analysis for global SHM—the assessment of whether or not a structure has been damaged (Lynch et al. 2006). They are currently the convention for dynamic testing or monitoring of large structures and have also been recognized for their efficacy in studies comparing new SHM methods against them (Hide et al.; Lynch et al. 2006; Gueguen et al. 2009). The ubiquity of accelerometers in SHM is shown by their use in studies examining more general aspects of SHM, in particular the shift from wired to wireless sensor arrays, such as in Whelan et al. (2007), Lynch and Loh (2006), and Masri et al. (2004). They can

obtain accuracies in acceleration measurements on the order of milligrams of loading (Lee et al. 2005).

3.2 Electrical Resistance

The electrical resistance method of SHM is a global, on-site, de-coupled technique for detecting defects even of modest size in composite materials and joints. Carbon-fiber polymer-matrix composites have been demonstrated to be a viable material for monitoring with this method, as they exhibit electrical properties which are affected by structural damage (Chung 2001). In addition, they are extremely strong, super-elastic, and possess piezoresistive qualities (Kang et al. 2006). In particular, as the conductivity in a certain direction of these composites is dependent on the number of carbon-fiber contacts, cracking can be detected by examination of the conductance (inverse of resistance) and its material characteristic, conductivity (inverse of resistivity). In general, fiber breakage is manifested as an increase in electrical resistivity. Measurements to determine such consist of using two electrodes for current injection into the composite lamina and two electrodes to measure the drop in voltage between two points on the lamina. From this measurement, the resistance between the two points can be calculated. This technique, sometimes dubbed electrical impedance tomography (EIT), has also been demonstrated to be effective at detecting temperature changes in conductive materials, as this is another parameter that affects measured resistance/conductance (Chung 2001). One disadvantage of this technique, however, is that it has low zero-stability, meaning that over time the measurand will drift (Ko and Ni 2005).

The electrical resistance of carbon fiber-reinforced polymer (CFRP) composites is influenced by fiber breakage, delamination, mechanical strain, and temperature, and applications for SHM must take all these factors into account even if they are not of interest for SHM concerns. Anisotropic effects must also be considered, as in CFRP laminates the carbon fibers are oriented in a specific direction. In these materials it is well understood that the electrical resistance is low (~0.022 mΩ·m) in the direction parallel to the fibers and high (~310 mΩ·m) in the transverse direction (Angelidis et al. 2004).

Calculating the electrical resistance in unidirectional laminates (carbon fibers oriented in one direction) is thus straightforward. In multidirectional laminates, however, the situation is more complicated, and the arrangement of fibers in a network must be considered. Angelidis et al. (2004) compared the electrical resistivity of unidirectional, cross-ply (two orthogonal fiber directions), and quasi-isotropic (two pairs of orthogonal fiber directions) CFRP laminates. Sample specimens were 60% fiber by volume, 2 mm thick, and 30 mm² in area. EIT with four or two contact points was used for resistance measurements. They were able to demonstrate that, for unidirectional laminates and homogeneous current injection (achievement of which is described in the paper),

resistance increases with positive strain in the lateral direction due to shrinking fiber diameter and in the transverse direction due to decreasing fiber contacts.

Wen and Chung (2000) demonstrated the use of electrical resistance measurements in measuring relative strain and the identifying damage under dynamic loading conditions. They employed EIT using silver paint and copper wire on the surfaces of plain cement, silica-fume cement, and latex cement pastes. They were able to observe changes in electrical resistance indicating both destructive plastic deformation as well as healing (e.g. closure of microcracks) in real-time. EIT was utilized by Schueler et al. (2001) in damage detection for CFRP composites with a resolution of 5 mm on a 50 mm by 50 mm grid with 1-mm spacing.

Song et al. (2006) demonstrated a revolutionary concept of a self-monitoring, self-healing concrete building. The building featured shape-memory alloys (SMAs), specifically martensite Nitinol cables, as reinforcement. When the SMA cables are resistively heated, they contract and close the cracks. Damage detection was accomplished with lead-zircontate-titanate (PZT) piezoelectric wafers which also estimated crack width based on the electrical resistance change in the SMA cables. Their concept was proofed with an SMA-reinforced concrete beam in which they produced a 0.47-inch wide crack under loading. They verified the monitoring and healing capabilities of their experimental setup and found that the electrical resistance value of an SMA cable changed by up to 27% in response to the opening crack.

Carbon nanotubes (CNTs) have also been studied in evaluations of the electrical resistance method of SHM. They are favored for their potential as actuators for high stress, high strain applications with low operating voltage. Due to their high tensile strength, they are also an attractive building material. The marriage of their architectural properties and their potential as stress/strain sensors presents a revolutionary potential for building self-monitoring _smart‘ structures.

3.3 Electromechanical Impedance

Electromechanical impedance (EMI) typically takes advantage of piezoelectric materials, which produce an electric field when subjected to mechanical stress. The effect also works in reverse in that piezoelectric materials will produce stress and/or strain when in the presence of an electric field. Obviously, this makes such materials extremely valuable for the detection and monitoring of strain in structures as a single piezoelectric device can act as both source and receiver. What is particularly innovative about the use of piezoelectric materials is that the electrical impedance measured in the circuit is directly related to the mechanical impedance of the host structure (Park et al. 2000), which makes absolute measurement possible. Mechanical impedance is directly related

to the fundamental characteristics of structures such as mass, stiffness, and damping—changes in which are indicators of structural damage (David et al. 2007).

A common EMI sensor is the piezoelectric wafer (patch), typically composed of piezoelectric-ceramic lead-zirconate-titanate (PZT), which is bonded to a structure or structural element to be monitored. By applying a voltage sweep signal—commonly in the kilohertz range—the PZT patch will induce vibrations in the structure. With an impedance analyzer connected to the wafer and controlling the voltage sweep signal, defects or deformations of the structure that are manifested as the electrical response of the PZT patch can be analyzed. By comparing conductance to frequency, a unique vibration signature of the structure is discovered which reveals structural characteristics like inherent stiffness, damping, and distribution of mass (Bhalla and Soh 2004).

Damage to the structure is especially apparent as changes in the structural stiffness and/or damping, so continuous monitoring that captures the dynamic behavior of the structure is most desirable. Such monitoring in real time can be achieved with the PZT wafer and numerous studies show how this sensor is successfully employed in permanent SHM networks (Lopes et al. 2000; Tanner et al. 2003; Lynch 2005; David et al. 2007). This method has been employed with great success and some studies have reported that it enabled the detection of cracks in concrete before they became visible, marking this technique as a clear improvement over standard, visual inspection methods.

3.4 Fiber Optics

Optical fibers are thin strands of dielectric material that trap light in a guided, low-velocity zone via total internal reflection, which is achieved by wrapping the waveguide or ―core" in a ―cladding"—a material with a lower refractive index. Optical fibers were first used for telecommunications and for endoscopy in medicine. By the late 1970‘s it was recognized that what distinguishes fiber optics best is that the materials are impervious to electromagnetic interference (Chang and Liu 2003) and so they began to be used as sensors; were also first used in concrete at the suggestion of Mendez et al. (1989). They are also attractive because they are lightweight and flexible, free from corrosion, allow for continuous monitoring, and possess very low signal transmission loss (Casas and Cruz 2003). Disadvantages presented by fiber optics are the cost and training required to decode optical signals.

One property of optical fiber that makes it ideal for use in SHM is that the light intensity of the optical signal decreases when the fiber is strained perpendicular to its length; light intensity can increase or decrease if the fiber is stretched or compressed (along its length). This enables fiber optics to be a valuable indicator of strain or displacement. To determine how much strain a fiber is experiencing, the signal‘s intensity is compared to that of an unstrained reference fiber of the same temperature. In

the case of displacement, the change in length of the fiber can also be determined by measuring the light intensity and travel-time or ―flight" time; this technique is called optical time-domain reflectometry (OTDR). These *intensity-modulated* sensing modes are examples of ―intrinsic" properties of fiber optics—responses characterized by changes in the optical fibers themselves (Casas and Cruz 2003) and consequently the intensity, frequency, polarization, or phase of the signal (Merzbacher et al. 1996). This is the most common application of fiber optics to SHM, as the ―extrinsic" case involves the use of fiber optics merely to convey an externally-generated signal (i.e. a signal from a computer or another sensor). Succinctly, extrinsic properties are those exploited by an independent sensor or computer while intrinsic properties are exploited when fiber optics serve as the sensor(s) themselves.

Fiber optics, particularly fiber Bragg grating (FBG) sensors, are also used as *spectrometric* sensors, which obtain absolute measurements of frequency changes in the optical signal in order to assess mechanical or thermal strain of the fiber. FBGs are manufactured fiber-optic cables that have the property of reflecting a finite wavelength band and passing all others. As the spectral width in reflected wavelength of the FBG is typically much smaller than the band of white light used in fiber optics, multiple Bragg gratings can be installed on the same fiber—a technique called *multiplexing* which allows the profiling of multiple parameters throughout a structure in real time on the same length of fiber cable (Chang and Liu 2003). Fiber-optic sensors without multiplexing are said to be *distributed* if they report conditions averaged along their entire length (i.e. if external forces along their length affect the signal) or *localized* if they report conditions only at a specific segment in the fiber (Lau 2003).

The advantages of absolute rather than relative measurement, wavelength-encoding, and an increased life span without calibration make spectrometric sensing preferable to intensity-modulated sensing. FBGs are sensitive to temperature and strain, however, the effects of which must be considered when using them to monitor any other parameters. Even when the desired measurement is strain, the strain of the structural member that is being monitored—both the load and thermal components—must be separated from the change in the optical properties of the fiber.

FBGs have also been used as inclinometers as they offer higher accuracy than other techniques and also possess the capability of multiplexing. In such applications, the temperature-dependence of strain is compensated for by having two distinct FBG sensors, for which dissimilar shifts in wavelength would be indicative of a change in the cable‘s inclination while identical shifts are known to be the product of temperature change (Casas and Cruz 2003) and can be ignored.

A third kind of fiber-optic sensor, *interferometric,* is also useful for monitoring strain and temperature variation. Most interferometers consist of two fiber wires—one acts as a reference wire—so that the signals can be compared. Various kinds of

interferometric fiber-optic sensors have been demonstrated including the common Mach-Zender configuration, the Michelson interferometer (based on the famous Michelson-Morley experiment), and the Fabry-Perot configuration, which unlike the others consists of only one fiber wire manipulated in such a way so as to form two parallel reflectors. Though early interferometric fiber-optic sensors were too slow for dynamic or continuous measuring, later developments enabled their signals to be demodulated at frequencies of up to 1 kHz (Inaudi and Glisic 2004).

Fiber-optic sensors of all kinds (spectrometric, interferometric, and intensity-modulated) can also be used in crack and displacement detection, which is otherwise performed through time-consuming and subjective visual inspection. Interferometric sensors sometimes operate as acoustic sensors—detecting the immediate development of a crack by the air wave it produces, which modulates the phase of the optical signal; this is described most notably by Ansari (2005). Most fiber-optic sensors used for this detection are interrogated with OTDR but the deployment of the sensors varies widely. The most successful application of fiber-optic sensors for crack detection involves embedding the sensors in a ―zigzag" shape. With the knowledge of where kinks in the fiber were placed, comparison of light intensity before a crack occurs and after a crack occurs can yield information about the location of the crack. The disadvantage of this method is that it requires an assumption about the direction of cracks (that will develop) in the structure to ensure that the kinked fiber-optic cables are aligned correctly. Similar success has been achieved in the realm of monitoring existing cracks as they develop and the associated change in load on structural elements (Kuang et al. 2003).

Other applications of fiber-optic sensors have been explored that lie outside the field of SHM but some are directly relevant. FBGs have been used simultaneously as a corrosion transducer and temperature sensor simply by adding a metal coating to one segment of the fiber (Lo and Xiao 1998). Others have reported on using FBGs as accelerometers in a spring-mass system not dissimilar to a seismometer (Krammer et al. 2000). Still other applications include using FBGs as load cells and for traffic monitoring and ice detection on decks (Casas and Cruz 2003) as well as pH-sensitive corrosion detection (Panova et al. 1997) and delamination identification (Ling et al. 2005).

In conclusion, fiber-optic sensors are ideal for the SHM of reinforced concrete because they are stable, either localized or distributed, possess adequate sensitivity and dynamic range, provide linear response, are sensitive to the direction of a measured parameter‘s change, are single-ended (minimal leads), insensitive to electromagnetic disturbance, capable of absolute measurement, nonperturbative to the structure, able to multiplex, easy to mass produce, and match the lifetime of the structure. Among the different types of fiber-optic sensors available, fiber Bragg grating sensors have the most distinct advantages in that they are intrinsic, have a linear response and require no calibration (Merzbacher et al. 1996).

3.5 GPS and Geodetic Measurements

Global positioning systems (GPS) offer an opportunity to make absolute displacement measurements of structures and structural elements in real time using the known positions of Department of Defense (DOD) satellites and the travel time of electromagnetic signals between them and the target. Due to the great distance of these satellites and, consequently, the great path length their signals travel through, GPS has, for much of its history, been unable to provide the necessary resolution for SHM, even after the policy of intentionally degrading the signals (for national security purposes) was lifted (Kijewski-Correa 2005). However, innovative signal processing techniques have enabled civilian users of GPS to obtain the resolution required for multiple applications including SHM.

For instance, although the ionosphere contributes significant time delay to these GPS signals, it does so at a rate proportional to their frequency. Therefore, estimates of this added delay can be made by comparing the arrival times of two signals of different frequencies—standardized as L1 (1.57542 GHz) and L2 (1.22760 GHz)—the latter of which can only be received by GPS units that are dubbed *dual frequency receivers*; others receive only one frequency (L1). Differential GPS (DGPS) further enables the user to correct for local environmental effects such as temperature and humidity by comparing signals of interest to those received at a reference station. The overall accuracy of such corrections is obviously proportional to the baseline separation between the target and the reference (Kijewski-Correa 2005). None of these corrections are able to overcome *multipathing*, however, where GPS signal reflections arrive later than the original signal—a phenomenon similar to ―ghost" images on television screens and the ability to hear one‘s own voice as feedback on a cellular telephone call. The multipath effect can be avoided, however, through the use of a specialized ―choke-ring" antenna that significantly reduces the strength of incoming signals, thereby preventing re-radiation of GPS signals (Huynh and Cheng 2000).

The accuracy attainable with these corrective procedures in place is within a few millimeters in near real-time (Knecht and Manetti 2001). One such system developed for SHM, described by Knecht and Manetti (2001) has as its goal a modular architecture, connectivity via the internet, and ease of installation, configuration and maintenance while the sensors themselves where desired to be of compact size, resistant to adverse environmental conditions, self-powered, and maintenance-free. The system consisted of mobile GPS receivers placed directly on the target object and a couple of reference receivers, identical to those installed directly on the target, which were placed at nearby locations, sometimes surveyed. The system demonstrated the capability of wireless link via radio or cellular modem. Solar panels and intelligent power-supply management of batteries provided the autonomous power required. All units communicated with a base station responsible for both data collection and processing and which also enabled remote

access and configuration via a web browser. Ultimately, decisions and alerts based on measured positions and displacements were automated by the base station.

Meng et al. (2007) demonstrated a technique for measuring bridge deflection and peak dynamic character by combining a GPS antenna and a triaxial accelerometer. The accelerometer was driven by time pulses from the GPS antenna at a rate of 1 Hz in order to synchronize its measurements with that of the GPS unit. A band-pass filter and fast Fourier transform (FFT) were used to precisely determine local, dominant frequencies. These determinations were compared to the predictions of a finite element (FE) model for the Wilford Bridge, a suspension footbridge. For example, they determined that dominant frequency over whole band is 1.732 Hz compared to the FE model‘s prediction of 1.740 Hz, the first natural frequency. They demonstrated an ability to extract structural modal parameters such as natural frequencies, mode shapes, and damping ratios from the GPS and accelerometer measurements of ambient vibrations.

3.6 Magnetic and Magneto-Elastic

The magnetic flux leakage (MFL) technique is used for the detection of flaws in small-diameter bridge hanger cables. This technique requires that the target under inspection be placed in or subjected to a homogeneous magnetic induction field in which the main axis of the field is along the cable‘s length. Any flaw such as a broken wire in the cable will be manifested as a perturbation of the magnetic field—or what is termed a *magnetic flux leakage*. The intensity of this leakage is determined by the size and position of the flaw. MFL requires an in-situ sensor system that travels along the length of the cable and requires anywhere from 10-20 minutes per cable to an entire day per cable. This technique is far from favorable due to the time required for completion, the heavy amount of preparation of cable surfaces, and the bulk and cost of equipment (Mehrabi 2006).

Elasto-magnetic technology is an innovative approach to measuring the strain within bridge cables. The technique is based on the magnetic properties of ferromagnetic materials. The conventional picture of these materials in the demagnetized state is that they are made up of a myriad of magnetic ―domains” each magnetized to saturation but possessing a random magnetization vector. The superposition of all of these random magnetization vectors results in a net magnetization of zero. In most scenarios, it is the application of an external magnetic field that changes the configuration of these domains by the movement of domain walls. However, mechanical stresses are also capable of moving domain walls and thereby stimulating the intrinsic magnetic field. By exploiting this relationship, the stresses that ferromagnetic materials are subjected to can be measured. An elasto-magnetic sensor, as proposed by Sumitro et al. (2002), consists of a hollow cylinder through which a steel (or other ferromagnetic material) structural element passes through. Ideally, this sensor should be installed during the construction.

The sensor itself contains primary, secondary, and compensating coils sealed with an insulating material. The life of this sensor is estimated to be no less than 50 years; it is weather-resistant and mechanically decoupled from the structural element.

The magnetic properties of steel are sensitive to temperature variations (on the order of 0.01 Wb/C), and careful correction for temperature changes is required while correlating magnetic field measurements to stress variations and corrosion in steel elements. Singh et al. (2004) attempted to detect corrosion of steel members by measuring the voltage induced in a conducting coil. Corrosion can be inferred from a change in cross-sectional area which is equal to the rate of change of magnetic flux. The rate of change of magnetic flux, in turn, is responsible for voltage induction in the coil. They calibrated their observations by varying the temperature of a sample through resistive heating and measuring magnetic flux every 5°C increase. The experimental setup was used for steel bars with varying mass% loss due to corrosion. They demonstrated how field measurements of steel elements can be compared to identical, non-corroded reference steel in order to quantify the amount of corrosion present.

Another magnetic technique applied to SHM is the use of a Superconducting Quantum Interference Device (SQUID). A SQUID is a highly sensitive magnetic flux-to-voltage transducer—it senses minute changes in magnetic flux and reports them by voltage changes. Advantages of SQUID as a measurement system include its high sensitivity (~10-100 fT $Hz^{-1/2}$), wide bandwidth, and broad dynamic range (>80 dB). In addition, as SQUIDs function at zero frequency they are able to achieve greater depth penetration than eddy-current sensors, as capable of detecting and monitoring the flow of steady-state corrosion currents, and can image static magnetization of paramagnetic materials (Jenks et al. 1997).

SQUIDs achieve their high sensitivity by utilizing superconducting materials. These materials, when cooled below a certain critical temperature T_C, exhibit zero resistance—hence, they are ~~"s~~uper-conducting" in that they allow current to persist indefinitely within them without any external power supply. SQUIDs are classified by the material that makes up their superconducting element, and these fall into two classes: superconductors with a high T_C and those with a low T_C. Both are used in SQUIDs but high-TC superconductors are favored because it is less difficult to reach their critical temperature. The cooling of high-T_C materials is often accomplished with liquid nitrogen, which is commonly available, easy to handle, and cheap compared to liquid helium—the staple for low-T_C superconductors. However, the best signal-to-noise ratio for SQUIDs is achieved with low-T_C superconductors, and they currently dominate the practice (Jenks et al. 1997).

Another curious property of superconducting materials is that they expel any internal magnetic fields—a phenomenon known as the Meissner effect—which means superconductors possess no internal magnetic fields. When superconductors are shaped

into a loop or are embedded so as to surround non-superconducting materials, however, they demonstrate yet another curious property: the quantization of magnetic flux. In all superconductors, regardless of their constituent materials, supercurrents (electrical currents that arise in superconductors) are arranged at the material boundaries in a way so that the induced magnetic flux is a multiple of the flux quantum. Furthermore, these supercurrents oppose any change in flux that may be applied to the superconducting loop.

The quantization of magnetic flux is what enables the SQUID to operate. As the supercurrents oppose any change in magnetic flux, such a change would be marked by a change in current flow across the superconductor. This results in a phase change, which can be detected in a Josephson junction—a pair of superconductors weakly connected across a junction of insulating material. SQUIDs are capable of making sensitive measurements of magnetic flux because they consist of one or two Josephson junctions.

In all SHM applications of SQUID, measurement begins with the imaging of the magnetic field distribution in the vicinity of the target. This is done either by monitoring intrinsic currents (e.g. galvanic currents in a corroded specimen) or external sources. The latter technique requires direct contact with the target when electrical excitation is used, however, excitation can be achieved without contact if a strong magnetic field is applied. Jenks et al. (1997) postulate that damage or failure prediction in steel elements may be possible with SQUIDs. They cite studies in which SQUIDs have been used for the detection of flaws in steel plates where a magnetic field was induced by a superconducting solenoid. Such a study found that machined voids as small as 2 by 1 mm^2 could be detected at a stand-off distance of 4.2 cm. They cite a more realistic study by Cochran et al. (1993) in which fatigue cracks in 12.5 mm-thick steel plates were identified. Krause et al. (2002) used four SQUIDs in conjunction with four Hall probes and four magnetoresistive sensors to detect breaks in reinforcing steel of a concrete bridge and were able to locate such defects to within ±5 cm. Applications of this technology for composite materials are described in Section 6.1 Fiber-Reinforced Polymer Composites.

3.7 Ultrasonic Emissions and Lamb Waves

Ultrasonic acoustic emission monitoring (ultrasonic AEM) is one of the most commonly used inspection techniques for steel structures. As with electromechanical impedance monitoring (described in Section 3.3 Electromechanical Impedance), an acoustic signal is induced in the structure from which reflections are interpreted in the search for defects (Chang and Liu 2003). More specific information about impedance monitoring can be found in Section 3.3 Electromechanical Impedance. The principle is the same in traditional SHM techniques like chain dragging and the tap test. Aside from the oft-

mentioned subjectivity of these traditional techniques, they are also limited to audible frequencies.

The distinct advantage of ultrasonic waves (generally, frequencies higher than 30 kHz) is due to the acoustoelastic effect, in which stress causes a change in ultrasonic wave velocity (ultrasonic pulse velocity or UPV). UPV techniques are affected by the inherent properties of the concrete, however, in addition to internal stresses; considerable computation time to address this complexity is required for most applications. Other modes of analysis, such as ultrasonic wave attenuation, are known to be indicators of microstructural features of interest, but there is a lack of consensus as to how the parameters should be measured.

In concrete, the impact-echo method has been employed with success in flaw detection. The method is based on the study of reflected stress waves that change in frequency character when transmitted through flawed material. It has been demonstrated to be effective in the detection of delamination, voids, and honeycombing (Chang and Liu 2003). At the forefront of AEM techniques are non-contact methods employing directional microphones, however, this method of noise reduction is ineffective at high noise levels or in complex sound fields (Zhang et al. 2010). The ambient noise that plagues acoustic evaluation is commonly encountered in the field where these techniques are applied on busy roads or highways.

Zhang et al. (2010) attempted to improve upon the problems that exist with AEM. They sought to address ambient noise by applying a modified independent component analysis (ICA) technique used to separate sounding (impact) signals from noisy recordings. They also eliminated subjectivity through the use of mel-frequency cepstral coefficients (MFCCs) for automatic detection—MFCCs are often used in acoustic signal processing for other applications. They were able to demonstrate high detection accuracy using MFCCs and a mutual information maximization algorithm. Though the performance decreased with increasing noise, they managed to compensate and improve detection at high noise levels with the modified ICA.

Global acoustic techniques typically involve spectral or time-domain analyses. These allow for feature extraction, frequency determination, and the vibration or displacement of structural elements. These can be determined from three distinct types of spectral analysis: Fourier, wavelet, and Hilbert-Huang transforms (HHT).

Lamb waves are a special case of elastic waves. As with electromechanical impedance techniques they are generated by piezoelectric transducers for the purpose structural health monitoring. Lamb waves are guided elastic waves whose particle motion occurs along the surface of a material in a plane described by the normal to the surface and the direction of propagation. They occur in materials with a uniform thickness on the order of a few wavelengths. They are in fact identical to Rayleigh waves in earthquake seismology—which propagate along the Earth‘s crust—with the exception

that Lamb waves are guided waves. Due to their relatively short wavelengths, they have shown promise in detecting highly localized defects (Crider 2007).

The methods commonly used for Lamb wave detection are *pitch-catch* and *pulse-echo*. The pitch-catch method uses two transducers—one for excitation and the other to receive signals—where damage is interpreted from the change in response. This is a global method where an insufficient number of transducer pairs are used, but can be deployed so as to locate damage specifically. The pulse-echo method uses only one transducer which acts both as source and receiver. The single transducer detects returns (echoes) from which the location of material defects can be inferred from the travel-time and the severity of damage from the amplitude of the reflection.

4.0 On-Site Monitoring Techniques

4.1 Eddy Currents

Eddy detection is conducted by the use of a probe coil—which may have either an empty, air core or a magnetic ferrite core—that induces electromagnetic currents in conducting materials. These currents nominally radiate from the coil in circular patterns (eddies). In the presence of a flaw in the material, however, these current patterns are disturbed at the site of the flaw, such as a crack. Although widely used in the inspection of surface and subsurface cracks as described, this technique requires the use of a differential probe when applied to weld metal due to the wide variation in magnetic material properties. The technique remains effective even when applied to surfaces with nonconductive coatings such as zinc-based primers and lead paint (Chang and Liu 2003).

The meandering winding magnetometer (MWM) is a special type of eddy current sensor that features a meandering primary coil for induction and numerous fully parallel, secondary coils for sensing. They are typically deployed in scanning arrays but are also used for a wide variety of applications in permanently-mounted arrays. MWM arrays are particularly well-suited for fatigue monitoring. In such an array, a drive winding, made up of linear drive segments, is stimulated by a current at anywhere from 1 kHz to 40 MHz to produce a time-varying magnetic field capable of inducing eddy currents in the pattern of the drive winding. MWM arrays achieve high resolution, usually down to 1 mm by 1 mm surface areas, with the use of numerous, tiny sensing coils (Zilberstein et al. 2003). Usually, these are adhered to a substrate allowing for the production of thin and flexible _chips‘ that serve as sensors. Their size and flexibility allows them to be permanently attached to or embedded in the element to be monitored under real load conditions. Micromachining enables the production of these chips so they are cheap and identical to one another.

Zilbertstein et al. (2003) describe the processing of MWM array data by inversion of the measurement grid, which converts sensor impedance magnitude and phase response into material properties such as electrical conductivity or magnetic permeability. They ran several cyclic loading tests on plain shot-peened plates and combination shot-peened-cadmium plates, letting some of the fatigue tests run to failure while others were terminated according to when the MWM array measurements of magnetic permeability indicated the onset of failure. Fatigue and cracks were identified using scanning electron microscopy (SEM). They surmised that gradual increases in magnetic permeability corresponded with fatigue damage prior to the formation of cracks that are much shorter than the grain size. They were able to detect the formation of cracks on the order of 250 μm or less in length. This capability has been previously demonstrated for aluminum alloys.

4.2 Electrical Time-Domain Reflectometry (TDR)

Bridge scour is a potentially devastating condition in which the adjacent and underlying sediments of bridge piers and abutments are removed due to erosion and related stream processes. The current method of predicting or assessing bridge scour relies on empirical scour prediction equations that have been generated from laboratory data. These equations generally do not adequately predict actual scour in the field, however (Yu and Yu 2009). Some field monitoring techniques have been developed from the use of a simple yardstick to more advanced methods such as ground-penetrating radar (GPR) and ultrasonic techniques. These methods do not allow for real-time monitoring, however, nor are they sufficiently rugged or automated.

Yu and Yu (2009) propose time-domain reflectometry (TDR) as an improvement over the current methods of predicting bridge scour. TDR has been used in other studies to the same end but the technique employed by Yu and Yu (2009) improves upon all of these earlier attempts and is capable of predicting scour depth, the density of sediment materials, and the electrical conductivity of river water.

TDR was first used by electrical engineers to locate discontinuities in electrical power and communication lines. It also provides a way of measuring the dielectric and electrical properties of materials. Specialized TDR devices that serve as pulse generator and sampler are used to send a fast-rising step pulse or impulse to the sensor probe. The TDR device measures the reflections due to either the change of system geometry or material dielectric permittivity. TDR is effective at discerning the sediment geometry and diagnosing bridge scour because of the large contrast in dielectric constant between water and air or sediment solids. These contrasts cause large reflections at the interfaces where they exist, such as the air-water boundary and material layers.

A real-time TDR scour-monitoring system consists of TDR probes permanently installed at the base of bridge piers and abutments. From the measurements made with these devices and the automated signal processing developed by Yu and Yu (2009), when scour depth exceeds the bottom of the structural element, a warning can be issued to bridge managers, allowing them to implement appropriate countermeasures to prevent catastrophic failure. There are some potential anomalies that have to be taken into consideration, however. Turbulent flow during storm or flood events, for instance, will affect the scour signal.

4.3 Infrared Thermography and Spectroscopy

Infrared thermography is the detection of electromagnetic waves in the infrared spectrum. More specifically, it is the detection of the strength and location of thermal anomalies and in the context of SHM these anomalies are (ideally) structural defects. This technique is

commonly applied directly to concrete and asphalt decks for the detection of thermal variances that are given by radiation, conduction, and convection (Maser and Roddis 1990). Infrared thermography has found favor in the SHM of transportation infrastructure because it requires shorter inspection time than many other methods which directly results in fewer or shorter traffic lane closures. Infrared thermography differs from infrared spectroscopy in that the spectrum of infrared radiation (the range of frequencies and their respective amplitudes) is only of significance in the latter.

Thermography is commonly used for the detection of concrete or asphalt delaminations, as surfaces with such underlying defects lack contact with bottom material that would otherwise act as a heat sink. Consequently, these delaminated areas will be warmer with respect to adjacent, full-bonded areas. A homogeneous material such as concrete cools quickly when it is warmer than its environment (e.g. after sunset). As it cools, the top surface of the concrete draws heat from lower layers. Defect areas, however, prevent or reduce this heat transfer and, as a result, surface areas above them cool more rapidly than surrounding areas. Conversely, when concrete is cooler than its environment, these surface areas warm at a slower rate than their surroundings (Howard et al. 2010). Passive thermography (i.e. the use of solar heating) has been described in the available literature as well as an active technique in which radiative heaters are used to heat (or cool) the target before infrared images are collected; both techniques are usually non-contact techniques (Alqennah 2000). Examples of radiation sources (and sinks) are hot air guns, quartz lamps, xenon flash lamps, hot (or cold) water, vortex tubes, and liquid nitrogen (Burleigh and Bohner 1999). As environmental conditions such as insolation (input solar radiation) and air temperature vary throughout the day, the thermal behavior of a concrete deck also fluctuates diurnally and thus requires compensation for these external factors.

A more complete list of factors influencing the thermal emission of a concrete deck includes: the deck‘s characteristic emissivity, deck surface temperature, ambient air temperature, deck thermal conductivity, deck volumetric heat, the thickness of the heated layer, solar radiation intensity, and air velocity (Maser and Roddis 1990). Thus, a simplified model of the physical system can be very useful for interpreting deck conditions. Maser and Roddis (1990) propose a model driven by an insolation function and ambient temperature. Between the concrete deck and the air temperature, some heat flux terms are linear (conduction) while others are non-linear (convection and radiation). For simplicity, they combine all three heat fluxes using the concept of a heat transfer coefficient. This linear approximation is valid to within ±5% for most cases. Their model included such physical approximations as modeling delamination by an air-filled crack, and this agreed with ground-truth data. Changes in the dimensions of this crack had a corresponding effect on the temperature difference observed. A much smaller difference in temperature between the solid deck and a water-filled crack was observed,

as the thermal conductivity of water is not substantially lower than that of concrete. In a similar study using this model, Maser and Roddis (1990) identified certain conditions (e.g. thick asphalt, small delamination width) under which the thermal anomalies are too small to detect. Alqennah (2000) reports that the method is insensitive to delaminations at deeper than half the thickness of the deck. This is consistent with the findings of another report by Howard et al. (2010).

During loading, a concrete deck may exhibit several thermo-mechanical effects—responses of a material‘s thermal properties to mechanical loading. Thermo-elasticity, heat dissipation by reversible anelastic dampening or by irreversible plastic deformation, and surface friction are all factors in temperature change during cyclical loading. Meyendorf et al. (2002) investigated the thermo-mechanical effects of loading and their applications to fatigue characterization. They measured the aforementioned thermo-mechanical effects as a function of accumulated fatigue cycles during interrupted fatigue tests conducted on cylindrical dog-bone specimens of machined titanium with 6% aluminum and 4% vanadium by weight. Thermal excitation was achieved, following fatigue loading, by high-frequency ultrasonic waves and low-frequency mechanical loading, alternately. They demonstrated that the temperature change per cycle ($\Delta\tau_{diss}$) is exceptionally sensitive to fatigue damage in its early stages. They also concluded that microstructural variations caused by fatigue could be identified by determining the dissipated heat per loading cycle.

Detection and quantification of chloride intrusion is one of the more difficult challenges for NDE as it is manifests as a regional, chemical property of the affected concrete structure. Infrared spectroscopy, however, has been used with success to identify chloride intrusion and evaluate chloride content (Kanada et al.). Such an application takes advantage of the fact that absorbance of thermal radiation increases with chloride content at a peak wavelength of 2266 nm. Kanada et al. found a correlation between difference spectra and chloride content as high as R^2=0.99. In their experiment, controls consisting of concrete cores with various, known chloride content were used to calibrate a field detection scheme. In a separate experiment, they extended this technique to the detection of carbonation and sulfate attack.

Alqennah (2000) reports on multiple thermography techniques that have been employed by others. (Winfree 1998) found that tailoring the shape of radiative heating can improve the sensitivity in detecting deep delaminations. Thermal inertia mapping is a thermography technique that measures the resistance of a material to temperature change, which is achieved by determining the inverse slope of the surface temperature versus the inverse square root of time. This technique was employed by (DelGrande and Durbin 1999) to detect delamination in reinforced concrete structures, and has also been successfully used to detect airframe material loss due to corrosion. They demonstrated

that the technique can determine the fractional area of delamination and can be applied to ―cluttered" (debris-strewn) concrete decks if a flash-heated stationary system is used.

Alqennah (2000) writes that while thermography has been useful in the detection of concrete deck conditions it has not yet been applied successfully to structures of composite materials. However, that account predates the reports of others who have used it to successfully detect damage in FRP composite structures (Bates et al. 2000; Hu et al. 2002; Meola et al. 2004; Halabe et al. 2005). For more information on such studies, consult Rao (2007) or Section 6.1 Fiber-Reinforced Polymer Composites in this paper.

Howard et al. (2010) describe the development of a commercial infrared imaging system for detecting concrete bridge deck delaminations. *BridgeGuard* rapidly evaluates deck conditions at typical driving speeds, immediately analyzing and storing the data within a data management system for future reference. The authors report that there are two ideal ‗windows' for infrared imaging, one beginning a few hours after sunset and the other beginning a few hours after sunrise. At these times, when skies are clear, the thermal properties of concrete can be exploited for maximum efficacy. In their initial report they found that 1600 hours offered maximum solar contrast while 0300 hours offered maximum non-solar contrast.

4.4 Laser Scanning

Terrestrial laser scanning (TLS) refers to the practice of illuminating target objects and structures with a ground-based (hence ‗terrestrial') laser. Airborne laser scanning (ALS) refers to the same when it is conducted by an airborne platform. Both are methods of light detection and ranging (LiDAR) and are used for the purpose of either detection and ranging or measurement of displacement and velocity. The common method of achieving the latter objective is through interferometry. Both TLS and ALS are discussed here.

The advantages of TLS lie in its ability to reach structures of any size or any structural members, the lack of dependence on natural light sources or supplementary illumination of the target, and that no wiring or in-situ sensors are required to be installed or maintained. As with ALS, the principle of 3D coordinate extraction is based on the travel-time of a pulse of light transmitted between instrument and a point on the structure or structural member of interest. By combining this information with the laser's rotation angle (both vertical and horizontal), coordinates are obtained without the need of any computational post-processing—they are obtained as absolute measurements from the emission of 10^2-10^6 laser pulses (Park et al. 2007).

Another boast of TLS and other laser scanning techniques is that they provide coordinate information in terms of the absolute position of the target (rather than relative deflections). Achieving this is not so straightforward, however. It requires the

transformation from the TLS coordinate system into the structural coordinate system by calculating *base vectors* which represent the distance to the target.

Commonly, laser scanning systems in SHM are used for the detection of shape changes or displacements. (Liu et al. 2010) have demonstrated that laser scanning is also capable of clearance detection, bridge load testing, and construction monitoring. In order to determine displacements or shape distortions of structural members with TLS, it is necessary to scan the target multiple times, ideally once before the structure is loaded or stressed and then at least once afterwards. In this fashion, the differences between the scans correspond to deformations or displacements of the structure. As with other innovative techniques for obtaining these measurements, results have been compared to those of established detection methods such as the use of linear variable displacement transducers (LVDTs) or accelerometers.

LiDAR usually refers to ALS exclusively rather than to both terrestrial and airborne methods. It is a popular technique in the fields of GIS and remote sensing as it allows three-dimensional location information of an entire object. Since its inception it has been used in these fields primarily to acquire topographic information, particular in the production of digital terrain models. When applied to SHM, LiDAR allows the measurement of displacement in three dimensions as well as shape deformation of specific structural elements. As a ―stand-off" method of monitoring, LiDAR has the advantage of not requiring any sensors, wiring, or supplementary illumination.

LiDAR operates in a similar fashion to radar, hence the similarity in the naming convention. LiDAR is more straightforward and enjoys more simplicity, however, in that the principle of three-dimensional coordinate extraction using LiDAR is based solely on travel time between the source of the laser pulse and the target object. High accuracy requires that the laser source be closer to the target object than other remote sensing modules (such as radar satellites), however. In general, for all laser scanning the source should not be farther than 350 m from a target with minimum reflectivity of 4% (Park et al. 2007). One study cites horizontal and vertical position errors of about 10 mm with distance errors of no more than 7 mm at a distance of 100 m from the target object (Lee et al. 2005). Errors were further reduced in this study by the application of the least squares method following coordinate transformation. Rice et al. (2010) report accuracy within 1 mm at a maximum range of 200 ft.

One important objective of LiDAR, be it terrestrial or airborne, is to determine the dynamic character of a structure. As such, ambient vibration methods have been investigated as a means of quantifying the elastic properties of buildings and evaluating the performance of structural retrofits. Although most ambient vibration surveys are conducted with accelerometers or velocimeters, Gueguen et al. (2009) argues that there is much to be gained from performing these surveys remotely (with LiDAR). They cite the ease in performing the survey without applying instruments directly to the structure and

the increased safety of assessing ambient vibrations remotely in the case of seismological hazards, particularly when aftershocks are expected. In their paper, they describe an experiment that compares the ambient vibration measurements of conventional, in-situ sensors with that of coherent LiDAR.

Coherent LiDAR exploits the Doppler effect to make precise measurements of micrometric vibrations over great distances. When illuminating a moving target with a laser source, the backscattered signal is shifted in frequency proportional to the difference in velocity between the target and the LiDAR platform. If the vibration of the LiDAR platform is separated out, the motion of the target can be effectively quantified. For simplicity, Gueguen et al. (2009) performed their experiment with the LiDAR platform inside the subject building with the instrument pointed at the ground. This way, the illuminated target was known to be stationary as opposed to if the building was illuminated from the ground. It is valid to assume that the same measurements will be obtained provided that there is no structural variability during the normal period. After comparing the LiDAR measurements to those of the in-situ velocimeter, they concluded that although the signal-to-noise ratio was lower for LiDAR, the techniques compared very well.

4.5 Nuclear Magnetic Resonance (NMR) Imaging

Nuclear magnetic resonance (NMR) is a phenomenon in which certain atomic nuclei in static magnetic fields, when exposed to oscillating electromagnetic (EM) radiation, absorb and re-radiate the energy at specific resonance frequencies. It is commonly applied in magnetic resonance imaging (MRI) to generate detailed images of biological tissues. The human body is composed mostly of water molecules and this is why MRI is such a successful investigative technique. Sensitivity to water is exactly why the technique has been adopted in SHM as well, though with some modifications.

Hydration is a key concern in concrete durability and tensile strength. Chloride ingress and corrosion of steel reinforcement are obvious consequences, however, there is also a danger of explosive spalling during fire with high moisture content. The inverse relationship between tensile strength and the water-to-cement ratio of concrete is well established. Compressive strength, too, is adversely affected by high water content (Li 2004). Porous concrete in northern climates is especially vulnerable to frost-wedging and other freeze-thaw degradation as water alternately freezes (and expands) or thaws (and contracts). Water content of cement paste is also a concern as concrete strength deteriorates due to the contraction associated with freeze-thaw events and other volumetric changes that exert pressure on pore walls. Excessive drying will also lead to shrinkage and subsequent cracking due to stress at the aggregate-paste interfaces. It has

been reported that moist curing followed by drying to a moisture content of less than 90% relative humidity boosts concrete‘s freeze-thaw resistance (Beyea et al. 1998).

The relaxation rate (how fast the nucleus‘ magnetic vector aligns with the main magnetic field initially or following tilt by radio-frequency pulse) of hydrogen atoms is often measured in NMR experiments, as it is strongly dependent on their mobility. This allows scientists to distinguish between frozen and non-frozen water, as one example. The spatial distribution of moisture content in concrete is determined by drying mechanisms, capillary flow, and molecular diffusion (provided the concrete is exposed to air). Careful application of MRI has allowed for the quantification of non-frozen water distribution in concrete samples. It has also been demonstrated that this technique could be applied under a variety of real weather conditions (Prado et al. 1997). It should be mentioned as a distinction from other SHM techniques described in this paper that NMR as described in the literature today is actually a destructive technique that admits only small samples taken from existing structures.

After hydrogen ^{1}H (because of its presence in water molecules), the most important nuclei for cement and concrete research are carbon ^{13}C, aluminum ^{27}Al, and silicon ^{29}Si. Carbon ^{13}C is found only in small quantities in cement as it is often applied only as an additive. Its use in NMR is primarily centered on its ability to distinguish between plasticizers, which may be an indication of what deterioration the concrete has experienced. Aluminum ^{27}Al may also be useful for identifying the presence of fly ash and zeolites. Zeolites are also indicated by the presence of silicon ^{29}Si, from which information about silicate hydration can also be derived. In short, NMR may be useful in SHM for studying clinker composition, the hydration kinetics of cement minerals, the influence of admixtures, the reactivity of pozzolanic materials, binder structure and degredation, frost mechanism, cement-polymer interaction, and for macro-pore imaging (Justnes et al. 1990).

Both Beyea et al. (1998) and Prado et al. (1997) describe the use of single-point imaging (SPI)—a technique that uses phase encoding instead of frequency encoding in order to spatially image a sample. SPI improves upon MRI in concrete applications because the relaxation rate of water in concrete is typically much too small. SPI is effective because the relaxation time for water is known to decrease with concrete pore size. The technique has been reported to achieve sub-millimeter accuracy with an excellent signal-to-noise ratio. It has been used in drying experiments, to provide on-demand imaging of lightweight concrete, to study the freeze-thaw and salt ingress processes, and even for high-resolution, 3D imaging of water distribution in both porous and non-porous aggregates.

4.6 Microwave Radar

Radio detection and ranging (RADAR, but now almost exclusively ~~"ra~~dar") is a well-established technique for measuring the range (distance to), altitude, direction, and speed of moving or stationary objects. This is achieved through the illumination and, commonly, the reflection off of an object with electromagnetic (EM) waves. Reflected EM waves are detected at the transmitter, making it both source and receiver. Otherwise, separate transmitting and receiving probes are used in *through-transmission* techniques. In most civil engineering applications, the reflective technique is used as it requires only one surface be accessible (Bungey 2004). Microwave, millimeter, and radio wave inspection techniques typically operate at frequencies ranging from 300 MHz to 300 GHz in dielectric (electrically insulating) materials (Chang and Liu 2003). In order to achieve 3D displacement measurements, radar measurements from independent directions must be made, as radar can only measure displacement in the range direction, parallel to transmission (Pieraccini et al. 2004). In the case of a fixed-position radar antenna, multiple targets at the same distance from the receiver (in the same *range resolution cell*) cannot be distinguished and are marked by one reflection for that *range bin.* Many of the principles discussed in this section hold true for all radar applications. In this paper, ground-penetrating radar (GPR) is discussed in Section 4.7 Ground-Penetrating Radar (GPR) while interferometric synthetic aperture radar (IfSAR) is discussed in Section 5.3 Interferometric Synthetic Aperture Radar (IfSAR).

Microwave and millimeter radar techniques first gained popularity in SHM because they offered more compact and less expensive equipment than GPR methods. Microwave radar is seen as a most promising SHM technique as it is able to penetrate deep inside concrete, attenuates much less due to scattering than acoustic methods, and offers excellent contrast between concrete and metal reinforcements. For concrete structures, the free-space reflection and transmission properties are a product of the material's behavior on the macroscopic level. Thus, they vary with the material's internal condition and superficial or deep elements of interest such as defects, reinforcement, moisture, and void spaces (Arunachalam et al. 2006).

There are many different techniques of operation for microwave radar in the near-field including diffraction tomography and open-ended waveguide measurements. These techniques require either direct contact or close-proximity to the target—generally much less than the transmission signal's wavelength—and, consequently, require some surface preparation or antenna positioning to avoid diffraction effects. The advantage of near-field techniques despite the rigors imposed by such requirements is their high sensitivity. Far-field techniques do not require such considerations and allow for a plane-wave assumption, which simplifies numerical models (Arunachalam et al. 2006).

Many microwave radar systems make use of a continuous-wave step-frequency (CW-SF) transceiver which emits continuous waves which step through discrete frequency values. CW-SF operation allows for the generation of deformation maps and the imaging of static displacements (Pieraccini et al. 2004). The use of CW-SF techniques imposes an upper limit on the range in which unambiguous range measurements can be made in accordance with the Nyquist-Shannon sampling theorem. Most development in this area has focused either on specific applications of CW-SF or making CW-SF systems respond fast enough for dynamic monitoring. In many radar applications, neural networks have great potential to automate the interpretation of results but, recently, success has been limited to simple cases such as the location of reinforcing bar (Bungey 2004).

4.7 Ground-Penetrating Radar (GPR)

GPR is the most commonly used radar technique in structural health monitoring. The technique is based on the emission of a very short time-duration (<1-20 ns) EM pulse in the frequency band of 10 MHz to 2.5 GHz; typically, no less than 500 MHz is used for practical applications. Antennae with a center frequency of a few hundred MHz or higher provide sufficiently high resolution detail of the shallow subsurface. However, as the Earth acts like a low-pass filter, these high-frequency antennae cannot penetrate farther than about 3 m depth. Penetration depth is achieved when the radar amplitude has been attenuated by a factor of e^{-1} though such a depth varies with attenuation factor and changes in the medium‘s electromagnetic properties. For deeper investigations, antennae with center frequencies below 100 MHz are used, though this sacrifices vertical resolution. 1 GHz antennae are well-suited for SHM goals such as crack detection, thickness estimation, and moisture detection (Arias et al. 2007).

Unlike other pulse radar systems that generate radio pulses at single, discrete frequencies, GPR operates in an ―ultra-wide band” where radio energy is transmitted over a wide frequency band. In GPR, the EM signal is emitted continuously or in discrete repetitions as the antenna passes over the ground. These pulses are reflected by changes in the medium‘s magnetic permittivity, electrical conductivity, and dielectric permittivity. The receiving unit records reflected signals as changes in voltage as a function of time, thereby generating an image of the shallow subsurface (Arias et al. 2007). This 2-dimensional image is referred to as a *radargram* and consists of one axis corresponding to antennae displacement and the other corresponding to the two-way travel time of the pulse emitted. Just as in seismic surveys, the y-axis corresponding to travel time is a proxy for depth and the two are related by the velocity of the medium. This graphic display of radar data is the most common preparation for interpretation as it presents a cross-section of subsurface structure.

GPR surveys are conducted with either *air-coupled* or *ground-coupled* antennae. Air-coupled antennae are typically suspended at about 25 cm above the target surface which allows them to be safely operated at highway speeds when mounted to the back of a survey vehicle (Morey 1998). Air-coupled antennae have been employed successfully for rapid bridge monitoring. The technique has reportedly been used to survey 134 bridge decks in 32 days without any lane closures or traffic interference (Maser and Bernhardt 2000). Ground-coupled antennae cannot be used in such a survey since they require direct contact with the ground. The advantage of ground-coupled surveys, however, lies in their improved depth penetration. Both ground-coupled and air-coupled GPR surveys can be conducted on either bare concrete decks or concrete decks with an asphalt overlay.

The spatial (plan) resolution of GPR is determined by the antenna frequency, achieved depth, and the electromagnetic properties of the medium. Sensitivity studies have shown that the horizontal resolution of GPR can be as fine as 3-4 cm in a high-velocity medium such as saturated concrete (Perez-Gracia 2008). When there is only small spacing between anomalies, it can be difficult to discern buried objects from one another due to interference effects, which become significant at a spacing of less than 10 cm in lower-velocity media. However, even at a separation of 3 cm, the shape of the anomaly is usually enough indication that the source may in fact be two distinct objects. Effects of interference can be minimized through the use of Kirchhoff migration but this may not result in a corresponding increase in spatial resolution. Spatial resolution is maximized when the antennae are placed directly over and close to the investigative surface (Van der Kruk 2003).

Sometimes, multiple GPR reflections can lead to false indications of a boundary or transition. At all times, the strength and polarity of the reflection is determined by the contrast in the dielectric properties of materials at the interface (Bungey 2004). For concrete and asphalt applications, the parameter most strongly affecting the dielectric permittivity is moisture, making it easiest to detect and measure with GPR. Of course, as free moisture in concrete and asphalt is contributed to by the presence of chloride ions, it is also an effective method of monitoring chloride ion distribution. Responses from saturation and chloride ion content are both due to the polarizing effect of an electromagnetic field. Delamination is also consistently distinguished from solid concrete and asphalt (Maser and Roddis 1990). Pavement substructure characteristics such as material type, layer thickness, and variability have been determined with specialized signal processing of GPR data (Brooks et al. 2007). In such applications, GPR is a well-established technique; by the end of the last millennium, over 260 papers, patents, and standards had been published on the subject (Olhoeft and Smith 2000).

Pavement thickness is easily determined by measuring the time difference between layer reflections if the propagation velocity within these layers is known or can also be measured. Depth and spacing of dowels in jointed concrete as well as iron bars in

reinforced concrete can be determined with radar tomography—one of the products of GPR. Scour refill in and around bridge supports and abutments can also be detected and its thickness quantified using GPR (Haeni et al. 1992). GPR has also been demonstrated as capable of detecting air- and water-filled voids with a threshold as small as 3 mm (Morey 1998).

In decreasing order of measurement reliability, the following is a list of some applications of GPR for structural concrete: thickness estimation from one surface, the location of reinforcing bars or other metallic objects, estimation of the depth of buried objects, location of moisture variations, location of voids, the dimensions of such voids, location of honeycombing or cracking, and an estimation of the size of reinforcing bars. Advantages of GPR are that it can rapidly and effectively investigate a large swath of one surface, it requires no coupling medium, it is continuous, results have a high potential to be improved through signal processing, and there are no special safety precautions required. Disadvantages include the requirement of highly specialized equipment, the need for calibration or _ground truth‘ corroboration, the expense of equipment and signal processing, and the inability to penetrate metal features (Bungey 2004).

In a 1998 questionnaire, the Transportation Research Board (TRB) surveyed the use and familiarity with GPR of every state and territorial transportation agency in the U.S. and all of the Canadian transportation agencies. From 51 responses, the TRB found that 33 agencies reported having some experience with GPR; 18 had no experience whatsoever with GPR. The most common applications of GPR employed by these agencies were pavement layer thickness (24 agencies), void detection (22 agencies), and bridge deck delamination (16 agencies). These agencies reported having been very successful in employing GPR for pavement layer thickness evaluation but reported less success using GPR in other applications (Morey 1998).

4.8 X-Ray, Gamma Ray, and Neutron Radiography

All radiographic techniques involve the use of a radiographic energy source on one side of an object and a sensitive film or other recording medium on the other side. Just as in medical or dental X-rays, the amount of radiation that impinges on the recording medium is determined by the density of the material it passes through. The result is a two-dimensional image of density variation within the structure, and while this technique has proved valuable in laboratories, it is not as viable for field use because the equipment is quite heavy and its power consumption large.

These devices commonly use either X-rays or gamma rays as the source and the techniques employed include measuring photoelectric absorption, Compton scattering of reflected gamma rays, and computational tomography (CT). CT requires the reposition

of the radiographic source at multiple orientations so that a computer can construct a 3D image of the target (Chang and Liu 2003).

Alternatively, X-ray fluorescence is a technique in which source and detector are on the same side of a target surface. The principle of X-ray fluorescence is exploited in many chemical analysis applications and in SHM it is no different. A primary X-ray is emitted at a certain, ionizing energy level—usually it is specifically chosen based on the chemical(s) under investigation. The primary X-ray has the effect of ionizing atoms in the target material. Under ionizing radiation, an atom‘s constituent electron(s) may be knocked out of orbit by the impinging photon (X-ray) or may be excited to a higher energy state. In either case, following removal of this electron by an energetic photon, another electron with a higher energy level drops down to fill its place. The difference in energy between the energy level of the electron ―hole” being filled and the energy level that the filling electron left is released as a fluorescent photon (X-ray). There are only a few ways in which this transition can take place depending on which outer shell gives an electron to fill the hole and each scenario results in the emission of a different (secondary) characteristic X-ray. Also, because each element has a unique set of energy levels there are different suites of characteristic X-rays for different elements. In addition, the intensity of these characteristic X-rays is directly proportional to the quantity of atoms in the sample.

Kanada et al. demonstrated this technique as a means of quantifying chloride content in concrete. They selected palladium (Pd) as the X-ray emission source because its Lα X-ray (2.838 keV) is highly effective at exciting chlorine atoms. They determined through trial and error that measurement should be done at low voltages to maximize the peak-background ratio and that X-ray filters (to reduce the background) could be discarded as chlorine is light enough to be excited by such weak X-rays. In their experiment, however, they were in direct contact with the sample and stipulated that this was necessary as X-ray fluorescence is attenuated through the air.

Gamma ray radiography offers a non-contact assessment of a material‘s thermophysical properties. Gamma rays are attenuated according to a material‘s density, just as with X-rays, but they are also attenuated by the presence of moisture in the material‘s pores. The relationship between gamma ray intensity and moisture content for a given material requires knowledge of the gamma ray intensity transmitted by that same material when it is dry. For materials with uniform thickness and porosity, the transmitted intensity of gamma rays is dependent only on the moisture content of the pores (Nizovtsev et al. 2008).

Neutron radiography, like X-ray radiography, is concerned with the variation in attenuation that makes up the object contrast in the resulting image. While in X-ray radiography this attenuation is determined mostly by the target material‘s density, attenuation in neutron radiography depends on the scattering and capturing potentialities

of the constituent elements (Michaloudaki et al. 2005). These differences have consequences for the applications of these techniques. X-ray radiography is favorable for investigating lighter (lower atomic number) elements because in these atoms X-rays interact mostly with the electrons in the atomic shell(s) in ways defined by Compton scattering, the photoelectric effect, and pair production. Neutrons penetrate much deeper than X-rays—interacting with the nucleons of the atom, ignoring electrons completely—and are more favorable for delineating heavier (higher atomic number) elements. There are two important mechanisms (as far as radiography is concerned) of neutron interaction in the atomic nucleus: absorption and scattering. While absorption prevents neutrons from reaching the detector, scattering often leaves a diffuse ~~"sk~~y shine" on the image.

Different elements absorb and scatter neutrons differently with no systematic bias. Consequently, neutron radiography is best used as a complement to X-ray radiography despite the similarities between them (Lehmann et al. 2006). This makes neutron radiography popular in SHM applications such as adhesive inspection and quantification of moisture content. Neutron radiography is used far less frequently than X-ray radiography because there are only a few sites in the world where neutrons can be obtained for such use. Typical sample sizes for neutron radiography range from 1 to 20 cm with spatial resolutions ranging from 10^{-5} to 10^{-3} m per pixel. Practical investigations usually achieve a nominal resolution of 0.1 mm on targets with outer dimensions up to 40 cm. The spatial resolution of neutron radiography is determined both by the detector and the beam width. A well-collimated beam that offers parallel beam geometry is really the only practical option, however, so in practice resolution is truly determined by the detector (Lehmann et al. 2006).

Da Silva et al. (2001) describe the development of a computer-automated means of radiographic pattern recognition, specifically for evaluating welding defects. They describe the following morphologic parameters that are observed in this context: geometric format, length, width, grey level (density) and location in the weld bead. The discriminating factors in classifying welding defect classification are a lack of penetration, undercutting, porosity, and linear and non-linear slag inclusions. By developing a hierarchical, linear classification method that expands upon previous success with non-hierarchical methods by treating those classes easiest to separate first, they were able to achieve 85% success in classification of welding defects.

5.0 Remote Monitoring Techniques

5.1 Electro-Optical Imagery and Photogrammetry

Electro-optical (EO) sensors are those electronic sensors which are sensitive to electromagnetic radiation in the visible spectrum. Charge-coupled devices (CCDs) are the most common electro-optical sensors and this section considers the contribution of even these simple digital camera components to structural health monitoring of bridges. Photogrammetry refers simply to the practice of making measurements from photographs and would currently include measurements made from both film photography and electro-optical (digital) photography. Digital photogrammetry has been demonstrated as a viable technique for generating 3D models of structures and structural elements such as medieval bridges and has also been shown to contribute specifically to damage monitoring of such (Arias et al. 2007). While that study did not utilize stereoscopic photogrammetric techniques, others, such as (Maas and Hampel 2006) did.

Aerial photography has long been studied as a method of SHM as it was the first remote sensing method to be developed for any application. Bridge inspection demands a higher resolution from aerial photography than is normally obtained for most applications. Though most aerial photography missions are flown at 5,000 ft and higher, lower altitudes are necessary to achieve the higher resolution (and consequently smaller area imaged) that is required. This technique is called small-format aerial photography (SFAP). While aerial photography is also usually orthorectified (intentionally distorted to more accurately represent ground coordinates with respect to topography), at such low altitudes (e.g. 1,000 ft), SFAP imagery does not need such post-processing (Rice et al. 2010). This technique is often useful only as a qualitative assessment of cracking, corrosion, deflection, or displacement. While feature recognition and qualitative assessment are viable using FSAP, attempts at more rigorous application of the technique have demonstrated its limitations, such as its coarse resolution (e.g. 1.2 cm) which prevent it from being useful for many SHM applications (Liu et al. 2010).

Digital cameras have been used most successfully for vertical displacement or vibration measurements. The advantage of using CCDs lies in their low cost and high sensitivity to light, although for some applications it can actually be cost-prohibitive or otherwise impossible to achieve the resolution required. One method involves image processing techniques such as pixel identification and edge detection (Chan et al. 2009) that amounts to ―blowing out" all background elements to accentuate the structural element of interest. The same study also refers to a ―sub-pixel displacement identification measurement" (SPDIM) method that boosts the accuracy of CCDs to that of traditional displacement transducers. Another study has demonstrated the viability and high-accuracy of real-time displacement measurement with image processing techniques

(Lee and Shinozuka 2006). Accuracy of this technique has been quantified to 0.1-1.0 mm for bridges with a fundamental frequency of up to 5 Hz (Olaszek 1999). Another survey using three CCDs measured displacements of a steel beam due to temperature variations of up to 1,200°C with an accuracy of 0.7-1.3 mm (Fraser and Riedel 2000).

Shearography is a full-field video imaging technique that was first developed for strain measurements and now is sufficient enough to do so in real-time over large areas. The technique measures out-of-plane deformation from a fringe pattern generated by two images, one of which is sheared or rotated from the other. The area of concern is illuminated by a laser once before and then after a structure element is loaded. If the element contains a flaw, then strain concentration is induced in that vicinity, and that in turn induces surface strain anomalies. These surface strain anomalies are measured as fringe anomalies and thus the location of the flaw, provided that it is not too deep, can be determined (Chang and Liu 2003). Shearography is related to speckle photography.

Fringe projection interferometry (FPI) is another optical technique is a technique very similar to speckle pattern interferometry (SPI), however, instead of producing an interference pattern from a coherent light source (as in SPI), an interference pattern is projected onto the target surface using an incoherent light source. FPI achieves temporal phase shifting, allowing for the determination of phase shifts in a set of images having introduced a known phase shift. For this technique, a camera is used to record at least as many images as there are interference patterns being projected; the camera-target geometry must be known. The final product of FPI, after phase unwrapping and transformation of the surface map, is an image of the target‘s surface topography. Typical distances to the target range from 10 to 70 feet and as distance increases there is an associated scaling upwards of pixel size (Krajewski 2006).

Multispectral/hyperspectral imagery, of either satellite or aerial origin, is similar to EO imagery but contains a much broader frequency band, providing images in the infrared and thermal bands in addition to those outside the narrow, visual spectrum. 16-band airborne multispectral imagery has been used in characterizing road surface type with up to 86% accuracy and could be extended to characterizing concrete decks on bridges (Brooks et al. 2007).

5.2 Speckle Photography and Speckle Pattern Interferometry

Speckle is a random, deterministic, interference pattern formed when coherent light is reflected from a surface and is typically regarded as undesirable noise in most fields where it is encountered. Speckle patterns are high-contrast, fine-scale, granular patterns with a random intensity (Anderson and Trahey 2006). Speckle is produced by light reflected from most rough surfaces in the real world. Here, the term ―rough” means most any material with microscopic imperfections that are on the scale of optical wavelengths.

This random, microscopic roughness contributes randomly phased, interfering radiation to the total observed field. This effect is strongest when monochromatic light is used to illuminate the surface, as speckle patterns produced by different wavelengths are of different dimensions and tend to average one another out. Although two different surfaces may appear to be identical on the macroscopic scale, their optical roughness is always unique on the microscopic scale to the effect that the two can be distinguished by their speckle patterns. Furthermore, speckle can be used to identify deformations or displacements by comparing speckle patterns of the same surface.

The speckle phenomenon can be observed in most any signal composed of independently-phased, additive components with both amplitude and phase information (e.g. coherent radar, ultrasound). The components of such a signal constitute a ―random walk" when they are added together provided they each have random directions in the complex plane. This can result in constructive or deconstructive interference and thus the observed signal may be large or small (Goodman 2004). There are three distinct ways in which speckle patterns change due to surface alterations: a displacement gradient (strain) or local rotation is induced, rigid translation (displacement) of the surface, or a morphological change under which the initial and final states are totally unrelated—this can consist of excessive elastic strain, surface tilt, plastic deformation, or translation or rotation of the target surface.

Applying speckle patterns to structural health monitoring began with *interferometric* techniques such as shearography and electronic speckle pattern interferometry (ESPI). In the latter, real-time fringe patterns are analyzed by comparing a live camera image with a stored reference speckle pattern. These interferometric or *correlation* techniques are contrasted with *speckle photography*, which involves the simple translation of speckle patterns with no use of phase information. The advantage of ESPI is that it has intrinsic resistance to ambient vibration and other sources of environmental noise. The technique utilizes a laser light split into two branches and then expanded in each. One is used to illuminate the target object while the other serves as the stored reference speckle pattern (after it is passed through a diffuser).

After collection, the two speckle patterns collected are made to interfere with one another. Complex calculations are required to deconvolve the output, but computers receiving output from camera CCDs can perform them rapidly. Pedrini and Tiziani (1994) describe a double-pulse ESPI with which three-dimensional deformation can be determined using three directions of illumination and one direction of observation (take two images closely space in time from one camera). Phase-shifting allows for improved signal-to-noise ratio and the real-time calculation of wrapped phase maps. However, these data remain esoteric to most users, including important end-users (e.g. civil engineers, bridge inspectors and managers). Post-processing techniques are necessary for phase unwrapping, ultimately generating ―snapshots" of discontinuities or

displacement/strain fields. Provided sufficient temporal resolution, temporal phase unwrapping (as opposed to spatial phase unwrapping) is preferred as it allows the extraction of high-quality phase maps and absolute (total since start of process) displacement fields. Coggrave and Huntley (2004) describe an innovative method of implementing these post-processing techniques in real-time by means of a pipeline image processor. Speckle patterns can also be preferentially improved by means of a high-pass filter, removing variations in mean speckle intensity.

In computer speckle interferometry (CSI), speckle patterns are imaged directly by a CCD array and post-processed by consecutive, two-dimensional fast Fourier transforms (FFTs). This derives the off-center peaks, corresponding to degree and direction of in-plane motion (Steckenrider and Wagner 1995). However, this requires certain assumptions about the loading conditions be met. In all speckle photography, the threshold of detection is of the size that individual points on a surface are displaced greater than the speckle size (this holds for speckle photography only and is not desirable for speckle correlation). However, this deformation should not be so great that it induces the local deformation of small regions or the deformation of the entire image. These conditions lead to decorrelation (distortion or loss of visibility of fringes) and the loss of accurate quantitative information about in-plane surface displacement. Steckenrider and Wagner (1995) describe a technique called computed speckle decorrelation (CSD) which combines CSI with intentional decorrelation to allow regions of deformation to be discerned as well as quantitative measurement of correlation. CSD boasts hardware-based image processing that allows for full-frame image analysis and display once every second. Partial-frame analysis can display images at rates approaching that of video frame rates (e.g. 30 frames per second). With the use of a long-distance microscope objective, resolution down to 10 μm can be achieved.

CSI and CSD are both variations of a more general speckle photography technique called digital speckle correlation (DSC) allows for the comparison of two speckle patterns captured at different points in time—say, before and after deformation has occurred—which does not require more than one camera. These two speckle patterns, when combined, are referred to as a *specklegram*. The relative displacement of the correlated patterns can be used to generate Young‘s fringes or isothetic fringes which allow for the calculation of displacement and displacement gradient (strain).

Speckle photography and speckle interferometry/correlation have been combined to overcome the limitations imposed by decorrelation. Effects such as mechanical play, rotations, and surface tilt are hard to avoid in engineering applications and they all result in the disappearance of fringes when speckle motion becomes too large. In some areas these effects can be controlled. Variation in laser output energy can be minimized through the use of pulsed lasers and pointing stability; cooled detectors also diminish thermal noise. When these controls are ineffective or irrelevant, other techniques have to

be employed. One is to use speckle photography to compensate for speckle motion before performing phase reconstruction in interferometry (Molin et al. 2004).

Other applications of speckle patterns have been investigated but few have been rigorously applied. Elsholz (2005) provides the theoretical groundwork necessary for describing the roughness of a surface based on coherent light scattering. Gulker et al. (2005) describes the use of ESPI in investigating the process of salt crystal growth and the deformation it induces in porous materials. Their experiment, however, was conducted on a very small scale with a microscope objective fitted to the ESPI and a scanning electron microscope (SEM) used for visualization. High-resolution ESPI has been employed in the detection of aircraft corrosion on a scale of 40 mm using both thermal and vacuum loading—the latter also allows for quantitative calculation of deformation fields as the load is well-defined (Jin and Chiang 1998).

In another experiment, the 3D displacement of a plate 4 cm² in area was measured using a pair of cameras in stereo and achieved a 4-11% error without coherent light. So-called ―white light" speckle interferometry in the frequency domain is popular in engineering applications due to its less stringent demands on measurement illumination and ambient vibration control. These and other interferometric techniques demonstrate the potential for 3D displacement measurements with simple binocular, stereoscopic imaging, eliminating the need for complex light paths used in speckle pattern correlations (Ji et al. 2008).

5.3 Interferometric Synthetic Aperture Radar (IfSAR)

IfSAR (sometimes InSAR) compares pixel-by-pixel differences in phase between two synthetic aperture radar (SAR) images in order to determine changes in surface deformation or ground topography during the time interval that occurred between the two images. Microwave differential interferometry is a very similar technique for mapping displacement phenomena.

Though many sophisticated SAR instrumentation is installed on Earth-orbiting satellites, many of these instruments are not practical for monitoring structures on Earth for despite their sufficient accuracy, they generally lack the resolution or imaging time required for SHM. Consequently, the techniques described here are ground-based (Pieraccini et al. 2004). Generating two SAR images for this purpose requires having two side-looking antennae, separated by a known baseline, ready to receive backscattered signals from a transmitting antenna. This enables the target to be scanned from two different antenna positions. The phase and amplitude of the backscattered signal is stored in each pixel, but it is the phase that reveals the most significant information for terrestrial scanning and SHM applications because it enables the generation of a digital surface model (DSM) or other 3D model (Baran 2009).

For IfSAR experiments in the SHM of bridges, the antenna needs to image multiple sections of the structure from different angles. Generally, displacement in a non-radial direction can be estimated from the displacement along the radar‘s line of sight (recall that static radar measurements represent movement only in this direction). Pulses are typically transmitted at a 20-50° look angle. As the pulse spreads geometrically from the antenna the reflections of this transmitted energy are recorded as time series. Consequently, different targets positioned at the same distance from the antenna cannot be distinguished (a phenomenon known by *foreshortening* and *layover*). EM *shadows* and multipathing are other limitations of IfSAR (Baran 2009). IfSAR is capable of operating under all weather conditions, however, due to the signal‘s generally long wavelength, though this can be altered to achieve different degrees of penetration.

Gentile et al. (2008) describe their IBIS-S (image by interferometric survey) sensor that is based on both wideband and interferometric techniques and was developed to measure the deflection of several points on a structure at a sensitivity of better than 0.02 mm—a goal which, if achieved, would make the system the most accurate, stand-off sensor system for the remote monitoring of displacement and deflection in civil engineering structures.

IBIS-S is a coherent radar system, meaning it preserves the phase information of received signals. The central frequency is 16.75 GHz and the antenna can be rotated in any direction. The bandwidth scanning rates are as high as 200 Hz and the sampling interval is 0.005 s. These characteristics make the system suitable for dynamic monitoring and waveform definition of acquired signals (Gentile et al. 2008). IBIS-S is available for commercial purchase and use by Olson Instruments, Inc.

6.0 Exceptional Materials and Structures

6.1 Fiber-Reinforced Polymer Composites

Fiber-reinforced polymer (FRP) composites vary in the composition of constituents but in general the matrix is made up of some polymer and the reinforcement consists of fibers. The most commonly used fiber types are glass (GFRP), carbon, and aramid synthetics (Kevlar); boron, silicon carbide, alumina, and others are used in more specialized applications. These reinforcement fibers are crucial to load transfer. The reinforcement properties are strongest in the direction of the fibers and weakest in directions perpendicular, or transverse, to them. In many applications, structures are not loaded in a single direction, and thus multiple *plies* of FRP composite are layered together randomly to produce a *laminate* consisting of fibers in multiple, random directions.

For the past 50 years, FRP composites have seen limited use in maintenance and construction of civil engineering structures. The corrosion of steel elements in traditional, reinforced concrete has generated interest in FRP as an alternative. Furthermore, FRP offers high strength, stiffness, and durability for low density. In addition to these advantages, FRP composites are easy to install, versatile, and are electromagnetically neutral. FRP composites have been used as pre-stressing tendons dowels in addition to their straightforward use as grid and bar reinforcements.

In maintenance applications, FRP laminates have been applied externally to structures such as reinforced concrete beams in order to increase their load carrying capacity. Li and Liu (2001) note that glass epoxy jackets are commonly used to reinforce concrete bridge collars. In new construction, FRP composites have not found widespread acceptance simply due to the lack of long-term studies of their reliability and structural integrity (Rao 2007). In order to assess their performance, monitoring techniques that are specific to this special material need to be developed, and that is the focus of this section.

Rao (2007) describes several signs of degradation that would be potential targets of structural health monitoring in FRP composites: cracks, matrix micro-cracks, fiber breakage, fiber/matrix debonding, and impact damage which manifests as delamination or large matrix cracks. Rao (2007) goes on to describe how infrared thermography, ultrasonic emissions, acoustic emission, microwave radar, ground-penetrating radar, magnetic, radiography, and optical non-destructive testing techniques have been employed to identify, characterize, and quantify damage to FRP composite structures. In this section, a small number of the studies considered by Rao (2007) have been briefly summarized.

Bates et al. (2000) demonstrated the use of ultrasonic and transient halogen lamp thermography in the inspection of impact damage in FRP composite materials. They found that lock-in thermography was more effective at detecting non-uniform radiation

than transient thermography, indicating that lock-in thermography is the preferred choice for curved or other surfaces where geometric effects make uniform heating harder to attain. In FRP composite structures, using infrared thermography, air blisters the size of 16-30 mm have been detected at a distance of up to 20 m (Hu et al. 2002) and delaminations and debonding on the order of 1/16 of an inch thick have been resolved (Halabe et al. 2005). Meola et al. (2004) carried out extensive tests of the geometrical limitations of defect detection in composites and concluded that carbon fibers permit deep investigation due to their higher conductivity and diffusivity and that, intuitively, decreasing size and increasing depth of defects lead to decreased contrast though thickness has a stronger, positive correlation with contrast then size or depth.

Doyum and Durer (2002) describe using the Automated Ultrasonic Scanning System (AUSS), a computer-controlled ultrasonic testing and data collection system, to identify and quantify the size of defects such as planar voids, core damages, and water/hydraulic intrusion in honeycomb composite structures. Hsu et al. (2002) also describe testing composite honeycomb structures—imaging the internal features and evaluating their conditions—using an air-coupled ultrasonic technique with piezoceramic transducers at 50, 120, and 400 kHz. Roth et al. (2003) demonstrated the ability to distinguish delamination, density variation, and microstructural variation in silicon infiltration, and crack space indication in SiC/SiC and C/SiC composites. Hosur et al. (2004) evaluated damage from a high-velocity impact in both stitched and unstitched woven carbon/epoxy composites and concluded that the damaged area is largest in satin weave laminates when compared to plain weave laminates. Imielinska et al. (2004) found that the air-coupled, ultrasonic C-scan technique is capable of detecting impact damage to carbon/epoxy plates as thin as 0.3 mm. Berketis and Hogg (2004), with GFRP composites that had been soaked continuously for two years to induce serious matrix damage, demonstrated how ineffective water-coupled ultrasonic emissions can be when evaluating saturated or water-immersed specimens as the water-damaged areas become invisible to ultrasound; use of an air-coupled ultrasound instead restored the ability to detect water-damaged areas. (Godinez-Azcuaga et al. 2004) used the ultrasonic C-scan technique to reveal debonding, cracks, and delamination in FRP-wrapped concrete columns and bridges.

Santulli (2000) used acoustic emissions to characterize defect areas in impacted glass-woven laminates 5 mm thick and concluded that a coarser weave cases damage to extend over a larger area while there is less damage in mat/polyester laminates of the same material. Amoroso et al. (2003) exhibited the detection and characterization of impact damage in FRP composites utilizing acoustic emission and were able to identify delamination, matrix microfracture, and fiber failure. Stepanova et al. (2004) used stress tests to monitor the fracture process in Organit-10T composite material and found that the onset of fracture could be anticipated from the distribution of acoustic amplitudes.

Zhang and Richardson (2005) demonstrated the sensitivity of optical measurements in detecting barely visible impact deformation; they used both ESPI and an Optical Deformation and Strain Measurement System (ODSMS) to identify the geometry of the damage and for strain classifications. Ambu et al. (2006) showed that holography and ESPI could be used to identify damage in thin FRP laminates with an efficient dependent on the through-thickness location of the delaminations, though the ESPI technique suffered from high noise that reduced the ability to quantify impact damage. Although holography demonstrated higher sensitivity than ESPI in this experiment, it was unable to resolve delaminations lying at interfaces more than 0.7 – 0.8 mm from the impacted surface. Hatta et al. (2005) compared three techniques including ESPI in the damage detection of carbon-carbon composites. With ESPI they were able to clearly observe delamination in carbon-carbon laminates as well as splitting, micro-cracking, and unstable zigzag crack extension.

Li and Liu (2001) used 10 GHz microwave radar and an algorithm for inverting dielectric constants to investigate air-filled voids (debonding) in glass epoxy jackets applied to concrete bridge collars. They achieved a resolution of 0.43 cm using dielectric lenses to focus the radar beams and it is likely that even higher resolution might be achieved at higher frequencies. Though their technique requires operation in extremely close proximity to the target, AbouKhousa and Qaddoumi (2004) have shown how microwave radar can be applied in the near-field to detect subsurface inclusions. Kharkovsky et al. (2006) also demonstrated a dual-polarized, near-field microwave reflectometer applied to carbon fiber-reinforced polymer (CFRP) composites and were able to detect debonding of a region 6 by 8 cm in size in a tilted (severe standoff distance variation) sample. Perhaps the most impressive achievement in this area is by Stephen et al. (2004) who utilized an automated scanning mechanism in conjunction with a near-field microwave reflectometer in the X-band and an open-ended rectangular waveguide to detect delamination between CFRP laminates and concrete substrate.

The efficacy of ground-penetrating radar (GPR) in this arena is highly variable with frequency. At lower frequencies (~1 GHz) the technique fails to resolve shallow defects but at higher frequencies (>2 GHz) the depth of penetration is compromised. Dutta (2006) utilized ground-coupled GPR at 1.5 GHz to detect water-filled voids down to 1.4 inches in diameter (the technique is incapable of detecting air-filled voids). Hing (2006) also used ground-coupled GPR at 1.5 GHz in addition to 2 GHz horn antennae for detection of defects in FRP bridge decks. The study reinforced the knowledge that neither antennae type could detect air-filled voids and that the 1.5 GHz ground-coupled antenna was superior to the 2 GHz horn antennae in detecting water-filled voids.

The field of structural health monitoring with radiographic techniques seems much less prolific than others, but Rao (2007) notes that X-ray radiography has been shown to be effective at detecting water intrusion, density change or deformation of the

core, and also air-filled voids. Doyum and Durer (2002) used X-ray radiography to characterize and classify defects unique to honeycomb structures and showed that the technique was much more effective than ultrasound.

Finally, Rao (2007) summarized defect detection done using a Superconducting Quantum Interference Device (SQUID), a very sensitive magnetic (three orders of magnitude more so than conventional magnetometers) flux-to-voltage transducer that utilizes the effect of quantum interference to detect internal flaws in both ferromagnetic and non-ferromagnetic conducting materials. SQUIDs come in two types, or two types of operation: low or high critical temperature (T_C). Hatta, Aly-Hassan (2005) used a low T_C SQUID to detect damage in notched carbon-carbon composites. This technique usually requires contact with the sample for current injection, but Hatsukade et al. (2002) demonstrated a non-contact SQUID technique in which they induced a current in the target using a U-shaped ferrite core and low-frequency current (150 mA at 300 Hz). The peak amplitude of the response they measured compared very well with the direct contact (current injection) method and they concluded the non-contact technique could be applied to very thick carbon fiber composites.

7.0 Case Studies

7.1 Commodore Barry Bridge, Philadelphia, PA

Described by Aktan et al. (2000), this 3288-ft long bridge consists of two anchor spans, two cantilever arms, and a central suspended span. The bridge is instrumented with environmental monitoring systems that report wind speed in three directions and ambient temperatures in several locations once every second. Additional sensors are in place to monitor the bridge‘s live load in real time. Aktan et al. (2000) also indicated that tilt and displacement sensors were being installed where inadvertent motion was anticipated; these would determine both the movement history and the displacement kinematics in three dimensions.

These and other data from controlled load tests and ambient vibration tests have been collected since the sensors were first installed in 1998. The data have been interpreted in terms of the bridge‘s mechanical characteristics and its loading and response environment with a 3D finite-element model. The controlled test data are used to calibrate and validate the analytical model (Aktan et al. 2000).

Plans exist to outfit the bridge with a new array of modern, remote sensors that will be part of a high-speed fiber-optic local-area network (LAN), communicating with two data acquisition systems at the towers which will communicate wirelessly with a bridge data server. This server will host real-time data streams and allow for the remote monitoring and manipulation of data acquisition, viewing of data and bridge imagery, as well as archival. Weigh-in-motion (WIM) and weather monitoring systems distant from the bridge itself will also communicate wirelessly with the bridge data server. Other planned sensor modalities include accelerometers, resistance strain gauges, vibrating wire strain gauges, thermistors (temperature-sensitive resistors), long-gauge fiber optic displacement wires, and vibrating wire crackmeters and tiltmeters.

Most interesting is the capability of corresponding video images of truck positions with WIM systems and the strains they report at those positions. Eventually, millimeter-level GPS and acoustic weld sensors will be incorporated to monitor the global geometry and welding fatigue, respectively.

These multiple data sources must be integrated in a meaningful way, and currently the Commodore Barry Bridge SHM relies on the LabView software program, graphical programming environment that allows for sophisticated data acquisition, instrument control, and signal processing. Deck and driving conditions and traffic levels as well as bridge element temperatures and strains are all monitored in real time using LabView. The goal of the user interface is to allow bridge managers to react to incidents and anomalies immediately by alerting them once certain conditions are detected. Images of the user interface are provided in Atkan et al. (2000) as well as a detailed

description of the phenomenological laboratory model being developed by Drexel University researchers.

7.2 Golden Gate Bridge, San Francisco, CA

(Kim et al. 2007) describe a wireless sensor network installed on the south tower and 4200-ft long main span of the iconic Golden Gate Bridge. Their installed sensor network consisted of 64 accelerometer sensors measuring ambient vibration accurately to 30 μG. The chosen sampling rate was 1 kHz with a time aperture of less than 10 μs and data were streamed at 441 B/s with pipelining.

One of the project requirements was the ability to detect signals with peak amplitudes as low as 500 μG. This was a serious constraint on the noise floor of the entire system, installation error, and temperature variation. To this end, each of the microelectronic mechanical systems (MEMS) that comprise an accelerometer node has a thermometer to measure acceleration temperature. The high sampling rate employed was also necessary in order to describe the local modes of vibration. The sensor software was based on TinyOS—an operating system specifically designed for MEMS.

7.3 Tsing Ma Bridge, Hong Kong, China

With a main span length of 1,377 m The Tsing Ma bridge has the distinction of being the longest suspension bridge to carry both highway and railway traffic (Chan et al. 2006). Highway traffic uses dual three-lane roads on top of a covered deck for two railway lines and two emergency roadways for use in periods of very high wind. Since the bridge was commissioned on May 22, 1997, the bridge has been monitored by the Wind and Structural Health Monitoring System (WASHMS), which is also used to monitor the conditions of two other cable-supported bridges in Hong Kong: the Ting Kau Bridge and the Kap Shui Mun Bridge.

WASHMS is comprised of a permanent sensor network of 774 nodes, making it—along with the Ting Kau and Kap Shui Mun bridges—one of the most heavily instrumented bridges in industry (Ko et al. 2000). These sensors include accelerometers, strain gauges (110 installed on the bridge deck), displacement transducers, level sensors, GPS sensors anemometers, temperature sensors, and weigh-in-motion (WIM) sensors all connected to a data acquisition and processing system. WASHMS has been used to test the efficacy of a new monitoring system using fiber Bragg grating (FBG) sensors developed by Hong Kong Polytechnic University. These FBG sensors are multiplexed and capable of simultaneous strain and temperature measurement as well as temperature-independent strain measurements. Their SHM system using FBG sensors is called DEMINSYS (demultiplexing/interrogation system) and boasts a resolution and accuracy of 1 pm and 10 pm, respectively, using a wavelength detection array comprised of

sensitive charge-coupled device (CCD) sensors. The system uses a broadband light source operating around 1550 nm and can achieve a sampling rate of up to 20 kHz. Chan et al. (2006) found that DEMINSYS can clearly and correctly detect dynamic strain responses to the passage of trains on the bridge(s).

7.4 Vernon Avenue Bridge, Barre, Massachusetts

This bridge is a 150 foot three-span continuous bridge that was built in the summer of 2009. The eight inch cast-in-place deck is supported by six steel girders. The sensors were placed on the structure during the construction process to capture the full strain history of the bridge. Vernon Avenue Bridge has a total of 100 strain gauges, 36 girder thermistors, 30 concrete thermistors, four bi-axial abutment tiltmeters and 16 biaxial accelerometers. These were placed at 13 different stations across the span of the bridge in which the data is collected using iSite® data acquisition boxes provided by Geocomp, INC. (Bell et al. 2010). This data was collected at different milestones during construction and has been collected ever 5 minutes since the concrete deck was poured.

Two different models are being created to model the bridge. The models are to model the actual response of the structure with the safety factors removed. The modeling of the bearing pads is difficult with defining the boundary conditions on the bridge, and all the different components of the bridge needed to be taken into account with the models to achieve the desired accuracy. One of the models is being drawn in great detail as a finite element model that makes use of solid elements to represent the concrete deck and shell elements to model the steel girders. This model was drawn in SAP2000® to be extruded along the length of the bridge. All assumptions are to be taken out of this model to try and provide the most accurate baseline available. Temperature gradients are also to be included in the model to allow the calibration with temperature. This model is to be created with all the components to provide the most realistic model possible (Bell et al. 2010).

The other model is being created using BrIM in SAP2000® to form the initial geometry for the bridge. The BrIM will then be turned off to change the model from designed based to monitoring based. This element is to be created with frame elements instead solid and shell elements of the previous model. With this model beam elements represent the girders and support piers, shells and/or brick elements represent the deck, and spring elements to represent boundary conditions. These two models than can be compared on how well they predict the behavior of the bridge compared to the amount of time used to create the model (Bell et al. 2010).

7.5 Cut River Bridge, Michigan

The Cut River Bridge was outfitted with different sensors in 2007 by Michigan Department of Transportation (MDOT). The Cut River Bridge is a steel truss bridge that is supported by two piers with a 125 foot anchor arm and a125 foot cantilever arm each for a total span of 500 feet. This was completed to go along with the Mackinac Bridge sensing system, so the data from the Cut River Bridge is sent wirelessly to the computers there in which MDOT has access to the data. The whole system is run from five solar panels which charge batteries until up to sixteen days of charge is available.

There are eight wireless fiber optic strain gages on each side of the bridge along with two temperature sensors for a total of sixteen fiber optic strain gages and four temperature sensors. The location of the strain gages can be seen in Figure 1 where the arrows are pointing to. There are two bridge deck environmental sensors placed on the bridge. The temperature and environmental sensors can be used to correlate their values to the strain gages to see how the strains are affected by temperature and other environmental factors. The bridge is also equipped with one wireless weigh-in-motion sensor along with two traffic monitoring sensors. This allows for the correlation of loads crossing the bridge with the strains on the bridge. Two close circuit television cameras are also in place on a seventy foot tower which can be used to confirm the values of the weigh-in-motion sensor and the traffic monitoring sensors.

Figure 1: Location of Sensors on Cut River Bridge

The data is to be used to develop correlations and comparisons between the actual bridge service loads and those used to design the bridge. MDOT is looking to establish a baseline from the data that they are collecting now to use in the future. They are hoping

to be able to examine future trends or changes in behavior and maintain the safety of the bridge along with being able to use the data to help with future maintenance planning for the bridge.

7.6 Field Monitoring of Four Integral Abutment Bridges, Pennsylvania

This study was the monitoring of four integral abutment bridges (IABs) for the use of

Table 4: Field Monitored IAB Description

Bridge No.	Girder Type	Integral Abutment	Abutment Height (ft-in)	Span Lengths Total Length (ft)	Number of Instruments
109	PennDOT 28/78*	Both	11-6	88-122-122-88 = 420	64
203	AASHTO V	North Only South Fixed	19-0	47-88-37 = 172	64
211	PennDOT 28/78*	Both	14-1	114	64
222	PennDOT 24/48*	Both	13-1	62	48

* PennDOT DM-4 (2007)
†Note: 1 inch = 0.0254 m, 1 ft = 0.3048 m.

gaining an understanding of different forces on these bridges. This studied looked at the time dependent and thermal effects on the bridge members. Due to environment concerns the four bridges weren't open for traffic for between 2 to 5 years from when the monitoring started. This allowed the study to look at just the effects of time and thermal changes to the bridges. The goal of the project was to determine how these effects could be better understood when designing IABs (Kim and Laman 2009).

There were a total of 240 sensors placed on the four bridges which were constructed from precast prestressed concrete girders with cast-in-place deck. The different properties of the bridge can be seen in the table below. There were multiple vibrating wire-based instruments placed on the bridge include: backfill pressure cells, abutment displacement extensometers, girder axial force and moment strain gages, girder tiltmeters, abutment tiltmeters, pile moment and axial force strain gages, and approach slab sister-bar strain gages.

The results of the extensometers for measuring displacement on the abutments showed that the top and bottom sensors had a wide range of movement for the given bridges. The maximum displacement ranges for the top were from 0.056 in to 1.935, and the bottom was from 0.186 in to 2.029 in over the period of when the bridge was completed as early as 2003 to 2009. The results of displacement are in a sinusoidal shape with the peak during the summer and the valley during the winter. Both abutment and

girder ration were measured using a tiltmeter. The results for the abutment rotation varied from 0.139 to 0.322 degrees for the interior location and 0.096 to 0.187 degrees for the exterior location. The results for the girder rotation varied from 0.157 to 0.225 degrees for the interior location and 0.135 to 0.255 degrees for the exterior location.

Other results found were pile moment and axial force, girder moment and axial force, approach slab strain, ambient temperature and structural temperature. With all these results the several conclusions could be reached. The temperature had the biggest affect on the different properties measured in this study. There was no significant change in the properties once traffic started showing that this wasn‘t a significant load on the bridge.

7.7 Bridge Monitoring TestBed

This case study consisted of four span 90 m long bridge that was out fitted with TestBed monitoring system along with a decision support system. The TestBed was developed at the University of California, San Diego. There are a total of 20 accelerometers placed in one of the box girders along the length of the bridge. These are wired to a data collection system that sends the information to a computer. There was also a camera set up to collect images of the traffic traveling over the bridge to allow the correlation of the accelerations values with the type of load crossing the bridge (Fraser et al 2010).

Using a decision support system they are able to correlate the load passing over the different sensor as well as the reading from the sensors to see how the load affected the structure. A website was developed to retrieve and disseminate the data for any time period desired. The web page can be seen in Figure 2. This system allows for the view of data from anytime period desired. They are developing a vehicle detection system in which the system can identify different vehicle sizes depending on how many pixels the vehicle takes up at know locations. This allows for the user to not have to identify the size of the vehicle since the system would do this.

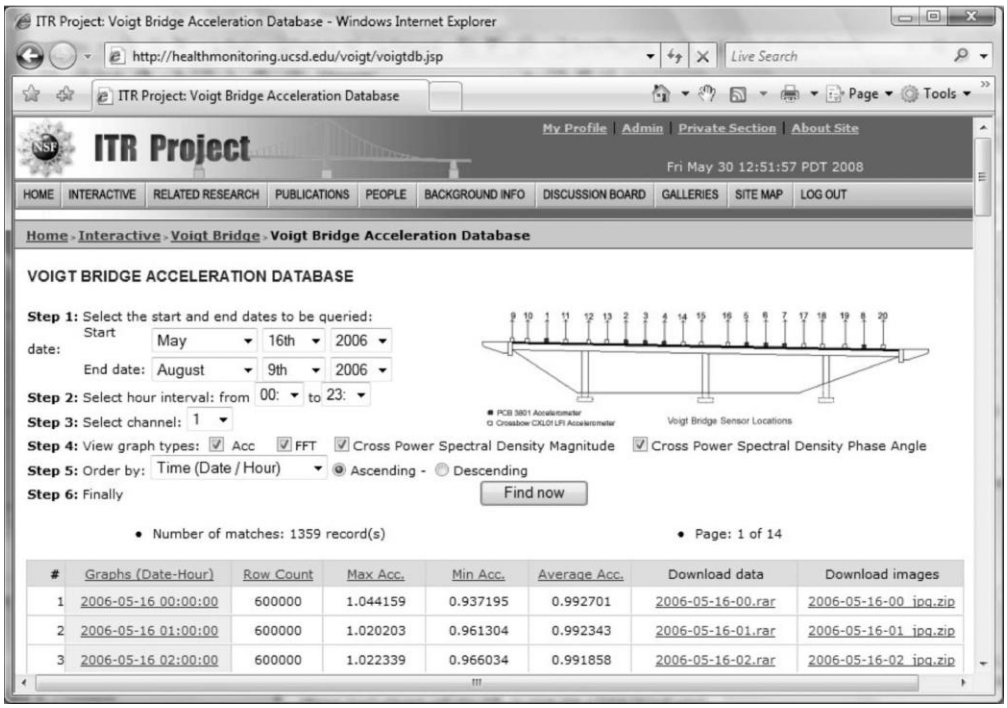

Figure 2: Web page for quering, browsing and downloading the recorded accelation and video data

8.0 References

AbouKhousa, M. and N. Qaddoumi (2004). Near-field microwave imaging of subsurface inclusions in laminated composite structures. 16th World Conference on Nondestructive Testing. Montreal, Canada.

Aktan, A. E., F. N. Catbas, M. Pervizpour, E. Kulcu, K. Grimmelsman, R. Barrish, X. Qin. (2000). Real-time bridge health-monitoring for management. Second Workshop on Advanced Technologies in Urban Earthquake Disaster Mitigation. Kyoto University, Drexel Intelligent Infrastructure Institute.

Alqennah, H. (2000). Detection of subsurface anomalies in composite bridge decks using infrared thermography. Department of Civil and Environmental Engineering. Morgantown, WV, West Virginia University. Master of Science in Civil Engineering: 95.

Ambu, R., F. Aymerich, F. Ginesu, P. Priolo. (2006). "Assessment of NDT interferometric techniques for impact damage detection in composite laminates." Composites Science and Technology 66(2): 199-205.

Amey, A. (2009). "Beyond State-Level Bridge Counts – Alternative Performance Measures for Evaluating Bridge Conditions." 2010 TRB Annual Meeting.

Amoroso, M. P., C. Caneva, F. Nanni, M. Valente. (2003). Acoustic emission performance for damage monitoring of impacted FRP composite laminates. Review of Progress in Quantitative Nondestructive Evaluation:Volume 22, Bellingham, Washington (USA), AIP.

Anderson, M. E. and G. E. Trahey. (2006, February 15, 2006). "A beginner's guide to speckle." A seminar on k-space applied to medical ultrasound Retrieved February 22, 2010, 2010, from http://dukemil.bme.duke.edu/Ultrasound/k-space/node5.html.

Angelidis, N., C. Y. Wei, P. E. Irving. (2004). "The electrical resistance response of continuous carbon fibre composite laminates to mechanical strain." Composites Part A: Applied Science and Manufacturing 35(10): 1135-1147.

Ansari, F. (2005). "Fiber optic health monitoring of civil structures using long gage and acoustic sensors." Smart Materials and Structures 14(3): S1-S7.

Arias, P., J. Armesto, D. Di-Capua, R. González-Drigo, H. Lorenzo, V. Pérez-Gracia. (2007). "Digital photogrammetry, GPR and computational analysis of structural damages in a mediaeval bridge." Engineering Failure Analysis 14(8): 1444-1457.

Arunachalam, K., V. R. Melapudi, L. Udpa, S. S. Udpa. (2006). "Microwave NDT of cement-based materials using far-field reflection coefficients." NDT & E International 39(7): 585-593.

ASCE, A. S. o. C. E. (2009). "Bridges | report card for America's infrastructure." Retrieved February 22, 2010, 2010, from http://www.infrastructurereportcard.org/fact-sheet/bridges.

Baran, I. (2009). Airborne InSAR and LiDAR compared.

Bates, D., D. Lu, G. F. Smith, J. Hewitt, (2000). Rapid NDT of composite aircraft components using lock-in ultrasonic and halogen lamp thermography. Nondestructive Evaluation of Aging Materials and Composites IV, Newport Beach, CA, USA, SPIE.

Bell, E., J. Sipple, P. Lefebvre, J. Phelps, B. Brenner, M. Sanayei. (2010). "Instrumentation, Modeling and Monitoring of a Concrete Bridge from Construction through Service." Transportation Research Board 2010 Annual Meeting.

Berketis, K. and P. J. Hogg (2004). "Effectiveness of non-contact ultrasonics for damage detection on wet GFRP composites."

Beyea, S. D., B. J. Balcom, T. W. Bremner, P. J. Prado, D. P. Green, R. L. Armstrong, P. E. Grattan-Bellew. (1998). "Magnetic resonance imaging and moisture content profiles of drying concrete." Cement and Concrete Research 28(3): 453-463.

Bhalla, S. and C. K. Soh (2004). "Structural health monitoring by piezo-impedance transducers I: modeling." Journal of Aerospace Engineering 17(4): 154-165.

Brooks, C., D. Schaub, B. Thelen, R. Shuchman, R. Powell, E. Keefauver, (2007). TARUT pilot studies technical details report. Deliverable 5.3-B. M. D. o. Transportation, Michigan Tech Research Institute.

Bungey, J. H. (2004). "Sub-surface radar testing of concrete: a review." Construction and Building Materials 18(1): 1-8.

Burleigh, D. D. and R. Bohner (1999). Thermal nondestructive testing (TNDT) of adhesively bonded composite reinforcements applied to concrete civil structures. Nondestructive Evaluation of Bridges and Highways III, Newport Beach, CA, USA, SPIE.

Casas, J. R. and P. J. S. Cruz (2003). "Fiber optic sensors for bridge monitoring." Journal of Bridge Engineering 8(6): 362-373.

Castro, T. A., D. V. Jáuregui, S. R. Maberry. (2009). "A Collaborative Approach for Load Rating of State Owned Bridges." TRB 2010 Annual Meeting.

Chan, T. H. T., D. B. Ashebo, H. Y. Tam, Y. Yu, T. F. Chan, P. C. Lee, E. Perez Gracia, (2009). "Vertical displacement measurements for bridges using optical fiber sensors and CCD cameras -- a preliminary study." Structural Health Monitoring **8**(3): 243-249 10.1177/1475921708102108: 10.1177/1475921708102108.

Chan, T. H. T., L. Yu, H. Y. Tam, Y. Q. Ni, S. Y. Liu, W. H. Chung, L. K. Cheng. (2006). "Fiber Bragg grating sensors for structural health monitoring of Tsing Ma bridge: Background and experimental observation." Engineering Structures 28(5): 648-659.

Chang, P. C., A. Flatau, S. C. Liu. (2003). "Review paper: health monitoring of civil infrastructure." Structural Health Monitoring 2(3): 257-267 10.1177/1475921703036169: 10.1177/1475921703036169.

Chang, P. C. and S. C. Liu (2003). "Recent research in nondestructive evaluation of civil infrastructures." Journal of Materials in Civil Engineering 15(3): 298-304.

Chong, K. P., N. J. Carino, G. Washer. (2003). "Health monitoring of civil infrastructures." Smart Materials and Structures 12(3): 483.

Chung, D. D. L. (2001). "Structural health monitoring by electrical resistance measurement." Smart Materials and Structures 10.

Cochran, A., G. B. Donaldson, L. N. C. Morgan, R. M. Bowman, K. J. Kirk. (1993). SQUIDS for NDT: the technology and its capabilities. Southend-on-Sea, ROYAUME-UNI, Non-Destructive Testing Society of Great Britain.

Coggrave, C. R. and J. M. Huntley (2004). "Real-time visualization of deformation fields using speckle interferometry and temporal phase unwrapping." Optics and Lasers in Engineering 41: 601-620.

Crider, J. S. (2007). Damage detection using Lamb waves for structural health monitoring. Wright-Patterson Air Force Base, Ohio, Air Force Institute of Technology.

da Silva, R. R., M. H. S. Siqueira, L. P. Caloba, J. M. A. Rebello. (2001). "Radiographics pattern recognition of welding defects using linear classifiers." Insight 43(10).

David, L. M., M. D. Todd, G. Park, C. R. Farrar. (2007). "Development of an impedance-based wireless sensor node for structural health monitoring." Smart Materials and Structures 16(6): 2137.

DelGrande, N. and P. F. Durbin (1999). Delamination detection in reinforced concrete using thermal inertia. Nondestructive Evaluation of Bridges and Highways III, Newport Beach, CA, USA, SPIE.

Doyum, A. B. and M. Durer. (2002). "Defect characterization of composite honeycomb panels by non-destructive inspection methods." from http://www.ndt.net/article/dgzfp02/papers/p36/p36.htm.

Dutta, S. S. (2006). Nondestructive evaluation of FRP wrapped concrete cylinders using infrared thermography and ground penetrating radar. Department of Civil and Environmental Engineering. Morgantown, West Virginia, West Virginia University. Master of Science in Civil Engineering: 128.

Elsholz, F. (2005). Rough surface characterization and determination of the RMS roughness from coherent light scattering.

Federal Highway Administration. (1995). "Recording and Coding Guide for the Structure Inventory and Appraisal of the Nation's Bridges." (FHWA-PD-96-001).

Federal Highway Administration. Deficient Bridges By Material Type of Structure by State, accessed at http://www.fhwa.dot.gov/BRIDGE/material.htm. July 7, 2010.

Fraser, C. S. and B. Riedel (2000). "Monitoring the thermal deformation of steel beams via vision metrology." ISPRS Journal of Photogrammetry and Remote Sensing **55**(4): 268-276.

Fraser, M., A. Elgamal, X. He, J. P. Conte. (2010). "Sensor Network for Structural Health Monitoring of a Highway Bridge." JOURNAL OF COMPUTING IN CIVIL ENGINEERING (January/Febuary).

Gentile, C., G. Bernardini, P. Ricci. (2008). "A new interferometric radar for full-scale testing of bridges: ambient vibration tests and operational modal analysis."

Godinez-Azcuaga, V. F., R. D. Gostautas, R. D. Finlayson, M. Miller. (2004). Nondestructive evaluation of FRP wrapped concrete columns and bridges. Structural Materials VI - An NDT Conference, Buffalo, NY, U.S.A.

Goodman, J. W. (2004). Speckle phenomena in optics: theory and applications.

Gueguen, P., V. Jolivet, C. Michel, A. Schveitzer. (2009). "Comparison of velocimeter and coherent LiDAR measurements for building frequency assessment." Bulletin of Earthquake Engineering.

Gulker, G., A. El Jarad, K. D. Hinsch, H. Juling, K. Linnow, M. Steiger, St. Bruggerhoff, D. Kirchner. (2005). Monitoring of deformations induced by crystal growth of salts in porous systems using microscopic speckle pattern interferometry. Lasers in the Conservation of Artwork, LACONA VI Proceedings. Vienna, Austria.

Haeni, F. P., G. Placzek, R. E. Trent. (1992). Use of ground penetrating radar to investigate refill scour holes at bridge foundations. Fourth International Conference on Ground Penetrating Radar, Rovaniemi, Finland.

Halabe, U. B., A. Vasudevan, H. V. S. GangaRao, P. Klinkhachorn, G. Lonkar. (2005). Subsurface defect detection in FRP composites using infrared thermography. Review of Progressive in Quantitative Nondestructive Evaluation, Golden, Colorado (USA), AIP.

Hatsukade, Y., N. Kasai, H. Takashima, A. Ishiyama. (2002). "Non-contact SQUID-NDT method using a ferrite core for carbon-fibre composites." Superconductor Science and Technology 15(12): 1728.

Hatta, H., M. S. Aly-Hassan, Y. Hatsukade, S. Wakayama, H. Suemasu, N. Kasai, (2005). "Damage detection of C/C composites using ESPI and SQUID techniques." Composites Science and Technology 65(7-8): 1098-1106.

Hide, C., S. Blake, X. Meng, G. W. Roberts, T. Moore, D. Park. "An investigation in the use of GPS and INS sensors for structural health monitoring."

Hing, C. L. (2006). Nondestructive evaluation of fiber reinforced polymer bridge decks using ground penetrating radar and infrared thermography. Department of Civil and Environmental Engineering. Morgantown, West Virginia, West Virginia University. Doctor of Philosophy in Civil Engineering.

Hosur, M. V., U. K. Vaidya, C. Ulven, S. Jeelani. (2004). "Performance of stitched/unstitched woven carbon/epoxy composites under high velocity impact loading." Composite Structures 64(3-4): 455-466.

Howard, G. B., C. P. Sturos, T. M. Ahlborn. (2010). "Detection of bridge deck de-laminations using thermal imaging." Roads and Bridges 98(2).

Hsu, D. K., D. J. Barnard, J. J. Peters, V. Dayal, V. Kommareddy.(2002). Nondestructive inspection of composites and their repairs. 6th Join AAA/DOD Aging Aircraft Conference, San Francisco, CA, U.S.A.

Hu, C. W., J. K. C. Shih, R. Delpak, D. B. Tann.(2002). Detection of air blisters and crack propagation in FRP-strengthened concrete elements using infrared thermography. Inframation - The Thermographer's Conference.

Huynh, S. H. and G. Cheng (2000). Low profile ceramic choke. United States, Antom Corporation. 6,040,805.

Imielinska, K., M. Casaings, R. Wojtyra, J. Haras, E. Le Clezio, B. Hosten.(2004). "Air coupled ultrasonic C scan technique in impact response testing of carbon fiber and hybrid composites." Journal of Materials Processing Technology 157(58): 513-522.

Inaudi, D. and B. Glisic (2004). "Combining static and dynamic deformation monitoring with long-gauge fiber optic sensors."

Jenks, W. G., S. S. H. Sadeghi, J. P. Wikswo.(1997). "SQUIDs for nondestructive evaluation." Journal of Physics D: Applied Physics 30(3): 293.

Jerry, J. S. and H. L. C. Roger (2000). Bridge Decks Inspection Using Chain Drag and Ground Penetrating Radar, ASCE.

Ji, X., X. Yang, C. Jinlong. (2008). "3D displacement measurement by white light digital image analysis in frequency domination area."

Jin, F. and F. P. Chiang (1998). "ESPI and digital speckle correlation applied to inspection of crevice corrosion on aging aircraft." Res Nondestr Eval 10: 63-73.

Justnes, H., I. Meland, J. O. Bjoergum, J. Krane, T. Skjetne.(1990). "Nuclear magnetic resonance (NMR)--a powerful tool in cement and concrete research." Advances in Cement Research **3**(11): 105-110.

Kanada, H., Y. Ishikawa, T. Uomoto."Measurement of chloride content in concrete using near-infrared spectroscopy and x-ray fluorescence analysis."

Kang, I., M. J. Schulz, J. H. Kim, V. Shanov, D. Shi.(2006). "A carbon nanotube strain sensor for structural health monitoring." Smart Materials and Structures 15(3): 737.

Kharkovsky, S., A. C. Ryley, V. Stephen, R. Zoughi.(2006). Dual-polarized microwave near-field reflectometer for non-invasive inspection of carbon fiber reinforced polymer (CFRP) strengthened structures. IMTC 2006 - Instrumentation and Measurement Technology Conference. Sorrento, Italy.

Kijewski-Correa, T. (2005). "GPS: a new tool for structural displacement measurements." APT Bulletin 36(1): 13-18.

Kim, W. and J. A. Laman (Nov. 15, 2009). "Long-term Field Monitoring of Four Integral Abutment Bridges." Transporation Research Board 2010 Annual Meeting.

Kim, S., S. Pakzad, D. Culler, J. Demmel, G. Fenves, S. D. Glaser, M. Turon. (2007). Health monitoring of civil infrastructures using wireless sensor networks. Proceedings of the 6th international conference on Information processing in sensor networks. Cambridge, Massachusetts, USA, ACM.

Knecht, A. and L. Manetti (2001). "Using GPS in structural health monitoring."

Ko, J. M. and Y. Q. Ni (2005). "Technology developments in structural health monitoring of large-scale bridges." Engineering Structures **27**(12): 1715-1725.

Ko, J. M., Y. Q. Ni, J. Y. Wang, Z. G. Sun, X. T. Zhou.(2000). "Studies of vibration-based damage detection of three cable-supported bridges in Hong Kong."

Krajewski, J. E. (2006). Bridge inspection and interferometry. Worcester, Massachusetts, Worcester Polytechnic Institute. Master of Science in Civil Engineering: 120.

Krammer, P., M. Willsch, N. Theune, M. Rothhardt.(2000). Novel fiber optic Bragg grating acceleration sensor detection scheme. Proceedings of SPIE, the International Society for Optical Engineering.

Krause, H. J., W. Wolf, W. Glaas, E. Zimmermann, M. I. Faley, G. Sawade, R. Mattheus, G. Neudert, U. Gampe, J. Krieger. (2002). "SQUID array for magnetic inspection of prestressed concrete bridges." Physica C: Superconductivity 368(1-4): 91-95.

Kuang, K. S. C., Akmaluddin, W. J. Cantwell, C. Thomas.(2003). "Crack detection and vertical deflection monitoring in concrete beams using plastic optical fibre sensors." Measurement Science and Technology 14(2): 205-216.

Lau, K.-t. (2003). "Fibre-optic sensors and smart composites for concrete applications." Magazine of Concrete Research 55(1): 16.

Lee, H. M., H. S. Park, I. Lee, H. Adeli.(2005). Displacement measuring model of continuous steel beams using terrestrial LiDAR. 4th World Conference on Structural Control and Monitoring.

Lee, J. and M. Shinozuka (2006). "Real-time displacement measurement of a flexible bridge using digital image processing techniques." Experimental Mechanics 46(1): 105-114.

Lehmann, E., P. Vontobel, R. Hassanein. (2006). Neutron tomography as tool for applied research and technical inspection. Advances in Solid State Physics**:** 389-405.

Li, G. (2004). The effect of moisture content on the tensile strength properties of concrete. Gainesville, Florida, U.S.A., University of Florida. Master of Engineering.

Li, J. and C. Liu (2001). "Noncontact detection of air voids under glass epoxy jackets using a microwave system." Subsurface Sensing Technologies and Applications 2(4): 411-423.

Ling, H.-y., K.-t. Lau, L. Cheng, W. Jin.(2005). "Fibre optic sensors for delamination identification in composite beams using a genetic algorithm." Smart Materials and Structures 14(1): 287-295.

Liu, W., S.-E. Chen, K. Dai, C. Rice, B. Phibrick, E. Hauser, Z. Hu, C. K. Huyck, C. Boyle.(2010). Bridge evaluation through advanced noncontact sensing techniques. Transportation Research Board 89th Annual Meeting. Washington, D.C., Transportation Research Board of IHF National Academies.

Lo, Y.-L. and F.-Y. Xiao (1998). "Measurement of corrosion and temperature using a single-pitch Bragg grating fiber sensor." Journal of Intelligent Material Systems and Structures 9(10): 800-807 10.1177/1045389x9800901003: 10.1177/1045389x9800901003.

Lopes, V., Jr., G. Park, H. H. Cudney, D. J. Inman.(2000). "Impedance-based structural health monitoring with artificial neural networks." Journal of Intelligent Material Systems and Structures 11(3): 206-214 10.1106/h0ev-7pwm-qyhw-e7vf: 10.1106/h0ev-7pwm-qyhw-e7vf.

Lynch, J. P. (2005). "Design of a wireless active sensing unit for localized structural health monitoring." Structural Control and Health Monitoring 12: 405-423.

Lynch, J. P. and K. J. Loh (2006). "A summary review of wireless sensors and sensor networks for structural health monitoring." The Shock and Vibration Digest 38(2): 91-128.

Lynch, J. P., Y. Wang, K. C. Lu, T. C. Hou, C. H. Loh.(2006). "Post-seismic damage assessment of steel structures instrumented with self-interrogating wireless sensors."

Maas, H.-G. and U. Hampel (2006). "Photogrammetric techniques in civil engineering material testing and structure monitoring." Photogrammetric Engineering & Remote Sensing **72**(1): 7.

Maser, K. R. and M. Bernhardt (2000). Statewide bridge deck survey using ground penetrating radar. Structural Materials Technology IV: An NDT Conference. S. Alampalli. Lancaster, PA, Technomic Publishing Company**:** 31-37.

Maser, K. R. and W. M. K. Roddis (1990). "Principles of thermography and radar for bridge deck assessment." Journal of Transportation Engineering 116(5): 583-601.

Masri, S. F., L. H. Sheng, J. P. Caffrey, R. L. Nigbor, M. Wahbeh, A. M. Abdel-Ghaffar.(2004). "Application of a Web-enabled real-time structural health monitoring system for civil infrastructure systems." Smart Materials and Structures 13(6): 1269-1283.

MBE 2008, Manual for Bridge Evaluation, American association of State Highway and Transportation Officials, Washington DC, U.S.A.

Mehrabi, A. B. (2006). "In-service evaluation of cable-stayed bridges, overview of available methods, and findings." Journal of Bridge Engineering 11(6): 716-724.

Meng, X., A. H. Dodson, G. W. Roberts.(2007). "Detecting bridge dynamics with GPS and triaxial accelerometers." Engineering Structures 29(11): 3178-3184.

Meola, C., G. M. Carlomagno, L. Giorleo.(2004). "Geometrical limitations to detection of defects in composites by means of infrared thermography." Journal of Nondestructive Evaluation 23(4): 125-132.

Merzbacher, C. I., A. D. Kersey, E. J. Friebele.(1996). "Fiber optic sensors in concrete structures: a review." Smart Materials and Structures 5(2): 196-208.

Meyendorf, N. G. H., H. Rösner, V. Kramb, S. Sathish.(2002). "Thermo-acoustic fatigue characterization." Ultrasonics 40(1-8): 427-434 10.1016/S0041-624X(02)00155-5: 10.1016/S0041-624X(02)00155-5.

Michaloudaki, M., E. Lehmann, D. Kosteas.(2005). "Neutron imaging as a tool for the non-destructive evaluation of adhesive joints in aluminium." International Journal of Adhesion and Adhesives 25(3): 257-267.

Molin, N. E., M. Sjodahl, P. Gren, A. Svanbro.(2004). "Speckle photography combined with speckle interferometry." Optics and Lasers in Engineering 41: 673-686.

Morey, R. M. (1998). Ground penetrating radar for evaluating subsurface conditions for transportation facilities.

Nizovtsev, M. I., S. V. Stankus, A. N. Sterlyagov, V. I. Terekhov, R. A. Khairulin.(2008). "Determination of moisture diffusivity in porous materials using gamma-method." International Journal of Heat and Mass Transfer 51(17-18): 4161-4167.

Olaszek, P. (1999). "Investigation of the dynamic characteristic of bridge structures using a computer vision method." Measurement 25(3): 227-236.

Olhoeft, G. R. and S. S. Smith (2000). "Automatic processing and modeling of GPR data for pavement thickness and properties."

Panova, A. A., P. Pantano, D. R. Walt.(1997). "In situ fluorescence imaging of localized corrosion with a pH-sensitive imaging fiber." Analytical Chemistry 69(8): 1635-1641 10.1021/ac961025c: 10.1021/ac961025c.

Park, G., H. H. Cudney, D. J. Inman. (2000). "Impedance-based health monitoring of civil structural components." Journal of Infrastructure Systems 6(4).

Park, H. S., H. M. Lee, H. Adeli. (2007). "A new approach for health monitoring of structures: terrestrial laser scanning." Computer-Aided Civil and Infrastructure Engineering 22.

Pedrini, G. and H. J. Tiziani (1994). "Double-pulse electronic interferometry for vibration analysis." Optical Society of America.

Perez-Gracia, V. (2008). "Horizontal resolution in a non-destructive shallow GPR survey: an experimental evaluation." NDT & E International 41: 611-620.

Pieraccini, M., M. Fratini, F. Parrini, G. Macaluso, C. Atze ni.(2004). "High-speed CW step-frequency coherent radar for dynamic monitoring of civil engineering structures." Electronics Letters 40(14): 907-908.

Pieraccini, M., G. Luzi, D. Mecatti, M. Fratini, L. Noferini, L. Carissimi, G. Franchioni, C. Atzeni, (2004). "Remote sensing of building structural displacements using a microwave interferometer with imaging capability." NDT & E International 37(7): 545-550.

Prado, P. J., B. J. Balcom, S. D. Beyea, R. L. Armstrong, T. W. Bremner. (1997). "Concrete thawing studied by single-point ramped imaging." Solid State Nuclear Magnetic Resonance 10(1-2): 1-8.

Rao, M. R. P. D. (2007). Review of nondestructive evaluation techniques for FRP composite structural components. Department of Civil and Environmental Engineering. Morgantown, WV, West Virginia University. Master of Science in Civil Engineering: 225.

Rice, C., S.-E. Chen, K. Dai, W. Liu, R. Eguchi, E. Hauser, C. Boyle, B. Phibrick. (2010). Remote sensing techniques for bridge inspections. Transportation Research Board 89th Annual Meeting. Washington, D.C., Transportation Research Board of IHF National Academies.

Roth, D. J., L. M. Cosgriff, R. E. Martin, M. J. Verrilli, R. T. Bhatt.(2003). Microstructural and defect characterization in ceramic composites using an ultrasonic guided wave scan system. 30th Annual Review of Quantitative Nondestructive Evaluation (QNDE). Green Bay, WI, U.S.A.

Ryan, T. W., R. A. Hartle, J. E. Mann, L. J. Danovich. (2006). "Bridge Inspector‘s Reference Manual." (FHWA NHI 03-001).

Santulli, C. (2000). Impact damage evaluation in woven composites using acoustic and thermoelastic techniques. Department of Engineering. Liverpool, U.K., University of Liverpool. Doctor of Philosophy: 253.

Schueler, R., S. P. Joshi, K. Schulte. (2001). "Damage detection in CFRP by electrical conductivity mapping." Composites Science and Technology 61(6): 921-930.Singh, V., G. M. Lloyd, M. L. Wang.(2004). "Effects of temperature and corrosion thickness and composition on magnetic measurements of structural steel wires." NDT & E International 37(7): 525-538.

Song, G., Y. L. Mo, K. Otero, H. Gu.(2006). "Health monitoring and rehabilitation of a concrete structure using intelligent materials." Smart Materials and Structures 15(2): 309.

Steckenrider, J. S. and J. W. Wagner (1995). "Computed speckle decorrelation (CSD) for the study of fatigue damage." Optics and Lasers in Engineering 22(1): 3-15.

Stepanova, L. N., E. Y. Lebedev, A. E. Kareev, V. N. Chaplygin, S. A. Katarushkin.(2004). "Use of the acoustic emission method in detecting the fracture process in specimens made of composite materials." Russian Journal of Nondestructive Testing 40(7): 455-461.

Stephen, V., S. Kharkovsky, J. Nadakuduti, R. Zoughi.(2004). "Microwave field measurement of delaminations in CFRP concrete members in a bridge." Journal of Materials in Civil Engineering.

Sumitro, S., A. Jarosevic, M. L. Wang.(2002). "Elasto-magnetic sensor utilization on steel cable stress measurement."

Tanner, N. A., J. R. Wait, C. R. Farrar, H. Sohn.(2003). "Structural health monitoring using modular wireless sensors." Journal of Intelligent Material Systems and Structures 14.

USDOT (2001). Highway Bridge Inspection: State-of-the-Practice Survey. T.-F. H. R. Center. Mclean, VA, U.S.A., U.S. Department of Transportation, Federal Highway Administration.

Van der Kruk, J. (2003). "Three-dimensional GPR imaging in the horizontal wavenumber domain for different heights of source and receiver antennae."

Wen, S. and D. D. L. Chung (2000). "Damage monitoring of cement paste by electrical resistance measurement." Cement and Concrete Research 30(12): 1979-1982.

Whelan, M. J., M. V. Gangone, K. D. Janoyan, K. Cross, R. Jha.(2007). "Reliable high-rate bridge monitoring using dense wireless sensor arrays." 8.

Winfree, W. P. (1998). "Enhanced thermographic detection of delaminations with computational pulse shaping." Review of Progresss in Quantitative Nondestructive Evaluation 17A: 441-447.

Yu, X. and X. Yu (2009). "Time domain reflectometry automatic bridge scour measurement system: principles and potentials." Structural Health Monitoring 8(6): 463-476 10.1177/1475921709340965: 10.1177/1475921709340965.

Zhang, G., R. S. Harichandran, P. Ramuhalli.(2010). NDE of concrete bridge deck delamination using enhanced acoustic method. Transportation Research Board 89th Annual Meeting. Washington, D.C., Transportation Research Board of IHF National Academies.

Zhang, Z. Y. and M. O. W. Richardson (2005). "Visualisation of barely visible impact damage in polymer matrix composites using an optical deformation and strain measurement system (ODSMS)." Composites Part A: Applied Science and Manufacturing 36(8): 1073-1078.

Zilberstein, V., K. Walrath, D. Grundy, D. Schlicker, N. Goldfine, E. Abramovici, T. Yentzer.(2003). "MWM eddy-current arrays for crack initiation and growth monitoring." International Journal of Fatigue 25(9-11): 1147-1155.

Appendix C – Technical Memorandums

MichiganTech Transportation Institute

Memo

To: L. Sutter, D. Harris, R. Shuchman, J. Burns, C. Brooks, R. Wallace

From: T. Ahlborn

CC: P. Hannon

Date: March 31, 2010

Technical Memorandum Number: 01

Re: Technical Advisory Council

Letters of invitation to join the BC/RS RITA team Technical Advisory Council have been sent to the transportation field members previously identified during our bi-weekly team meetings. A request for an answer by April 9, 2010 was noted as seen in the attached sample letter.

In addition to the letter of invitation, each potential TAC member received a copy of the project abstract to provide them additional information about the project as well as a list of duties and purpose of membership in the TAC. These documents are also attached.

Letters of invite were sent to the following:

Steve Cook, Michigan DOT (accepted)
Roger Surdahl and Krishna Verma, FHWA
Amy Trahey, Great Lakes Engineering Group (accepted)
Carin Roberts-Wollman, Virginia Tech (accepted)
Kelley Rehm, AASHTO (declined due to conflict of interest with UNC project)*
Duane Otter, Transportation Technology Center, Inc. (accepted)
Doug Couto, Transportation Research Board
David Hohmann, Texas DOT (declined and recommended a better qualified candidate)**
Peter Sweatman, University of Michigan Transportation Research Institute (accepted)
Brent Bair, Road Commission for Oakland County***
Dan Johnston, South Dakota DOT (accepted)
Charles Ishee, Florida DOT

*Kelly Rehm recommended Michael Johnson, CALTRANS
**David Hohmann recommended Keith Ramsey, Texas DOT (accepted)
***Brent Bair will be replaced with Dennis Kolar per Brent's suggestion (accepted)

The first TAC meeting is scheduled to be held in Ann Arbor, MI in May 2010.

MichiganTech Transportation Institute

Memo

To: T. Ahlborn, L. Sutter, D. Harris, R. Shuchman, C. Brooks, J. Burns, R. Wallace

From: P. Hannon

CC: K.A. Endsley, K. Vaghefi, D.C. Evans, R. Oats

Date: June 1, 2010

Technical Memorandum Number: 02 (revised)

Re: TAC Meeting

The first meeting of our Technical Advisory Council is scheduled for June 16-17, 2010 at the MTRI offices in Ann Arbor MI. This location will allow for easier travel for our council members than traveling to our Houghton campus.

The TAC members are:

Steve Cook – Michigan Department of Transportation
Roger Surdahl – Federal Highway Administration
Krishna Verma – Federal Highway Administration
Amy Trahey – Great Lakes Engineering Group
Carin Roberts-Wollmann – Virginia Tech
Keith Ramsey – Texas Department of Transportation
Michael Johnson – CalTrans
Duane Otter – Transportation Technology Center, Inc.
C. Douglas Couto – Transportation Research Board
Peter Sweatman – University of Michigan Transportation Research Institute
Dennis Kolar – The Road Commission for Oakland County
Dan Johnston – Independent Materials Consultant
Charles Ishee – Florida Department of Transportation

A detailed agenda is currently being developed. The meeting will begin on Wednesday evening with a short social, followed by a full a day of activities on Thursday and adjourning so that council members can travel back that evening. Details of the agenda will be discussed in our upcoming bi-weekly team conference call.

MichiganTech Transportation Institute

Memo

To: T. Ahlborn, L. Sutter, D. Harris, R. Shuchman, J. Burns, R. Wallace

From: C. Brooks

CC: P. Hannon

Date: March 31, 2010

Technical Memorandum Number: 03

Re: State of the Practice Synthesis

Progress on Deliverable 2-A: State of the Practice Synthesis Report

The project team has been reviewing and summarizing the state of the practice for bridge sensing technologies in preparation of submitting the first deliverable for the Bridge Condition Characterization task. This State of the Practice Synthesis Report will review existing and newer technologies being used for structural health monitoring of bridges. Our draft report is under development, and we have divided into eight sections, described below, with three main sections describing sensing technologies that are in-situ, on-site ("local") remote sensing technologies, and remote monitoring technologies typically not collected onsite. The draft eight reports sections are:

1. Abstract
2. Overview
3. In-Situ Monitoring Techniques
4. On-Site Monitoring Techniques
5. Remote Monitoring Techniques
6. Sensing of Exceptional Materials and Structures
7. Case Studies
8. References

Note that as part of the references section, we are building a detailed EndNote electronic reference database that we anticipate sharing via the project website as a supplement to the Synthesis Report. This should be of high interest and value to the research community as so far it contains over 360 references of book chapters, conference papers, journal articles, government reports, theses, web pages, and patents relevant to structural health monitoring of bridges.

Sections 3, 4, and 5 are the main body of the report. Section 3, on in-situ monitoring techniques, currently includes reviews of the following sensing technologies:

3.1 Accelerometers and Velocimeters
3.2 Electrical Resistance
3.3 Electromechanical Impedance
3.4 Fiber Optics
3.5 GPS and Geodetic Measurements
3.6 Magnetic and Magneto-Elastic
3.7 Ultrasonic Emissions and Lamb Waves

Section 4, for on-site monitoring techniques, includes reviews of the following sensing technologies:

4.1 Eddy Currents
4.2 Electrical Time-Domain Reflectometry (TDR)
4.3 Infrared Thermography and Spectroscopy
4.4 Laser Scanning
4.5 Nuclear Magnetic Resonance (NMR) Imaging
4.6 Microwave Radar
4.7 Ground-Penetrating Radar (GPR)
4.8 X-Ray, Gamma Ray, and Neutron Radiography

Section 5, on "remote" monitoring technologies, includes reviews of the following sensing technologies:

5.1 Electro-Optical Imagery and Photogrammetry (includes aerial photography and satellite imagery)
5.2 Speckle Photography and Speckle Pattern Interferometry
5.3 Interferometric Synthetic Aperture Radar (IfSAR)

We will be improving the current draft of the report by ensuring that a reasonably comprehensive list of sensing technologies has been included and that the technologies have

been described with appropriate level of detail at a synthesis level to be of use to transportation professionals and the research community. We anticipate that this document will be of enough interest and quality to be formatted into a peer-reviewed publication submission. The Synthesis Report will be made available through the project website at http://www.mtti.mtu.edu/bridgecondition (under "Tasks and Deliverables"), once approved by USDOT-RITA.

MichiganTech Transportation Institute

Memo

To: T. Ahlborn, L. Sutter, B. Shuchman, D. Harris, J. Burns, C. Brooks

From: D. Evans

CC: P. Hannon, K. Vaghefi, K. A. Endsley, R. Oats

Date: June 30, 2010

Technical Memo Number: 04

Re: State of the Practice Synthesis

The State-of-the-Practice of Modern Structural Health Monitoring for Bridges: A Comprehensive Review is now centrally located on the Wiki site. The report will be included in the second quarterly report due to the USDOT-RITA by July 15, 2010. This report will also be posted on the project web site as a stand-alone document once it is approved by the project manager.

MichiganTech Transportation Institute

Memo

To: L. Sutter, D. Harris, D. Evans, R. Oats, K. Vaghefi

From: T. Ahlborn

CC: R. Shuchman, J. Burns, C. Brooks, K.A. Endsley, C. Roussi, B. Hart, P. Hannon

Date: July 14, 2010

Technical Memo Number: 05

Re: Laboratory Work Plans and Specimen Fabrication

Attached are four laboratory work plans as proposed by our MTRI team members.

1. Experimental Plan for Field Spectra Data Collection to support Bridge Surface Condition Assessment

2. Experimental Plan for High-Resolution Digital Image Analysis to support Bridge Surface Condition Assessment

3. Experimental Plan for Preliminary Investigation of Radar Applications for Bridge Deck Sensing

4. Experimental Plan for Digital Image Correlation and Tracking for Measuring Displacement of a Structural Element

It is necessary to review these plans for completeness and provide feedback to MTRI. The review will be completed on two levels. First, a review and discussion will be conducted to ensure that these plans fulfill and encompass the overall objectives of the project and second, that the details (specification size, quantity, etc.) are adequate to address the individual plan goals.

Discussion of these plans will continue during our next bi-weekly conference call such that feedback can be incorporated. These sample work plans are to be considered as living documents, and will continue to be revised as we progress.

Also attached are the specimen fabrication details of the thin-slab specimens that were cast in our structures and materials laboratory in April, 2010.

Experimental Plan for Field Spectra Data Collection to support Bridge Surface Condition Assessment

Rick Powell and Colin Brooks, MTRI
Version of 3/30/2010
Revised 7/14/10, Tess Ahlborn, MTTI

Overview and Objective

The current state of knowledge about the spectral characteristics of bridge surface condition, and the relationship of these characteristics to indicators of bridge condition, is inadequate. The availability of high spatial resolution multispectral and hyperspectral remote-sensing systems, with the potential to cost-effectively enhance current bridge inspection practices, drives the need to conduct a detailed study of spectral properties of a variety of bridge surface conditions. Surface defects such as spalling, scaling, cracking, and other observable defects that present themselves in the field are the primary focus of the study. We will focus on these indicators of bridge condition, while investigating other targets of opportunity within focused field data collections.

Our objective is to develop a library of the spectral characteristics of various bridge surface defects, conduct a quantitative assessment of spectral separability, and an evaluation of which wavelengths are most suitable for spectral separation of critical bridge condition features. The results are intended both to identify the specifications of an optimal sensor for bridge condition assessment, and to asses the potential for field spectral reflectance units (such as spectroradiometers) to become part of a future bridge inspection process.

The study will be conducted in both the field and in the lab. Bridges with known surface defects in Washtenaw and Oakland counties in Michigan will be used to collect measurements with the assistance of the respective Road Commissions. We propose that the Michigan Tech Structures and Materials Laboratories will develop concrete blocks of identical shapes, size, and composition to evaluate the spectral response of surface defects over time.

Spectroradiometer Measurements

Spectra will be acquired with an Analytical Spectral Devices (ASD) FieldSpec3 spectroradiometer (Analytical Spectral Devices, Boulder, CO). The spectroradiometer samples a spectral range of 350–2500 nm. The instrument uses three detectors spanning the visible and near-infrared (VNIR) and short-wave infrared (SWIR1 and SWIR2), with a spectral sampling interval of 1.4 nm for the VNIR detector and 2.0 nm for the SWIR detectors. Field-based bridge surface measurements will be taken within two hours of solar noon and bracketed by Spectralon (Labsphere, North Sutton, NH) 100% reflective standard. The unit is GPS-enabled and records

the location of each sample in a format suitable for mapping and relating to remote sensing imagery.

Field spectra of relatively large bridge surface defects such as spalling (holes, roughness) and cracks will be captured at nadir from a height of 1 m using the bare fiber optic input, which provides a field of view of approximately 43 cm in diameter. Moderate and smaller sized surface defects will be acquired from the same height using the unit's 8° foreoptic, with a field of view of approximately 30cm. Select targets of opportunity will be acquired from nadir, 5°, 30°, 45°, and 60° using bare fiber and the 8° foreoptic mounted to a tripod to evaluate the Bidirectoral Reflectance Distribution Function (BRDF) of the surface defects and explore if better spectral separation of conditions can be achieved at off-nadir viewing geometries.

Preliminary Field Data Collection and Exploratory Analysis:

A preliminary set of spectroradiometer measurements, as described above, will be collected at three local bridges representing a variety of bridge deck surface conditions. These include a recently constructed bridge deck with no observable surface defects, a bridge deck surface with some moderate surface defects, and an older bridge deck with significant amounts of surface roughness. MDOT safety procedures will be used on any roadway or bridge data collections. Field data collection procedures will be implemented and evaluated for utility, and may be revised for future data collections. An exploratory data analysis of the preliminary data collection will be performed to evaluate the spectral response of the various levels of bridge surface deck deterioration. The results of the preliminary data analysis may be used to inform and revise future field data collections, including target selection, and analysis techniques. We anticipate a 2-week period to complete this exploratory analysis.

Lab Sampling Procedure:

To investigate the effect of chloride contamination on bridge surfaces, concrete samples would be artificially degraded and the spectrum measured periodically.

We propose that the Michigan Tech Structures and Materials Laboratories would develop 4 concrete blocks of identical shapes, size (30 x 30 x 6 cm^3), and composition (curing, cure temperature, and aggregate materials) identical to that used in bridge surfaces. One sample will be retained as control. The other 3 samples will be exposed to a 10% solution of chloride for 12 weeks. Spectral measurements will be collected every week for the 12 week period. Sampling the blocks during the exposure period will be collected as well when feasible.

The Fieldspec3 spectroradiometer (ASD Inc.) with a spectral range of 350–2500 nm will be used to collect reflectance spectra of the concrete blocks in the laboratory with a quartz–tungsten–halogen (QTH) lamp as a light source. Diffused light from the 100 W light source will be used to illuminate the concrete block at 45° angles when spectra are collected in the laboratory. The foreoptic of the spectroradiometer will be aligned vertically, and the height of the foreoptics from the top of the concrete block will be adjusted so that reflected light only from the surface of

the concrete block will fill the field of view (FOV) of the instrument. Spectra will be collected at a height of at 30 cm from the surface of each concrete block. The Spectralon (Labsphere, North Sutton, NH) 100% reflective standard will be used to calibrate before recording each concrete spectra.

Correlation between degradation level and spectral response:
We will analyze the statistical relationship between degradation (as known from lab samples, or as visible in the field) and the spectral response measured by the Fieldspec3. We will also perform an analysis to investigate the relationship between degradation depth (such as chloride penetration) and spectral response. This will include having samples analyzed in Houghton for degradation depth. We will calculate a first order derivative for change at each wavelength over time of degradation (estimates degradation), and compare estimates to actual degradation.

Time Period

Field data collection should occur during the spring and summer seasons (late April-August) when solar radiation and angle are optimal. Lab-based measurement may occur at any period, but we recommend starting in the Spring so that lab samples can be created. Field data collection, analysis, and reporting is estimated to be completed within 60 days, with primary labor support for Rick Powell (at ¼ time), Rick Dobson (at ¼ time), plus a ½ time intern, with limited coordination support (1 day per pay period) for Colin Brooks. Limited additional time would be needed to collect the spectral profiles of the concrete samples, in coordination with the Michigan Tech lab.

Sampling Procedure:

For each sampling point:

1. **Measure Reflectance Spectra.**

   For each sample site, the instrument will be optimized and calibrated to white reference.

   Spectral reflectance will be collected.

   Five samples will be collected for each measurement.

   Each sample will consist of the average of 25 scans.

   Field Spectra Sampling Form (Appendix A) will be completed for each location in the field and for each concrete sample block.

2. **Digital Photographs** Surface, weather conditions and context will be recorded with GPS attributed photographs at each sampling location.

3. **GPS Point:** Although the spectroradiometer instrument controller will be configured to record GPS location, the high-resolution Trimble GeoExplorer GPS unit will be used to record the point as backup.

Required Resources:

1. 100 W quartz–tungsten–halogen (QTH) lamp
2. 2- person crew
3. Map of study sites
4. ASD FieldSpec3 Spectroradiometer with Instrument Controller.
5. Two GPS units (WAAS enabled Garmin & differential correction-capable Trimble unit)
6. Data forms (FieldSpec)
7. Pencils, clipboard, black markers
8. Digital camera
9. Safety equipment (including orange blazer, steel-toed boots, car light, hard hat) for data collections on or near roadways and bridges; safe data collection procedures will be used for all data collections.

MichiganTech Research Institute

Appendix A. Spectrometer Field Data Collection Form.

FIELD SPECTROMETER DATA					
PROJECT NAME:					
DATE/TIME:					
SITE:				OBSERVER:	
PHOTO REFERENCE:					
COORDINATES	X:			Y:	
INSTRUMENT ID:			# OF SCANS AVG:		
GEOMETRY OF OBSERVER'S POSITION RELATIVE TO INCIDENT RADIATION *sketch or description*					
HEIGHT OF INSTRUMENT ABOVE GROUND:				ABOVE TARGET:	
SCAN NO.	TARGET	TIME	SKY CONDITION		COMMENT

Experimental Plan for High-Resolution Digital Image Analysis to support Bridge Surface Condition Assessment

Colin Brooks, Rick Powell, Rick Dobson, MTRI
Version of 3/30/2010

Overview and Objective

Understanding the surface condition of bridge decks is a priority method of evaluating bridge condition for transportation departments. One measure used by MDOT, amongst others, is to assess the percentage of a bridge deck that has visible delamination. One example trigger level for indicating a significant problem described by MDOT at our February 5th, 2010 kickoff meeting was greater than 30% deck delamination. Greater than 10% delamination was described a trigger for an in-depth inspection. Major deck cracking is an additional problem described by MDOT.

To sense and analyze these problems, we propose to perform a high-resolution digital photograph collection taken from above the bridge deck at sufficient height to collect overlapping stereo-capable images. Our primary objective is to demonstrate the capability of using custom image processing algorithms developed by MTRI to rapidly estimate the frequency, size, depth, and distribution of delamination features on a bridge deck. Demonstrating capability for automatic recognition and characterization of major deck cracking, at resolutions higher than is capable with aerial photography or satellite imagery, is a secondary objective. Both of these objectives serve the larger project focus of demonstrating where remote sensing can effectively and efficiently be used to assess bridge condition.

The study will primarily be field-focused, using local and State bridges with visible surface defects in the southeast Michigan area. Lab-created control samples will be sensed on a representative basis. Based on available maps, proximity, and our relationships with local road commissions, we will focus on Washtenaw and Oakland counties in Michigan, with the assistance of the respective Road Commissions and MDOT.

Digital Imagery Collection

We will use a digital SLR (DSLR) camera to collect the high-resolution photographs needed for this study. The Spatial Analysis Lab currently has a Nikon D40 DSLR available for check-out; other high-resolution cameras could be used as purchased or loaned to the study. The Nikon D40 (http://www.nikonusa.com/Find-Your-Nikon/ProductDetail.page?pid=25420) is a recent and advanced DSLR appropriate for use in the study. Its relevant specifications are:

Focal Length: 18-135mm (we will use 18mm for the project)
Focal Length Multiplier: 1.5
Field-of-View (FOV) Horizontal: 67.4 Deg

FOV Vertical: 47.9 Deg
FOV Diagonal: 77.4 Deg
6.1 megapixels resolution (3008 x 2000 pixels)
DX-format CCD image sensor, 15.6 x 23.7 mm size

As we are proposing to do both image processing for feature analysis and stereo-pair analysis to characterize delamination depth, we will require collection from an appropriate height to capture these data. For a single-camera, single photo system, the horizontal field-of-view (FOV) of the camera can be used in a simple trigonometric equation to calculate the height at which photos need to be collected to capture a certain width of road area. Similarly, for a two-camera system set up to simultaneously acquire the 60% overlap normally used for stereo photography (Falkner, 1995), the camera height required for this overlap for certain widths can be calculated. Table 1 shows the camera height needed for a single-camera, single-photo system. Table 2 shows the height needed for the two-camera, 60% overlap system we propose to apply for this study, under the assumption we can implement one inexpensively. Note that typical lane widths are highlighted in the figures. We have also calculated the heights needed for a system where a single camera would take three photos across the roadway.

Table 1: Collection heights required for a single-camera system:

Nikon D40

Focal Length	18mm
Focal Length Multiplier	1.5
FOV Horizontal	67.4 Deg
FOV Vertical	47.9 Deg
FOV Diagonal	77.4 Deg

FOV-H = Field of View - Horizontal
FOV-V = Field of View - Vertical
FOV-D = Field of View - Diagonal

These calculations are for a single camera.

FOV-H (ft)	Camera Height (ft)	Camera Height (m)	FOV-V (ft)	FOV-D (ft)	
1	0.75	0.23	0.89	1.60	
2	1.50	0.46	1.78	3.20	
3	2.25	0.69	2.67	4.81	
4	3.00	0.91	3.55	6.41	
5	3.75	1.14	4.44	8.01	
6	4.50	1.37	5.33	9.61	
7	5.25	1.60	6.22	11.22	
8	6.00	1.83	7.11	12.82	
9	6.75	2.06	8.00	14.42	
10	7.50	2.29	8.88	16.02	
11	8.25	2.51	9.77	17.63	
12	9.00	2.74	10.66	19.23	**Single Lane**
13	9.75	2.97	11.55	20.83	
14	10.50	3.20	12.44	22.43	
15	11.25	3.43	13.33	24.03	
16	12.00	3.66	14.21	25.64	
17	12.75	3.88	15.10	27.24	
18	13.49	4.11	15.99	28.84	**Single Lane with Shoulder**
19	14.24	4.34	16.88	30.44	
20	14.99	4.57	17.77	32.05	
21	15.74	4.80	18.66	33.65	
22	16.49	5.03	19.54	35.25	
23	17.24	5.26	20.43	36.85	
24	17.99	5.48	21.32	38.46	**Two Lanes**
25	18.74	5.71	22.21	40.06	
26	19.49	5.94	23.10	41.66	
27	20.24	6.17	23.99	43.26	
28	20.99	6.40	24.87	44.86	
29	21.74	6.63	25.76	46.47	
30	22.49	6.86	26.65	48.07	**Two Lanes with Shoulder**
31	23.24	7.08	27.54	49.67	
32	23.99	7.31	28.43	51.27	
33	24.74	7.54	29.32	52.88	
34	25.49	7.77	30.20	54.48	
35	26.24	8.00	31.09	56.08	
36	26.99	8.23	31.98	57.68	**Three Lanes or Two Lanes with two Shoulders**
37	27.74	8.46	32.87	59.29	
38	28.49	8.68	33.76	60.89	
39	29.24	8.91	34.65	62.49	
40	29.99	9.14	35.53	64.09	
41	30.74	9.37	36.42	65.69	
42	31.49	9.60	37.31	67.30	**Three Lanes with Shoulder**
43	32.24	9.83	38.20	68.90	
44	32.99	10.05	39.09	70.50	
45	33.74	10.28	39.98	72.10	
46	34.49	10.51	40.86	73.71	
47	35.24	10.74	41.75	75.31	
48	35.99	10.97	42.64	76.91	**Three Lanes with Two Shoulders**

Table 2: Collection heights required for a dual-camera system with 60% overlap.

Nikon D40

Focal Length	18mm
Focal Length Multiplier	1.5
FOV Horizontal	67.4 Deg
FOV Vertical	47.9 Deg
FOV Diagonal	77.4 Deg

FOV-H = Field of View - Horizontal
FOV-V = Field of View - Vertical
FOV-D = Field of View - Diagonal

These calculations are for a 2 camera system.

60% Overlap Width (ft)	Camera Height (ft)	Camera Height (m)	Total FOV-H (ft)	FOV-V (ft)	FOV-D (ft)	
1	1.25	0.38	2.33	1.11	2.58	
2	2.50	0.76	4.67	2.22	5.17	
3	3.75	1.14	7.00	3.33	7.75	
4	5.00	1.52	9.33	4.44	10.34	
5	6.25	1.90	11.67	5.55	12.92	
6	7.50	2.29	14.00	6.66	15.50	
7	8.75	2.67	16.33	7.77	18.09	
8	10.00	3.05	18.67	8.88	20.67	
9	11.25	3.43	21.00	9.99	23.26	
10	12.50	3.81	23.33	11.10	25.84	
11	13.74	4.19	25.67	12.21	28.42	
12	14.99	4.57	28.00	13.32	31.01	**Single Lane**
13	16.24	4.95	30.33	14.43	33.59	
14	17.49	5.33	32.67	15.54	36.17	
15	18.74	5.71	35.00	16.65	38.76	
16	19.99	6.09	37.33	17.76	41.34	
17	21.24	6.47	39.67	18.87	43.93	
18	22.49	6.86	42.00	19.98	46.51	**Single Lane with Shoulder**
19	23.74	7.24	44.33	21.09	49.09	
20	24.99	7.62	46.67	22.20	51.68	
21	26.24	8.00	49.00	23.31	54.26	
22	27.49	8.38	51.33	24.42	56.85	
23	28.74	8.76	53.67	25.53	59.43	
24	29.99	9.14	56.00	26.64	62.01	**Two Lanes**
25	31.24	9.52	58.33	27.75	64.60	
26	32.49	9.90	60.67	28.86	67.18	
27	33.74	10.28	63.00	29.97	69.77	
28	34.99	10.66	65.33	31.08	72.35	
29	36.24	11.04	67.67	32.19	74.93	
30	37.49	11.43	70.00	33.30	77.52	**Two Lanes with Shoulder**
31	38.74	11.81	72.33	34.41	80.10	
32	39.98	12.19	74.67	35.52	82.69	
33	41.23	12.57	77.00	36.63	85.27	
34	42.48	12.95	79.33	37.74	87.85	
35	43.73	13.33	81.67	38.85	90.44	
36	44.98	13.71	84.00	39.96	93.02	**Three Lanes or Two Lanes with two Shoulders**
37	46.23	14.09	86.33	41.07	95.60	
38	47.48	14.47	88.67	42.18	98.19	
39	48.73	14.85	91.00	43.29	100.77	
40	49.98	15.23	93.33	44.40	103.36	
41	51.23	15.62	95.67	45.51	105.94	
42	52.48	16.00	98.00	46.62	108.52	**Three Lanes with Shoulder**
43	53.73	16.38	100.33	47.73	111.11	
44	54.98	16.76	102.67	48.84	113.69	
45	56.23	17.14	105.00	49.95	116.28	
46	57.48	17.52	107.33	51.06	118.86	
47	58.73	17.90	109.67	52.17	121.44	
48	59.98	18.28	112.00	53.28	124.03	**Three Lanes with Two Shoulders**

Using a two-lane roadway on a bridge with shoulder as our representative collection scenario, we would need a height of 11.43 meters (37.49 feet) for a dual-camera, 60%-overlap data collection for a system travelling down the roadway. For a single-camera system, taken from the side of the road with 60% overlap, with manual placing of the camera to get the next overlapping photo, the one-camera height of 6.86 meters (22.49 feet) would suffice. We are anticipating that this would require access to a "cherry picker" (boom lift), except in rare cases where a nearby overpass or building would provide the equivalent needed height and view of a bridge deck surface. It is our intention that this scenario would represent a future "real-world" data collection methodology for use by Departments of Transportation, which is a focus of the project sponsor.

To create the stereo photography and resulting high-resolution digital elevation model (DEM), we will use the advanced capabilities of the new ERDAS 2010 software now available in the MTRI Spatial Analysis Lab. While designed to produce DEMs from aerial photography with dedicated aerial cameras, it has also been used to generate DEMs from DSLRs. We will test this

capability with an initial experiment using a height from a local building or other height (such as the top of a truck rented for another project data collection). We will also test feasibility on at least two samples created by the MTTI lab with controlled delamination and spalling issues. The custom DEM created through this process would also help in confirming that a feature is a delamination with a measurable depth of deck loss.

For analyzing the frequency, size, and distribution of delaminations, we propose to develop and apply a combination of custom algorithms in MATLAB, ENVI+IDL, and Definiens. It is noteworthy that even with the application of commercial image processing software, we will still be developing a custom algorithm for delamination characterization. We will not be applying just "out-of-the-box" software for our analysis. These algorithms should form part of the input for the Bridge Condition Assessment Decision Support System that will result from the larger project. MATLAB's image processing capabilities, the pixel-based strengths of ENVI that are customizable with IDL, and Definiens' capability to enable custom algorithm development will all be used, as appropriate, for our algorithm creation.

For automatic recognition and characterization of major deck cracking, we propose to develop a custom algorithm using the advanced object-based capabilities of our image processing software. We will use this opportunity to assess if our recent reliance on the object-based image classification capabilities of Definiens are still the best tool for algorithm development, given other new software developments. ENVI now has the "Feature Extraction Module" while ERDAS has the "IMAGINE Objective" tool that appears appropriate for this study based on our review of its capabilities. In particular, the capability to encode custom algorithms in the Feature Models capability of IMAGINE Objective makes that tool appropriate.

Time Period

We are proposing a 3-month project for this experiment plan. Month 1 would be focused on field data collection and collectionsystem design. Month 2 would be focused on algorithm development and testing. Month 3 would be for algorithm adjustment and any final data collections needed to fine-tune the final algorithms. To keep costs reasonable, we propose to take advantage of the presence of 1-2 summer interns to assist with the field data collection, under appropriate supervision.

Preliminary Field Data Collection and Exploratory Analysis:

To test the feasibility of our proposed method, we will rapidly gather a set of high-resolution digital photographs taken from above a bridge using another overpass, from the top of a local building, or from the top of a truck rented by MTRI for other data collections, so we can gather the imagery needed for delamination characterization and depth characterization. MDOT safety procedures will be used on any roadway or bridge data collections. If sufficient time remains, we would take a first pass at high-resolution crack characterization as well. We estimate that this initial data collection would take two days of field collection and four days of analysis.

Sampling Procedure:

For each sampling point, with development of custom analysis algorithms:

In the field:

1. **Visit study sites to find optimal locations to collect data.**
2. **Obtain the help of MDOT or the local road commission for making the bridge available for data collection, and availability of a boom lift if needed.**
3. **Use safety equipment (including orange blazer, steel-toed boots, car light, hard hat) and safe data collection procedures for data collections on or near roadways and bridges.**
4. **Take digital photographs from appropriate height.**
5. **Record the GPS location of each photograph.**

In the Spatial Analysis Lab:

6. **Process photos into stereo pairs for DEM extraction.**
7. **Characterize depth of delamination areas.**
8. **Use custom image analysis algorithm for characterizing the frequency, size, and distribution of delamination areas.**

Required Resources:

1. 2- person crew for field data collection (MTRI researcher - Dobson + intern)
2. Image analyst (Powell with Brooks)
3. Map of study sites
4. Permission to collect at bridge locations
5. Available method of reaching needed height (cherry picker, above bridge structure)
6. Image analysis software (MATLAB, Definiens, ERDAS, ENVI, as determined through the study)
7. GPS unit (Trimble when available, Garmin 76 Csx WAAS-capable unit or equivalent)
8. Two DSLR cameras similar to available Nikon D40.
9. Safety equipment (including orange blazer, steel-toed boots, car light, hard hat) for data collections near roadways or bridges.
10. For lab testing: Two or more lab-controlled samples with spalling and/or delamination problems.

We propose to use Powell at 1/5 time, Brooks at 1/5 time, Dobson at ¼ time, and an intern at ½ time during the 3-month duration of the experiment. This will provide a focused time period and set of hours to complete the experiment design in a timely manner.

References:

Falkner, E. 1995. Aerial Mapping: Methods and Applications. CRC Press – Lewis Publishers, Boca Raton, FL. 322 pp.

Experimental Plan for Preliminary Investigation of Radar Applications for Bridge Deck Sensing

K. Arthur Endsley and Ben Hart, MTRI
Version of 7/14/2010

Overview and Objective

Radio detection and ranging (radar) is a technology in broad-use for measuring the distance to and direction and speed of targets. Radar involves the use of electromagnetic (EM) waves, either pulsed or continuously transmitted, for measurement. In through-transmission techniques the signal changes as it propagates from source to receiver. In most applications, however, a single antenna is used as both source and receiver, and it is the reflected signal that is measured. Changes in the radar signal consist of phase, frequency, or amplitude shifts which might be caused by the target's motion or the dielectric properties of both the target's material and the medium of transmission. Radar emissions vary in these parameters as well depending on the application. By adjusting the emission frequency, the technology has the potential to provide information on a target's composition and internal structure.

There are a variety of techniques applying radar signals to different ends, and several of these have viable transportation applications. Ground-penetrating radar (GPR) is a well-established technique for sensing subsurface features and defects in concrete structures. Some state DOTs even have the equipment and the expertise to perform GPR surveys in-house. Generalized microwave and millimeter-wave radar techniques have become popular in structural health monitoring (SHM) because they offer more compact and less expensive equipment than commercial GPR equipment. Synthetic aperture radar (SAR) is a process that generally involves a scanning or moving radar take multiple measurements along a transect line. By applying range migration processing to these measurements it is possible to derive a 2D projection of 3D reflectivity in the scene. SAR makes it possible to achieve spatial resolution not only in the range direction but also along the transect line. Furthermore, in range compression, a long EM pulse with encoded phase information can be used for enhanced resolution. GPR typically does not involve coherent processing; only time-delay information is used and so real target dimensions cannot be known.

We are interested in determining whether or not we can detect subsurface defects such as delamination, inclusions, or changes in a concrete deck's composition such as increasing chloride and/or water content. These measurements cannot be made directly without penetrating and thereby destroying the concrete deck. Optical methods that are limited to what can be sense in the visible spectrum have no way of detecting embedded features. In this report we describe an experiment in which we investigated the use of SAR collection and processing techniques to image concrete slabs. The preliminary results describe how

deep we can penetrate concrete slabs in the laboratory and, consequently, whether or not we can image re-bar embedded in the slabs.

Radar Measurements

The AKELA radar is a fairly sophisticated radar system with innovative features such as range-gating, a low-noise amplifier, and position encoder. This system has a frequency range of 300-3000 MHz. Any values in that range can be chosen as the first and last frequencies of the radar scan. The number of evenly spaced samples over the selected range can also be chosen, 512 is what we choose. The sampling rate can also be adjusted. This parameter affects the signal-to-noise ratio, and, when the antenna is in motion, the spatial sampling distance. We chose 45 kHz as the sample rate for these measurements.

The antennas for the radar are chosen to have a radiation pattern such that only the target is being illuminated by the radar. We use two antennas mounted together, one for transmission and the other for receiving the reflected signal. To create a two dimensional radar image, these antennas must be moved and radar measurements made at evenly spaced intervals along the direction of motion. To achieve this motion a garage door opener was modified and the antennas mounted to the carriage on the rail. This solution provides a stable direction of motion and constant speed. A position encoder has been mounted to the motor and connected to the AKELA radar unit to record the position of the antennas for each measurement sweep.

Laboratory Sampling Procedure

The most basic determination necessary to assess the feasibility of using radar in the detection of subsurface flaws is to determine the effective resolution that can be achieved. Another objective is to determine whether or not we can resolve specific features or flaws based on their position (depth) within the concrete slab. In our facility, we used concrete pavers as “slabs” of a concrete deck and thin metal rods inserted in between two slabs to simulate re-bar. A reflective plate was placed at the bottom of the stack to provide a definite “bottom” for deepest reflections. Data have also been collected on actual concrete samples provided by MTTI in Houghton. These samples were representative of actual bridge surfaces with and without defects.

To make a measurement, the antenna translation system is mounted above, or to the side of the sample, depending on the desired look angle. The cables between the antenna, radar, and computer are routed out of the antenna beam so that they will not be included in the measurement. The software is then set up for a 20 second collection. Once the radar is running, the garage door button is pushed and the antennas move along the rail while the radar is running. At the end of the collection the data file is saved, manually or automatically depending on settings. The antennas are brought back to their starting position and the process may be repeated.

Time Period

This whole process is relatively quick. It takes two people 30 minutes to set up the system for measurement. Each data collection takes about a minute from beginning to end. The data processing is automated as well. Software takes the radar data files and processes them into MATLAB-friendly formats. A MATLAB script reads these files and creates the images for visual interpretation.

Required Resources

1. AKELA Radar System
2. Garage door opener translation system
3. Laptop running AKELA APRD software
4. Two antennas with adequate cabling and connectors
5. Calibration targets
6. Miscellaneous tools

Experimental Plan for Digital Image Correlation and Tracking for Measuring Displacement of a Structural Element

K. Arthur Endsley, MTRI
Version of 7/14/2010

Overview and Objective

Digital image correlation and tracking is a straightforward approach to measuring structural condition and dynamic character using recognizable features on a target surface. In this technique, deflection and vibration are sensed optically from structured-light photographs. Fiducial marks projected or applied to the target surface are correlated between multiple photographs. Their motion from frame to frame can be tracked to calculate the direction and speed of an object's motion. For structural health monitoring applications, a reference photograph can be used for comparison with subsequent still images or a series of photographs can be taken at regular intervals to characterize structural dynamics.

Displacement of the target is calculated at the pixel scale based on the displacement of individual fiducial marks. A wide size distribution in these marks is required in order to prevent aliasing; to ensure that a wide range of rigid displacements can be detected. The technique is capable of measuring both in-plane and out-of-plane displacement for an effectively 3D measurement of displacement and/or vibration. Most bridge dynamics can be optically sensed and this technique, in particular, allows for very fine accuracy. The resolution is dependent on the distance to the target, but dynamics such as displacement and strain can be measured at sub-pixel accuracy.

This document describes an early attempt to measure the deflection and vibration of a steel I-beam using digital image correlation and tracking. We planned to determine the resolution that can be achieved using this method to measure displacement and to ultimately determine whether or not the technique is useful for monitoring real-world bridge deflection.

Pattern Application

Our implementation of this technique consisted of spray-painting a pattern of white dots on the structural I-beam to be measured. Through experimentation, we found that the appropriate size distribution can be achieved by obstructing the direct flow of paint from the nozzle by using one's finger placed 0.5-1 inch in front of the nozzle opening.

Loading the Structural Element

The structural I-beam was stressed by dual hydraulic rams, operated synchronously, capable of generating a fixed displacement per input volt (for this model, 1 volt resulted in 0.5 inches of piston displacement). Based on the output results, it seems clear that the steel beam from which the rams are suspended was being pushed upwards as the ram was in operation. This is not surprising, as the steel I-beam is almost identical to the steel beams that support the rams; the steel I-beam is just as rigid as the steel beams supporting the rams. In addition to static loading, dynamic tests were also conducted in which a sinusoidal signal was used to induce alternating motion of the pistons.

Digital Image Collection

A series of digital images were taken at fixed intervals using a Nikon D300s, 12-megapixel, digital SLR camera with a 150 mm lens attached. The camera was placed 2 m from the target surface on a rigid tripod. The area of the beam in the camera's field of view was 5 by 5 inches. The maximum optical resolution that can be achieved with this setup is 0.0014 inches/pixel; We achieved an effective resolution of 0.0058 inches/pixel. The images are numbered automatically by the camera's firmware, and each of the images was correlated with the known load applied to the I-beam at that time. Table 1 shows the static load conditions when each frame was taken.

Digital Image(s)	Load Condition	Displacement Sensed
033	No load	
040	0.85 kips	0.08 in
104	5 kips	
129	10 kips	
140	15 kips	0.50 in
146	17 kips	0.50 in
158		0.60 in
183		0.70 in
198	22.8 kips	0.75 in
199-225	Unloading	
226-232	No load	

Digital Image Processing

Camera images were processed in MATLAB using software created by Christoph Eberl from Johns Hopkins University. This software subdivides each image into a grid of grids. Cross-correlation of each subgrid with the corresponding subgrid in the next image in succession is then performed. A displacement vector is calculated for each subgrid, effectively producing a displacement field for the entire image. The amplitudes of these vectors were extracted and plotted by the x and y positions for each image, rendering a plot of displacement over the 2D image surface for different loading conditions. At one point during loading the hydraulic rams reported a displacement of 0.2 inches, yet we calculated a displacement of 0.104 inches from the imagery. This most likely indicates

the hydrualic rams' support beams were being displaced as they pushed down on the steel I-beam.

Time Period

The experiment required 2 hours of work in the laboratory stressing the steel I-beam and collecting the images. Processing in MATLAB required 10-15 minutes for about 150 images and the total job of processing and interpreting the results required one engineer at full time for half a day.

Required Resources

1. High-resolution digital SLR camera
2. Stable tripod with swivel head
3. Can of white spraypaint
4. Dual hydraulic ram
5. Computer capable of running MATLAB software
6. MATLAB software

Memorandum

To: Dr. Tess Ahlborn, P.E

CC:

From: Darrin Evans

Date: 6/8/2010

Re: Thin Slab Specimens

Test Slab AB

This test specimen consists of a 4'x4'x5 ½" slab of concrete with different "defects" placed inside the concrete. The concrete used is a MDOT Grade D deck mix design. Tests on the concrete determined the following properties 2.75" slump, 5% air content and a 5500 psi compressive strength. The relative humidity was measured to be 88.8% with a temperature of 20.1 degrees Celsius. This was measured with a HM44 at 12 days after casting.

Several "defects" are placed in the concrete slab at variable locations. Attached is a document showing the location and depths at which the different items are placed in slab AB. Along the A side of the slab different sized rebar are located at two different depths. Several rebar are stacked on top of one another to see if the bottom layer can be located or if just the top layer is visible.

In order to simulate delamination in the concrete slab, a plastic bag is situated along the B side of the slab as well as card boards which are located at different depths inside the slab. A plastic bottle is included to simulate a void in the concrete, but as the concrete was leveled managed to make its way to the surface. This leaves the bottle not in the original location that it was placed in but just under the surface. Ping pong balls are also used to simulate voids, but had the same situation as the plastic bottle with the locations changing after they were placed.

Test Slab CD

This test specimen is constructed the same as the previous slab with the only changes being what material is added to simulate "defects." The properties for this slab were not tested, but the same mix design was ordered. This specimen has several sensors including thermo wire to detect the temperature at several different depths. These depths should be just under the surface and two and four inches from the surface at the center of the slab. This specimen also has two imbedded humidity sensors. One is placed near the center and the other is near the edge. The relative humidity was measure to be 93.5% with a temperature of 19.2 degrees Celsius. The relative humidity was measured with a HM44 at 4 days after casting.

Attached document shows where the different items are located in the concrete slab. Along the C side of the slab a piece of scrap wood is located. A corroded steel plate was also included to simulate

distressed steel as well as an uncorroded steel plate for reference. Finally a couple of odd pieces of metal are placed in the slab.

On the D side of the slab are a segment of epoxy coated #3 rebar along with a segment of regular #3 rebar for comparison. Two different sized pieces of Styrofoam are placed at two different depths. The Styrofoam was used to simulate a void in the concrete. A piece of plastic is placed about an inch below the surface to simulate a delamination in the concrete. This likely moved once more concrete was placed in the slab to finish the surface.

Attached:

Final Concrete Slab AB Layout

Final Concrete Slab CD Layout

Final Concrete Slab Layout for AB

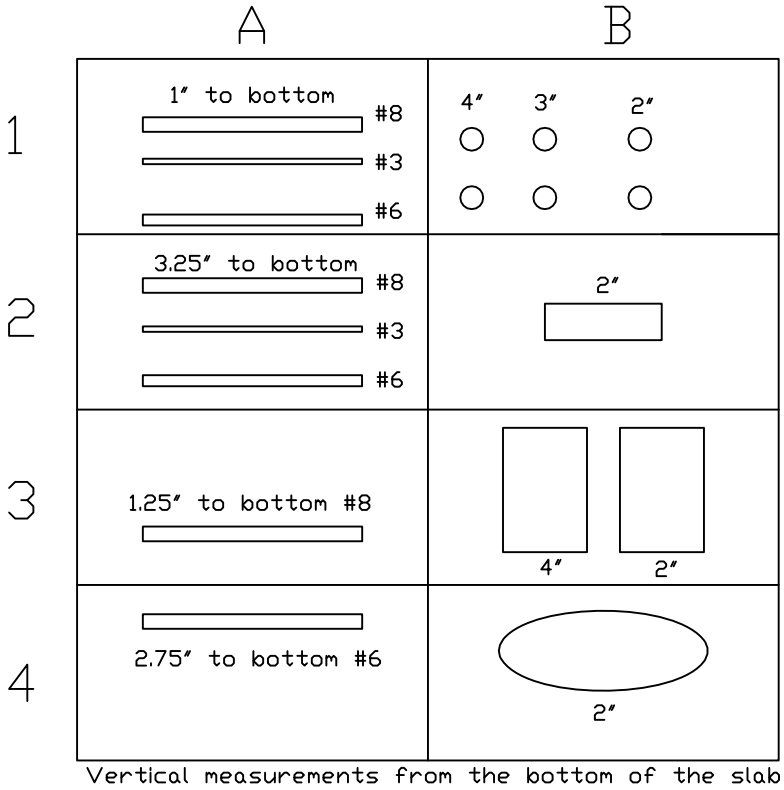

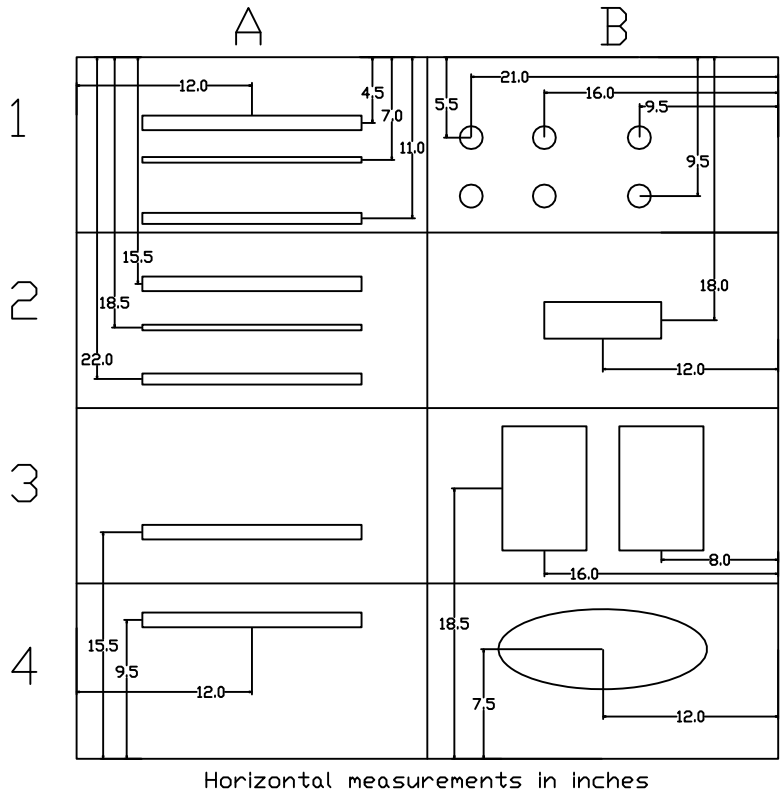

The slab was made into a grid pattern like the one shown. Each grid space is approximately 1 ft by 2 ft. The labeling of the grid was done as shown so locations can be referred to as A2 or B4 for easy reference. The top slab shows the depths of the items in the slab while the bottom one shows the horizontal location from the outside of the slab.

A1: Three rebar which were #3, #6 and #8 were placed at the same level. Rebar were 15" in length.

A2:Three rebar which were #3, #6 and #8 were placed at the same level.

A3 and A4: A #6 bar was placed directly above a #8 bar.

B1: 6 Ping pong balls were placed at different locations which probably don't correlate with the actual position. Diameter was 1.57".

B2: Plastic 16 fluid once bottle that floated to just under the surface. Diameter 2.5" x 8" in length.

B3: Cardboard placed at two different depths. Dimensions are 5.75" x 8.5" and 0.05" thick.

B4: Plastic shopping bag approximately 7"x 15" and 0.003" thick.

Final Concrete Slab Layout for CD

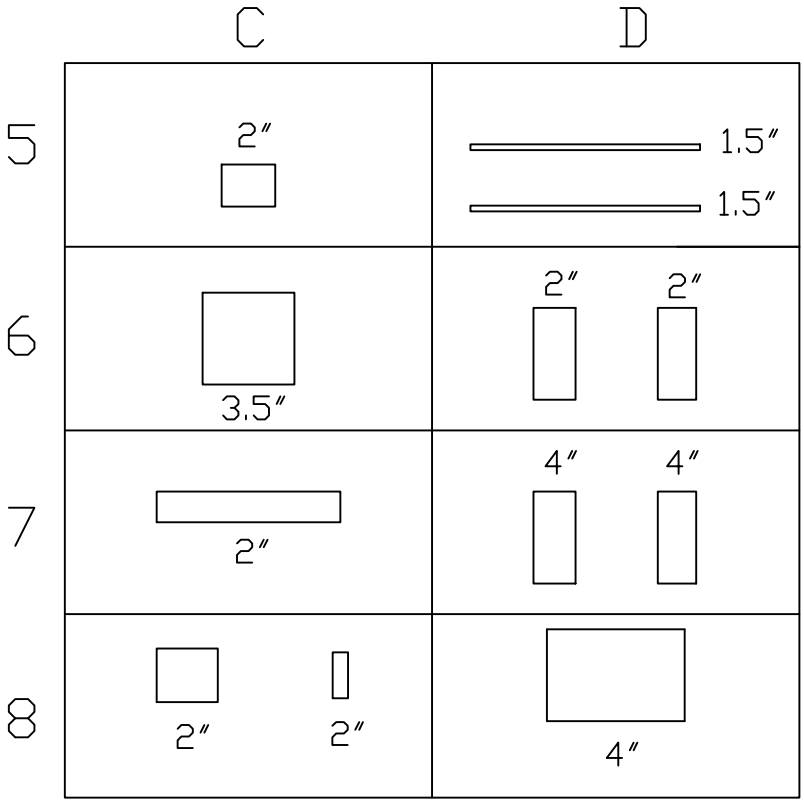

Vertical measurements from the bottom of the slab

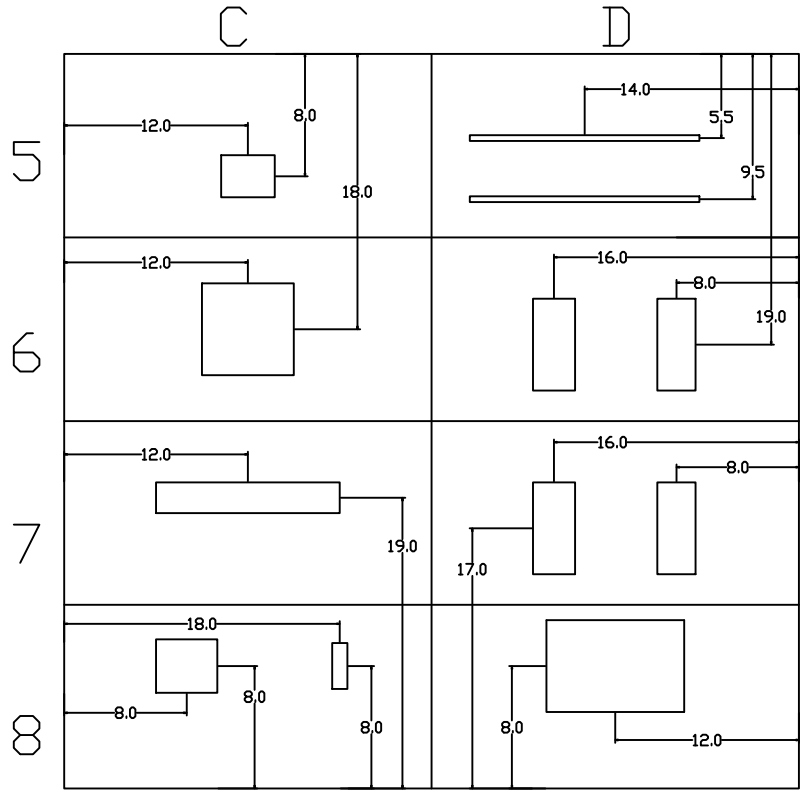

Horizontal measurements in inches

The slab was made into a grid pattern like the one shown. Each grid space is approximately 1 ft by 2 ft. The labeling of the grid was done as shown so locations can be referred to as C5 or D7 for easy reference. The top drawing shows the depths of the items in the slab while the bottom one shows the horizontal location from the outside of the slab.

C5: A piece of wood 3.5" x 2.75" and 1.5" thickness.

C6: A corroded plate 6" x 6" and .25" thickness. This plate also has a piece that extended to the bottom directly underneath of it.

C7: Contains a metal bar 2" x 12" and 1/8" thick. It has several holes along its length.

C8: Galvanized scrap metal 4" x 3.5" with 1.5" sides sticking up along two sides. The other piece of scrap metal was 1" x 3" and 0.5" thick with a hollow area in the center.

D5: This included 2 # 3 rebar one which was epoxy coated and the other one wasn't. The epoxy coated one was closest to the edge.

D6 and D7: Two different size pieces of Styrofoam with the larger one being closest to the outside edge. The smallest is 2.75" x 6" and 5/8" thickness. The larger one is 2.5" x 6" and 1.5" thick.

D8: Plastic bag shopping bag. With dimensions approximately 6" by 9" and 0.003" thick.

Memo

To: T. Ahlborn, L. Sutter, D. Harris, R. Shuchman, J. Burns, C. Brooks, R. Wallace

From: K. Arthur Endsley

CC: P. Hannon

Date: 06/28/10

Technical Memorandum Number: 06

Re: Progress report on Commercial Sensor Evaluations

Commercial Sensor Evaluation Report

In the course of this study thus far, we have evaluated several remote sensing technologies for their suitability in the structural health monitoring of bridges. These technologies not only reflect the domain expertise of the Michigan Tech Research Institute staff but are also most promising for broad, practical implementation in a bridge condition assessment strategy. Other technologies have been evaluated and other will continue to be evaluated, but the techniques specified here represent those that best fit the objectives of the project.

Digital Image Correlation and Tracking

Digital image correlation and tracking is a straightforward approach to measuring structural condition and dynamic character using recognizable features on a target surface. The most reliable implementation involves the use of several fiducial marks of variable sizes. These marks are either projected from a light source or painted directly on the target surface. Once marked, high-resolution photographs of the target surface and the superimposed pattern of markings. A reference photograph can be used for comparison with subsequent still images or a series of photographs can be taken at regular intervals to characterize structural dynamics. Displacement of the target is calculated at the pixel scale based on the displacement of individual marks.

The technique is attractive as it requires no expensive, sophisticated equipment—high-resolution digital SLR cameras are available commercially for less than $1000. The data collected and the processing required to derive measurements of interest are easy to understand and have real-world meaning. Though the fiducial marks can be applied rather easily to the target object, it can be time-consuming as the scale and number of structures to be evaluated increases. Other drawbacks to this technique include its inability to sense changes

in a bridge or other structure that do not manifest as deflection and that it is hindered by poor weather, aberration of the optics (such as dirt), and cannot be performed in darkness.

Our implementation of this technique consisted of painting a pattern of dots with a wide size distribution directly on concrete or steel structural elements. A wide size distribution is required in order to prevent aliasing; to ensure that a wide range of rigid displacements can be detected. It is capable of measuring both in-plane and out-of-plane displacement for an effectively 3D measurement of displacement and/or vibration. Most bridge dynamics can be optically sensed and this technique, in particular, allows for very fine accuracy. The resolution is dependent on the distance to the target, but dynamics such as displacement and strain can be measured at sub-pixel accuracy. In laboratory testing of this technique on a steel I-beam, we were able to measure displacement as small as 1/10 of an inch, however, it is possible to measure displacement down to 1/1000 of an inch by controlling spot size, optics selection, and distance to the target. With the appropriate optics, long standoff distances are possible, and these may be more practical for implementation. We expect to rigorously explore the relationship between sensor-target geometry and effective resolution and to demonstrate the technique's flexibility in this respect during field deployments.

Synthetic Aperture Radar (SAR)

Radio detection and ranging (radar) is a familiar but complex remote sensing technique that can measure a target's displacement, speed, frequency of oscillation, modes of vibration, size, distance, and even its material properties. The emission and reflection of electromagnetic (EM) waves is the basis of radar measurement.

In the previous phase of this study, several applications of radar for bridge condition assessment were identified including measuring gross displacement of bridge structure, vibration of the bridge structure, penetrative imaging for the detection of defects, inclusions, or material changes, and the characterization of surface roughness. We have already identified what aspect of the radar signal these measurements will be based upon. Displacement can be measured directly using conductive markers attached to the bridge—these strongly reflect EM energy and their position can be easily calculated from radar returns. Material changes will manifest as changes in the dielectric constant. Surface roughness can be quantified from coherent speckle (sometimes considered to be noise in radar images) as it is proportional to the contrast.

Synthetic aperture radar (SAR) is a technique that combines radar returns from multiple tiny apertures for the purpose of simulating one measurement from a very large aperture. The term

aperture here refers to the radar antenna's beam width and, as a rule; larger antennas have narrower beam widths. Consequently, to increase the resolution with which a target surface is imaged a larger antenna is needed. This is obviously inefficient and even impractical for applications with high-resolution requirements. Instead, the effect of using a large aperture can be achieved by post-processing the returns from multiple radar measurements at different positions along a transect line over the target. One tremendous advantage of SAR over GPR in this arena is that the radar returns have real dimensions unlike the singular peaks associated with GPR data. This enables us to measure the dimensions of subsurface features such as rebar—when looking for corrosion—or defects such as delamination when we're interested in specifying the condition of a bridge deck.

We have conducted an investigation into the application of range-compressed radar measurements for detecting and characterizing concrete-embedded features and defects. In a laboratory test, concrete slabs with improvised reinforcing bar inserted in between were imaged using a new radar system featuring range gating, a low-noise amplifier, and position encoder. The slabs were illuminated by EM energy from 500 to 2,000 MHz and we were able to achieve a resolution of 10 cm. The resulting image enabled us to locate the position of the rebar and even distinguish the discontinuities between separate concrete slabs.

Acknowledging that radar images are not easy to interpret, we plan to develop algorithms that would extract features important for characterizing a bridge deck. These algorithms would be fully automated and lend themselves to implementation in a decision support system we conceived for reporting bridge condition and developing bridge "signatures" that help bridge managers make informed decisions about maintenance and safety.

Photogrammetry and 3D Modeling

Photogrammetry, broadly defined, is the science of making accurate measurements by means of photography. This technique achieves accurate 3D measurements of surfaces and terrain through the use of stereo pair imagery. Stereo pairs are comprised of two images with at least 60% overlap and are almost always collected by an aerial photography platform. Stereophotogrammetry as a means of measuring depth in addition to planar extents was first advocated and developed in the 19th century. Since its inception it has matured from a recreational curiosity (i.e. the stereoscopes of the Victorian era) to a well-established remote sensing technique.

Acquisition of stereo pairs is commonly achieved by taking successive still photographs as the camera traverses a straight line over the target. In this way, multiple stereopairs are

generated that cover a wide area of the target surface. Modern commercial software such as the Leica Photogrammetry Suite can rapidly generate 3D models from stereo pairs, and our team has extensive experience with this particular product. We have explored the use of stereophotogrammetry as a means of calculating the depth and extent of surficial features and defects on concrete bridge decks. Laboratory research has demonstrated the efficacy of creating 3D models of concrete slabs imaged from two angles. With our considerable experience in digital image processing and feature extraction we are capable of automating the calculation of feature extent and depth from these models.

Further development of this technique will involve the collection of photographs covering an entire road lane using a vehicle-mounted system. We have parameterized the collection of stereo pairs and calculated the necessary camera geometry in order to generate 3D models that will provide accurate and detailed measurements of concrete deck condition. We found that in order to image a road lane on a bridge the camera system must be elevated to total height of 15 feet off the ground. Though the system is limited to detecting only visible features and defects, it offers a rapid and automated method of evaluating bridge deck condition that does not interfere with traffic or require lane closures that might put bridge inspectors at risk.

Spectral Reflectance

Visible and infrared light can be used to characterize a target surface for representation and evaluation in an automated routine. That different materials reflect light differently is intuitive to us—it is the basis of our eyesight. This difference can be quantified, however, and represented in a way that enables us to make reasonable comparisons. Spectral reflectance is such a representation, as it is a measure of the amount of light reflected across the visible and infrared spectrums. Reflectance spectra are plotted as waveforms showing the continuous response of a material to illumination by visible and thermal energy.

Our hypothesis is that different conditions of bridge elements (which can be optically sensed) can be identified by their spectral reflectance. For example, as a concrete bridge deck ages and develops signs of wear its appearance—and therefore spectral reflectance—should change. Different levels of oxidation, chloride intrusion, and leachate issues should also contribute to differences in spectral reflectance. We have attempted to demonstrate the potential of this technology for fairly rapid bridge deck evaluations, conceiving of a vehicle-mounted system capable of capturing reflectance spectra and analyzing them on the fly, performing feature extraction and identification.

We tested our hypothesis in the field using a portable spectroradiometer capable of collecting reflectance spectra from 350 to 2500 nm (ultraviolet to near infrared). This device consists of a backpack unit that communicates wirelessly with a small laptop for data collection. The optical device integrates reflectance spectra from everything within its field of view. At a height of 1 m above the target surface, this amounts to a spot size (footprint) of 30 cm. Data at three bridges in southeast Michigan were collected. The bridges varied in age with concrete deck surfaces that were 47, 39, and 6 years old. Spectral reflectance was collected from the bridge deck surface, both large cracks and hairline cracks, spalls, and asphalt patches. One bridge in particular had areas with visible oxidation, leachate, and exposed rebar.

The reflectance spectra showed considerable difference between the youngest concrete bridge deck and the two far older decks. This difference was marked by a spike from 10 to 40% reflectance in the range of 1000 to 1750 nm. Spalls, oxidation, and leachate all showed appreciably distinctive reflectance curves though exposed rebar and degraded concrete spectra were not appreciably different from areas without defects. The Kolmogorov-Smirnov (KS) test was utilized to quantify the differentiation between spectra curves from different bridges. The test indicated that each bridge's spectral reflectance curve was different from one another, even in the case of the two oldest bridges where the difference between the curves could not be appreciably discerned by eye. This seems to suggest the KS test is not sensitive enough for these distributions. However, the test's D-statistic was considerably higher when comparing either of the older bridges to the younger one and was sufficiently low when they were compared to each other. This would suggest that it is the D-statistic itself and not the acceptance/rejection criteria of the test that should be used to determine if two spectra are sufficiently different.

Though this technique is limited to elements of bridge condition that can be optically sensed, it offers distinct advantages over traditional, visual inspection methods. Most importantly, the measurement processes itself and the data that are collected enable automation of the evaluation and replace subjective assessment with objective characterization.

Memo

To: USDOT/RITA research team members

From: C. Brooks, D. Evans

CC: P. Hannon

Date: October 15th, 2010

Number: 07

Re: Work plans – progress to date

The following summarizes the work plans associated with our proof-of-concept feasibility studies.

Spectral Reflectance

The assessment of spectral reflectance will be completed using representative, *in situ* measurements along with several specimens made in the lab as needed beyond the initial testing done at two southeastern Michigan bridges. These samples could include several different types of depressions to simulate a flaw in the surface. Samples containing different levels of chloride will also be measured to see if spectra could indeed be used for sensing chloride ingress. The results of these multiple samples will be compiled in a database of reflectance curves. Once this is completed, a field demonstration will be performed to assess whether or not the curves correlate to actual defects in bridge elements. This will establish if spectral analysis is indeed an effective method to detect and distinguish bridge surface conditions and defects. The project leader will review progress on this area to see if additional lab testing is needed beyond what has already been completed.

3D Optics (including Photogrammetry)

The overall optical processing is expected to comprise techniques that are both 2- and 3-dimensional in nature for this work plan. Much useful information is present in 2D images, and these are both easier to collect and easier to process, and are part of the process of creating 3-D data. Our plan will be to use the 2D images to form a preliminary analysis of the surface, and based on those results, determine if the more complicated (and more informative) 3D processing is needed.

For 2D analysis parts of this work plan, we expect to use a variety of standard image processing algorithms, including (but not limited to), edge-detection, image morphology (e.g. dilation and erosion), statistical analysis (e.g. histograms), and other segmentation algorithms. These will be used to determine the nature of the surface (cracked, spalled, etc.) in a general way, and to make decisions about further processing.

For the 3D processing of optical imagery, we have identified three methods. All use multiple realizations of 2D images collected by standard digital SLR cameras to extract 3D information, rather than using the direct (but much more expensive) 3D sensors (such as LiDAR). For all three methods, we will perform an assessment on how capable the methods are of producing useful assessments of bridge deck surface indicators, such as spalling and cracking, first by using a lab specimen displaying various levels of these indicators. These three methods are:

1. Standard stereo-photogrammetry, including an accurate lighting model to be able to deal with hole/bump ambiguities. We will test both commercial and MTRI in-house photogrammetric processing tools as part of the lab work plan.

2. 3D point-cloud generations from multiple images, followed by surface finding (using, for example, Marching Cubes or Marching Tetrahedra) and then surface characterization (in terms of roughness, cracking, etc.). Software implementing these methods has been developed at MTRI for other programs, and is available for this application. The implicit surface-finding algorithm, Marching Tetrahedra, takes 4 points in 3-space that form a cube, divides that cube into 6 tetraheda by cutting diagonally through the cube, and the points in the clouds nearest each of these vertices are found. The resulting associated triangular facets are then used to form the surface. Because adjacent cubes share all edges in the connected surface, there will be no "holes" in the surface where edges do not match, and the surface normals are available for each facet (allowing immediate analysis of the surface variability).

3. Plenoptic processing, in which a series of 2D images is used to be able to extract detailed depth-of-field information, and thus full 3D characterization of the surface. There are commercial sensors available for this: http://www.petapixel.com/2010/09/23/the-first-plenoptic-camera-on-the-market/ or existing cameras may be fitted with a custom lens:

http://www.raytrix.de/index.php/rx.html to make these measurements. Commercial software also exists allowing processing of these 3D images. Assessing the capabilities of commercial tools to help in 3-D assessment is a goal of this work plan.

Digital Image Correlation

Digital image correlation is to first be tested in the laboratory on a steel beam to determine whether further field testing should be completed. Test preparation requires applying a pattern of fiducial marks; in this case, white paint dots were sprayed on the beam during an initial lab study. Pictures of the beam are then taken using a digital SLR camera while the beam is loaded. The images are then processed in MATLAB; from the displacement of the dots on the beam the deflection can be measured along with vibrations of the beam. If the tests in the lab show promising results the testing will continue on bridges in the field. The project leader will review progress on this area to see if additional lab testing is needed beyond what has already been completed.

Radar Testing

The radar testing will be completed using an AKELA radar unit that is moved along a track at a constant speed for collection of SAR data in the laboratory. The first test was completed at MTRI using concrete blocks with metal rods placed under them to determine the depth at which the radar can penetrate. The radar will then be tested on several slab specimens that have simulated defects in order to assess the technology's capability of detecting them. The radar will also be tested on several concrete beam samples that are at various stages of degradation. These tests will allow for the determination of the technology's applicability for detecting defects in the field. Initial work has started on this lab experiment and results will be reported in the coming quarter.

EO Airborne / Satellite Imagery

The assessment of EO (electro-optical) airborne/satellite imagery for detecting bridge condition indicators was determined by the project team to be more practical for a field demonstration rather than an individual laboratory test. The work plan will be included with the field demonstration plan. We will also include a review of the work done as part of the www.tarut.org study by Brooks, Shuchman, and others on using visible and near-infrared satellite imagery to assess road condition.

LiDAR, Acoustics

LiDAR is not going to be assessed in the field or laboratory in this project due to the USDOT-RITA-funded work being done at The University of North Carolina at Charlotte. It was also

determined at this point that acoustics would be difficult to assess within the bounds of study and that because the technology is not strictly remote sensing it would not be considered for this study beyond the initial performance evaluation.

Optical Interferometry

The testing of optical interferometry includes both the testing of speckle pattern interferometry (SPI) and shearography. The SPI measuring process is performed using a high-resolution digital SLR with a coherent light source (laser light) illuminating the target. In this experiment a sheet of paper covering a hole is flexed under illumination in order to assess the technique's ability to measure strain gradients and displacements of the paper. These data are processed quickly by computer programs. Shearography was assessed using a Michelson interferometer to capture the deformations or displacements of a target surface. Shearography data are analyzed by looking for phase shifts that result from these tiny deformations or displacements. Data was collected at a very fine scale (sub-millimeter) during an initial test. The data will be reviewed by the project leader in collaboration with the remote sensing experts at MTRI to see if any further testing should be done beyond the current demonstration.

Thermal IR

The assessment of thermal IR, as with EO airborne/satellite imagery, will be part of the upcoming field demonstration as the project team is still coordinating with a potential commercial partner on a field demonstration which could also include a lab testing component. Additional information will be assessed and included in the next quarterly report.

StreetView-Style Photography

StreetView-Style Photography, or panoramic photography that is projected into a 3D coordinate system, will be assessed in the future as both an individual test and as part of the field demonstration. We will assess the ease of extending MTRI's existing vehicle-mounted multi-camera image capture for higher resolution photography. From the bridges in the greater Ann Arbor area and possibly Oakland County, one or more will be selected for a drive-by data collect. The images will be processed at MTRI to tie geospatial coordinates to each image. These images will be displayed in a simple GIS such as Google Earth and analysts will assess whether or not the technology allows for convenient and rapid evaluation of bridge condition from the office. We will also assess the potential to demonstrate an existing commercial system as part of either a lab or field study, such as the Trimble MX8 system (http://www.trimble.com/geospatial/Trimble-MX8.aspx?dtID=overview&).

InSAR

Based on our commercial sensor evaluation, InSAR is of value in detecting displacement and potentially vibration of the bridge as a whole. The assessment of this technology will involve the acquisition of SAR images from a commercial currently-available platform. MTRI will leverage its expertise in SAR processing to improve upon the permanent scatterers technique, in which structural elements of a bridge that respond brightly to radar illumination will be tracked in the interferograms for enhanced spatial resolution. If it is determined that existing structural elements will not be sufficiently bright to be used as permanent scatterers, then corner reflectors will need to be installed on a target bridge. This investigation will be conducted during the field demonstration.

Memo

To: T. Ahlborn, L. Sutter, B. Shuchman, D. Harris, J. Burns, C. Brooks, K. A. Endsley

From: R. Oats

CC: P. Hannon, K. Vaghefi, D. Evans

Date: October 8th, 2010

Number: 08

Re: Structural Modeling Development

To date, the finite element simulation task is progressing as expected, with models being developed and validated. The validation stages are critical for future model development, as they provide confidence in the modeling approaches used. Validation allows the models to be extended with confidence and functional to applications in which they may not have been specifically validated. The models under development focus on structural components of a bridge and are expected to be combined to form a full bridge model. For comparison to current progress, the expected outcome of the finite element modeling tasks will be capable of correlating with evaluating the global challenges highlighted in the commercial sensor evaluation report.

Memo

To: T. Ahlborn, L. Sutter, B. Shuchman, D. Harris, J. Burns, C. Brooks, C. Roussi, R. Wallace

From: D. Evans

CC: P. Hannon, K. Vaghefi, K. A. Endsley, R. Oats, M. Forester, R. Dobson

Date: October 15th, 2010

Technical Memo Number: 09

Re: Commercial Sensor Evaluation Report

The commercial sensor evaluation report, titled *An Evaluation of Commercially Available Remote Sensors for Assessing Highway Bridge Condition*, is now centrally located on the project Wiki site.

This report is also posted on the project web site as a stand-alone document <www.mtti.mtu.edu/bridgecondition>.

And the report will be referenced in the third quarterly report due to the USDOT/RITA office by October 15, 2010.

Memo

To: USDOT/RITA research team members

From: C.N. Brooks

CC: P. Hannon

Date: October 15, 2010

Number: 10

Re: Decision Support System update

The initial software development for the decision support system (DSS), including how we will be creating code for integrating sensor data and normalcy models for sensor response, is described below.

For beginning the development of the DSS, our work on the Commercial Sensor Evaluation (Deliverable 3-A), has provided important guidance to our DSS design. This will continue as we assess technologies as part of our lab work plans and eventual field testing. The framework we designed and applied to rating remote sensing technologies (repeated in the figure below) will be important to the DSS as well. Remote sensing technologies that already appear to be promising to evaluate particular bridge condition indicators, or could do so with focused additional investigation as part of this study, will be important to integrate into a DSS, as allowed by study funding. As recommended by the TAC, making sure any DSS demonstration ties into existing bridge management tools and methods is also critical.

Location	Challenges	Indicator	Desired Measurement Sensitivity	GPR	Spectra	3D Photo-grammetry	EO Airborne/ Satellite Imagery	Optical Inter-ferometry	LiDAR	Thermal IR	Acoustics	DIC	Radar (Backscatter/ Speckle)	InSAR	Streetview-Style Photography
				Rating Based, in Part, on Theoretical Sensitivity for Measurement Technologies											
Deck Surface	Expansion Joint	**Torn/Missing Seal**		0	8	14	12	11	13	11	0	0	9	0	13
		Armored Plated Damage		0	0	14	12	11	13	11	0	0	0	0	13
		Cracks within 2 Feet	0.8 mm to 4.8 mm (1/32" to 3/16") width	0	8	14	0	12	12	11	0	0	9	0	13
		Spalls within 2 Feet	6.0 mm to 25.0 mm (1/4" to 1") depth	0	8	14	12	12	12	11	0	0	9	0	13
		Chemical Leaching on Bottom		0	11	0	0	0	0	0	0	0	0	0	0
	Map Cracking	Surface Cracks	0.8 mm to 4.8 mm (1/32" to 3/16") width	0	8	14	12	12	12	11	8	0	9	0	13
	Scaling	Depression in Surface	6.0 mm to 25.0 mm (1/4" to 1") depth	0	8	14	12	12	12	11	0	0	9	0	13
	Spalling	Depression with Parallel Fracture	6.0 mm to 25.0 mm (1/4" to 1") depth	0	8	14	12	12	12	11	0	0	9	0	13
	Delamination	**Surface Cracks**	0.8 mm to 4.8 mm (1/32" to 3/16") width	0	8	14	0	12	12	11	8	0	0	0	13
Deck Subsurface	**Expansion Joint**	**Material in Joint**		0	0	0	0	11	0	0	0	0	0	0	0
	Delamination	**Moisture in Cracks**	Change in moisture content	11	0	0	0	0	0	11	0	0	0	0	0
		Internal Horizontal Crack	Approximately 0.1 mm (0.004") level	0	0	0	0	0	0	11	8	0	0	0	0
		Hollow Sound		0	0	0	0	0	0	0	8	0	0	0	0
		Fracture Planes / Open Spaces	Change in signal from integrated volume	12	0	0	0	0	0	0	8	0	12	0	0
	Scaling	Depression in Surface	6.0 mm to 25.0 mm (1/4" to 1") depth	12	0	0	0	0	0	11	0	0	0	0	0
	Spalling	Depression with Parallel Fracture	6.0 mm to 25.0 mm (1/4" to 1") depth	12	0	0	0	0	0	11	0	0	0	0	0
	Corrosion	Corrosion Rate (Resistivity)	5 to 20 kΩ-cm	0	0	0	0	0	0	0	0	0	0	0	0
		Change in Cross-Sectional Area	Amplitude of signal from rebar	13	0	0	0	0	0	0	8	0	13	0	0
	Choride Ingress	Choride Content through the Depth	0.4 to 1.0 % chloride by mass of cement	12	0	0	0	0	0	0	0	0	12	0	0
Girder Surface	**Steel Structural Cracking**	Surface Cracks	< 0.1 mm (.004"), hairline	0	8	11	0	12	0	11	0	0	0	0	0
	Concr. Structural Cracking	Surface Cracks	.1 mm (.004")	0	8	11	0	12	0	11	8	0	0	0	0
	Steel Section Loss	Change in Cross-Sectional Area	Percent thickness of web or flange	0	0	11	12	0	13	11	0	0	11	0	0
	Paint	**Paint Condition**	Amount of missing paint (X %)	0	9	0	0	0	0	11	0	0	0	0	0
	Concrete Section Loss	Change in Cross-Sectional Area	Percent volume per foot	0	0	11	12	0	13	11	7	0	11	0	0
Girder Subsurface	**Concr. Structural Cracking**	Internal Cracks (e.g. Box Beam)	Approx 0.8 mm (1/32")	0	0	0	0	0	0	11	8	0	0	0	0
	Concrete Section Loss	Change in Cross-Sectional Area	Percent volume per foot	0	0	0	0	0	0	0	7	0	11	0	0
	Prestress Strand Breakage	Change in Cross-Sectional Area	Wire 2 mm or strand 9.5 mm diameter	9	0	0	0	0	0	0	8	0	9	0	0
	Corrosion	Corrosion Rate (Resistivity)	5 to 20 kΩ-cm	0	0	0	0	0	0	0	0	0	0	0	0
		Change in Cross-Sectional Area	Amplitude of signal from rebar	8	0	0	0	0	0	0	8	0	13	0	0
	Choride Ingress	Choride Content through the Depth	0.4 to 1.0 % Chloride by mass of cement	10	0	0	0	0	0	0	0	0	11	0	0
Global Metrics	Bridge Length	**Change in Bridge Length**	Accuracy to 30 mm (0.1ft) (smaller)	0	0	15	13	0	0	0	0	9	0	12	0
	Bridge Settlement	Vertical Movement of Bridge	Approximately 6 mm to 12 mm	0	0	12	0	0	12	0	0	9	0	12	0
	Bridge Movement	**Transverse Directions**	Approximately 6 mm to 12 mm	0	0	12	0	0	12	0	0	9	0	12	0
	Surface Roughness	Surface Roughness	Change over time	0	9	14	13	12	12	0	0	0	11	13	13
	Vibration	Vibration	.5 -20 Hz, amplitude?	0	0	0	0	12	0	0	0	10	12	12	0

Performance ratings of commercial remote sensing technologies, from *An Evaluation of Commercially Available Remote Sensors for Evaluating Highway Bridge Condition* (Deliverable 3-A). Note: Higher scores equal higher ratings for a particular combination of technologies, needed measurements, and bridge condition indicators. For a detailed description of how these ratings were arrived at, please see the Deliverable 3-A at *www.mtti.mtu.edu/bridgecondition/Tasks_and_Deliverables.html*

Our visits to four bridges on two days with Michigan DOT bridge inspectors were also informing for our DSS design. We learned that any DSS that reaches the field needs to be mobile and rugged to survive environments where sometimes uneven and steep surfaces must be traversed. The idea of an application available in a ruggedized iPad type computer was discussed by the inspectors and the project team (rugged cases are now becoming available – see the "iPad defender" for an example at http://www.otterbox.com/ipad-cases/ipad-defender-series-case/). A rugged, lightweight, and easy-to-use computer such as the iPad would form the hardware base for a tool that the inspectors would use out in the field. The tool would provide bridge locations and bridge inspection data in an easy-to-use graphical mapping interface such as Google Earth. As most bridges do not have typical resolvable street addresses, the DSS application would direct inspectors to the bridge location based on the latitude and longitude of the bridge. With almost 1,000 bridges in MDOT's University Region

(which our inspectors operate out of), this was described a significant need that we had not expected. The DSS interface would then bring up historical inspection reports about a bridge, and provide the ability to enter new bridge inspection data, which would get automatically integrated with MDOT's Bridge Management System. In addition to this sketch of useful DSS provided by our MDOT bridge inspectors, we recommend including the results of any remote sensing analyses performed prior to visiting a bridge, such as an InSAR satellite imagery analysis that could have indicated bridge settlement since the last inspection. The DSS would also then be capable of integrating remote sensing results incorporated as part of inspections, where such tools to become part of standard or enhanced inspections and little further processing was needed. For example, high-resolution digital Streetview-style photography could be linked into the DSS on the iPad-like device so that any noteworthy indicators of interest (such as significant spalling) would always have a photograph attached to notes about the indicator, and the locations where those photos were taken. The idea of a DSS being useful before field work (for mission planning) and in the field also integrates well with the TAC recommendation that a DSS be able to highlight locations with "red light / green light" indicators of bridge problems based on traditional bridge inspection and remote sensing data.

Over the next quarter, we will be turning these ideas into a demonstration set of code that will be able to display sensor data tied to bridge condition indicators, using desired measurement sensitivities tied to NBI Condition Ratings where possible. This should prove the more quantitative way of tying remote sensing measurements into actual indicators of bridge condition. Because we expect to learn a great deal from both lab testing and field demonstrations, we are now anticipating that the Decision Support System period may have to end coincidentally with Task 5, the Field Demonstration. This would provide an additional six months to create a practical and useful DSS demonstration as part of this project. We will produce a status report at the current deadline (April 2011), but would like to have the flexibility to produce an enhanced DSS nearer the end of the study once more information is available.

Memo

To: USDOT/RITA research team members

From: H. de Melo e Silva, C. Brooks, R. Dobson, J. Ebling, D. Evans, B. Hart, R. Oats, C. Roussi, K. Vaghefi

CC: P. Hannon

Date: January 14, 2011

Number: 11

Re: Laboratory Study Progress Update

The fourth quarter afforded significant progress in our feasibility studies for promising remote sensing technologies. Activities for each commercially available technology that is being investigated are summarized below.

3D PHOTOGRAMMETRY

3D photogrammetry is the generation of 3D models from stereo pairs of imagery in order to obtain depth and height information, and is part of the 3D optics technology assessment. Stereo images have to be collected with a 60% overlap in order to generate these models. Challenges being looked at include spalling, scaling, cracking and surface roughness. Along with assessing the accuracy of the technique two different modeling programs will be compared to see how they affect the outcomes of the measurements.

AgiSoft PhotoScan is a 3D modeling commercial software program that can generate 3D models with minimal digital photographic inputs. Once photos are uploaded, the software processes them without having to calibrate cameras, user input of camera parameters or manually aligning the photos. While extensive calibration is required with Eos PhotoModeler, this

software package will also be considered. The cameras used to record the images are two different digital single lens reflex (DSLR) models; a Nikon D5000 and a Canon EOS 7D.

Preliminary Studies

Various experiments were performed to test the cameras and software limitations using a piece of foam board, which was used for its ease to shape and attach extra pieces. A wedge shape was carved into the board that allowed us to determine the horizontal resolution of the program, which relates to the width of cracks on bridges. Pieces of cardboard were arranged in a stair-step fashion that shows the programs limit to resolve height or depth measurements. Finally, different colored spheres were added (see Figure 1a) to show if there would be problems with generating accurate models due to poor contrast and the different sizes show what the resolution is with respect to generating rounded features.

The camera was mounted directly above the board at a translation stage that allowed photos to be taken at precise intervals across the length of the board. This initial experiment showed that this program has a resolution of about 4mm in both the horizontal and vertical directions within this setup. Tests were also conducted with a single light source that illuminated the board from various angles to determine how the lighting and resulting shadows affected the model. All of the tests produced similar results and demonstrated that photos can be taken throughout daylight hours without concern over reducing resolution or accuracy.

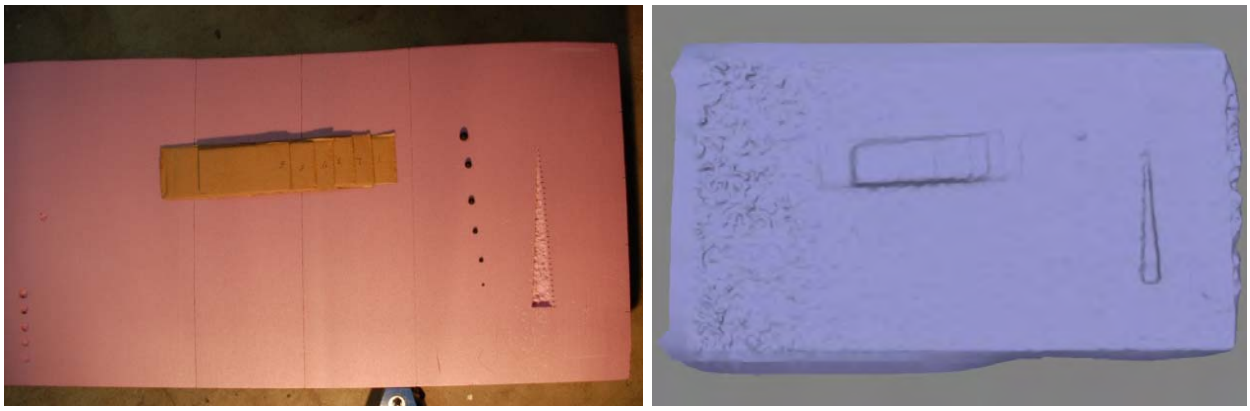

Figures 1a & 2a: First experiment with foam board in the lab with original photo on the left and 3D model on the right.

Test runs were also performed to consider how the quantity of photos affected the resulting model. Models were generated using three, 20, and then 48 photos. This experiment showed

that increasing the number of photos noise was reduced and produced a clearer more accurate model without a change in resolution. Also differences in contrast did not appear to play a significant role in generating a model as all spheres greater than 10mm in diameter were discernable in the 3D model for all colors (see Figures 3a & 4a).

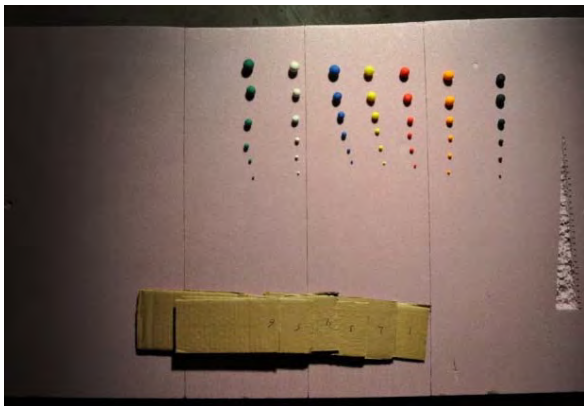

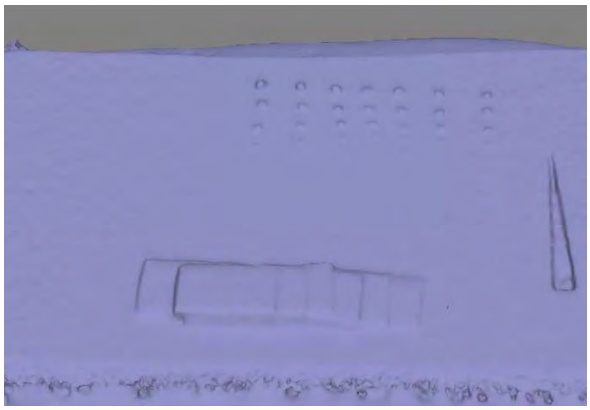

Figures 3a & 4a: Next set of experiments to determine contrast relevance and using different illumination angles with original photo is on the left and model on the right.

The first in-field test was conducted by taking the camera and capturing spalls on the underside of the 6 Mile Bridge over US-23 north of Ann Arbor, MI (see Figures 5a and 6a). 3D models of spalls were generated by taking four to six photos in a line, with the spalls being located approximately 2.5 meters above where the photo was taken (see Figures 7a & 8a). Spalls at a distance were of importance to demonstrate how a 3D setup could be deployed to measure the length, width, and depth of spalls that would otherwise require equipment to reach. Calculations of resolution attained by this camera, distance, and number of photos are currently being related that to desired measurement sensitivities.

Figures 5a & 6a: Researcher taking photos of the underside of 6 Mile Bridge at US-23 near Brighton, MI. The distance from the camera to the spalls was approximately 2.5 meters (8 feet). Photo taken of spall on deck bottom surface from the field test shown above at 6 Mile/US-23 Bridge.

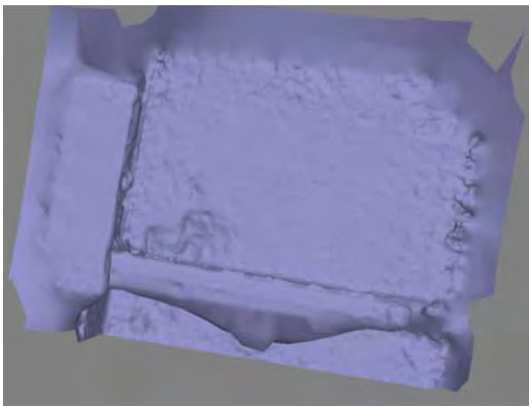

Figures 7a & 8a: Models generated from the infield photos with textured model on the left and shaded model output from PhotoScan on the right.

What's next for 3D Photogrammetry

Testing will continue with fundamental experiments to determine what size defects can be seen and processed by the equipment and software using specimens of multiple sizes with various types of challenges. Given success with these tests, other factors will be looked at in a more rigorous fashion.

Through testing with this technology we are hoping to gain a better understanding of the capabilities that can be provided in assessing the condition of the bridge deck. This will be completed through the different works expected to be completed in the future.

After laboratory testing is done, it is also planned that a camera will be mounted to the rear of a vehicle that will take photos at a predetermined rate that will allow for a 60% overlap of the images. The camera will be driven over the bridge in both directions covering one lane at a time. A 3D model will then be generated for the whole bridge. Some of the issues that will be looked at:

- What size crack can be seen
- What size spall or scalling can be seen
- Measure surface roughness
- Change shooting distance to determine what affect that has
- Look at how on-the-field shooting angles affects the accuracy
- Look at different light conditions
- What would be the right amount of photos for appropriate accuracy

Turning a 3D model into a "good, medium, poor" rating for sections of the bridge deck, as described in the technical memorandum nº 10 Decision Support System (DSS) description, will be another future step. The goal is to demonstrate the capabilities and limitations of 3D optics, tune the setup to ensure needed indicators are being measured, and to generate information for inclusion in the DSS, while keeping within an inexpensive system that could be easily and rapidly deployed by a Department of Transportation to bridges of interest.

THERMAL INFRARED

Thermal infrared (IR) inspection technique is based on measuring the radiant temperature of the concrete deck by using a thermal IR camera. The concept behind this technique is that the anomalies and subsurface delaminations interrupt the heat/energy transfer through the concrete. Thus, surface delaminations will appear as hot or cold spots on the thermal IR image.

Determining the subsurface anomalies within concrete slabs and depth of the delaminated areas are objectives in this experimental plan. Experiments were performed using a FLIR SC-640 Thermal IR camera (research & development grade), a digital thermal hygrometer (measuring ambient temperature & humidity), and proprietary software.

Preliminary Studies

Laboratory testing was conducted on the thin concrete slabs which were built with simulated delaminations. These slabs are 'filled' with impurities such as rebar, plastic bags, ping-pong balls, a plastic bottle, and so on. The layout of the impurities and size of these specimens are detailed in technical memorandum nº 5.

The slabs were placed outside in the cold where they spent over 24 hours. They were then brought in to the lab, which has a significantly higher temperature than outside and thermal IR images were taken inside the lab as the specimens warmed up. Test set up shown in Figures 1b & 2b.

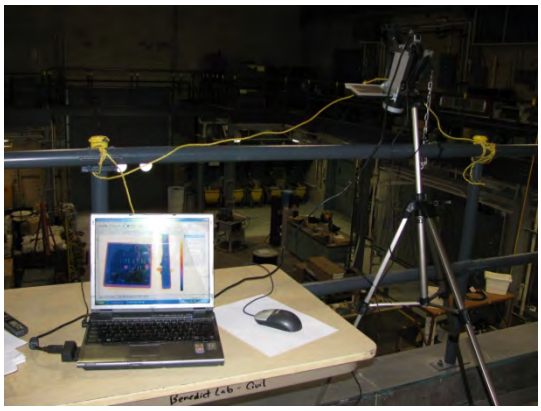

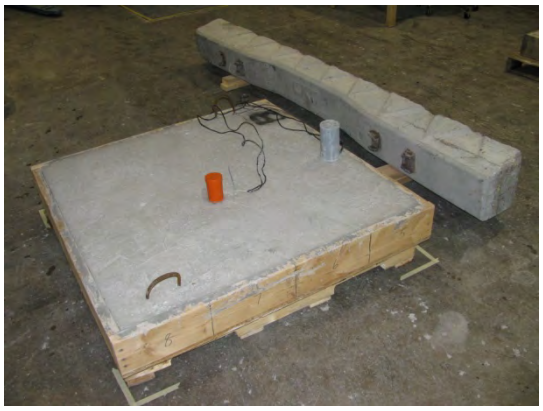

Figures 1b & 2b: Laptop, FLIR camera, one of the slabs, and a concrete railroad tie.

Slab AB (12-07-2010)

A thermal IR camera was set up at a distance of 15.2ft from the slab to take images every ten minutes during a six-and-a-half hour period (8:27am to 4:00pm). The lab temperature was around 69.8˚F and the relative humidity was 9.8%. The emissivity was considered 0.95 for the concrete slab. Figures 3b and 4b below are the two images, which were taken at 8:27am and 11:58am respectively.

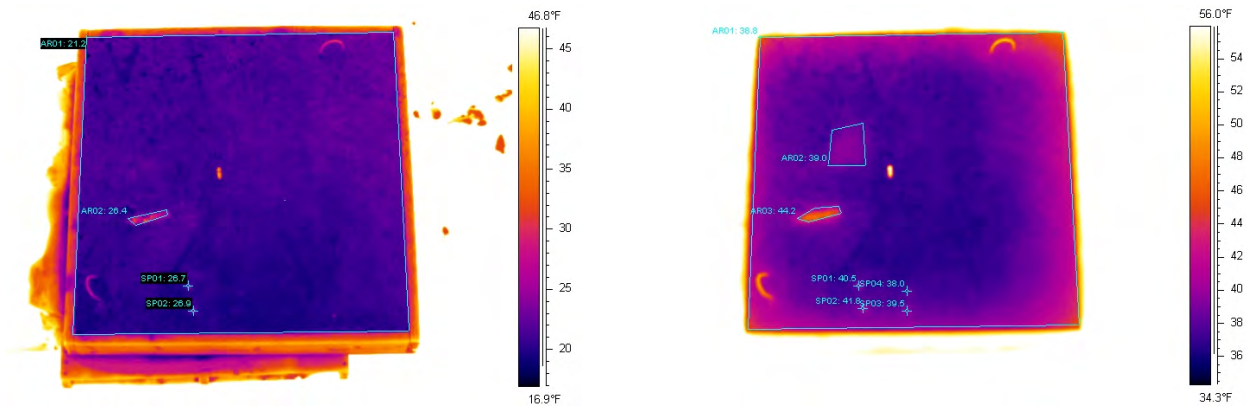

Figures 3b & 4b: Images taken at 8:27am and 11:58am respectively.

As shown in these images, the plastic bottle (which is very close to the surface) and ping-pong balls appear as hot spots in the thermal IR images and indicated delaminated areas close to the surface. Other delaminations, which were deeper appeared in the thermal IR images after a few hours, but they have lower thermal contrast compared to the ones closer to the surface.

Slab CD (12-17-2010)

The thermal IR camera was set up at a distance of 16.67ft from the slab to take images every 10 minutes during a seven hour period (9:28am to 4:30pm). The lab temperature was around 72.3˚F and the relative humidity was 13%. The emissivity was considered 0.95 for the concrete slab.

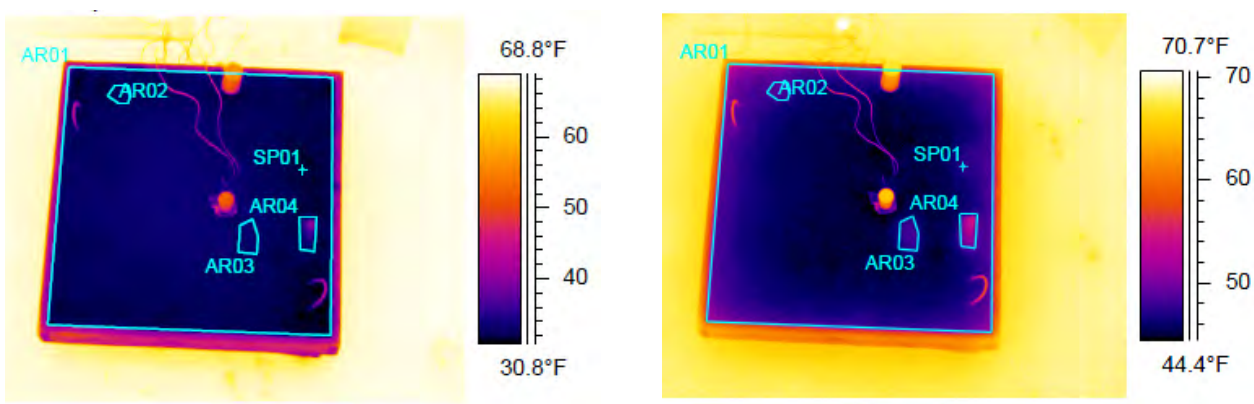

Figures 5b & 6b: Images taken at 9:28am and 12:58pm respectively.

Figures 5b and 6b are thermal IR images of the slab CD, which were taken at the start of the experiment and after three-and-a-half hours respectively. Areas three and four on these images shows defect D7, which is two pieces of Styrofoam 5/8 and 1.5 inches thick located four inches from the bottom of the slabs. Figure 7b is a graph of the average temperatures of these areas during the seven hour experiment period.

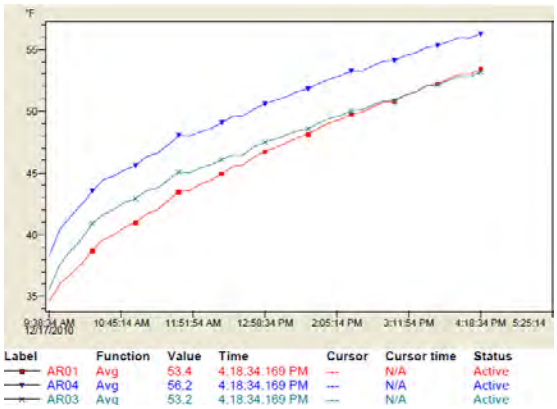

Figure 7b: Average temp vs time for areas 3 and 4.

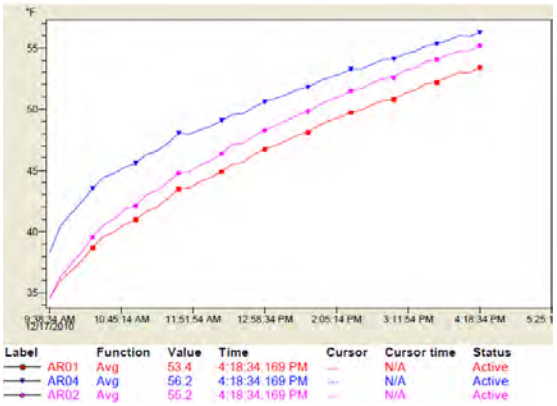

Figure 8b: Average temp vs time for area 2.

This graph shows that the maximum contrast between the delaminated areas and the average temperature of the slab appears after approximately 2.5 hours. Figure 8b shows the same graph for area two, which is a piece of wood 1.5" thick. Comparison of Figures 7b and 8b shows the difference in thermal conductivity between Styrofoam and wood, which causes the different heat/energy flow through the impurity and temperature contrast in the thermal IR image.

What's next for Thermal IR

With these experiments we expect to get a better understanding of the thermal IR technology and how to employ this technology for detecting bridge deck challenges. Future work with this technology will include further testing, determining the percentage and depth of the delaminated areas, collecting thermal IR information at highway speeds, and determining how different environmental conditions can affect the results.

DIGITAL IMAGE CORRELATION

Digital Image Correlation (DIC) is an optical based remote sensing technology suggested for challenges on the global metric level of the bridge system. Digital images before and after loading are optically compared and details about the structure's deformation and/or rotation information are determined. DIC will be employed for conducting laboratory experiments to verify methodology of the technology and apply it towards bridge condition assessment measurements of dynamic and static bridge behavior.

The overview plan involves laboratory testing of different structure samples such as W-shape structural steel members and concrete bridge pylons (concrete filled pipes) to determine static and dynamic behavior as emulated from bridge structures. Figure 1c below shows the pylons (note steel and concrete) and Figure 2c shows the sample bridge pylon during a compression test.

Preliminary Studies

To date, there has been much preparation for these laboratory tests to be completed in order to measure these particular bridge challenges associated with global-metric bridge interaction. This technique involves taking high resolution digital images and using computer algorithms. For the high resolution digital images, a Canon EOS 7D digital single lens reflex camera (DSLR) was selected for the photo recording device. This camera has been researched and used in image testing in order to gain an understanding of the camera's capabilities and functions.

Figures 1c & 2c: Bridge pylons on a pallet and pylon before a compression test.

In these tests, the standoff distances of the camera will be compared at short distances (within 5 to 10 feet), long distances (greater than 10 feet) and from vertical distances (from the top of the structures at different angles). Unique marks applied to the specimen's surface will enable detection of movement or rotation of the structure. This will allow the method to be analyzed for different displacement measurements in relation to bridge settlement, bridge movement and bridge length. The testing will also be applied to vibration testing in which a corresponding sampling rate for the images with be used for frequency detection. This sample testing involves 2D analysis, but can be further expanded to 3D image analysis with an additional camera implemented in the setup.

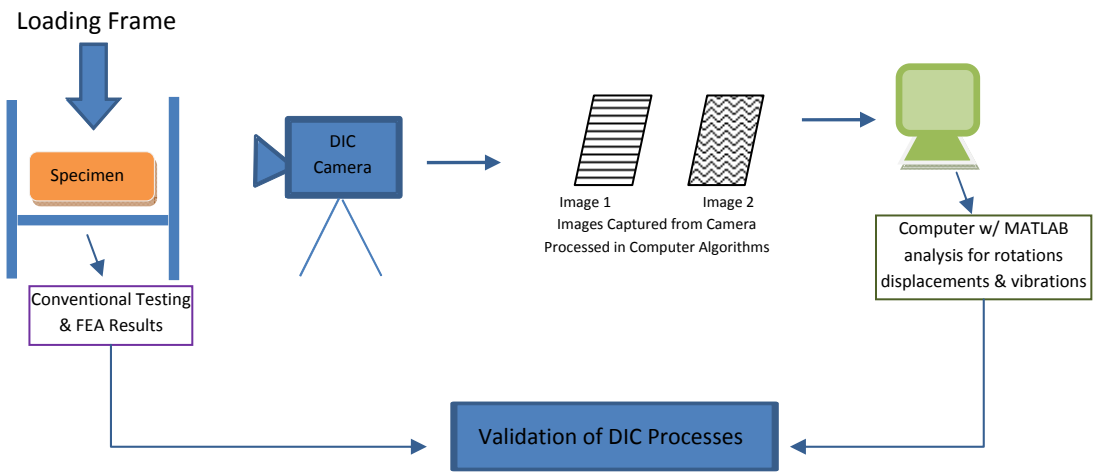

Figure 3c: Concept of Laboratory Setup

What's next for Digital Image Correlation

As stated this camera is used in conjunction with MATLAB computer processing and also involves a certain level of understanding for usage. MATLAB will process the images in a defined pixel by pixel grid analysis. Sample MATLAB program files have been reviewed and altered to correspond to the measurements needed for laboratory tests in measuring these global metric indicators. This correlation technique will be verified with finite element modeling using ANSYS. Modeling of the loading frame setup has been initiated for validation of the DIC measurements. The mechanical behavior and the "global metric challenges" measurements will also be collaborated (see Figure 3c) with computer modeling to compare the measurement results and calibrate the modeling itself. More information on finite element modeling can be found in Technical Memo 13.

RADAR

The goal of this exercise is to investigate the feasibility of utilizing an inexpensive radar system for non-destructive testing of concrete box-beams, girders, and decks to evaluate defects.

First, efforts would be restricted to investigating and understanding the phenomenology of the radar/box beam interaction and develop techniques to enhance features of interest. The next phase would identify the subset of useful techniques which would be evaluated for feasibility of field application and tested for efficacy under field conditions.

Although radar image resolutions are generally insufficient, concluding that the inexpensive radar is not an appropriate measurement system might be premature, since data products other than images can be formed. This is born out by the wealth of literature showing that the application of higher performance, more expensive radar using more standard techniques. Part of the purpose is to demonstrate that useful data products can be generated through less expensive radar systems.

Preliminary Studies

A modified Synthetic Aperture Radar (SAR) processing-code for forming images from the Akela radar was used. The code applies a method known as “Range Migration”, which takes into account the wavefront curvature resulting from the collection geometry. The processing code was modified and tested using data collected from well-known, point scatterers with impulsive response characteristics (corner reflectors) in a controlled environment (the MTRI antenna chamber).

This involved setting up equipment in the chamber to translate the antenna, allowing imaging in the cross range direction (see Figure 1d). The resulting images were used to tune collection parameters in the code to match precisely the collection geometry. The results were well focused images of the point scatterer, as seen in Figure 2d.

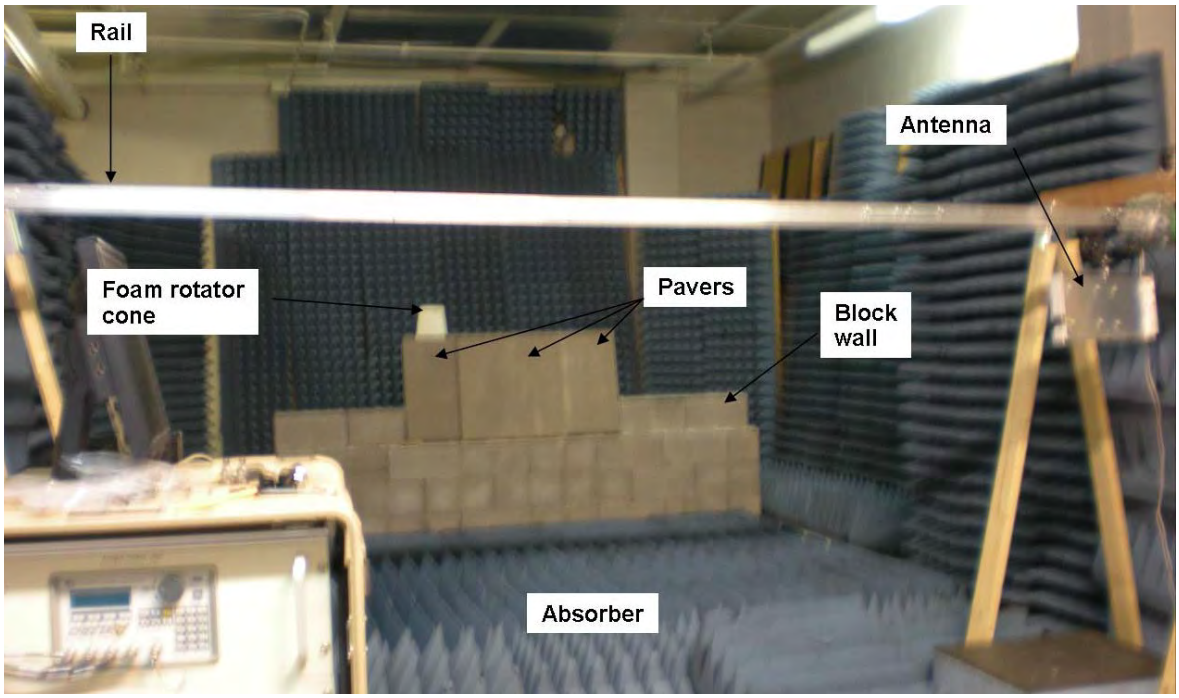

Figure 1d: MTRI antenna chamber with Lab Genie set up.

De-trending was successfully used to reduce noise from internal leakage and some residual chamber artifacts. With de-trending any linear trend is removed from each frequency step over the synthetic aperture. This removes artifacts that are stationary relative to the antenna motion such as internal noise and some artifacts in the scene (see Figure 2d). Some residual "non-stationary clutter" from the chamber that was still evident was reduced by employing background subtraction. In this technique, the scene is imaged with no targets of interest (image of clutter background), then targets of interest are introduced, and the scene is re-imaged. The clutter background data is subtracted coherently from the target data, resulting in better suppression of clutter as well as internal radar noise as evident in Figure 3d (software was developed to perform this task).

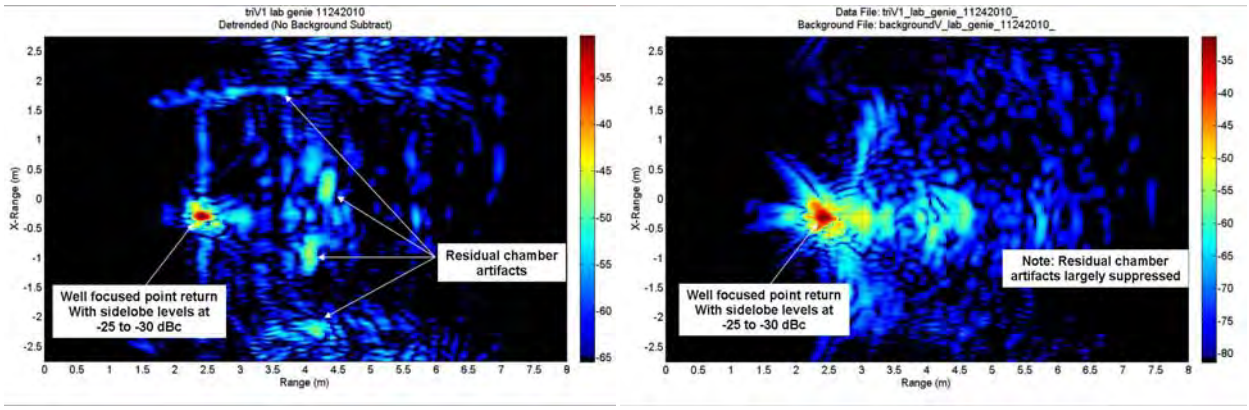

Figures 2d & 3d: Example of focused point scatterer with residual chamber noise and Point scatterer image employing background subtraction.

A concrete block wall was imaged to simulate the front surface of a box beam. Resulting images revealed internal structure of the hollows and solid areas (Figure 4d) of the wall and were consistent with Xpatch simulations of cinder-block walls in the literature[1].

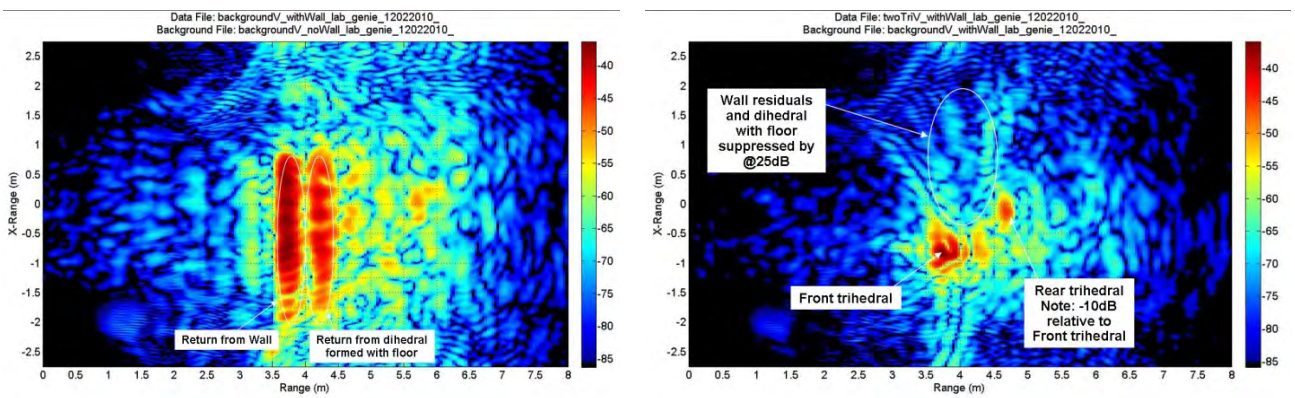

Figures 4d & 5d: Block wall with background subtraction and Corners in front of and behind block wall.

Imaging 2'x2'x2" concrete pavers, as being more representative of actual box beam construction, allowed us to simulate cracks and hollows by careful placement of the pavers. The radar was configured to provide 6cm spatial resolution in both range and cross-range. We imaged two pavers under several conditions; in close edge contact, with a 1mm gap between them, with a 25mm gap between them, and with Ø0.5in rebar in the gap and behind them. We

1 Traian Dogaru, Le, Calvin, "SAR Images of Rooms and Buildings Based on FDTD Computer Models", IEEE Transactions on Geoscience and Remote Sensing, Vol. 47, No. 5, May 2009

also imaged three pavers with the third paver being placed over the gap/seam between the other two pavers. As seen in Figure 6d, the background subtracted images correctly depict the two pavers, but the sub-resolution cell sized gaps (i.e. smaller than 6cm) were not readily distinguished. In Figure 7d, the 3 pavers are all readily distinguished as separate entities, despite the third paver being laid directly against the other two (extremely small seams). The reinforcing bar was visible to a trained eye.

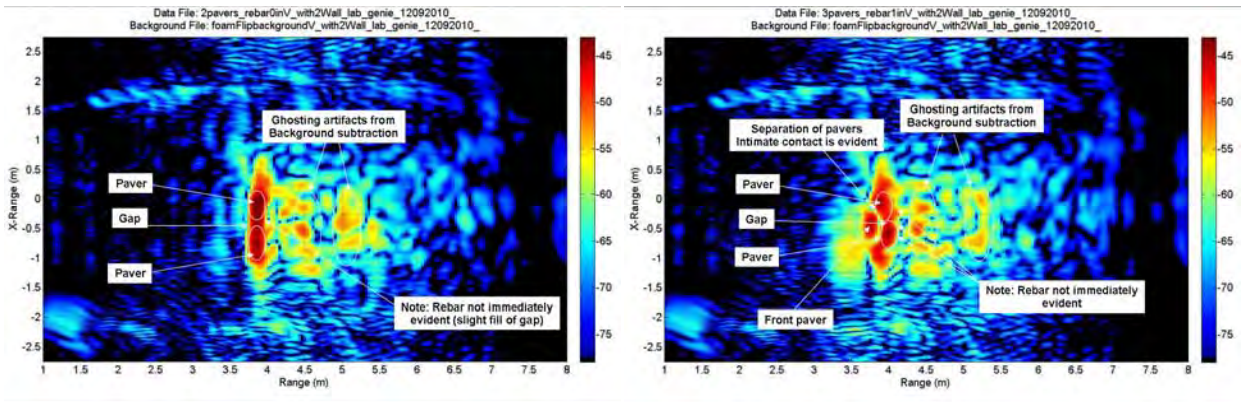

Figures 6d & 7d: Background subtracted image of two pavers with rebar behind and Background subtracted image of three pavers with rebar behind.

As expected, the radar could not clearly highlight gaps smaller than the resolution limit between the pavers (which simulated cracks). This prompted us to apply another technique to the processing known as “coherent change detection”. This technique is comparable to background subtraction, however it is typically employed by imaging a scene, then re-imaging that scene at some time later then coherently subtracting the later image from the original image of the scene. In this way, changes of a fraction of wavelength can be highlighted due to the radar’s inherent sensitivity to phase.

To illustrate the technique, we chose an image of the two adjacent pavers as the background image, and an image of the two pavers positioned with a 1mm gap between them. Figure 7d shows that the gap and the paver that was moved are clearly shown. This shows potential for inexpensive radar to clearly indicate physical changes that are significantly smaller than its resolution cell size (~3in^2).

What's next for Radar

The results show that the inexpensive Akela radar is capable of penetrating concrete, and the measured attenuation is consistent with the expected values for this material. Also, background subtraction processing is clearly preferable to de-trending when background data is available, although de-trending is readily applicable in the field while background subtraction may or may not be.

Performance could be improved by compensating for frequency/phase non-linearities of the system/antenna. This could make relatively low cross-section targets (such as rebar and small chunks of concrete) more readily observable in the presence of the strong return from the main structure of walls/beams. A higher gain antenna could improve system signal-to-noise ratio and improve detection of smaller cross section features of interest.

Extending background subtraction to employ change detection could be a powerful tool, although, as with background subtraction, spatial registration of the images used must be achieved to within a fraction of a wavelength of the radar signal. This means repeating measurements to within this accuracy, or measuring the errors to this accuracy. There may also be some means to do registration in software using prominent scatterers in the scene such as the large return from the face of the concrete. Combining the radar data with some of the optical techniques being explored could also prove to be extremely powerful.

Finally, we were somewhat limited in gaining good understanding of the phenomenology of the problem by not having an actual box beam available. Getting measurements of an actual box beam will help our understanding, and allow development of processing techniques better tuned toward extraction of features of interest. The following are considered necessary next steps:

- Improve calibration of the radar/antenna
- Investigate higher gain/better frequency response antennas
- Make field measurements of true box beam with and without flaws
- Evaluate whether these methods have practical application in the field
- Demonstrate how the processed radar data can be displayed in a way that is easily understandable to non-experts as part of the project's Decision Support System

Memo

To: USDOT/RITA research team members

From: R. Oats

CC: T. Ahlborn, D. Harris, C. Brooks, R. Dobson, J. Ebling, H. de Melo e Silva, D. Evans, B. Hart, C. Roussi, K. Vaghefi, P. Hannon

Date: January 14, 2011

Number: 12

Re: Structural Modeling

To date, the structural model development is continuing to progress as expected. Since the completion the Commercial Sensor Evaluation Report (Q3 2010), the direction of the finite element model development has continued to focus on simulating global system response of bridge structures. This finite element global system response is expected to align directly with some of the global metrics challenges observed by the selected remote sensing technologies described in the Commercial Sensor Evaluation Report such as: Digital Image Correlation (DIC), Interferometric Synthetic Aperture Radar (InSAR), 3D Photogrammetry, Radar, and Optical Interferometry.

In some cases, these global metrics may directly indicate a problem or damage (e.g. bridge settlement, or surface roughness); however, in other scenarios damage is inferred (e.g. vibration or deflection) from these observed metrics using damage identification technique. Finite element analysis (FEA) allows for the integration of these indicators into the models; however, the results (e.g. displacement, rotation, and vibration) from the developed finite element models align most appropriately with the technologies capable of observing global behavior responses. Other global characteristics such as surface roughness and degradation mechanisms (e.g. girder section loss or strand breakage and deck deterioration – spalls and delaminations) can be integrated into the models, but the output results will still be as a global system responses such as displacement, rotations, vibrations, stresses and strains. The integration of these global characteristics has significant value when considering damage

identification techniques that could be employed using the global response measurements, but this is beyond the scope of this study.

The finite element method is being used to simulate structural response to load, particularly those related to the multi-directional global level responses related to bridge movement. The models under development will be used to correlate with laboratory tests being performed in the Michigan Tech Structural Testing Facility. For these tests, a finite element model of the structural facility's loading frame has been created to appropriately calibrate the testing environment for the sample specimens. This is shown in Figure 1a and 1b. This allows for precise calibration of the structural model to ensure the expected results are determined and the accuracy of the loading frame. The measured results using traditional instrumentation techniques will then be used for calibration of the finite element models.

The laboratory tests will also be used as test bed for an expanded feasibility study particularly on DIC testing. The laboratory tests will focus on component testing that can be used to validate the model approach and compare with the DIC measurements. The calibrated finite element model is a simulation of the structure's behavior and global responses that will be validated through the DIC tests. The schematic of this idea is shown in Figure 2. These results can in turn be extrapolated to the development of a full bridge model for simulating global responses. Following the completion of the laboratory studies, the structural simulation studies will enable progression toward full scale bridge finite element simulation that will be used as part of the field demonstration phase. The models developed for this stage will aid in determining where measurements for global system response will be collected and for result comparisons.

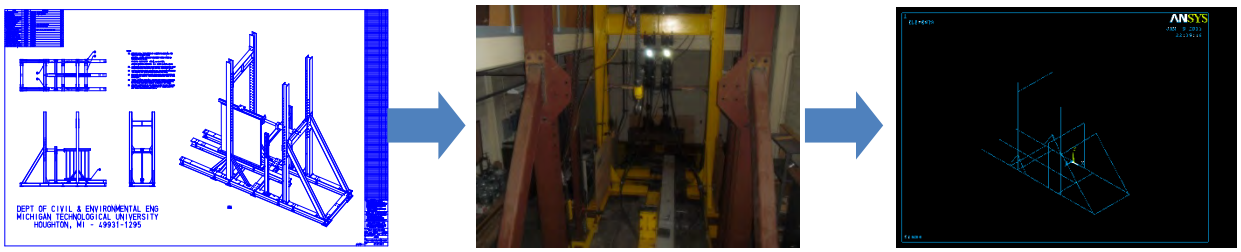

Drawing of Frame Picture of Frame Model of Frame

Figure 1a. Finite Element Model Creation of the structural facility's loading frame

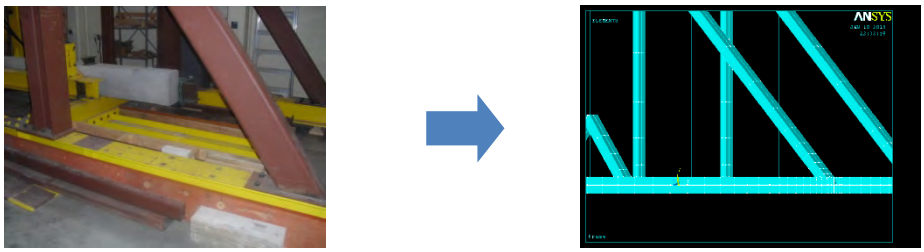

Figure1b. Close up of meshing capability in finite element model compared to digital photo image

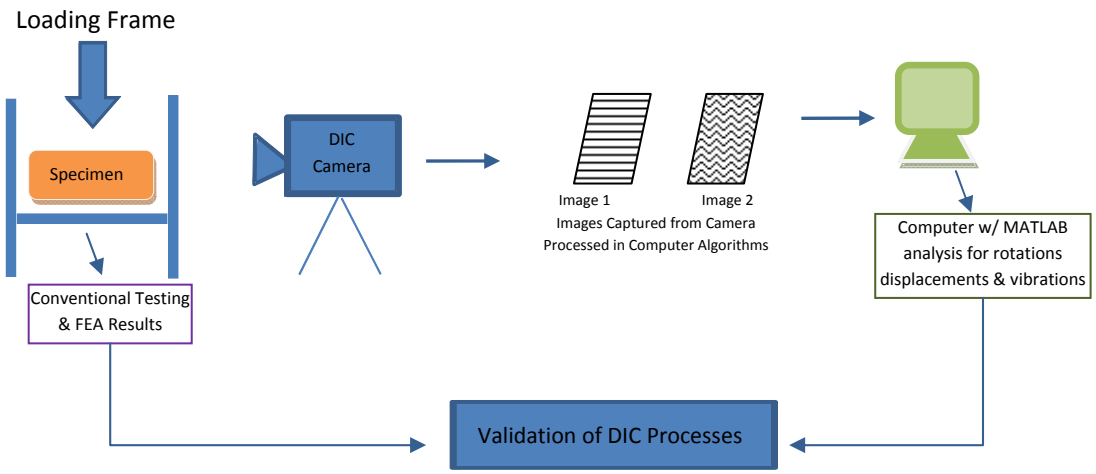

Figure 2. Schematic of DIC Processes Used in Collaboration with FEA Measurements

Michigan Tech Transportation Institute

Memo

To: L. Sutter, D. Harris, B. Shuchman, J. Burns, C. Brooks

From: Pam Hannon

CC: Tess Ahlborn

Date: December 22, 2010

Number: 13

Re: Technical Advisory Council Update

A summary report of the project's 3rd quarter activities was sent to all Technical Advisory Council members today for their review, along with a reminder that updates are posted to the website.

A tentative SAVE THE DATE meeting invitation was also included in the email. Our next TAC meeting will be held on **March 3, 2011** at the MTRI offices in Ann Arbor, MI.

Also, our annual project team meeting is scheduled for Wednesday, February 23, 2011. We will have a technical meeting with our colleagues at MDOT on Thursday, February 24. Both meetings will be held at the MTRI facilities in Ann Arbor, MI.

Memo

To: USDOT/RITA research team members

From: C.Brooks, K.A. Endsley, R. Shuchman,

CC: P. Hannon

Date: January 7, 2011

Number: 14

Re: DSS Update – 4th Quarter

The 4th Quarter Report summary describes the current three-tiered design that the Bridge Condition Assessment using Remote Sensors Decision Support System (BCARS DSS), which is:

1. Providing a field data interface to allow DOT users to access existing bridge condition information and to enter bridge condition data while out in the field.
2. The ability to display already-processed remote sensing data from previous collects in an intelligent, easy-to-use format and DSS tool interface.
3. The ability to integrate, analyze, and display remote sensing data for bridge condition indicators collected "live" in the field.

As stated previously, DSS design efforts in quarters 3 and 4 have focused on the first two tiers, which are within the scope and timeline of this two-year project. The third tier, integrating remote sensing data "live" into a DSS, is a logical next step for DSS development.

Tier 1 is a near-term goal of the DSS because many state departments of transportation, such as Michigan's (MDOT), already have web-based information tools that provide access to a database of bridge condition information. MDOT's Michigan Bridge Reference System (MBRS) provides a web-based interface to the data collected during previous bridge inspections, and is used by inspectors to plan for upcoming inspections and to prioritize repair work assignments after collection of field data. The Michigan Bridge Information System (MBIS) provides a web-based interface to enter (and retrieve) bridge inspection data in a format that looks very similar to the printed bridge inspection reports that

are currently taken out into the field. Providing access to these sorts of databases while out in the field, with the ability to navigate to the next bridge of interest, is our recommended first step in building an effective and useful DSS.

The current project work to design and test remote sensing technology demonstrations and practical field data collection methods will provide the example data needed to design and code the new software part of the DSS, which is our second and newly started tier. For example, we plan to integrate data from the current radar, 3-D optics, thermal IR, and digital image correlation lab work into the DSS. The data will be represented in the DSS as having been already collected for bridges of interest and translated into useful indicators of bridge condition for the inspectors and state-level planners to use in their bridge repair and Asset Management efforts. For example, using 3-D optics, a three-dimensional surface of a bridge could be analyzed and interpreted into a surface roughness per unit area value, which could be translated into a indicator of condition similar to the National Bridge Inventory rating system. We anticipate that a similar rating could be derived for the number of spalls per unit area for the deck bottom surface. Such quantities might be visualized as a color-coded overlay on a photograph of the bridge surface. A radar-based sensing of delamination presence or crack width could be displayed on a digital photo of that part of the bridge and integrated into a larger NBI-style indicator of condition.

A key point to remember when doing this translation of data into decision-supporting information is that the strengths of remote sensing are in being able to gain a wide spatial and temporal coverage while not necessarily obtaining the same resolution as manual, close-up methods. The benefits of this approach are realized when assessing the condition of bridges at the scale of a region or state through a geographic information system (GIS) that codes bridge condition and recent changes for a large number of bridges in a given region. The ability to integrate large amounts of data and then monitor change over time is another traditional strength of remote sensing-based technologies that this project and the DSS need to take advantage of. Taking the remote sensing data and creating indicators of relatively good, medium, relatively poor condition is another key goal. Presenting those overall ratings to the bridge condition community through the DSS to help make economically-efficient decisions on which bridges to focus on in a budget-limited repair environment is part of that goal. Highlighting changes in those conditions so that users represented by our Technical Advisory Committee can have the “red light / green light” indicators of problem bridges that they requested is another part of that goal. Figure A below shows an example of displaying bridge condition information (from Michigan’s Transportation Management System) this is also available through the MBIS) with a green-to-red (relatively good to relatively bad) condition state for the bridge deck, with a highlight on those the “Fair” (NBI rating of 5 or 6) condition that are typically the focus of MDOT repair efforts. This could easily represent a

highlighting of those bridges where the condition has recently changed based on traditional inspections combined with new remote sensing-based data.

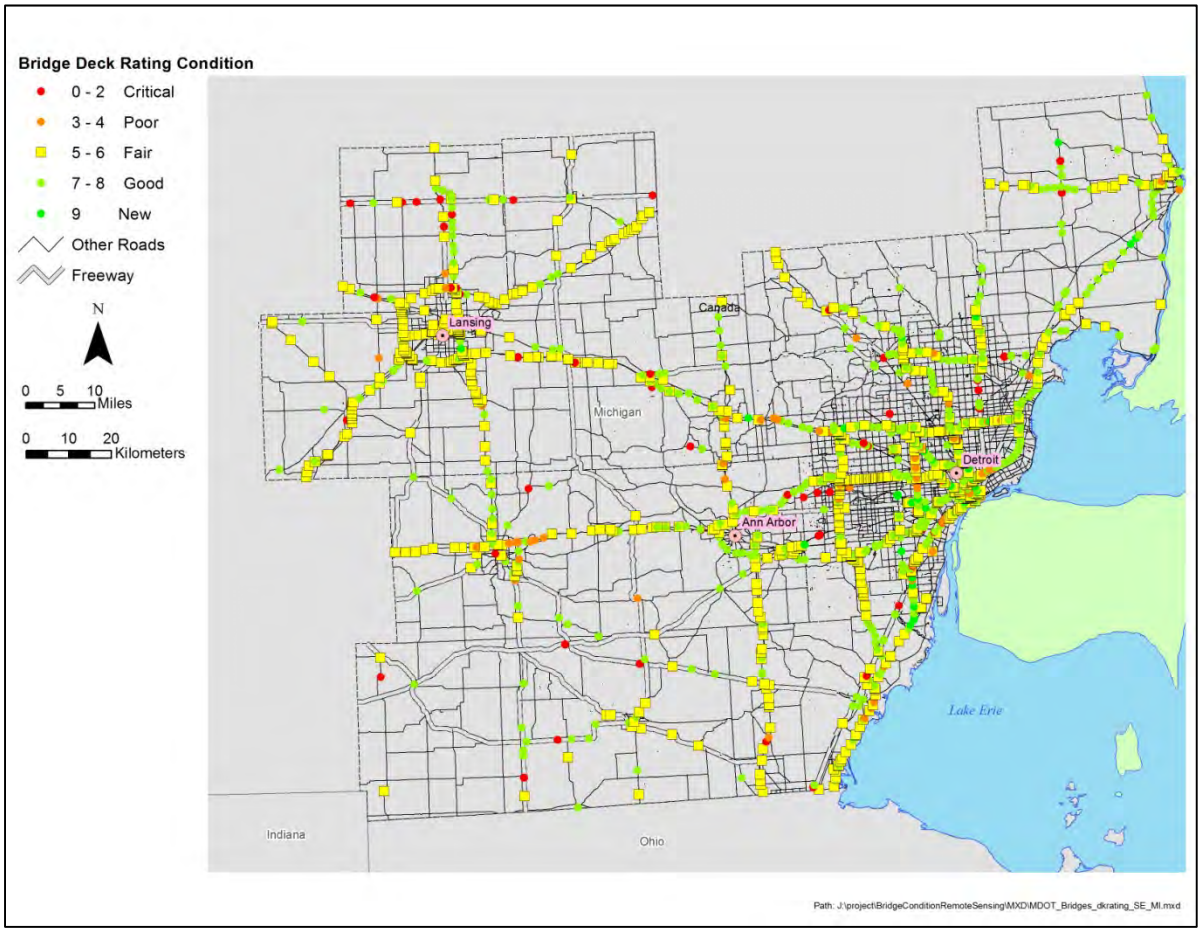

Figure A: A representation of Michigan's bridge condition data for southeast Michigan, using the deck rating as of March 2010, to show one way that remote sensing-based condition data could be presented to DSS users when integrated with traditional inspection data.

As stated in Tech Memo 10, we are now working on the DSS task as having a coincident end with the Field Demonstration (Task 5) so that we can integrate more data into it, enhance the interface and analysis algorithms based on the field demonstration data, and gain more information from ongoing lab work. We propose to deliver an interim report at the original deadline of April 2011 (end of Quarter 5) and a final, revised deliverable with the end of Task 5 (Quarter 7).

Memo

To: T. Ahlborn, D. Harris, L. Sutter, B. Shuchman, C. Brooks, J. Burns

From: H. (Kiko) de Melo e Silva, C. Brooks, J. Ebling

CC: A. Endsley, D. Evans, R. Oats, K. Vaghefi, R. Hoensheid, C. Roussi, R. Dobson

Date: April 14, 2011

Number: 15

Re: UPDATE – lab progress, structural modeling and remote sensing response correlation

---

3D PHOTOGRAMMETRY

The 3D photogrammetry investigation has been transitioning from lab testing to field demonstration in the last quarter. Validation was completed through the collection of high-resolution three-dimensional information on bridge spalls and bridge deck surface condition using inexpensive, commercially-available digital single-lens reflex (DSLR) cameras such as the Nikon D5000 and the Canon EOS 7D.

Cracks of different widths and depths were imaged to determine the minimum size the technology would be able to resolve. Figure 1a displays surface models of different cracks, each produced from multiple photographs taken at different angles and the resulting 3D point-cloud generated with the AgiSoft PhotoScan software. Each surface model was ported to ESRI ArcGIS as a Digital Elevation Model (DEM) in which the vertical information could be categorized on a pixel-by-pixel basis. The resulting images are shown in Figure 2a where each color represents an elevation change of two millimeters.

While the models from PhotoScan are useful, they are improved by post-processing in ArcGIS due to the added value from categorizing the elevation information and producing derivative products such as elevation contours. Using the DEM to estimate different crack widths, it can be seen that the 0.125 inch crack was visible.

Scaling and spalling of concrete (concrete loss or volume reduction) was also investigated using both image processing programs. Figure 3a shows a typical scaling/spalling problem found on a

concrete sidewalk which was, like the cracks, captured with the EOS 7D, pre-processed in PhotoScan, and post-processed using ArcGIS as shown in Figure 4a.

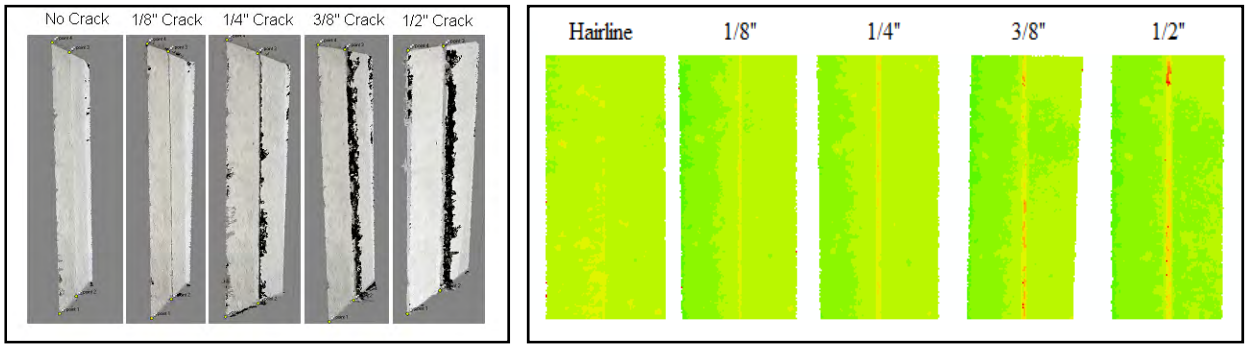

Figures 1a & 2a: PhotoScan models of each crack and DEM of the same cracks shown in ArcGIS.

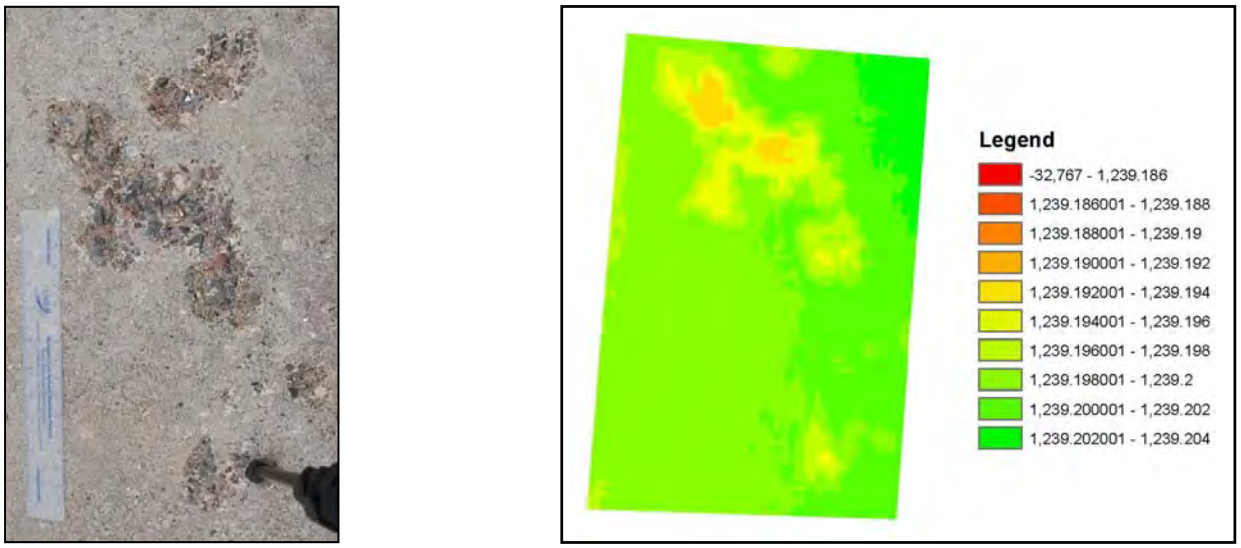

Figures 3a & 4a: Actual picture of sidewalk and DEM of spall.

Each model's points (pixels) can be grouped within an elevation range and the number used to calculate the area of that elevation range on the model, so given the number of points of a certain range, the overall area that is scaled or spalled can be calculated. The percent area that is scaled or spalled is simply calculated taking the total number of points per elevation range over the entire number of points for the image.

Specifically, to calculate the area of spall in the model above any value below 1239.198 meters was taken as a scale using the point information from the histogram shown in Figure 5a. This percentage was calculated to be 15.4 percent on the sidewalk model.

#	Colors	Text	Bar
0		-32767 - 1239.1859999999999	1
1		1239.1859999999999 - 1239.1880000000001	0
2		1239.1880000000001 - 1239.1900000000001	0
3		1239.1900000000001 - 1239.192	0
4		1239.192 - 1239.194	9,121
5		1239.194 - 1239.1959999999999	24,683
6		1239.1959999999999 - 1239.1980000000001	51,682
7		1239.1980000000001 - 1239.2	297,361
8		1239.2 - 1239.202	143,537
9		1239.202 - 1239.204	29,302

Figure 5a: Histogram of elevation points showing 10 ranges for sidewalk test.

Figure 6a shows another picture that was collected over an asphalt-overlaid parking lot. In addition to the PhotoScan model, the figure also displays the DEM, the deviations from the plane in ArcGIS, and the average deviations from the same plane.

Classification of surface roughness and percentage of “deck out-of-plane” can be easily registered, cataloged, and compared not only for bridge decks, but for any highway surface.

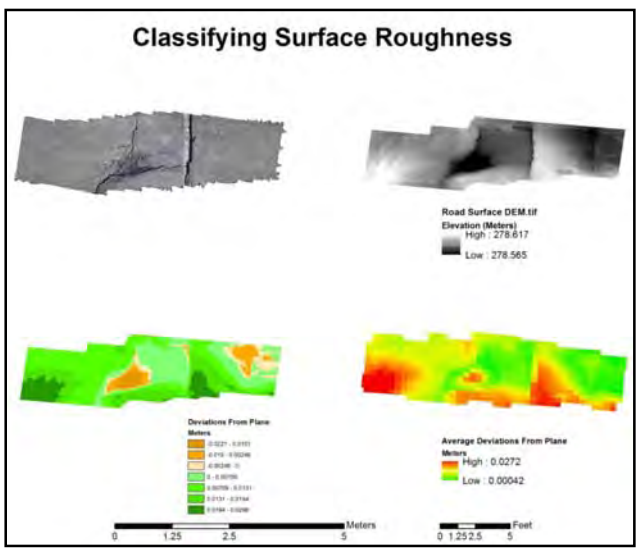

Figure 6a: An example of a damaged surface converted into an overall indicator of condition based on elevation deviation and average deviation.

To build from the work that has already been accomplished, a vehicle camera mount has been constructed to provide the necessary vertical offset (height above the ground) to collect data over one-lane’s width (~12 feet) per pass on a bridge deck for the creation of a 3D model of the surface. The vehicle mount fits in the bed of a pick-up truck and elevates the camera to a minimum of nine feet above the road surface as shown in Figure 7a.

Testing of this set-up has been completed in a parking lot and adjustments are being made in preparation for testing on the 6-Mile over US-23 bridge, where the most recent bridge inspection report is available for correlation purposes.

Figure 7a: Demonstration of close-range photogrammetry image collection system for bridge deck surface condition evaluation, currently undergoing further testing.

Next Steps for 3D Photogrammetry

- Test the vehicle-mounted elevated camera system on an example bridge, such as the 6-Mile over US-23 bridge.
- Based on testing, make refinements to the camera mount system possibly designing a mount to accommodate two cameras and varying heights.
- Prepare test data for integration into the Decision Support System (DSS)
- Plan for the upcoming field demonstration due to take place in the summer 2011

STREETVIEW-STYLE PHOTOGRAPHY

During this past quarter the StreetView-Style Photography focus was set on improving the practical deployment of a low-cost GPS-tagged photo collection system. The team's "BridgeViewer Remote Camera System" or RCS uses commercial digital cameras (such as the Canon PowerShot SX110 IS and the Nikon D5000) and sub-$500 GPS units to create a photolog-like inventory of bridge photos with geographic coordinates, allowing for easy viewing in existing GIS software such as ArcGIS or 3D globe viewers such as Google Earth.

The inspiration for this approach came from the inventory of street photography that has been made available by Google called StreetView. The practical extension of this concept for bridge condition assessment is the eventual deployment of a low-cost system for state and/or local DOTs to create a continuously-updated photo-record of a bridge. Recent efforts have included the attempt to increase the frame capture rate of the RCS; to take photos more frequently for the creation of a denser set of photographs which would allow for a more complete photo inventory to be generated, particularly when passing underneath a bridge at highway speeds.

Figures 1b and 2b show an example of the points where photos were taken using the RCS when passing over the 6-Mile over US-23 bridge near Ann Arbor, MI with a link to one of the GPS-tagged photos processed using the commercially available GPS PhotoLink software.

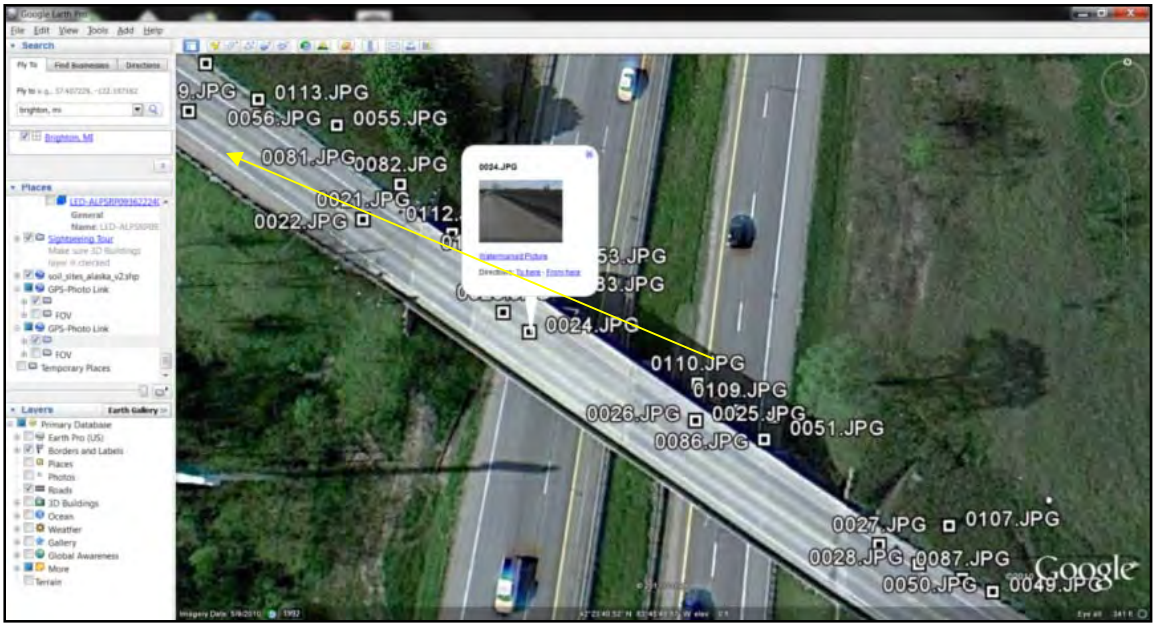

Figure 1b: An example of a GPS-tagged photo inventory created when driving over the 6-Mile over US-23 bridge shown here using Google Earth Pro.

Figure 2b: A GPS-tagged photo created when driving over the 6-Mile over US-23 bridge using the BridgeViewer Remote Camera System.

While investigating the application of these high-density photo inventories, the value of user-friendly visualizations was considered. The hardware necessary to collect a "gigapixel" (1,000 megapixels) photo (see <http://www.gigapxl.org/> and <http://www.gigapan.org/>) was previously purchased (~$800) and a study investigating the usefulness of viewing large amounts of photos of a location through Microsoft's Photosynth software <http://photosynth.net/> was performed. A fixed collection of photos was processed into a single 110 megapixel equivalent photo; the most recent hardware version is available for $895 at <http://www.gigapansystems.com/>.

These types of high-resolution photos could be taken easily and rapidly whenever a DOT needs to create a photo-based inventory of a bridge and use it to help compare changes over time. The Photosynth results are available at <http://photosynth.net/view.aspx?cid=260692da-9e0a-4d2d-bdec-a63776a7ab6b> and/or <http://bit.ly/dHWk2N>.

What's next for StreetView-Style Photography

- Refining the RCS to work at closer to highway speeds
- Refining the RCS to be able to take a frequent-enough series of photos to capture the underside of a bridge
- Demonstrating integration of the RCS, gigapixel, and Photosynth views of bridge data into the DSS

THERMAL INFRARED

Further Thermal Infrared (ThIR) testing has been done on the 80x45x9 (inches) slab prepared and reported on previously. This nine inch thick slab approximates the actual thickness of a bridge deck, providing a better representation of heat flow through concrete decks. The ThIR camera used in this experiment (FLIR SC640) was the same camera used in previous tests (see technical memorandum nº 11). Figure 1c shows the plan layout of the slab with simulated defects.

	#1	#2	#3	#4	#5
#6	#7	#8	#9	#10	#11

#1: 6"x6"x¼" Styrofoam located at 1 inch from the top surface
#2: 6"x6"x¼" Styrofoam located at 3 inch from the top surface
#3: 6"x6"x¼" Styrofoam located at 5 inch from the top surface
#4: 6"x6"x¼" Styrofoam located at 7 inch from the top surface
#5: 6"x6"x¼" Styrofoam located at 9 inch from the top surface
#6: pop can located at 9 inch from the top surface
#7: cardboard located at 7 inch from the top surface
#8: Plywood located at 5 inch from the top surface
#9: Surface scratch located at the top surface
#10: 0.7 mm plastic sheet located at 1 inch from the top surface
#11: pencil located at 1 inch from the top surface

Figure 1c: Concrete test slab layout showing 11 different types of defects and/or problems.

The test procedure was similar to what was done in the previous quarter. The slab (see Figure 2c) was placed outside and was brought in the lab, which had a higher temperature than the outside, and ThIR images were taken inside as the specimen warmed up. Figure 3c shows the ThIR image taken after 3.5 hours. Lab temperature was around 69.4 degrees Fahrenheit with a relative humidity of 6.8 percent. Defects numbers one and two were shown as hot areas on the image. Comparing the temperature results between similar defects in different levels show that defects located three inches below, or closer, to the top surface are more likely to appear as 'hot areas' on the ThIR image.

Determining the percentage of delaminated areas is one of the objectives of this study and will provide valuable input for the DSS. During the data processing, it was determined that taking ThIR images at a normal angle (camera perpendicular to the slab) will provide more accurate

results. In fact, viewing the slab from any other angle will reduce the number of pixels on the slab.

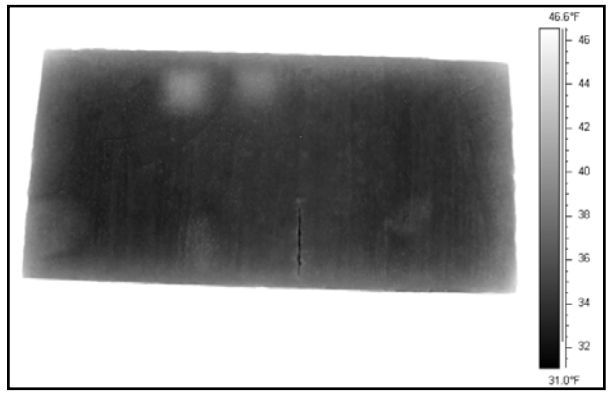

Figures 2c & 3c: Normal (optical) image and ThIR image of the nine inches thick slab after being warmed up for 3.5 hours inside the laboratory.

ThIR tests on slab CD (see technical memorandum nº 11) were repeated with a new lab setting to take perpendicular images. Also, noise reduction was turned off on the camera in order to collect raw data. Figures 4c and 5c show the test set up for taking perpendicular images. The plan layout and size of this specimen was attached in technical memorandum nº 5.

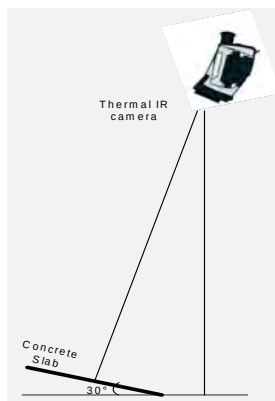

Figures 4c & 5c: ThIR lab test set up showing camera and slab perpendicular to each other.

Two approaches were taken to calculate the percentage of delaminated areas. The first one was using the FLIR ThIR software to draw the box around the hot areas and count the number of pixels within the box. The percentage of delaminated area in this test was determined by using the formula below.

$$\text{Percentage of delaminated areas} = \frac{\text{Number of pixels within the hot area}}{\text{Number of pixels within the slab}} \times 100$$

The second approach was saving the data as a comma-separated value file and using an MS Excel spreadsheet to count the number of pixels. In this test, the spreadsheet was set up to highlight and count the number of pixels within a specific temperature range that best shows the delaminations. One error that appeared in this test was the effect of the thermal gradient from the slab's edges which makes it difficult to assign a pixel to the outer most delaminated areas. Test results are shown in Figures 4c and 5c. The percentage of delaminated areas can be calculated by using the same equation as the first method as shown in Table 1c.

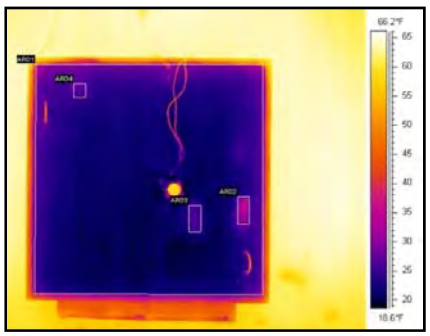

Percentage of Delamination		
Actual	Software	MS Excel
1.78	1.61	1.84

Figures 4c & 5c / Table 1c: Results of calculating the percentage of delaminated areas on the concrete slab using three different methods.

Previous studies on ThIR applications for bridge deck assessment show that the most suitable time for collecting the data is a few hours after sunrise. Another experiment was performed to compare ThIR images at different times of the day. The camera used for this experiment was a handheld FLIR i7.

Slab CD was placed outside during the night and ThIR images were taken the next day between one and three hours after sunrise during a very sunny day. Figures 7c, 8c, 9c, and 10c show the results of this experiment.

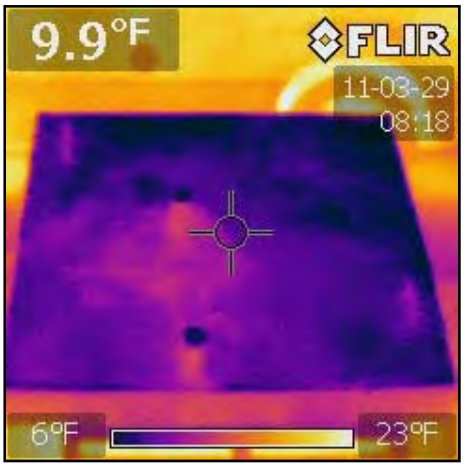

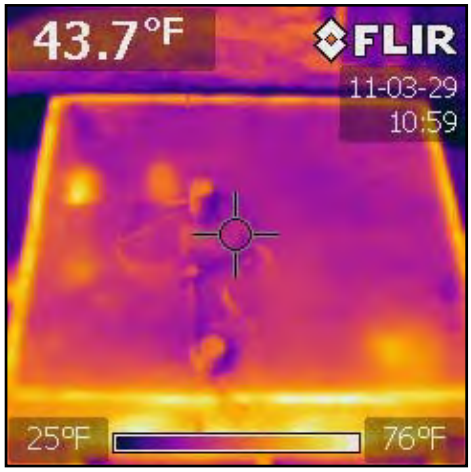

Figures 7c & 8c: Comparing ThIR images of the concrete slab at 8:18am and 10:59am.

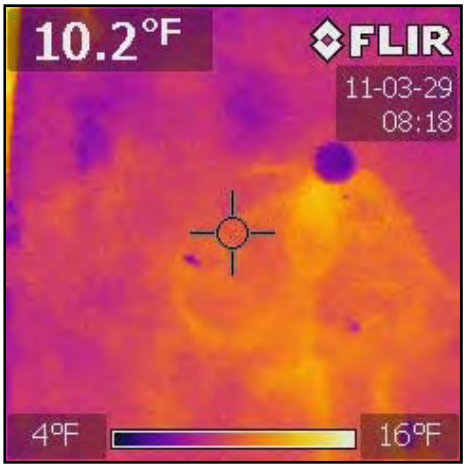

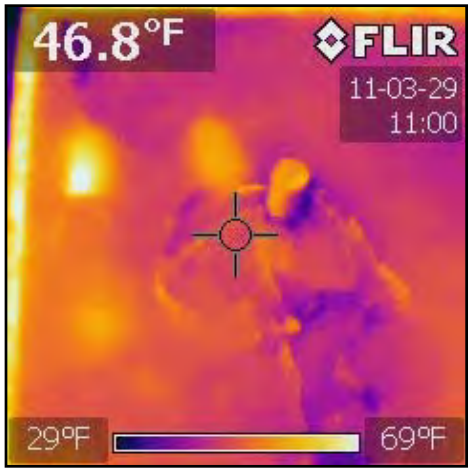

Figures 9c & 10c: Comparing ThIR images of the concrete slab at 8:18am and 11:00am.

Next Stesps for Thermal Infrared

- Collecting delamination data at various depths down to around five inches
- More involved data post-processing to obtain clearer images, including a focus on algorithm development for use in processing results appropriate for use in the DSS
- Collecting ThIR images at highway speeds
- Determining the factors that can influence the data collection and results
- Determining the best way to transfer the data/results to the DSS

DIGITAL IMAGE CORRELATION

Digital Image Correlation (DIC) has been investigated for its application toward bridge condition assessment measurements of dynamic and static bridge behavior. This technique involves taking high-resolution digital images using the selected Canon EOS 7D DSLR and using computer algorithms developed in MATLAB to process the images.

To date, there has been much investigation in the laboratory to measure dynamic and static bridge behavior associated with bridge global-metrics. Preliminary testing involved compression tests on bridge pylons (concrete-filled pipes) to determine correlation between optical images. An 18 inches tall section of a bridge pylon (Figure 1d) was placed in a compression-testing load frame and was subjected to a force of over 1,000 kip. The camera captured images at a ~12 inches standoff distance. In the analysis, the MATLAB software divided each image into a grid-of-grids; the sub-grids were then compared between images. Figure 2d shows the displacement field of the defined sub-grid on the images versus X- and Y-positions. Figure 3d shows the determined raw strain in the X-position found using the computer software. These measured values can be fine-tuned further by the specification of areas-of-interest on the images themselves.

Figure 1d: Section of a bridge pylon (concrete-filled pipe) in load frame compression test.

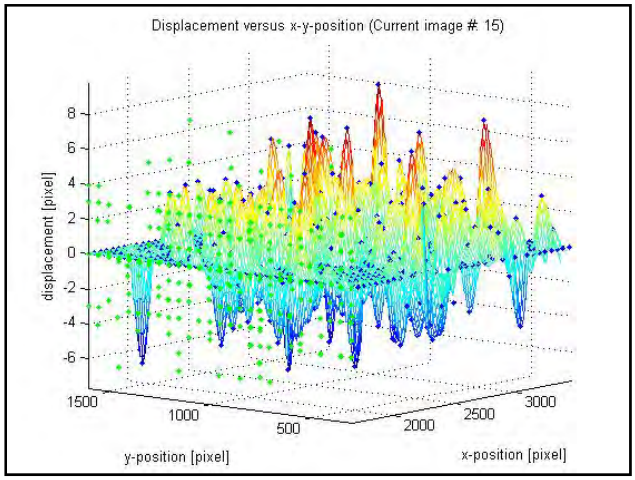

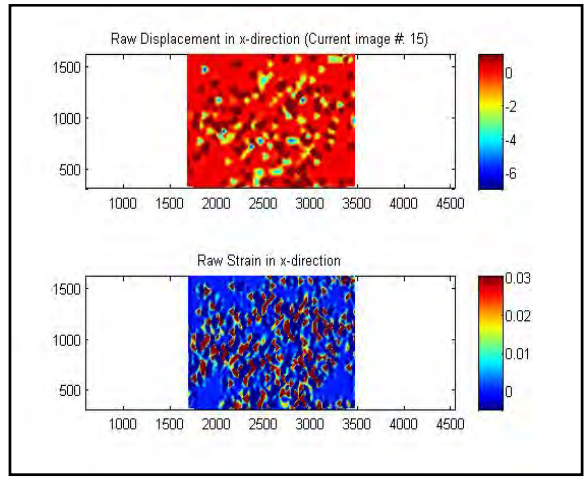

Figures 2d & 3d: Results of the compression tests for the bridge pylon.

Additional analysis of the digital image correlation technique involved looking at vertical displacement in comparison to the rotation of a specimen. A blue Styrofoam board sprayed with a random black and yellow pattern was tested focusing on movement, in particular, the displacement in both the X- and Y-directions (rotation about the Z-axis). The camera was placed ~two feet from the board which was subjected to rotation of around four degrees counter-clockwise. The images were post-processed in MATLAB and the computed results compared with the actual movement of the blue board about the Z-axis. Figure 4d shows the foam board and Figure 5d shows the measured displacement field results from the fully-rotated image. Additional post-processing techniques can reveal more defined results such as displacements within two specified markers from one image to the next.

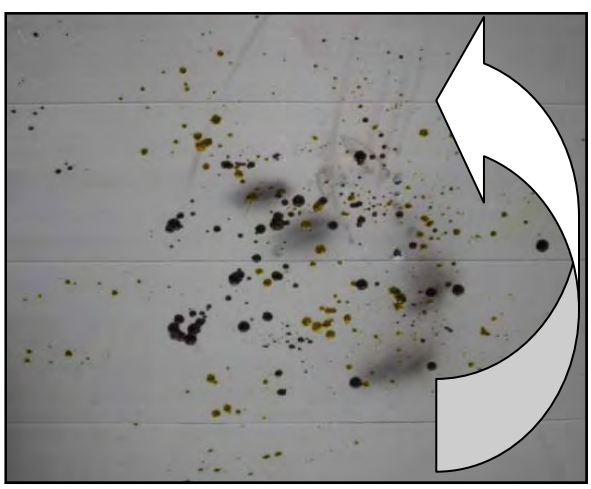

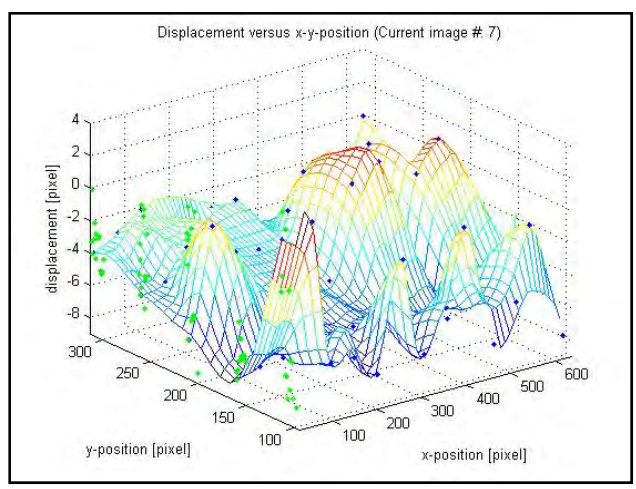

Figures 4d & 5d: Pictures of the Styrofoam board (showing direction of rotation) and its measured response.

To further understand flexural behavior, a simple flexure test was also conducted using a "two-by-four" wood specimen with a distinct surface pattern. In these tests, the viewing angle was varied (in both X- and Y-directions) to test the capabilities of this process. Variations in the software and camera settings were also explored. Figure 6d shows the wood specimen in the experimental setup with the flexure point in the center of the photograph. Additional investigation of these distances in relation to detection measurement will be correlated and examined.

Figure 6d: Picture of "two-by-four" wood specimen in testing machine.

Next Steps for Digital Image Correlation

- Additional post-processing will be completed on pictures to extract specific data from the image sets
- Continuation of flexure tests to ensure mobile flexibility with the camera and a comparison to field testing; various standoff distances and angles
- Testing of specimens in the structural self-reacting load frame in which distances and angles to the testing specimen can be manipulated for measurement detection
- Consideration of how results could be included in the DSS
- Correlation technique will be verified with finite element modeling using ANSYS (see Structural Finite Element Modeling section)

SYNTHETIC APERTURE RADAR

Prior to the field demonstration, a radar experiment involving a box beam is planned. One such box-beam, leftover from a bridge being demolished due to its poor condition, has been

identified. Access to the Silverbell bridge beam nº 12 (center beam) was acquired at one of the yards of the Oakland County Road Commission in southeast Michigan (see Figure 1e).

Contact with this box-beam highlighted the need for making measurements on 'good structures' and 'bad structures' (both with known defects) in order to be able to make quantitative assessments of condition. The box-beam not only provided an appreciation for the types of structures to be measured it also granted insight into the concept of operations for the field implementation.

Better calibration of the radar was also emphasized in Q5. Compensating for fluctuations in magnitude over frequency was found to be straightforward and will be implemented and tested using existing data. Phase linearity of the commercial Akela radar was found to be very good, but will primarily depend on the antenna phase response and the stability of the translator; characterization of the phase response for a few selected antennas with linearity correction are underway. While correcting for the phase non-linearities in the system should result in better focusing of the image products, it will be largely impossible to completely remove phase perturbations due to instability in the translator. The radar is especially sensitive to motion in the range dimension. If performing tests at higher frequencies is desired the translator would need to maintain accuracies consistent with the smaller wavelengths.

Figure 1e: Silverbell bridge box-beam saved for radar sensing work by the Oakland County Road Commission after the bridge was recently removed from service due to poor beam condition.

Due to the need for developing future field operations, focus was directed on analyzing the methods for making the field measurements more extensively, and on designing a better implementation of the imaging radar system. This has resulted in what is a rather novel method for collection of bridge deck surfaces using a 2D scanning approach and taking advantage of the known geometries for resolving ambiguities in the measurements. This method has a very desirable concept of operations (con-ops) that could possibly be extended to deployment on

board an Unmanned Aerial Vehicle (UAV) which could result in an extremely safe, cost-effective means of bridge deck assessment.

Using this approach, the radar antennas would be scanned along a linear track with a 2D range/cross-range image formed using the same range migration algorithm used for the lab experiments. The antennas would be located above the deck of the bridge, pointing down at the deck at an angle that would minimize the surface return to the radar, thus enhancing sensitivity to subsurface features. Note that surface defects would still be visible to the radar.

This method of collection has the potential advantage that the radar could eventually be mounted on the side of a vehicle and image a lane while driving in an adjacent lane. The vehicle's motion would provide the requisite translation for the 2D imaging. As mentioned previously there is a possibility of mounting the radar on an UAV to allow for more efficient data collection, at least for non-covered/obscured bridges. An experiment plan was developed for field experiments to attempt to validate the approach. A concern has been finding an area with no defects to image, then causing a known defect and patching it, while leaving subsurface defects. The area would then be re-imaged to determine if the subsurface features are visible.

A preliminary analysis of the box-beam was conducted but due to the geometries involved, a full 3D image would be required. In order to do this, an accurate 2D translator would need to be procured. Also required would be a ‘known good’ beam to image. The ‘known bad’ beam has been identified (the Silverbell box-beam) and an investigation is currently underway to ascertain if the components of a 2D translator with the requisite accuracy can be assembled economically.

Next Steps for Synthetic Aperture Radar

- Improve calibration of the radar/antenna and apply frequency response correction
- Conduct 2D imaging experiment in a controlled field test to investigate efficacy of technique to bridge deck evaluation
- Measure phase response and apply correction as necessary
- Evaluate efficacy of implementing 3D imaging apparatus and imaging of box beams
- Schedule/make measurements of both a pristine box-beam and one with defects
- Consideration of how results could be represented in the DSS

FINITE ELEMENT ANALYSIS MODELING

Finite Element Analysis (FEA) modeling is being used to simulate structural response to loading, particularly those related to the multi-directional, global-level responses related to bridge movement. For these tests, a finite element model of Michigan Tech’s structural facility’s self-reacting load frame has been created in ANSYS Structural to appropriately calibrate the testing environment for sample steel I-beam and W-shape specimens (see Figures 1f and 2f). The testing frame has been under review and configurations are being finalized for the testing of specimens under given loads to further collaborate with the finite element analysis model.

The FEA model of the frame has been evaluated under simulated loading for comparison with conventional loading frame measurements as demonstrated in Figures 3f and 4f. Sample outputs of this simulation detail global system responses such as displacements, stresses and strains as expected in this global behavior analysis.

Additional configurations of the FEA model are continuously implemented to maintain an up-to-date emulation of the structural frame. The laboratory tests will also be used as a test bed for an expanded feasibility study particularly on DIC testing as reported in the schematic process in technical memorandum nº 12. Ideally, these structural simulation studies will enable progression toward full-scale bridge finite element simulation that will be used as part of the field demonstration phase.

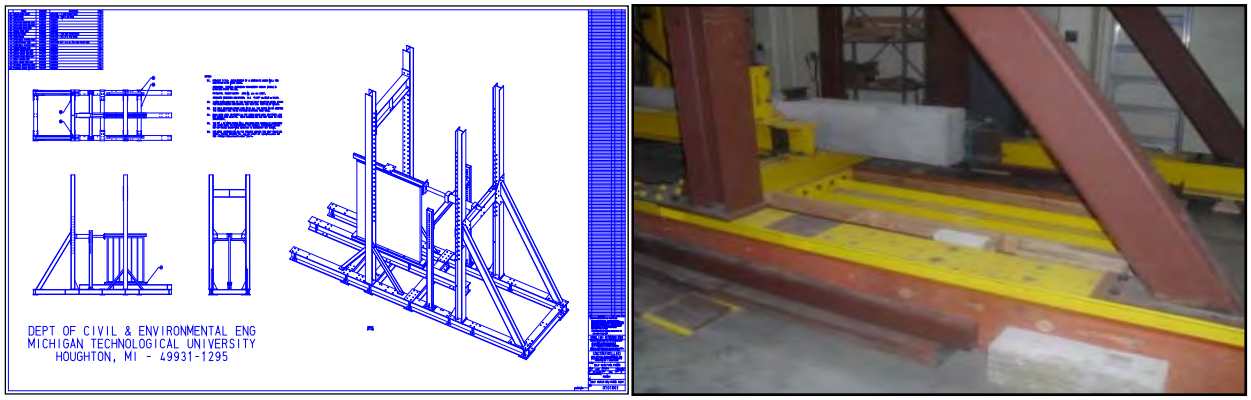

Figures 1f & 2f: Blue-print layout and picture of structural self-reacting load frame.

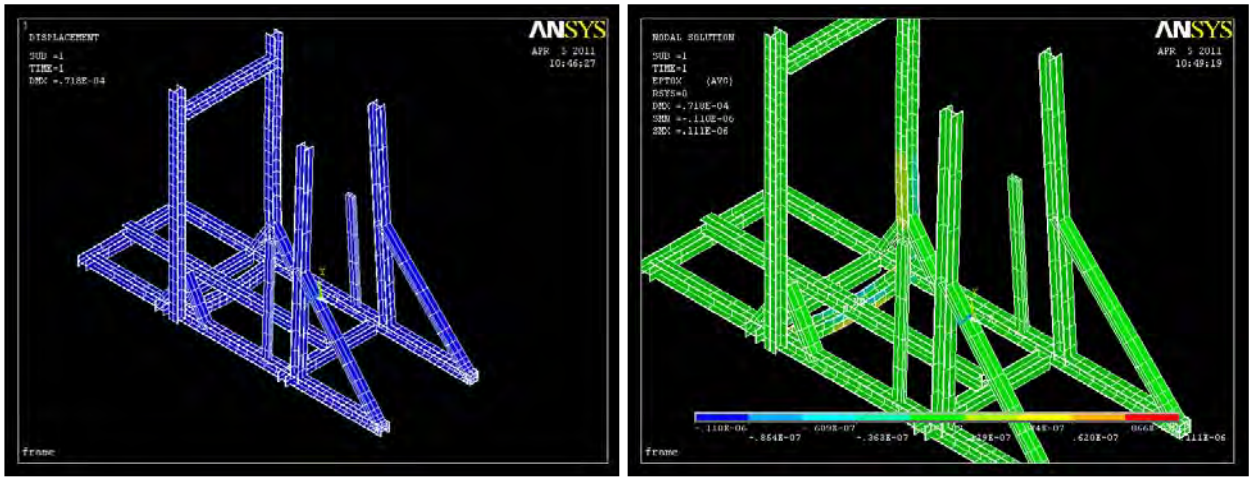

Figures 3f & 4f: Finite element model creation of the structural facility's loading frame; measured responses of displacement and strains are shown under simulated loading.

Next Steps for Structural Finite Element Modeling

- Continued configurations will be implemented to the FEA model to maintain an up to date emulation of the structural frame
- FEA modeling simulations in comparison with structural frame load tests in detection of displacements, strains, and other global systems responses
- FEA modeling of the selected bridge structures that will be tested in field demonstrations of remote sensing technologies
- Create a test bed for an expanded feasibility study on digital image correlation technique

REMOTE SENSING RESPONSE CORRELATION

A report with updates of the response correlation of the various remote sensing techniques and the respective data can be found in technical memorandum number16 being submitted together with this technical memo in the Q5 report. This will be a major focus over the next quarter.

Memo

To: T. Ahlborn, D. Harris, L. Sutter, R. Shuchman, J. Burns

From: C. Brooks, K.A. Endsley, M. Forster

CC: D. Evans, R. Oats, K. Vaghefi, R. Hoensheid, de Melo e Silva

Date: March 21, 2011

Number: 16

Re: DSS update - integration of bridge health indicators and development of the bridge condition signature

---

The first and second primary goals of our project, as stated in the proposal's Technical Approach, are as follows:

1. Establish remotely sensed bridge health indicators.
2. Develop a baseline bridge performance metric, the "signature," for benchmarking overall bridge condition.

The first goal is an ongoing effort to validate remote sensing technologies for bridge health applications which involves all members of the project team and includes activities such as laboratory testing of remote sensing technologies. These efforts have milestones such as the Commercial Sensor Evaluation Report (as posted to http://www.mtri.org/bridgecondition/Tasks_and_Deliverables.html) and the numerous experiment plans, collection procedures, and data processing workflows generated along the way. The next step towards achieving this goal involves integrating what remotely sensed bridge health indicators we have established so far into the decision support system (DSS) and linking them to traditional metrics of bridge condition.

The second goal, to develop a comprehensive metric of bridge condition, is a desired outcome of the DSS design and development. The Bridge Condition Decision Support System, currently under development and recently displayed at the Technical Advisory Committee meeting, will include the ability to apply algorithms used to extract and combine relevant condition information from sensor data, compare current sensor data to historical data in order to establish trends, and make recommendations to ensure optimal bridge health using cost-effective maintenance and repair protocols. Central to its utility will be the ability to synthesize measures of bridge condition from the disparate remote sensing, historical and inventory datasets. This effort will require insightful modeling and display of the data and careful design of the underlying DSS database.

A Survey of the Datasets and their Parameters

The following datasets are currently planned for integration with the DSS, depending on the level of development and practicality they reach through lab studies and the field demonstration:

1. Existing bridge inventory data (e.g. MDOT's bridge inspection data)
2. Radar imagery and analysis outputs
3. 3D optics models and analysis outputs
4. "StreetView-style" photography
5. Thermal infrared analysis results
6. Digital image correlation analysis results
7. Satellite imagery and aerial photography analysis results
8. Representative LiDAR data

Of these technologies, currently the 3D optics, StreetView-style photography, thermal infrared and radar imagery analyses are the furthest along towards a summer 2011 field demonstration. In late March 2011 we received a “snapshot” of the full bridge condition database used in MDOT’s bridge management system (BMS).

The remote sensing datasets will initially be comprised of specially-processed data, each with their own representation of bridge health indicators. It is the interpretation that arises from analysis of these outputs that must be represented in the database in a consistent and meaningful way. Meaningful indicators such as width of cracks, depth of spalls and area of delamination must be extracted from these outputs.

Starting with the existing bridge inventory data (in this case, from MDOT), the following parameters are those which are likely to be informed or updated by other datasets:

- Deck rating
- Substructure rating
- Superstructure rating
- Culvert rating (if any)
- Sufficiency rating
- Bridge length
- Deck width
- Clearance

The other fields in the existing bridge inventory data represent parameters that are not likely to be captured or updated by any other type of investigation. These bridge *metadata* signify that the table(s) of existing bridge inventory data will also serve as *lookup tables* for contextual information. This context includes bridge data that never change during the life of the bridge (e.g. year built, location) or bridge metrics that change only with human intervention

(construction and maintenance) such as the number of lanes and spans and the dates of maintenance activities. In addition, the existing bridge inventory of a state DOT contains the ratings (e.g. superstructure, substructure, culvert) given to the structure, and an approximately 10 to 12-year record of those ratings, according to a description of the database from MDOT. We are currently investigating the bridge condition database to gain a fuller understanding of all the details and time periods contained within it, and will be meeting with our DSS focus group to continue this process in April 2011. Included below is an overview of the technologies investigated during this project and the bridge condition indicators it is anticipated they can collect information about. The metrics of bridge condition to be extracted from these indicators are detailed as well.

The outputs from radar data collection (i.e. coherent radar images) initially cannot be represented as table(s) in a database. Feature/information extraction will deliver metrics of bridge condition that can be incorporated into the database and compared to other measures of bridge condition. Based on our laboratory testing and the Commercial Sensor Evaluation Report, radar is capable of resolving the following bridge condition indicators: deck cracking, delaminations, and corrosion of rebar. While the processed radar images will be made available separately within the DSS, parameters such as width of deck cracks, measured area, depth and extent (percentage of total area) of delamination, and crack density are expected to be derived from the analysis.

The outputs from 3D optics will include digital surface models and original high-resolution photographs. Final results and interpretations of 3D optics will be available through the DSS within the current constraints of web browsers. The major limitation to analyzing these data is that the digital surface models cannot be viewed within the web browser in 3D. Instead, 2D projections of these surface models might be made available for viewing. Analysis of the 3D models, through feature extraction algorithms not exposed in the DSS, should provide parameters of bridge condition assessment which will be incorporated into the DSS including depth, area, extent (percentage of total area), and volume of spalls, section loss and potholes.

Outputs from the "Street-View Style" photography will be a series of photographs or photographic panoramas. These will be made available in the DSS through a GIS, where the data are tied to their geospatial context. While feature extraction is not planned to be a part of the analysis of these data, they might have important metadata associated with them such as date/time of collection, collection rate, and vehicle speed in addition to the foreign key (NBI bridge identification) which ties the data to the established (inventory) metadata. These high-resolution "photolog"-type inventories allow state DOTs to efficiently monitor how a bridge has changed visually over time.

Thermal infrared imaging outputs are in the form of a series of photographs reflecting the changes in thermal radiation of the target over time. As with radar and other remote sensing modalities, the post-processed images will be available in the DSS for the power-user's interpretation and analysis. In addition, the following parameters of bridge condition will be

extracted and tabulated for comparison and visualization in the DSS: the depth, area, and extent (percentage of total area) of spalls, section loss, and potholes as well as the extent of deck cracks and map cracking. Since these metrics would also be extracted from the radar dataset(s), the DSS would offer multiple, equally-valid (presumably) measurements of bridge condition indicators which could be substituted for one another or used to complete a time series history of bridge condition.

The application of digital image correlation (DIC) to bridge condition assessment will produce numerous plots of the strain field over time as well as maps of rigid displacements. These outputs, generated by special processing algorithms, will also be available in the DSS (again, for power-users). The tabular metrics to be extracted from the post-processed data include the offset of bridge settlement or transverse bridge movement, and the amplitude, frequency, and modes of vibration.

Processed aerial and satellite electro-optical (EO) images, as with the images collected and processed through other remote sensing techniques, will be available for viewing within the DSS. The metrics to be extracted (through algorithms not exposed in the DSS) include measurements of bridge length, surface roughness, width of deck cracks, area and extent (percentage of total area) of map cracking and surface depressions as well as length of seal/expansion joint damage.

Based on what LiDAR data will be available for use in the demonstration DSS, the anticipated outputs, like those from 3D optics, will not be directly included in the DSS. Rather, the metrics extracted from these indicators will be included for analysis and comparison with other datasets within the DSS; these metrics include: width and depth of deck cracks, area and extent of map cracking and surface depressions as well as depth of depressions, volume of section loss and, possibly, the global metrics transverse bridge movement and bridge settlement offsets.

Integrating Multiple Indicators through Identifying Commonalities in Data Models

All of the datasets have some characteristics in common. As regards the database, they are each dynamic in that their respective tables within the database will be continuously updated with new records in the future. This is especially true for the existing inventory data which are based on routine bridge inspections. How are these metrics to be represented as a time series in the database? Are they best represented as a series of successive tables or as individual records in one table?

In the demonstration DSS, time series are likely to be represented by individual records that encapsulate an observation in time. The date/time stamp and the metrics obtained from a remote sensing data collection will be fields included with every record. Unless multiple observations are stitched together and a single, representative metric is produced, the granularity of records will be based on how many individual observations were obtained during a

survey (e.g. multiple snapshots of bridge deck captured by 3D optics camera system, thermal infrared camera, or scanning radar). This means that one bridge may have multiple observations (records) on the same day over the duration of a single survey of that bridge. To obtain the average deck crack width of a single bridge at a single point in time, say, extracted from multiple 3D surface models, aggregation of these records for the given time period would be performed. This “average deck crack width at the given time” could then be plotted in a series of similar measurements for the same bridge or multiple different bridges to extrapolate desired decision criteria of any kind (e.g. average crack width changes over time or distribution of crack widths in an inventory at a given time).

Another thing these datasets have in common, necessarily so, is their primary key. Identifying the primary key for a bridge database requires a consideration of the problem domain context. At a national level, every bridge in the U.S. has unique bridge identification (ID). In some state DOT's Bridge Management Systems, every bridge may also be identified by a structure number which is unique to every bridge in that state but is not necessarily unique outside of that state. For scalability, we have decided to use the national bridge ID as the primary key identifying unique bridges in our database. Each observation of a bridge condition indicator through any remote sensor is then tied to a specific bridge at a specific time. It is the temporal and spatial queries executed on these observations that derive the decision criteria of interest and allow for integration of multiple bridge condition indicators into a user-defined, comprehensive bridge signature.

Representing Bridge Condition Indicators through Established Ratings of Bridge Condition

In order to convey bridge condition in a meaningful way to bridge inspectors and manager, it is important to represent metrics of bridge condition through established rating systems (e.g. NBI). To this end, we will be using the current references and standards materials prepared for and by state DOTs, national transportation agencies and our representative DOT partner (Michigan). These are likely to include, but will not be limited to:

- AASHTO Guide Manual for Bridge Element Inspection - 2011, First Edition. https://bookstore.transportation.org/collection_detail.aspx?ID=97
- MDOT Project Scoping Manual - October 2009. http://www.michigan.gov/mdot/0,1607,7-151-9622_11044_11367-243045--,00.html
- MDOT Prestressed Concrete Box-Beam Superstructure Evaluation Handbook. April 2011. Available from the Michigan Tech Transportation Institute Tech and the MDOT Bridge Operations Unit.
- Recording and Coding Guide for the Structure Inventory and Appraisal of the Nation's Bridge. 1995. USDOT FHWA Report No. FHWA-PD-96-001.

- Reports and updates posted to the National Bridge Inventory web page (http://www.fhwa.dot.gov/bridge/nbi.htm).
- MDOT's Asset Management program information, especially as it relates to bridge condition information, such as the Bridge Management System of the Transportation Management System (BMS, http://www.michigan.gov/mdot/0,1607,7-151-9621_15757---,00.html).
- MDOT's Michigan Structure Inventory and Appraisal Guide (http://www.michigan.gov/documents/MDOT-Bridge-SIAMANUAL-2_87989_7.pdf)

To the extent that condition indicators for a bridge overall and bridge structural elements described in these and other relevant publications can be linked to remote sensing, this project will be able to demonstrate how remote sensing can be used to assess bridge condition and an overall bridge signature. The effort to synthesize a comprehensive bridge signature from the different bridge condition indicators is currently underway and will continue through the next quarter in both the bridge characterization task and the DSS development task. Our spreadsheet entitled "Performance Rating of Commercial Remote Sensing Technologies", as shown in Table 3 of the Commercial Sensor Evaluation report, was the start of that process. That spreadsheet and also an example of measurable bridge indicators tied to established ratings based on the Michigan Structure Inventory and Appraisal Guide, are attached to this memorandum.

Table 3: Performance Rating of Commercial Remote Sensing Technologies

Location	Challenges	Indicator	Desired Measurement Sensitivity	Rating Based, in Part, on Theoretical Sensitivity for Measurement Technologies											
				GPR	Spectra	3D Photo-grammetry	EO Airborne/ Satellite Imagery	Optical Inter-ferometry	LiDAR	Thermal IR	Acoustics	DIC	Radar (Backscatter/ Speckle)	InSAR	Streetview-Style Photography
Deck Surface	Expansion Joint	**Torn/Missing Seal**		0	8	14	12	11	13	11	0	0	9	0	13
		Armored Plated Damage		0	0	14	12	11	13	11	0	0	0	0	13
		Cracks within 2 Feet	0.8 mm to 4.8 mm (1/32" to 3/16") width	0	8	14	0	12	12	11	0	0	9	0	13
		Spalls within 2 Feet	6.0 mm to 25.0 mm (1/4" to 1") depth	0	8	14	12	12	12	11	0	0	9	0	13
		Chemical Leaching on Bottom		0	11	0	0	0	0	0	0	0	0	0	0
	Map Cracking	Surface Cracks	0.8 mm to 4.8 mm (1/32" to 3/16") width	0	8	14	12	12	12	11	8	0	9	0	13
	Scaling	Depression in Surface	6.0 mm to 25.0 mm (1/4" to 1") depth	0	8	14	12	12	12	11	0	0	9	0	13
	Spalling	Depression with Parallel Fracture	6.0 mm to 25.0 mm (1/4" to 1") depth	0	8	14	12	12	12	11	0	0	9	0	13
	Delamination	**Surface Cracks**	0.8 mm to 4.8 mm (1/32" to 3/16") width	0	8	14	0	12	12	11	8	0	0	0	13
Deck Subsurface	**Expansion Joint**	**Material in Joint**		0	0	0	0	11	0	0	0	0	0	0	0
	Delamination	**Moisture in Cracks**	Change in moisture content	11	0	0	0	0	0	11	0	0	0	0	0
		Internal Horizontal Crack	Approximately 0.1 mm (0.004") level	0	0	0	0	0	0	11	8	0	0	0	0
		Hollow Sound		0	0	0	0	0	0	0	8	0	0	0	0
		Fracture Planes / Open Spaces	Change in signal from integrated volume	12	0	0	0	0	0	0	8	0	12	0	0
	Scaling	Depression in Surface	6.0 mm to 25.0 mm (1/4" to 1") depth	12	0	0	0	0	0	11	0	0	0	0	0
	Spalling	Depression with Parallel Fracture	6.0 mm to 25.0 mm (1/4" to 1") depth	12	0	0	0	0	0	11	0	0	0	0	0
	Corrosion	Corrosion Rate (Resistivity)	5 to 20 kΩ-cm	0	0	0	0	0	0	0	0	0	0	0	0
		Change in Cross-Sectional Area	Amplitude of signal from rebar	13	0	0	0	0	0	0	8	0	13	0	0
	Choride Ingress	Choride Content through the Depth	0.4 to 1.0 % chloride by mass of cement	12	0	0	0	0	0	0	0	0	12	0	0
Girder Surface	**Steel Structural Cracking**	Surface Cracks	< 0.1 mm (.004"), hairline	0	8	11	0	12	0	11	0	0	0	0	0
	Concr. Structural Cracking	Surface Cracks	.1 mm (.004")	0	8	11	0	12	0	11	8	0	0	0	0
	Steel Section Loss	Change in Cross-Sectional Area	Percent thickness of web or flange	0	0	11	12	0	13	11	0	0	11	0	0
	Paint	**Paint Condition**	Amount of missing paint (X %)	0	9	0	0	0	0	11	0	0	0	0	0
	Concrete Section Loss	Change in Cross-Sectional Area	Percent volume per foot	0	0	11	12	0	13	11	7	0	11	0	0
Girder Subsurface	**Concr. Structural Cracking**	Internal Cracks (e.g. Box Beam)	Approx 0.8 mm (1/32")	0	0	0	0	0	0	11	8	0	0	0	0
	Concrete Section Loss	Change in Cross-Sectional Area	Percent volume per foot	0	0	0	0	0	0	0	7	0	11	0	0
	Prestress Strand Breakage	Change in Cross-Sectional Area	Wire 2 mm or strand 9.5 mm diameter	9	0	0	0	0	0	0	8	0	9	0	0
	Corrosion	Corrosion Rate (Resistivity)	5 to 20 kΩ-cm	0	0	0	0	0	0	0	0	0	0	0	0
		Change in Cross-Sectional Area	Amplitude of signal from rebar	8	0	0	0	0	0	0	8	0	13	0	0
	Choride Ingress	Choride Content through the Depth	0.4 to 1.0 % Chloride by mass of cement	10	0	0	0	0	0	0	0	0	11	0	0
Global Metrics	Bridge Length	**Change in Bridge Length**	Accuracy to 30 mm (0.1ft) (smaller)	0	0	15	13	0	0	0	0	9	0	12	0
	Bridge Settlement	Vertical Movement of Bridge	Approximately 6 mm to 12 mm	0	0	12	0	0	12	0	0	9	0	12	0
	Bridge Movement	**Transverse Directions**	Approximately 6 mm to 12 mm	0	0	12	0	0	12	0	0	9	0	12	0
	Surface Roughness	Surface Roughness	Change over time	0	9	14	13	12	12	0	0	0	11	13	13
	Vibration	Vibration	.5 -20 Hz, amplitude?	0	0	0	0	12	0	0	0	10	12	12	0

Example of Object Bridge Metrics for Applying Established Rating

		Percent of...	Concrete Deck (Top)			Concrete Deck (Bottom)				Steel/Paint Corrosion		Bearings		Expansion Joints
			Cracking		Spalling	Map Cracking		Spalling	Rust	Joint Cracks	Paint Weather	Section Loss	Coating Failure	Water Leakage
			Width	Spacing	Depth	Width	Spacing	Depth	Extent	Width, Proximity	Extent			Adhesion/Seal Failure
9	Excellent	< 2%	NONE	NONE	NONE	NONE	NONE	NONE	NONE	NONE	NONE	NONE	NONE	
8	Very Good	< 2%	< 0.8 mm		NONE	< 0.8 mm		NONE	NONE		"minor"		"minor"	NONE
7	Good	< 2%	< 1.6 mm	> 10 ft	"shallow"	< 1.6 mm	> 10 ft	"shallow"	NONE	< 0.8 mm within 2 ft of joint	"minor"		"minor"	NONE
	Good	0 - 2%	< 1.6 mm	> 10 ft	"shallow"	< 1.6 mm	> 10 ft	"shallow"	NONE		"minor"		"minor"	NONE
6	Satisfactory	< 2%	> 1.6 mm	< 5ft	6.4 - 13 mm	> 1.6 mm	< 5 ft	6.4 - 13 mm	< 2 %	> 0.8 mm within 2 ft of joint	< 1%	"minor"	"minor"	NONE
	Satisfactory	0 - 2%	> 1.6 mm	< 5ft	6.4 - 13 mm	> 1.6 mm	< 5 ft	6.4 - 13 mm	< 2 %		< 1%	"minor"	"minor"	NONE
	Satisfactory	2 - 10%	N/A		N/A	N/A		N/A	N/A		< 1%	"minor"	"minor"	N/A
5	Fair	< 2%	N/A		N/A	N/A		N/A	N/A		1 - 5%	"minor"	"moderate"	N/A
	Fair	0 - 2%	"excessive"		13 - 26 mm	N/A		N/A	N/A		1 - 5%	"minor"	"moderate"	< 5% of length
	Fair	2 - 10%	"excessive"		13 - 26 mm	"heavily map cracked"		13 - 26 mm	2 - 10%		1 - 5%	"minor"	"moderate"	< 5% of length
	Fair	10 - 25%	N/A		N/A	N/A		N/A	N/A		1 - 5%	"minor"	"moderate"	N/A
4	Poor	0 - 2%	N/A		N/A	N/A		N/A	N/A		5 - 10%	< 10%	"considerable"	N/A
	Poor	2 - 10%	N/A		N/A	N/A		N/A	N/A		5 - 10%	< 10%	"considerable"	N/A
	Poor	10 - 25%	"excessive"			"heavily map cracked"			10 - 25%		5 - 10%	< 10%	"considerable"	> 5% of length
	Poor	25 - 50%	N/A		N/A	N/A		N/A	N/A		5 - 10%	< 10%	"considerable"	N/A
3	Serious	2 - 10%	N/A		N/A	N/A		N/A	N/A		> 15%	< 25%	"considerable"	
	Serious	10 - 25%	N/A		N/A	N/A		N/A	N/A		> 15%	< 25%	"considerable"	"most of device leaking or loose"
	Serious	25 - 50%							> 25%		> 15%	< 25%	"considerable"	
	Serious	> 50%							> 25%		> 15%	< 25%	"considerable"	
2	Critical										> 50%			
1	Imminent Failure													
0	Failed													
	Source:	FHWA	MDOT		MDOT	MDOT		MDOT	MDOT	MDOT	MDOT		MDOT	MDOT

References: Michigan Structure Inventory and Appraisal Guide (MDOT), FHWA Specifications for the National Bridge Inventory (FHWA)

Memo

To: T. Ahlborn, D. Harris, L. Sutter, B. Shuchman, J. Burns

From: K.A. Endsley, M. Forster, C. Brooks

CC: D. Evans, R. Oats, K. Vaghefi, R. Hoensheid, de Melo e Silva

Date: March 30, 2011

Number: 17

Re: DSS development and decision criteria, beta version testing

---

The Decision Support System (DSS), a tool for helping bridge inspectors and managers to make informed and cost-efficient decisions about bridge maintenance, will be designed for flexibility with the multiple types of data generated by technologies evaluated in the course of this USDOT-RITA project. The relational database on the back-end is already capable of working with different datasets including geospatial data. We have already ingested a snapshot of the database used by MDOT in their bridge management system (BMS). This historical database of bridge condition information includes the following parameters that are accessible as decision criteria:

- Latitude
- Longitude
- Year built
- Year reconstructed (if any)
- Year painted (if any)
- Year overlaid (if any)
- Deck rating
- Substructure rating
- Superstructure rating
- Culvert rating (if any)
- Sufficiency rating
- Number of lanes
- Number of spans
- Material used in construction
- Paint type
- Deck width
- Bridge length

The DSS will incorporate multiple heuristics as needed to support bridge managers and other decision makers in evaluating bridge condition at an inventory level. A modular, web-based interface will allow the user to select only the decision from among different data

presentations. Decision criteria will be presented one of four ways, or data “views” for the user: in a geographic information system (GIS), in an interactive chart, in a table, or in a custom "remote sensing view" for photographs and other metadata or a custom remote sensing data view (e.g. interpreted radar images).

Visualizing Bridge Condition Data in a GIS

The GIS view will allow for the categorization of various elements of bridge condition, displaying all bridges in an inventory symbolized or color-coded by such inputs as deck condition rating or date built. Its most basic contribution to decision support will be the identification of bridges based on their location—a “spatial query.” This will be enhanced by the symbolism of different bridge condition parameters or "attributes" at the inventory scale—in effect, the "color coding" of bridges on a map. More advanced visualizations can be derived from position and attribute information by contouring or gridding a large number of bridges. This will allow for more complex relationships to be compared in more than two dimensions; that is, geography and single attribute relationships captured by simply color-coding bridges on a map would be improved by the ability to compare geography and more than one attribute (e.g. color-coded bridges for one attribute overlain on a contour map of another attribute). Here are just a few examples of the kinds of decision criteria a GIS could present in this context:

- **Categorization**: Deck condition of all bridges in an inventory, region, or city
- **Generalization**: Contour or "heat maps" of year built (and, by extension, age of infrastructure)
- **Distance, cost or path analysis**: Minimum distance to another bridge of a given or similar condition, age, etc...
- **Spatial aggregation**: Number of bridges within a certain distance of a given point (e.g. MDOT regional office) or radius within a certain number of bridges matching the given criteria are found
- **Interpolation**: Metropolitan infrastructure with deck condition interpolated along roadways for dense, adjacent bridges

Visualizing Bridge Condition Data in Charts, Graphs, Plots

The chart view will provide the usual benefits that come from plotting data points—specifically, the visualization of the relationship between two or more parameters. In many cases, one of these parameters will be time. At a recent team meeting with MDOT (in Ann Arbor, on February 24), an MDOT bridge inspector expressed interest in viewing the deterioration rate for bridges. Deterioration rate plotted as a curve against time would represent a repeatable database query of interest—the kind of functionality that can be programmed into the DSS for repeat access. Trend analysis of a time series might not be very useful for this application as the trends are generally well known: bridge condition deteriorates over time, bridges get older over time, and maintenance of bridges at regular intervals improves their condition over time. However, curve fitting might allow for the estimation of deterioration rate at

multiple scales. Decision criteria *at the inventory scale* that will be enabled by this presentation include:

- **Scatter plots**: Deck condition vs age, deck condition vs length, year built vs year reconstructed, paint type vs year painted, superstructure condition vs substructure condition...
- **Histograms**: Frequency of any bridge condition metrics
- **Pie charts**: Number of bridges given each rating for their deck, substructure, or superstructure; number of bridges in the inventory with virtually any parameter

For individual bridges, too, trend analysis of a time series is generally not as useful (as trend is known: bridges deteriorate over time). Again, the rate of bridge or structural element degradation might, however, be estimated from curve-fitting, an area investigated by MDOT Bridge Operations Engineer Dave Juntunen. Here are some decision criteria *at the scale of individual bridges* that will be enabled by this presentation:

- **Scatter/line plots**: Deck, superstructure, substructure or culvert condition of a bridge over time; plot of individual structural element ratings together
- **Trend analysis (if significant)**: Rate of bridge (whole) and bridge element deterioration
- **Multiple curve comparison**: Condition changes compared over time for bridge as whole; condition rating over time of every structural element
- **Pie charts**: Percentages of structural elements receiving various ratings throughout inspection history

Representing Bridge Condition Data in a Table or Grid

Despite the rich visualizations offered by the GIS and chart data views, a table of raw bridge metrics is still important for decision making as it offers insight into further relationships between data points and parameters that are not exposed the same way in a map or on a plot. Sorting, filtering, and aggregating records will be the most basic and essential functionality built into these data grids, offering insight into decision criteria that include the following:

- **Ranking**: Sorting records on any field finds the bridges built earliest, built most recently, in best/worst condition, with the most lanes or spans, etc.
- **Classification**: Multiple sorting of fields allows more complex classification such as the oldest bridges with the worst deck condition ratings or the bridges with the greatest number of both lanes and spans.
- **Exclusion/inclusion**: *Filtering* or querying records on multiple fields allows for very narrow categorization of bridges such as "bridges with a deck rating of less than 6 with no more than 2 lanes built before 1970 without paint type 3" to be found quickly.
- **Aggregation**: Fields can be summarized and totaled for any parameter such as the average deck condition rating of all bridges selected, the standard deviation of

sufficiency ratings, the most common year built or most common condition rating in an inventory...

Visualization of Bridge Condition Remote Sensing Data

The three views described so far make up the bulk of data presentation in a wide variety of fields for a number of applications. We have determined, however, that alone they are not quite sufficient for the representation of some datasets that are planned for incorporation in this study, namely remote sensing datasets. These data typically consist of imagery and other spatial representations in localized (i.e. individual bridge) coordinate systems. Here is a brief list of the kinds of data and their representation that should be enabled by the "remote sensing" view:

- **Radar image analysis**: Radar images of bridge decks, substructures or structural elements will be accessible in both their raw "blob" form and with advanced analysis techniques applied for feature extraction and/or defect identification; the latter results should be displayed on top of photos of the measured bridge, with annotations about detected cracks, delaminations, and their metrics; in many cases these overlays might be applied to a photograph of the bridge.
- **3D optical analysis**: 3D models derived from photogrammetry will be available in sa user-friendly form; the intended platform of the DSS (a web browser) is not currently a good environment for 3D modeling so it is likely that snapshots of 3D models or raster imagery of surface models will be made available instead, with the appropriate annotation about volume of spalls, depth of cracks, etc.

DSS Development: Moving from the Desktop to Mobile Devices

Our Decision Support System (DSS) will consist of a client-side interface developed in Javascript using the ExtJS library (http://www.sencha.com/products/extjs/). This library allows for the development of rich user interfaces in Javascript. When a website written with the ExtJS library is accessed from a browser, the HTML elements that make up the page, complete with dynamic behavior and event handlers, are rendered upon execution of the Javascript. As the library was designed for compatibility with all major desktop browsers on the market (e.g., Internet Explorer, Chrome, Safari, Firefox), it is during the execution of the Javascript code that the library dynamically responds to the client environment. Failsafe browser and OS detection is used when instantiating HTML elements and their associated behaviors so that only syntax compatible with that environment is used. The library exposes these detection schemes as a set of global Booleans (e.g. Ext.isIE6, Ext.isSafari) so that the developer can add additional, browser-dependent behavioral constraints (e.g. if (Ext.isIE) {// Code executed only for IE browsers}). Unfortunately, there is not Ext.isMobile to detect mobile browsers.

While the library is extremely reliable for desktop browsers, the library's performance on mobile browsers is not clear. For compatibility with the DSS, any candidate browser must be capable of:

- Understanding and executing Javascript
- Accessing Javascript files from external domains (e.g. Google Maps API)
- Performing GET and POST HTTP requests
- Receiving Javascript Object Notation (JSON) data in the body of an HTTP response

Additional features that are desirable, though not required, for candidate browsers include:

- Accepting and properly handling gzip-compressed (Javascript) files

From an independent developer's report (http://www.twintechs.com/blog?p=103), it appears that both browsers we tested here (iOS Safari and the built-in Android browser) support gzip compression.

Initial testing was conducted with our iOS (iPad/iPhone) and Android (Samsung Galaxy Tab) testbeds. With each device, we accessed web applications developed by MTRI using the same technologies that we plan to leverage for the DSS. These web applications are mostly (www.MichiganTechLakeSuperior.org/data) or entirely functional on mobile devices, though they obviously would benefit from design that was informed with a mobile browser in mind. Evaluation of the performance of these testbeds was largely based on our experience with the aforementioned web applications, as mobile devices do not offer the same developer's tools (e.g. Firebug) that desktop browsers do which would enable a more rigorous investigation. As it stands, our preliminary investigation reveals the following about critical feature support of mobile browsers:

	Safari on iOS	(Built-In Browser) Android
Understands and executes Javascript?	Yes	Yes
Access external Javascript?	Yes	Yes
Perform GET requests?	Yes	Yes
Perform POST requests?	Yes	Yes?
Receive JSON data?	Yes	Yes
Works with Highcharts library?	Yes	No?
Buttons, fields, drop-down menus work?	Yes	Yes
Scrolls overflow into view?	No	No

The lack of support for the Highcharts library on the Android testbed is not yet understood. There is no clear reason as to why one Javascript library works while another does not. The problem is likely one of available memory, instead, as the Android testbed seems to have initiated the process of drawing Highcharts charts (it displayed the "Loading..." waiting message) but never actually rendered a chart.

Beyond the initial critical features we identified, we discovered some additional user-interface (UI) constraints of mobile browsers in our investigation. With the Samsung Galaxy Tab in particular, which is much smaller than the iPad, screen size or "real estate" affects the functionality of UI components which were designed with the desktop in mind. Smaller buttons used to close or collapse windows were extremely difficult to click on using your finger on a touch-screen (Figure 1). In addition, regardless of screen size, the display of overflow (content that needs to be scrolled into view) is not as expected on mobile browsers. In fact, in most cases, the option to scroll hidden content into view was simply not available. This needs to be addressed when developing with the ExtJS library. It is obvious that a separate interface will be needed for mobile devices—one with a user-interface tailored for the touch-screen environment (e.g. bigger buttons, no need for scrolling).

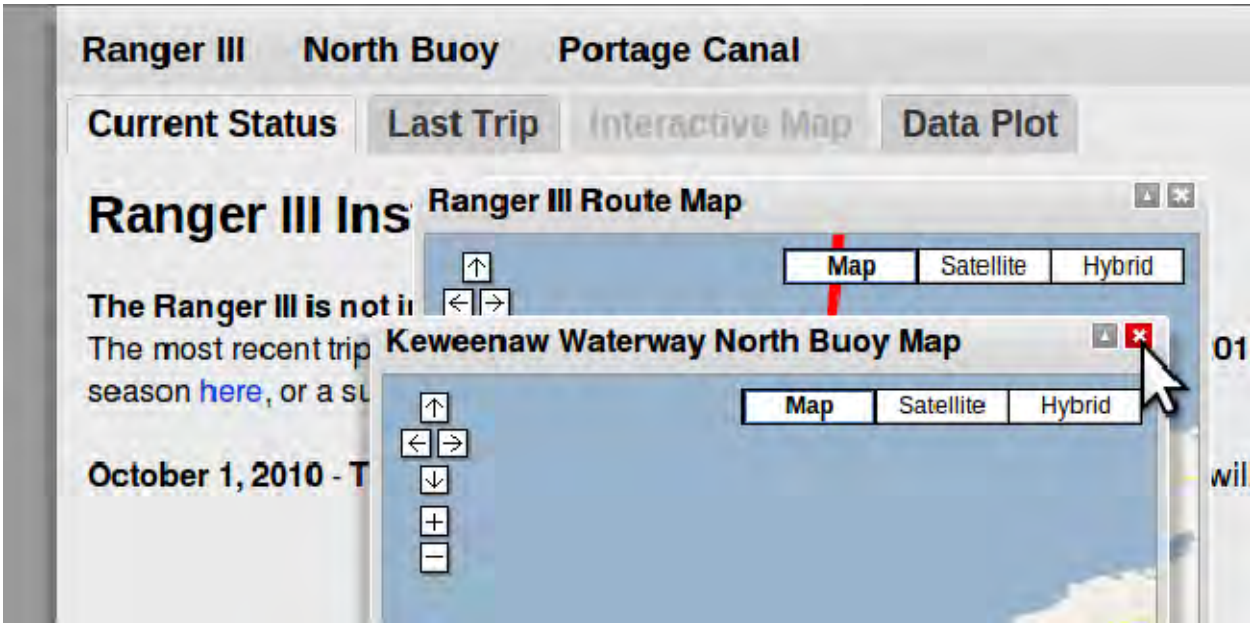

Figure 1: While the buttons to close or collapse windows are an appropriate size for desktop users, they are extremely small targets for a human finger on a mobile, touch-screen interface, as shown on this screenshot from www.MichiganTechLakeSuperior.org/data

While it is certainly an option to develop only one interface, intended for both the desktop and mobile client but with an interface optimized for mobile users, such an interface would hinder the desktop user's experience; in particular, it would be an inefficient use of screen real-

estate. There are also other advantages to having separate desktop and mobile interfaces. Not only would they each cater to the strengths of their respective environments, but the overall size of the application (in bytes) would be reduced significantly compared to directing mobile and desktop users to the same website which must include the code for both interfaces. A desktop-focused interface would also work on smaller "netbook" type computers; our MDOT partners have recently experimented with making these available in their bridge engineer pickup trucks. We will investigate this platform in addition to the tablet devices and more traditional laptop or desktop computers.

It is important to note that developing two interfaces does not necessarily involve duplication of effort. In our opinion, the development workflow in ExtJS supports development of a desktop interface first. The real functionality and working components of the DSS will not be rewritten for the mobile interface. Rather, the user interface, once completed for the desktop, would then be optimized for a mobile environment. The changes required should not include functional (i.e. algorithm or data processing) changes. We anticipate that dimensions, position, appearance, and some minimal behavioral changes to the desktop interface are all that are required to produce a mobile-optimized interface.

In the event that the interface cannot be optimized for mobile devices using the ExtJS library due to unavoidable technical constraints (e.g. overflow scrolling), we have the option to develop a reliable, intuitive mobile interface using the Sencha Touch (http://www.sencha.com/products/touch/style-design/) library. As both ExtJS and Sencha Touch are created by the same developer and are both written in Javascript it is likely there will be minimal duplication of effort. Ideally, we wish to develop a desktop DSS in ExtJS and then modify it for mobile devices using the same library. Performance on mobile devices will be a consideration throughout desktop DSS development. Regardless of how they are developed, both the mobile and the desktop interfaces would provide, necessarily, the same functionality and capacity for decision support tailored for their respective operating environments.

MichiganTech Transportation Institute

Memo

To: T. Ahlborn, C. Brooks, L. Sutter, B. Shuchman, J. Burns

From: D. Harris and R. Hoensheid

CC: A. Endsley, D. Evans, R. Oats, and K. Vaghefi

Date: March 30, 2011

Number: 18

Re: Site identification for the field demonstration and preliminary field instrumentation plan

---

As part of the field demonstration task of the project, a site selection process was initiated in Quarter 5. The aim of the site selection process is to identify potential bridges that can be evaluated using the suite of remote sensing technologies identified in this study. A primary goal of the site selection is to identify bridges that have varying degrees of degradation which have the potential to be identified and quantified using the remote sensing technologies. The end goal of the site selection is to identify two bridges within the State of Michigan that can be inspected (visual and detailed), tested, and evaluated using both traditional structural health monitoring techniques (strain gauges, deflectometers, live load vehicles, etc.) as well as remote sensing technologies (thermal IR, 3D optics, radar, etc.).

Preliminary site selection criteria were established during meetings with the Michigan Department of Transportation (MDOT) project panel on February 23rd, 2011 and our project Technical Advisory Council on March 3rd, 2011. These criteria include the aspects of bridge condition manifest in the bridge(s), the applicability of sensing technology to features of interest, schedule, proximity of the site to Ann Arbor (i.e. MTRI and CAR), safety, feature crossing, and interruption of traffic. Additionally, during the meeting it was concluded that the site selection should not be narrowed down to one bridge, but two bridges; that the first bridge possessed characteristics of a structurally deficient system (deck rating < 4) and another of slightly higher quality (4 < deck rating < 6). Other key characteristics include highway-over-highway bridges with span lengths greater than 20 feet, a concrete deck surface and no HMA overlay.

Current efforts are focused on refining the site identification protocol and selecting candidate bridges for further consideration. Presently, the selection process has been refined to include 300 candidate bridges and further refinements to the site identification process will continue in the coming quarter. Final selection will be made in conjunction with MDOT input. In addition to the site selection process, future quarter activities will include the formal development of a field instrumentation plan that will highlight procedures, equipment, personnel requirements, logistics and details of the proposed testing program. This instrumentation plan is expected to serve as a

guide for all of the field demonstrations and will also aid MDOT with coordination of traffic control and lane closures.

Memo

To: RITA Project Team

From: D. Harris

CC:

Date: July 13, 2011

Number: 19

Re: Lab progress, structural modeling and remote sensing response correlation

---

Since the previous quarter, activities in the lab and the structural modeling have shifted focus to the field demonstration planned for Quarter 7 (August 2011). A summary of the field deployment plan is presented in Technical Memo 20, which emphasizes field instrumentation installation and calibration as well as the field deployment. This memo describes the laboratory and structural modeling progress that was made with the following technologies in Quarter 6.

Digital Image Correlation

The application of digital image correlation in this project has historically used non-proprietary MATLab code, but in the past quarter the project team has shifted to a commercially available software package (Correlated Solutions Vic2D) which was much more user friendly and applicable to the global system measurements of interests. The team has had success in using our existing digital SLR cameras with this software package and is currently testing the limitations for field application of the technology. Efforts have focused on establishing the sensitivity of the technology as compared to traditional methods, testing of the influence of aspects such as angle of measurement and lighting, and final equipment requirements for field testing (e.g. lenses, lighting, and marking pattern). It is expected that digital image correlation will be deployed on one of the three proposed bridge sites with a focus on measuring global deflection for further correlation with finite element results and tradition deflection measurement tools.

LiDAR

The application of LiDAR was not originally included in the assessment plan, but collaboration with a current Michigan Tech faculty member, who purchased a LiDAR system, prompted

reconsideration. In the past quarter, the LiDAR system was evaluated on a trial basis collect sample data that could be included in the beta Decision Support System. In addition to the MTU owned system, the project team has also initiated discussions with Michigan Department of Transportation (MDOT) for acquisition of LiDAR data collected by MDOT's surveying group with MDOT owned equipment. The data sets from both of these collaborations have proven useful to the project and as a result, plans have been initiated to incorporate LiDAR data collections in the field deployment plan. The proposed activities include collection with both LiDAR systems for comparison to other technologies being deployed (e.g. deck surface features using 3D photogrammetry and deflection measurements using digital image correlation).

Additional progress has been made on other technologies including thermal IR, 3D optics, and streetview-style photography, synthetic aperture radar (SAR), and interferometric synthetic aperture radar (InSAR), but these efforts have primarily centered on challenges and logistics associated with field deployment and are not presented herein.

STRUCTURAL MODELING

The finite element modeling in this project has consistently been coupled with global response metrics and as a result aligns well with technologies that assess global response such as digital image correlation and the recently added LiDAR. In the past quarter, the finite element model development has been limited due to preparations for the field deployment; however it is expected that results from the field deployment, specifically digital image correlation and LiDAR results, will be compared against finite element model simulations of the bridge response. Future activities will include the development of models for the bridges that will be evaluated for global system response (see Technical Memo 20 which describes the field deployment plan). While the models will be capable of simulating the response of the bridge to a variety of loading scenarios, the results from the field deployment will be limited to specific locations and loading scenarios and as a result will not provide sufficient detail for model updating techniques.

REMOTE SENSING CORRELATION

When considering the overall objectives of this study, the primary emphasis has been placed on establishing an indicator of global health of bridges. In the initial stages of the project, a decision was made to focus on indicators of health that can likely be observed using classical and non-classical remote sensing technologies. With consideration of the guidance provided by the project partners (MDOT) and our TAC, the focus of the project shifted to challenges of deterioration and condition monitoring on a temporal basis rather than structural safety (e.g. engineering behavior and safety). As a result of this focus shift, the project team recognized that the concept of a bridge health signature is extremely useful to a decision-maker, but the components of this signature are unique to each user and beyond the scope of this limited study. In lieu of developing a unique signature, the project team will focus efforts to provide ground truth of the various remote sensing technologies with traditional methods of evaluation and developing a highly adaptable decision support system that provides the user with indicators of condition upon which to make decisions to implement into the development a unique bridge signature.

Memo

To: T. Ahlborn, D. Harris, L. Sutter, R. Shuchman, J. Burns

From: H. de Melo e Silva, C. Brooks

CC: A. Endsley, R. Oats, K. Vaghefi, R. Hoensheid, R. Dobson, J. Ebling

Date: July 14, 2011

Number: 20

Re: Field Deployment and Instrument Installation and Calibration Plan

---

SELECTION CRITERIA

The aim of the site selection process was to identify bridges that have varying degrees of degradation with potential to be identified and quantified using the remote sensing technologies. The end goal of the site selection was to identify three bridges within the State of Michigan that can be inspected (visual and detailed), tested, and evaluated using both traditional structural health monitoring techniques (strain gauges, deflectometers, accelerometers, live load vehicles, hammer-sounding, chain-drag, etc.) for correlation as well as remote sensing technologies (thermal infrared, 3D optics, radar, etc.).

To allow for a more comprehensive assessment of each technology, the selection criteria was defined accordingly by using the National Bridge Inventory (NBI) rating scale (see Table 1) along with current MDOT assessment practices. The “poor”, “fair”, and “satisfactory” selections were determined by correlating NBI deck ratings of four, five and six (or better) respectively. Finally, the remaining candidate bridges were separated by item “43: Main span(s) material type” of the Michigan Department of Transportation (MDOT) structure inventory and appraisal form (such as pre-stressed concrete box beam versus steel continuous). To further refine the selection process preliminary site visits and appraisals were conducted allowing for visual observation and validation of documented deficiencies recorded in past inspection reports.

Following the completion of the preliminary site visits, photographs were collected and organized. This image database was then used to generate discussion about each particular

bridge and the suite of technologies' implementation capability. All the technologies were judged individually for each bridge with a focus on four criteria; (1) presence of sensing deficiencies, (2) accessibility, (3) setup, and (4) sampling. During this process the deck top surface, bottom surface and bridge superstructure were of particular importance. Additionally, three supplemental bridges had been selected, one for each category in case of unforeseen issues will the selected bridges.

National Bridge Inventory Rating Scale:

9-Excellent Condition

8-Very Good Condition: No problems noted

7-Good Condition: Some minor problems

6- Satisfactory Condition: Structural elements show minor deterioration

5-Fair Condition: All primary structural elements are sound, but may have minor corrosion, cracking, or chipping. May include minor erosion on bridge piers.

4-Poor Condition: Advanced corrosion, deterioration, cracking, or chipping. Also, significant erosion of concrete bridge piers

3-Serious Condition: Corrosion, deterioration, cracking and chipping, or erosion of concrete bridge piers have seriously affected deck, superstructure, or substructure. Local failures possible.

2-Critical Condition: Advanced deterioration of deck, superstructure, or substructure. May have cracks in steel or concrete, or erosion may have removed substructure support. It may be necessary to close bridge until corrective action is taken.

1-"Imminent" Failure Condition: major deterioration or corrosion in deck, superstructure, or substructure, or obvious vertical or horizontal movement affecting structure stability. Bridge is closed to traffic, but corrective action may put it back in light service.

0-Failed Condition: Out of service, beyond corrective action.

Table 1: Table showing National Bridge Inventory (NBI) rating scale (0-to-9) and brief description.

The following deployment sites have been selected for field demonstration of remote sensing technologies (see the 'A', 'B', and 'C' pins in Figure 1):

- 'A' – MDOT structure n° 1713 – Mannsiding Road over US-127 north bound
- 'B' – MDOT structure n° 10892 – Willow Road over US-23
- 'C' – MDOT structure n° 10940 – Freer Road over I-94

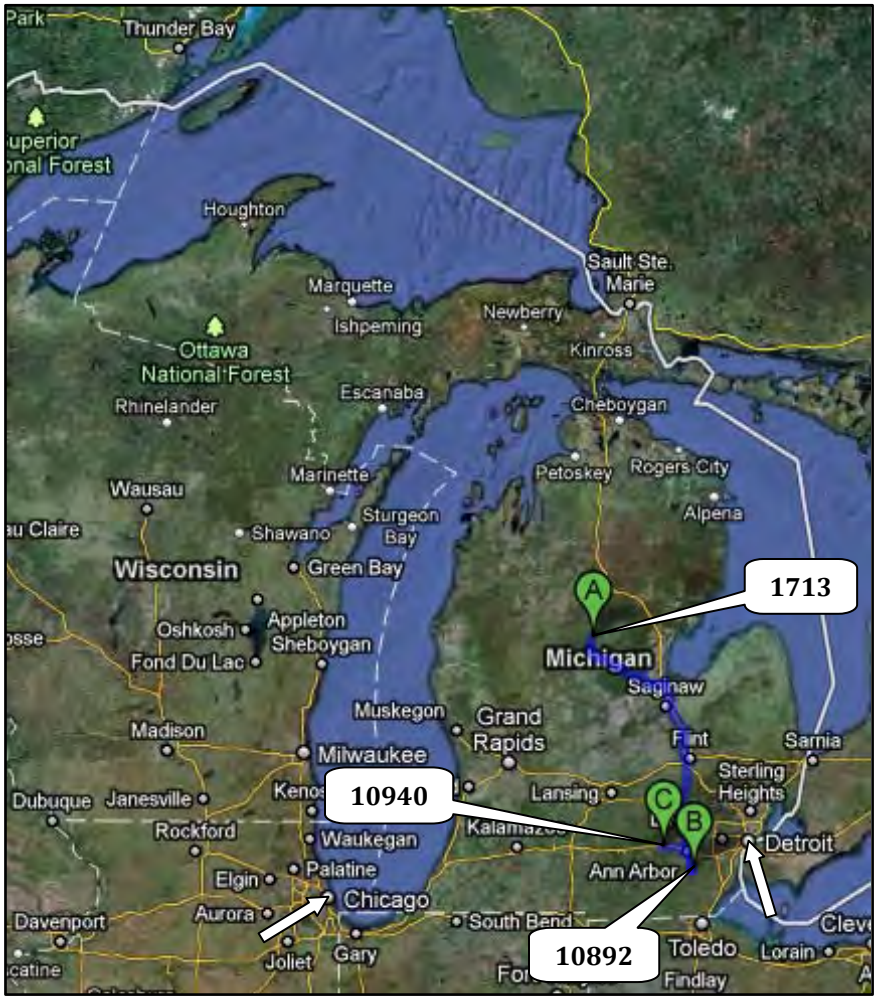

Figure 1: Location of all three bridges (poor 'A', fair 'B', & satisfactory 'C') in relationship to the State of Michigan and the cities of Chicago and Detroit.

"Poor Bridge" Selection

MDOT structure n° 1713 – Mannsiding Road over US-127 north bound; located in Clare County approximately 10 miles north of Clare, Michigan was determined to be the best candidate for field demonstration (see Figure 2).

The field demonstration candidate structure serves Mannsiding Road; a "Major Collector" road. The bridge was constructed in 1966 and is a 3-span pre-stressed concrete multi-I-beam composite structure. The structure is 130'-6" in length, 31'-5" in width, which translate into 26' of open roadway riding surface. During 1996 the average daily traffic (ADT) over the structure was found to be 1,000 with 3 % being commercial.

Figure 2: Aerial view of MDOT structure № 1713 – Mannsiding Road over US-127 north bound.

Currently the bridge has no posted speed limit restriction. The crossing spans north bound US-127; a National Highway System (NHS) route that is not within any federal-aid urban boundary. The bridge doesn't meet the desired minimum vertical clearance for NHS routes. This is located 2.3 miles south of M-61 or approximately 5.5 miles south of Harrison on US-127. The structure is part of an interchange serving the greater Harrison area, which is considered to be a rural environment. Figures 3 and 4 show two photos of the bridge - one taken in 2008 during a MDOT scoping/inspection that provided detailed condition information, and the other by the research team during a site visit in June 2011. The structure is located in Hatton Township within Clare County.

The current condition of the deck surface is an area of major focus and concern; it's rated at a "4" on the NBI scale. In 2008, a detailed inspection and scoping were completed of the top and bottom of the deck surface (project team has access to this report from MDOT). The scoping revealed that on the top surface of the concrete deck 176 ft^2 or 4.4 % of the deck was delaminated. Additional testing on the bottom surface revealed that 623 ft^2 or 15 % of the deck was in distress. The deck also possesses light scaling throughout and numerous transverse, longitudinal and diagonal cracks are present. In concern with the superstructure several high-load hits have resulted in scrapes and spalls but currently there is no sign of exposed reinforcing steel or pre-stressing strands. The bridge is scheduled for complete replacement in 2012/13.

Figures 3 & 4: Photos of the Mannsiding Road bridge, from a 2008 MDOT scoping report (left), and from a June 2011 site visit (right).

Due to the location and low ADT over the bridge, Mannsiding Road is very suitable for deployment of multiple technologies. Pertaining to the two major structural components of concern in this research project, the deck (top and bottom surface) and superstructure six technologies can be instituted. These six technologies that work for both deck and superstructure are;

- 3D Optics (3DO)
- Street-view Style Photography (SVSP)
- Thermal Infrared (ThIR)
- Digital Image Correlation (DIC)
- Light Detection and Ranging (LiDAR)
- Synthetic Aperture Radar (SAR)

"Fair Bridge" Selection

MDOT structure n° 10892 – Willow Road over US-23; located in Washtenaw Country approximately 3 miles north of Milan, Michigan was determined to be the best candidate for field demonstration (see Figure 5).

The field demonstration choice structure serves Willow Road; a "Major Collector" road. The bridge was constructed in 1962 and is a 4-span pre-stressed concrete multi-I-beam composite structure structure. The structure is 209' in length, 30'-10" in width, which translate into 26' of

open roadway riding surface with no availably for shoulder room. During 1997 the ADT over the structure was found to be 2,220 with 3 % being commercial.

Currently the bridge has no posted speed limit restriction. The crossing spans both north and south bound US-23; a NHS route that is not within any federal-aid urban boundary. The bridge does not meet the desired minimum vertical clearance for NHS routes. The structure is located in York Township within Washtenaw County.

Figure 5: Aerial view of MDOT structure № 10892 – Willow Road over US-23.

The current condition of the deck surface is rated at a "5" on the NBI scale. In 2010, the inspection report indicates that open transverse cracks, diagonal cracks and areas of delamination are present throughout the deck. Concrete patching has been done to help minimize deterioration and prolong the service life of the bridge. Additionally areas on the bridge superstructure display desired sensing deficiencies over both the north and south bound lanes. This is attributed to several high-load hits which have resulted in scrapes and spalls but currently there is no sign of exposed reinforcing steel or pre-stressing strands. Figure 6 shows a photo of the bridge deck.

Figure 6: An example photo of the bridge deck of the Willow Road bridge taken on May 13, 2011 (note the variety of visible deck surface defects).

Due to the location and low ADT over the bridge, Willow Road is very suitable for deployment of multiple technologies. Pertaining to the two major structural components of concern in this research project, the deck (top and bottom surface) and superstructure five technologies can be instituted. These five technologies that work for both deck and superstructure are:

- 3D Optics (3DO)
- Street-view Style Photography (SVSP)
- Thermal Infrared (ThIR)
- Light Detection and Ranging (LiDAR)
- Synthetic Aperture Radar (SAR)

"Satisfactory Bridge" Selection

MDOT structure n° 10940 – Freer Road over I-94; located in Washtenaw County approximately 1 mile east of M-52 in Chelsea, Michigan was determined to be the best candidate for field demonstration (see Figure 7).

The field demonstration candidate structure serves Freer Road; a "Major Collector" road. The bridge was constructed in 1960 and is a 4-span pre-stressed concrete multi-I-beam composite

structure. The structure possesses dimensions of 209’ in length, 30’-10” in width, which translate into 26’ of open roadway riding surface with no availably for shoulder room. During 1997 the ADT over the structure was found to be 150 with 3 % being commercial.

Figure 7: Aerial view of MDOT structure nº 10940 – Freer Road over I-94.

Due to its low ADT, this structure will be the first to be tested which allows for researchers to work in an even safer environment while causing minimal disruption to local traffic going over the bridge.

Currently the bridge has no posted speed limit restriction. The crossing spans both east and west bound I-94; a NHS route that is not within any federal-aid urban boundary. The bridge does meet the desired minimum vertical clearance for NHS routes with a measured clearance of 16’. The structure is located in Lima Township within Washtenaw County.

The current condition of the deck surface is rated at a “6” on NBI scale. In 2010, the inspection report indicates that there were several areas of concrete patching accompanied by few tight transverse and diagonal cracks present on the deck. Concrete patches have been applied to help minimize deterioration and prolong the service life of the bridge. The report indicates that

there are also areas of interest on the superstructure where the concrete material has spalled and cracked. These areas of interest are located at the beam-end locations on the bottom flange. None of the spalled sections are currently deep enough to expose any reinforcing steel or pre-stressing strands (Figures 8 and 9 show two sample photos of the bridge).

Figures 8 & 9: Two sample photos taken of the Freer Road bridge over I-94 on May 13, 2011.

Due to the location and low ADT over the bridge, Freer Road is highly suitable for deployment of multiple technologies. Pertaining to the two major structural components of concern in this research project, the deck (top and bottom surface) and superstructure five technologies can be instituted. These five technologies that work for both deck and superstructure are:

- 3D Optics (3DO)
- Street-view Style Photography (SVSP)
- Thermal Infrared (ThIR)
- Light Detection and Ranging (LiDAR)
- Synthetic Aperture Radar (SAR)

FIELD DEMONSTRATION DESIGN

The proposed field demonstration time has been narrowed down to the first two weeks of August; actual days are pending weather and closure timing and availability. The first structure to be tested is planned to be the “satisfactory” condition bridge (MDOT nº 10940), followed the “fair” condition bridge (MDOT nº 10892), and the “poor” condition bridge (MDOT nº 1713) respectively (see Figure 10).

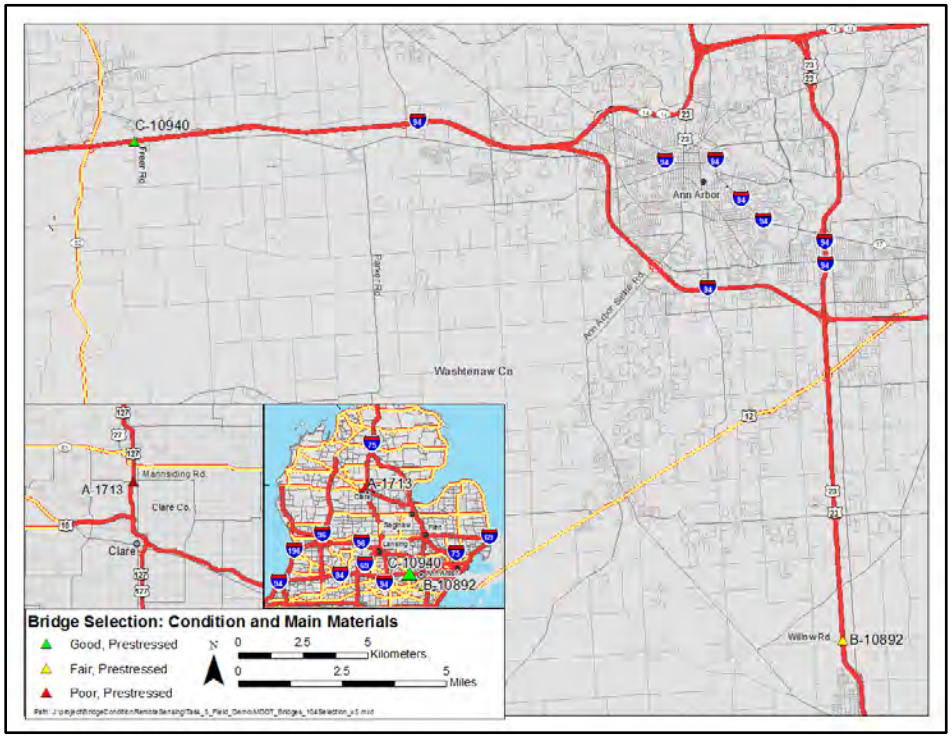

Figure 10: Close up of the locations of all three bridges shown in the Decision Support System (DSS) interface in relationship to Ann Arbor and the State of Michigan.

The projected schedule currently estimates that at a minimum one day per bridge will be necessary to gather all data in a timely fashion since not all technologies can be deployed at the same time including some that are restricted by the time of day and the need to have the bridge deck clear of all personnel and equipment. Up to three days per bridge, if needed, are currently available thanks to MDOT. Additional days may be requested and scheduled if revisits are needed to collected additional or more refined data.

For establishing ground-truth, the research team is requesting that a MDOT certified bridge inspector be present during the field testing and inspect the entire structure for correlation purposes (e.g., delamination maps, spall maps, crack maps, roughness, etc) with all the remote sensing technologies being deployed on the three selected bridges.

3D Optics (3DO)

In order for the team's optical Nikon D5000 digital single lens reflect (DSLR) camera to capture the sharpest image of the suspect deck surface, lighting is a critical parameter. The conditions for optimal image capture are as follows: sun or artificial light source, a preferably dry surface,

no foreign surface containments and limited vehicle/pedestrian interference. It is not necessary for the lighting to stay consistent throughout the image collection process, but for best results it is preferred. This has been validated from previous testing completed at the Michigan Tech Research Institute (MTRI) showing that the sharpest three-dimensional models are generated by proper and consistent lighting conditions. This is associated with the post-processing software's ability to more accurately distinguish points of commonality between stereo pairs.

The MDOT certified inspector present would generate a scaled deck spall and roughness map allowing for the post-processed 3D photogrammetric data to be correlated with the inspection results. The team will follow the following steps for field deployment of the 3D optics system:

- Assemble the vehicle mount (see Figures 11 and 12)
- Attach the Nikon D5000 camera being used for the field test
- Drive across the bridge at a speed around 2 mph (4x4 low at idle speed)
- As the truck drives across bridge, camera will take photos at 1 fps
- Repeat pass on the other lane of the bridge

Once at the site, the vehicle mount for the 3D system is put together, the camera is mounted and the vehicle mount is strapped down to the bed of a truck. The camera is then connected to the computer and then tested to make sure there is a good connection and everything is working properly. Once everything is ready, the truck drives along the bridge at a slow speed (currently 1-to-3 mph); this has been achieved by putting the truck into 4x4 low and letting it idle across (see Figures 11 and 12). Note that potential future systems would be able to cross at higher speeds if more advanced digital cameras are used.

Figures 11 & 12: 3D Optics (3DO) data collection system deployed for pre-field demonstrations trials.

The camera is set to take photos once per second (1 fps) during the collects. The combination of the vehicle speed and the camera's continuous shooting allows for at least a 60 % overlap in the photos (which is necessary for 3D photogrammetry) and due to the height of the camera we are able to cover one full lane width on a bridge. On the selected bridges, we would need two passes to cover the entire bridge.

Street-view Style Photography (SVSP)

For field deployment of the team's SVSP system, the BridgeViewer Remote Camera System (RCS), two sets of steps are needed. The BridgeViewer RCS comes in two versions developed by MTRI, a (1) "Bridge Deck" version for imaging the surface of the deck, and a (2) "Bridge Underside" version for taking more rapid photography while traveling under a bridge to image the underside.

The deployment steps for bridge-deck version are:

- Take a picture of Garmin GPS unit being used to geo-tag the photos later
- Mount the cameras to the hood of the car (see Figure 13)
- Align the cameras so that their field of views overlap in the center of the lane
- Drive over bridge at 5 mph while capturing images once every four seconds

And the deployment steps for bridge-underside version are:

- Take a picture of Garmin GPS unit being used to geo-tag the photos later
- Assemble vehicle mount with camera and lights (see Figure 14)
- When approaching the bridge, turn on the lights and start taking photos at 1 fps
- Drive along both lanes to collect full coverage under the bridge

Both systems can be deployed during the field demonstrations and finished with data collection in less than 30 minutes each. Data will be processed in the MTRI GIS lab into a geo-tagged photo inventory of each bridge for inclusion in the Decision Support System (DSS) (see Figure 10).

Figures 13 & 14: Example deployments of the "Bridge Deck" (left) and "Bridge Underside" (right) versions of the BridgeViewer Remote Camera System (RCS).

Thermal Infrared (ThIR)

Several factors need to be considered for the FLIR SC640 or FLIR i7 ThIR cameras to capture the temperature differential on the concrete deck. These factors include: clear sky, sun, dry surface, no foreign surface containments and limited vehicle/pedestrian interference.

When all the provided criteria are satisfied, the image should be captured during the mid-morning to mid-day sun (10 am to 2 pm) for best results. This has been validated through previous laboratory testing completed at Michigan Technological University (MTU) showing that the largest radiant temperature differential occurs during this time period exposing anomalies and subsurface delaminations. This is associated with the disruption of heat transfer through the concrete deck in defective areas allowing for the defective areas to warm up sooner than areas with no defects and thus generating an area with higher temperature compared to an area of intact concrete.

For establishing ground-truth, the MDOT certified bridge inspector present during field demonstration would perform a hammer-sounding and/or a chain-drag on the deck surface. The inspector would also generate a scaled deck delamination map allowing for the post-processed infrared data to be correlated with the MDOT delamination survey results.

A pair of both ThIR and optical images are to be collected at predetermined intervals along the bridge deck using the SC640 and/or i7 for ThIR imaging and a Canon EOS 7D and/or Nikon

D5000 DSLR cameras for optical imaging (SC640 can also be used for taking optical photos and videos of the surface).

The SC640 camera will be mounted on a moving cart at an appropriate height to capture the required field-of-view (FOV). Table 2 includes the horizontal and vertical FOV for each specific height for the SC640 camera and the time intervals of taking images based on the speed of the camera. The number of required images in transverse and longitudinal direction can be determined based on horizontal and vertical FOV of the camera at the specific height, respectively.

Height (ft)	HFOV (ft)	VFOV (ft)	Speed (mph)	period of taking images (s)	freq (Hz)	Frames (n°)
24	10.32	7.68	5	1.0450944	0.956851	1
12	5.16	3.84	5	0.5225472	1.913703	2
10	4.3	3.2	5	0.435456	2.296443	3
7	3.01	2.24	45	0.0338688	29.5257	30
7	3.01	2.24	6	0.254016	3.93676	4
7	3.01	2.24	1.5	1.016064	0.98419	1
6.5	2.795	2.08	1.4	1.01088	0.989237	1
6.2	2.666	1.984	1.3	1.038395077	0.963025	1
6	2.58	1.92	5	0.2612736	3.827405	4
6	2.58	1.92	1.3	1.004898462	0.995125	1
5	2.15	1.6	5	0.217728	4.592887	5

Table 2: HFOV and VFOV of the FLIR SC640 ThIR camera at various heights.

The ThIR camera can be set to take a sequence of images on specific time intervals or frame rate. Corresponding optical images can be captured either by the DSLR camera or by converting optical video captured by FLIR camera into images. Optical videos should be converted to images based on the specific time intervals to cover the required vertical FOV. Each of the images has to be correlated with their respective counterparts and assembled into a comprehensive “bridge deck photograph” revealing to the user all subsurface anomalies layered over an optical rendering.

The ThIR images will need to be stitched together to create a delamination map of the deck surface. The FLIR ThermaCAM software will be used to create boxes around the delaminated areas and calculate the area based on the number of pixels. The area of delamination can also

be calculated by comparing the boxed area to a reference area on the bridge deck. Figure 15 shows the cart with fabricated wooden frame for collecting the ThIR images. The height of the camera lens to the deck surface should be ~6.2 ft giving about a 2.67 ft by 1.98 ft FOV (5.29 ft^2), allowing for the ThIR camera to take images 1 fps while the cart rolls along at ~1.3 mph.

Figure 15: FLIR SC640 ThIR camera mounted on the cart for field demo.

Chalk lines will be drawn on the deck top surface to facilitate the data collection procedure. Figure 16 shows a diagram of the deck. As it can be seen in this figure, data collection of the whole bridge requires 8 passes. Duration of data collection will be approximately 20 minutes for Freer Road and Willow Road and 15 minutes for Mannsiding Road. This excludes the time duration between each pass.

For taking the ThIR images of the deck bottom surface, the height of the camera varies depending on the standing point (on the shoulders or on the highway below). ThIR images can be taken between each girder and stringer. Any false decking has to be removed prior to inspection. ThIR images can also be taken from pre-stressed concrete girders and stringers and can be saved based on the girder's number.

The experiment requires one hour of preparation and installation of equipments on the bridge deck. Once the installations are completed ThIR and optical image collection will commence, which is estimated to take up to four hours between 10 am to 2 pm.

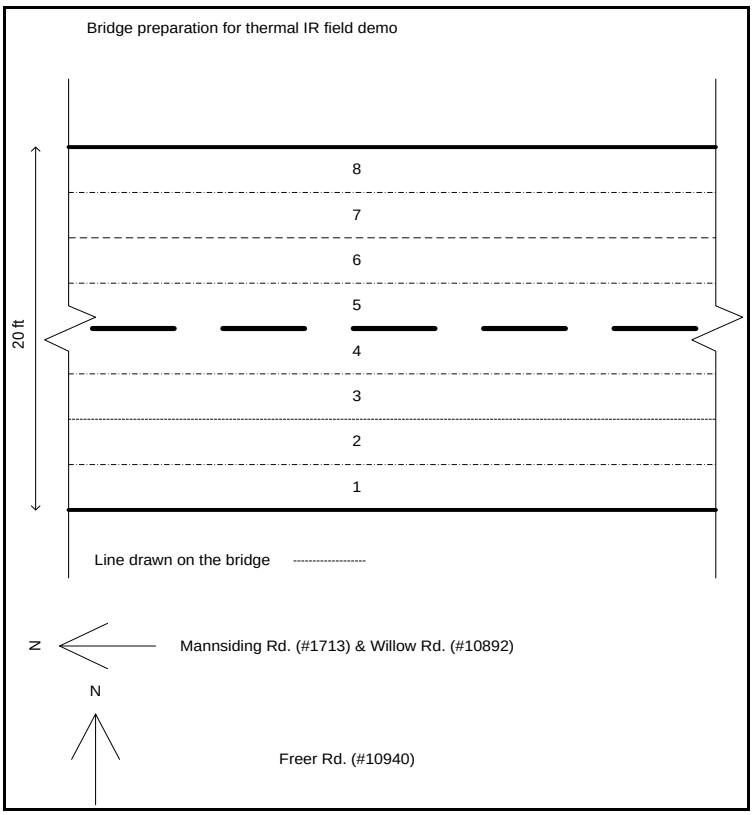

Figure 16: Diagram of the deck surface showing lanes which ThIR camera-equipped cart will travel on.

Digital Image Correlation (DIC)

DIC will be used on MDOT structure n$^{\underline{o}}$ 1713 – Mannsiding Road over US-127 north bound. The Mannsiding Road bridge will be used to verify the capabilities of the technique and application for structural health measurements such as displacement and strains. DIC will not be deployed on the two other bridges due to the involved permitting process for live-load testing. Procedures involved in the field demonstration consist of:

- Field setup design
- Deployment of field instrumentation
- Live load testing (loaded trucks)
- DIC testing (image collection)
- Post-processing of data

Mannsiding Road bridge has 3 major spans; to prepare for the load test, the bridge will be instrumented with traditional equipment such as deflectometers for deflection monitoring; and gauges for strain data collection. Several accelerometers will be placed near the testing locations to monitor the frequency range on the bridge. The instrumentation plan originally focused on the midspan and quarter point locations of the span. Since the midspan is over highway, US-127, and if the center of the midspan is not accessible, testing locations are suggested for the side spans and near the quarter points of the midspan. Therefore, each testing location would have a deflectometer and two strain gauges for validation measurements.

Implementation of DIC consists of markers or a spray-paint pattern of contrasting dots on the structural I-beam span to be measured. Through experimentation, it is suggested that the appropriate size distribution can be achieved by obstructing the direct flow of paint from the nozzle by using one's finger placed 0.5-to-1 inch in front of the nozzle opening.

A pre-determined bridge span is to be stressed by both a quasi-static and dynamic live-load generated by a live-load test truck. During loading, images will be captured by a Canon EOS 7D DSLR on the exterior girder of the superstructure at the quarter points of the midspan and on the side span near the abutment locations. In order to establish ground-truth with DIC tests, deflectometers and strain gages will be mounted at the previously discussed locations of interest along the exterior girder on the extreme tension face of the bottom flange of the girder for deflection and strain measurements.

The quasi-static test is to evaluate static deflection of a structural element through both remote sensing instrumentation and traditional sensing technology, then correlating the results. There will be a weighted truck of (e.g., 37.5 kip) for the load testing on Mannsiding Road. All of the quasi-static tests are to be performed at "crawl" speeds of 10 mph or less, to minimize the dynamic amplification and allow the truck to follow lines marked on the bridge deck. The required recording rate for the displacement and strain data is 20 Hz, which covers the entire spectrum of the predicted truck crossing. The dynamic test will be performed to determine how accurately the remote sensing technology can capture an optically sense bridge vibration. The dynamic tests are to be performed at posted speed to mimic actual service conditions. For this test situation the displacement and strain data sample rate is to be set at 200 Hz to cover the entire spectrum produce by highway speeds. A minimum of three repetitions per load combination is requested for both the quasi-static and dynamic load testing with the truck crossing in the same direction as previously.

A series of digital images per location of interest are to be collected at fixed intervals using the EOS 7D with a zoom capable lens (e.g., 300 mm). The camera is to be placed 15 ft (which can

vary) from the target surface on a rigid tripod at no more than a horizontal angle of 180° and a vertical angle of 90°. The images are numbered automatically by the camera's firmware, and each of the images is to be correlated with the known load applied during the load test to the bridge span at that time.

The experiment requires 3-to-4 hours of preparation work applying and calibrating the required deflectometers and strain gages on the selected bridge span. Once bridge preparations are completed, live-load stressing of the bridge span, collecting optical images and displacement and strain data will take nearly 2-to-4 hours.

Data collected from the conventional instrumentation and DIC procedures from the load test will be processed and analyzed. The information gathered from the cameras will be processed in computer software tools such as The MathWorks MATLAB and Correlated Solutions Vic-2D for strain and displacement measurements. This will be verified with the conventional strain gauge sensors and deflectometer devices used on the bridge. This data will also be correlated with an FEM of Mannsiding Road to compare simulated behavior with actual bridge response.

Light Detecting and Ranging (LiDAR)

Compared to traditional surveying equipment, a LiDAR instrument can collect millions of data points in a single pass of a suspect object allowing for detailed analysis to be completed. The issue arises when the object has many faces producing "shadows" or "blind spots" in the instrumentation field of sight. This line of sight issue can be resolved by repositioning the device allowing for the hidden sections of the object to be revealed. This allows for a full three dimensional rendering of the object after the multiple collection points are fused together. Lastly, since light is absorbed by water LiDAR cannot penetrate any water barrier, so the bridge surface should be dry allowing for limited interference.

For establishing ground-truth, the research team is requesting that a MDOT certified bridge inspector be present during field demonstration and performs a visual inspection of the surface condition. Cracking, scaling, and spalling should be identified and documented allowing for the research team to correlate the inspection results with the post-processed three dimensional LiDAR rendering.

Prior to initializing the LiDAR data collection, a minimum of four points of commonality must be established in order to triangulate and validate a local coordinate system. By establishing these points of commonality the independent LiDAR images can be referenced in a common local

coordinate system allowing for a layered three-dimensional rendering eliminating the presence of “shadows”. For this particular field demonstration, six retro reflective prisms should be used to generate the required points of commonality. The reasoning for instituting two additional points of commonality is attributed to the increased flexibility and accuracy of the data collection process. To clarify, the two additional points allows the LiDAR unit to be located anywhere within the area of concern where a minimum of four points were in direct line of sight to the device. Additionally, when all six points are visible in retrospect to the LiDAR unit’s position, data accuracy of the scanned bridge will increased.

Once a local coordinate system is established the optical camera mounted on the LiDAR unit will have to be adjusted for lighting conditions. The purpose of this optical camera is to allow the integration of a color scale into the generated LiDAR rendering.

Testing should last roughly four hours, which includes setup, six to eight separate scan locations and demobilization. A simple survey location map has been constructed to help accelerate the actual selection during data collection (see Figure 17). To be more precise, once the crew is on-site it will 30 minutes to assemble, and position the Riegl LMS-Z210ii LiDAR unit (see Figure 18) in the first scanning location along with the six retro reflective prisms for the points of commonality. Note the opportunity to gain access to MDOT's terrestrial Leica LiDAR system for deployment at the three bridge sites, in coordination with MDOT LiDAR experts is being investigated.

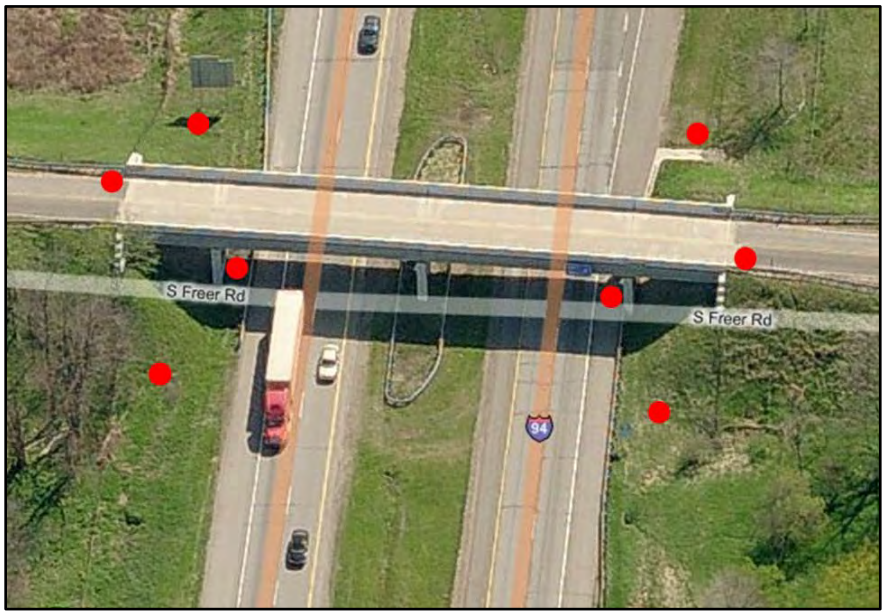

Figure 17: Possible survey points for Freer Road bridge.

When the equipment positions is fixed, an initial LiDAR scan lasting approximately five minutes of the entire surrounding area must be completed allowing for the technician to establish the points of commonality within the image by identifying the center of the retro reflective prisms. Once the points are located, a more detail scan at a higher resolution lasting approximately ten minutes is completed by selecting a window on interest from the initial rendered image. The previously discussed process is to then be repeated five to seven additional times allowing for a final three-dimensional rendering of the subject bridge.

Additional to the bridge surface condition scanning, MTU is planning on utilizing the equipment to measure deflections during live load testing in correlation with DIC. This portion of the data collection is expedited to take an additional 30 minutes for data collection.

Figure 18: Typical Reigl LiDAR unit setup.

The experiment requires one hour of preparation and installation of equipments on-site. Once the installations are completed the LiDAR survey and optical image collection is estimated to take around four hours.

Synthetic Aperture Radar (SAR)

MTRI's 2D Radar will look at bridge deck top surface to detect sub-surface delaminations. The radar will be setup in one lane and image the other lane, requiring blocking of two lanes (see Figure 19). No vehicle or pedestrian traffic should be present on the bridge during data collection.

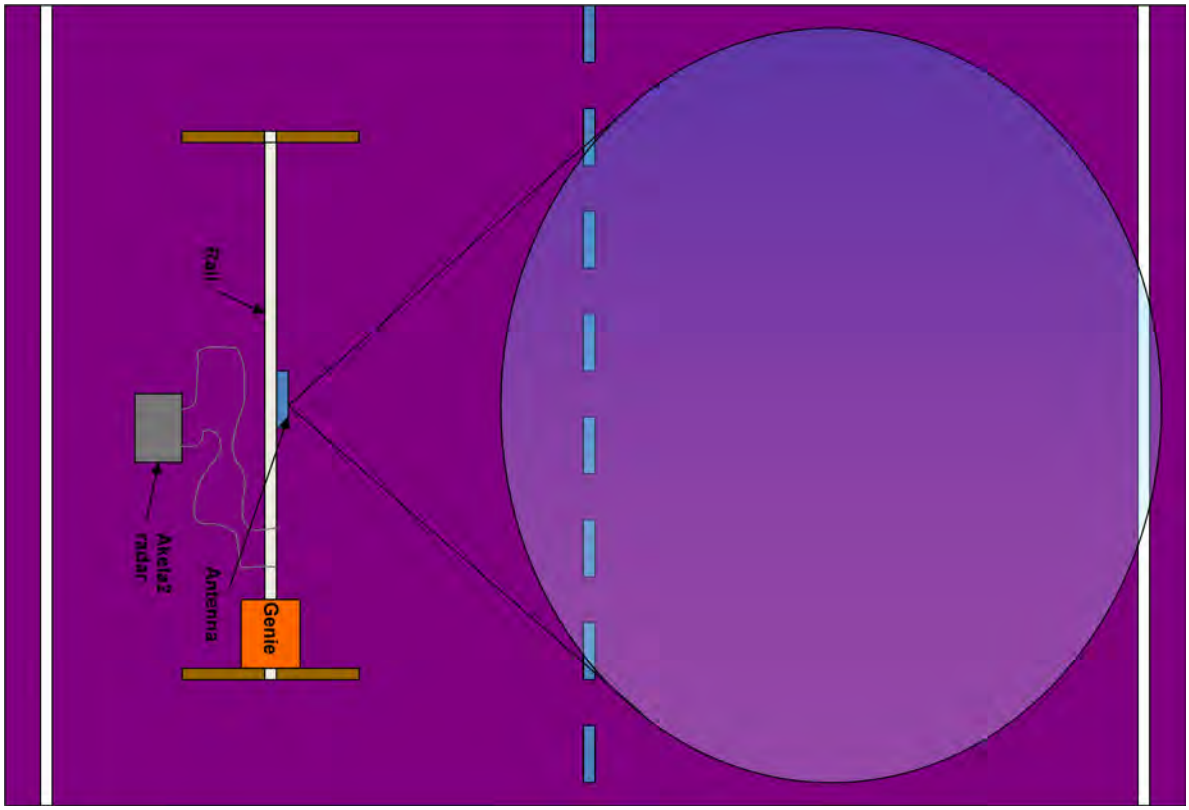

Figure 19: The setup of the project's 2D radar sensing system for detecting bridge delaminations.

Initial translator setup and radar calibration is anticipated to take approximately one hour. These steps include assembling translator fixture with radar antenna, cabling radar to the antenna, cable power from a generator, and setting up fiducials. This will be at a minimum a two person job.

Data collection for three 5 m by 10 m (50 m^2) scenes will take approximately two hours. Multiple passes at two heights will be done. Moving to a new patch will require minimal time (about 15 minutes). The translator can be moved without breaking down the unit. The radar itself is disconnected, moved, and re-connected at the next patch to be scanned.

Equipment break-down and removal is expected to take one hour. Total collection time for three scenes will be about four hours (including setup and break-down). Environmental requirements are dry, but no time of day constraint (radar data can be collected at day or night). Ground-truth of bridge delamination will be needed, from chain-drag surveys and possible deck coring.

Interferometric Synthetic Aperture Radar (InSAR)

InSAR analysis methods are currently underway for the project, but are being used at three bridges that have undergone an elevation change (e.g., settlement, heave) and can be detected through the use of multiple SAR satellite images. As this does not need any deployment of equipment or personnel for this satellite imagery-based analysis, no further deployment planning is needed for this field study.

SAFETY PLAN

For actual field demonstration the United States Department of Transportation (USDOT) and MDOT require the wear of personal protective equipment (PPE) at all times. The use of PPE on site will follow, and be in accordance with, USDOT and MDOT's PPE policies. Instructions and adequate training will be provided prior to actual field test date.

In order to ensure inspector, researcher, traffic, and pedestrian safety during field demonstration a MDOT, Washtenaw-, and Clare-County Road Commission approved traffic plan will be instituted with full- and or partial-bridge and lane closures enforced were necessary to guarantee a safe and undisturbed work site. Hood mounted amber warning lights will also be deployed where necessary (e.g., data collection vehicles traveling below posted speed limit).

In all, municipal, county, state, and federal laws, safety and other wise, will be followed.

Memo

To: T. Ahlborn, D. Harris, L. Sutter, R. Shuchman, J. Burns

From: H. de Melo e Silva, C. Brooks

CC: A. Endsley, R. Oats, K. Vaghefi, R. Hoensheid, R. Dobson, J. Ebling, D. Dean

Date: October 13, 2011

Number: 21

Re: Summary of Field Demonstration Including Sensor Evaluation and Update of the DSS.

3D OPTICAL BRIDGE-EVALUATION SYSTEM (3DOBS)

The 3DOBS, a demonstration of 3D optics technology, was successfully deployed to all field demonstration bridges to collect 3D bridge surface data. The field system consisted of a Nikon D5000 digital single lens reflex (DSLR) camera, vehicle mount, and a camera triggering device. The camera triggering device was programmed at the Michigan Tech Research Institute (MTRI) to enable the camera to capture photos at one frame per second (fps).

Easily transported in the bed of a light duty pickup truck the 3DOBS took 15 minutes to setup. For collecting the imagery, the truck was geared down to “4x4 low” and idled across the bridges at a speed of about 1 mph (see Figures 1 and 2 for the system in data collection mode). This allowed for at least 60% overlap of the resulting photos with the camera mounted 9 ft above the bridge deck surface, needed for photogrammetric image collection. The total time needed to make a full collect (two passes, one pass per lane) of the bridge was about 10 minutes. Breakdown of the system took another 10 minutes which translates to total collect time of 35 minutes per bridge (see Figure 3 for an example of the 3DOBS when broken down into its parts). With a faster camera that could take more frequent images, the speed of data collection could be increased and the data collection time could be decreased to less than 10 minutes per bridge for a full collection.

Figures 1 & 2: The 3DOBS being deployed on Willow Road bridge over US-23 during August, 2011 field demonstrations.

Figure 3: The disassembled 3DOBS being transported to bridge field demonstration sites.

The resulting photos from the Willow Road bridge (see Figure 4) were processed in the commercial software package Agisoft PhotoScan Professional to generate 3D models of the bridge deck surface. Using the labeled bridge locations from the team's onsite bridge grid system, the models were given a coordinate system and were then exported out of PhotoScan Professional as a Digital Elevation Models (DEM) seen in Figure 5. The bridge DEM is being used

in Esri ArcGIS to calculate the size and volume of individual spalls as well as generate a map showing the spalled areas and calculating the percent of the bridge that is spalled. These are the types of condition data that will be integrated into an overall bridge health signature. The same post-processing described here for Willow Road bridge will completed for the Mannsiding and Freer Road bridges within the next few weeks.

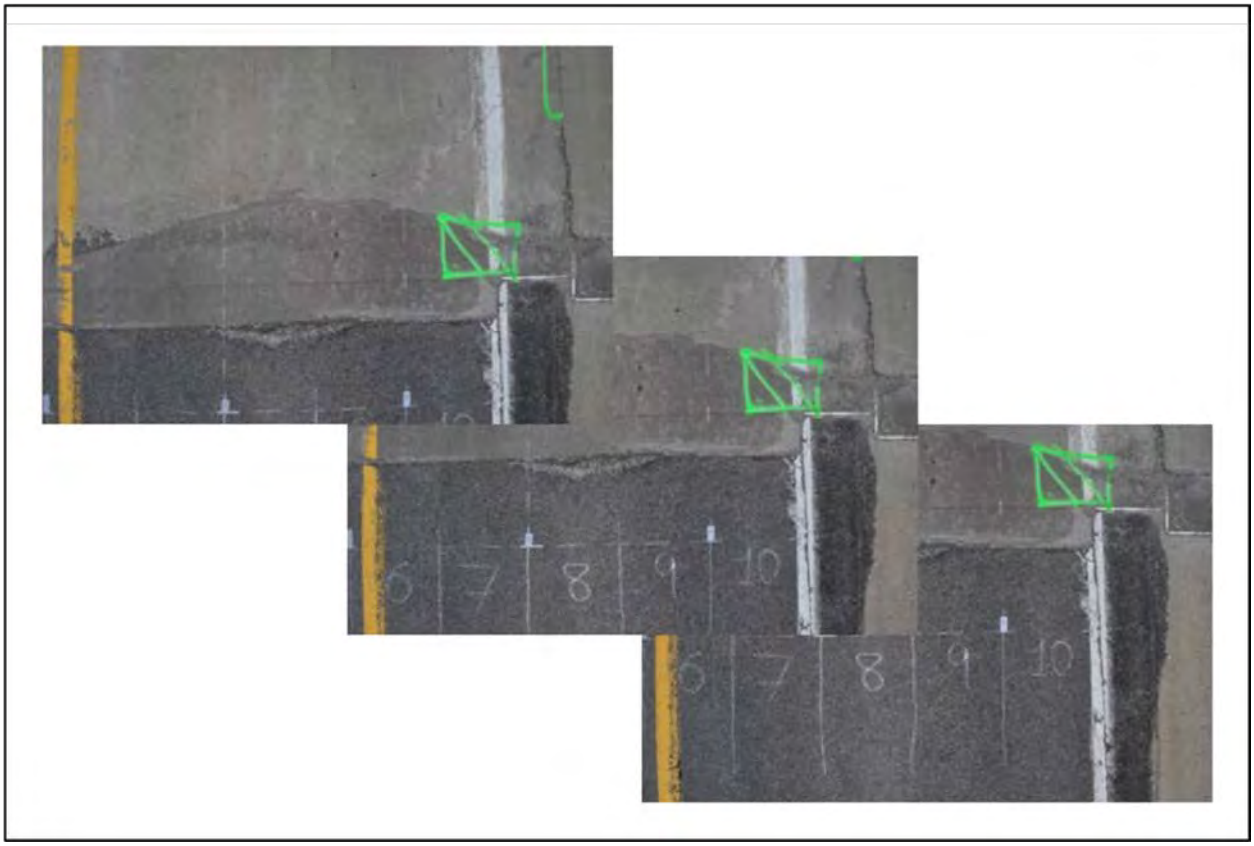

Figure 4: Photos of Willow Road bridge taken with the 3DOBS showing a 60% picture overlap for photogrammetric image creation.

As shown in Figure 6, it is possible to calculate the volume and area of spalls on the bridge deck using data collected by the 3DOBS. The output above has a 5 mm by 5 mm (~0.04 in^2) horizontal resolution and appears to be detecting vertical changes as small as 2 mm (smaller then 1/12 of an inch). The analysis team is currently investigating ways to automate the calculation of this type of bridge deck condition data that will be used as part of the overall bridge signature. During the next quarter, the team will be completing of these analyses, and processed data, that helps to indicate bridge superstructure condition, will be included in the project's Decision Support System (DSS).

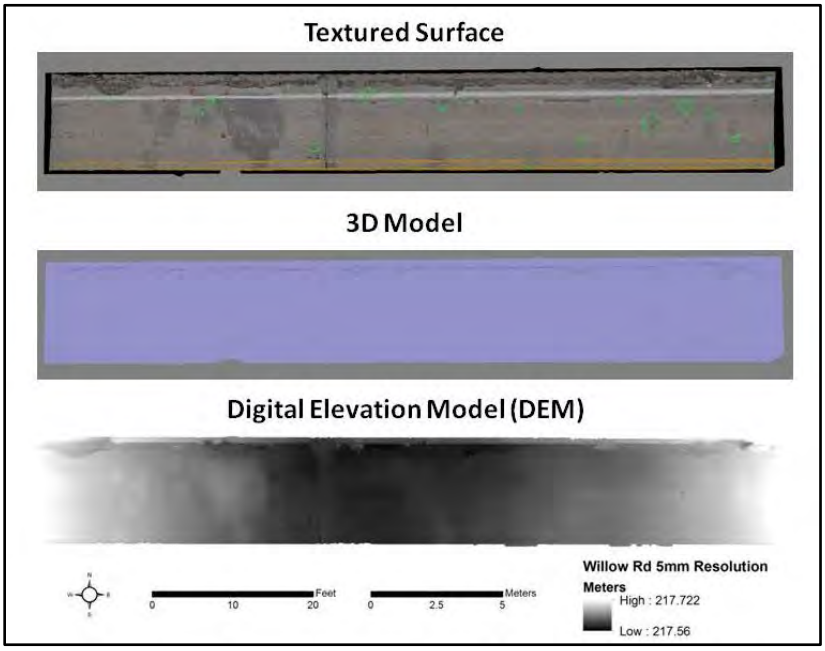

Figure 5: Examples of the PhotoScan Professional output. A textured surface and 3D model are generated from the photos with no additional user input needed. A DEM is generated after the user sets up a coordinate system by adding reference points.

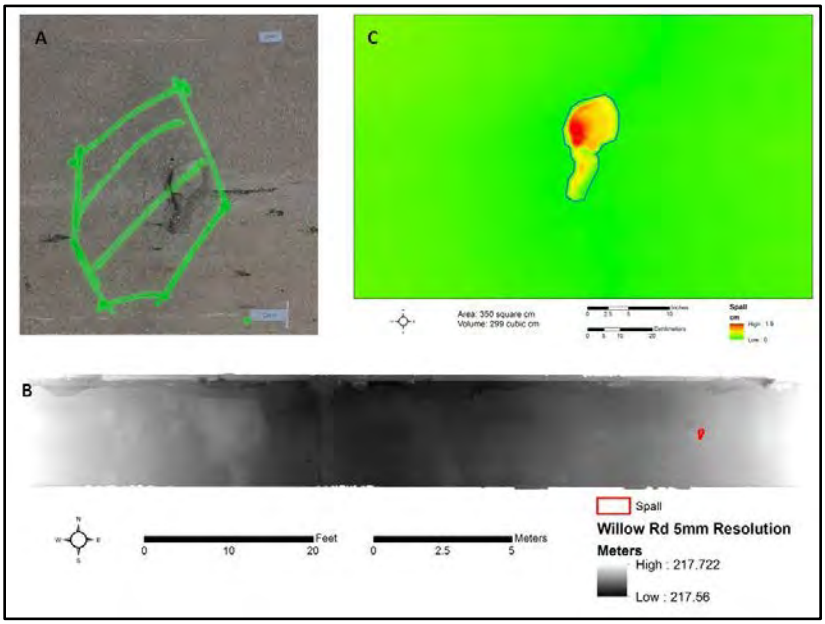

Figure 6: Analysis of a spall on Willow Road bridge based on 3D data collected with the 3DOBS at Willow Road bridge. A spall ('A' – within the green area marked by the Michigan Department of Transportation (MDOT) as a delamination) can be located on the DEM of the west bound lane ('B' – red area). Area and volume estimates can be calculated in Spatial Analyst (see 'C'). The spall above has an area of 350 cm^2 and a volume of 299 cm^3.

The total percent of spalled area was also calculated and analyzed using ArcGIS Spatial Analyst with the 3D data collected. Figure 7 shows an example of the 3D bridge deck data having been analyzed and categorized into spalled versus unspalled areas. The total spalled area is 6.08% of the total bridge surface. As an example of additional data that can be calculated, the average area of a spall is 673 cm^2 (~104 in^2) and 0.8% of the area within 7.5 cm (~3 in) of a bridge joint is spalled; 5% of the area outside of this bridge joint area is spalled. As stated, the analysis team is now focusing on automating these types of analysis so that remote sensing results can be transformed into metrics for inclusion in an overall bridge signature.

Figure 7: Example of calculating percent spalled area for Willow Road bridge using the 3DOBS data as the input and ArcGIS as the analysis software.

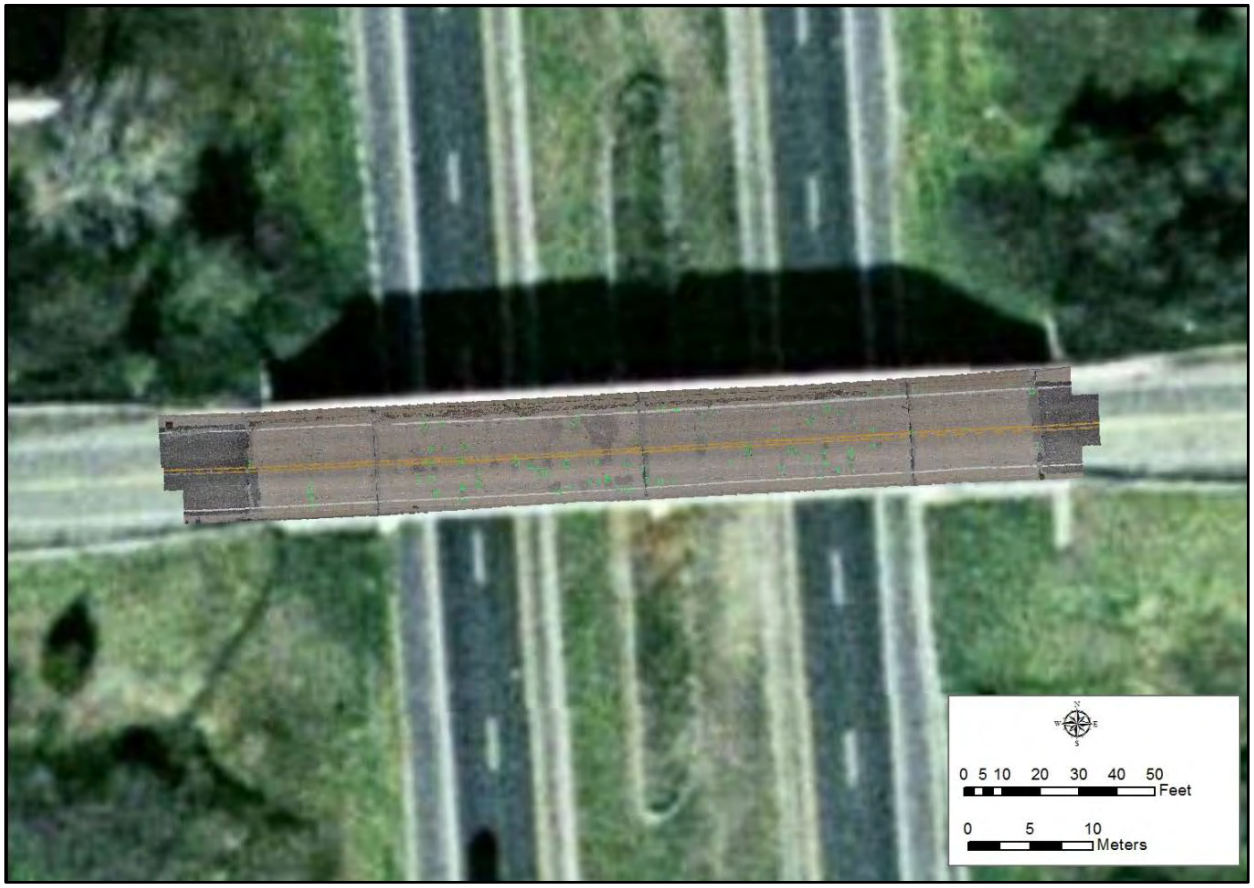

Figure 8: A composite image of Willow Road bridge deck that can be used to evaluate its condition as serve as a reference to understand deterioration over time, as collected by the 3DOBS.

Benefits, Limitations, and Next Steps

The primary benefits of the 3DOBS are: low cost to purchase components, rapid deployment, limited time needed to collect data on the bridge, and that the team has demonstrated how to derive useful metrics of bridge deck condition, such as percent of spall plus volume and area of spalls. The total system cost ($4,320) as currently developed is: $3,500 for Photoscan Professional, $700 for the D5000 (including default kit lens), $20 for the camera triggering device, and $100 for the vehicle mount. A department of transportation (DOT) could purchase a single license (or other limited number) of Photoscan Professional to process the data while deploying several hardware setups at a cost of $820 per system. A higher-end camera capable of more frames per second such as the Canon EOS 7D, with kit 28-135 mm lens ($1,700), would enable faster data collection.

The primary limitation on the current system is the speed at which data can be collected. Ultimately, the goal would be to gather data at full standard, 24 fps (some cameras can now exceed this speed). However, the highest resolution high definition video (1,920 pixels by 1,080 pixels) is still only equivalent to 2 megapixels (mp), versus a 12.3 mp photo from the D5000 or a 18 mp photo from the EOS 7D, meaning a significant sacrifice would be made in image quality and resulting resolution of the DEM products. For the time being, a deployable system that can resolve features 5 mm (~0.2 in) or smaller would need to be a DSLR camera.

Also limiting practical deployment, but being actively worked on, is the automation of analyzed output that is meaningful to bridge inspectors and that can be rapidly included in a bridge condition DSS. This is anticipated to be resolved within the next quarter.

The 3DOBS system can be deployed as developed and demonstrated through this project, and has in the team's opinion already reached a level beyond the research stage. Additional development during this study will improve the current system with more automated output. Future development beyond this stage would be intended to lead to a completely field-ready system that a DOT could purchase from a vendor (if desired) or assembled by a DOT itself, with a software tool that works with existing DOT software to create bridge deck condition indicator data such as percent of spall by surface area for a bridge. The team proposes to write a "How to Deploy the 3DOBS" manual depending on project sponsor input and Technical Advisory Committee (TAC) interest, as a logical next step for reaching a field ready system.

As demonstrated at the recent Association of Environmental and Engineering Geologists (AEG) Conference in September, 2011, it is noteworthy that a United States government agency, the U.S. Bureau of Reclamation, has developed and deployed a similar system on a practical basis for mapping 3D surfaces of dam spillways; for an example output from their pole- and balloon-mounted systems, see <http://www.usbr.gov/pmts/geology/3dphotogrammetry.pdf>. This is a technology that is now practical to deploy thanks with less expensive cameras, cheaper and more powerful close-range photogrammetric processing software, and an understanding of the value of 3D data in end-users.

BRIDGE VIEWER REMOTE CAMERA SYSTEM (BVRCS)

The BVRCS, a demonstration of Google Street View style photography technology, deployment consisted of two Canon PowerShot SX110 IS cameras, a Garmin GPSMAP 76CSx GPS unit, and a laptop installed with Breeze Systems PSRemote camera control software. The cameras were mounted to the front of the vehicle and oriented so that the overall field of view would capture an entire lane width (see Figures 9 and 10). The vehicle was driven at a speed of less than 5

mph while the cameras took pictures once every 4 seconds in order to capture the entire bridge using the PowerShot SX110 IS cameras (see Figures 11 and 12). This allowed the team to ensure that the digital photographs were not blurred and the detail of the bridge deck was preserved through in-focus photographs. Lighting conditions at the bridge did not affect the quality of the photos captured; these conditions ranged from sunny to completely overcast skies.

Figures 9 & 10: The BVRCS being deployed on Freer Road bridge to capture a photo inventory.

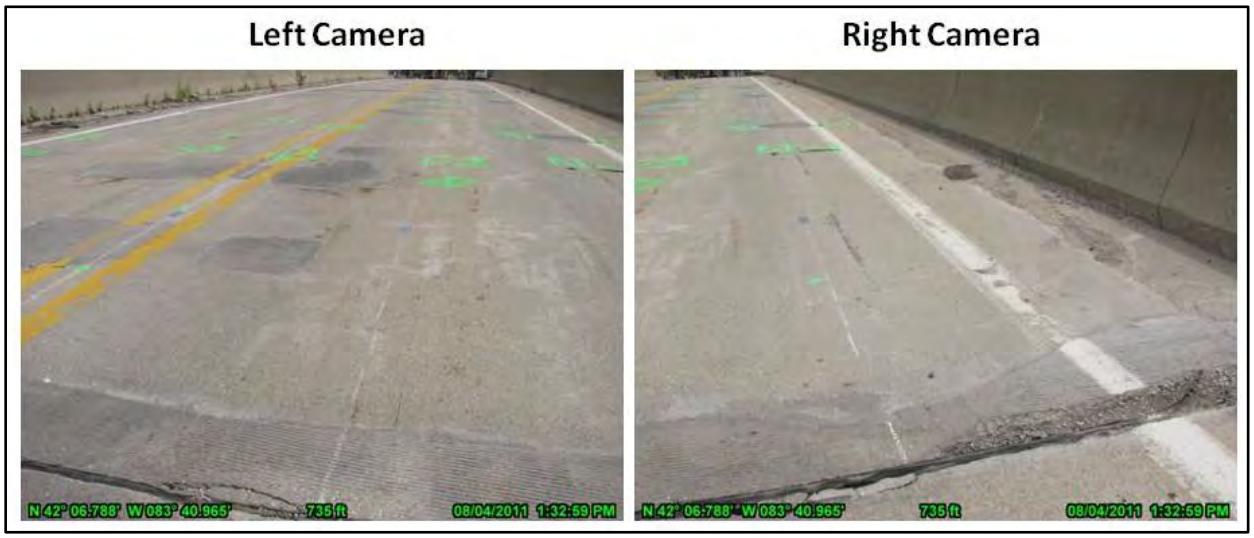

Figures 11 & 12: Example photos taken with the BVRCS of Freer Road field demonstration bridge. Photos show that a full lane width was captured including overlap of the center of the right lane.

The set-up, deployment, and breakdown of the BVRCS at each of the field demonstration sites happened within a 30 minute time-frame. The purpose of the BVRCS is to capture a location-tagged set of photographs of a bridge so that bridge inspectors can easily and inexpensively

review a bridge at a later point and over time as more photo inventories are taken, while working from the office. This is intended to optimize field time and enable review of high-resolution photos of a bridge, especially its deck.

Once the photographs were taken, they were processed into a location-tagged, geographical information system (GIS) and Google Earth-compatible files (e.g., shapefiles and Keyhole Markup Language (KML) files) using the commercially available GeoSpatial Experts GPS-Photo Link software. The photo locations were displayed within ArcGIS and Google Earth and included hyperlinks to the full-resolution original photos; other geospatial software that can read shapefiles and KML files would also be able to use these data. Figure 13 shows an example of the GPS-Photo Link output being displayed in Google Earth, including the ability to see a preview of the photo before linking to the original full-resolution photo. A "watermarked" version including the GPS coordinates, date, and time showing where and when the photo was taken can also be linked to, as also shown in Figure 13. The photos can reside on a DOT desktop computer, a server for multiple-user access within an office, or made accessible to a web server so they can be accessed in the field or from remote offices. The project team is currently working on including the location-tagged bridge photos from the demonstration bridges in the DSS to demonstrate how they can help understand the condition of multiple parts of a bridge at a point in, and over, time.

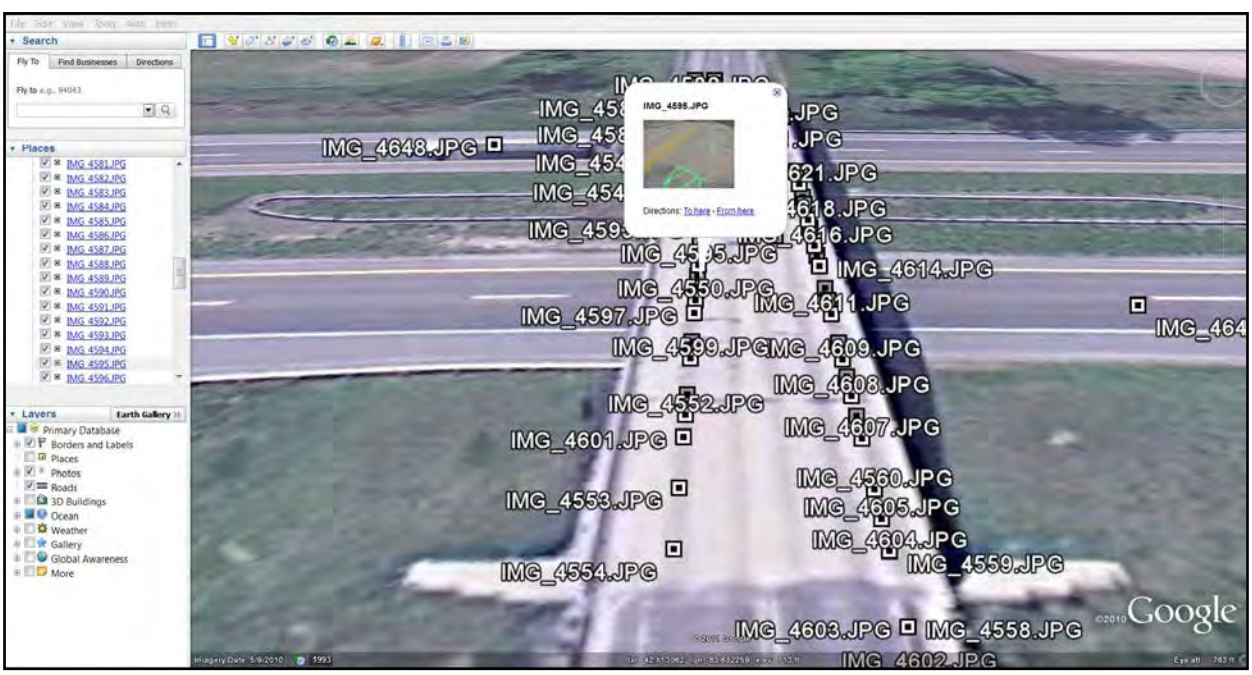

Figure 13: Example of the location of the digital photographs being displayed in Google Earth; each box contains a hyperlink to a full-resolution view of the photo taken at that location.

The project team also developed an additional version of the BVRCS that could capture a photo inventory of the underside of a bridge. In order to accomplish this task, the BVRCS was modified so that a camera faced straight-up, and a lighting source was added to address potential shadow areas. The BVRCS-Underside was developed by the project team and deployed at all bridges. This system was mounted in the bed of a truck and used the same base as the 3DOBS. An attachment was added that had two 500 watt work-lights with one of the D5000 cameras mounted to it. Due to being underneath a bridge with the sky blocked, collection of exact location-data with a GPS was not practical with the BVRCS-Underside.The same 3DOBS camera triggering device was also used. Again the truck drove at a speed of about one mph and captured photos at a rate of one fps (see Figure 14). Similar to that system, a faster camera would enable increased driving speeds. This system was easily transported and was set up, deployed and broken down within 25 minutes.

Figure 14: Example photos taken with the BVRCS-Underside of Willow Road bridge.

Benefits, Limitations, and Next Steps

The primary benefits of the current version of the BVRCS (both bridge deck and underside versions) is that they can be deployed using inexpensive hardware, they can quickly set up and taken down (10 minutes or less to collect data), they existing commercially-available software for photo processing, and that this system creates an easily viewable photo inventory of the condition of a bridge that can be compared to future photos. For the bridge deck version, the photos are location-tagged using GPS and can be accessed and queried using commonly available geospatial software such as ArcGIS and Google Earth. The total system cost ($1,140)

as currently developed is: $500 for the two PowerShot SX100 IS cameras, $190 for PSRemote camera control software, and $350 for the GPS-Photo Link software.

The primary limitations of the setup include data collection speed, the need to assemble a working system from separate parts, and the use of non-high-end GPS. Similar to the team's 3DOBS, higher-end cameras would enable faster data collection. However, the PSRemote software only works with certain cameras and cannot take photos faster than about once every four seconds (with the cost being $95 for the Canon version and $175 for the Nikon version, see <http://www.breezesys.com/>). The team's solution for the BVRCS-Underside, as for 3DOBS, has been to adapt some existing MTRI camera control software to take photos at a rate of 1 fps. Ideally, the combined camera hardware, control, and photo processing system would be available from vendors that a DOT could contract with for services for field deployment.

In the meantime, a working and immediately useful system can be assembled based on the results of the current project. The team proposes to write a "How to Deploy the BVRCS" manual depending on project sponsor input and TAC interest, as a logical next step for reaching a field ready system.

GIGAPAN SYSTEM (GigaPan)

Collecting multiple digital photographs and stitching them into a single gigapixel (or larger) image was not previously considered as a bridge condition assessment technology. However, the MTRI team had a GigaPan available from a previous, non-bridge related project. As the system is capable of creating gigapixel (1,000 megapixels or more) high-resolution photos that can be used to help inventory a bridge's visual condition at a particular point in time, the project team decided to deploy it along with the other technologies while out at the field demonstration bridges.

The GigaPan consisted of a GigaPan EPIC robotic camera mount, a PowerShot SX110 IS, and a camera tripod (see Figure 15). This system was deployed at all three bridges and collected both side (fascia) profiles and undersides of the bridges. The setup and break down times for the GigaPan were both less than 10 minutes. Collection times ranged from 20 minutes up to 4 hours, depending upon the size of the area being captured and the amount of photos taken. The end results were between 1- and 10-gigapixel photos for a particular part of a bridge, such as its fascia (see Figure 16).

While the resulting images are very large in size (hundreds of megabytes to several gigabytes), the GigaPan website provides the ability to share the full-resolution versions of these images at no current cost. The project team has loaded two gigapixel examples onto the <http://www.gigapan.org/> website for easy example access, and to make it possible to rapidly integrate the results into the DSS. This type of image hosting could be provided through an existing DOT or contractor website, but using the <http://www.gigapan.org/> website means that an already optimized streaming service for these high-resolution images can be used for at least demonstration of a method of implementation. These two links provide access to full-resolution gigapixel-equivalent example photos taken at two of the selected bridges: Willow underside <http://gigapan.org/gigapans/84465> and Mannsiding looking north along south-bound US-127 <http://gigapan.org/gigapans/84462>.

Figure 15: An example of the GigaPan being used to collect high-resolution bridge inventory photos during August, 2011 field demonstrations at Willow Road bridge.

Figure 16: Profile view of Willow Road bridge looking south along US-23 from a GigaPan image. The full resolution version of this photo captures the entire side of the bridge at very high resolution in a gigapixel image.

Benefits, Limitations, and Next Steps

A primary benefit of the GigaPan is that it uses relatively inexpensive hardware to create a high-resolution photo inventory of parts of a bridge, available as a single gigapixel image stitched together from many hundreds or thousands of digital photos. The EPIC camera mount owned by MTRI costs $299; a higher-end version with faster robotic arm and capable of using more cameras costs $895 (see <http://www.gigapansystems.com/>). The EPIC camera mount comes with the GigaPan Stitch software that easily stitches together the multiple single images into a single larger image. The project team used one of its $250 PowerShot SX110 IS cameras while newer systems can use DSLR cameras.

A primary limitation is the length of time it can take to collect the photos needed to create a gigapixel image. Some of the image collections during field demonstrations took the team slightly over three hours. Also, the resulting number of images takes storage space capable of holding 1,000 or more 7-to-12+ megapixel images. It also takes approximately 4-to-6 hours to stitch together the images. Making the data available to end users requires a server that can stream large images to end users, although fortunately so far the GigaPan project (see <http://www.gigapan.org/>) is providing this service free of charge. If a very high-resolution photo inventory of various parts of a bridge is valuable to a DOT within these limits, then the GigaPan is ready for deployment at the current time. With server space, processor power, and data streaming speeds generally increasing, then the large size of files generating through GigaPan data-collection should be less of a limitation in the near future.

The team proposes to write a "How to Deploy the GigaPan" manual depending on project sponsor input and TAC interest, as a logical next step for having a user-ready system. A review of GigaPan capabilities and practicality in the near future is recommended once new versions have been released and DOTs have increased their computer and server capabilities.

THERMAL INFRARED (ThIR)

Field demonstration of ThIR imagery was conducted on the selected pre-stressed concrete bridges using the data collection procedure based on the proposed method in technical memorandum nº 20. ThIR images were collected on the top of the bridge deck by pulling the cart with a “homemade tripod” over the bridge (see Figure 17) on the specific grid pattern (see Figures 18 and 19) that was drawn on each bridge prior to data collection. This cart system can be adapted to a vehicle-based mount.

Figures 17 & 18: ThIR camera mounted on the cart with "homemade tripod" system and chalk and duct tape grid layout on Freer Road bridge.

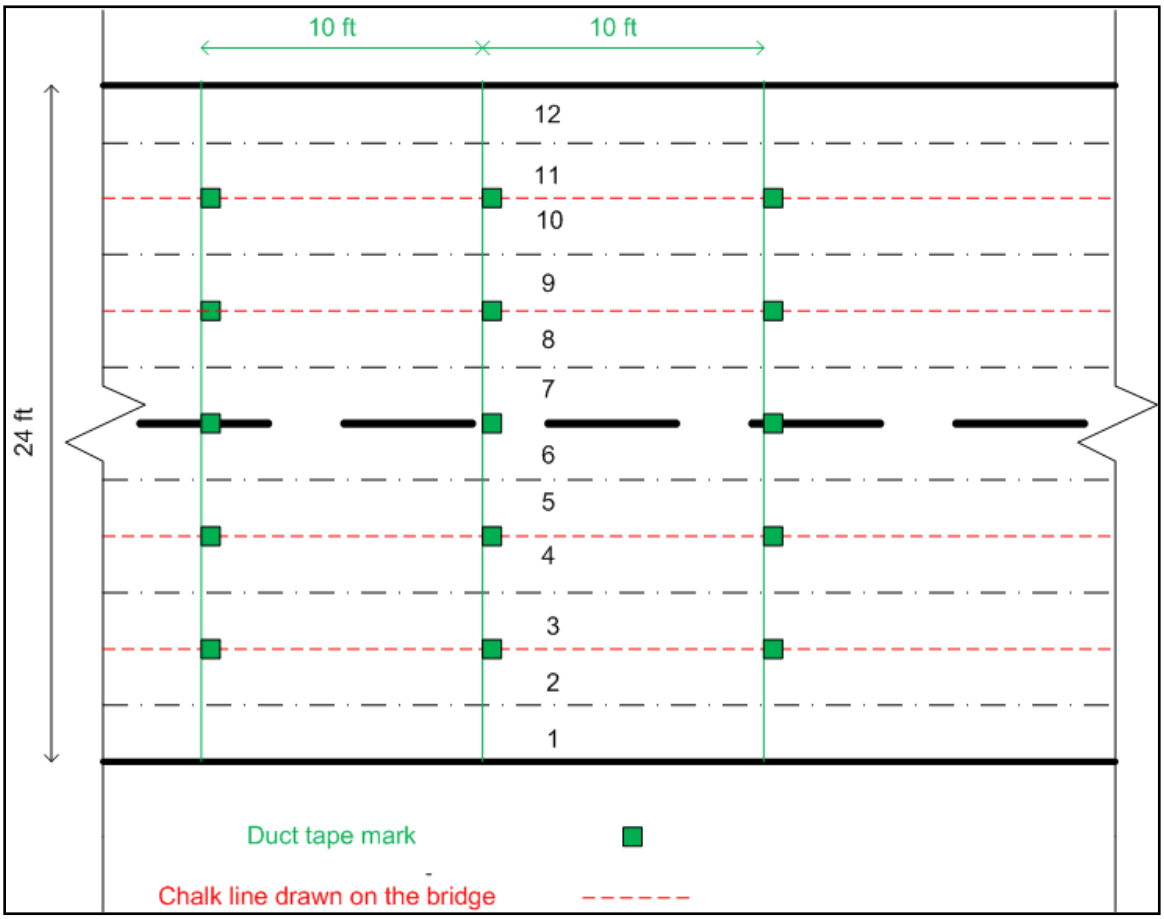

Figure 19: General grid pattern what was used on each of the bridge decks.

Collecting ThIR images from the bottom of the bridge was done by standing on the shoulders or closed lanes underneath each bridge using the FLIR ThermaCAM SC640 camera and by using a bucket truck and the FLIR i7 camera to get closer to the surfaces of interest and compare the differences.

The first approach to ThIR data analysis after the bridge deck data collection was to stitch all the images together to get the overview of the entire deck. Figure 20 shows the results of this approach for the Freer Road bridge. Calculating the percentage of delamination was the next step in the process which was accomplished by analyzing each image in Microsoft Excel (this method was discussed in technical memorandum nº 15) and calculating the total percentage of delamination by adding the percentage of delamination for each image. Table 1 shows the result of this calculation for the Freer Road bridge. This bridge was rated as a "satisfactory bridge" based on the most recent inspection in June, 2010.

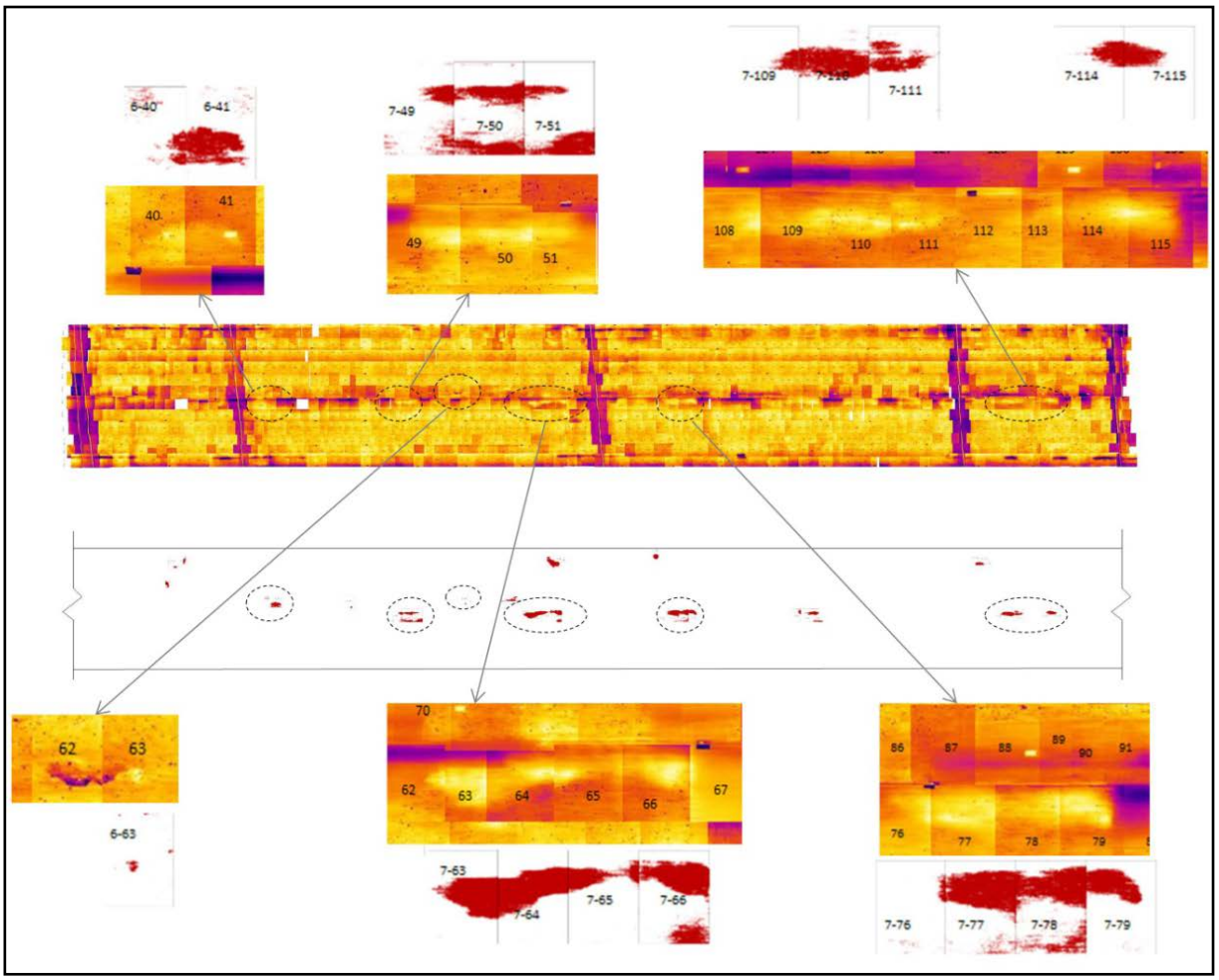

Figure 20: Free Road bridge deck delamination map created by ThIR images and Excel spreadsheet.

Total Delaminated Area (ft^2)	22.95
Total Bridge Area (ft^2)	5,015.75
Percentage of Delamination (%)	0.46

Table 1: Percentage of delamination calculation for Freer Road bridge.

The delamination map created can help bridge inspectors locate and quantify the delaminations on a bridge deck, however this method is labor intensive and require an operator to move images around to find the correct location of the image. Also, it needs reference points such as pieces of duct tape on the surface to help in the stitching procedure. Another method being developed by the project team is using The MathWorks MATLAB to automatically stitch the photos and calculate the area of delamination.

Possible delaminated areas on bridge piers and under the deck were visible on several of the ThIR images taken from these locations, however calculating the area of delaminations based on number of pixels is not accurate because the cameras were not completely perpendicular to the surfaces. However, current bridge inspection practice under the bridge involves lane closure and use of a bucket truck, which does not occur on a biennial base. Therefore, locating these areas can be helpful to bridge inspectors identifying these areas without lane closures.

Figures 21 and 22 show the delaminated areas on a bridge pier of Willow Road bridge. All the four inspected bridges were pre-stressed I-beam bridges which did not have many delamination problems on the girders; problems that have been observed by the research team were mostly located on the deck bottom surface and piers.

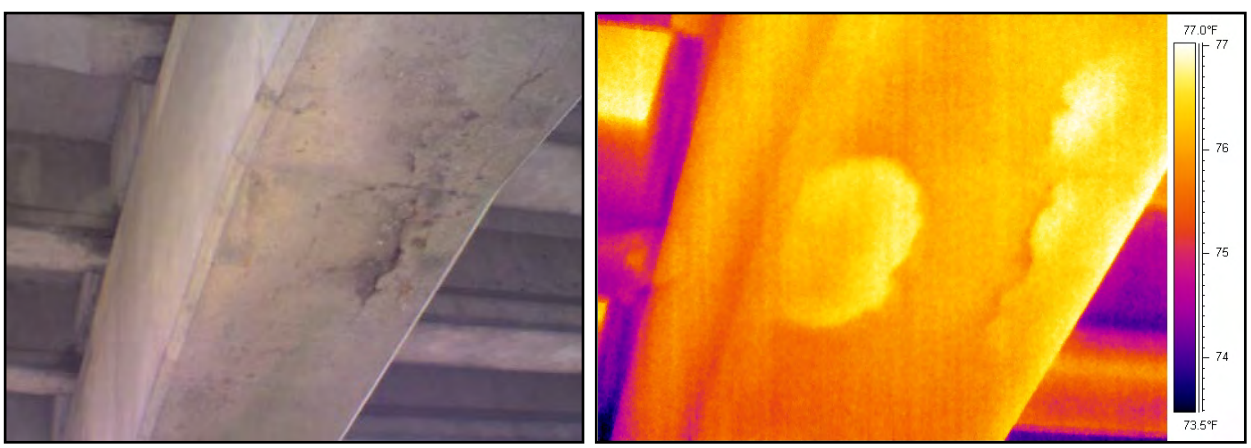

Figures 21 & 22: Optical and ThIR images showing delaminated area on a Willow Road bridge pier.

Benefits, Limitations, and Next Steps

Detecting delaminations on a concrete bridge is a major challenge for DOT inspectors as the current practice methods, hammer sound and chain drag, are labor intensive, time consuming, and require lane closures over and under the bridge. ThIR imagery is a technology that can assist bridge inspectors with detecting delaminations faster and easier than what is currently being done, which is the primary advantage for deploying this technology.

As it has been mentioned in technical memorandum nº 20, weather conditions and the time of day play an important role in having an accurate data set. During this field demo for all selected bridges, weather condition was partially to mostly cloudy. Data collection time was between 10:30 am and 2 pm as planned. More research is required in this field to improve the system by possibly adding heaters and use active thermography method.

The i7 ThIR camera is a handheld device which costs around $1,995. Although this camera is easy to use and has the ability to produce similar results as the more expensive cameras, it is not as efficient. This camera has smaller field of view (FOV) and lower resolution (14,400 pixels) than the more expensive cameras. Not having the options of taking ThIR images at time increments and taking optical images as well as ThIR images are the main disadvantages of this model. The ability of a camera to take images at time increments is necessary to use this technology at any rolling speed. Taking optical images of the bridge as well as ThIR images is one of the important components of data collection to help bridge inspectors re-visit the collected data at a later time and separate the noise and surface staining from the delaminated areas. FLIR software is not included in the price of this camera and it has to be purchased separately. A hand-held FLIR option that has higher resolution (19,200 pixels) including both optical and ThIR imaging capability is the E40 at around $4,195. Comparable FLUKE options are the Ti10 and the TiR; either for around $4,495.

The ThermaCAM SC640 (307,200 pixels) has the option to collect data at time increments up to 30 fps which helps in collecting the data at rolling speeds and creates a sequence of images for each pass. Also, this camera has the option to collect optical images as well as ThIR images which can be stored one device. The proprietary software of this camera has the option to analyze the images and help in detecting and calculating the area of delaminations. While not being part of FLIR's current line-up, this research and development camera is estimated to cost around $40,000.

Although this technology is promising in identifying delaminations (see Figures 21 and 22), this method of data collection is not completely practical for bridges at the current stage of

development. The field demonstration data collection method was designed based on the available ThIR cameras and their limitations. The lens on the ThermaCAM SC640 has a focal-length of 40 mm which limits the horizontal field of view of this camera to about 2.7 ft wide at a height of 6.2 ft. This FOV limits the possibility of installing the camera on the back of the truck (similar to the 3DOBS) – the camera would be to be installed at a height of 24 ft (very impractical) to be able to capture a lane that is about 10 ft wide. The lens on this camera can be replaced with a calibrated 19 mm lens at the cost of about $10,000; which would increase the FOV to a width of 10 ft at a more sensible height of about 12 ft. However, using the 19 mm lens can cause image distortion along the edges which can create inaccuracy in the pixel analysis of the image.

The first approach of data analysis (originally proposed in technical memorandum nº 15) is labor intensive and time consuming for analyzing the large amounts of data. While MATLAB programming is in progress for processing large amounts of data it requires more research time to make it applicable for bridge inspection practices. Although the ThIR camera and the proprietary software is commercially available, a package which is specific for bridge data analysis and delamination detection is not currently developed and requires further research in this area.

There is a future in using ThIR to detect bridge delaminations, but simultaneous development in data collection procedure and a specific software package need to happen to make this technology user ready for bridge inspectors and transportation authorities.

DIGITAL IMAGE CORRELATION (DIC)

DIC was implemented on MDOT structure nº 1713 – Mannsiding Road over US-127 north-bound. The objective with this field deployment was to verify the capabilities of the technique and application for structural health measurements such as displacement and strains. The complete north-bound Mannsiding Road bridge system has three major spans; two approach spans over each shoulder and a center-span over the US-127 north bound lanes.

While part of the original plan, traditional instrumentation (e.g., deflectometers, accelerometers, strain gauges) for correlation purposes was not deployed as planned. However Light Detecting and Ranging (LiDAR) was used as a possible validation technique for DIC deflection measurements.

Implementation of DIC consisted of a creating a contrasting dot pattern on the structural I-beam span (of the center-span), and setting up an elevated (at center-span) camera-lens system. Before testing began, the half-point and quarter-point locations on the 60.25 ft center-span north-most girder were marked with duct tape to easily identify the testing locations before a washable water-based spray-paint was used for the creation of a speckle pattern on the exterior girder. A MDOT bucket truck was used for the creation of these larger and smaller refined marks constituting the speckle pattern which are necessary for tracking pixel movement using DIC (see Figures 23 and 24).

The camera was placed at a 20 ft standoff distance from the target surface on a rigid tripod (4.25 ft) located on a scaffolding platform (10 ft). The overall height of 14.25 ft placed the camera perpendicular with the exterior girder (see Figures 23, 25, and 26).

Figures 23 & 24: DIC setup at Mannsiding Road bridge and detail of girder with speckle patterns.

The predetermined bridge span was stressed by both a quasi-static and dynamic live-load generated by a live-load test truck. A live load truck with a weight of around 57 kip (see Figure 25) was used during load testing. The truck was guided along the exterior lane path at a crawl speed below 10 mph. During loading, images were captured by a Canon EOS 7D DSLR with the EF 70-200 mm f/2.8L USM lens on the exterior girder at the quarter span location. This test was repeated three more times with two of those trials remaining at focal length of around 85 mm and the third was at a focus length of around 135 mm.

The camera was then moved horizontally to capture images at a 45° angle to the girder surface at the half-point. This test was repeated three times at crawl speeds at a focal length of around 135 mm and the third was a focal length of around 200 mm. The speed on the truck was increased to about 40 mph and a series of images were taken at this speed shooting at the

more defined speckle pattern quarter-point location. To conclude this testing, a static test was performed with the truck parked at the quarter-point location. Additionally, a series of static tests were done on the bridge as well with no truck (load) on the bridge.

Figures 25 & 26: Load truck going over bridge and close-up of camera and tripod setup on scaffolding.

The dynamic test was performed to determine how accurately DIC can optically sense, and capture, bridge vibration. The dynamic tests performed at posted speed were completed to mimic actual service conditions. The images were numbered automatically by the camera's firmware, and each of the images was correlated with the known load applied to the bridge span at that time. All of the truck measurements and distances on the bridge were collected to be able to use further in finite element analysis (FEA) bridge model. The field experiment with scaffolding preparation and image capturing from loading on the exterior girder took about an hour. The total time for the application of the speckle pattern took about 15 minutes.

The images gathered with the camera were processed in Correlated Solutions Vic-2D for strain and displacement measurements. The next step involved formatting and processing the images into Vic-2D. Expected results from this testing would expect to show quasi-static behavior where there is a higher value that drops due to displacement from the loading truck and then returns back or near the point of origin as the truck drove across and off of the half-point and quarter-point locations. The values of the change in position (displacement) the images file numbers (time elapse) are quite varied from set to set. Figure 27 shows a sample graph from the raw data of the quarter-point set from one of the crawl speed run series.

From this graph, very erratic movement is shown. With all this noise and variation displayed, trend lines and linear graphical relations were attempted to characterize the movement. This approach was used in all sets with not a lot of consistency between them. Looking at Figure 27,

it reveals a change in displacement of at least four inches (down vertical direction). Now, with all conditions considered such as a standoff distance of 20 ft and a slight degree movement of the camera from a wind disturbance, the camera could easily move and correlation could indicate larger movement than what actually occurred (perhaps, something as large as four inches). This leads to further investigation of the data files being produced in the VIC software. A re-examination of the 'V' (vertical displacement) of the pixel location, 'c' as interpreted through the software was investigated to ensure the data presented is the data that is expected.

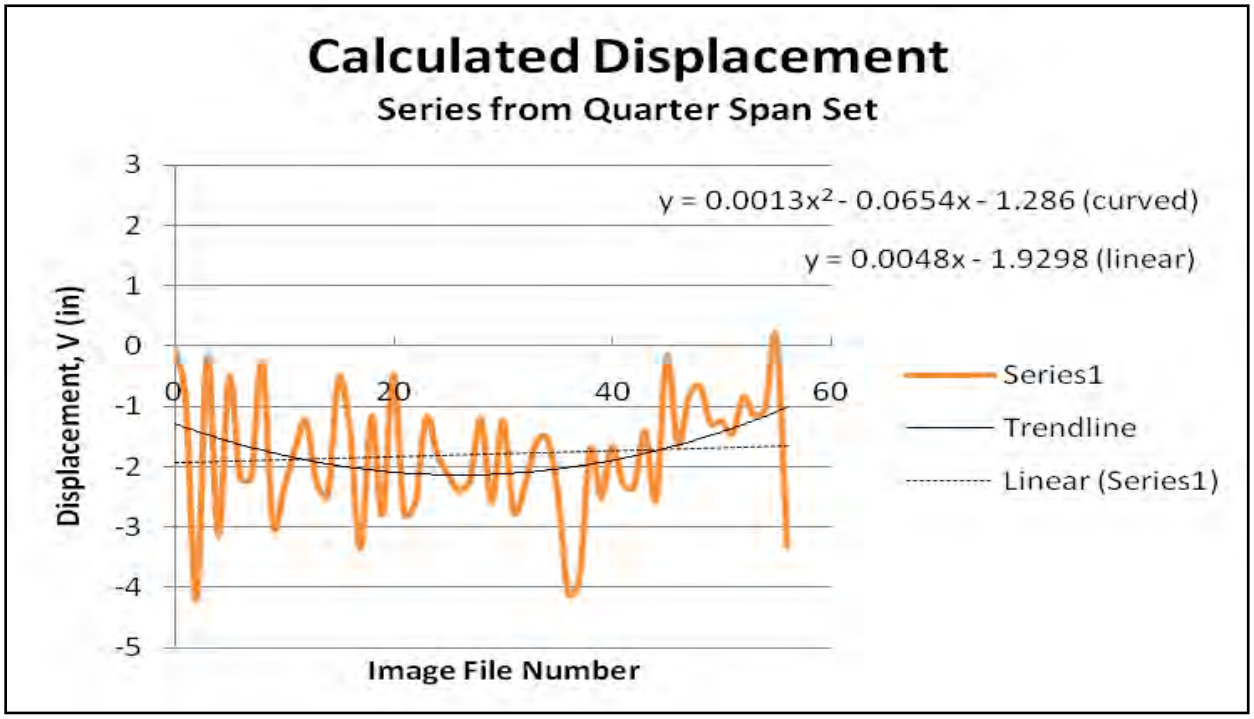

Figure 27: Vic-2D graphical plot of calculated displacement for a test series.

Through this investigation, it was evident that this random graph display was presented in all the sets due to various environmental effects endured in field testing. During the tests, there still was one lane of traffic next to the camera system on the scaffolding platform which is shown in Figure 23.

Therefore, the wind and vibration effects of the passing traffic were a factor throughout the testing. In addition, other wind movement in the air could impact camera and lens stability as well as movement to the scaffolding itself especially since it was elevated 10 ft for alignment with the bridge girder height. The noise is an issue that was considered and an attempt to factor out or single out somehow was used which in explained in the next section. Additionally,

this testing data will be compared with the LiDAR point cloud data collection that was taken both with the truck and without the load truck once this data is thoroughly processed. Furthermore, this data will also be correlated with a finite element model (FEM) of the Mannsiding Road bridge comparing simulated behavior with actual bridge response. A simple model was created of the bridge girder and the truck loading configurations which were correlated under the maximum value deflection that can be endured with this bridge's measurements. This analysis will be explored further while considering distribution factor analysis for a combined bridge girder- and deck-system.

As discussed, additional laboratory testing was also done to see how well Vic-2D captures movement together with also identifying the dynamic effects of wind and other "outdoor" effects in the camera system as experienced previously in the field. With the same lens settings, tripod, and camera system a series of tests were completed. A rectangular piece of plywood with a distinct speckle pattern was used at 2 ft and 32 ft from the camera; it was subjected to cyclic movements at two varied displacements on an MTS 810 Material Test System. Figures 28 and 29 show the setup of the speckled board and camera at the two different distances.

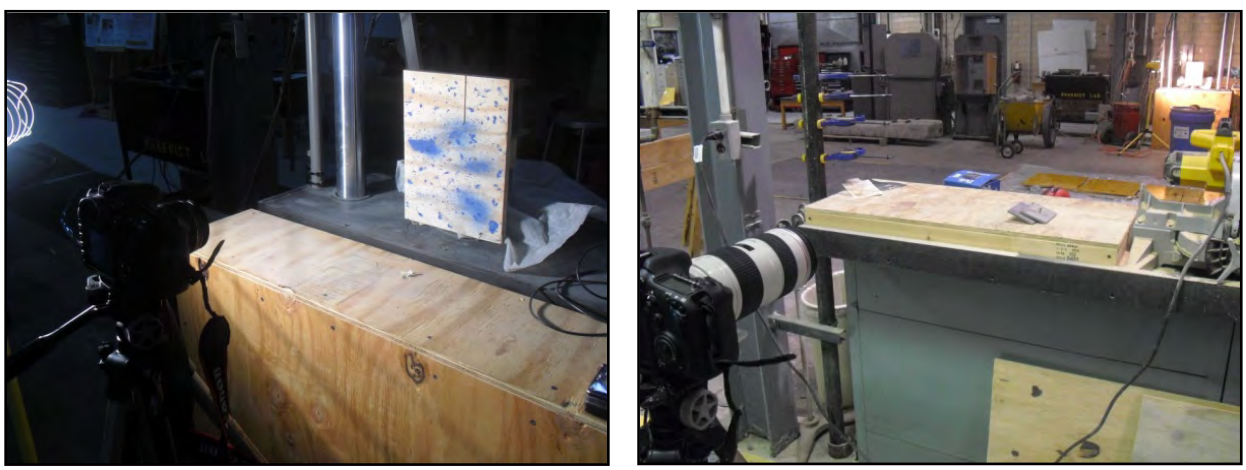

Figures 28 & 29: Benedict lab testing setups at 2 ft and at 32 ft.

At the closest distance, 2 ft, two different trials were completed; with (fan on camera) and without wind. Table 2 shows the percent difference in displacement values as calculated in Vic-2D software as compared to the data collection from the 810 Material Test System; the values had little error at 1.8%, but with wind simulation the change in displacement increased almost by half. For the 32 ft testing scenario, the camera was placed on the loading platform of a Fairbanks-Morse floor scale located on the MTU's Benedict Laboratory (see Figure 30).

Test Number/Type	Test Frequency	Expected Displacement	MTS Measurements	Vic-2D Measurements	Percent Difference
T1 - no wind	0.25 Hz	0.25 in	0.2468 in	0.2515 in	1.8%
T2 - wind	0.25 Hz	0.25 in	0.2462 in	0.2521 in	2.4%

Table 2: Test measurement comparisons at 2 ft with wind and no wind.

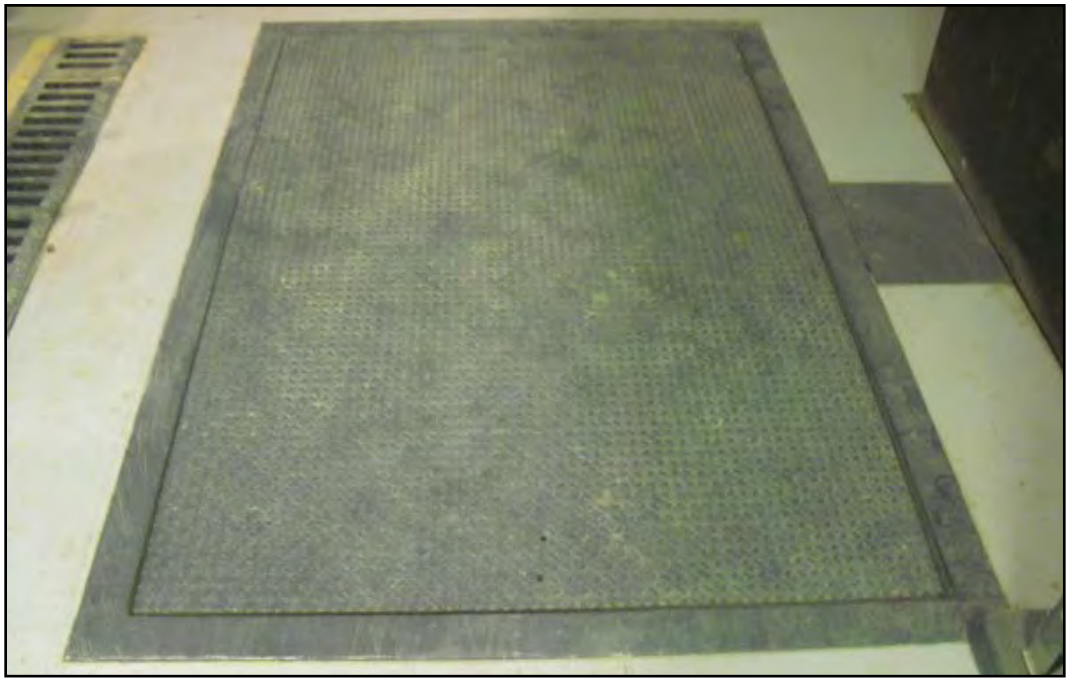

Figure 30: Floor scale loading platform used to simulate scaffolding movement.

The floor scale platform can easily move with a person walking or a simple shift of weight by objects. The camera and tripod were placed on the platform and images were taken of the rectangle speckled board. This test was repeated with a person moving on the platform to demonstrate a field like simulation of the scaffolding setup. Table 3 shows the results from the processed images in Vic-2D compared to the 810 Material Test System data and the percent differences.

In this battery of tests, it was shown that the displacement values differ drastically when tests are repeated with and without movement. In Test 4, there was so much movement that the data could not be compared. This graphical representation is shown in Figure 31. Again, Tables 2 and 3, show the re-examined approach of the 'V' (vertical displacement) of the pixel location, 'c' as interpreted through the software. These tests are very comparable to the same type of noise identified in the field results.

Test Number/Type	Test Frequency	Expected Displacement	MTS Measurements	Vic-2D Measurements	Percent Difference
T1 – without movement	0.25 Hz	0.25 in	0.2457 in	0.2578 in	4.8%
T2 – without movement	0.25 Hz	0.50 in	0.4966 in	0.5070 in	2.1%
T3 – with movement	0.25 Hz	0.50 in	0.4974 in	0.7414 in	39%
T4 – with movement	0.25 Hz	0.25 in	0.2482 in	-----	-----

Table 3: Test measurement comparisons at 32 ft; movement and no movement.

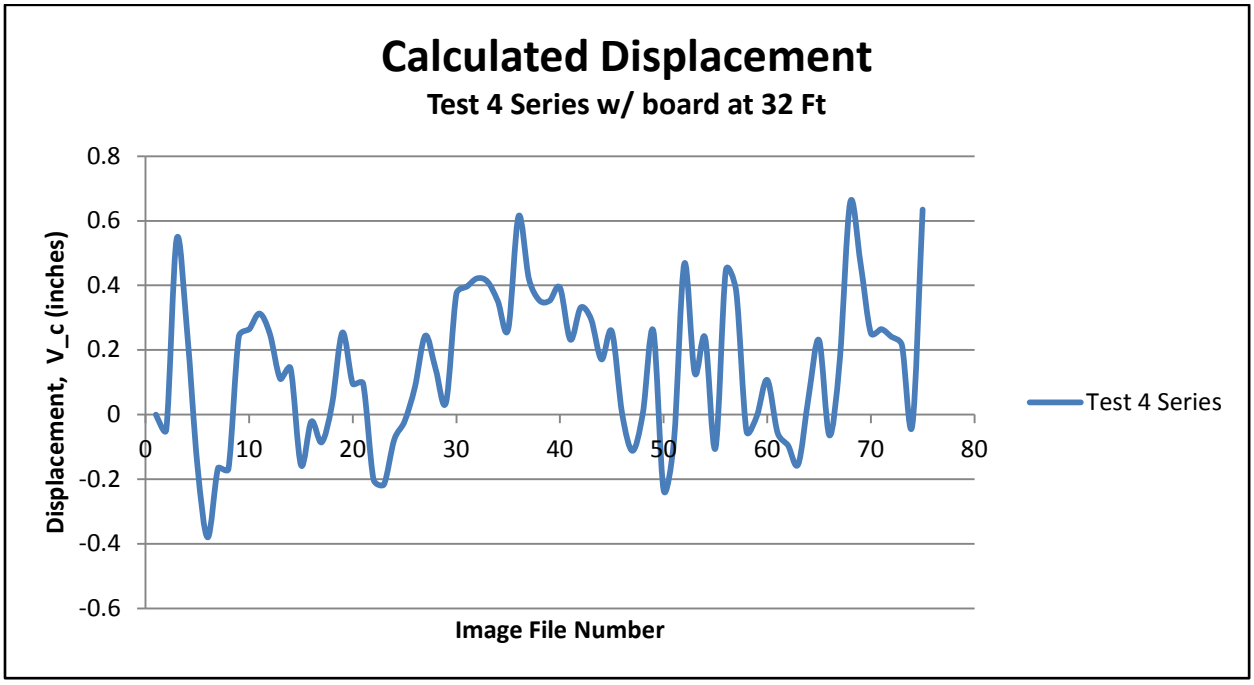

Figure 31: Test 4 results from the 32 ft series testing; test performed with floor scale movement.

Benefits, Limitations, and Next Steps

The benefits of DIC include the flexibility in location for testing as well as time-of-day for image collection (depending on requirements), use of available software for analysis and ability to provide load performance details with single tests.

The total cost of this system currently consists of; ~$12,000 for Vic-2D, $3,000 camera and lens system, $1,000 scaffolding system, $100 tripod, and $15 for washable spray-paint. Much of the

DIC system cost depends on the requirements needed for particular testing being conducted (e.g., higher grade lens or camera, different paint used for pattern, better more stable tripod).

The limitations of the software consist of the compatibility with the camera-lens system in the testing environment, the applicability of the speckle pattern to be detected (enough contrast), and actual software specifications. This technology has the capability to obtain the measurements expected (shown in a controlled laboratory setting) but needs further development for field deployment. Ideally, continued testing with better adjusted system setup and instrumentation data correlation would be beneficial in meticulously tracking down displacement in images with time-stamps to track movement incurring on a bridge.

When considering additional testing, it is suggested that both the system performance and system algorithms details may need to be revised. Initially, when applying the pattern, there needs to be assurance that the pattern will be detected at the imposed standoff distance; a "pre-test" needs to be performed to insure this. One of the trial runs for the quarter-point series did not correlate pixels from image-to-image; this gave a non-readable data set for that series. The exact causes of this non-readable set is not known but it is speculated that sunlight during that particular series produced non-desired contrasts with between the speckle pattern and the concrete face on the girder.

Specific to hardware, a more stable testing platform could be used together with a shorter and sturdier surveying-style tripod reducing much noise. Also surrounding the camera and lens with a "shield" could possibly eliminate certain wind conditions. Note that accurately assessing wind and vibration factors is very important. The movement of the camera lens could be tracked using an accelerometers and an algorithm; this could allow for lens movement to be possibly factored out in displacement analysis. A gyroscopically-compensated camera mount, such as one of the Kenyon Laboratories Gyro Stabilizers, could also help in keeping the camera still. Reduction of the standoff distance would certainly reduce the effects of wind and vibration.

There are also numerous changeable parameters within the software that can alter the results. Algorithm details may require further investigation considering bias errors in the accuracy or precision of the software analysis. Bias interpolation of these results can translate into incorrectly interpreted testing data. More investigation into parameters and how they affect results is a major component of the post-processing data analysis.

While DIC has hardware and software that is commercially available and ready for deployment, it is a technology that is currently best suited for laboratory work where most-all conditions

(e.g., wind, vibration) can be controlled. There is a future in using DIC in the field when but there needs to be much hardware development specific for bridge condition tests outdoors.

LIGHT DETECTING AND RANGING (LiDAR)

The field demonstration for LiDAR imagery was conducted on the three pre-stressed concrete bridges, selected in the previous quarter. Data collection procedure for all of these bridges was based on the proposed method in technical memorandum nº 20. Multiple scan positions were sampled allowing for the equipment to illuminate any "shadows" due to the technologies limitation regarding light of sight measurement. Approximately 8-to-12 scans positions were needed to allow for a complete a 3D point cloud rendering of the numerous faces of the bridge structure. A typical scan position layout is provided to help show where data collection generally took place during the field demonstration (see Figure 32).

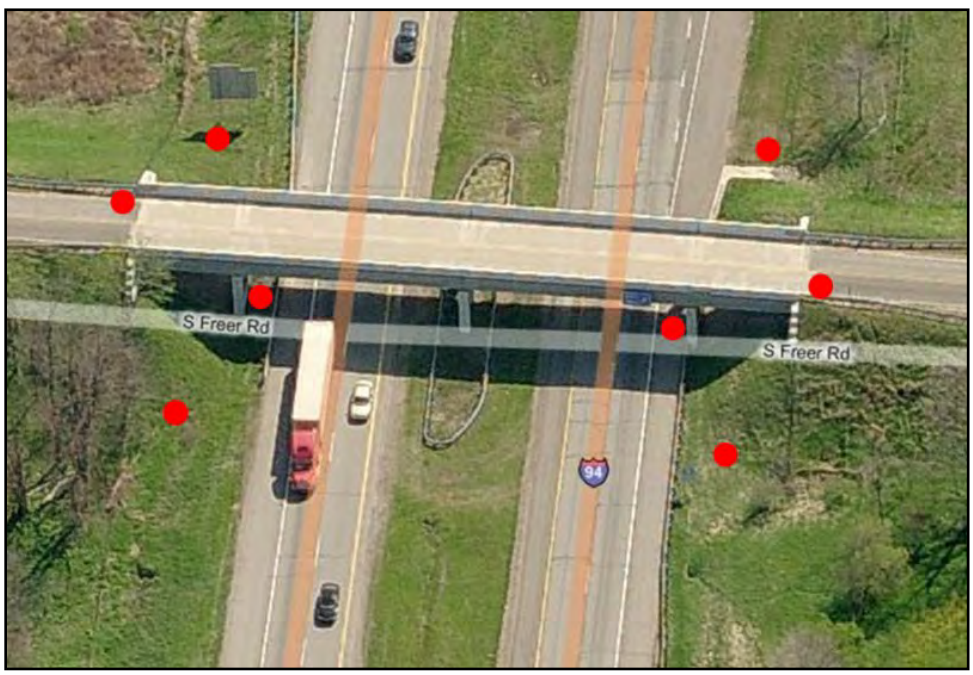

Figure 32: Red dots showing general locations for LiDAR scans to be performed.

Individual collection scans were completed utilizing two separate LiDAR surveying units; a MDOT owned Leica ScanStation C10 and a MTU owned RIEGL LMS-Z210ii (see Figures 33 and 34). The most obvious difference between to the two units is the built-in user interface of the ScanStation C10 compared to the required computer connection of the LMS-Z210ii allowing for the ScanStation C10 to be easily re-positioned by a single individual. Scan data is currently

being process to determine individual accuracy of defect detection for each unit. Note that for the first two field demonstration locations in Washtenaw county (Free Road and Willow Road bridges) MDOT's ScanStation C10 was the only source of data collection.

Figures 33 & 34: MDOT's Leica ScanStation C10 and MTU's RIEGL LMS-Z210ii.

Both data streams are being imported into three post-processing programs: Certainty 3D TopoDOT (a Bently MicroStation application), Applied Imagery Quick Terrain Modeler, and the University of North Carolina at Charlotte (UNC Charlotte) Light Detection and Ranging-based Bridge Evaluation (LiBE) surface damage detection algorithm. Usable 3D data is being created that can be analyzed for condition information using other commonly available software such as ArcGIS.

The ScanStation C10 data was collected by MDOT's Geodetic Surveying, Topographic, and Aerial Mapping Services Unit to help understand the capability of this data source in evaluation indicators of bridge condition. Regarding the LMS-Z210ii (which was deployed only at Mannsiding Road bridge) the collected scans were individually stored using RIEGL RiSCAN PRO which allows for the user to view the data collection in real-time insuring the user that the scan captured all desired features. Once all selected scan locations were scanned, post-processing began immediately on-site by combining the single scans into one master image to ensure cohesiveness (see Figure 35).

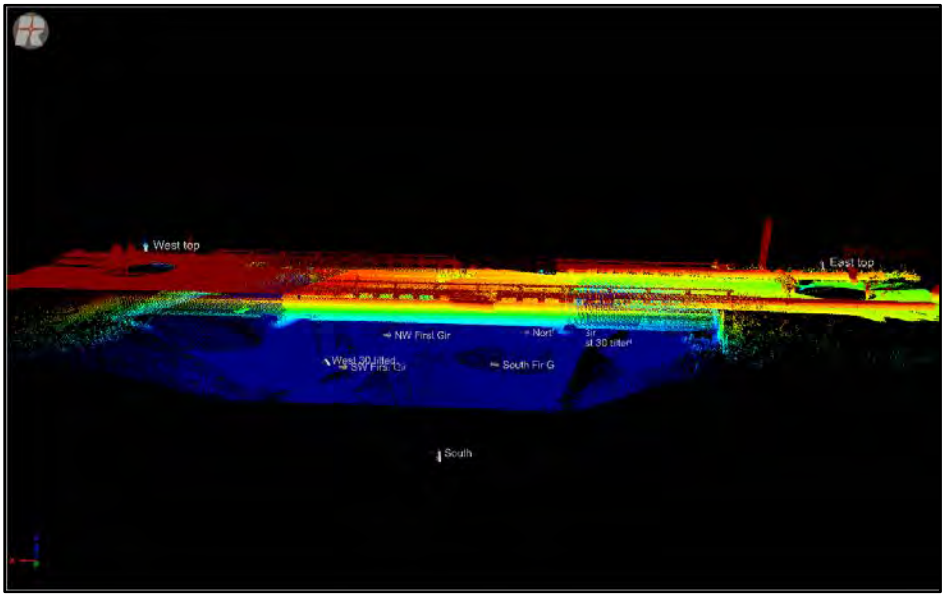

Figure 35: Master scan data image from the LMS-Z210ii and RiSCAN PRO.

While the project team waits for data processing to be completed, they are processing sample data from previous MDOT surveys shared by MDOT in order to establish a documented workflow for processing the LiDAR data into. The current generation of LiDAR sensors, such as the ScanStation C10, can extract data on XYZ location, 8 bit intensity of the return and red, green, and blue (RGB) values from each laser pulse-return.

Another commercial LiDAR processing software package, Cardinal Systems VrOne together with VrLiDAR and was also evaluated by the project team for data analysis processing and analysis capabilities. Based on ease of use so far, Quick Terrain Modeler appears to a practical piece of software for taking LAS-format LiDAR data from MDOT and converting into elevation data that can be analyzed within ArcGIS for bridge condition assessment. MDOT uses a combination of MicroStation and TopoDOT software to process and view its LiDAR data; the project team is investigating if this software can be acquired at a reasonable cost and in a timely manner.

Results from processing of MDOT sample data support the ability of LiDAR data to detect defects in the bridge deck. The combination of XYZ location, return intensity and RGB values provide a dataset sufficient to extract usable information on bridge deck condition. Note that the following scans are from a single LiDAR scan setup; MDOT frequently gathers multiple scans at a bridge in order to form a more complete picture of the bridge environment. Anomalies resulting from passing traffic, decreasing return density with distance from the scanner and buildups of debris on the bridge deck (at the lower right) are evident in the sample images. Multiple scans, additional data processing and site preparation prior to scanning can help

correct these anomalies; Figures 36, 37, 38, and 39 show examples of LiDAR data being displayed with Quick Terrain Modeler so that bridge surface condition indicators, such as the location and depth of spalls can be easily seen and detected.

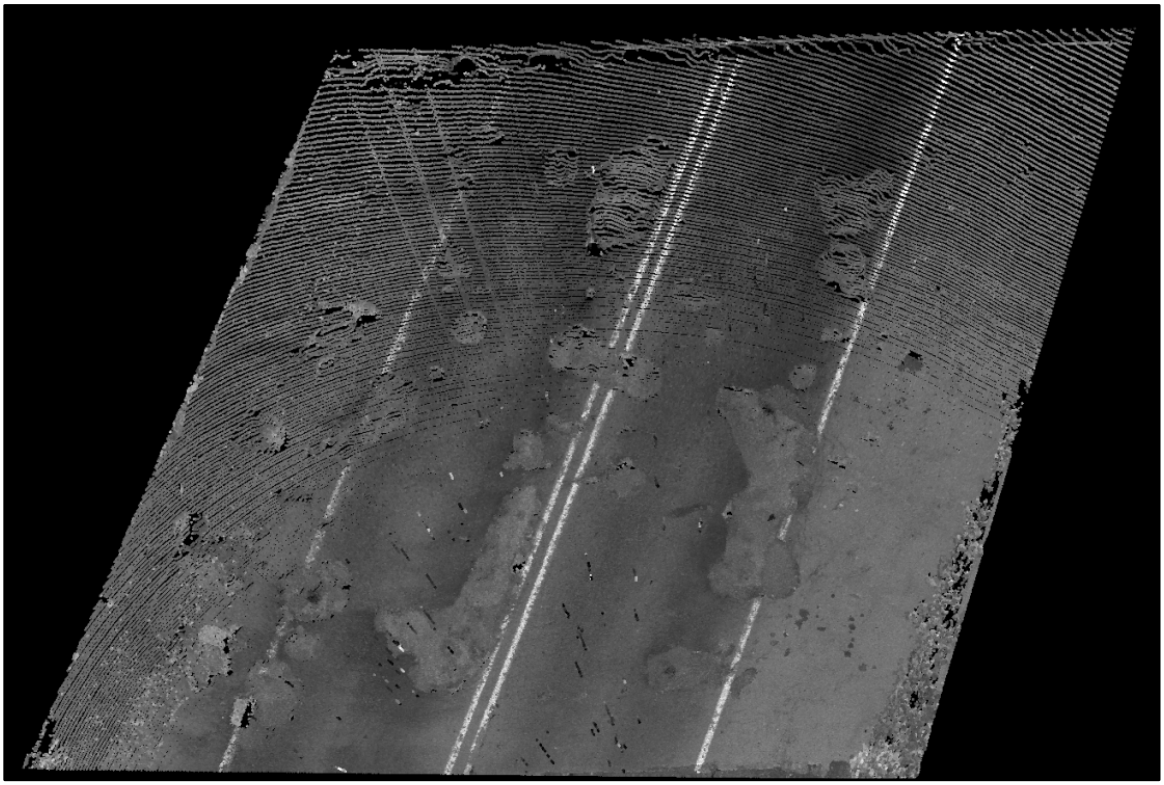

Figure 36: A LiDAR intensity image extracted from an MDOT sample data set (Warren Road over I-275). Deck condition is clearly visible as is increasing point spacing with distance from the scanner.

Figure 39 shows how an MDOT LiDAR survey has captured the presence and depth of an example bridge spall. The project team's added-value to these data is taking them and converting them into indicators of bridge condition that can be integrated into the overall bridge health signature, such as percent spalled, and location and volume of spalls, similar to what can be evaluated with the 3D optical 3DOBS. The LiDAR point clouds will be co-registered to other datasets collected at each study, allowing comparison of different remotely sensed data such as the ThIR imagery and 3D optical DEM. Initial steps have been taken to develop procedures to extract information documenting the area and volume of spalls on bridge decks and support structures from the LiDAR datasets. Fortunately, the team anticipates that spall analysis routines developed for the 3DOBS data can be used with LiDAR data as well, helping with project efficiency and eventual deployment.

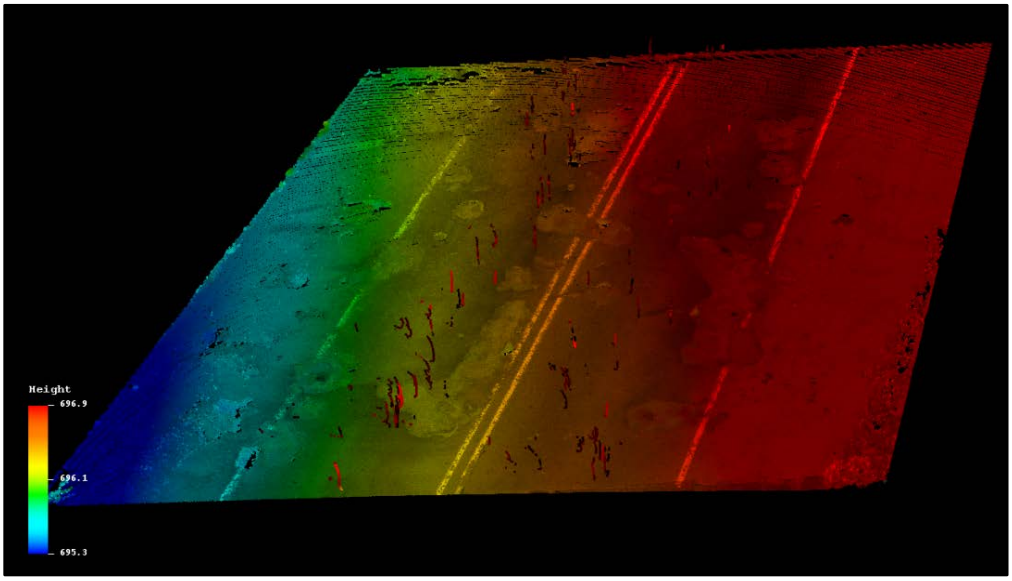

Figure 37: Composite LiDAR elevation and intensity image; deck condition can still be assessed from the intensity image. The bridge deck slopes from upper right to lower left with a total elevation change of about 48 cm.

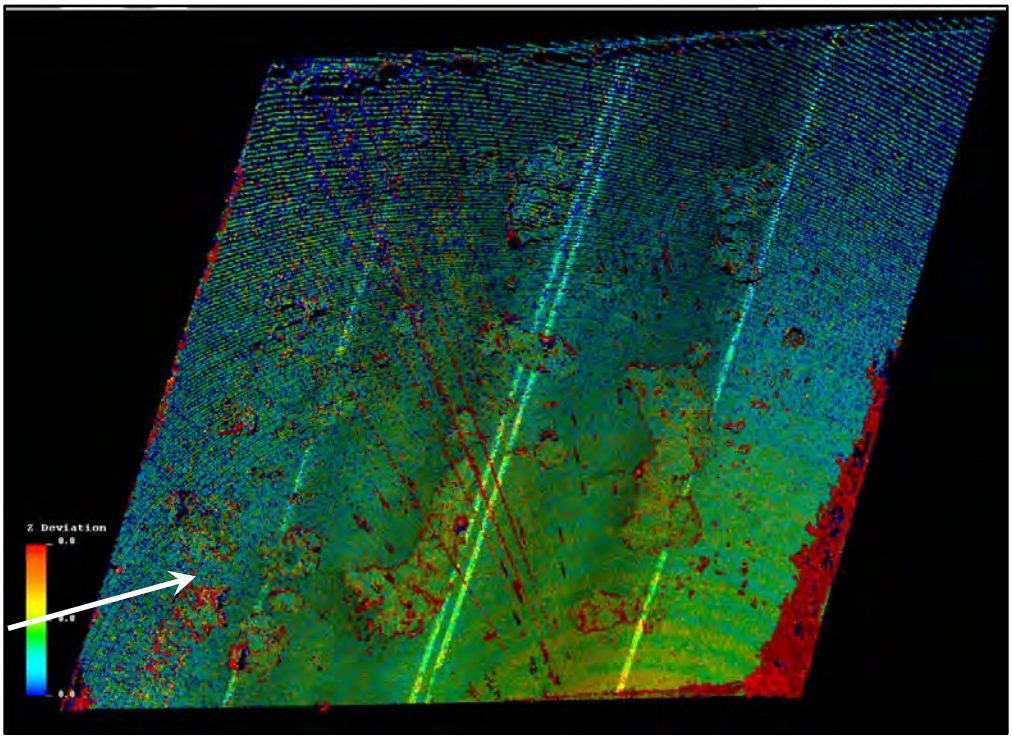

Figure 38: A composite Z-deviation and intensity image showing sharp changes in elevation between returns (red pixels). Outlines of potholes are visible as irregular shapes outlined in red. The large triangle of red pixels at the lower left is an accumulation of debris on the bridge deck. The red lines radiating from the lower right are returns from passing cars that have not yet been filtered out.

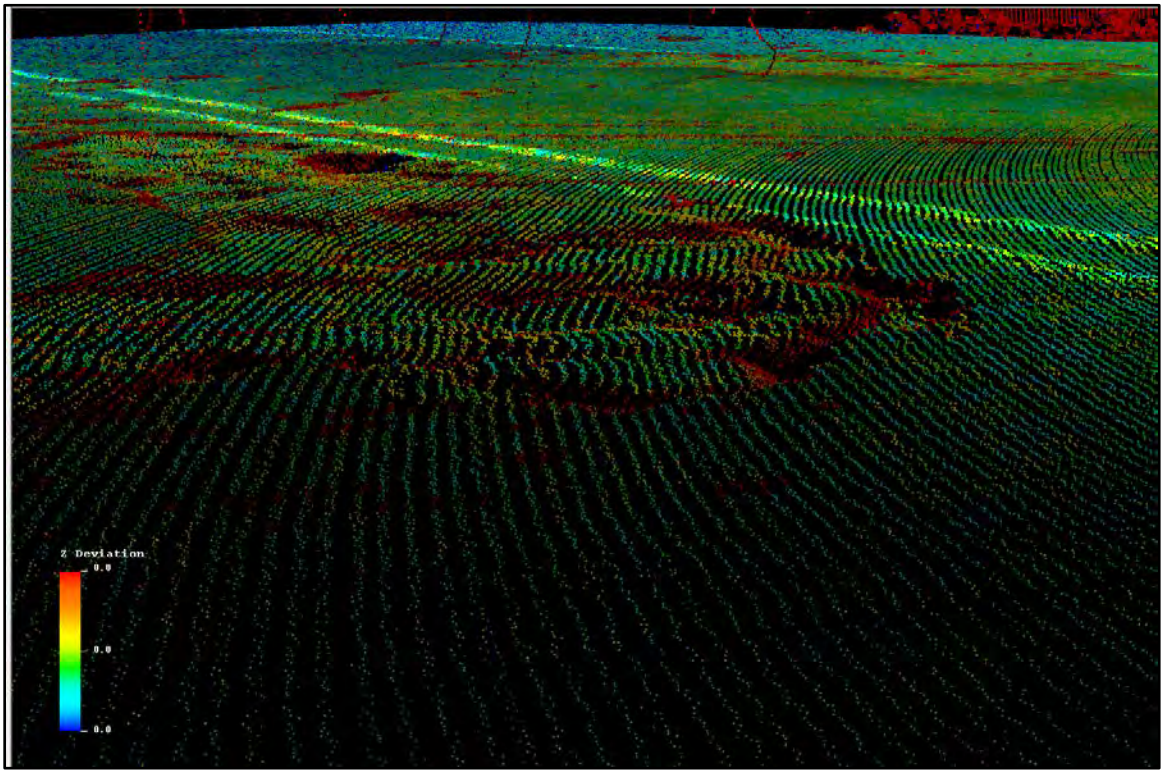

Figure 39: Demonstration of how LiDAR has captured the location and elevation values for a bridge spall. View is from the lower left looking toward the center right (white arrow) of the image. As in Figure 38, red pixels indicate rapid elevation change between returns. Further processing is expected to be able to extract deck damage area and volume values from the data.

A side by side comparison of a Google Street View image with the LiDAR intensity and Z-Deviation image demonstrates that under certain circumstances, Street View and similar data sources (such as data from the BVRCS) can be useful to validate interpretation of the LiDAR images (see Figures 40 and 41). The LiDAR data were collected fall, 2010 by MDOT but the collection date of the Street View image, while appearing recent, is unknown.

Figure 42 shows the same LiDAR data as in the previous figures, but now converted into an elevation raster file being used and displayed within ArcGIS. ArcGIS was selected because the same type of spall analysis routines developed for 3DOBS data can be used with LiDAR elevation data. The project team is currently further developing these routines with the goal of making them as automated as possible. Anticipated inputs into the bridge health signature include percent spalled for a bridge deck surface, amount spalled for bridge structure supports, and volume and location of spalls.

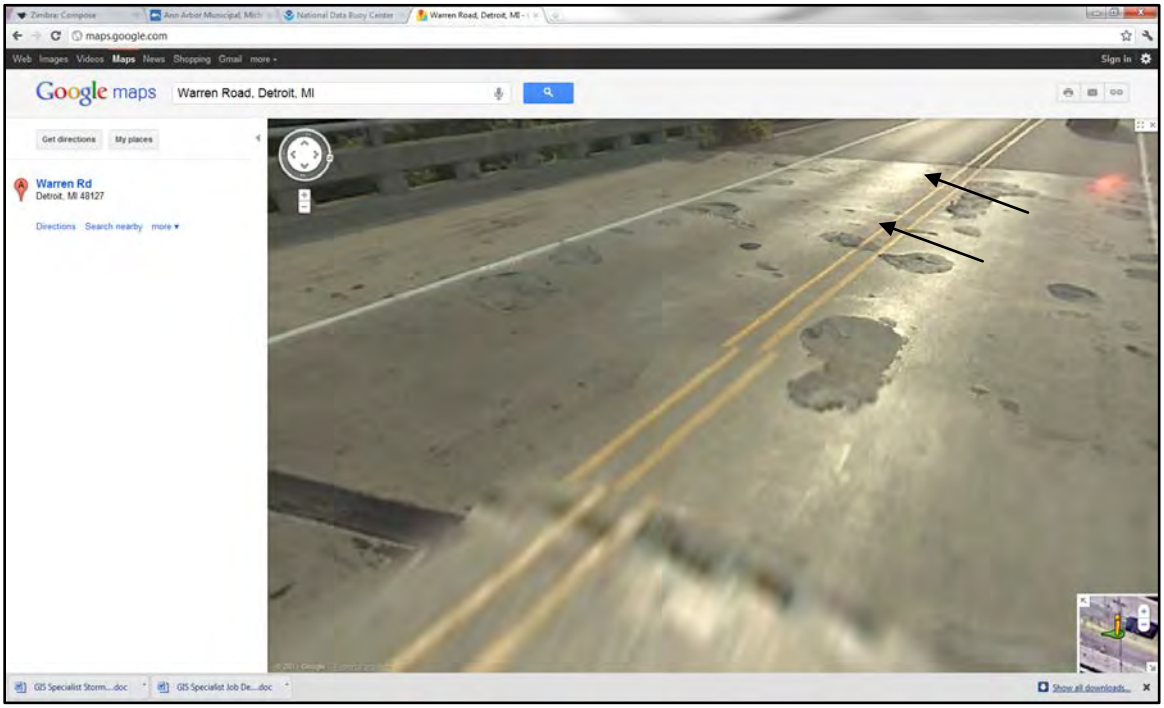

Figure 40: Street View image of the western-most span of the Warren Road bridge showing patches on the bridge deck.

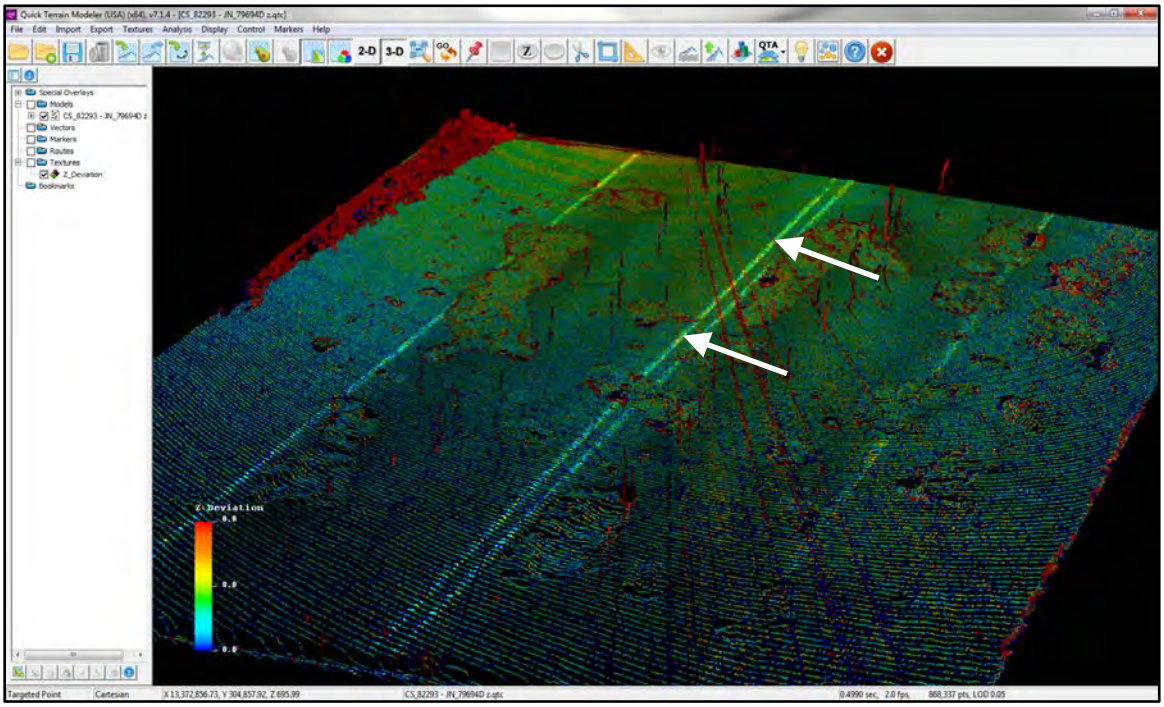

Figure 41: LiDAR intensity and Z-deviation image of the westernmost span of the Warren Road bridge from a similar perspective as Figure 40. Arrows point to the same features in each image.

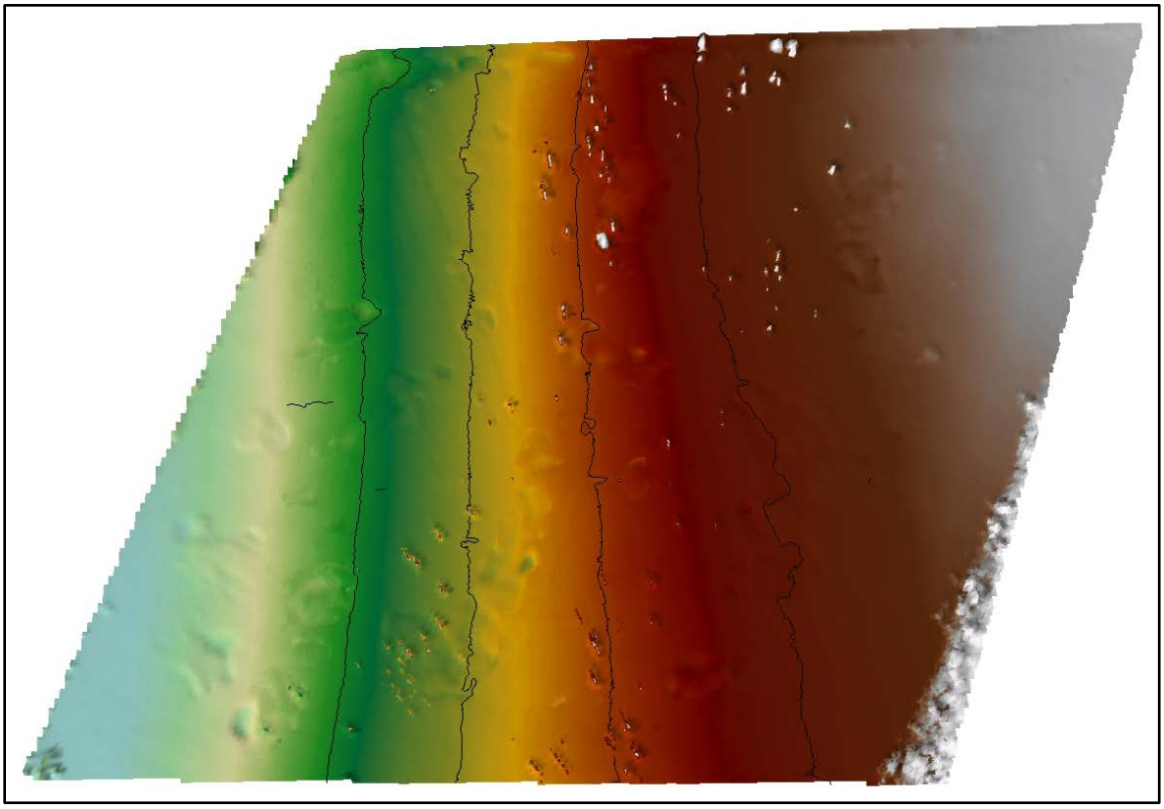

Figure 42: DEM derived from LiDAR data, exported from Quick Terrain Modeler and displayed in ArcGIS Arc Scene. Low-high is from lower left to upper-right. Generally, positive deviations from surrounding bridge deck are returns from passing vehicles, negative deviations are considered to be spalls. Orientation of this scene is similar to the previous LiDAR figures.

Benefits, Limitations, and Next Steps

As it has been mentioned in technical memorandum nº 20, LiDAR is a line of sight instrument and requires repositioning to illuminate shadowed areas increasing collection time and required labor. However the primary limitation of LiDAR is that systems are expensive; the ScanStation C10 system used by MDOT cost around $125,000. Multiple detailed scans to inventory most of a bridge can also take several hours, including set up time for geo-registration points. This technology has two main variables affecting practical use for bridge condition assessment, beyond system cost: resolution and collection time. To achieve desired feature resolution with the current models, increased collection time is required. Processing of LiDAR data into an initial usable form can also take significant time (two weeks or more depending on data-set size). Also, a workflow into bridge condition information for LiDAR data needs to be established as it not has typically been used for this purpose, but this project is

working on that process. LiDAR data has more commonly been used for inventory of information such as bridge clearance; our team's value is to analyze its capability to help developed bridge condition metrics.

The primary benefit of using LiDAR is that DOTs are already acquiring and using LiDAR systems as part of their day-to-day operations, or obtaining these services regularly from established vendors. Adding another reason to collect data (to help evaluate bridge condition) could be a relatively easy addition to existing DOT activities. The project team is providing a demonstration of how LiDAR data can be converted into bridge condition information by establishing a documented workflow whose eventual goal is integration of the analyzed data into the project's DSS.

Once the team has completed this development of LiDAR data to bridge condition workflow, the next step will be to assess the technical and financial feasibility of implementation of such a system in DOT operations. Because this technology is already used by DOTs, it may stand a better chance of being implemented that other technologies that would be new to most DOTs, such as the 3DOBS. The critical part will be establish and document a practical workflow that uses software tools commonly available to DOTs, such as ArcGIS, or that may be new but are not overly expensive, such as Quick Terrain Modeler ($995 for a license that can operate on multiple computers).

Note that LiDAR units are developing quickly and current models provide more practical resolution to data collection time results. The RIEGL VZ-4000 has the potential to reduce collection time by 75% while maintaining similar scan clarity. Trying to compare similar systems, the LMS-Z210ii requires a hard data connection to a laptop reducing mobility while the VZ-4000 has an integrated touch screen eliminating the mobility issue. Additionally, the LMS-Z210ii requires tie points to fuse the individual scans together while the VZ-4000 has an on-board GPS eliminating the need for tie points. The current state of the practice regarding LiDAR only shows that with the ever advancing field of technology will continue to shrink the gap between research grade and practical application.

The VZ-4000 has an associated capital cost of around $150,000. Since the equipment is in current uses by numerous DOTs as an inventory and surveying tool the trained individuals are already in place within the agencies to operate the unit. Additionally, the movement to mobile LiDAR platforms is already occurring. Private consulting firms nation-wide have begun to notice the potential and mobile LiDAR units traveling at slower than highway speeds are currently being deployed, such as the Optech Lynx Mobile Mapper and the Ambercore TITAN Mobile Laser Scanning System.

ULTRA WIDE BAND IMAGING RADAR SYSTEM (UWBIRS)

To assess the utility of UWBIRS, a demonstration of synthetic aperture radar, measurements to sense the interior of concrete bridge component structures and identify potential structural defects such as delaminations, two types of imaging radar measurements were collected at the test sites. In the 2D imaging modality, the radar sensor obliquely illuminated the bridge deck surface as it was moved along a linear path parallel to the deck surface. This type of data collect produces a 2D map of the radar reflectivity of the deck, which may indicate areas of internal defect and/or delamination. This type of collection is consistent with a concept of operation that has a radar system mounted on a moving vehicle to produce maps of deck radar reflectivity that identify areas of concern. This type of collection could also be performed by a standoff airborne sensor.

In the 3D imaging modality, the radar illuminates the bridge at a normal angle of incidence, and the radar is scanned over a two dimensional plane parallel to the bridge structure under test. Data from this form of collection can be used to produce a three dimensional map of the radar reflectivity, which may indicate areas of internal defect. This type of data collection is consistent with a concept of operation that uses the radar system to make a detailed internal survey of a suspect area.

A portable UWBIRS was developed at MTRI to emulate the performance of commercial radar sensors for the field demonstrations. The radar system consists of a commercially available AKELA RF Vector Signal Generator and Measurement Unit (AVMU), connected to a pair of wideband exponential taper horns. The AVMU operates in a stepped frequency continuous wave (SFCW) mode, with pulse modulation to bind the time delays over which data are collected. The AVWU collects data over 387.5 MHz to 3,000 MHz, with a nominal output power of 17 dBm. The 1.1 lb unit can operate using portable power sources. The radar is controlled using a laptop computer, and all of the instrument's operating parameters are under user control via a graphical user interface. As discussed below, the radar system was deployed on a portable, reconfigurable translation fixture to collect frequency diverse data as the radar sensor was scanned in one and two spatial dimensions at the field demonstrations.

A 2D radar data collection refers to a measurement where the radar collects electromagnetic backscattering measurements over a range of radio frequencies as the radar is moved linearly along one spatial dimension. The resulting data set is a two dimensional array of scene backscattering measurements as a function of frequency and sensor location.

To collect 2D radar data an apparatus was constructed at MTRI which moves the radar antenna along one dimension, parallel to the object being measured. This system is made using aluminum framing and an electric motor drive system for consistent sensor motion. The rail along which the radar antenna is translated allows for approximately 2.8 m of sensor motion, which is only limited by the current size of the side support rails and motor drive mechanism (see Figure 43).

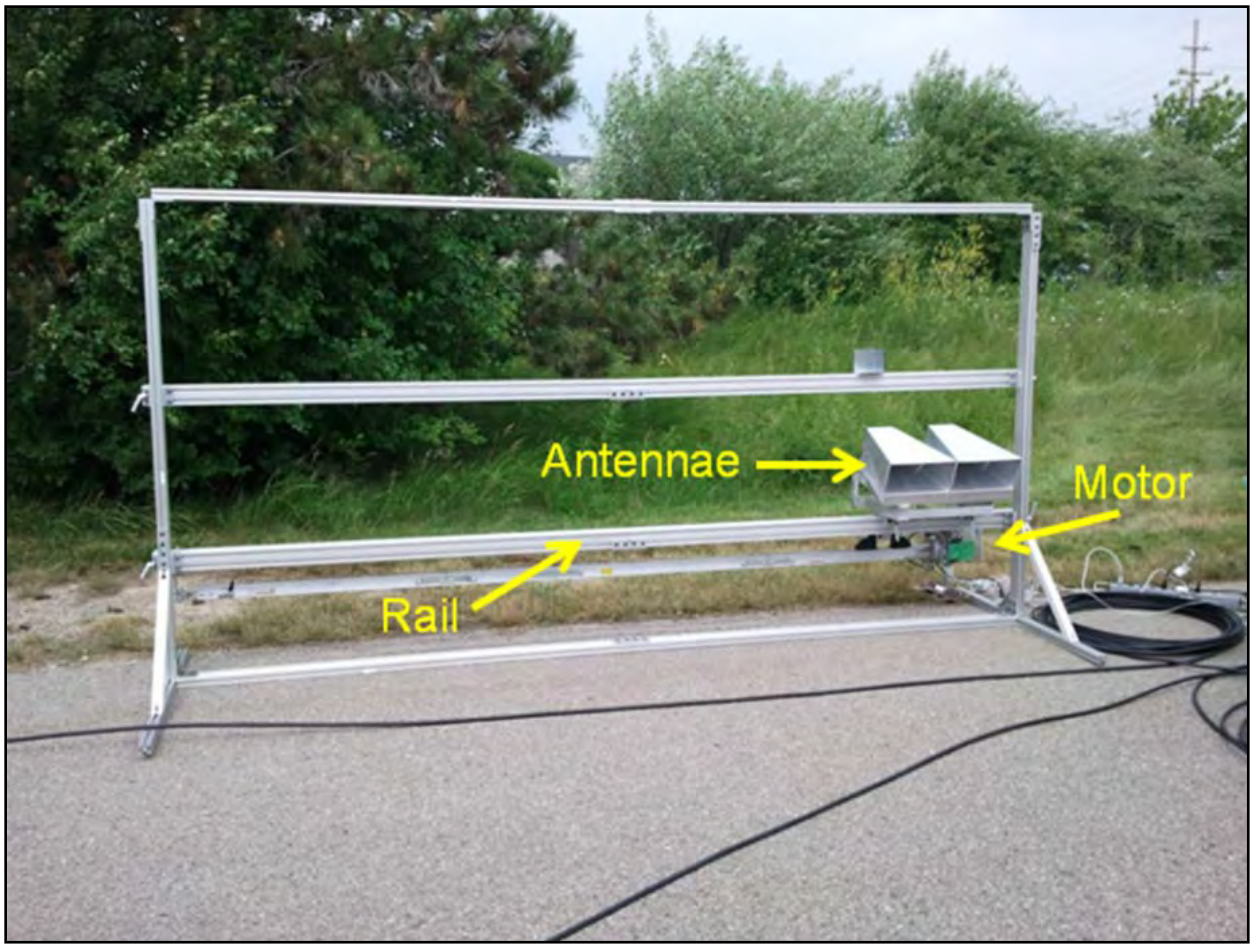

Figure 43: 2D Radar translator apparatus.

An optical position encoder is attached to the motor to record antenna along-track positions at the start of each radar frequency sweep. The operating parameters of the radar AVMU are configured to illuminate a constrained area of the scene to be imaged via appropriate time gating, and to have the appropriate settings for the particular measurement (e.g., frequency span, gain, etc.). In operation, the radar sweeps frequency and collects scene backscattering measurements as the antenna translates down the rail. After the measurement has finished,

the 2D data (e.g. scene backscattering verse frequency and sensor location) are saved and post-processed into imagery and/or other products.

A 3D radar data collection refers to a measurement where the radar collects electromagnetic backscattering measurements over a range of radio frequencies as the radar is moved linearly along two spatial dimensions. The resulting data set is a three dimensional array of scene backscattering measurements as a function of frequency and the sensor position in two spatial dimensions.

The 3D apparatus is identical to the 2D setup, except the side support rails are lengthened allowing for approximately 2.5 m of translation in that dimension (normal to the motorized rail direction). This added length is necessary to achieve roughly equivalent spatial resolution in this dimension as in the along rail dimension. This 2D translation of the radar sensor results in 3D data – frequency and sensor position in two spatial directions corresponding to the two translation directions. In this configuration the motor drive rail system is set at one end of the side support rails, data are collected in the same manner as the 2D scan, and then the drive rail system is repositioned by a specified amount for the next measurement. These data are saved and then post processed into a 3D radar image.

The 3D apparatus can be oriented with the side support rails either vertical, with the antennas pointing horizontally (at various angles), or horizontal, with the antennas pointing either up or down. This allows 3D measurements to be made of vertical structures such as walls, as well as horizontal structures, such as the underside of bridge structures, in order to attempt to evaluate their sub-surface features. In the vertical configuration the translator apparatus moves the antennas in a plane perpendicular to the ground, while in the horizontal configuration, the translator apparatus moves the antennas in a plane parallel to the ground. The horizontal orientation was utilized to make measurements of the underside of the bridge deck. Post processing is identical in either orientation. Figure 44 shows the translator apparatus in the horizontal orientation.

The first set of measurements occurred on the Freer Road bridge. Over the course of three days, 2D bridge deck measurements and 3D measurements of a section of the bridge underside were made using the portable imaging radar system described above.

2D measurements of the entire bridge deck were made by setting up the translator apparatus in its vertical orientation such that the radar antenna would be moved parallel to the direction of travel on the road. A measurement was taken with three fiducial corner reflectors set in the area to be imaged, and then this measurement was repeated with the fiducials removed. The

translator apparatus was then moved 10 ft (~3.05 m) further along the bridge deck and these measurements were repeated. This method of moving the translation apparatus along the road at intervals also served to simulate mounting of the radar to a vehicle and driving in one lane while imaging another.

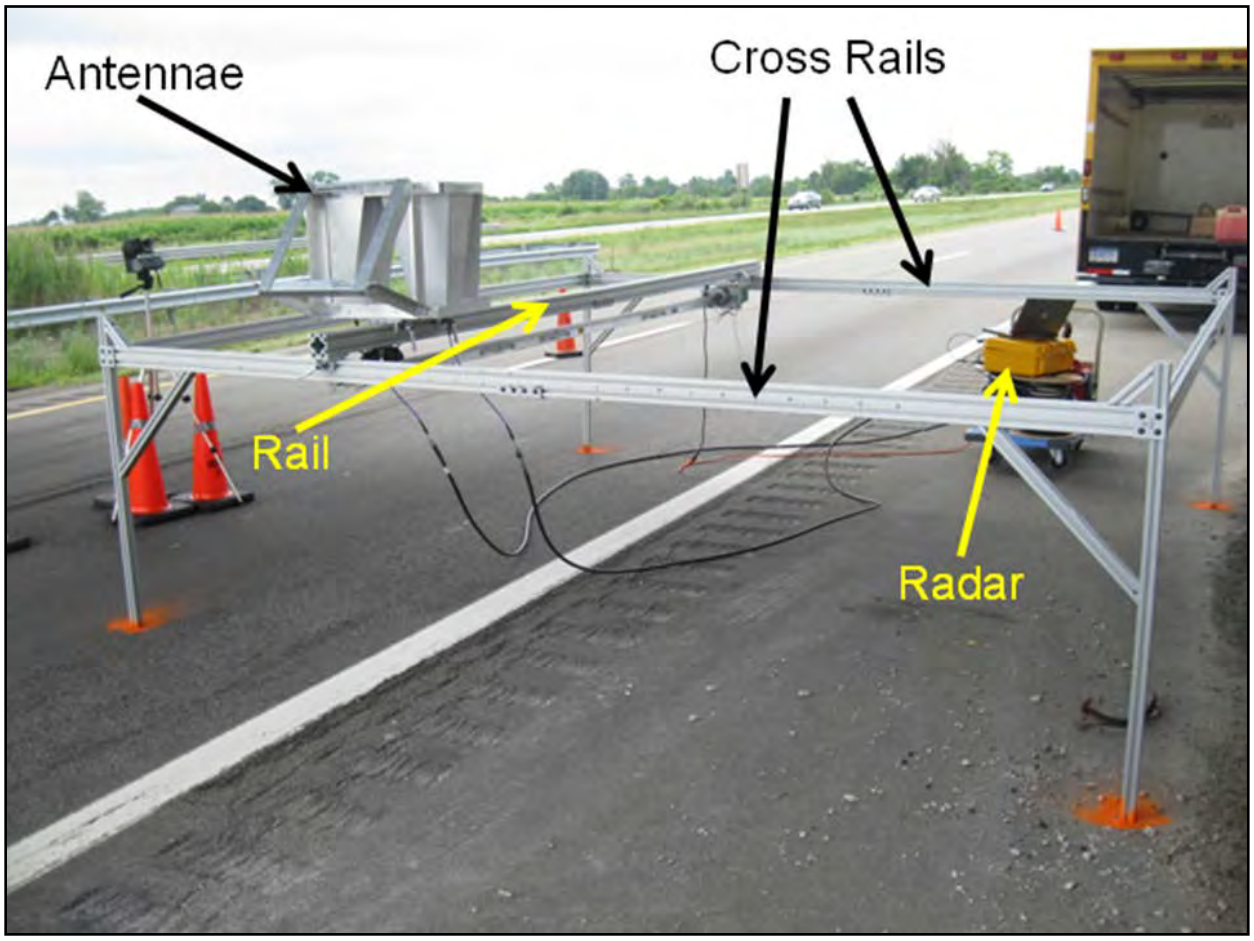

Figure 44: Translator apparatus configured for 3D imaging in horizontal orientation.

The 2 ft (~0.61 m) by 10 ft (~3.05 m) grid system (see Figures 19 and 45) that was laid-out on the bridge deck was useful for it served as a locator by placing one corner of the translator apparatus, as well as the fiducials on grid markings (see ThIR section). Care was also taken to orient the translator along the selected grid line. The selected grid line for the translator apparatus positioning was close to the center of the bridge, but representative of where a vehicle mounted radar antenna would travel. In this way, the individual images taken at each 10 ft interval along the bridge could not only be stitched together, but also features in the resultant images could be registered to locations on the bridge deck. Figure 45 shows a sketch representing the grid markings laid out on the Freer Road bridge.

The translator apparatus was placed and moved along the grid line 'c' with the antennas pointing west at the Freer Road bridge. The radar timing gates were set such the center line of the road all the way to the guard rail barrier was in the scene. The south-most corner of the translator apparatus was placed on successive 10 ft grid markings such that it was moved along the road from south to north. The along-road grids from 0 to 160 were imaged.

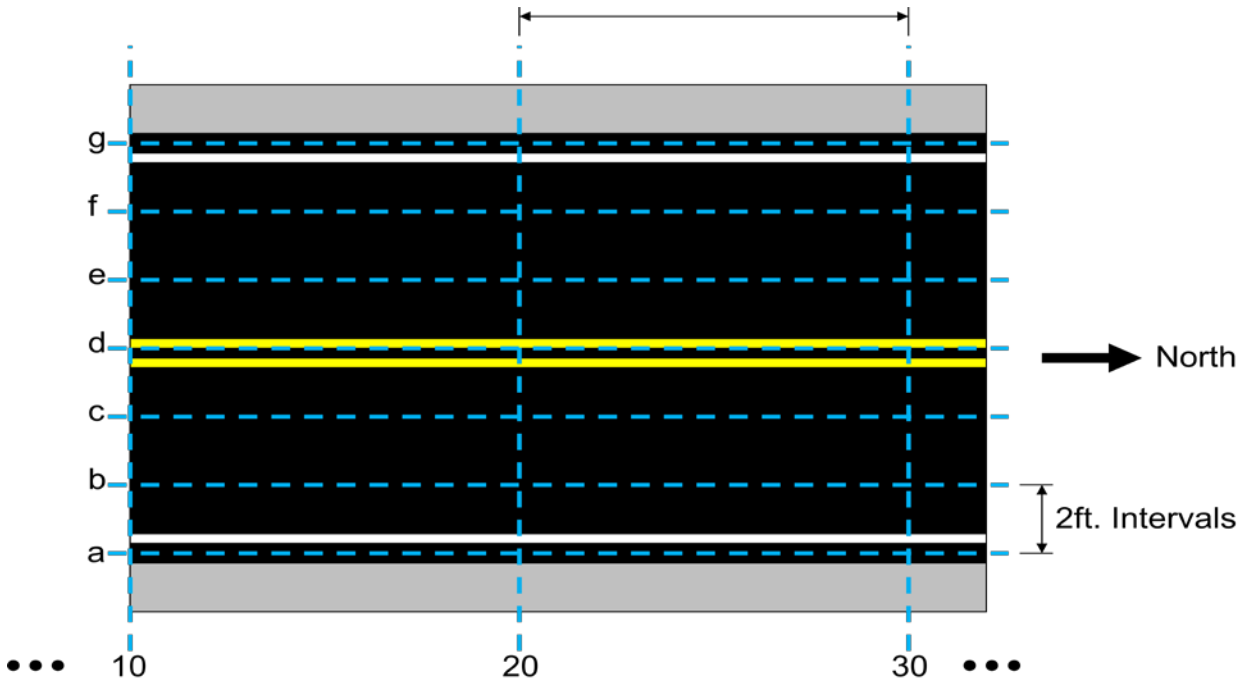

Figure 45: Representation of Freer Road bridge grid markings.

For the collection on August 2nd, two furniture dollies where employed to roll the translator apparatus from one grid mark to the next. Further, the other equipment (radar, cables, generator, and laptop) was placed on a small wheeled cart. In this way the apparatus and equipment could be much more easily moved along the bridge, allowing for more efficient data collection. The translator apparatus with the furniture dollies is shown in Figure 46. It also provided a concept of operation for how such a system could be adapted for use on a moving vehicle, such as DOT data collection vehicle (see Figure 46).

The east half of the Freer Road bridge was imaged. The translator apparatus was moved along the 'e' cross-road grid line from along-road grids 0 to 160. Prior to making the measurements the gate settings from previous day were configured and checked to ensure scene covered the center of the road to the edge with some overlap. The antennas were pointed east and the east (north-bound) lane of the bridge deck was imaged.

3D imaging of a portion of the underside of the Freer Road bridge was undertaken. To accomplish this, the translator apparatus was configured in its extended, horizontal orientation below the bridge with the antennas pointing up at the underside of the bridge. The motorized rail was placed such that it translated the antennas in the cross-road direction (relative to the road on the bridge above). Every effort was made to attempt to keep this direction of travel normal to the along-road direction (relative to the road on the bridge above). The set up of the translator apparatus is shown in Figure 46. Note that the apparatus was set up at the south end of the bridge, extending into right hand, east-bound lane of I-94.

Figure 46: More "mobile" translator apparatus and radar equipment. It is easy to view how such a system could be adapted for use on a moving vehicle.

Prior to commencing measurements, the radar time gating was adjusted such that the nearest part of the underside of bridge was just within scene, and the farthest end of the range gate was set to be approximately 5.8 m farther down-range.

Beginning with the motorized rail at the position furthest from the bridge supporting structure, a measurement was made by translating the antennas along the rail. The motorized rail was then successively moved by 2 cm closer to the bridge support structure and measurements made each time. Unfortunately, rain on the morning of August 3rd delayed the beginning of the measurements until approximately 11 am. Since the road closure on I-94 had to be removed by 2 pm, the apparatus had to be disassembled beginning at 1:30 pm. Therefore, only a partial data set was collected.

Radar measurements were collected at the Willow Road bridge. Over the course of two days, 2D bridge deck measurements and 3D measurements of a section of the bridge underside were made using the portable imaging radar system described above.

2D radar measurements were collected over the entire Willow Road bridge deck. The translator apparatus was moved along the 'b' cross-road grid line from along-road grids 0 to 220 with the antennas pointed to the north and along the 'd' cross-road grid line from 220 back to 0 with the antennas pointed to the south. Prior to making the measurements the gate settings were configured and checked to ensure the scene covered the center of the road to the edge with some overlap. As before, images were made at each position with, and without, fiducials in order to aid in image registration.

3D radar measurements of a portion of the underside of the Willow Road bridge were collected. To accomplish this, the translator apparatus was configured in its extended, horizontal orientation below the bridge with the antennas pointing up at the underside of the bridge. The motorized rail was placed such that it translated the antennas in the cross-road direction (relative to the road on the overpass above). Every effort was made to attempt to keep this direction of travel normal to the along-road direction (relative to the road on the overpass above). Note that the apparatus was set up at the west-end of the bridge, extending into the right-hand, south-bound lane of US-23. Figure 47 shows the geometric orientation of the translator apparatus relative to the bridge support structure.

Prior to commencing measurements, the radar time gating was adjusted such that the nearest part of the underside of bridge was just within scene, and the farthest end of the range gate was set to be approximately 5.8 m farther downrange.

Beginning with the motorized rail at the position furthest from the bridge supporting structure, a measurement was made by translating the antennas along the rail. The motorized rail was then successively moved by 2 cm closer to the bridge support structure and measurements made each time. A complete 3D set of measurements was taken within the 9 am to 4 pm road

closure constraints. The portable system was also deployed at the Mannsiding Road bridge. However, equipment malfunctions prevented collection of any useable radar data during the scheduled lane closures.

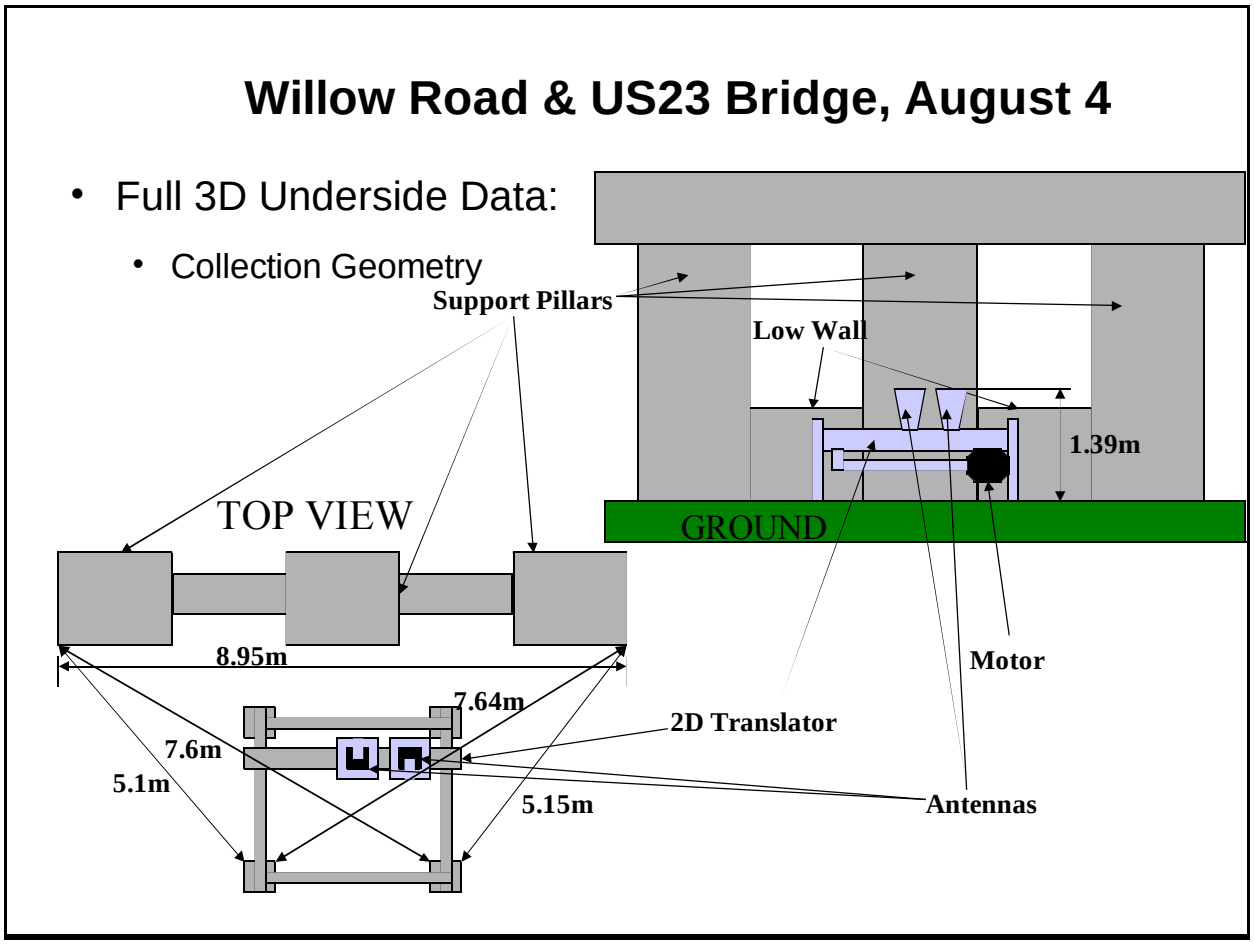

Figure 47: Geometric orientation of translator apparatus for Willow Road bridge structure.

The scene backscattering measurements collected as a function of frequency and sensor location can be processed into spatial maps (images) of radar reflectivity using back-projection or range migration algorithms. Range migration algorithms were selected for the initial processing since they are computationally more efficient than the back-projection approach.

Two dimension radar measurements of the scene, specifically radar backscattering measurements as a function of frequency and radar sensor location along a straight line can be processed into a 2D map of radar reflectivity using the 2D Range Migration Algorithm (2DRMA). The algorithm is outlined in Figure 48 and derivation is given in Carrara, et al. (1995).

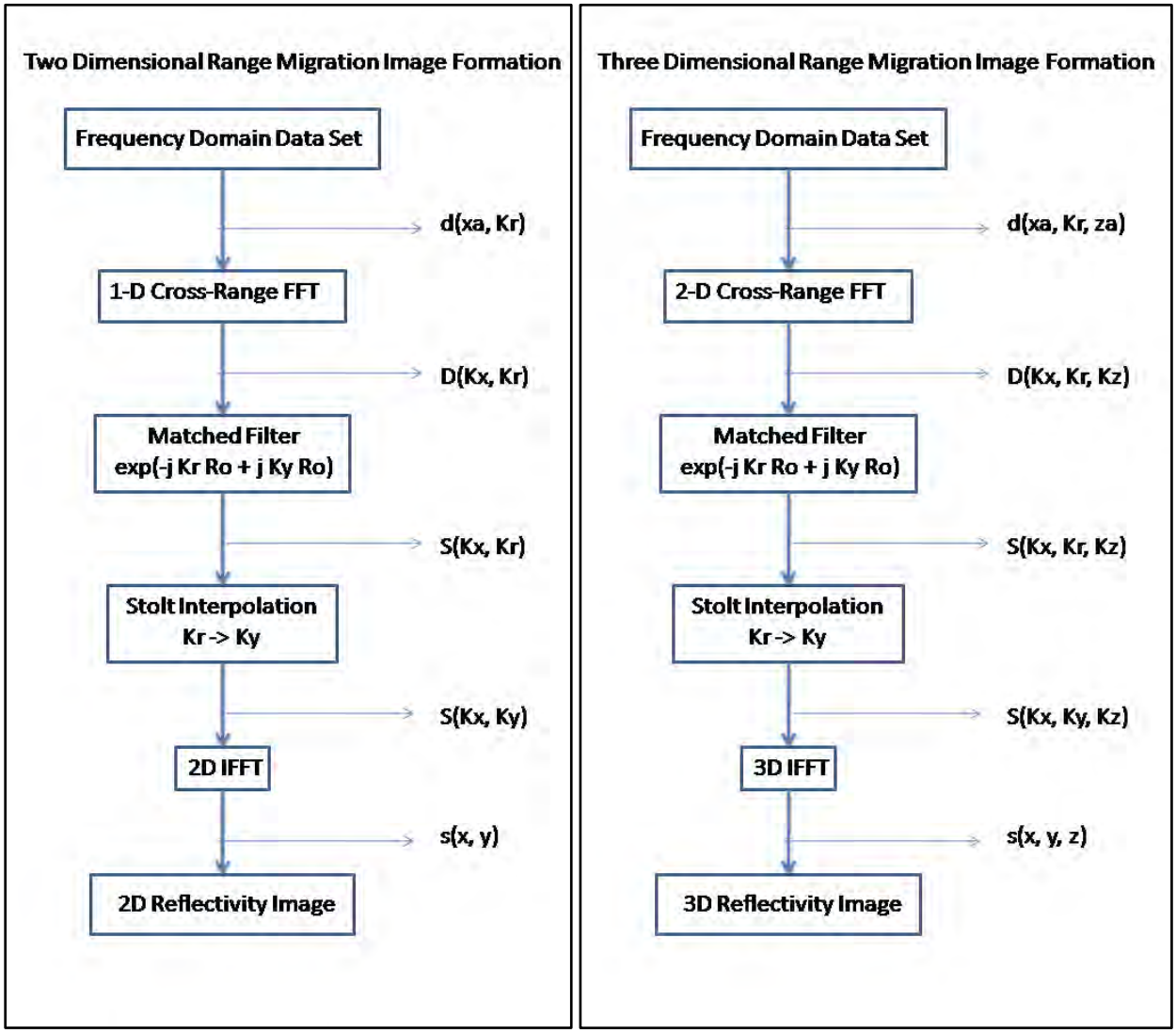

Figures 48 & 49: 2D and 3D range migration image formation algorithm.

Given the radar measurements as a function of position and frequency, the Fourier transform of the data is taken along position, and are multiplied by a matched filter. The resulting data are interpolated in the frequency direction to form an estimate of the image spectrum that is uniformly sampled in spatial frequency space. The 2D Fourier transform is then taken to produce a 2D reflectivity map of the scene. The 2DRMA algorithm has been implemented in MATLAB by the project team, and functioning of the code has been verified both using simulated sensor data and actual radar measurements of test arrays.

3D radar measurements of the scene, specifically radar backscattering measurements as a function of frequency and sensor location scanned over a 2D plane can be processed into a 3D

map of radar reflectivity using the 3D Range Migration Algorithm (3DRMA). The algorithm is outlined in Figure 49 and derivation is given in in Lopez-Sanchez and Fortuny-Guasch (2000).

The algorithm is very similar to the 2D approach. Given the radar measurements as a function of 2D position and frequency, a 2D Fourier transform of the data is taken along the two position directions, and are multiplied by a matched filter. The resulting data are interpolated in the frequency direction to form an estimate of the image spectrum that is uniformly sampled in spatial frequency space. The 3D Fourier transform is then taken to produce a 3D reflectivity map of the scene. The 3DRMA algorithm has been implemented in MATLAB, and functioning of the code has been verified both using simulated sensor data.

Data from the 2D and 3D radar data collections from Freer and Willow Road bridges, have been processed using the algorithms described earlier. The 2D radar measurements of the bridge deck have been processed into radar reflectivity maps of the bridge deck. Analysis of the 3D radar measurements of the bridge substructure is in progress.

2D radar reflectively maps (images) were produced using the range migration algorithm. Data from each of the translation stage measurements were combined, and the resulting single data file was processed as if the data came from a radar sensor on a moving vehicle. Images of the two lanes of the Willow Road bridge deck when calibration reflectors were placed in the scene are shown in Figure 8. The figure shows the Willow Road deck geometry, with potential delamination sites from the ground truth survey, to the left. It is these types of analyzed radar results that the project team plans to integrate into the DSS to show where radar has detected these likely delamination results, as well as the locations and percent of delamination. These data will contribute to the overall bridge health signature being developed for this project.

The 2D radar reflectivity map on a 35 dB color scale in the center, and the amp with the delamination site superimposed to the right. These images were generated from radar backscattering measurements spanning the full 750-to-3,000 MHz frequency range. The point-like returns in the images are the localized returns from the calibration reflectors. The point-like response of the calibration reflectors in the images verify that the collected data have been successfully processed into imagery. The variable, distributed returns are the returns from the deck subsurface (see Figure 50).

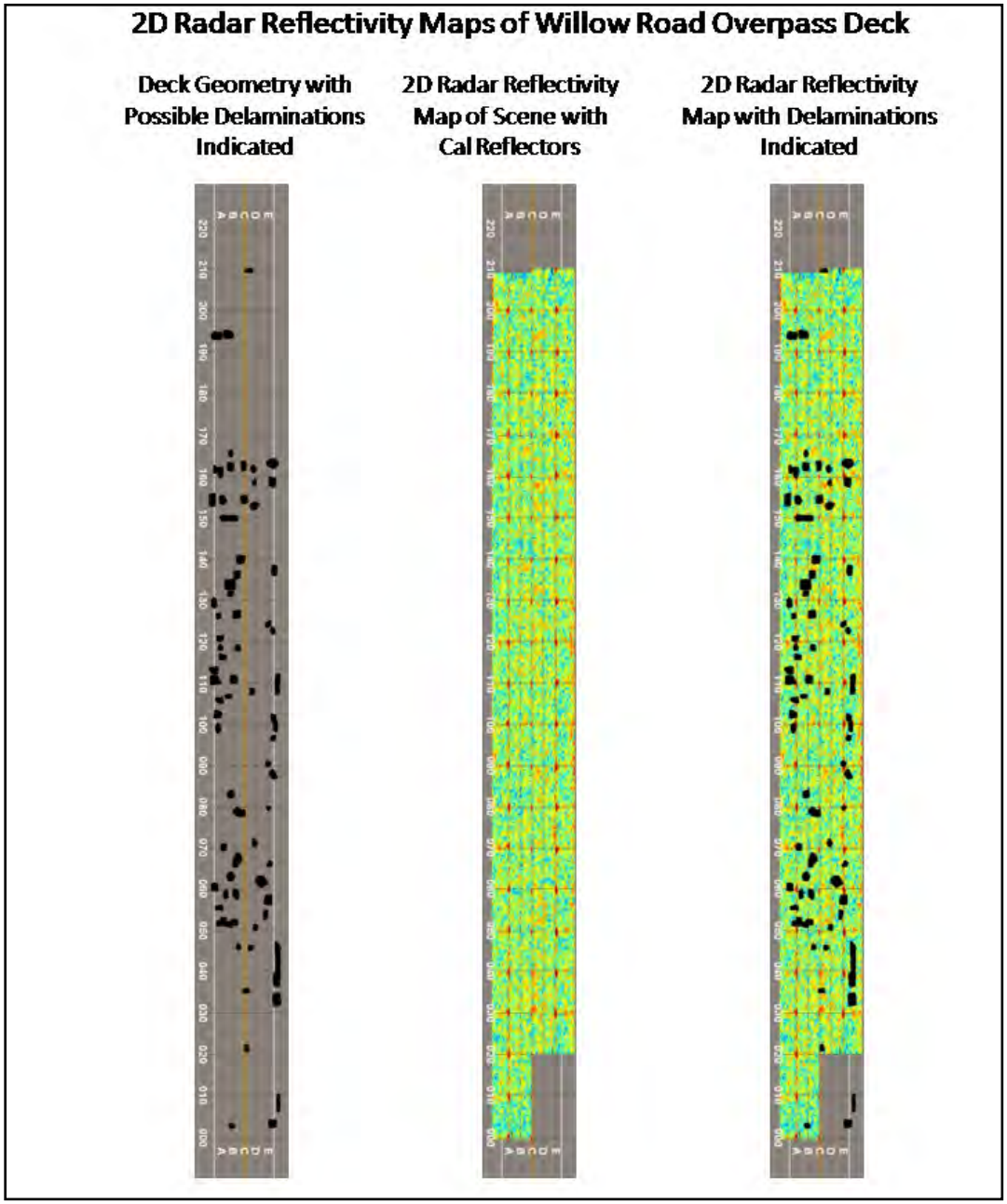

Figure 50: 2D radar reflectivity maps of the Willow Road bridge deck with calibration reflectors. These results are examples of what will be integrated into the DSS, such as locations and amounts of likely delaminations.

Images of the two lanes of the deck without calibration reflectors are shown in Figure 51. These images show just the returns from the deck. In upcoming work, these images will be quantitatively compared with the ground truth data to see if the variations in the distributed

radar returns can be correlated with suspected areas of delamination. 2D radar reflectively maps (images) were also produced from data collected at the Freer Road bridge with the same process used for the Willow Road bridge data. However, an initial assess of the result suggest that collected data were of poorer quality, and the data are currently being reprocessed to try to improve the resulting imagery.

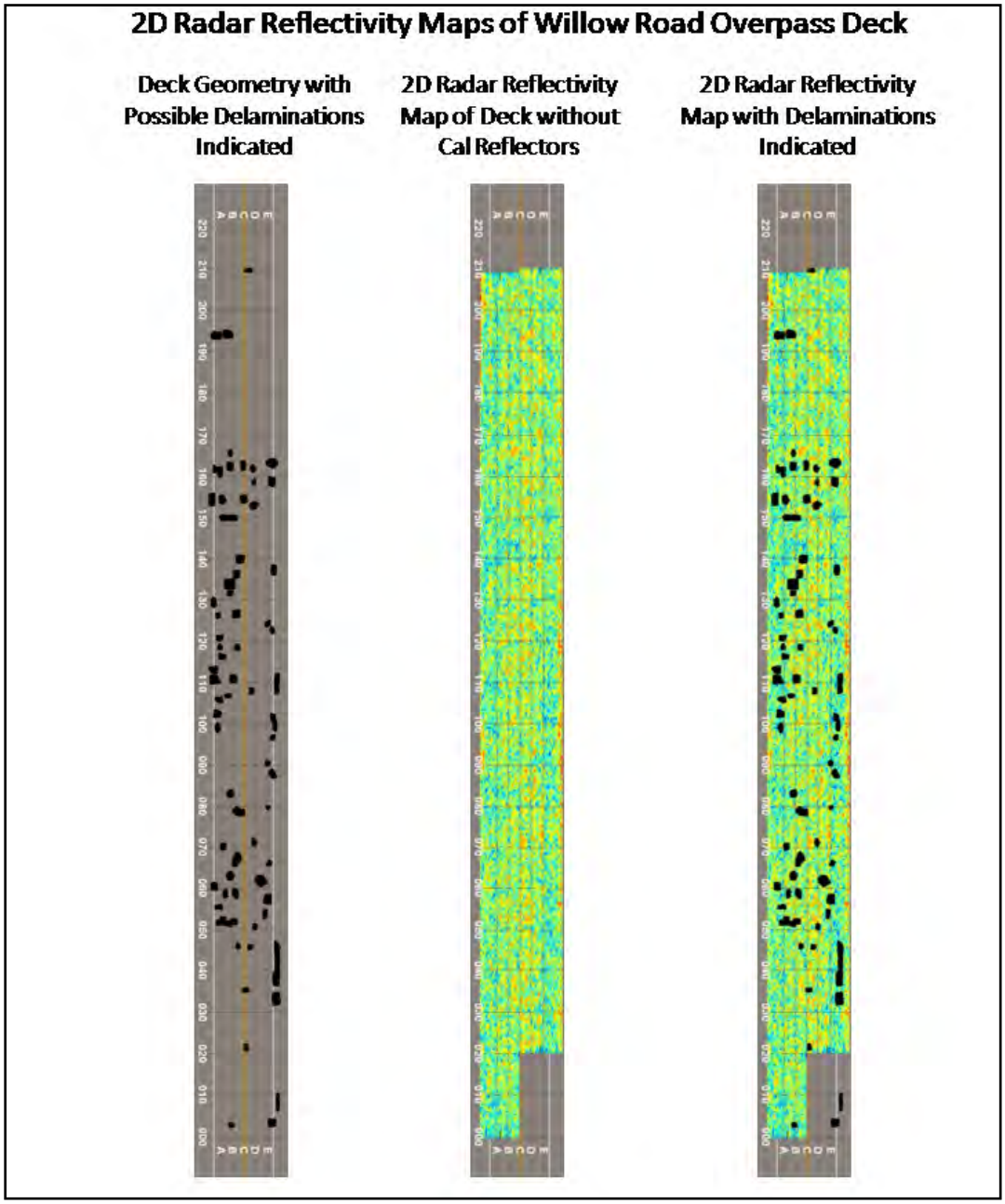

Figure 51: 2D radar reflectivity maps of the Willow Road bridge deck without calibration reflectors.

Benefits, Limitations, and Next Steps

2D and 3D radar measurements of concrete bridge deck and substructure were collected during the field demonstrations at Freer Road and Willow Road bridges using a portable UWBIRS. The data collected at Willow Road bridge were of higher quality and than that collected at Freer Road bridge; thus, the Willow Road bridge data have been processed into 2D imagery. The Freer Road bridge analysis is continuing in the next quarter. Data were not collected at Mannsiding Road bridge due to hardware problems.

Software has been developed to produce both radar reflectivity maps from both 2D and 3D radar data collections. The implementation of the software has been validated on both simulated data and test target measurements.

The primary benefit at this point in the data analysis is that the 2D radar reflectivity maps generated from data collected at Willow Road bridge show variation in intensity potentially due to bridge deck internal structure and/or defects. The team's next step will be to complete the upcoming work on quantitatively comparing the radar reflectivity maps to the ground truth information gathered during the field demonstrations, in order to evaluate the utility of the radar data and system for deck condition assessment The team also plans to investigate the use of alternate imaging parameters and/or post-processing to enhance measurement performance.

The primary limitation at this point is that the overall system would need continued development in order to become a commercially available setup for DOTs and bridge inspectors. Additional work on making a vehicle mounted 2D system would be needed and such a system would have to be developed in a future stage of a bridge condition-related project. Additionally, MTRI is continuing to develop software-based algorithms to analyze and compare the data to ground truth. The team anticipates moving the analysis software tools forward significantly during the next quarter to complete production of results useful for the DSS and the overall bridge health signature.

ADDITIONAL TECHNOLOGIES UNDER EVALUATION

In addition to the primary technologies described above, there are four additional technological applications of remote sensing that continue to undergo evaluation as part of the study. These are technologies that are not tied to the same locations and field time limits as the field demonstrations due to the inherent capabilities of the remote sensing technologies themselves,

so have not been further detailed in this technical memorandum which is focused on the field demonstration results. While the evaluation process of these technologies was not a focus during the field demonstration, a more detailed effort will be the focus of the end of this quarter and the beginning of the next so their capabilities can be documented for USDOT-RITA. They are briefly reviewed here. The technologies and their applications are:

- Using Synthetic Aperture Radar (SAR) speckle to assess bridge deck condition and also to image the interior of a box-beam.
- Using Interferometric Synthetic Aperture Radar (InSAR) to assess bridge settlement.
- Using Multispectral Satellite Imagery (MSI) to assess bridge deck condition.

Synthetic Aperture Radar (SAR)

In the Transportation Applications of Restricted Use Technology (TARUT) study (see <http://www.tarut.org/>), C. Roussi, R. Shuchman, and C. Brooks from MTRI published a method to use complex InSAR data from the commercial Intermap corporation to assess road condition via remote sensing (Brooks et al. 2007). The Intermap corporation's InSAR data collection platform is airplane based, giving the potential to assess large number of bridges with a single data collection. To build from the TARUT study methods, the remote sensing team has obtained the necessary InSAR data for the field demonstration bridges so that they can compare their SAR speckle-based technique to the field data and MDOT inspection results, providing critical ground truth. Previously, using SAR speckle retrieved higher-resolution road condition results than traditional methods such as the International Roughness Index (IRI) or the Pavement Surface and Evaluation Rating (PASER) system. With the necessary data now in hand, the analysis of this information is currently underway to derive a bridge deck surface condition indicator that can be rapidly derived for multiple bridges.

To assess the utility of radar to image the interior of concrete box-beam, radar measurements of a box-beam salvaged from a recent bridge demolition were collected in September, 2011 at the Oakland County Road Commission facility in Waterford, Michigan. This works builds from the UWBIRS being tested for this project, and adds value to by reusing technology developed for assessing other parts of bridge structures. The collected data will be processed into a 3D map of radar reflectivity, which will be compared to knowledge of standard beam construction to determine if the interior structure and/or defects can be observed.

The measurement setup is shown in Figure 52, along with a side view of the salvaged box-beam. The portable aluminum frame used to scan the radar antenna over a 2D plane (horizontal and

vertical to the ground) parallel to the side surface of the beam is shown in the figure in the position used to image the beam.

The data were collected using the same hardware and setup in the UWBIRS described earlier in the document. The analysis of the radar data collected in September, 2011 and the resulting 3D radar imagery are currently under evaluation to extract box-beam condition information.

Figure 52: Portable UWBIRS mounted on a 2D translation stage parallel to side of salvaged concrete box-beam at Oakland County Road Commission site in Waterford, MI.

Interferometric Synthetic Aperture Radar (InSAR)

The MTRI remote sensing team is currently investigating the feasibility of using two-pass SAR interferometry to detect bridge deck settlement (i.e., centimeter-level elevation changes). Recent work has indicated that interferometric radar holds promise for being able to measure settlement for features as small as buildings and bridges (Pieraccini et al. 2008 and 2000). Thanks to the TAC, the team has identified three bridge locations (two in Colorado and one in Michigan) for which degree and timing of changes in bridge elevation are known, and are using

before- and after-settlement ERS-2 SAR images to evaluate if those changes can be accurately detected. ITT Visual Information Solutions ENVI SARscape Interferometry Module is being used to conduct the analysis. Results from this analysis are expected during the next quarter.

Multispectral Satellite Imagery (MSI)

Another TARUT study method that showed promise was using high-resolution multispectral remote sensing data from satellites and aerial systems to rapidly assess road condition. These methods are being updated by the remote sensing team to see if they can be used on a practical basis to assess bridge deck condition without the need for additional field work. In the TARUT study, the team was able to map road sufficiency rating with 88% accuracy for asphalt roads and 80% accuracy for concrete roads. The primary investigation will be to see if the analysis methods can be applied for features as small as bridges, and if modern high-resolution imagery such as WorldView-2 data can be applied for bridge deck condition assessment. The previous work (Brooks et al. 2007) used a blue imagery band and an infrared imagery band to analyze road condition and these exists in a wide variety of satellite and aerial based imagery collection platforms. Condition results that match available MSI field data will be assessed for inclusion into the DSS.

DECISION SUPPORT SYSTEM (DSS)

This section serves as a detailed review of progress in developing the DSS since the previous quarterly report. Since development began in March, 2011, two data primary bridge data sources, both provided by the project cost-share partner MDOT, have been used in prototyping the bridge condition DSS functionality. One source is the Transportation Management System (TMS) database BRIDGE table export provided by Bob Kelley, TMS database manager at MDOT, which is referred to within the DSS as the “MDOT Bridge Inventory (MDOTBI)” as it contains a unique record with attributes for all 4,405 MDOT-owned bridges. The other source came from Dave Juntunen, MDOT engineer of Bridge Operations, as an Excel-based application for visualizing bridge condition deterioration over time. The table of data that drive the spreadsheet application was imported into the DSS database as the “MDOT Bridge History (MDOTBH)” dataset since it contains non-unique records of bridge condition ratings for each of the MDOT-owned bridges back to circa 2000.

While the MDOTBI (see Table 4) and MDOTBH (see Table 5) tables do not match an existing Pontis bridge inventory database schema, they were the only data then made available earlier this year by MDOT when DSS development began. Nonetheless, the MDOTBI and MDOTBH tables represent two necessary views of important bridge condition data: inventory-level

bridge-to-bridge comparisons of the current infrastructure, and single-bridge condition assessment for individual maintenance decisions. Now that direct read access of MDOT's TMS database has been established, it is apparent that the MDOTBI currently used in the DSS is an export of the TMS database's BRIDGE table with some additional TMS data.

Furthermore, since the fields of the MDOTBI match many of the fields in the BRIDGE table, it should be simple for the DSS team to replace the MDOTBI in the DSS with a proper, Pontis-compliant export from the TMS BRIDGE table. It is important that the underlying database of the DSS be an effective prototype for state transportation agencies throughout the United States. As such, a standard schema is needed or, at the very least, a server framework which emphasizes a standard schema. The Pontis tables from the TMS database appear to the DSS development team to be such a standard. The tables available to the project team in the TMS database are currently being considered for inclusion in the DSS database.

Investigation is ongoing to assess whether or not the TMS database can be directly read by the DSS instead of doing periodic exports of the data from TMS into the DSS. This would substantially reduce the effort to get MDOT data into the DSS and would not require updating as changes to TMS database content would be automatically reflected in DSS queries and visualizations. However, as the TMS database is an Oracle database and the project team does not have an expensive Oracle installation, this may not be possible within this project. In order for the DSS server framework to communicate with the Oracle database it requires certain files which seem to be available only with an Oracle client installation. The free client SQL Developer, which has been used to read the TMS database in a graphical user environment, may not suffice.

Nonetheless, it is possible to easily and rapidly copy TMS database objects to the project team's PostGIS/PostgreSQL database which is used for the DSS. The team's plan is to regularly update the DSS bridge database with queried exports from TMS, and then to clearly label the date of the most recent export to users of the DSS so they will understand how up-to-date the bridge inventory data are that they are using.

The DSS application in the web browser communicates with the server and receives data through various data services. These are resources on the web with an established Uniform Resource Indentifiers (URIs or URLs) at which requests for data are received. The data services corresponding to these various datasets are currently implemented in the Django web framework through a RESTful interface. REST refers to Representational State Transfer, a set of documented principles for web development that require stateless communications between server and client use the Hyper Text Transfer Protocol (HTTP) according to certain conventions. These interfaces are currently configured only for delivering data to the DSS as they emit

compact data in Javascript Object Notation (JSON) tailored for the DSS application. In the near future these services could offer XML in an established standard for sharing such data on the web (such as a Web Feature Service or WFS). In addition to separate web services for inventory metrics and historical data (MDOTBI and MDOTBH data, respectively), a third web service has been implemented for client-side applications requiring a distribution of National Bridge Inventory (NBI) ratings, such as the pie chart showing inventory-wide NBI rating distributions.

Field Name	Description	Field Name	Description
region	MDOT region	subrating	NBI substructure rating
brkey	Pontis bridge ID	culvrating	NBI culvert rating
strc_num	MDOT bridge ID	servtypund	Type of service under bridge
facility	Facility carried	sd_fo	Being determined
featint	Being determined	suff_rate	Sufficiency rating
location	Location	materialmain	Material
latitude	Latitude	designmain	Main design type
longitude	Longitude	lanes	Number of lanes
yearbuilt	Year bridge built	num_spans	Number of spans
yearrecon	Year bridge reconstructed	left_sw_width	Left sidewalk width
yearpntd	Year bridge last painted	right_sw_width	Right sidewalk width
yearovly	Year of last bridge overlay	deck_width	Bridge deck width
compute_0012	Not determined	length	Bridge length
dkrating	NBI deck rating	adttotal	Average daily traffic
suprating	NBI superstructure rating	painttyp_cd	Paint type

Table 4: Field names and descriptions for the MDOT Bridge Inventory table.

Field Name	Description	Field Name	Description
region	MDOT Region	pier_rtg	Pier condition rating
brkey	Pontis bridge ID	culvert_rtg	Culvert condition rating
strc_num	MDOT bridge ID	low_maj_rtg	Lowest major rating
cs_strno	Being determined	superst_rtg	NBI superstructure rating
insp_date	Date of inspection	paint_rtg	Paint condition rating
deck_rtg	NBI deck rating	section_loss	Section loss rating
deck_surf_rtg	Deck surface rating	subst_rtg	NBI substructure rating
deck_bott_rtg	Deck bottom rating	abut_rtg	Abutment condition rating

Table 12: Field names and descriptions for the MDOT Bridge History table.

Recent screenshots of the DSS at its current level of development is shown in Figures 53 through 55. A list of the current features in the DSS:

- Quick links to various MDOT TMS-related websites are available from the top toolbar.
- Tabular data supports multiple column-sorting and -filtering so that complex queries can be constructed within the table. These queries are performed on the server (remote filtering), not merely on the 30 records visible in the table (local filtering).
- The distribution of NBI ratings throughout the inventory or a particular MDOT region can be viewed as an interactive pie chart to be printed or saved to a file with the click of a button.
- The rows of the bridge metrics table can be color-coded by NBI or sufficiency ratings.
- Map markers can be color-coded by NBI or sufficiency ratings. The appropriate will appear based on the symbology.
- The InfoWindow that appears when a bridge's map marker is clicked contains links to automatically zoom to the bridge or launch a directions utility.
- The directions utility provides directions to a bridge from user-specified latitude and longitude coordinates, a street address or an MDOT region office. Turn-by-turn text directions are provided in addition to a route layer on the map.

- Map overlays of MDOT regions and Michigan counties are available.
- Bridges can be spatially filtered by drawing a polygon on the map or by quickly querying the map viewer's current extent.

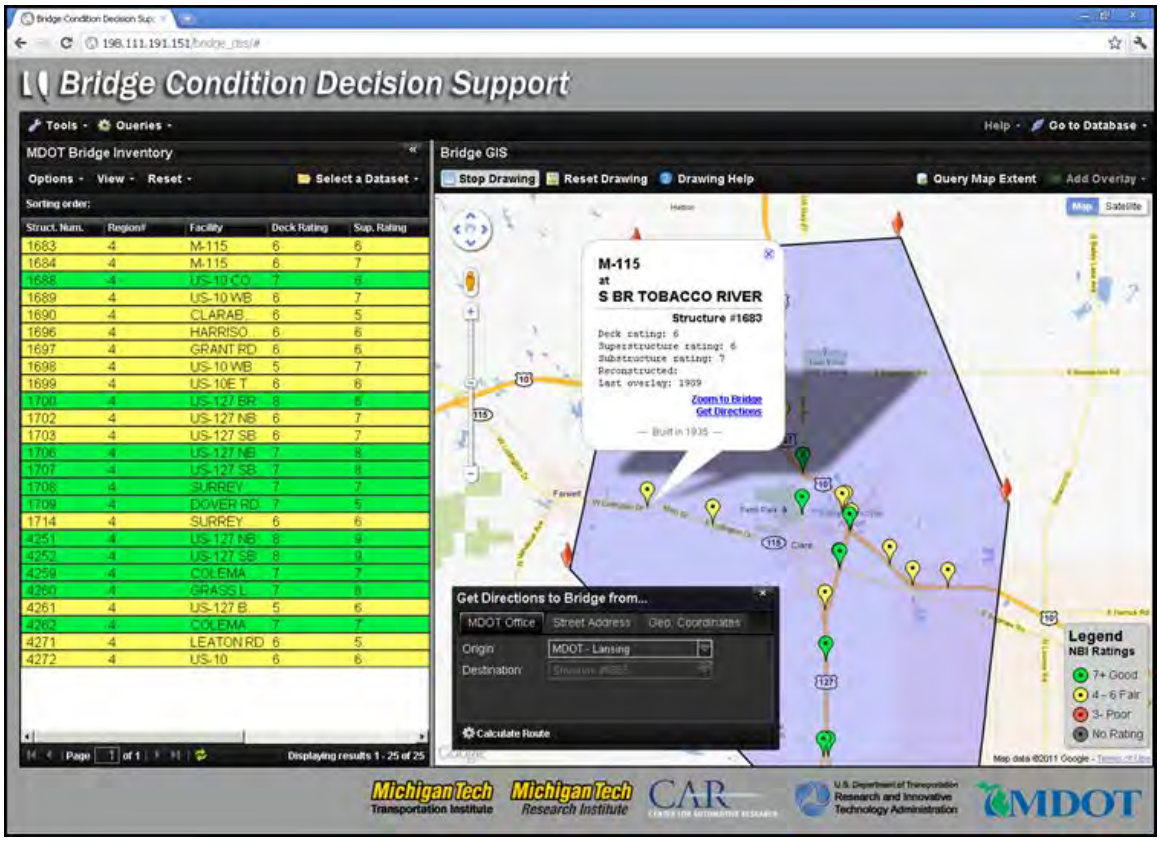

Figure 53: Screenshot of the DSS showcasing several functional elements including table highlighting by NBI rating, map marker coloring by NBI rating, a directions service, InfoWindows for each bridge showing its parameters and links to 'zoom' and 'directions', and spatial filtering on the map by drawing a polygon (shown here in translucent purple).

Some features not yet implemented have been identified and documented in a task-tracking database. These are listed below with some discussion about how each will be implemented over the next quarter:

- In addition to aggregating inventory-wide and by MDOT region, display the distribution of NBI ratings for any Michigan county.
- Link to Street View and the BVRCS results of, or for, a bridge from its InfoWindow.

- Display a detail (summary) view of a bridge's attributes at the bottom of the table when a bridge is selected.
- Showcase bridge photos and recent inspection reports and how they are accessed for the field demonstration set of bridges.
- Allow for charting and plotting of any bridge parameters over time as available in the MDOTBH dataset.
- Allow for parameter (scatter) plots of any two parameters to be displayed.
- Display remote sensing data results in the web browser, such as 3D models of bridges from LiDAR data in the web browser. 3D data will require the use of another software library in the client to support 3D rendering. Ultimately, this feature will most likely launch a separate application, outside of the DSS, to improve its performance.
- Add a utility for visualizing MDOT's strategic goal for bridges. This will require an effective representation of the key elements of this strategic goal within the database; currently, not all required elements are captured in the DSS database.

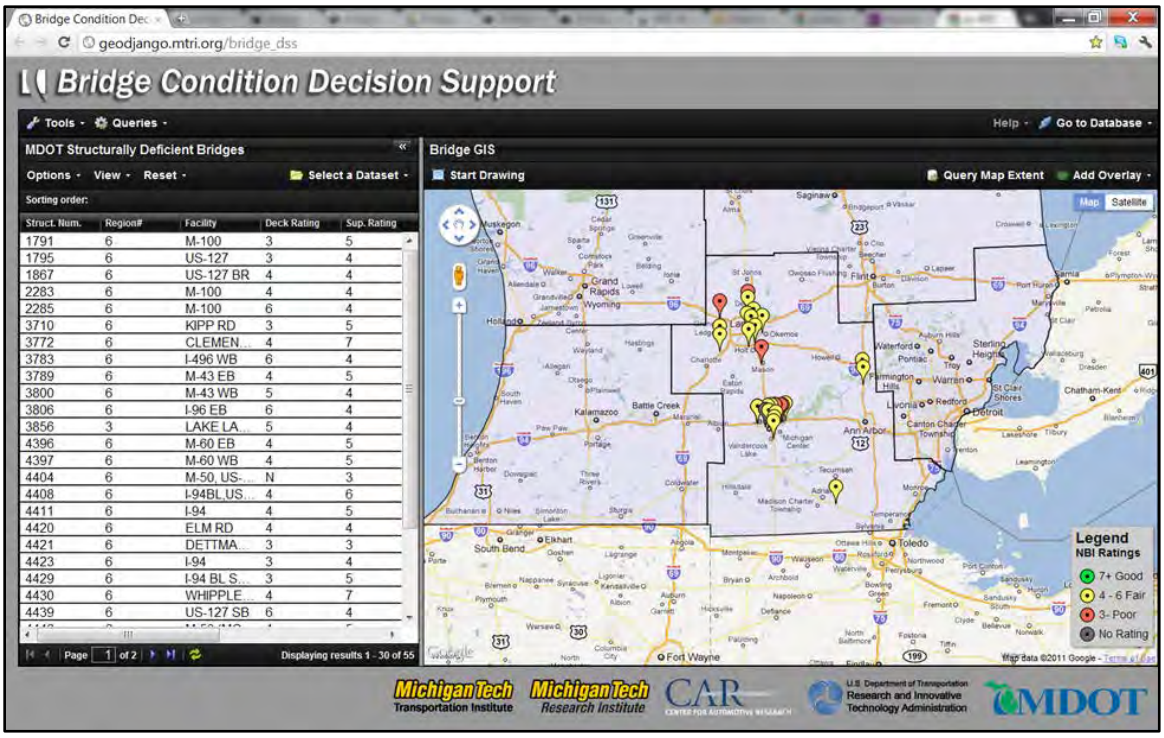

Struct. Num.	Region#	Facility	Deck Rating	Sup. Rating
1791	6	M-100	3	5
1795	6	US-127	3	4
1867	6	US-127 BR	4	4
2283	6	M-100	4	4
2285	6	M-100	6	4
3710	6	KIPP RD	3	5
3772	6	CLEMEN...	4	7
3783	6	I-496 WB	6	4
3789	6	M-43 EB	4	5
3800	6	M-43 WB	5	4
3806	6	I-96 EB	6	4
3856	3	LAKE LA...	5	4
4396	6	M-60 EB	4	5
4397	6	M-60 WB	4	5
4404	6	M-50, US-...	N	3
4408	6	I-94BL,US...	4	6
4411	6	I-94	4	5
4420	6	ELM RD	4	4
4421	6	DETTMA...	3	3
4423	6	I-94	3	4
4429	6	I-94 BL S...	3	5
4430	6	WHIPPLE...	4	7
4439	6	US-127 SB	6	4

Figure 54: Second screenshot of the Bridge Condition DSS, showing the database of only structurally deficient bridges available in a particular MDOT region.

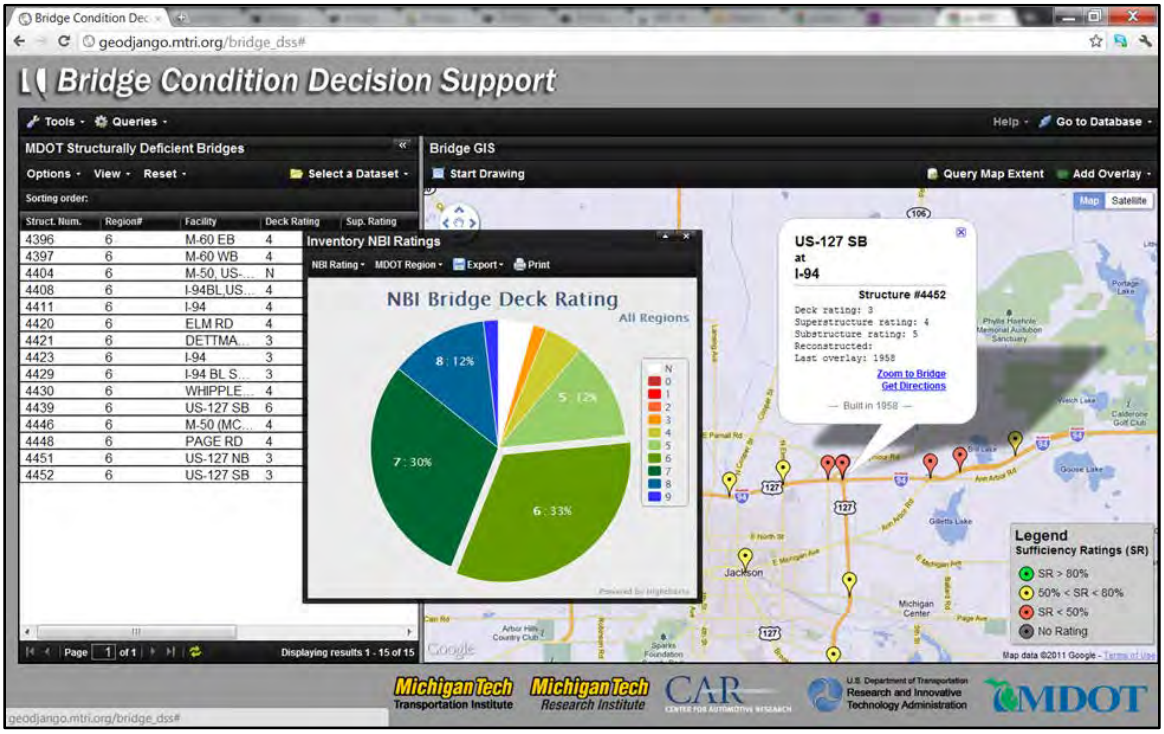

Figure 55: A third screenshot of the current Bridge Condition DSS, showing the DSS's graphping capabilities by displaying NBI bridge deck rating of the structurally deficient bridges selected by the user for Jackson County, Michigan.

Benefits, Limitations, and Next Steps

Of these "next features," the most critical one for development over the remainder of the project is to integrate into the DSS the indicators of bridge condition analyzed and extracted from the various remote sensing technologies deployed in the August, 2011 field demonstrations. From ThIR data, based on results so far, the project team anticipates obtaining percent and amount of delaminated area for all field demonstration bridges. The UWBIRS work also should yield location and amount of delamination. It is encouraging that multiple potential methods could available to a DOT to assess this important bridge condition indicator. The 3DOBS is yielding percent spalled, and volume and location of spalls on the bridge deck by creating a 3D model of the bridge surface using an inexpensive data collection system. DIC can provide the latest information on the loading capacity performance of the structure. The BVRCS and GigaPan are creating a location-tagged high-resolution photo inventory of bridges that can be referenced over time for bridge decks, undersides, and fascia.

LiDAR data is also being used to create a 3D model of the bridge deck surface, calculate volume, location, and amounts of spalls, as well as creating 3D imaging of structural components such as

bridge supports. All of these data have the likelihood of being integrated into an overall bridge health signature, a major goal of this project and a focus area for the remainder of the project. The DSS is intended to provide access to these condition metrics (such as percent spalled or delaminated), representations of the actual remote sensing data (such as a ThIR delamination map or 3D bridge surface), as well as an overall bridge health signature that integrates these remote sensing data, as well as traditional bridge inventory condition data such as recent bridge inspection condition results. This DSS work will continue over the next quarter, but may well require additional time to fully integrate the analyzed remote sensing results once they are all completed, and then to develop logical, easily-understandable ways of representing the data and bridge health signature to DOT users. Fortunately the current DSS level of development provides a strong foundation to make this data representation possible.

This type of DSS development and completion will require interactive TAC, MDOT, and sponsor input and is another reason that additional time may be needed to complete a practical, user-friendly, and easily extendable DSS tool.

REFERENCES

Carrara WG, Goodman RS, Majewski RM (1995), Range Migration Algorithm, Chapter 10 in Spotlight Synthetic Aperture Radar: Signal Processing Algorithms, Artech House, Boston, pp. 401-442.

Lopez-Sanchez, JM, Fortuny-Guasch, J (2000), 3-D Radar Imaging Using Range Migration Techniques, IEEE Trans. Antennas and Propagat., Vol., 48, No. 5, pp. 728-737.

Brooks, C., D. Schaub, B. Thelen, R. Shuchman, R. Powell and E. Keefauver (2007). TARUT pilot studies technical details report. Deliverable 5.3-B. M. D. o. Transportation, Michigan Tech Research Institute.

Pieraccini, M., M. Fratini, F. Parrini, C. Atzeni and G. Bartoli (2008). "Interferometric radar versus accelerometer for dynamic monitoring of large structures: An experimental comparison." NDT & E International 41(4): 258-264.

Pieraccini, M., D. Tarchi, H. Rudolf, D. Leva, G. Luzi, G. Bartoli and C. Atzeni (2000). "Structural static testing by interferometric synthetic radar." NDT & E International 33(8): 565-570.

Memo

To: T. Ahlborn, D. Harris, L. Sutter, R. Shuchman, J. Burns

From: Q. Hong, R. Wallace, C. Brooks, A. Endsley,
M. Forster, M. Birmingham, H. de Melo e Silva

CC: C. Singh

Date: October 13, 2011

Number: 22

Subject: Task 6 – Technical Assessment and Economic Valuation Update

---

Michigan Technological University (MTU) currently is leading an investigation of the utility of using remote-sensing technology for bridge condition assessment. This project, under contract to the USDOT, includes the field testing of several technologies for bridge condition assessment. As part of Task 6 of the study, Michigan Tech Research Institute (MTRI, part of MTU) will perform a technical assessment and evaluation of the bridge condition Decision Support System (DSS) tools and its software and sensor components. The Center for Automotive Research (CAR), a subcontractor to MTU, has the task of conducting an economic evaluation of the cost-effectiveness of a broad deployment of remote sensing techniques for bridge condition assessment. This assessment is designed to provide insights into which techniques tested are good candidates for adoption into standard bridge management practice by state and potentially other department of transportation (DOT). This memo provides an update on the status of DSS tools, software, and sensor components, as well as a description of the team's research findings pertaining to bridge inspection cost data and analysis and a discussion of future activities planned to complete Task 6.

DSS TOOLS, SOFTWARE, AND SENSOR COMPONENTS UPDATE

> *TM-22 is to include the DSS in "discussing technical and economic approach for evaluation of commercial remote sensors for bridge condition assessment".*

The DSS is being developed as a user-friendly, on-line web mapping tool focused on the needs of the bridge assessment community. It has been designed to be able to integrate existing

historical bridge condition data typically collected and used by DOTs, as well as integrate the analyzed remote sensing results from the technology assessments that have been underway to this point. A next focus is to integrate these existing and new data sources into one or more overall bridge health signatures using the DSS. Also upcoming is a version of the DSS that displays clearly in mobile table-computers such as the Apple iPad and others running the Android operating system to make the DSS readily available to bridge inspectors and engineers in the field.

Figure 1 shows an example of the current version of the DSS displaying existing Pontis-style bridge condition data, as shared by the Michigan Department of Transportation (MDOT). In this example, the user has zoomed to an area of interest, drawn a polygon around the area for which they wish to see bridge condition data, and then clicked on a bridge of interest to see its existing bridge data. This capability is new for our primary DOT partner, MDOT. The user can also get directions to the bridge by using the DSS (using the "Get Directions" link seen below), which is a requested feature by MDOT, as bridges can be difficult to navigate to in the field by bridge inspection crews because they do not have traditional street addresses that work in tools such as Google Maps. However, these types of data displays are not the only major focus points of the DSS. Integrating the remote sensing results into the DSS is the next major focus of the DSS development.

Various technologies are described below in the economic evaluation, including 3D Optics, Thermal Infrared, Digital Image Correlation, Radar (including SAR and InSAR), Street View-style Photography in the form of the Bridge Viewer Remote Camera System, GigaPan System, LiDAR, and various forms of satellite imagery and aerial photography analysis. Most of these systems were tested during an intensive summer 2011 field demonstration period, and the data from these field tests are now being analyzed to produce indicators of bridge condition.

Once the analysis of these data is complete, the DSS will be able to display both the remote sensing results and their integration into an overall bridge health signature or set of signatures. It is this integration that will help provide the necessary environment for helping Departments of Transportation understand if the remote sensing technologies can provide the information needed to help advance bridge condition assessment in a cost-effective economic manner. Full use of the DSS to help with technical and economic assessment of the results will be possible once the remote sensing data and interpreted results have been integrated into the DSS, which is a major focus for the next part of the study.

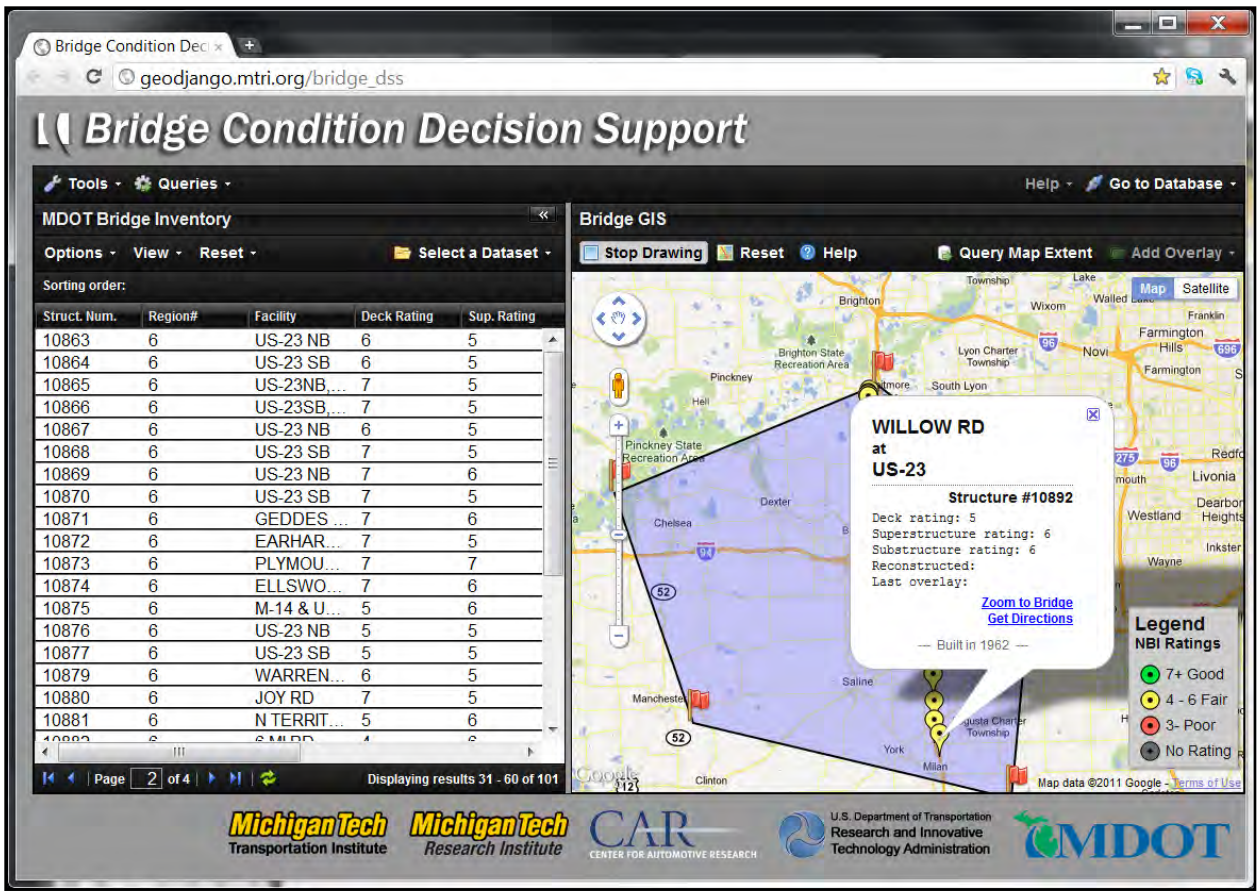

Figure 1: An example screenshot of the current version of the DSS that will be able to display existing Pontis-type bridge condition data (shown) and newer remote sensing-based bridge condition indicators (under development).

ECONOMIC VALUATION OF BRIDGE CONDITION ASSESSMENT USING REMOTE SENSING TECHNOLOGIES

The quality and performance of transportation infrastructure, including highway bridges, are vital to the nation's economy and social well-being. Federal investment in the Highway Bridge Program (HBP) totaled $4.95 billion in 2009, representing 15% of total expenditures of federal funds administered by the Federal Highway Administration (FHWA).[1] Over the past three decades, the HBP (previously the Highway Bridge Replacement & Rehabilitation Program or HBRRP) received more than $81 billion federal funds and the funding level is moving higher (see Figure 2).

[1] USDOT Federal Highway Administration. Highway Statistics 2009, Table FA-3. http://www.fhwa.dot.gov/policyinformation/statistics/2009/

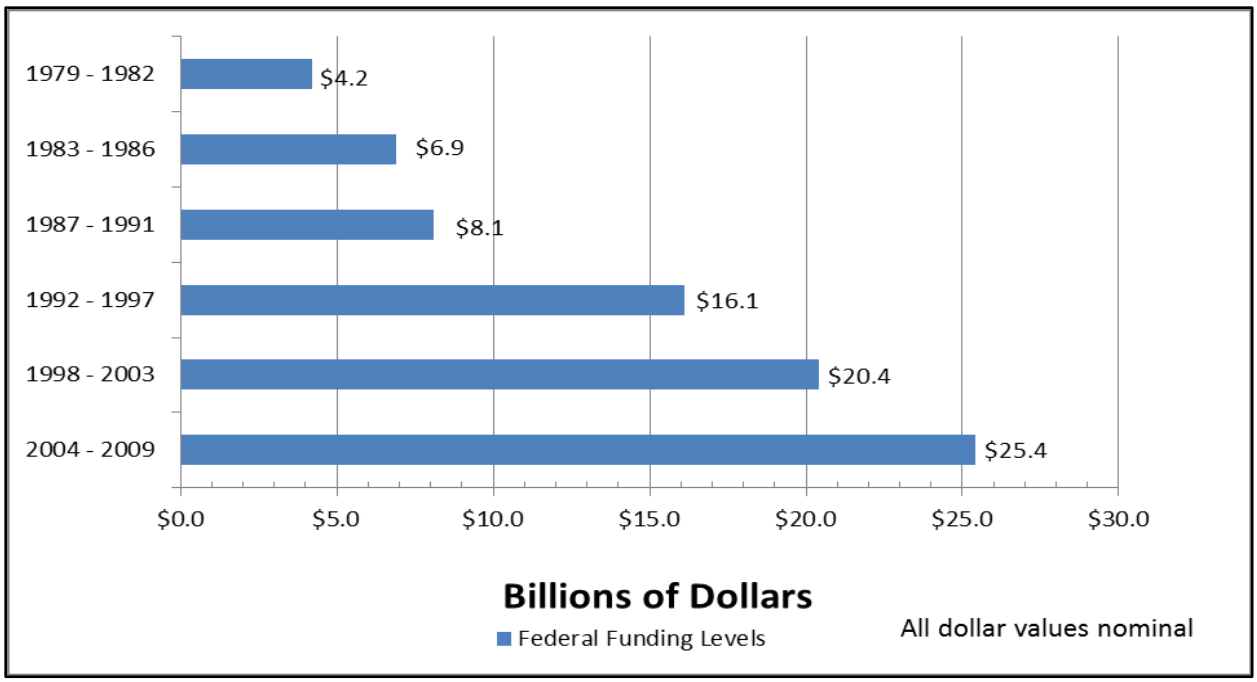

Figure 2: Funding levels of the HBP (1979-2009). Data source: 1979 - 2003 data from Bridge Inspector's Manual; 2004-2009 data from USDOT Office of Highway Policy Information website <http://www.fhwa.dot.gov/policyinformation/statistics.cfm>.

Fiscal sustainability of a national HBP remains a challenge as the Highway Trust Fund (HTF), which funds the HBP and other highway programs, is projected to incur significant deficits in the years ahead. Further, the purchasing power of funding currently available for bridge maintenance, rehabilitation, and replacement is also declining (GAO, 2010).

Addressing the scope of deficient bridges will be a bigger challenge as larger numbers of bridges built after 1950 reach the age at which they are increasingly likely to need to be rehabilitated or replaced; as shown in Figure 3, the correlation between bridge age and condition is strong. About 21% of nation's bridges were built before 1950 or are more than 60 years of age, and more than 40% of these "old" bridges were either structurally deficient or functionally obsolete (see Figure 4). Bridge repair and replacement needs soon will exceed available funding from federal and state sources.

An increasing pressure to increase economic efficiency of expenditures has created the necessity of bridge management systems (BMSs) and effective life-cycle cost management. National Cooperative Highway Research Program (NCHRP) recently conducted a domestic scan focusing on practices among DOTs for identification, prioritization, and execution of programs for management of highway bridges. One of the scan team's key recommendations for bridge management decision-making is to adopt element-level bridge inspection programs and

establish standard condition states, quantities, and recommended actions (i.e., maintenance, preservation, rehabilitation, and replacement) to match the operational characteristics of the agency maintenance and preservation program (TRB, 2009).

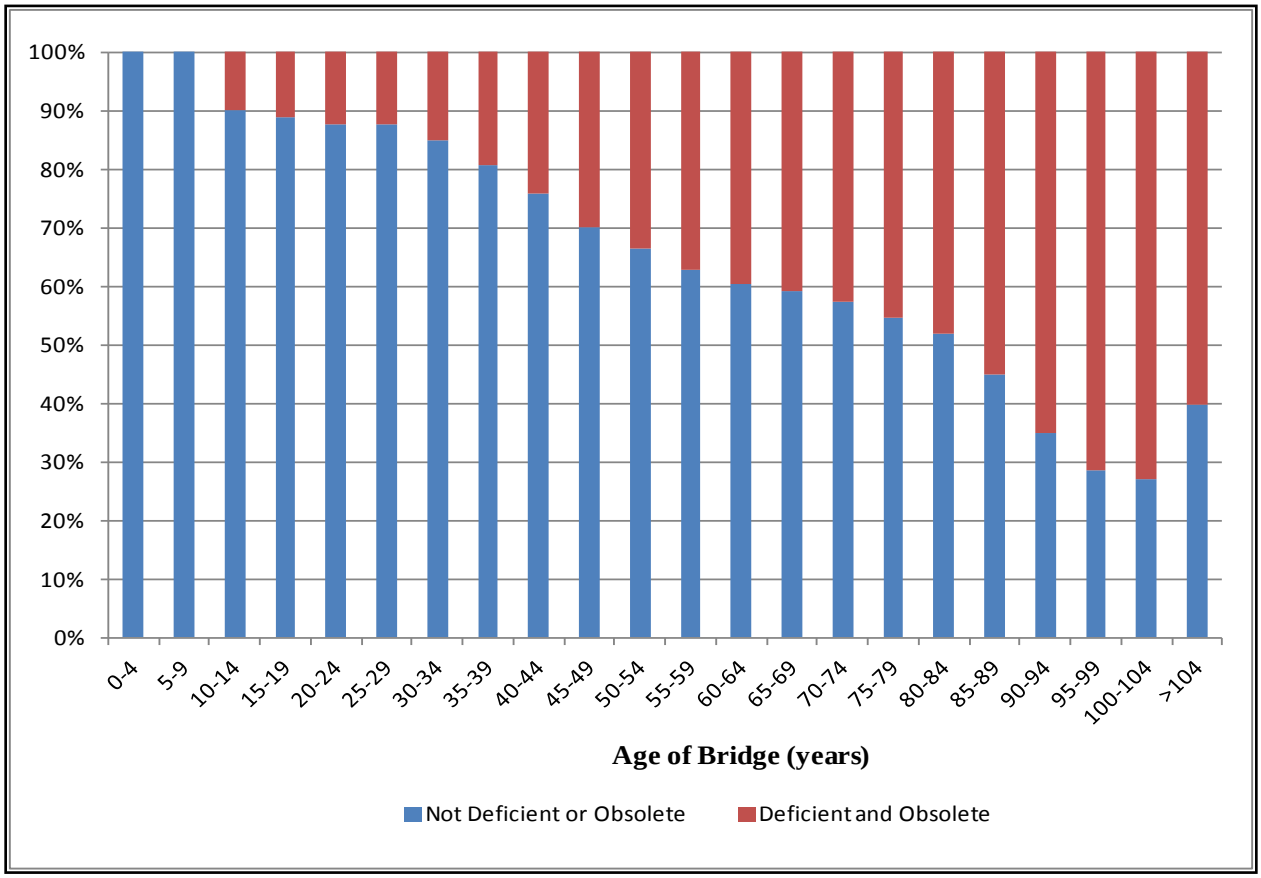

Figure 3: Age of bridge strongly correlated with condition (deficient or not). Data source: 2010 National Bridge Inventory (NBI) data.

Bridge management systems are data-driven and based on a strategic, systematic, and balanced approach to managing bridge preservation and replacement needs. The main components of bridge management are condition assessment, planning, life-cycle analysis, and maintenance management. Bridge inspection data and condition rankings are essential to BMSs to in order optimize the use of available funds and help local, state, and federal agencies make smart maintenance and rehabilitation decisions. Research suggests that preventive maintenance (PM) is a cost-effective way of extending the service of highway bridges. For every dollar spent on the PM program, $4 to $10 was saved in the rehabilitation program (Adams, 2008).

The team's DSS has the goal to take traditional BMS data and making it more valuable and user-friendly through a geospatial web interface that integrates newer remote sensing data. This is intended to enhance the usability of BMS data and advance the technologies that can be displayed through BMS-related decision support interfaces.

Furthermore, a new bridge safety initiative was introduced recently by FHWA to improve bridge inspection and management practices. The new process is based on objective, statistical data, providing for greater consistency in bridge inspections and more strategic approaches to identifying problem areas by using defined criteria for 23 key metrics.[2] Such strategy is in align with the process and basics of a bridge management systems and will improve bridge investment decisions at all levels.

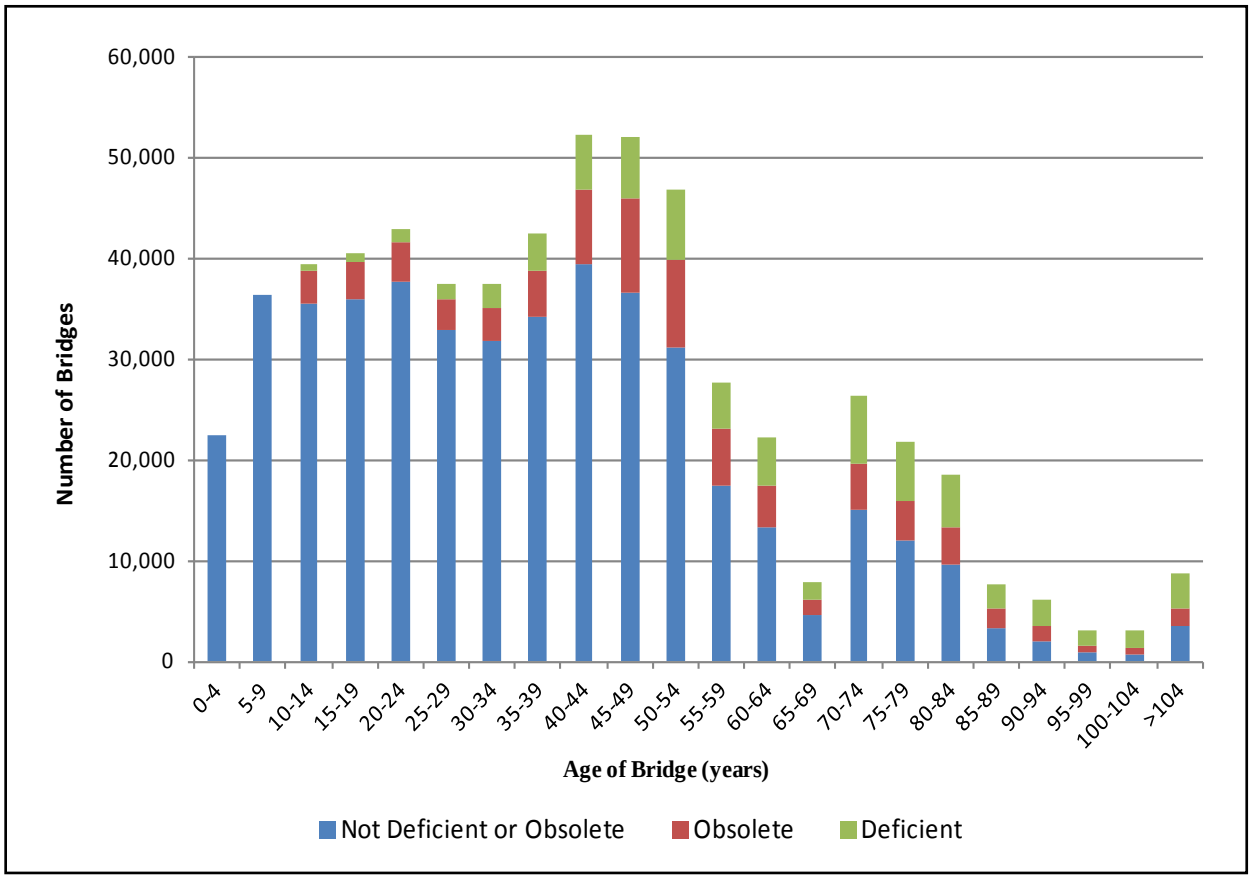

Figure 4: High percentage of older bridges are obsolete or deficient. Data source: 2010 National Bridge Inventory (NBI) data.

[2] USDOT Federal Highway Administration. *FOCUS*. August 2011. Retrieved from http://www.fhwa.dot.gov/publications/focus/index.cfm

OVERVIEW OF CURRENT BRIDGE INSPECTION PRACTICES

U.S. federal regulations define eight types of bridge inspections (routine, fracture-critical, underwater, damage, hands-on, in-depth, initial, and special). Three of these, routine, fracture-critical, and underwater inspection occur at intervals set by regulation (TRB, 2007). In most cases, the National Bridge Inspection Standards (NBIS) suggests a 24-month interval for routine inspections. Some states, such as Minnesota and Ohio, require routine inspection at 12-month intervals. Bridges with condition problems can be inspected on 6-month or even 3-month intervals. The current state of the practice was also reviewed in the team's Deliverable 2-A, available on the project website can be found at <http://www.mtri.org/bridgecondition/doc/State-of-PracticeSHMforBridges(July2010).pdf> (see "Bridge Evaluation Process" section).

Routine inspection is described as “regularly scheduled inspection consisting of observations and/or measurements needed to determine the physical and functional condition of the bridge, to identify any changes from initial or previously recorded conditions, and to ensure that the structure continues to satisfy present service requirements” (see TRB NCHRP SYNTHESIS 375).

All routine bridge inspections, by federal mandate, require rating five major bridge components, including bridge deck, superstructure, substructure, channel and channel protection, and culvert condition. Most transportation agencies and owners go beyond the NBIS and federal mandates to collect more information to support their bridge management program (Alampalli, 2010).

Currently most inspections are visual based, even though non-destructive evaluation (NDE) methods are becoming popular in augmenting the visual inspections and subsequent evaluations advocated. Traditional structural health monitoring techniques include:

- Strain gauges.
- Deflectometers.
- Accelerometers.
- Live load vehicles.
- Hammer-sounding.
- Chain-drag.

U.S. federal regulations identify four staff positions for bridge inspection programs:

- *Program manager:* The individual in charge of bridge inspection, reporting, and inventory.
- *Team leader:* The individual in charge of an inspection team and responsible for planning, performing, and reporting field inspections.
- *Load rater:* The individual with the overall responsibility for bridge load rating.
- *Underwater bridge inspection diver:* Individual(s) performing inspections, by diving, of submerged components of bridges.

State DOTs may use different staff titles for each of the above four positions. For example, Michigan has one state bridge inspection manager, 7 region bridge engineer, 15 bridge inspectors, and 15 inspection assistants.

U.S. federal regulations require training for program managers and inspection team leaders in an FHWA-approved comprehensive course in bridge inspection. Federal regulations do not establish qualifications for inspection team members working under the direction of an inspection team leader (TRB, 2007). In Michigan, professional engineers must complete the National Highway Institute (NHI) two week training class. A non-professional engineer needs 2 years of training in addition to the two week training class. After obtaining 5 years of inspection experience, non-technical inspectors can become an inspection team leader.

Most state DOTs use two-person inspection team, including Michigan. Local agencies and consultants often use single-person teams.

COST ESTIMATES OF CURRENT BRIDGE INSPECTION TECHNIQUES

Estimating bridge inspection costs is a very complicate issue since the data is not readily available in most cases. Agency experience or budgets are the only practical source for costs estimates. As previously discussed, state DOTs are required by federal law to inspect all bridges owned and maintained by the states at least once every 24 months. Most DOTs include regularly scheduled inspections costs in their “normal” or “preventive” maintenance budget since bridge inspection is often part of a DOT’s overall highway maintenance, repair, and traffic operations program (TRB, 2003). The CAR research team used a combined approach, namely through extensive literature review and face-to-face interview with MDOT partners, to establish realistic agency cost estimates of current bridge inspections. The initial findings of the research are presented below.

Inspection Costs by State, County, and City

The average inspection cost per bridge varies significantly from place to place. For example, Connecticut's DOT oversees inspection of about 5,300 highway bridges and 330 railway spans in the state, and spent around $22.9 million on private bridge inspection services and in-house inspection for FY 2010[3]. On average, this translates into an annual inspection cost of $8,135 per bridge in Connecticut (assuming 50% or 2,815 bridges were inspected each year).

In 2008, Wisconsin Legislative Audit Bureau conducted a limited-scope review of WisDOT's bridge inspection program that included FY 2006-07 bridge inspection expenditures by state staff and consultants ($1.31 million and $1.01 million, respectively). There are 5,188 state-owned bridges in Wisconsin and the on-time inspection rate is 98% or 2,542 bridges were actually inspected. As a result, the average inspection cost is $917 per bridge for FY2006 - 07.[4]

State/County/City	Bridge Inspection Cost	# of Bridges Inspected Annually	Period	Annual Inspection Cost Per Bridge	Type of Inspection Services
Connecticut	$22.9 million	2,815	FY2010	$8,135	$15.8M for contractors; $7.1M for in-house
Wisconsin	$2.32 million	2,542	FY 2006-07	$917	$1.01M for contractors; $1.31M for in-house
Armstrong County, Penn	$482,172	34	2010 to 2015	$2,398	Contract service with PennDOT
City of Tulsa, Oklahoma	$98,000	256	2007 - 2008	$383	Contract service
City of Tulsa, Oklahoma	$130,000	256	2005 - 2006	$508	Contract service
Tulsa County, Oklahoma	$70,000	195	2007 - 2008	$359	Contract service
City of Sapulpa, Oklahoma	$4,500	11	2009 - 2010	$409	Contract service
Coal County, Oklahoma	$18,300	52	2009 - 2010	$352	Contract service
Garvin County, Oklahoma	$73,200	272	2009 - 2010	$269	Contract service
Logan County, Oklahoma	$88,000	231	2007 - 2008	$381	Contract service
Oklahoma Turnpike	$150,000	399	Since 1998	$376	Contract service

Table 3: Bridge inspection costs by state, county, and city.

Armstrong County in Pennsylvania recently signed bridge inspection contract with PennDOT from 2010 through 2015. The average inspection cost is $2,398 per bridge.

A long-time bridge inspection service provider in Oklahoma charged from $269 to $508 per bridge for state, county, and city-owned bridges.[5] The inspections are for the NBIS inspection program, and include updating the Pontis database, reviewing the load ratings and updating

[3] http://www.ct.gov/scsb/lib/scsb/Cost_Benefit_Analysis_attachments.pdf
[4] Wisconsin Legislative Audit Bureau. Bridge Inspection Program. February 2008. http://legis.wisconsin.gov/lab/reports/08-bridgeinspectionprogram_ltr.pdf. (accessed August 15, 2011)
[5] http://www.okladot.state.ok.us/projmgmt/off_system_bridge_inspection_consultants/EC-1321%20-%20The%20Benham%20Companies%20LLC.pdf. (accessed August 15, 2011)

where necessary, preparing reports with Pontis data and work candidates, and coordinating load postings and overhead clearance signage. These bridge inspection cost information is summarized in Table 3.

Time Spent on Inspections

While the time required for a bridge inspection varies according to the type and design of the bridge, the Inspection Manual published by Ontario Ministry of Transportation (MTO) states that an inspector should plan to spend at least two to three hours at a typical bridge site to adequately assess the condition of all elements. Insufficient time spent on inspections increases the risk that serious deficiencies will be missed, especially in older structures and bridges that have a history of problems. On average, inspectors conducted three to five inspections in a single day. Larger bridges take longer to inspect.[6]

In Wisconsin, most routine inspections take less than one day to complete, and some take less than an hour, although inspections of bridges with complex designs or structural problems can last several days. [7]

Another study points out that visual inspections rely upon the inspector having access to all components of a bridge and, therefore, methods of gaining access to an elevated bridge are critical to inspection times. The two primary access methods are access equipment and vehicular (aerial) lifts. Access equipment includes ladders, rigging and scaffolds. Typical vehicular lifts are Manlifts, bucket trucks, and under-bridge inspection vehicles. Usually, employing a vehicular lift will be less time-consuming than deploying access equipment; however, the time savings will be offset by the higher costs associated with operating vehicular lifts.[8]

Findings from Interview with Bridge Inspection and Management Experts

A preliminary discussion on the assessment task of the project was initiated at the MDOT partner meeting and the TAC meeting in February 2011. The discussion focused primarily on the challenges associated with the assessment and the inputs required from project partners to allow for a realistic assessment. Therefore, follow-up interviews with bridge inspection and

---

[6] Ministry of Transportation, Ontario. Bridge Inspection and Maintenance. 2009. http://www.auditor.on.ca/en/reports_en/en09/302en09.pdf. Accessed in August 2011.
[7] Wisconsin Legislative Audit Bureau. Bridge Inspection Program. February 2008. http://legis.wisconsin.gov/lab/reports/08-bridgeinspectionprogram_ltr.pdf. Accessed in August 2011.
[8] Brian Leshko. Access Methods for Bridge Inspections. Structure Magazine, October 2008.

management experts, including MDOT partners, were conducted in August and September, 2011.

The purpose of the interviews is to quantify costs of traditional bridge inspection methods, such as time and labor requirements for bridge inspection, equipment needs, costs of special bridge inspection, and overall annual budget for bridge inspection program in Michigan. Another round of interviews are necessary in order to measure the benefits of new bridge inspection technologies, as well as incentives or barriers to their implementation, after the field demonstration data and analytical results become available. Following is a summary of the interviews.

Michigan has 4,465 state-owned bridges. For routine bridge inspections, almost 100% are done by MDOT inspectors. MDOT also owns about 200 over-water bridges that often require consultants help in inspection. On-time inspection rate at MDOT is 99.8%. Only a few bridges may be delayed due to their special conditions. Meantime, special needs bridges may be inspected more frequently, at less than 24-month intervals. Annually inspected bridges include:

- Moveable Bridges.
- Fracture Critical and Fatigue Sensitive Bridges.
- Special Needs Bridges.
- Complex and/or Large Bridges.
- Underwater Bridge Inspections.

Michigan's annual budget for bridge operations is $185 million, increased from $28 million since one cent per gallon gas tax increase goes directly to MDOT to fix seriously deficient bridges on the state road system in 1997. The annual budget for in-house and contract service is about $2 million, which includes inspection, the bridge asset management program, and contract services. This translates into an inspection cost of $896 per bridge.

Typically, preparation for inspection (e.g., review historical inspection reports) requires about 10-20% of total inspection time. The actual field inspection requires about 70-80% of the total inspection time. Data entry requires the remaining 10% of bridge inspection time.

A typical 3-5 span bridge will require 4-6 hours inspection time. The deck, superstructure, and substructure will each take about 30% of the total inspection time. The remaining 10% of time is spent on approaches. All routine inspections can be done without interrupting the traffic.

For list of interviewees, interview questions, and MDOT partners' responses, see **Appendix A**.

COST ESTIMATES AND DATA COLLECTION OF USING REMOTE SENSING TECHNOLOGIES

While cost-benefit analysis can be straightforward in cases with known or measurable costs and benefits, analysis of remote sensing technologies is complex because neither the true benefits nor true costs can be measured with certainty. Additionally, the current technologies are being assessed as part of an applied research project. Once implemented on a commercial basis, the cost of these technologies is likely to fall significantly. One important approach used for this study is to collect and analyze cost data through field demonstration and associated technical assessment of these technologies.

Three MDOT bridges were selected for field demonstration in August 2011. The bridges provides a variety of conditions from poor to good and are the same type (pre-stressed concrete I-beam with concrete deck) to provide comparability between remote sensing results but under different condition ratings. The 2011 field demonstration bridges, their location, and dates are:

- MDOT structure nº 10940 – Freer Road over I-94, Washtenaw County, August 1-3.
- MDOT structure nº 10892 – Willow Road over US-23, Washtenaw County, August 3-5.
- MDOT structure nº 1713 – Mannsiding Road over US-127, Clare County, August 8-10.

The remote sensing technologies and the specific systems used to deploy these technologies on the three selected bridges include:

- 3D Optics (3DO), in the form of a 3D Optical Bridge-evaluation System (3DOBS).
- Street View Style Photography (SVSP), in the form a Bridge Viewer Remote Camera System (BVRCS).
- Thermal Infrared (ThIR) Imaging.
- Digital Image Correlation (DIC).
- Light Detecting and Ranging (LiDAR).

- Synthetic Aperture Radar (SAR) in the form of an Ultra Wide Band Imaging Radar System (UWBIRDS).

- GigaPan (gigapixel panoramic photograpy).

A field demonstration cost data collection form was developed with a purpose of documenting detailed inspection activities on the bridge, including types of technology and equipment use, personnel, set-up time, running time, traffic closure etc.

The use and quantitative analysis of the cost data collected through field demonstration will be conducted in combination with ongoing data processing steps, software needs, and final technical assessment and performance of remote sensing technologies, which will be available to CAR research team at a later stage of the study. The detailed field demonstration activities and notes (from day one through day eight) are presented in **Appendix B**.

NEXT STEPS

CAR researchers will continue to work closely with MTTI and MTRI teams to complete a thorough and comprehensive economic valuation and assessment of the cost-effectiveness of the new technologies and bridge monitoring system, including signatures and the DSS. Specifically, CAR researchers will next focus on following areas:

- Quantify costs of using remote sensing technologies (labor, equipment, software etc.) into monetary values and link the costs to the performance and detection capability of the technologies. Careful analysis will need to be performed to estimate the cost of these technologies once at a commercially available stage, as research costs are not typically representative of implemented technology costs.

- Collect user costs data. Current routine bridge inspections usually do not require traffic lane closures. Several remote sensing technologies, however, will need to close the traffic. User costs will be included in final analysis, such as traffic delay and accidents rates.

- Benefit estimates of DSS. In general, inspection costs are not that significant comparing to bridge investment since they represent less than 4% of bridge life-cycle costs (construction, maintenance, and rehabilitation etc.)[9] The greater value of remote sensing technologies is likely the benefits of a more efficient bridge management system and DSS that will lead to timelier detection of problems,

[9] Hank Bonstedt. Life Cycle Cost Analysis for Bridges. http://caba-bridges.org/Presentations/files/LCCA.ppt. (accessed September 28, 2011)

resulting in substantial cost savings and longer asset life – if these technologies become practical and cost-effective. The Bridge Condition DSS described above, and technical memorandum nº 21 in greater detail, will be used to understand and evaluate this value.

- Conduct scenario analyses and prepare final report. This will include considerations of alternative scenarios, time period, scale of implementation, and valuing outcomes. Because each of the remote sensing technologies has its own advantages and disadvantages, combining several methods may yield better results and take advantage of the unique strengths of each individual technology. As a result, development of scenarios to a large extent will rely on the outcomes of technical assessment of the technologies.

REFERENCES

Adams, T. M., M. Kang, and J. A. Pincheira (2008). *A Systematic Process for Using Federal Aid to Support Bridge Preventive Maintenance*. Midwest Regional University Transportation Center. Project 07-14.

Alampalli, S. *Special Issue on Bridge Inspection and Evaluation*. Journal of Bridge Engineering. July/August 2010.

Transportation Research Board (2003). *Bridge Life-Cycle Cost Analysis*. NCHRP Report 483.

Transportation Research Board (2007). *Bridge Inspection Practices*. NCHRP SYNTHESIS 375.

Transportation Research Board (2009). *Best Practices in Bridge Management Decision-Makin*g. NCHRP Project 20-68A.

USDOT (2006). *Bridge Inspector's Reference Manual (BIRM)*. U.S. Department of Transportation, Federal Highway Administration. Publication No. FHWA-NHI-03-001.

USDOT (2011). *Bridge Preservation Guide: Maintaining State of Good Repair Using Cost Effective Investment Strategies.* U.S. Department of Transportation, Federal Highway Administration. Publication No. FHWA-HIF-11-042.

U.S. Government Accountability Office (GAO) (2008). *HIGHWAY BRIDGE PROGRAM: Clearer Goals and Performance Measures Needed for a More Focused and Sustainable Program*. GAO-08-1043.

U.S. Government Accountability Office (GAO) (2010). *HIGHWAY BRIDGE PROGRAM: Condition of Nation's Bridges Shows Limited Improvement, but Further Actions Could Enhance the Impact of Federal Investment*. GAO-10-930T.

APPENDIX A: INTERVIEW WITH BRIDGE INSPECTION AND MANAGEMENT EXPERTS

Interview dates: August 31 and September 2, 2011

Interviewees: Amy Trahey, Great Lakes Engineering Group

Rich Kathrens, MDOT

Dave Juntunen, MDOT

Steve Cook, MDOT

Jason DeRuyver, MDOT

Purpose: 1) To quantify the costs of traditional bridge inspection methods, such as time and labor requirements, equipment needs, cost of special bridge inspections, and develop an estimate of the overall annual budget for bridge inspection programs in Michigan.

2) To measure the benefits of new bridge inspection technologies, as well as incentives or barriers to their implementation (we will schedule a separate interview on this topic after field demonstration data becomes available in October);

3) To obtain results that will be in the white paper "Economic Valuation of Commercial Remote Sensing and Spatial Information for Bridge Health Monitoring."

General Questions About MDOT Bridge Inspection Program

1. How many people are on the bridge inspection team at MDOT? How many years of experience does a typical bridge inspector have? What are the qualifications for bridge inspection?

The type of inspection drives the need for and number of inspectors. For MDOT, there are always two inspectors in each inspecting team. Local agencies vary and a lot time there is only one inspector.

There are seven regions that have 2-3 dedicated bridge inspectors per region, making a total of 21-24 inspectors in MDOT. There is also an 8th group of inspectors based in Lansing that are called in when bridge inspections require special services. They are responsible for following bridges:

- Fracture Critical Bridges
- Complex Large Deck and Large Superstructure
- Underwater Fatigue Sensitive and Removable

Qualifications: There are several different ways to become a Qualified Team Leader. Professional engineers must complete the National Highway Institute (NHI) two week training class. A non-professional engineer needs 2 years of training in addition to the two week training class. After obtaining 5 years of inspection experience, non-technical inspectors can become an inspection team leader. Also the Federal Highway Administration (FHWA) has guidelines for bridge inspector's qualifications.

2. Of the 4,465 state-owned bridges, how many of them require specialized inspection services by private consultants? What are the determining factors for hiring a private consultant (e.g., special equipment, expertise, in-house staff shortage etc.)?

For routine bridge inspections, almost 100% are done by MDOT inspectors. By contrast, about 90% of local bridges are contracted out to consultants. For scoping inspections, about half are done in-house and the other half by consultants. There are about 260 total scoping inspections done by MDOT each year. MODT also owns about 200 under water bridges that often require consultants help in inspection. Almost 100% of underwater bridge inspections are hired out.

Most scoping in the University Region is hired out, with an average cost of about $10,000 per bridge.

3. What is the percentage of state-owned bridges that are inspected at least once every 24 months? What factors cause this to be less than 100%?

On-time inspection rate at MDOT is 99.8%. Only a few bridges may be delayed due to their special conditions. Meantime, special needs bridges may be inspected more frequently, at less than 24-month intervals. Annually inspected bridges include:

- Moveable Bridges.
- Fracture Critical and Fatigue Sensitive Bridges.
- Special Needs Bridges.
- Complex and/or Large Bridges.
- Underwater Bridge Inspections.

4. What is the breakdown of bridgework funding at MDOT (e.g., capital scheduled maintenance, capital preventive maintenance, bridge rehabilitation, and bridge replacement)? How much is provided by federal and state governments, respectively?

Michigan's annual budget for bridge operations is $185 million. This increased from $28 million due to the gas tax increase.

- $163 million is distributed to DOT regions for replacements (48%), rehabilitations (32%), and preventive maintenance (20%).
- $16 million is allocated to the Big Bridge Program.
- $3 million is allocated to special needs, such as emergency maintenance.
- $3 million is allocated to Michigan's emerging technology program for trial applications of new materials and methods.

U.S. Federal Highway Bridge Program (HBP) funds make up $110 million of Michigan's bridge operations budget, about 60% of total. Other federal programs, such as interstate maintenance, surface transportation, and national highway system funds, are also used to fund bridge preservation projects.

Funds are distributed across state regions based on their proportion of statewide bridge inventory in each work category. For each region, the inventory of bridges in each work category (i.e., prevention, rehabilitation, and replacement) is computed. The work categories have significantly different costs. The average cost of a bridge preventive maintenance project is $450,000. Replacing a bridge deck will cost $1.7 million for a 5-lane deck. The average cost of bridge replacement is $2.2 million. In 2009, Michigan will execute 118 preventive maintenance projects, 87 rehabilitation projects, and 51 replacement projects.

5. Over the next ten years, how important are each of the followings to MDOT's bridge inspection program?

- *Funding limitations for bridge inspection programs*

Funding is always an issue, but as long as the inspection is completed on-time, the cost will be reimbursed from the Federal Government. In that sense, funding is not an issue.

- *Not enough qualified bridge inspectors*

It's not an issue since MDOT has a lot engineers with potential to become bridge inspectors after training. But on the other hand, some specific regions (e.g. metro region) may have a hard time to fill a vacancy.

- *Applying new technologies*

New technologies are the future, and they are a potential solution to many challenges. If a new technology saves time, saves money long term, helps makes bridge inspectors safer, or interrupts traffic less, then it could be a good and attractive investment.

New technologies will have more impact on bridge construction and management than on bridge inspection itself. Examples of new tools:

- Optimize bridge data management system
- Hand-held tablets
- Uploading photos when on-site
- Online system that can track real-time maintenance records
- Consolidating/streamlining various paper files
- Fit in MDOT overall IT strategies

- *Increasing maintenance and improvements costs*
- *Optimizing bridge inspection and repair programs*
- *Meeting federal regulations and inspection guidelines*

This is a critical component of bridge inspection policy. We have to comply with Federal requirements.

Costs of Current Inspection Techniques

6. What are the annual budgets for in-house and contract service of bridge inspections at MDOT?

The annual budget for in-house and contract service is about $1.5 – $2.1 million, which includes inspection, the bridge asset management program, and contract services.
(Metro and University Regions spend about 1.5 million on scoping each year.)

7. What are the current inspection techniques and related equipment requirements for a typical bridge? Is there any way to examine the inspection accuracy of these techniques?

The accuracy of current methods used in the bridge inspection process is reliant on the skills of the bridge inspector. Interpreting the results from the inspection methods is subjective, so it takes a keen sense to accomplish the inspection process with a good degree of accuracy.

8. On average, what is the percent share of annual hours a bridge inspector spends on preparation for inspection, conducting field inspection, data entry and reporting, training, and other activities (such as providing local support)?

Preparation for inspection requires about 20% of total inspection time.
The actual field inspection requires about 70% of the total inspection time.
Data entry requires the remaining 10% of bridge inspection time.

As made clear above, three activities account for 90% of an inspector's hours. The remaining 10% are spent on other activities, such as training and supporting local programs. MDOT bridge inspectors are required to accept 24 hours training every five years.

Preparation for inspection takes about 15 minutes a bridge.
Field inspection takes about 90 to 120 minutes a bridge.
Data entry takes about 30 minutes a bridge.

Normally we can do about 4-5 bridges a day. There are no field inspections from December to March, but we undertake other activities such as maintenance.

9. When conducting a field inspection, which element-level inspection requires most of the inspector's time (including inspection and equipment set-up and break-down hours): the deck, superstructure, substructure, or approach?

It depends on a bridge's condition and type. For steal-beam bridges, the superstructure takes most time, followed by decks, substructure, and approach. A typical 3-5 span bridge will require 4-6 hours inspection time. The deck, superstructure, and substructure will each take about 30% of the total inspection time. The remaining 10% of time is spent on approaches. Hours spent on element-level inspection:

a. The Deck – 1.5 hrs.
b. Superstructure – 1.5 hrs.
c. Substructure – 1.5 hrs.
d. Approach – 0.5 hrs.

Completing all the component steps in deck inspection takes a lot of time.

10. How difficult is it to close traffic lanes when conducting field inspections? How often do closures take place? What is the average expense of deploying traffic lane closures?

The cost to set up of traffic closures ranges from $2,000 to $30,000, depending on how many levels of magnitude. The typical cost range is between $2,000 and $3,000. The set-up time usually only requires 15–20 minutes. Switch the closure to another lane will also take about 15 minutes. We usually do not close traffic unless we have to. There are other restrictions too, such as hours, for traffic control. Usually lane closures occur from 10:00 am to 2:00 pm for inspection purpose.

Traffic closures never happen during routine inspections. After routine inspection, 5-7% of the bridges will require in-depth inspections, which then require traffic control. We spent about one million contract dollars on in-depth inspections in the Metro Region.

11. How much time did it take your team to complete inspections for following bridges? Did you need special access equipment? If so, how much time did it take to set up? Did the inspections require traffic control?

- *Freer Road over I-94:* 30 minutes for preparation
  90 to 120 minutes for inspection
  30 minutes for data entry

- *Willow Road over US-23:* 15 minutes for preparation
  One to two hour for inspection
  30 minutes for data entry

- *Mannsiding Road over US-127:* 30 minutes for preparation
  Two to Three hours for inspection
  30 minutes for data entry

Usually it takes about 4-6 hours per bridge; contractors try to have it done within two hours

Benefits and Limitations of New Technologies

12. We will conduct a second-round interview on this topic later. But based on what you have observed from the BCAURS field demonstration, how much potential do you see for using remote sensing technologies for bridge condition assessment?

Thermal IR seems promising. It can allow us to get deck bottom delamination data without closing traffic. Kansas and the University of Missouri may be using these applications already. 3D photos are also useful. They are useful in creating a reliable record that can be compared with damages caused by accidents.
GPS tagging is not very promising because it takes too much time to do it.

13. One last question: what technical capabilities would the remote sensing technologies have to have to supplement or even replace current bridge inspection techniques?

Remote Sensing has great potential, as long as it is easy to use, easy to deploy, and easy to interpret the data/results. If it meets all these criteria then we will go for it. It's our goal to use less money to do more things, and using technologies definitely will help us achieve this goal. On top of that, remote sensing will not only support the bridge management system (MBI and Pontis), but also TMS.

If remote sensing inspection could get the results currently obtained through scoping, and if it's cost effective, then the new technology will be a great value to us.

APPENDIX B: FIELD COST DATA COLLECTION SPREADSHEETS

Bridge Name: Freer Rd over I - 94						
	3D Optics (3DO)	**Street-view Style Photography (SVSP)**	**Thermal Infrared (ThIR)**	**Light Detection and Ranging (LiDAR)**	**Synthetic Aperture Radar (SAR)**	**Digital Image Correlation (DIC)**
Inspection date 8/1/11						
# of persons operating the equipment	2	2	4-5 for grid creation 2-3 for Camera cart setup 1-2 to operate			
Equipment #1	Nikon D5000	Cannon SX110IS	FLIR i7 (Hand-Held)	LEICA C-10 ($140K)	Synthetic Aperture Radar	Canon EOS 7D
Equipment #2	Ford F-150	Cannon SX110IS	FLIR SC 640	8 Trimax	Laptop	70-200 MM lens
Equipment #3	8 bit controller	Laptop	Laptop			
Equipment #4		Ford F-150	Cart			
Equipment #5						
Equipment #6						
Equipment set-up starts	10:35	9:00				
Equipment set-up ends	10:55	9:15				
1st run starts	11:10	10:00				
1st run ends	11:12	10:10				
Position, direction, and coverage area	SE > NE (1 Lane)	SE > NE (1lane)				
# of traffic lanes closed	Both	Both				
2nd run starts	11:14	10:11				
2nd run ends	11:16	10:13				
Position, direction, and coverage area	NW > SW (1 Lane)	NW > SW (1lane)				
# of traffic lanes closed	Both	Both				
3rd run starts	11:17	10:13				
3rd run ends	11:20	10:15				
Position, direction, and coverage area	SE > NE (1 Lane)	SE > NE (1lane)				
# of traffic lanes closed	Both	Both				
4th run starts	11:21	10:14				
4th run ends	11:24	10:15				
Position, direction, and coverage area	NW > SW (1 Lane)	NW > SW (1lane)				
# of traffic lanes closed	Both	Both				
5th run starts			**Underside of Bridge inspeciton** 18 min to gear up 45 min to use handheld LiDAR Unit for underside			
5th run ends						
Position, direction, and coverage area						
# of traffic lanes closed						
Equipment break-up starts						
Equipment break-up ends						

Table B1: Day 1 Field Demonstration.

Bridge Name: Freer Rd. Bridge over I-94							
	3D Optics (3DO)	Street-view Style Photography (SVSP)	Thermal Infrared (ThIR)	Light Detection and Ranging (LiDAR)	Synthetic Aperture Radar (SAR)	Digital Image Correlation (DIC)	GIGAPAN (Panoramic)
Inspection date 8/2/11							
# of persons operating the equipment	2	2	4-5 for grid creation 2-3 for Camera cart setup 1-2 to operate	2	2 or 3		1
Equipment #1	Nikon D5000	Cannon SX110IS	FLIR i7 (Hand-Held)	Leica C-10	Synthetic Aperture Radar	Canon EOS 7D	Cannon SX110IS
Equipment #2	Ford F-150	Cannon SX110IS	FLIR SC 640	Built in Lieca GPS	Laptop	70-200 MM lens	GigaPan
Equipment #3	8 bit controller	Laptop	Laptop	Control Targets			
Equipment #4		Ford F-150	Cart				
Equipment #5						``	
Equipment #6							
Topside, Underside, or Profileof Bridge	**Topside**	**Underside**		**Underside and Profile**	**Topside**		Underside
Equipment set-up starts			**Underside of Bridge inspeciton** **18 min to gear up** **45 min to use handheld Thermal IR Flir i7** **Unit for underside**	10:17 AM	10:11 AM		10 min
Equipment set-up ends				11:08	11:12 AM		
1st run starts				**11:15**	Started at 1:00 pm		9:30 AM
1st run ends				12:37	Ends at 3:30		10:15 AM
Position, direction, and coverage area				North Face			South Face of Bridge
# of traffic lanes closed				1 Lane			1 Lane
2nd run starts				12:38			11:00
2nd run ends				13:52			11:52
Position, direction, and coverage area				North East Face			North Face of Bridge
# of traffic lanes closed				1 Lane			
3rd run starts				2:17 PM			
3rd run ends				3:30 PM			
Position, direction, and coverage area				South Face			
# of traffic lanes closed				1 Lane			
4th run starts							
4th run ends							
Position, direction, and coverage area							
# of traffic lanes closed							
5th run starts			**Underside of Bridge inspeciton** 18 min to gear up 45 min to use handheld LiDAR Unit for underside				
5th run ends							
Position, direction, and coverage area							
# of traffic lanes closed							
Equipment break-up starts							
Equipment break-up ends							

Table B2: Day 2 Field Demonstration.

Bridge Name: Willow Rd. Bridge over US 23							
	3D Optics (3DO)	Street-view Style Photography (SVSP)	Thermal Infrared (ThIR)	Light Detection and Ranging (LiDAR)	Synthetic Aperture Radar (SAR)	Digital Image Correlation (DIC)	GIGAPAN (Panoramic)
Inspection date 8/3/11			Insufficent Light				
# of persons operating the equipment	2	2		2	2		1
Equipment #1	Nikon D5000	Cannon SX110IS		Leica C-10	Radar	Canon EOS 7D	Cannon SX110IS
Equipment #2	Ford F-150	Cannon SX110IS		Built in Lieca GPS	Generator	70-200 MM lens	GigaPan
Equipment #3	8 bit controller	Laptop		Control Targets	Laptop		
Equipment #4		Ford F-150			Special Radar Cable		
Equipment #5					Supporting Structure		
Equipment #6					Antenna Above		
Topside, Underside, or Profileof Bridge	Topside	Topside		Underside and Profile	Underside		Underside
Equipment set-up starts	11:37	9:30					5 min
Equipment set-up ends	11:45	9:45					
1st run starts	12:09	10:07			9:30		9:30 AM
1st run ends	12:10	10:10			1:30 PM		10:15 AM
Position, direction, and coverage area	NW > NE (1 Lane)	SE > NE (1lane)			2 centimeter horizontal increments per scan. Scans are still 10 ft per		North Bound (Underside)
# of traffic lanes closed	Both	Both					
2nd run starts	12:13	10:11					
2nd run ends	12:15	10:13					
Position, direction, and coverage area	SE > SW (1 Lane)	NW > SW (1lane)					
# of traffic lanes closed	Both	Both					
3rd run starts	12:17	10:13					
3rd run ends	12:19	10:15					
Position, direction, and coverage area	NW > NE (1 Lane)	SE > NE (1lane)					
# of traffic lanes closed	Both	Both					
4th run starts	12:21	10:14					
4th run ends	12:24	10:15					
Position, direction, and coverage area	SE > SW (1 Lane)	NW > SW (1lane)					
# of traffic lanes closed	Both	Both					
5th run starts							
5th run ends							
Position, direction, and coverage area							
# of traffic lanes closed							
Equipment break-up starts							
Equipment break-up ends							

Table B3: Day 3 Field Demonstration.

Bridge Name: Willow Rd. Bridge over US 23							
	3D Optics (3DO)	Street-view Style Photography (SVSP)	Thermal Infrared (ThIR)	Light Detection and Ranging (LiDAR)	Synthetic Aperture Radar (SAR)	Digital Image Correlation (DIC)	GIGAPAN (Panoramic)
Inspection date 8/4/11			Insufficent Light				
# of persons operating the equipment	2	2		2	2		1
Equipment #1	Nikon D5000	Cannon SX110IS		LEICA C-10 ($140K)	Radar	Canon EOS 7D	Cannon SX110IS
Equipment #2	Ford F-150	Cannon SX110IS		8 Trimax	Generator	70-200 MM lens	GigaPan
Equipment #3	8 bit controller	Laptop		Control Targets	Laptop		
Equipment #4		Ford F-150			Special Radar Cable		
Equipment #5					Supporting Structure		
Equipment #6					Antenna Above		
Topside, Underside, or Profileof Bridge	Underside	Underside		Underside and Profile	Underside		Underside
Equipment set-up starts	11:45	9:30			11:15 AM		5 min
Equipment set-up ends	12:01	9:45			11:40 AM		
1st run starts	12:07	10:07		11:54	12:00a		2:30 PM
1st run ends	12:12	10:10		12:37	1:30 PM		4:00 PM
Position, direction, and coverage area	NW > NE (1 Lane)	SE > NE (1lane)		Underside and Profile of So	2 centimeter horizontal increments per scan. Scans are still 10 ft per		South Bound (Underside)
# of traffic lanes closed	Both	Both		1 Lane	Lane Closer Ends at 1:30, Radar Stops Prematurely.		
2nd run starts	12:14	10:11					
2nd run ends	12:16	10:13					
Position, direction, and coverage area	SE > SW (1 Lane)	NW > SW (1lane)					
# of traffic lanes closed	Both	Both					
3rd run starts	12:17	10:13					
3rd run ends	12:20	10:15					
Position, direction, and coverage area	NW > NE (1 Lane)	SE > NE (1lane)					
# of traffic lanes closed	Both	Both					
4th run starts	12:21	10:14					
4th run ends	12:24	10:15					
Position, direction, and coverage area	SE > SW (1 Lane)	NW > SW (1lane)					
# of traffic lanes closed	Both	Both					
5th run starts							
5th run ends							
Position, direction, and coverage area							
# of traffic lanes closed							
Equipment break-up starts							
Equipment break-up ends							

Table B4: Day 4 Field Demonstration.

Bridge Name: Willow Rd. Bridge over US 23							
	3D Optics (3DO)	Street-view Style Photography (SVSP)	Thermal Infrared (ThIR)	Light Detection and Ranging (LiDAR)	Synthetic Aperture Radar (SAR)	Digital Image Correlation (DIC)	GIGAPAN (Panoramic)
Inspection date 8/5/11							
# of persons operating the equipment							
Equipment #1							
Equipment #2							
Equipment #3							
Equipment #4							
Equipment #5							
Equipment #6							
Topside, Underside, or Profileof Bridge							
Equipment set-up starts				Crew arrives around 15:45:00 for one scan			Crew arrives around 15:45:00 for one scan
Equipment set-up ends							
1st run starts							
1st run ends							
Position, direction, and coverage area							
# of traffic lanes closed							
2nd run starts							
2nd run ends							
Position, direction, and coverage area							
# of traffic lanes closed							
3rd run starts							
3rd run ends							
Position, direction, and coverage area							
# of traffic lanes closed							
4th run starts							
4th run ends							
Position, direction, and coverage area							
# of traffic lanes closed							
5th run starts							
5th run ends							
Position, direction, and coverage area							
# of traffic lanes closed							
Equipment break-up starts							
Equipment break-up ends							

Table B5: Day 5 Field Demonstration.

Bridge Name: Mannsiding Rd over US-127								
	3D Optics (3DO)	Street-view Style Photography (SVSP)	Thermal Infrared (ThIR)	Light Detection and Ranging (LiDAR) - MDOT	Light Detection and Ranging (LiDAR) - Mich Tech	Synthetic Aperture Radar (SAR)	Digital Image Correlation (DIC)	GIGPAN
Inspection date 8/8/2011								
# of persons operating the equipment	2	2	4-5 for grid creation 2-3 for Camera cart setup 1-2 to operate	1-2		2		1
Equipment #1	Nikon D5000	Cannon SX110IS	FLIR i7 (Hand-Held)	LEICA C-10	RIEGL	Synthetic Aperture Radar	Canon EOS 7D	Cannon SX110IS
Equipment #2	Ford F-150	Cannon SX110IS	FLIR SC 640	8 Trimax	Nikon D30	Laptop	70-200 MM lens	Gigapan (need model)
Equipment #3	8 bit controller	Laptop	Laptop		Calibrated Lens			
Equipment #4		Ford F-150	Cart		8 Trimax			
Equipment #5					Dell Computer			
Equipment #6								
	Topside	Topside	Topside					
Equipment set-up starts	11:10	15 Min	Grid Creation 9:30 am	Initial Setup 11:30 am		30 min		10 Min
Equipment set-up ends	11:25		10:15 am	12:30 pm				
1st run starts	11:30	12:10	11:48	1:05 pm		2:45		10:30
1st run ends	11:33	12:14	12:10	2:05 pm		3:45		11:00
Position, direction, and coverage area	Mannsiding Rd WB (NB Bridge)	Mannsiding Rd WB (NB Bridge)	Mannsiding Rd. WB (NB Bridge)	US-127 NB south side		Mannsiding Rd. EB (NB Bridge)		South Face of SB Bridge
# of traffic lanes closed	1 Lane	1 Lane	1 Lane	1 Lane		1 Lane		1 Lane
2nd run starts	11:34	12:15	12:40	2:30 pm				
2nd run ends	11:37	12:20	12:52	3:15 pm				
Position, direction, and coverage area	Mannsiding Rd EB (NB Bridge)	Mannsiding Rd WB (NB Bridge)	Mannsiding Rd. WB (SB Bridge)	US-127 SB south side				
# of traffic lanes closed	1 Lane	1 Lane	1 Lane	1 Lane				
3rd run starts	3:20	3:00						
3rd run ends	3:24	3:07						
Position, direction, and coverage area	Mannsiding Rd WB (SB Bridge)	Mannsiding Rd WB (SB Bridge)						
# of traffic lanes closed	1 Lane	1 Lane						
4th run starts	3:25	3:08						
4th run ends	3:27	3:12						
Position, direction, and coverage area	Mannsiding Rd WB (SB Bridge)	Mannsiding Rd WB (SB Bridge)						
# of traffic lanes closed	1 Lane	1 Lane						
5th run starts								
5th run ends								
Position, direction, and coverage area								
# of traffic lanes closed								
Equipment break-up starts								
Equipment break-up ends								

Table B6: Day 6 Field Demonstration.

Bridge Name: Mannsiding Rd over US-127								
	3D Optics (3DO)	Street-view Style Photography (SVSP)	Thermal Infrared (ThIR)	Light Detection and Ranging (LiDAR) - MDOT	Light Detection and Ranging (LiDAR) - Mich Tech	Synthetic Aperture Radar (SAR)	Digital Image Correlation (DIC)	GIGPAN
Inspection date 8/9/2011								
# of persons operating the equipment	2	2	4-5 for grid creation 2-3 for Camera cart setup 1-2 to operate	2	2	3	1-3	1-3
Equipment #1	Nikon D5000	Cannon SX110IS	FLIR i7 (Hand-Held)	LEICA C-10 ($140K)	RIEGL	Synthetic Aperture Radar	Canon EOS 7D	Cannon SX110IS
Equipment #2	Ford F-150	Cannon SX110IS	FLIR SC 640	8 Trimax	Nikon D30	Laptop	70-200 MM lens	Gigapan (need model)
Equipment #3	8 bit controller	Laptop	Laptop		Calibrated Lens			
Equipment #4		Ford F-150	Cart		8 Trimax			
Equipment #5					Dell Computer			
Equipment #6								
Equipment set-up starts	11:30	8:30	8:30	10:30	8:30	8:30	90 minutes to set up, inlcuding marks	
Equipment set-up ends	11:55	8:55	9:50	11:00	10:30	9:30		
1st run starts	12:00	10:58	10:00	11:00	10:30	Did not start due to failed motor. It will take about 30 minutes to run both directions of the top bridge. To complete the 10 ft x 10 ft 3D scan, it will require 4 - 5 hours.	Survey did not start due to rain	
1st run ends	12:05	11:00	10:15	11:45	11:15			
Position, direction, and coverage area	Mannsiding Rd WB (E. Section)	US-127 NB Right Lane	Mannsiding Rd WB E. Section	US-127 NB north side	US-127 NB north side		US-127 NB north side	
# of traffic lanes closed	1	1	1	1	1		1	
2nd run starts	12:05	11:01	Each lane was divided into four segments and it takes about 2 hours to complete all eight segments of Mannsiding Rd (east section)					
2nd run ends	12:10	11:03						
Position, direction, and coverage area	Mannsiding Rd WB (E. Section)	US-127 NB Right Lane						
# of traffic lanes closed	1	1						
3rd run starts								
3rd run ends								
Position, direction, and coverage area								
# of traffic lanes closed								
4th run starts			Takes about 30 minutes to complete under-the-bridge photography (NB US-127)					
4th run ends								
Position, direction, and coverage area								
# of traffic lanes closed								
5th run starts				Depending on resolutions, each scan will take about 5-30 minutes. # of scans for each bridge will depend on the configurations. For example, Mannsiding Rd will need 22 scans. No wet condition				
5th run ends								
Position, direction, and coverage area								
# of traffic lanes closed								
Equipment break-up starts			Takes about 15 minutes to break-up					
Equipment break-up ends								

Table B7: Day 7 Field Demonstration.

Bridge Name: Mannsiding Rd over US-127								
	3D Optics (3DO)	Street-view Style Photography (SVSP)	Thermal Infrared (ThIR)	Light Detection and Ranging (LiDAR) - MDOT	Light Detection and Ranging (LiDAR) - Mich Tech	Synthetic Aperture Radar (SAR)	Digital Image Correlation (DIC)	GIGPAN
Inspection date 8/10/2011								
# of persons operating the equipment	2-3		4-5 for grid creation 2-3 for Camera cart setup 1-2 to operate	2	2	3	1-4	
Equipment #1	Nikon D5000	Cannon SX110IS	FLIR i7 (Hand-Held)	LEICA C-10 ($140K)	RIEGL	Synthetic Aperture Radar	Canon EOS 7D	Cannon SX110IS
Equipment #2	Ford F-150	Cannon SX110IS	FLIR SC 640	8 Trimax	Nikon D30	Laptop	70-200 MM lens	Gigapan (need model)
Equipment #3	8 bit controller	Laptop	Laptop		Calibrated Lens			
Equipment #4		Ford F-150	Cart		8 Trimax			
Equipment #5					Dell Computer			
Equipment #6								
Equipment set-up starts	10:10			12:00	8:30	8:30	8:30	
Equipment set-up ends	10:30			12:30	9:15	1:00	9:00	
1st run starts	10:33			12:30	9:15	1:00	9:10	
1st run ends	10:35			1:00	Seventh scan ends at 2:30?	Completed three transmission measurements at 1:25	9:40	
Position, direction, and coverage area	Mannsiding Rd WB (E. Section)			US-127 NB under the bridge	US-127 NB under the bridge	Mannsiding Rd WB (E. Section)	US-127 NB north side face	
# of traffic lanes closed	1			1	1	1+1	1 +1	
2nd run starts	10:35			1:00	7 scans today. Each will take about 30-45 minutes (including 1-2 minutes initial scan, 3 minutes target scan, and 15 minutes final scan)		Truck from Clare County Road Commision makes eight runs on top of bridge, lasting about one hour (9:10 - 10:10)	
2nd run ends	10:37			1:30				
Position, direction, and coverage area	Mannsiding Rd WB (E. Section)			US-127 NB under the bridge				
# of traffic lanes closed	2			1				
3rd run starts	10:45			1:30				
3rd run ends	10:47			1:50				
Position, direction, and coverage area	Mannsiding Rd WB (E. Section)			US-127 NB under the bridge				
# of traffic lanes closed	2			1				
4th run starts	10:55							
4th run ends	10:57							
Position, direction, and coverage area	Mannsiding Rd EB (E. Section)							
# of traffic lanes closed	1							
5th run starts				9 scans on Monday, 7 scans on Tuesday, and 6 scans on Wednesday				
5th run ends								
Position, direction, and coverage area								
# of traffic lanes closed								

Table B8: Day 8 Field Demonstration.

PAGE INTENTIONALLY LEFT BLANK

Memo

To: D. Harris, L. Sutter, R. Shuchman, and rest of Project Team

From: T. Ahlborn, H. de Melo e Silva

CC: C. Singh

Date: January 13, 2012

Number: 23

Subject: Update for No-cost Time Extension and Final Report Outline

---

This is to inform the project team of two items critical to the completion of our project using remote-sensing technologies for bridge condition assessment.

First, the project has been granted a no-cost time extension, with a new completion date of September 30, 2012. As such, quarterly reports items and dates for deliverables must be adjusted to meet the new completion date. Below is an updated list and timeline of our project deliverables (as of December 8, 2011), including additional information for content of technical memorandums (starting on page TM#23 - 1).

Second, an outline (as of December 8, 2011) of our final report has been developed and can also be found below (starting on page TM#23 - 3).

DELIVERABLES

Quarter 8 (September-December 2011)

Items 28 – 30: Due to the United States Department of Transportation (USDOT) within twenty-four (24) months of the effective date of the Agreement (due 1/15/12).

28. Technical memorandum nº 23 provides an update for the timeline and deliverables for this project in light of the no-cost time extension (thru September 30, 2012). This memorandum also includes the outline of the final report.
29. Technical memorandum nº 24 describing health indicators for each technology with progress related to the Decision Support System (DSS) as well as a DSS progress update.
30. Technical memorandum nº 25 reporting on progress of the economic valuation of the technologies and the DSS tool, software and components for bridge condition assessment.

Quarter 9 (January-March 2012)

Items 31 – 32: Due to USDOT within twenty-seven (27) months of the effective date of the Agreement (due 4/15/12).

31. Technical memorandum nº 26 describing final papers developed for each technology and the economic evaluation.
32. Technical memorandum nº 27 explaining the DSS beta version evaluation by our Michigan Department of Transportation focus group and by our Technical Advisory Committee (TAC) through a secure web-portal, summarizing the capabilities of the DSS for integrated bridge assessment as well as the DSS.

Quarter 10 (April-June 2012)

Items 33 – 34: Due to USDOT within thirty (30) months of the effective date of the Agreement (due 7/15/12).

33. Technical memorandum nº 28 describing the assessment from the comprehensive project review workshop.
34. Final draft report submitted to USDOT June 30, 2012 (internal deadline May 15, 2012).

Quarter 11 (July-September 2012)

Items 35 – 36: Due to USDOT within thirty-three (33) months of the effective date of the Agreement (due 9/30/12).

35. Conduct *Remote Sensing Workshop*, following American Society for Nondestructive Testing NDE/NDT for Highway and Bridges: Structural Materials Technology (SMT) <http://www.asnt.org/events/conferences/smt12/smt12.htm>, August 24, 2012 – New York, NY.
36. Deliver Final report, incorporating comments received from USDOT and TAC members by September 30, 2012.

FINAL REPORT OUTLINE

Project Documentation Page

Executive Summary

Acknowledgments

Disclaimer

Table of Contents

List of Figures
List of Tables
List of Appendices

Chapter 1 – Introduction, Project Overview

Chapter 2 – Selected RS literature review, cite Appendix A (CSE report)

Chapter 3 – State of the Practice, cite Appendix B (SOA report)

Retool the SOP report: selection for our project focus

Chapter 4 – Methodology

Lab work, field demonstration (general)

Chapter 5 – Technology Performance and Evaluation

Each technology here: lab work, field performance, complementing technologies

Chapter 6 – Decision Support System

Development, layout, framework
Condition data integration (existing NBI, RS and other inspection techniques)

Chapter 7 – Economic valuation

Chapter 8 – Implementation and Field Readiness

Combine complementing technologies discussion

Chapter 9 – Conclusions and the Path Forward

Note About Chapter Five

Chapter 5 will be written as a series of papers for the following topics:

3D Opitical Bridge-evaluation System (3DOBS)
Bridge Viewer Remote Camera System (BVRCS)
GigaPan System (GigaPan)
Thermal Infrard (ThIR)
Digital Image Correlation (DIC)
Light Detecting and Ranging (LiDAR)
Ultra Wide Band Imaging Radar System (UWBIRS) / Ground Penetrating Radar (GPR)
Synthetic Aperture Radar (SAR)
Interferometric Synthetic Aperture Radar (InSAR)
Multispectral Satellite Imagery (MSI)

Each paper/sub-chapter includes intro/background/details on lab and field work, applications, results/pros/cons, limitations for implementation, costing comments, integration into the DSS, combining with other technologies (surface, subsurface, global, etcetera).

Other papers include a “combined field deployment or R/S technologies” and “economic evaluation for R/S technologies for bridge inspection”.

Memo

To: T. Ahlborn, D. Harris, L. Sutter, R. Shuchman, and rest of Project Team

From: H. de Melo e Silva, C. Brooks, D. Banach, J. Burns, D. Dean, R. Dobson, A. Endsley, R. Hoensheid, R. Oats, K. Vaghefi

CC: C. Singh

Date: January 13, 2012

Number: 24

Subject: Project Progress Update Relating Technologies and Decision Support System to Health Indicators for Bridge Condition Assessment.

3D OPTICAL BRIDGE-EVALUATION SYSTEM (3DOBS)

The 3DOBS, a demonstration of 3D optics technology that uses close range photogrammetric principles, was successfully deployed to all field demonstration bridges to collect 3D bridge surface, as previously described in technical memorandum nº 21. The remote sensing team has focused on extending the maximum value from this successful demonstration of a practical, low cost remote sensing system that can characterize bridge deck surfaces with high-resolution elevation data.

An example of extending the value of the high-resolution Digital Elevation Model (DEM) data being generated for each bridge out of the 3DOBS is calculating the International Roughness Index (IRI) for all the field demonstration bridges. The IRI data is being incorporated into this project to help assess the overall health conditions of the pavement for the three tested bridges, which can be used as a component of the overall bridge health signature. The IRI profiling index has ratings ranging from 0 m/km (or mm/m) to 20 m/km; indicating a perfectly smooth surface and an extremely rough unpaved surface, respectively. The ratings are based on a longitudinal profile of the pavement, which is then processed through the quarter-car and 250 mm wavelength models to simulate how a single wheel of a vehicle would react to the condition of a pavement.

Normally the longitudinal profile is created from a series of measurements made by an altimeter connected to a car, which is driven across the pavement. However, for the purposes of this project, the elevation measurements were collected using a remote sensing methodology to determine where the three bridges would be positioned on the IRI graph (Figure 1) and to validate if the results were similar to their real-world conditions.

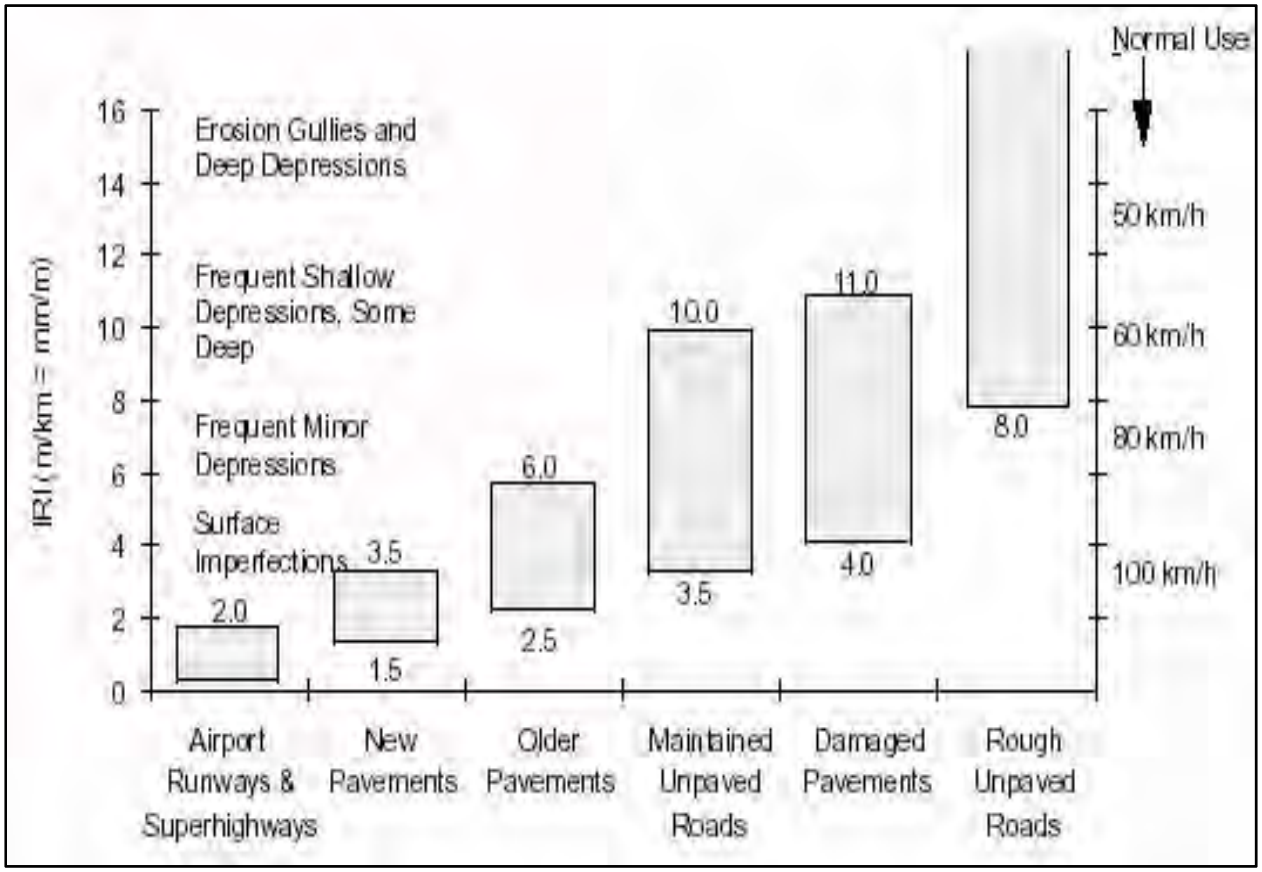

Figure 1: The International Roughness Index graph.

Collecting the pavement's elevation changes on the Freer Road bridge involved using a DEM created using the 3DOBS. This process contained the necessary data to create a zero plane, in which all elevation deviations were based on. The profiling data was then formatted into an Engineering Research Division (ERD) file format that was imported into a computer program, The Transtec Group ProVAL, used to view and analyze pavement profiles. ProVAL then graphed the longitudinal profile, which was processed through the two models. The end result is an IRI value that is indicative of a single wheel path across the bridge.

Figures 2 and 3 demonstrate the longitudinal profiles of two tire tracks for each side of the Freer Road bridge. The bridge deck-joints elevation data were removed from the profiles because they would misrepresent depressions on the bridge. After being processed through the two models, the northbound left tire track data produced an IRI value of 3.59 m/km, while the northbound right tire track data had an IRI value of 4.26 m/km. In addition, the southbound left tire track produced an IRI value of 4.14 m/km, and the southbound right tire track had an IRI value of 3.71 m/km (see Table 1). All of these roughness values were classified as "older pavements" according to the IRI graph. To validate the results, they were compared against what was known about the bridge. Similar to the IRI graph, the Freer Road bridge has an older pavement, has frequent minor depressions, and is a paved surface.

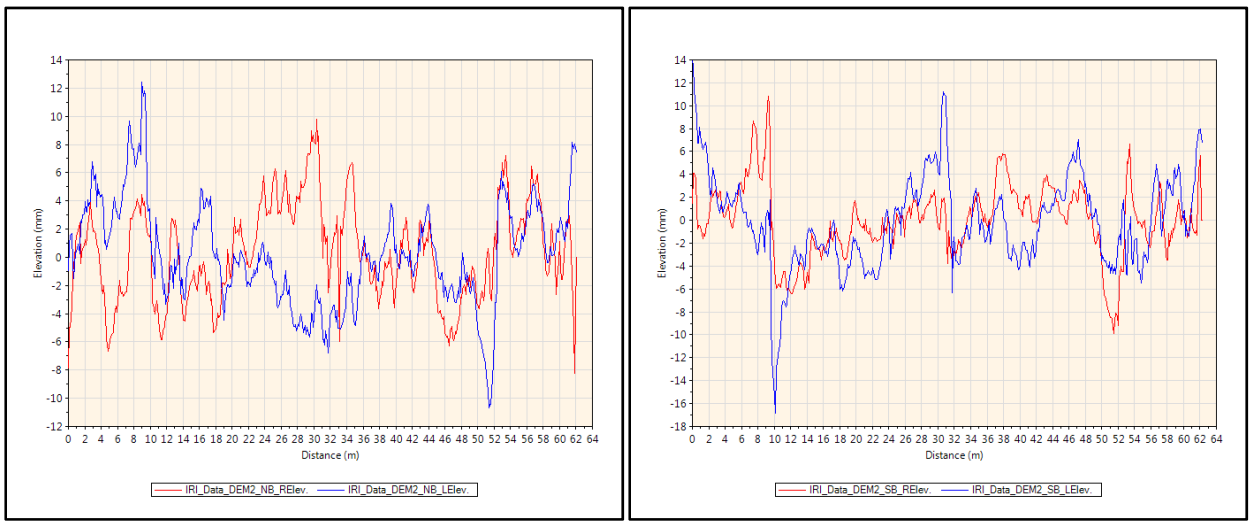

Figures 2 & 3: The longitudinal profiles of the bridge at Freer Road. Each indicates two tire tracks on the northbound (left) and southbound (right) lanes.

File	Profile	IRI (m/km)
IRI_Data_DEM2_NB	LElev.	3.59
IRI_Data_DEM2_NB	RElev.	4.26
IRI_Data_DEM2_SB	LElev.	4.14
IRI_Data_DEM2_SB	RElev.	3.71

Table 1: IRI values for each tire track on Freer Road.

In addition to this new IRI data analysis, the project team has continued to use the 3DOBS-derived bridge deck elevation data for detecting a variety of bridge condition indicators. The

team has been able to determine the percent spalled of a bridge deck, location, area and volume of individual spalls, total area, and volume spalled. All of these are derived from a DEM that was generated from a single, inexpensive, rapidly-deployable vehicle mounted system.

An algorithm was created for the 3DOBS to automatically detect spalls from the DEM and calculates area and volume using focal statistics. This enabled rapid calculation of useful data to integrate into the Decision Support System (DSS) and has been labeled the "MTRI (Michigan Tech Research Institute) 3DOBS spall detection algorithm". One feature of the algorithm is that users can specify the minimum size of spall that they are interested in. With the use of the high resolution DEM produced by the 3DOBS (as detailed in technical memorandum nº 21), the remote sensing team is able to manually find spalls that are less than 10 cm^2 (1.55 in^2, or a circle having ∅1.41 in). However, at such a small size, there are artifacts in the DEM around a similar size. Theses artifacts would be difficult for an automated algorithm to differentiate from "real spalls" and therefore possibly produce incorrect results.

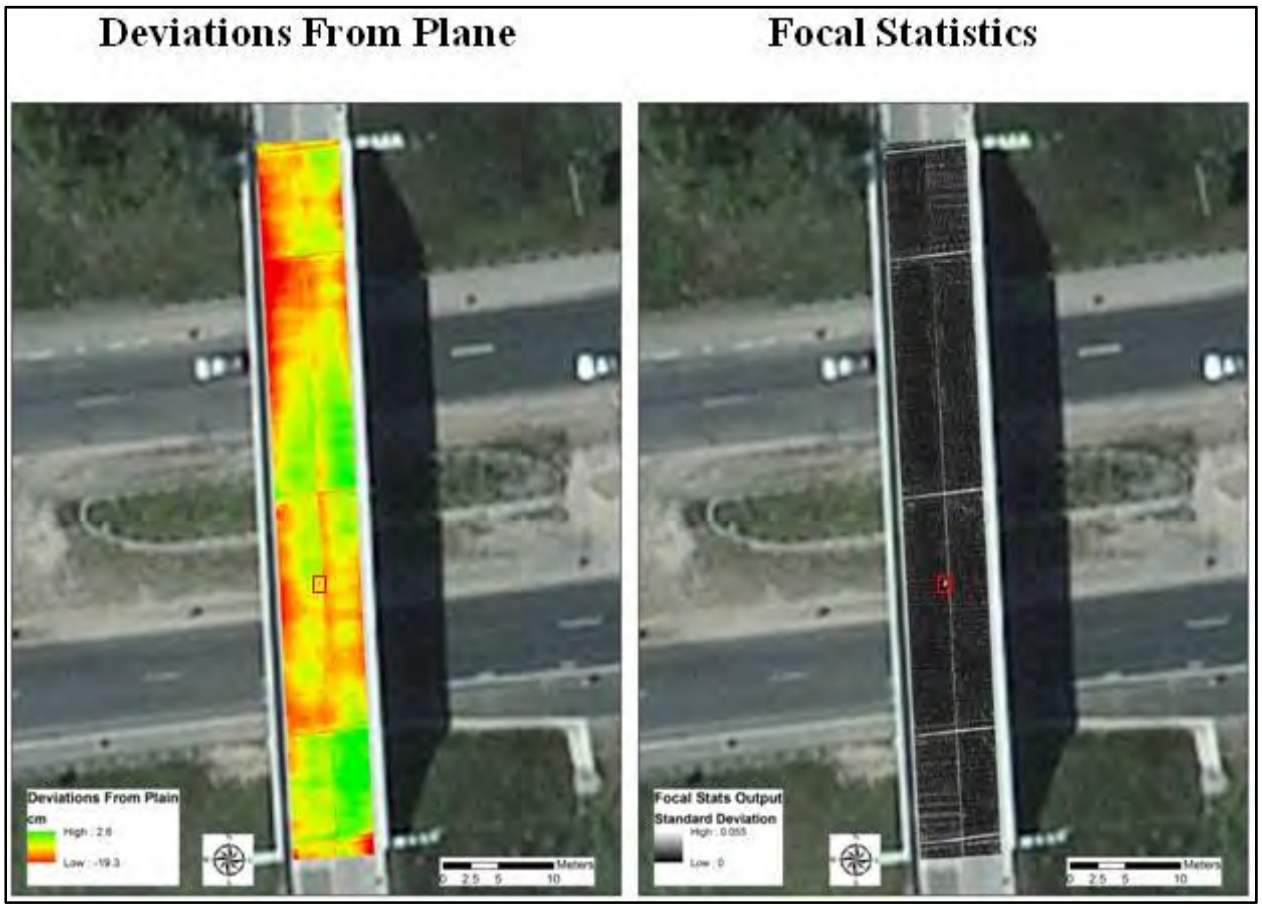

Figure 4: Comparison of the DEM and Focal Statistics output for the Freer Rd bridge.

The 3DOBS spall detection algorithm uses the focal statistics function found in Esri ArcGIS to locate spalls. This function determines the change in cell values as it relates to a specified "neighborhood" of cells. Figure 4 shows an example of the focal statistics output as it relates to the DEM. The red box on both the DEM and the focal statistics output shows the location of a rather large spall on the Freer Road bridge. This spall has a size of 11,429 cm^2 (12.3 ft^2). Figures 5 shows examples of the different sizes of the neighborhood that could be set within the focal statistics function. The top two are examples of a rectangular neighborhood and the bottom two are examples of a circular neighborhood with a specified radius of cells.

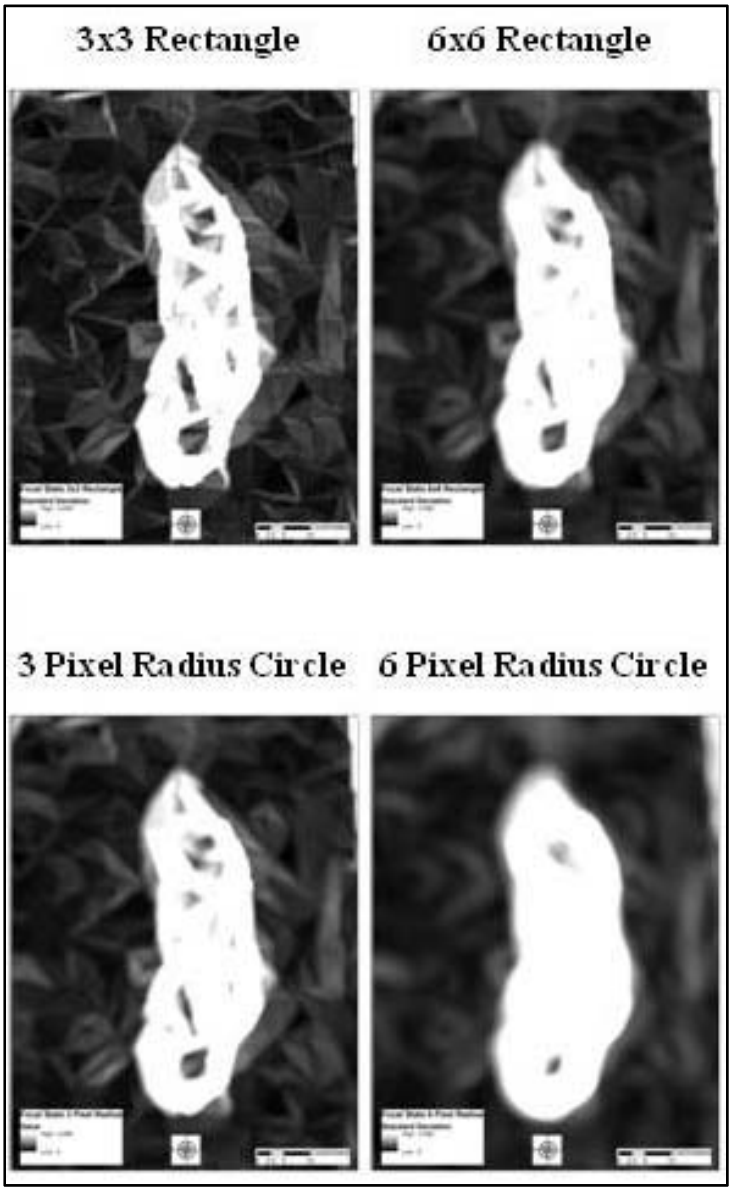

Figure 5: Comparison of the different "neighborhood" sizes and type that can be calculated.

Since the 3DOBS-derived elevation data can detect spalls at various minimum sizes, testing was done to see at what minimum size was optimal for accurately detecting spalls. Figure 6 shows an example of three different minimum sizes that were used. These minimum sizes were 10 cm^2, 100 cm^2 and 1,000 cm^2. From this testing, we determined that a minimum detection size of about 40 cm^2 (6.2 in^2) would be optimal.

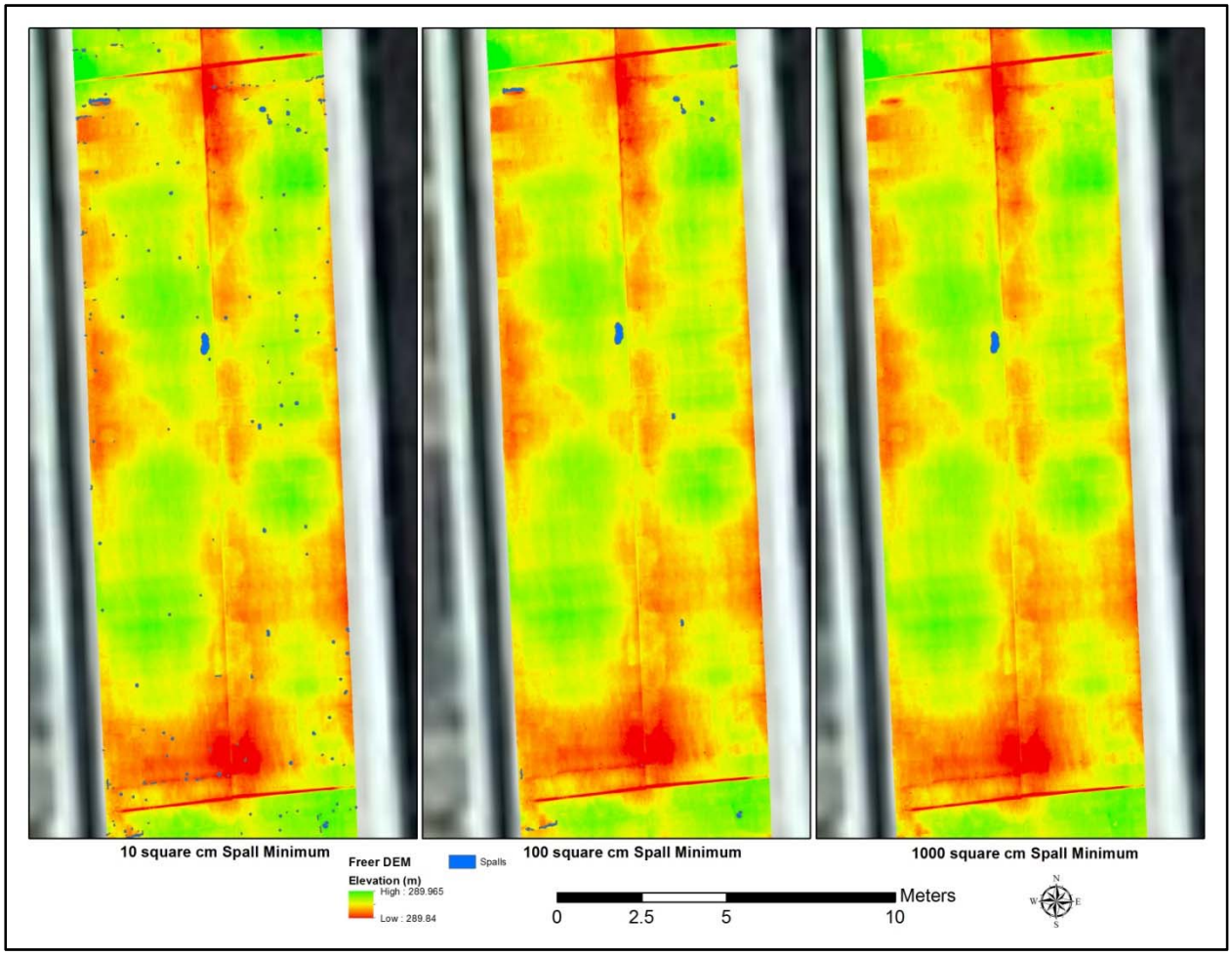

Figure 6: Comparison of three different minimum spall output sizes from the 3DOBS spall detection algorithm.

Table 2 is an example of the detailed output from the spall detection algorithm. This example is from the Freer Road bridge over I-94. The minimum spall size set for the algorithm is 40 cm^2, which is at a sufficient size to remove the artifacts. There were a total of 267 spalls detected with a total area of 48,141 cm^2 and a total volume of 80,700 cm^3. This means that Freer Road bridge is 0.85% spalled.

Another bridge that was visited was the Willow Road bridge over US-23 was somewhat different from the Freer Road bridge. There was a significant amount of spalling that was outside but adjacent to the driving area. Due to the field of view of the camera used for the 3DOBS, this area was represented in the DEM and subsequently in the algorithm analysis. If the total bridge is included in the calculation then the total spalled area is 369,814 cm^2 and volume is 1,980,300 cm^3 and the bridge would be 6.99% spalled. If, however, only the driving area of the bridge is then the total spalled area is 21,838 cm^2 and volume is 20,600 cm^3. The percent spalled drops to just 0.41% which is less than the Freer Road bridge.

ID	GRIDCODE	ORIG_FID	AREA	MAX	MIN	SP_VOLUME	SP_AREA
92	2	91	11883.75	289.96	289.84	0.0485	1.1429
983	2	982	5130.50	289.94	289.91	0.0079	0.5206
991	2	990	21092.50	289.95	289.91	0.0079	0.5282
1008	2	1007	1967.75	289.94	289.92	0.0028	0.1923
989	2	988	1840.75	289.94	289.91	0.0016	0.1796
1009	2	1008	1279.00	289.93	289.91	0.0013	0.1232
47	2	46	965.25	289.95	289.92	0.0012	0.1100
616	2	615	1208.75	289.94	289.91	0.0012	0.1264
942	2	941	872.50	289.95	289.94	0.0007	0.0873
75	2	74	2173.75	289.93	289.90	0.0007	0.0710
519	2	518	549.50	289.95	289.93	0.0005	0.0550
288	2	287	350.00	289.93	289.92	0.0003	0.0350
46	2	45	404.25	289.95	289.93	0.0002	0.0404
987	2	986	263.25	289.94	289.92	0.0002	0.0258
527	2	526	234.75	289.95	289.93	0.0002	0.0240
536	2	535	185.50	289.95	289.94	0.0002	0.0440
11	2	10	407.00	289.93	289.91	0.0002	0.0403
184	2	183	168.00	289.94	289.93	0.0001	0.0168
290	2	289	95.25	289.94	289.92	0.0001	0.0095
682	2	681	88.00	289.95	289.93	0.0001	0.0086

Table 2: Example output from the 3DOBS spall detection algorithm. The columns labeled "SP_VOLUME" and "SP_AREA" are the calculated volume and area measurements in m^3 and m^2.

Next Steps

During the next quarter of this project, the team's new ability to derive IRI data will be applied to the Willow Road bridge and both of the Mannsiding Road bridges. Each will have a digital

elevation model built for them using the 3DOBS, upon which elevation data can be extracted. The end result will be IRI values for each of the bridges that should not only match the description given on the IRI graph but also be indicative of the deck surface condition health. The team will also complete the derivation of the 3DOBS DEM for the Mannsiding Road bridges, now that Freer and Willow Roads bridges are complete.

Technical memorandum nº 21 described the primary benefits of the 3DOBS as: low cost to purchase components, rapid deployment, limited time needed to collect data on the bridge, and that the team has demonstrated how to derive useful metrics of bridge deck condition. The ability to extract out additional useful metrics such as IRI can now be added.

The project team anticipates that transportation agencies will find additional uses for a very high resolution deck surface elevation data set that can be created rapidly and inexpensively.

BRIDGE VIEWER REMOTE CAMERA SYSTEM (BVRCS)

Additional work with the BVRCS was not needed during the past quarter. It continues to be an inexpensive, easily deployable way of collecting location-tagged photo inventories of a bridge and its environs, deployable at any time a transportation agency would like to do so. The current level of technology could be deployed by a local or state transportation agency, and fully commercial system could easily be derived from this project's version. As a practical demonstration of Google Street View-style photography technology, further development is not anticipated in this project. The project team is now at the point that the photo inventory is being integrated into the DSS as a demonstration of how the photos could be used to visually assess current conditions and to future photo inventories as they become available.

GIGAPAN SYSTEM (GigaPan)

Similarly, the project team did not consider additional development of the GigaPan System necessary during the past quarter. Instead, the DSS part of the team has started to integrate the high-resolution photo inventory into the DSS so that transportation agencies can more easily understand how they can use this bridge photo inventory method. GigaPan continues to serve as a demonstration of a relatively inexpensive hardware that creates a high-resolution photo inventory of parts of a bridge, available as a single gigapixel image stitched together from hundreds or thousands of digital photos, with the limitation of the time needed to process the images into a single photo, as described in technical memorandum nº 21.

THERMAL INFRARED (ThIR)

In this quarter, preliminary ThIR results for the Freer Road bridge were compared with the Michigan Department of Transportation (MDOT) hammer sounding technique. In this method, a photo of the whole bridge was created and imported into ArcGIS to show the boundaries of delaminations that were marked by bridge inspectors on site (see Figure 26). By creating a layer for these areas, the total area of delamination can be calculated in ArcGIS. The total "hammer sounding" area calculated was 101 ft^2 compared to 29 ft^2 using the ThIR method (corrected from 22.95 ft^2, see technical memorandum nº 21). The difference is mainly because of the limitation for identifying the exact boundaries of each delamination by inspectors on site and/or not having good quality images for some areas.

There were two main problems for this bridge; (1) delaminations around the construction joints on the center of the bridge and (2) the painted centerline stripe overlapping delaminated areas. Because the ThIR camera works with reflective energy, the paint affects readings, having at times an adverse effect on the interpretation of the images in this area. Figure 7 shows delaminations around centerline area and Figure 8 shows the difference between boundaries of MDOT marked area and ThIR images.

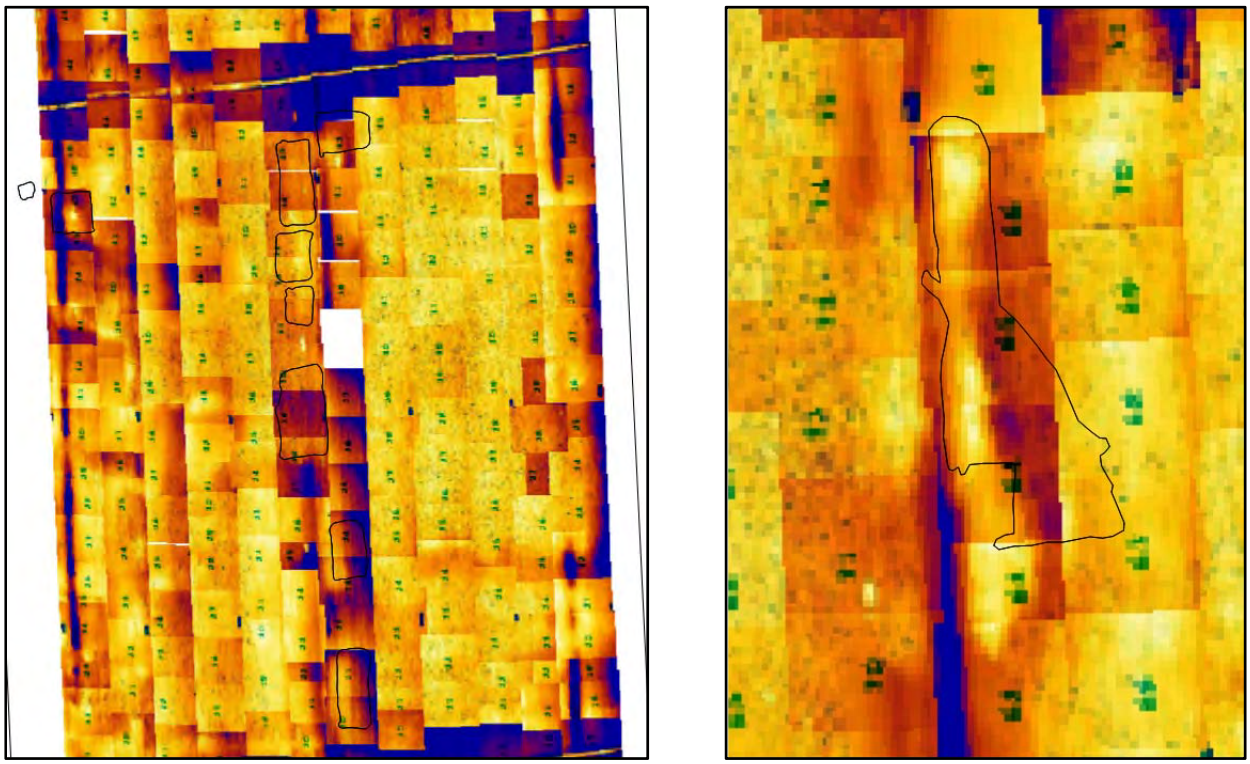

Figures 7 & 8: MDOT delamination map and ThIR image superimposed on each other.

The ThIR data for the Willow Road bridge has been analyzed with the same method that was discussed in technical memorandum nº 21 for the Freer Road bridge. Shoulders of this bridge were in bad condition at the time of inspection, therefore the total area of delamination was calculated without considering the images taken from the shoulders. Table 3 summarizes the results of this calculation.

Total Delaminated Area (ft^2)	140.95
Total Bridge Area (ft^2)	5,015.75
Percentage of delamination (%)	2.81

Table 3: Willow Road bridge ThIR preliminary results.

Figure 9 shows the ThIR image(s) of the Willow Road bridge and Figure 10 shows the MDOT-marked areas of delamination which were imported into the ArcGIS environment (see Figure 26). The total area of delamination based on one of MDOT's current practices (hammer sound) was calculated to be 159.54 ft^2 using ArcGIS. This indicates that 3.18% of the bridge deck is delaminated. Based on the ThIR images the delaminated area of the bridge deck was calculated to be 141 ft^2. This corresponds to 2.81% of the bridge deck being delaminated. Note that the spray-painted areas marking the delamitations are possibly 'over marked'.

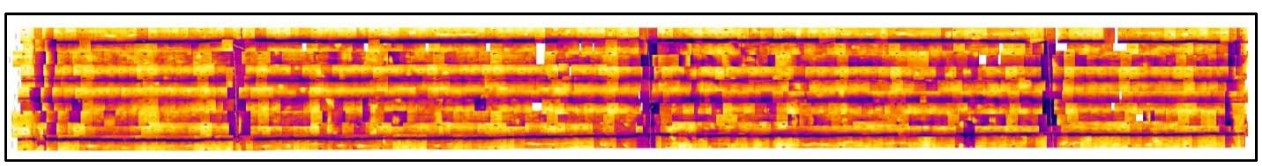

Figure 9: Willow Road bridge ThIR image.

Figure 10: Willow Road bridge MDOT hammer sounding delamination survey.

Next Steps

Next quarter of this project will be focused on extracting delamination information from ThIR images for Mannsiding Road bridges and summarizing the results based on percent delamination that can be imported and displayed in the DSS to help bridge inspectors. In parallel the project team is still developing a The MathWorks MATLAB algorithm to process large amounts of data, automatically stitch the photos, and calculate the area of delamination. Limitations of applying this technology on a bridge has been discussed in technical memorandum nº 21 and investigations are under consideration to overcome those barriers and improve data collection methods and results.

DIGITAL IMAGE CORRELATION (DIC)

As discussed previously in technical memorandum nº 21, DIC was implemented during field demonstrations and revealed to have many benefits and limitations. Additionally, the limitations initiated more investigation of this method's processing algorithms and a more stable data collection system. The overall goal of additional investigation will allow for improvements on analysis of bridge health indicators at the global behavior level.

In previous tests, the 318.25 MTS 810 Material Test System was used for DIC measurements. This testing machine was implemented again to monitor movement with a PCB Piezotronics 333B50 piezoelectric accelerometer and transform (integrate) those readings into displacement. Measuring this data can enable a measurement of environmental noise (i.e., vibration or movement on the camera) that can be factored out to capture the true bridge movement measurement (see Figure 11).

In the previous set of tests as reported in technical memorandum nº 21, there was substantial noise encountered in the set due to environmental conditions. Using the MTS system, a known displacement measurement can be used and therefore an easier integration into displacement measurements can be obtained. The accelerometers were connected to a Campbell Scientific CR9000X measurement and control system in which results were collected, filtered through, and presented graphically. The results of this test showed us that this method can allow for movement tracking using accelerometer data and integrating into position (displaced movement) measurements. A sample of this acceleration data plot is shown in Figure 12. These plots show the data from the raw accelerometer measurements and the expected displacement measurements determined using a MATLAB algorithm. In Figure 13, the calculated displacement plot of the test data is shown with units of meters and seconds. The measured displacement graph reveals the sinusoidal wave that was expected as

the MTS system testing platform was moved in a cyclic motion for measurement comparisons. More investigation is being done to ensure the output data is correctly producing what is expected from the inputs. In this investigation, correct filtering procedures are evaluated as well as appropriate unit conversion. Both measurements are plotted versus the time.

Figure 11: Accelerometers on MTS testing machine.

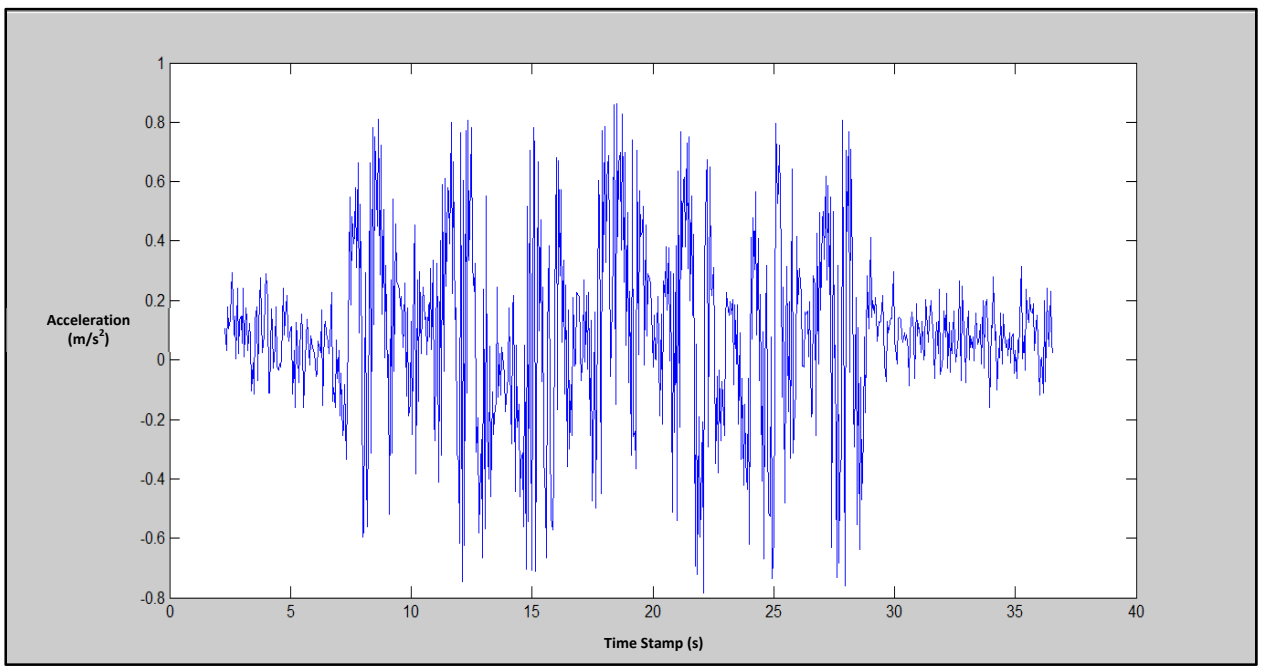

Figure 12: Plots of Acceleration and calculated displacement measurements.

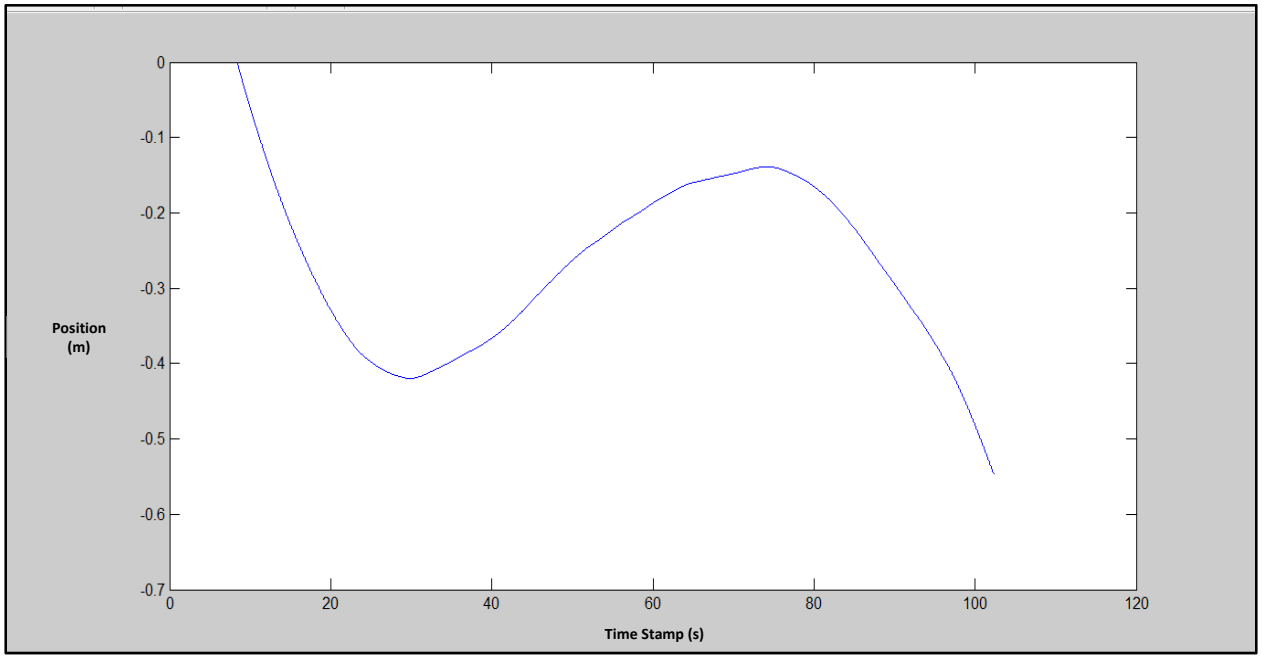

Figure 13: Plots of Acceleration and calculated displacement measurements.

As the generic method for capturing motion into displacement measurements on the MTS system, this was further configured for the camera-lens system. The camera-lens system (as used in DIC system) was connected with an accelerometer in order to measure the excessive movement endured and computed the movement as displacement. In this setup, a more stable and heavier surveying tripod as well as a wooden base ensuring a flat secure platform for the camera–lens system was employed. An additional accelerometer was also placed at the bottom of the tripod for location comparisons at the top and bottom of the tripod. These figures of the tripod and camera-lens setup can be shown in Figures 14 and 15.

The measurement of the camera movement(s) have shown similar results as in the testing system's data, but there were more unknown factors to consider in the acceleration measurement. The calculated position (displacement) measurement for this scenario reveals some alteration in what is expected and other parameters may have to be recognized in the setup and even in considering algorithms such as the input of the constant "c" values from the integration of the acceleration of the data (i.e., $\int$(acceleration) = velocity + "c" and similar in the integration of velocity for position) . This method allows for noise to be captured in measurements, but also may require an additional program to account for noise and other parameters associated with system inputs and obtaining correct bridge structure movement.

Moreover, stabilizing systems are being considered and should be implemented in the future. As an example, a gyroscopically-compensated camera mount, such as one of the Kenyon

Laboratories (<http://www.ken-lab.com/>), could help in keeping the camera stable and minimized movement within the camera-lens system. Reduction of the standoff distance would certainly reduce the effects of excessive wind and vibration on the camera-lens system.

Figures 14 & 15: Camera on stable tripod and detailed of mounted accelerometer.

Next Steps

The benefits of the DIC system definitely show great promise for bridge health indicators, but alterations in data collection procedures and in the analysis algorithms can improve the measurements. As mentioned, DIC is beneficial in allowing flexibility in testing location and use of available software analysis. However, the software analysis is dependent on the inputs of the testing system and calibration of the testing environment (in which noise will have to be considered). For the DIC method, a more integral algorithm is being investigated that would accurately tracked the movement using optical images that also will consider noise movement as previously mentioned. Depending on the software used for analysis whether it is commercial (Correlated Solutions Vic-2D) or not (MATLAB), more adjustments should be considered for accurate displacement measurements bearing in mind noise issues.

For future bridge comparison, a walking bridge (Figure 16) located in the Michigan Technological University (MTU) Benedict laboratory would provide a great case for

implementation for testing alterations and variations of the DIC system and developed algorithms. In addition, equipment instrumentation on the walking bridge would be complemented in the future test scheme.

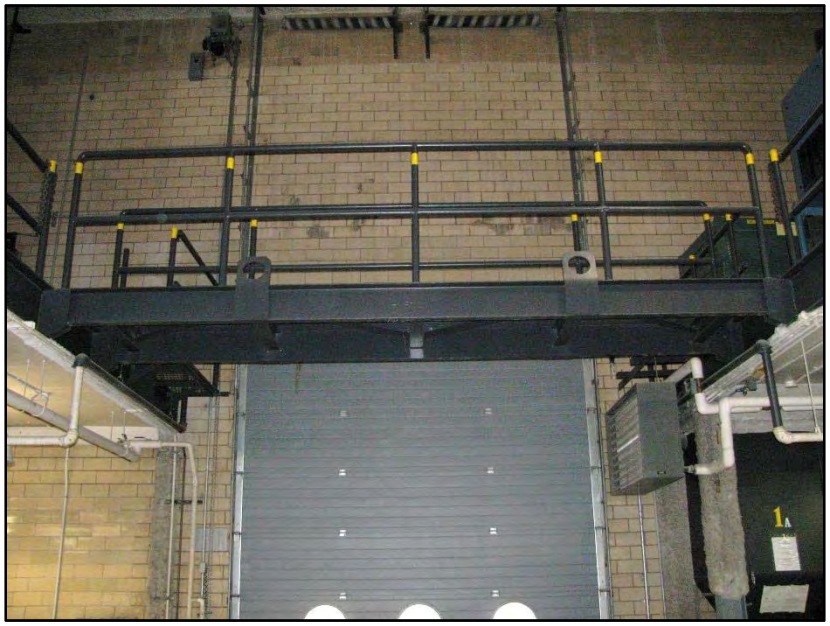

Figure 16: Walking bridge located in Benedict laboratory at MTU.

LIGHT DETECTING AND RANGING (LiDAR)

The remote sensing team has been focusing on extracting out useful bridge condition metrics out of the LiDAR scans of the study areas that were performed by an MDOT LiDAR crew (Kelvin Wixtrom and Shawn Roy) during the field campaigns in August, 2011 at Freer Road, Willow Road, and Mannsiding Road bridges (see Figure 17). Twenty scanner setups were performed at the Freer Road site, 18 setups were performed at Willow Road, and 12 setups each were performed for Mannsiding Road over northbound and southbound lanes of US-127. LiDAR scans were post processed by MDOT.

Certainty 3D TopoDOT, Applied Imagery Quick Terrain Modeler, and the University of North Carolina at Charlotte (UNC Charlotte) Light Detection and Ranging-based Bridge Evaluation (LiBE) surface damage detection algorithm were a few of the promising post-processing platforms under consideration. Currently, the majority of data refinement has been completed with TopoDOT. This was primarily due to the product's availability and prior understanding of the basic operating platform, Bentley MicroStation.

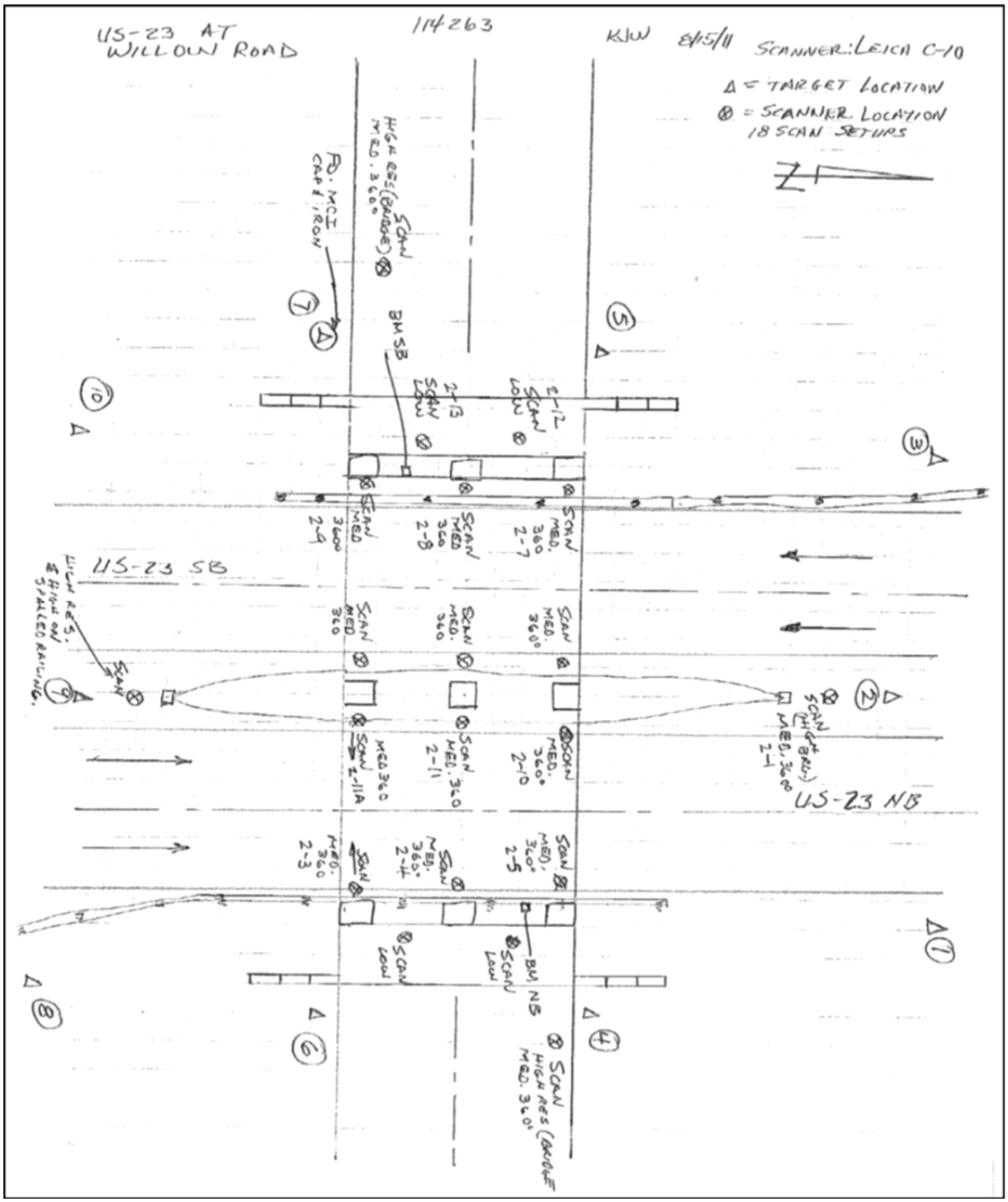

Figure 17: Field sketch for the LiDAR data collection made by the MDOT survey crew on the Willow Road bridge. The sketch documents the site configuration, scan locations, location of retro-reflectors and bench marks (used to register the individual scans to each other) and the resolution of the scans along with other information.

LiDAR data from setups at each site were merged together into a single registered and geo-referenced point cloud. The point cloud then was cropped to the area of interest (the bridge structures), reducing the file size and eliminating extra data. Attributes in the data include return intensity and elevation. MTRI staff has subset the data in order to analyze only the bridge deck surface and extract out condition information into separate LAS (Log ASCII Standard) files, such as the percent of the deck surface, underside, or support columns that are spalled.

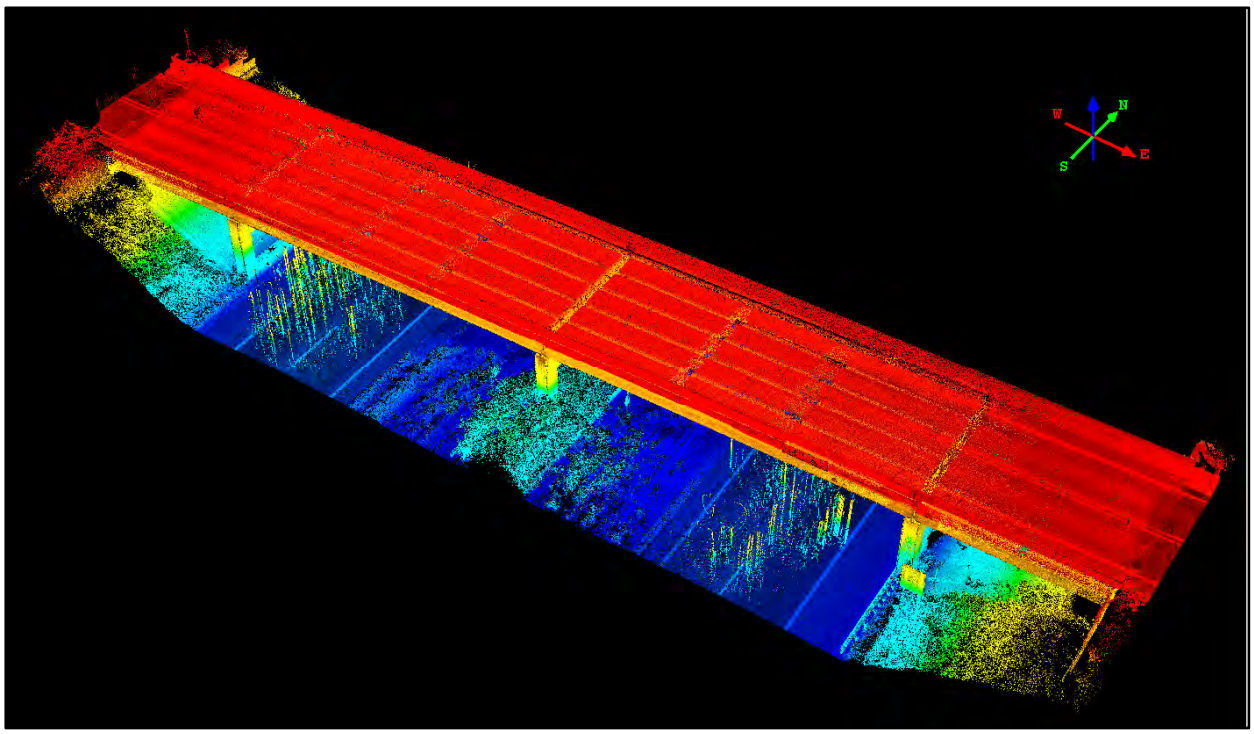

Figure 18: Registered, geo-referenced LiDAR point cloud of the Willow Road as collected by MDOT for this project. Point elevation (color) and intensity are displayed. This LiDAR point cloud contains more than 186 million points. The Willow Road bridge is approximately 209 ft long (63.7 m). Applied Imagery Quick Terrain Modeler software was used to generate the point clouds and DEMs.

Because the point clouds were so large, data collected at Willow Road bridge (and other sites) has been broken into subsets by bridge span to alleviate processing difficulties (see Figures 19, 20, and 21). Arch and crown in the bridge structure and deck may require sub-setting the data to separate the points on the bridge deck from the supporting structures. The quantity and location of the scanner setups can significantly affect the point density on the target surface. A point density image of the span of the Willow Road bridge over southbound US-23 shows the dramatic drop in point density with distance from the scanner, which was set up on the west approach of the bridge (see Figure 22).

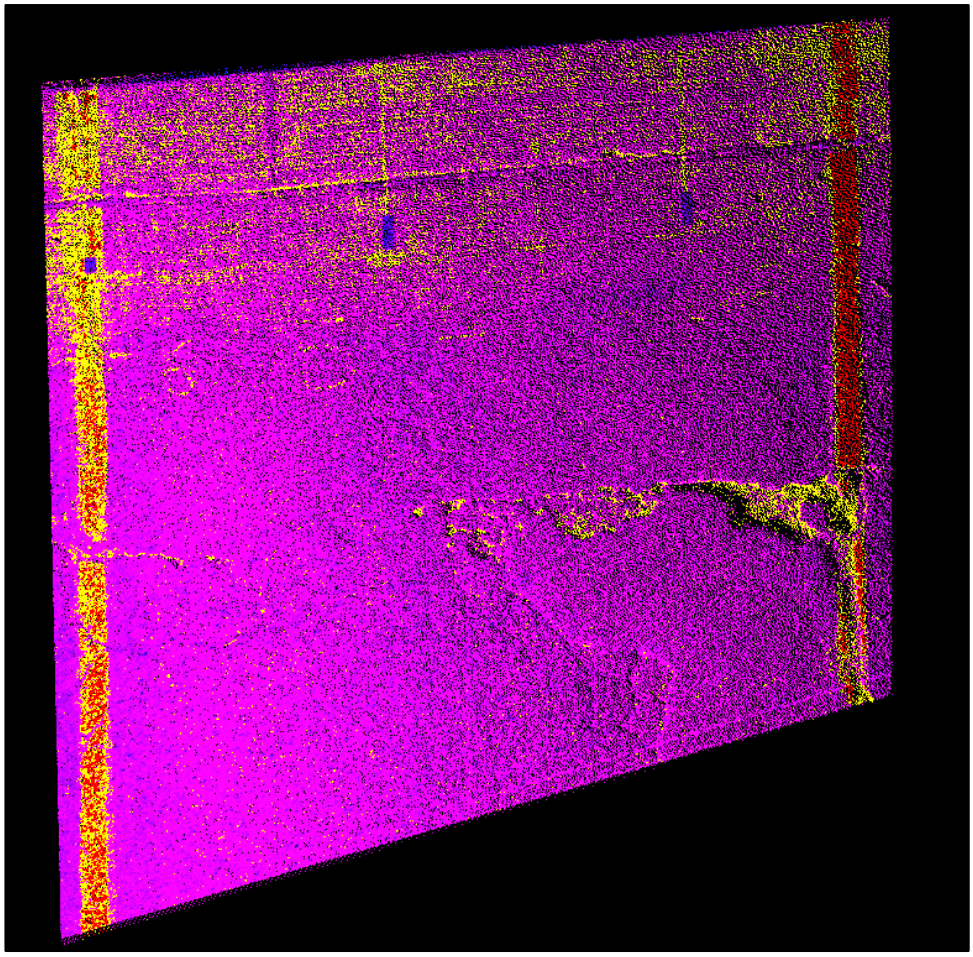

Figure 19: TopoDOT data of Willow Road bridge subset deck extraction, color intensity display.

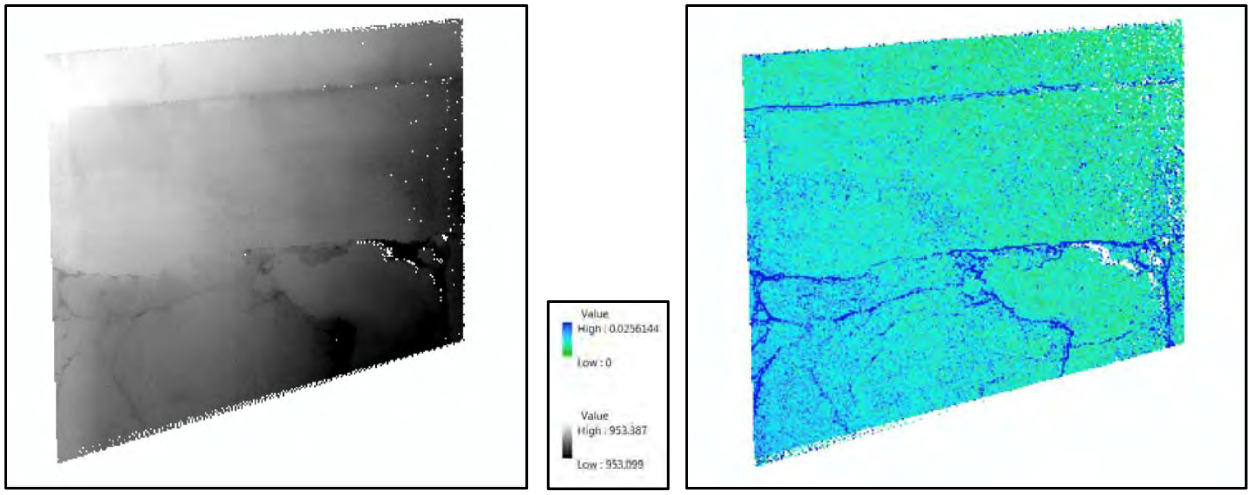

Figures 20 & 21: ArcGIS ArcMap Willow Road bridge subset deck DEM displaying point elevation (ft) and standard deviation from plane.

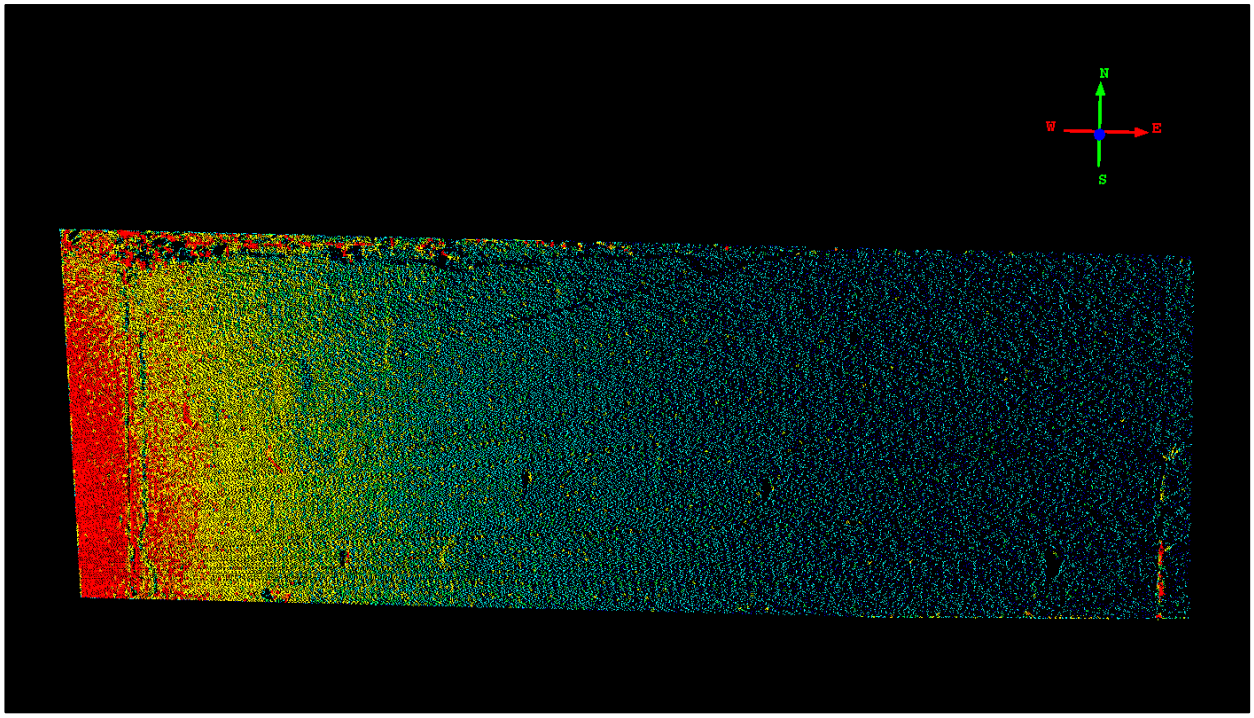

Figure 22: Point density image of Willow Road bridge span over southbound US-23. Note the dramatic fall-off in density of points from left to right (red to blue, high to low).

The color ramp is from red (high density) to blue (low density) which represents a range from approximately 25 points per 20 cm^2 (1.25 points/cm^2) grid cell to approximately 300 points per cell (15 points/cm^2). The distance between the LiDAR scanner and the left edge of this subset of the scan is approximately 50 ft (16.5 m). The scan resolution, slope of the surface to be scanned toward or away from the scanner and size of and distance to the features to be resolved are all important attributes to be considered when designing how many times and where the scanner is set up at a site. Potential shadowing and orientation of features to the scanner must be considered when placing the LiDAR scanner. Even small features can be affected by shadowing and scanner setup location should take that into account. Figure 22 is an example of the fall-off in point density as distance from the scanner increases. In this example, the scanner is approximately 51 ft from the left edge of the image. Features in the bridge deck that are closer to the scanner have a higher point density and can be more easily resolved than similar features further away from the scanner.

LiDAR returns usually include attributes such as RGB (red, green, and blue) and intensity (brightness) values in addition to X, Y, and Z location information. The MDOT LiDAR data processed here also contains 8 bit intensity information which is useful when interpreting the elevation data. Information about the relative reflectivity (intensity) of the bridge deck can be combined with color coded elevation data to provide clearer picture of the study area.

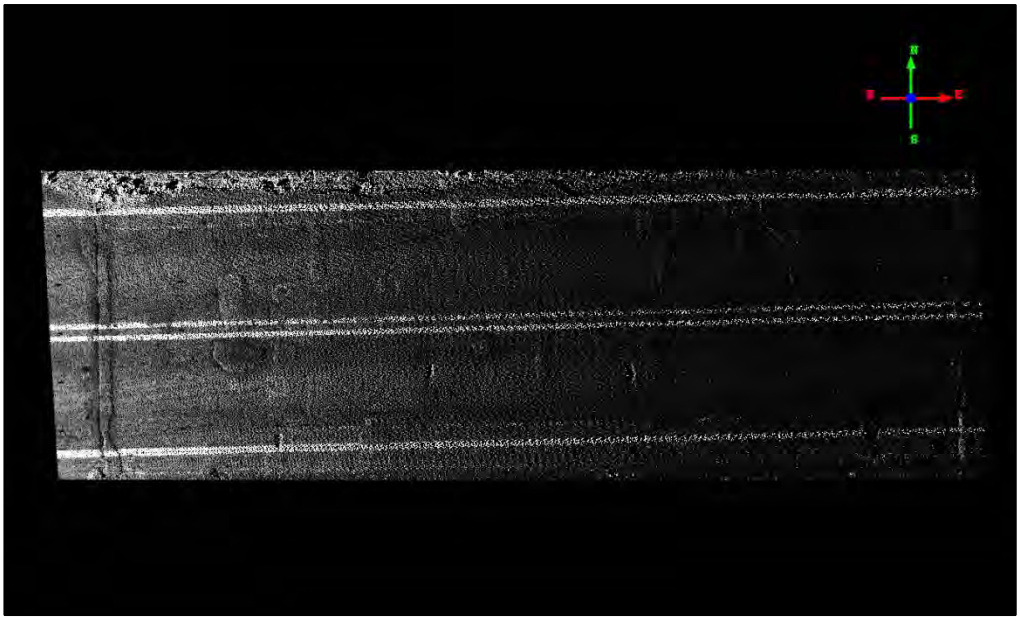

Figure 23: LiDAR intensity image of the Willow Road bridge span over southbound US-23.

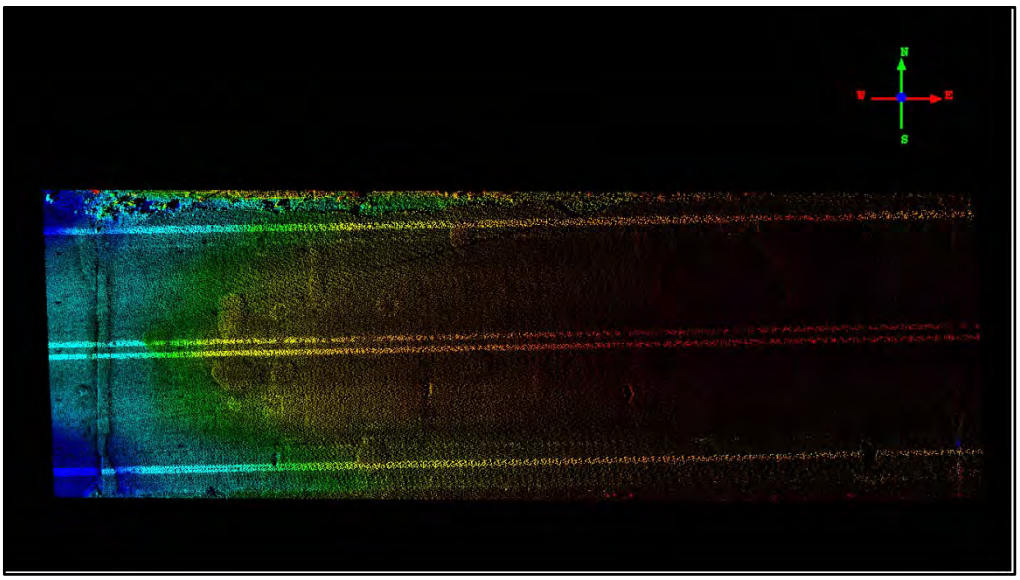

Figure 24: LiDAR intensity and elevation data displayed together provide a clearer picture of the condition of the bridge deck. This segment of the bridge deck is approximately 77 ft long. Total elevation change from left (low) to right (high) is 0.71 ft.

Deck specific information was then transferred into ArcGIS ArcMap, where the LAS file was converted to a working multipoint feature class, which allowed the user to build a terrain data set for the LiDAR points. From that working feature class the user was able to develop a DEM.

Currently, the DEM is being used as an input file for the spall detection algorithm. Figure 25 shows an example of highlighted defects (shown in red).

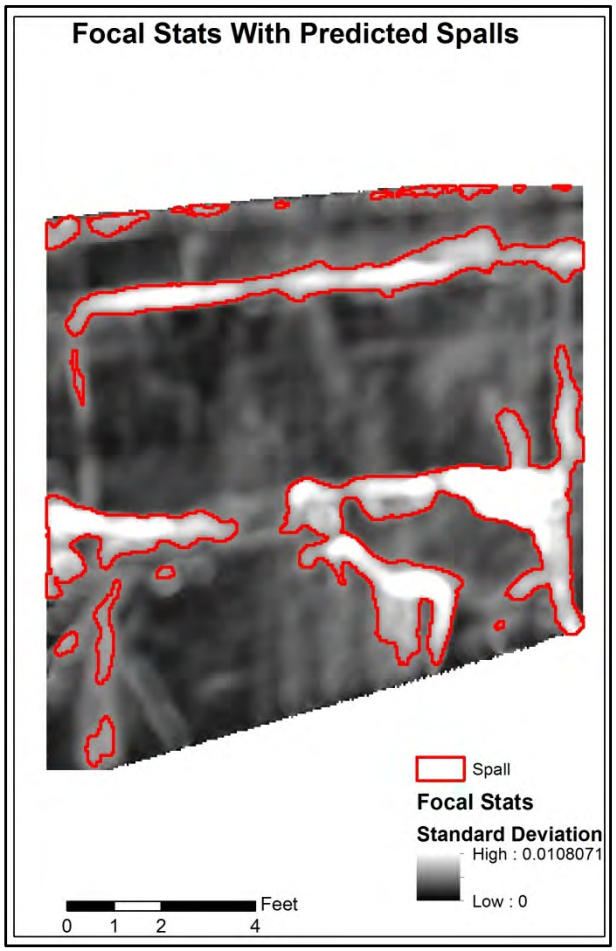

Figure 25: Willow Road subset deck focal statistic algorithm output highlighting predicted spall regions.

The DEM derived from the LiDAR data overlaid on ortho-photographs of the bridge is a useful technique to verify visual and quantitative analysis of the data. In this example a geo-referenced mosaic of bridge deck images captured by the 3DOBS system is used to help confirm the analysis of the deck condition seen in the LiDAR data. In Figures 26 and 27 patches made to the bridge deck that are not flush with the existing deck can be seen (arrows) as areas of slightly higher elevation. A spall can also be seen in Figures 26 and 27 as an area somewhat lower in height than the surrounding bridge deck. The patches are 0.25-to-0.625 in (0.635-to-1.59 cm) higher than the surrounding bridge deck and the spall at its deepest point is about 0.375 (0.953 cm) deep.

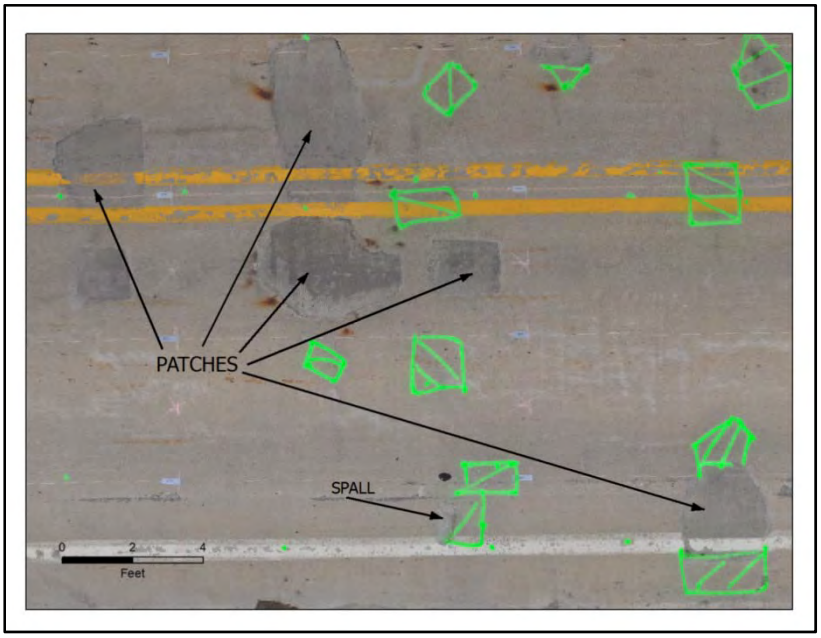

Figure 26: Section of the ortho-photo of the Willow Road bridge deck illustrating patches and a spall. The green pavement markings outline areas of subsurface delamination as determined by sounding performed by MDOT bridge inspectors with the hammer (rod) sounding technique.

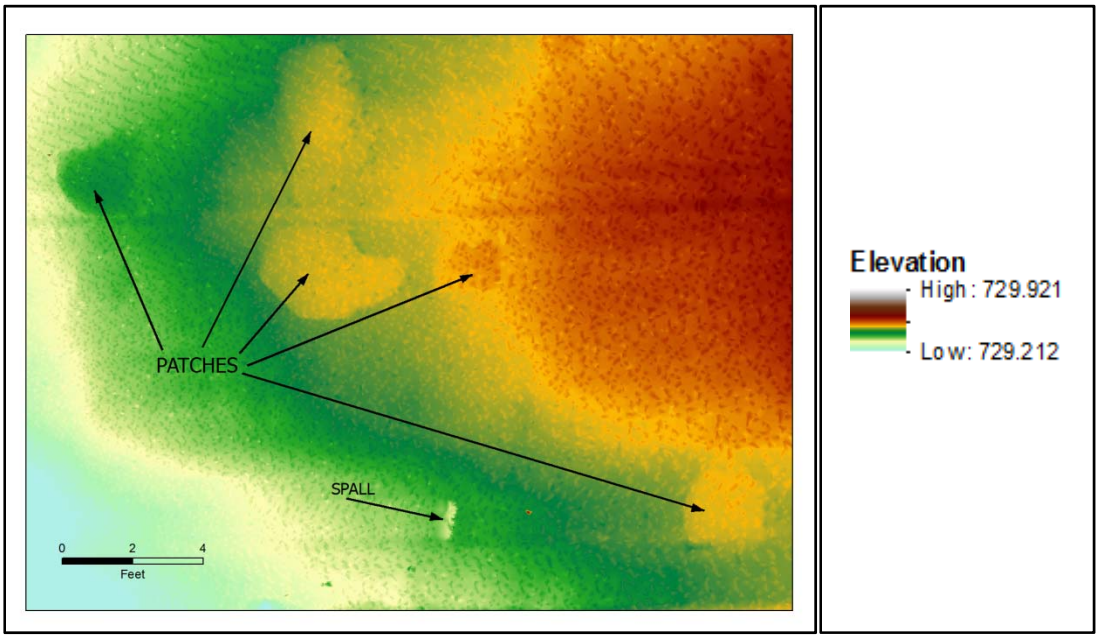

Figure 27: DEM with a color ramp applied of the same area of the Willow Road bridge deck. Note that the higher areas of the concrete patches and missing material from the spall correlate well between the ortho-photo and DEM. The patches (correctly) appear higher than the surrounding bridge deck and the spall appears lower than surrounding deck.

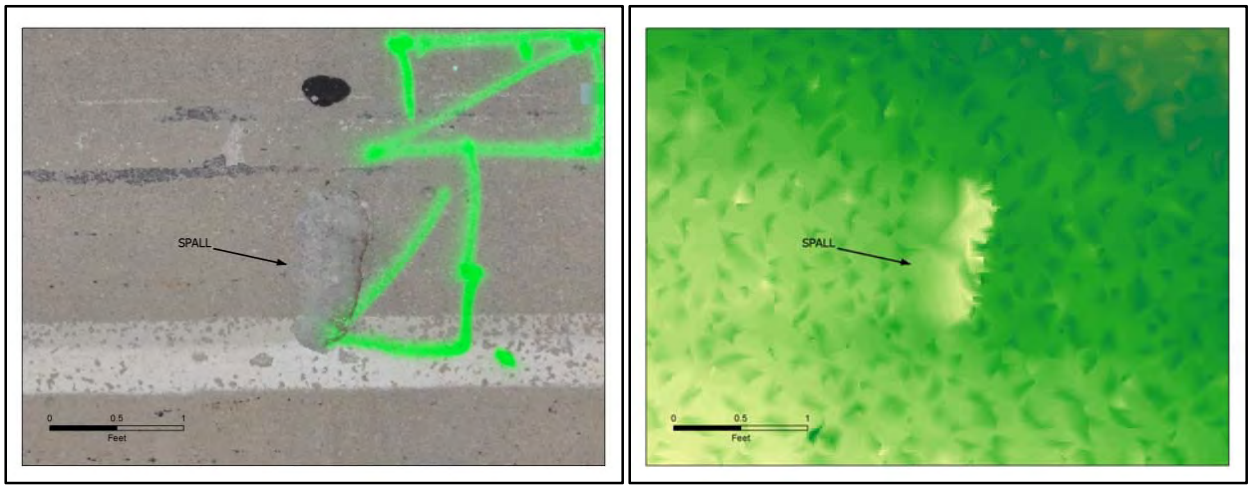

Figure 28: Close up of the spall on the Willow Road bridge deck. The spall is clearly visible in the ortho-photo as well as in the DEM (the light yellow color is lower than the green).

Next Steps

For LiDAR data processing, the next step is to take the DEMs of sections of the bridge deck that have been exported and process them in the 3DOBS spall detection algorithm. Adjustments to the DEMs will be made based on the results of the processing until the best possible result is obtained during the next quarter.

As it has been mentioned in technical memorandums nº 20 and nº 21, LiDAR is a line of sight instrument and requires repositioning to illuminate shadowed areas, increasing collection time and required labor. The line-of-sight issue meant for the terrestrial LiDAR system used by MDOT, areas further away from the collection point were characterized with fewer points. A mobile LiDAR system could address such an issue, although mobile LiDAR systems generally have lower overall accuracy capabilities than fixed terrestrial LiDAR systems, at least compared to areas near the fixed LiDAR system itself. Mobile LiDAR has the potential to reduce the collection time and increase the resolution as discussed in technical memorandum nº 21. Surveying Solutions (<http://www.ssi-mi.com/>) has scanned the I-96 and US-23 interchange in southeast Michigan using mobile LiDAR and MTRI is in the process of acquiring that dataset. The resolution and coverage of the dataset is unknown at this time; however, once acquired, the data will be assessed in a similar manner to the terrestrial LiDAR for its potential as a tool for bridge condition assessment.

As results of processing of DEMs are evaluated, a recommended LiDAR data collection and processing workflow will be developed to create the final condition metric, which is anticipated to be at least the percent spalled area of the bridge deck surfaces. Because the terrestrial LiDAR system can be positioned almost anywhere near or under a bridge (which was demonstrated during MDOT's data collection), it may be possible to characterize the number and volume of spalls in other parts of the bridge infrastructure as well, such as bridge piers and the deck underside. This is being investigated in the next quarter.

The high-resolution elevation profile created through the 3DOBS is an alternative to intensive LiDAR data collection and analysis process; it creates consistent, high resolution data across the entire deck surface without the need for a mobile or fixed LiDAR system. An evaluation (both technical and economic) of LiDAR elevation data versus the 3DOBS elevation data in creating useful bridge condition data is expected to be a very useful outcome of this project.

ULTRA WIDE BAND IMAGING RADAR SYSTEM (UWBIRS)

Most commercially available ground penetrating radar (GPR) systems for bridge deck assessment use arrays of antennas pointed perpendicular to the deck to probe the subsurface. As noted in the Commercial Sensor Evaluation report (<http://www.mtri.org/bridgecondition/doc/RITA_BCRS_Commercial_Sensor_Evaluation.pdf>), these systems can sense subsurface defects, but can require substantial time to survey the deck. These commercial systems can provide output products for use in the DSS, such as the location of delaminations. To potentially improve data collection efficiency, the current project has been investigating the idea of using side-looking, low cost ultra wide band imaging GPR, now referred to as UWBIRS. This type of collection is consistent with a concept of operation that has a radar system mounted on a moving vehicle to produce maps of deck radar reflectivity that identify areas of concern. This type of collection could also be performed by a standoff airborne sensor. An issue with this approach is whether or not the subsurface deck defects will be uniquely indicated when the deck is illuminated obliquely by the radar.

Side-looking imaging GPR measurements of concrete bridge decks were conducted in August, 2011 as part of the field demonstrations. Specifically, data were collected at the Freer Road bridge and the Willow Road bridge. The field measurements and radar equipment were recently well summarized in technical memorandum nº 21. In the 2D imaging modality, the radar sensor obliquely illuminated the bridge deck surface as it was moved along a linear path parallel to the deck surface. This type of data collect produces a 2D map of the radar reflectivity of the deck, which may indicate areas of internal defect and/or delamination. The deck measurements at

the Freer Road bridge were repeated on December, 2011 to fill in some missing data areas from the earlier August, 2011 collect.

The primary activity during the reporting period was to processed the collected radar data into radar images, geo-reference the images so that they could be displayed with other sensor products in the DSS, and finally compare the images to polygon overlays that indicate potential delamination areas, which were identified by MDOT using the hammer sounding technique during the August, 2011 data collection. Images of the two lanes of the Willow Road bridge deck when calibration reflectors were placed in the scene are shown in Figure 29 with potential delamination sites from the ground truth survey overlaid. It is these types of analyzed radar results that the project team has been planning to integrate into the DSS to show where radar has detected these likely delamination results, as well as the locations and percent of delamination. These data would contribute to the overall bridge health signature being developed for this project.

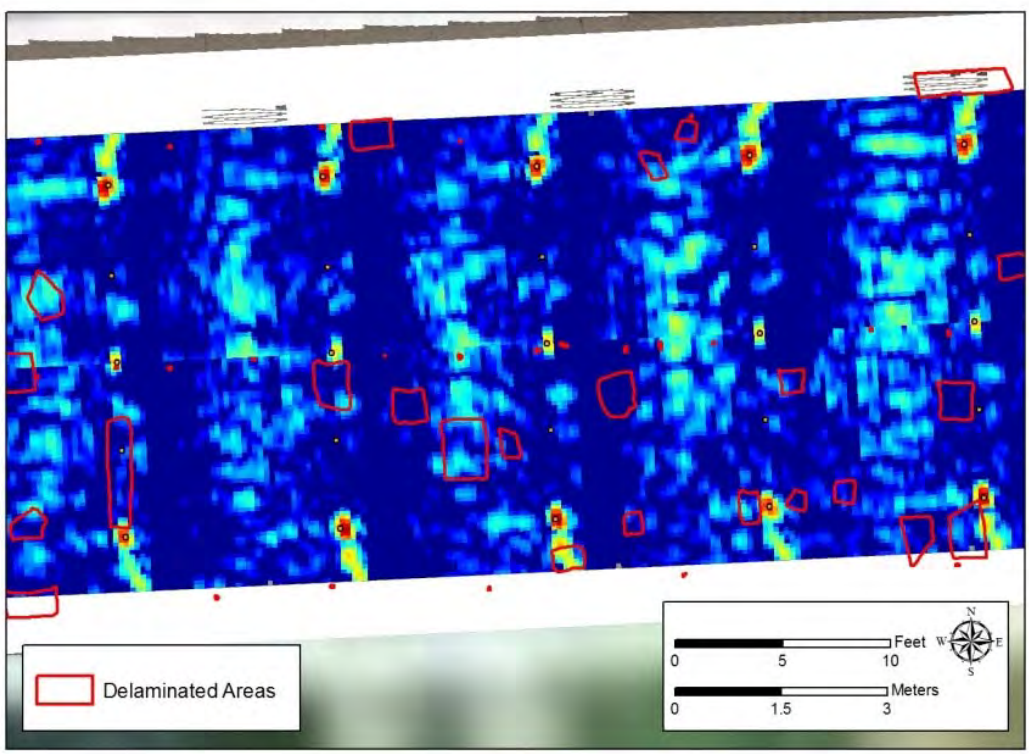

Figure 29: Radar image of Willow Road bridge deck with delamination areas indicated by red polygons.

Next Steps

Even though the side looking GPR images show variation that is likely due to variation in the bridge structure, an initial qualitative comparison of the side looking GPR images with the delamination ground truth suggests that the high return areas in the radar images do not uniquely identify the delamination areas. This preliminary result suggests that a limitation of obliquely illuminating the bridge deck is that near surface delaminations cannot be uniquely separated from other variations in the bridge substructure. The next step in the analysis will be to quantitatively compare the variations in the radar images to the ground truth information in order to evaluate the utility of the radar data and system for deck assessment. The team also plans to investigate the use of alternate imaging parameters and/or post-processing to enhance measurement performance.

UWBGPR data from conventional commercially available systems can provide delamination information for use in the DSS, albeit at the cost of more data collection time, even if the side-looking concept investigated through this project does not prove viable. The Commercial Sensor Evaluation noted the HERMES system (Scott et al. 2001 at <http://www.fhwa.dot.gov/publications/research/nde/pdfs/01090.pdf> and <https://www.llnl.gov/str/Hernandez.html>), described as the "bridge diagnosis at 55 mph" system focused on delamination detection.

A related system is the Roadscanners commercial GPR data analysis system, which characterizes bridge decks including areas of subsurface deterioration (see <http://www.roadscanners.com/uploads/PDF/Bridge_web.pdf>). Based on these descriptions the Roadscanners system and of HERMES and its successor, the PERES Bridge Inspector (<http://ntl.bts.gov/DOCS/peres.htm >), the project team anticipates that data from such a system could provide the needed delamination data for inclusion in the DSS. As a next step, the project team is pursuing contacts with the HERMES/PERES team at FHWA and Lawrence Livermore National Lab and Roadscanners to see if a representative delamination data set could be shared to serve as a firm example of the type of result that could be included in the DSS.

ADDITIONAL TECHNOLOGIES UNDER EVALUATION

During the past quarter, major additional work was not pursued for the "additional technologies" of using Synthetic Aperture Radar (SAR) for evaluating the inside of concrete box beams, using Interferometric Synthetic Aperture Radar (InSAR) for bridge deck settlement, using InSAR data for deck condition, and using Multispectral Satellite Imagery (MSI) for bridge deck condition evaluation.

Instead, the team focused on the main technologies such as the 3DOBS, ThIR, DIC, LiDAR, and the UWBIRS. The project team expects to conclude and write up these additional technology investigations during the next quarter.

DECISION SUPPORT SYSTEM (DSS)

Since the last quarterly report, a number of improvements have been made to the DSS and development is ready to focus on the last major feature, the integration of remote sensing data, before testing and mobile app versioning. These include refactoring the server-side data models based on the Pontis schema, importing data from MDOT's Transportation Management System (TMS), and the utilization of new bridge information derived from remote sensing in the DSS through new features.

Migration to the Pontis Database Schema

A few months ago, the DSS team gained direct read access to MDOT's TMS database, an Oracle database based, in part, on the Pontis schema. When DSS development began in March, 2011, MTRI only had partial database exports shared by MDOT to use in designing the server and database schema. As a result, the schema that was developed and much of the client-side architecture were based on a data model that MDOT bridge managers and inspectors were used to working with. This data model was also amenable to visualization in a Geographic Information System (GIS), a planned feature for the DSS.

The DSS team members have since decided, however, that this data model, while amenable to geo-spatial visualization, is not as flexible, extensible and informative to end users as it ought to be. In particular, this data model could not answer questions such as "*How does, for instance, the Texas Department of Transportation load their bridge data into the DSS?*" and, more generally, "*How would transportation agencies in other states make sense of bridge data in the DSS?*" Furthermore, this data model limited attempts to update the DSS with new bridge condition information. The DSS team had intended to accomplish this through regular data exports from TMS. However, without the queries used by MDOT employees to generate the tables the DSS team had based our data model on, it was not practical to export usable data from the TMS. Consequently, the DSS would go without updates.

As being able to have frequently updated bridge condition information is important even for a demonstration tool, the DSS team decided a data model consistent with the TMS was needed. Within Pontis, the National Bridge Inspection System (NBIS) lays out a national standard for

storing bridge inspection data and bridge metadata. The TMS database uses this standard for its relevant bridge tables. To facilitate quick DSS updates from the TMS database, the DSS team decided to modify its initial data models to match that of the bridge tables in the TMS.

There are always challenges to redesigning a database schema, particularly relatively late in the life of a software project using a database application programming interface (API). Many technical challenges arose simply because the DSS and the full TMS database use different database management systems (DBMS); the DSS is based on a flexible, open source PostgreSQL database while TMS uses an Oracle database. The most fundamental obstacle this posed was that it prevented the DSS from reading the TMS database directly: data would have to be exported form the TMS and inserted into our database. Different DBMSs led to irreconcilable differences between the TMS database schema and what would eventually be used in the DSS, such as the lack of a distinction between *null* and *blank* fields in Oracle, differing data types, and the implication of foreign keys in the TMS database that are never actually used. Overall, these differences are relatively trivial obstacles. However, the most serious and persistent obstacle for development of effective data models of bridge condition was the mismatch between the representation of data in the application (front-end) and service (back-end) layers. This mismatch is often referred to as *object-relational impedance mismatch* because it arises when object-oriented frameworks, such as the Ext JS framework used to develop the client-side web application and the Python language used to support server programming, are used in conjunction with relational databases.

The DSS was designed to represent the latest condition information for multiple bridges at a time using bridge attributes such as facility carried, latitude, and longitude. In the TMS, under the Pontis schema, condition information and bridge attributes are stored in different tables which are not related. This requires the developer to make a decision about how the DSS will access the information stored in both tables quickly (whenever users make a query) and comprehensively. The DSS team realized there were only two practical solutions: run the "*What's the latest condition of each bridge?*" query in real time, every time, or create an intermediate table to store this query. The former would be slow and expensive but the latter would store redundant data in the database. The DSS team decided to create an intermediate table because its contents would need to be accessed too frequently to justify the expensive calculations involved in a *virtual table* created from querying the database in real time.

New Bridge Attributes and the Value Added

Despite the aforementioned obstacles, migrating to the Pontis schema enables new, meaningful and up-to-date bridge attributes to be exposed through the DSS, and leads to a

system that could be used across multiple states for bridge condition assessment. In the original small MDOT bridge data export, even simple attributes like the county a bridge is located in were not available (since it was not part of the data exports given to us) before data from TMS were integrated. These new attributes led to the development of a new feature: attribute tables for each bridge (Figure 30). These tables correspond to the new tables available from Pontis. While most of the information they contain is unnecessary or inappropriate to display in the metrics table to the left, it is still extremely valuable and of interest to the bridge manager or inspector. Accessing these data through an *attribute table* is a workflow borrowed from GIS that seems very appropriate when the user is capable of visualizing up to 12,000 bridges.

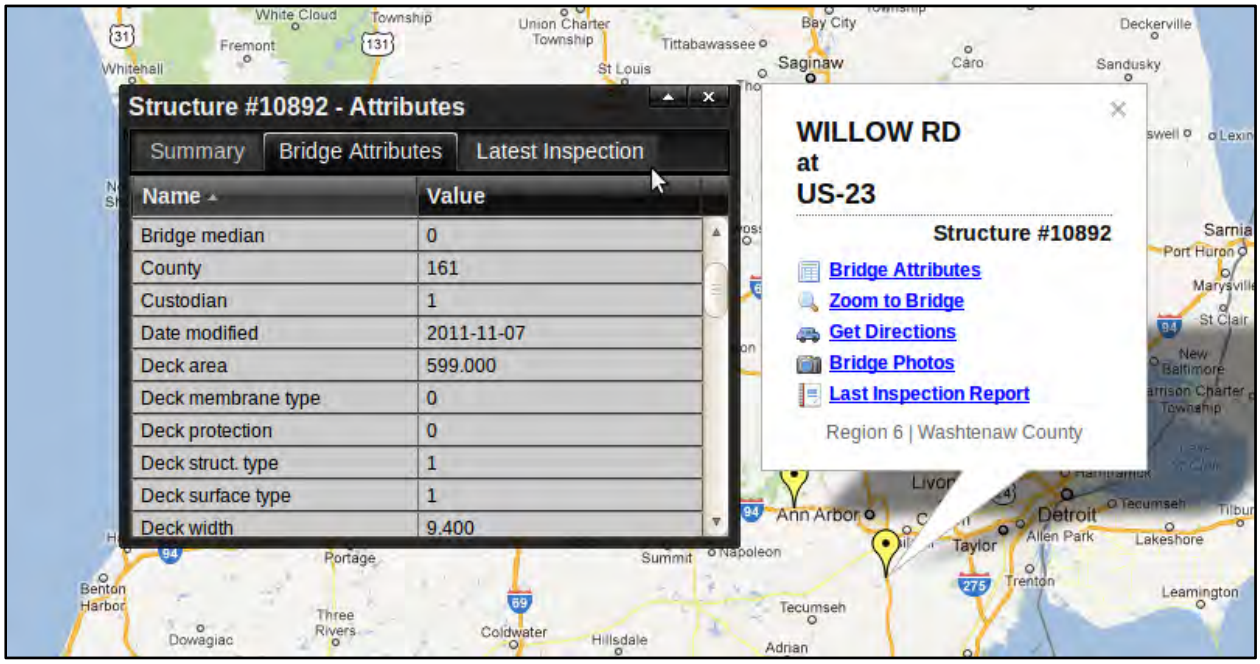

Figure 30: Migrating to the Pontis schema has made new data available; though in separate tables, they can be accessed individually through the "Bridge Attributes" utility.

In addition to the "Bridge Attributes" table, a link to the "Bridge Photos" utility is also now available through the DSS' Bridge GIS plane. The "Bridge Photos" utility displays location-tagged photographs of the bridge deck, approach and underside that were taken with the BVRCS. These photos are displayed both as thumbnails and a points layer in Bridge GIS showing the position from which they were taken (Figure 31). A full-resolution version of the geo-referenced photos is available through both.

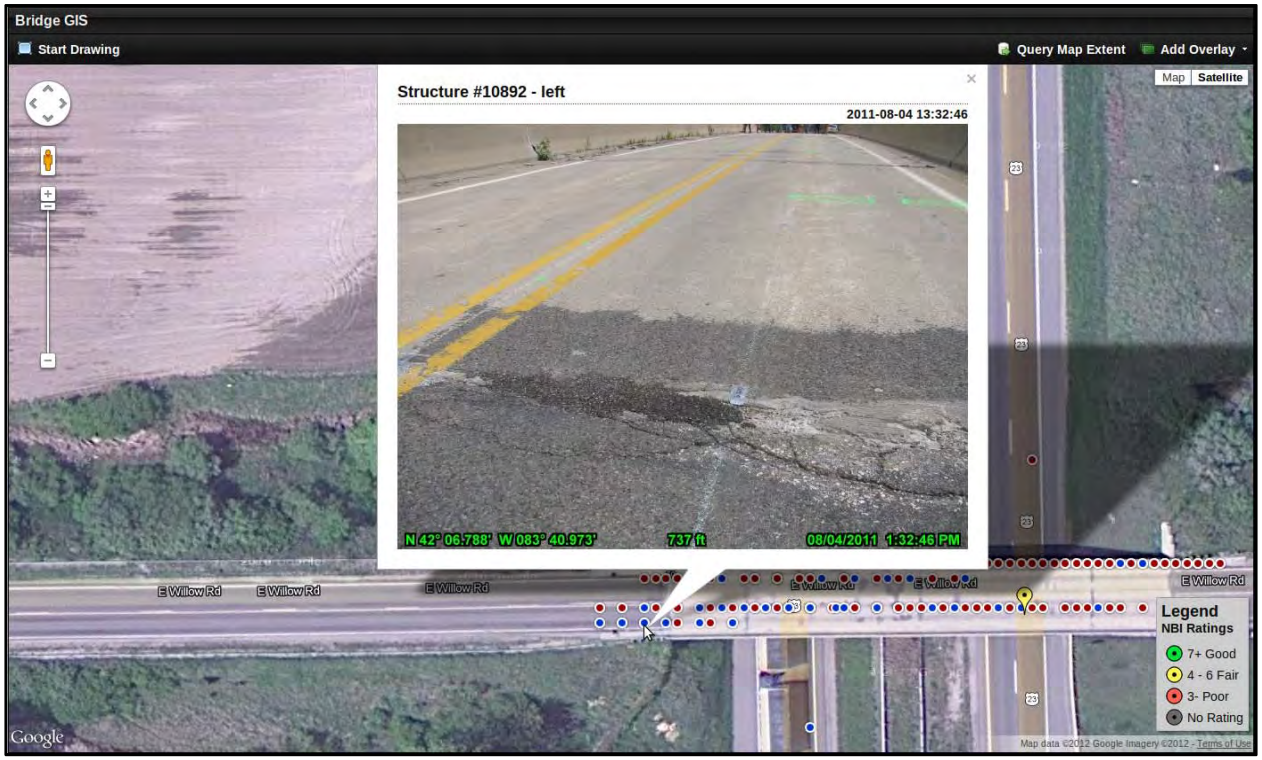

Figure 31: Geo-tagged photographs from the BVRCS are available as a Points layer in Bridge GIS; clicking on a point shows you the photograph taken there.

Integrating Data and Deriving the Bridge Condition Signature

The next major phase of the DSS development has begun with the integration of the remote sensing data like the BVRCS photographs. These photos are an example of a "points" layer representation of remote sensing inputs for bridge condition. Other examples can be seen in the concept diagram, Figure 32, including examples of "polygon" datasets (such as areas of spalls collected by the 3DOBS) and extremely high-resolution georeferenced composite images of the deck surfaces (also created through the 3DOBS). This refers to how these datasets will be represented in the DSS. The more important question, however, is how will these datasets be integrated with each other and important metrics of bridge condition derived from them?

The summary data (Figure 32) the project team can now expect to derive from bridge remote sensing data include the percent spalled, the percent delaminated, the roughness (as an IRI score), and potentially crack density and count. Deflection amount and settlement may be possible to integrate depending on final remote sensing results. These should be related to NBI condition indicators wherever possible, such as the amount of spalling that results in a certain NBI rating. These will be integrated in what has been referred to from the project's beginning as

the bridge condition *signature*. An example formula to derive such a notion for a bridge deck surface rating (BDSR) is given below, where "a, b, c, and d" are user-defined weights:

$$BDSR = a \cdot [\%\ spalled] + b \cdot [\%\ delamination] + c \cdot [roughness\ index] + d \cdot [crack\ density]$$

Next Steps

With the remote sensing technologies producing results such as percent spalled, percent delaminated, and bridge deck roughness, the project has reached the intended stage of integration-usable indicators of bridge condition into a decision support system. This is a critical step to having an overall bridge condition assessment system (technologies plus the DSS) that is practical to use by transportation agencies. The next Quarterly Report will update the team's progress on reaching this important project milestone.

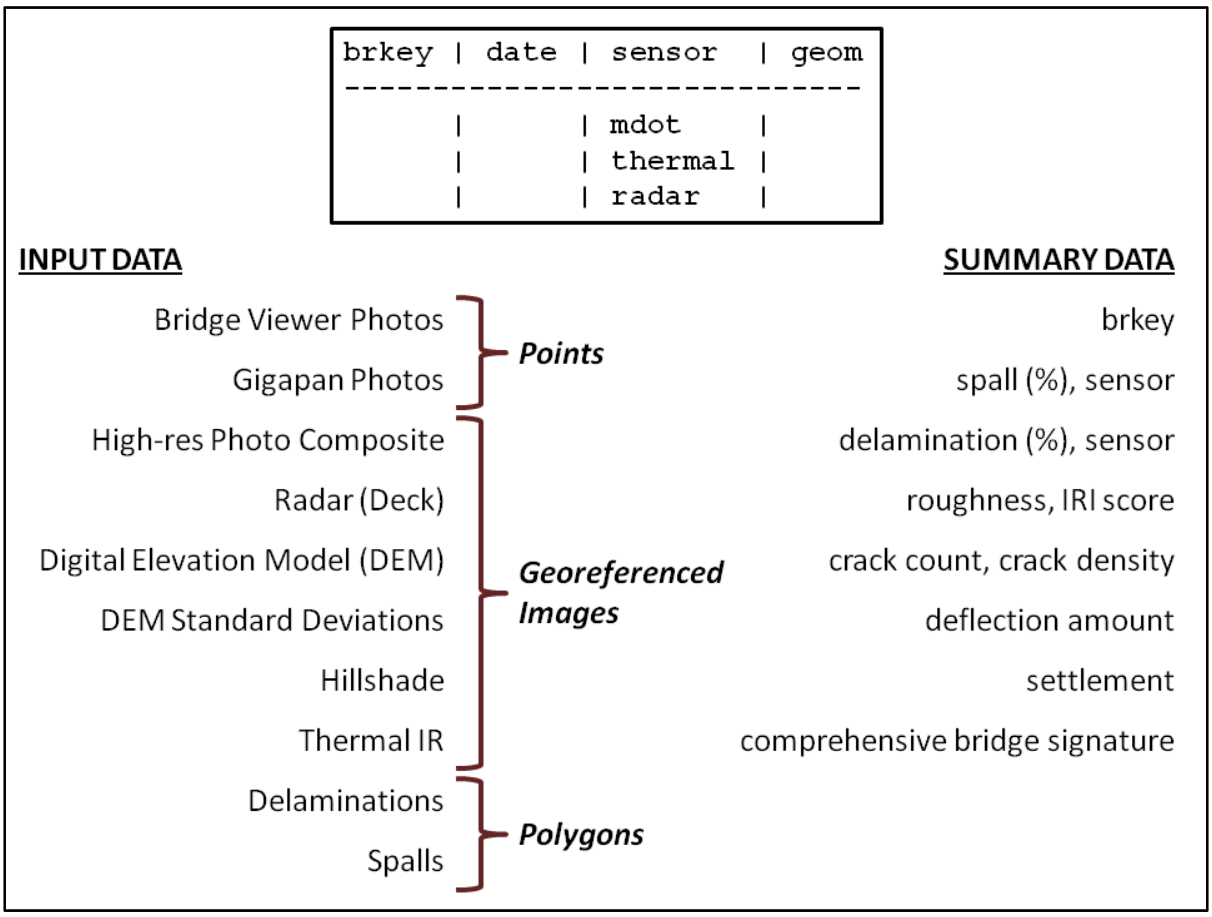

Figure 32: Concept diagram for remote sensing datasets and their role in the DSS.

REFERENCES

Scott, Michael, Ali Rezaizadeh, Mark Moore. 2001. Phenomenology Study of HERMES Ground Penetrating Radar Technology for Detection and Identification of Common Bridge Deck Features. FHWA Report No. FHWA-RD-01-090, Turner-Fairbank Highway Research Center, 33 pgs. Retrieved at <http://www.fhwa.dot.gov/publications/research/nde/pdfs/01090.pdf>.

Memo

To: T. Ahlborn, D. Harris, L. Sutter, R. Shuchman, and rest of Project Team

From: Q. Hong, R. Wallace, M. Forster, C. Brooks, A. Endsley, H. de Melo e Silva

CC: C. Singh

Date: January 13, 2012

Number: 25

Subject: Project Progress Update on the Economic Valuation of Technologies and Decision Support System for Bridge Condition Assessment.

In technical memorandum nº 22, the Bridge Condition Assessment Using Remote Sensors (BCAURS) team summarized research findings related to the national bridge program in the context of shrinking transportation revenue, current bridge inspection practices and cost estimates, field cost data collection using remote sensing technologies, and outcomes of the Michigan Department of Transportation (MDOT) stakeholder interviews (available at <http://www.mtri.org/bridgecondition/Tasks_and_Deliverables.html>). Since then, our major activities in Quarter 8 (September-December, 2011) for Task 6 focused on (1) reviewing economic evaluation methods, (2) estimating costs of using remote sensing technologies, (3) estimating costs to road users, and (4) documenting costs of bridge scoping. This memorandum contains a brief summary of each of these four activities.

ECONOMIC EVALUATION METHODS

The decision to integrate remote sensing technologies into bridge inspection practices can be viewed as an investment strategy for both the public and private sectors. The economic indices (e.g., capital and operational costs) are critical for quantifying and qualifying the ability of the proposed new technologies to meet the functional and operational needs of the bridge inspection process. Therefore, a high quality economic evaluation should provide "value for money" information to those making decisions about the investment of new technologies and the allocation of limited bridge inspection resources.

While the resulting information is of value to practitioners and researcher alike, the economic evaluation of remote sensing technologies tends to be very complex, because the task of

evaluation involves determining the value of rapidly evolving technologies or products (both hardware and software) in an environment in which market data from real-world practices is very limited. Second, the outcome indicators of traditional bridge inspections and those derived from using remote sensing technologies are not always identical; thus, it is often difficult to create head-to-head comparisons.

For example, some remote sensing technologies are creating higher-resolution indicators of bridge condition than have traditionally been available to transportation agencies, such as the bridge deck digital elevation model (DEM) created through the 3D Optical Bridge-evaluation System (3DOBS). Third, the benefits of using remote sensing technologies and the associated Decision Support System (DSS) are not easily assigned a monetary value without linking them to a broader context, such as life-cycle cost of bridge analysis and the benefits of optimized bridge management system.

The Center for Automotive Research (CAR) team reviewed various economic evaluation techniques, including cost-utility analysis (CUA), cost-effectiveness analysis (CEA), cost-minimization analysis (CMA), cost-benefit analysis (CBA) and cost-consequence analysis (CCA). None of these techniques is absolutely perfect for application to the bridge condition assessment using remote sensors context due to the unique research questions raised, the condition of interest, and the availability of data on outcomes.

To address these challenges, the CAR research team will rely on the BCAUR team's technical assessment of each technology, a second set of interviews with MDOT stakeholders, previous research findings, and field cost collection, as well as a forecast of field costs once tested technologies have been incorporated into a standard concepts of operations (CON-OPS) for bridge assessment to develop application scenarios and conduct relative cost analysis, similar to what the cost would be once these technologies were implemented on a commercial basis. During the analysis process, the team intends to highlight the factors explored below that will influence our final evaluation approaches.

Adoption Curve

The adoption of new technology tends to follow similar patterns, and this can be expected to apply to bridge condition assessment technology as well. Thus, these technologies are likely to be adopted over time following familiar patterns, such as the one shown in Figure 1 based on theoretical models for the diffusion of innovations. This general model, of course, leaves open the questions of how many users at the top of the curve and the length of the uptake time needed to reach the peak.

Time Period of Analysis

The time period for an economic evaluation should maximize the anticipated economic efficiency of the alternatives. The capital costs should be spread over their economic life (e.g., 10 years or longer, depending on the technology). To a large extent, the time period will be determined by the technical or functional obsolescence of a product, especially when new products become available on the market. Considering the rapid development of sensing and communication technologies, the equipment replacement frequency could be as short as a few years; this frequency can be longer when transportation agencies make use of purchased technology for as long as possible in budget-limited environments. We will develop several different time-period options based on technological and equipment types, such as 5 years, 10 years, and 15 years.

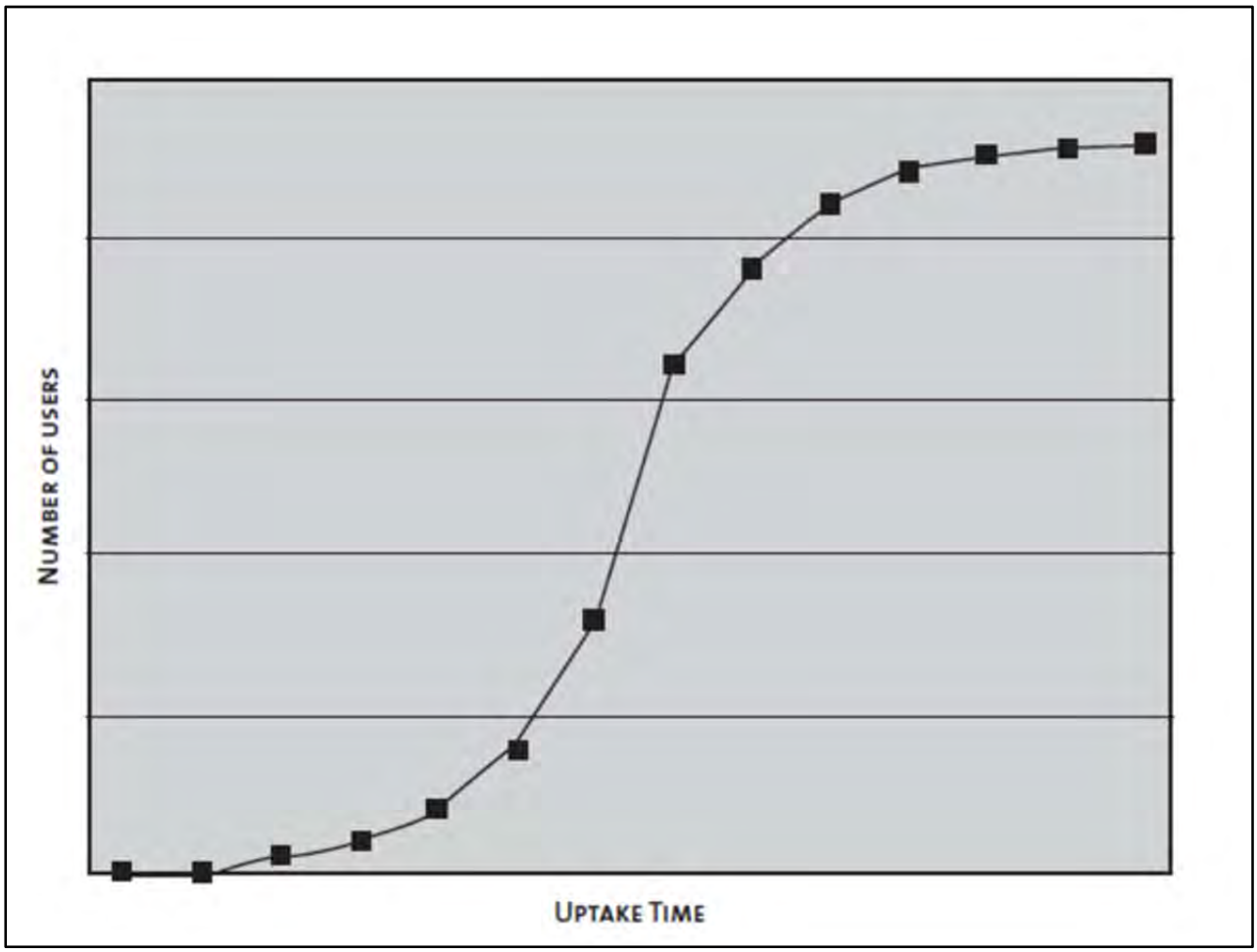

Figure 1: Generalized adoption curve for a new product or technology. Source: Robert H. Potter, Technology Valuation: An Introduction <http://www.iphandbook.org/handbook/ch09/p02/>, 2007.

Geographic Scope of the Analysis

The area included in the analysis will be the State of Michigan, which has 4,465 state-owned National Bridge Inventory (NBI) length bridges and 6,500 local NBI-length bridges. As new bridge condition assessment technologies are adopted, we can expect them to be applied to more and more bridges over time related to the adoption rate discussed previously. We can also assess the potential for broad deployment in adjacent states, such as Indiana, Illinois, Wisconsin, and Ohio, to reduce marginal costs. This latter approach is particularly useful if the likely CON-OPS is for departments of transportation (DOTs) to contract out remote sensing services for bridge condition assessment, as needed, rather than engage in an outright purchase of hardware. DOTs frequently contract out current remote sensing data needs, such as high-resolution aerial photography collection and LiDAR data collection, from commercial services firms such as Woolpert (<http://www.woolpert.com/>) and Aerocon (<http://www.aerocon.com/>), and may choose to do so for new remote sensing technologies as well. These two possibilities – to purchase hardware or to purchase services – may well be the most important distinction in developing the CON-OPS; and the recommended option may vary by technology.

CALCULATION OF COSTS

Many factors must be considered during the process of estimating the costs of using remote sensing technologies, such as technology costs (e.g., equipment and or hardware), labor costs (e.g., operation of sensors, analysis of data), software costs (e.g., needed analytic tools), scheduled maintenance of equipment and hardware, additional costs for data storage and transfer, and road user costs due to traffic disruption.

Some of the above cost elements are relatively straightforward to be measured based on available market data and our field demonstration cost data collection efforts. Other ones with greater uncertainty are not very easy to be measured, such as final labor costs associated with inspection and data processing times. We propose to distinguish experimental or research-stage costs and concept of operations (CON-OPS) costs for real-world applications, and would expect CON-OPS costs to come down when technologies mature.

One example of these cost estimates is presented in Table 1 for the Thermal Infrared (ThIR) bridge condition assessment technology. Similar analyses are planned for development for the other project technologies, such as the 3DOBS, Ultra Wide Band Imaging Radar System (UWBIRS), Digital Image Correlation (DIC), the Bridge Viewer Remote Camera System (BVRCS), and Light Detecting and Ranging (LiDAR).

Road User Costs

Currently, routine bridge inspections generally do not require traffic lane closures. Several remote sensing technologies, however, will need to close the traffic, at least based on currently developed implementations. The user costs represent the inconvenience and expenses incurred by the bridge users due to lane closures and traffic disruption, which include the travel delay costs, vehicle-operating costs (VOC), and crash costs. These costs could be minimized as remote sensing technologies such as the 3DOBS are improved to work at highway speeds.

Thermal Infrared	Cost Elements	Research-Stage Cost Measurement	CONOPS Cost Estimates
Equipment	FLIR SC640 Thermal IR Camera (307,200 pixels)	$20,000 - $40,000	$20,000
	or FLIR i7 Thermal IR Camera (handheld, 14,400 pixels)	$2,000	$2,000
	or FLIR optical and ThIR Camera (handheld, 19,200 pixels)	$4,195	$4,000
	or FLUKE Ti10	$4,495	$4,000
	Cart with fabricated hitch (height=6.2ft)	$100	$100
	GPS installed on the cart	$100	$100
	Laptop computer	$800	$800
Software	ThermaCAM software (professional edition)	$7,000	$7,000
Labor	# of persons to do the survey	2 persons	One person
	Set-up time	60 minutes	15 minutes
	Running (3 span, 2-lane bridge)	90 minutes	30 Minutes
	Break-up	20 minutes	15 minutes
	Total hours	2.5	1.0
Road user costs	Traffic disruption	ThIR camera mounted on a cart; one lane closed each time	ThIR camera mounted on a vehicle that is driven at a lower speed
Post-processing hours	To quantify surface condition by creating delamination map and calculating percentage of delamination etc.	> 40 hours	< 8 hours

Table 1: Cost estimates for using ThIR technology.

Calculations of road user costs require much location-specific information, such as length of highway affected by the activity, traffic speed during activity, normal traffic speed, annual average daily traffic (AADT), annual average daily truck traffic (AADTT), work zone crash rates, vehicle operating costs, etc. The CAR research team will rely on existing research findings and apply them accordingly to the scenarios we are going to develop. For example, one study suggested that road user cost due to bridge inspections could range from $20,000 to $32,000 per occurrence.[1]

Another example is the lane rental fee, which appears to be more appropriate for our analysis. Lane rental is commonly used in the roadway construction contracting process, meaning that

[1] Hank Bonstedt. Life Cycle Cost Analysis for Bridges <http://caba-bridges.org/Presentations/files/LCCA.ppt>. Accessed on December 8, 2011.

the contractor has to pay for the time or right to use lanes during construction operations. This time component is converted to a cost to the contractor based on estimated road user costs, depending on, for example, whether one lane is occupied as opposed to a lane and a shoulder. In addition, rental rates can be different depending on the time of day (e.g., peak or off-peak travel hours). A detailed example of a lane rental fee is presented in Table 2 (year 2000 dollars).

Lane Type	Daily Fees (dollars/day)	Hourly Fees (6:30 a.m.-9:00 a.m.) (dollars/h)	Hourly Fees (9:00 a.m.-3:00 p.m.) (dollars/h)
One lane	20,000	2,000	500
One shoulder	5,000	500	125
One lane and shoulder	25,500	2,500	625
Two lanes	45,000	4,500	1,250
Two lanes and shoulder	50,000	5,000	1,375

Table 2: Example Lane Rental Fees. Source: Transportation Research Board, Reducing and Mitigating Impacts of Lane Occupancy During Construction and Maintenance: A Synthesis of Highway Practice NCHRP SYNTHESIS 293, 2000.

BRIDGE SCOPING AND THE BENEFITS OF REMOTE SENSING TECHNOLOGIES

Bridge scoping is a more in-depth bridge inspection process than the standard bridge inspections that evaluate a bridge for various repair alternatives and recommend the most economical rehabilitation or treatment, then develop a scope of work and cost estimate for the selected alternative. The work for each bridge scoping includes two major steps: site review and engineering analysis.[2] According to MDOT, about 167 state-owned bridges were scoped in 2010 at a total cost of $1,557,960, or $9,329 per bridge, on average. All bridge scoping was conducted by engineering contractors (that is, none was done in house).

The outcome indicators of several of the remote sensing technologies field tested are similar to the outputs required in bridge scoping, such as measures of extent of delamination, spalling, and crack areas, and calculation of deterioration percentage. These measures are critical input in developing repair strategies and cost estimates and certainly should be included in benefit estimates in our economic evaluation process.

[2] Great Lakes Engineering Group, LLC <http://www.glengineering.com/services_scoping.htm>. Accessed on December 28, 2011.

DSS AND ITS ROLE IN ECONOMIC EVALUATION

As described in technical memorandum nº 22, the DSS will provide the necessary environment for helping transportation agencies understand if the remote sensing technologies evaluated through this project can provide the information needed to help advance cost-effective bridge condition assessment. During this past quarter, the project team focused on improving the functionality and user-friendliness of the DSS interface, integrating direct exports of current bridge condition data from the MDOT Transportation Management System, generating an example bridge condition health signature, and the starting of integration of remote sensing results such as geo-tagged photo inventory points and the high-resolution bridge deck DEM. Figure 2 shows an example of integrating the BVRCS photo inventory points into the DSS.

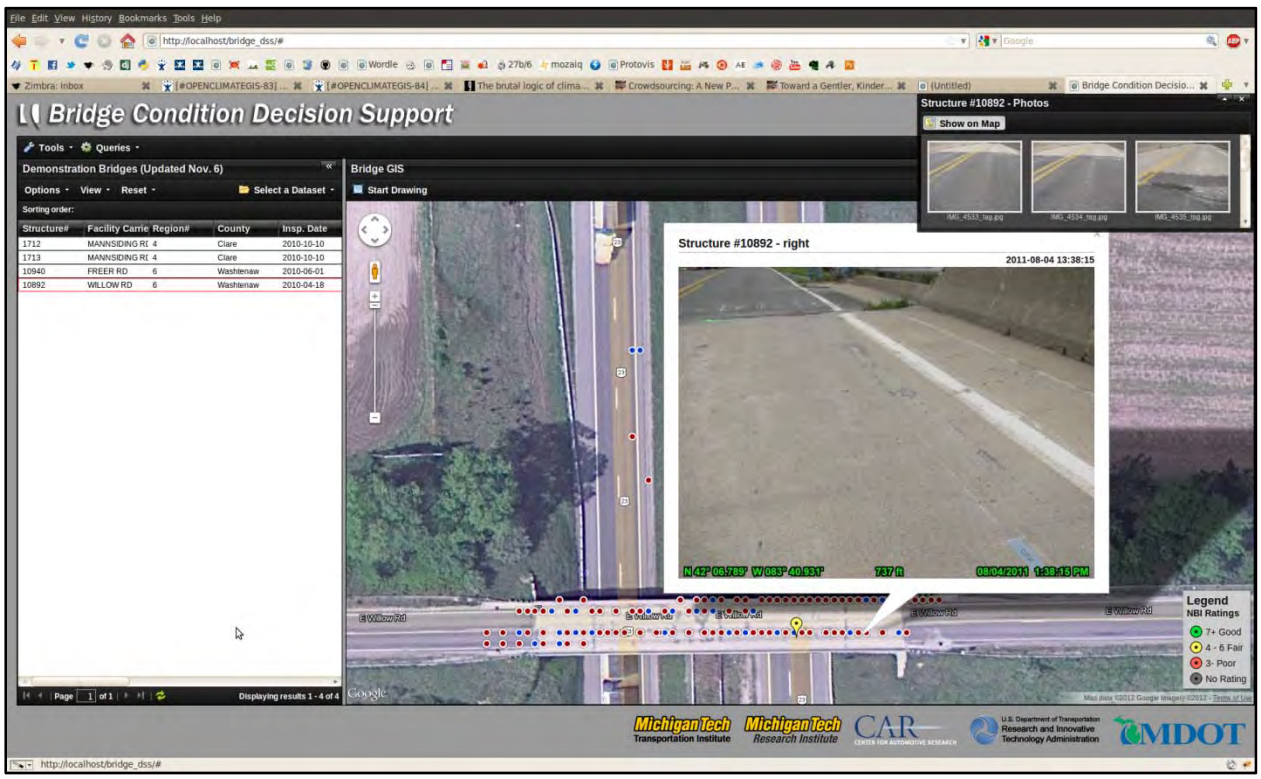

Figure 2: An example of the BVRCS geo-tagged photo inventory points being integrated into the updated DSS. Work on integrating advanced remote sensing results such as 3D optical spall detection data and ThIR delamination detection data is continuing.

Once the DSS development is completed, especially the integration of remote sensing indicators of bridge condition, then the DSS can be used for helping with the technical and economic assessment of the project results. A major focus of the next January-March quarter is taking the DSS as far as possible towards completion, although work in the following quarter is also anticipated. A meeting with the DSS focus group, established at the recommendation of

the project Technical Advisory Committee, is planned for early March, 2012. A major updated release of the DSS will be made available for that meeting and it is anticipated that this version of the DSS will be sufficiently advanced to help with economic evaluation. For example, it should be possible to estimate the productivity savings of MDOT for its bridge condition evaluation processes if they were using the DSS as part of their day-to-day bridge asset management and bridge repair planning methods. It is that type of economic evaluation that the project team anticipates completing with help of the DSS.

NEXT STEPS

The CAR research team will continue to work closely with the Michigan Tech Transportation Institute and the Michigan Tech Research Institute to complete Task 6: Economic Evaluation of Remote Sensing Technologies. Specifically, CAR researchers will focus on following steps to complete this effort:

- Finalize cost estimates (both research stage and within a CON-OPS for sustainable adoption within a bridge operations and maintenance program).

- Finalize assumptions, application scenarios, and evaluation approaches.

- Conduct second-round interviews with MDOT stakeholders in March, 2012, with a focus on agency valuation of the outputs of the tested remote sensing technologies.

- Analyze how the DSS can enable more cost-efficient bridge asset management if used as part of MDOT planning processes.

- Prepare a final study report that compares costs and benefits and provides recommendations on cost-effective use of remote sensing for bridge condition assessment (i.e., documents which technologies provide the highest added value per implementation and operation cost).

MichiganTech Transportation Institute

Memo

To: T. Ahlborn, D. Harris, L. Sutter, R. Shuchman, and the rest of the Project Team

From: H. de Melo e Silva, C. Brooks, D. Banach, J. Burns, D. Dean, R. Dobson, A. Endsley, R. Hoensheid, R. Oats, K. Vaghefi

CC: C. Singh

Date: April 11, 2012

Number: 26

Subject: Outline of chapters 5 and 7 (final report) and abstracts of final papers developed for each technology and the economic evaluation.

The final report of the *Bridge Condition Using Remote Sensors* project includes sections for each technology (chapter 5) and the economic evaluation (chapter 7). Each section for the technologies will follow the general outline listed below.

- **Introduction;** technology overview, literature review, and state of practice of the technology.
- **Methodology;** laboratory testing, proof of concept, software description, and field deployment.
- **Results and Discussion;** field demonstration results and discussion, pros and cons, and integration into the Decision Support System.
- **Implementation and Next Steps;** challenges for implementation, costing comments, merging (data fusion) with other technologies, and future plans.

These sections are described in the form of abstracts which are being developed into papers to be included in the final report. The abstracts for each technology can be found below. Chapter 7 of the final report will include the economic evaluation, following its own outline described later in the "Economic Evaluation" section of this memorandum.

3D OPTICAL BRIDGE-EVALUATION SYSTEM (3DOBS)

"Designing and Deploying the 3D Optical Bridge-evaluation System to Assess Bridge Deck Surface Condition"

3DOBS (3D Optical Bridge-evaluation System) uses 3D optical photogrammetric methods to produce high-resolution Digital Elevation Models (DEM) of bridge decks and other bridge elements, and includes automatic detection of surface spalls and their characteristics. Currently, the calculation of the National Bridge Inspection (NBI) rating for a bridge deck is done by inspectors visually inspecting the bridge deck. 3D optical photogrammetry is an innovative technology that can help assess bridge deck condition while at the same time enhance the ability to compare data for future reference and decision making. This technology is also less expensive than other modeling technologies, such as LiDAR (Light Detection and Ranging), and it can provide high resolution results (down to 5 mm 'x' and 'y' and 2 mm 'z').

3DOBS was developed by taking a Digital Single Lens Reflex camera (DSLR), mounting it to a truck and driving it across a bridge at appropriate speeds. The resulting photos were then processed in a close range photogrammetry software that produced a DEM of the bridge deck for four bridges in Michigan. The DEMs were then run through an automated spall detection algorithm developed at the Michigan Tech Research Institute (MTRI). The algorithm located spalls, calculated area and volume of individual spalls, and the percent of the total bridge deck that is spalled. For example, one bridge was calculated to have 6.99% surface spalling using 3DOBS. A version for assessing the underside of bridge deck was also developed.

While the current version of the system has been successful in producing surface DEMs and locating spalls, it was limited by the speed of the collection setup to 1-2 mph, which means that lanes would have to be closed for collects. Upgrades are described to enable faster data collection at near-highway speeds of at least 40 mph by upgrading the camera component of the system.

BRIDGE VIEWER REMOTE CAMERA SYSTEM (BVRCS)

"Deployment of the vehicle mounted Bridge Viewer Remote Camera System to Generate a Geospatially Referenced Photo Inventory for Bridge Decks"

The Bridge Viewer Remote Camera System (BVRCS) is an optical assessment technology that was developed and deployed by mounting low-cost cameras on a vehicle to capture a location-tagged photo inventory of a bridge deck. Currently bridges are inspected by field crews visiting bridges and taking photos of only major problems that are found during inspections. There are companies with dedicated equipment that will deploy dedicated vehicles to take a photo inventory, however the cost per deployment can be expensive. BVRCS costs less than $1,000 to deploy and can be mounted to any vehicle for deployment to multiple bridges without additional cost. This technology is composed of two point-and-shoot cameras, a low-cost global positioning system (GPS), and a laptop with software that is used to trigger the cameras. The cameras are mounted to the front of the vehicle and in the current version of BVRCS are driven at a speed of less than 5 mph.

Because the cameras capture regularly spaced photos of the bridge deck, a photo inventory of the entire bridge is generated. After the collection, the photos are processed in a GPS photo tagging software that spatially references the photos as Google Earth KML layers and Esri shapefiles. While this system is very effective at generating a photo inventory of the bridge deck, the current setup is limited by how slow the vehicle has to drive. Despite the speed, it took less than 30 minutes for setup, collect both lanes of a two lane bridge and breakdown of the system. This can be avoided by upgrading the cameras and future versions of this technology could be implemented without disrupting traffic by collecting at near-highway speeds of at least 40 mph.

GIGAPAN SYSTEM (GigaPan)

"GigaPan System: A High-resolution Photo Inventory Tool for Bridge Structures"

GigaPan is an optical assessment tool capable of creating high-resolution photo inventories of bridge structure components such as fascia and deck undersides. The original GigaPan project was a collaboration between Carnegie Mellon University and the National Aeronautics and Space Administration (NASA), with funding provided by Google, with the intent of creating a commercially viable, low-cost photographic robot and software package to catalogue the world (see <http://www.gigapan.com/>). The GigaPan EPIC hardware (costing about $800) with a Canon PowerShot SX110 IS camera ($250) was deployed to capture a very high-resolution composite photo image of the fascia and underside of four bridges in Michigan.

The GigaPan Stitch software compiled the individual images and produced high-resolution panoramic images that can be used for condition evaluation, especially to visually assess

changes over time, and are easily accessible via any web browser despite typically being over one gigabyte in size. The resulting location and time-stamped composite photos have been made available to transportation agency end-users through the overall project's web-based bridge condition Decision Support System (DSS).

THERMAL INFRARED (ThIR)

"Implementation of Thermal Infrared Imagery for Concrete Bridge Inspection"

Accurate inspection and assessment of the transportation infrastructure has become a critical issue for bridge inspectors and transportation authorities in recent years. Specifically in concrete bridge components, the accurate assessment of subsurface delaminations and cracks has become a burden due to the difficulties in detecting these types of defects during the biannual visual inspections. Subsurface delaminations mostly occur within reinforced concrete bridges and eventually develop into spalls on the bridge. This evolution of decay highlights the importance of detecting this type of deterioration. Thermal infrared (ThIR) imagery has been recognized as a useful tool for detecting delaminations and subsurface defects that are not visible to the human eye. This technology collects surface radiant temperature and presents the results as a ThIR image. During the day, delaminated areas within the concrete will appear as higher temperature areas within the thermal infrared image compared to the sound concrete area around them.

This remote sensing technology can yield both qualitative and quantitative indicators of condition. A delamination map, created from the outputs of a ThIR bridge inspection, can help to document delaminations in a format useful to transportation agencies. Total area of delamination on the entire bridge deck can be calculated from the ThIR images and can be reported as a percentage of delamination over the entire bridge deck. The purpose of this paper is to summarize the results of the laboratory study and deployment of this technology on three concrete bridge decks in Michigan as well as discuss the challenges that a bridge inspector may face during data collection and processing and how these challenges could be overcome for practical deployment. Applying this technology can provide transportation agencies with useful measures for maintenance and repair decision making.

DIGITAL IMAGE CORRELATION (DIC)

"Using Digital Image Correlation for Condition Assessment of Global Behavior Measurements on Bridge Members"

Digital Image Correlation (DIC) is an optical based remote sensing technology suggested for condition assessment of challenges on the global metric level of a bridge system. DIC has been primarily deployed in controlled laboratory environments, but the technique holds great promise for implementation in field environments for in-service bridge performance evaluation. With DIC, sequential digital images before and after loading are compared optically using computer processing algorithms where pixel movement is tracked. The resulting pixel movement is then correlated to displacement and deformation which can be related to the structure's translation, rotation, and/or deformation.

The computer algorithms used for DIC comprised of (1) a commercially available code and (2) a The MathWorks MATLAB developed routine with features specific to bridge testing such as relative referencing for minimizing effects of camera movement and element scaling to provide reference measurements within tracked images. In this investigation, DIC was employed in a series of laboratory experiments using a variety of specimens, under both static and dynamic conditions. This method encompasses many variables in its analysis that were investigated in detailed laboratory evaluation and experimental setups. In the series of experiments, the variables that were considered included: lighting, surface pattern, camera stability, loading, measurement distance, and angle, in an effort to mimic conditions that would be observed in a field test of an in-service bridge. Results from the laboratory investigation confirmed the performance of the technique while allowing for consideration of factors that would be present in a field environment (wind/vibration, lighting, and measurement distance/angle).

These additional laboratory studies allowed for the creation of an improved in-field deployable system for the DIC. The benefits of the DIC definitely show great potential for bridge health indicators, as well as providing performance measurements of global behavior of bridges.

LIGHT DETECTING AND RANGING (LiDAR)

"The Evaluation of Surface Defect Detection using Light Detection and Ranging for Bridge Structural Health Monitoring"

Routine bridge inspections require labor intensive and subjective visual interpretation to determine bridge deck surface condition. Light Detection and Ranging (LiDAR), a relatively new class of survey instrument, has become a popular and increasingly used technology for providing as-built and inventory data in civil applications. While an increasing number of private and governmental agencies possess terrestrial and mobile LiDAR systems, an understanding of the technology's capabilities and potential applications continues to evolve.

LiDAR is a line-of-sight instrument and as such, care must be taken when establishing scan locations and resolution to allow the capture of data at an adequate resolution for defining features that contribute to the analysis of bridge deck surface condition. Information such as the location, area, and volume of spalling on deck surfaces, undersides, and support columns can be derived from properly collected LiDAR point clouds. The LiDAR point clouds contain information that can provide quantitative surface condition information, resulting in more accurate structural health monitoring. LiDAR scans were collected at four study bridges, each of which displayed a varying degree of degradation. A variety of commercially available analysis tools and an independently developed algorithm written in Esri ArcGIS Python (ArcPy) were used to locate and quantify surface defects such as location, volume, and area of spalls. The results were visual and numerically displayed in a user-friendly web-based decision support tool integrating prior bridge condition metrics for comparison. LiDAR data processing procedures along with strengths and limitations of point clouds for defining features useful for assessing bridge deck condition are discussed. Point cloud density and incidence angle are two attributes that must be managed carefully to ensure data collected are of high quality and useful for bridge condition evaluation. Mobile LiDAR datasets are evaluated and compared to terrestrial LiDAR data as a potential data source for bridge condition evaluation. When collected properly to ensure effective evaluation of bridge surface condition, LiDAR data can be analyzed to provide a useful data set from which to derive bridge deck condition information.

ULTRA WIDE BAND IMAGING RADAR SYSTEM (UWBIRS)

"Applications of Ground Penetrating Radar for Assessment of Subsurface Bridge Condition Indicators"

While optical remote sensing technologies provide information about the surface condition of bridge decks, radar systems, employing low frequency electromagnetic waves that penetrate the deck material, provide information about the deck interior. Previous studies have demonstrated that down-looking, low frequency, ground penetrating radar (GPR) can image delaminations, defects, and rebar within concrete bridge decks. Several commercial companies have developed production systems to produce reflectivity maps that are indicative of deck defects such as subsurface delaminations. These maps, or more specifically metrics derived from these maps, can be used within the Decision Support System (DSS) to provide quantitative measures of deck condition which contribute to the overall bridge condition metric. The current program reviewed available commercial systems for compatibility and utility with the DSS and conducted a limited set of radar measurements to extend the use of radar technology for bridge assessment.

Radar measurements conducted under this program as part of the field testing aimed to extend use of radar technology for bridge assessment in two ways. First, current commercial radar systems used to survey deck condition utilize arrays of truck or cart mounted antennas that are scanned at a vertical oriented close to the deck surface. These systems operate in close proximity to the deck and may require the bridge to be closed for extended periods of time to complete the scan. To mitigate these limitations, an alternate imaging approach where a single radar antenna viewing the deck surface at an oblique angle from the side was investigated as part of a potentially less-expensive Ultra Wide Band Imaging Radar System (UWBIRS). This approach would allow a vehicle mounted radar travelling in one lane to produce a two-dimensional image of an adjacent lane, and thus, potentially reducing data collection time and interference with traffic. The imaging geometry is also similar to the geometry that would be provided by a standoff airborne radar, so the data collection provided information for assessing the potential utility of a standoff airborne sensor.

The second radar application investigated as part of the field demonstration was the use of low frequency radar to image the interior of concrete box beams. Lack of visual access to the interior of box beams makes condition assessment difficult. Low frequency, 3D imaging radar potentially provides a means of interrogating the structure interior. For each application, a prototype low frequency, wideband radar system was developed using a commercially available transmitter/receiver unit. These systems were used to image bridge structures as part of the

summer field demonstrations, and resulting data were evaluated for their utility for bridge condition assessment. In this section, currently available commercial radar systems will first be reviewed, and their applicability to the DSS will be discussed. Subsequently, the exploratory radar measurements conducted as part of the field demonstrations will be reviewed. The radar systems and experiments conducted as part of the field demonstrations will be described, and the results of the experimental collections and their utility for structure assessment will be summarized. Advantages and limitations of the approaches will be presented, along with recommendations for potential future work.

SYNTHETIC APERTURE RADAR (SAR)

"Synthetic Aperture Radar Speckle for Bridge Deck Condition Assessment"

In this investigation, the project team attempted to correlate bridge surface roughness as measured using Synthetic Aperature Radar (SAR) airborne imagery with bridge deck condition from established techniques, namely the NBI (National Bridge Inventory) inspection. Coherence speckle, often observed as "graininess" in radar backscatter images, is produced due to phase differences between picture elements (pixels) in the scene. In turn, these phase differences in the image correspond to phase differences between scattering elements in the scene such as height differences on the order of the radar wavelength (or optical wavelength in the case of optical speckle from coherent light sources). If a surface is rough at that scale then the speckle pattern observed may contain a measure of that roughness.

Airborne SAR data were obtained for three demonstration bridges in Michigan. Due to inadequate collection geometry in the available satellite imagery, the imagery from all but one of the bridges could not be analyzed. The project team applied a technique first developed under a previous study, Transportation Applications of Restricted-Use Technologies (TARUT), but, lacking timely ground data for the bridge(s), was not able to assess the performance of the technique. The report lays out the steps needed for validation of the technique, describes the methodology employed, and comments on the commercial viability and practicality of the technique.

INTERFEROMETRIC SYNTHETIC APERTURE RADAR (InSAR)

"Assessing the Use of Commercial Interferometric Aperture Radar Imagery for Detection of Bridge Settlement"

Interferometric Synthetic Aparture Radar (InSAR) displacement mapping (D-InSAR) techniques have demonstrated utility in detecting sub-centimeter resolution elevation changes over time in studies of land subsidence and in studies of smaller-scale targets such as buildings. In this analysis it was sought to assess the potential to detect bridge settlement for two bridges where known elevation changes have occurred by using two-pass D-InSAR with commercially available SAR (Synthetic Aperture Radar) imagery from the ERS-2 satellite.

Imagery for each bridge was acquired before and after known elevation changes and processed using ERDAS IMAGINE's D-InSAR module. The resulting displacement maps did not definitively reflect the known changes in elevation for either bridge. The principal conclusion was that the commercial SAR imagery used in this task was not optimal for detection of bridge settlement due to relatively coarse horizontal resolution (> 4 m) which affected the vertical resolution change detection. Additionally, displacement detection may have been hampered by low radar return of paved roads. Other projects using D-InSAR methods to detect settlement of relatively small target features are reviewed for comparison.

MULTISPECTRAL SATELLITE IMAGERY (MSI)

"Assessing the Overall Condition of Bridge Decks by Using Commercial High-resolution Multispectral Satellite Imagery"

Commercial high-resolution multispectral satellite imagery, such as WorldView-2, IKONOS, and GeoEye-1, has a spatial resolution of up to 0.5 m which is a relatively coarse resolution when compared to other more "onsite" remote sensing techniques. Therefore this technology was used to evaluate the overall condition of the bridge deck rather than individual areas, as was done for the Transportation Applications of Restricted-Use Technologies (TARUT) study. For testing this technology, archived imagery from IKONOS and WorldView-2 was used for the field demonstration sites. The imagery was first pan-sharpened before the analysis was run to increase the resolution of the spectral bands to match the higher-resolution panchromatic band. Based on previous work at the Michigan Tech Research Institute (MTRI), the VIS2-band differencing technique was adapted for evaluating bridge condition.

In this technique an input integer was generated for each bridge by subtracting band 1 from band 4 for IKONOS imagery and band 2 from band 8 in WorldView-2 imagery and then averaging the pixel values of each bridge. This value was used to correlate to the condition of the bridge deck as determined by the inspection reports. With this technology an overall condition indicator for a bridge deck can be calculated without closing lanes or disrupting traffic. However, despite this advantage, satellite imagery is more expensive than some other technologies and it is dependent on whether the satellite is over the target site when clouds are not present, and does not provide detailed condition information.

ECONOMIC EVALUATION

The decision to integrate remote sensing technologies into bridge inspection practices can be viewed as an investment strategy for both the public and private sectors. The economic indices (e.g., capital and operational costs) are critical for quantifying and qualifying the ability of the proposed new technologies to meet the functional and operational needs of the bridge inspection process. This economic assessment is designed to assess the cost effectiveness of remote sensing technologies by comparing marginal costs of employing sensor technologies to the marginal enhancements that they provide, and therefore to ensure a practical, cost-effective product to be integrated into transportation agency operations.

Input data was obtained from field demonstrations, vendor interviews, and two rounds of interviews with the Michigan Department of Transportation (MDOT) stakeholders. The cost benefit analysis was conducted based on several assumptions (e.g., adoption curve of new technologies, time period of analysis, and geographic coverage) and deployment scenarios of remote sensing technologies (e.g., combinations of technologies and service types). This evaluation also examines the benefits of the project's Decision Support System (DSS) integrated with remote sensing indicators of bridge conditions. Finally, this evaluation recommends strategies to achieve cost effectiveness of remote sensing technologies.

Chapter 7 of the final report of the *Bridge Condition Using Remote Sensors* project will include the economic evaluation of commercial remote sensing technologies considered and the DSS for bridge health monitoring. The chapter will follow an outline which is different than the outline of the technologies above. It is listed below.

- **Introduction**
- **Bridge Inspection and Maintenance in the Context of Shrinking Transportation Revenue**

- **Description of Existing Bridge Inspection Practices**
- **Remote Sensing Technologies for Bridge Condition Assessment**
- **Economic Evaluation of Bridge Inspection Using Remote Sensing Technologies**
- **Summary and Discussions**

MichiganTech Transportation Institute

Memo

To: T. Ahlborn, D. Harris, L. Sutter, R. Shuchman, and the rest of the Project Team

From: A. Endsley, M. Forster, C. Brooks, H. de Melo e Silva

CC: C. Singh

Date: April 11, 2012

Number: 27

Subject: Description of the Decision Support System (DSS) evaluation by the Michigan Department of Transportation and the Technical Advisory Committee capabilities of the DSS for integrated bridge assessment as well as the DSS itself.

The Decision Support System (DSS) focus group reconvened on March 1, 2012 at the Michigan Tech Research Institute (MTRI) office in Ann Arbor, MI. Invited from the Michigan Department of Transportation (MDOT) were; Jason DeRuyver, David Juntunen, Rich Kathrens, Steve Cook, and Bob Kelley. From the Technical Advisory Committee, Amy Trahey from Great Lakes Engineering Group, a contractor, was also invited.

Under the suggestion of Jason DeRuyver, Melissa Knauff from MDOT was invited but ultimately could not make it. Beckie Curtis (MDOT Bridge Management Engineer) attended on behalf of Dave Juntunen. The attendance list from the March 1 meeting is as follows:

- Jason DeRuyver, MDOT
- Rich Kathrens, MDOT
- Beckie Curtis, MDOT
- Richard Wallace, CAR
- Mike Forster, CAR
- Qiang Hong, CAR
- Amy Trahey, GLEG
- Larry Sutter, MTTI
- Colin Brooks, MTRI
- Jim Ebling, MTRI
- Bob Shuchman, MTRI
- Arthur Endsley, MTRI
- Rick Dobson, MTRI
- David Dean, MTRI

The morning session consisted of presentations by team members, followed by a live demonstration of the DSS. The progress in research and commercial evaluation of remote sensing technologies for bridges, highlighting the most promising technologies that have emerged from the 2-year study was also presented. A presentation outlining the progress made in developing the DSS and the anticipated outcomes of the focus group was presented as well:

- Feedback on the functionality, completeness, ease-of-use, and relevance of the demonstration DSS.
- Feature requests for any missing or incomplete functionality.
- Identification of obstacles to implementation at a state transportation agency.
- Identification of barriers to user adoption (adoption by decision-makers).

The DSS live demonstration was projected onto a screen for the entire group to follow along. The complete functionality of the DSS was demonstrated, highlighting important features such as:

- Plotting bridges across the inventory on a map.
- Filtering the bridge inventory (e.g., all bridges in the Metro Region; all bridges with a bridge deck rating less than 4) and viewing a subset on the map.
- Obtaining driving directions to a bridge from an MDOT office, postal address, or arbitrary latitude-longitude pair (Figure 1).
- Viewing highway traffic condition symbolized on the map.
- Spatial filtering by predefined areas of interest (e.g., counties, regions) through map overlays.
- Spatial filtering by arbitrary polygons drawn on the map (e.g., filter to bridges along a traffic corridor, see Figure 1).
- Spatial filtering by the current map extent (i.e., filter to all bridge in current map view only).

- Changing symbology of table-rows, bridge markers on map to symbolize NBI bridge deck, superstructure, substructure, or culvert ratings or sufficiency ratings.
- Zooming to individual or multiple bridges by table selection.
- Viewing Bridge Viewer Remote Camera System (BVRCS) photos in the DSS; a visualization experience similar to Google StreetView (Figure 2).
- Viewing GigaPan System photographs and where they were taken from.
- Viewing remote sensing data as map overlays, including delamination and spall feature maps and digital elevation models (DEMs, see Figure 2).
- Accessing remote sensing metrics such as percent spalled, percent delaminated, and International Roughness Index (IRI) calculations from 3D optics through a custom "Bridge Deck Health Signature" scoring table (Figure 2).
- Executing arbitrary queries on Pontis data (Figure 1).

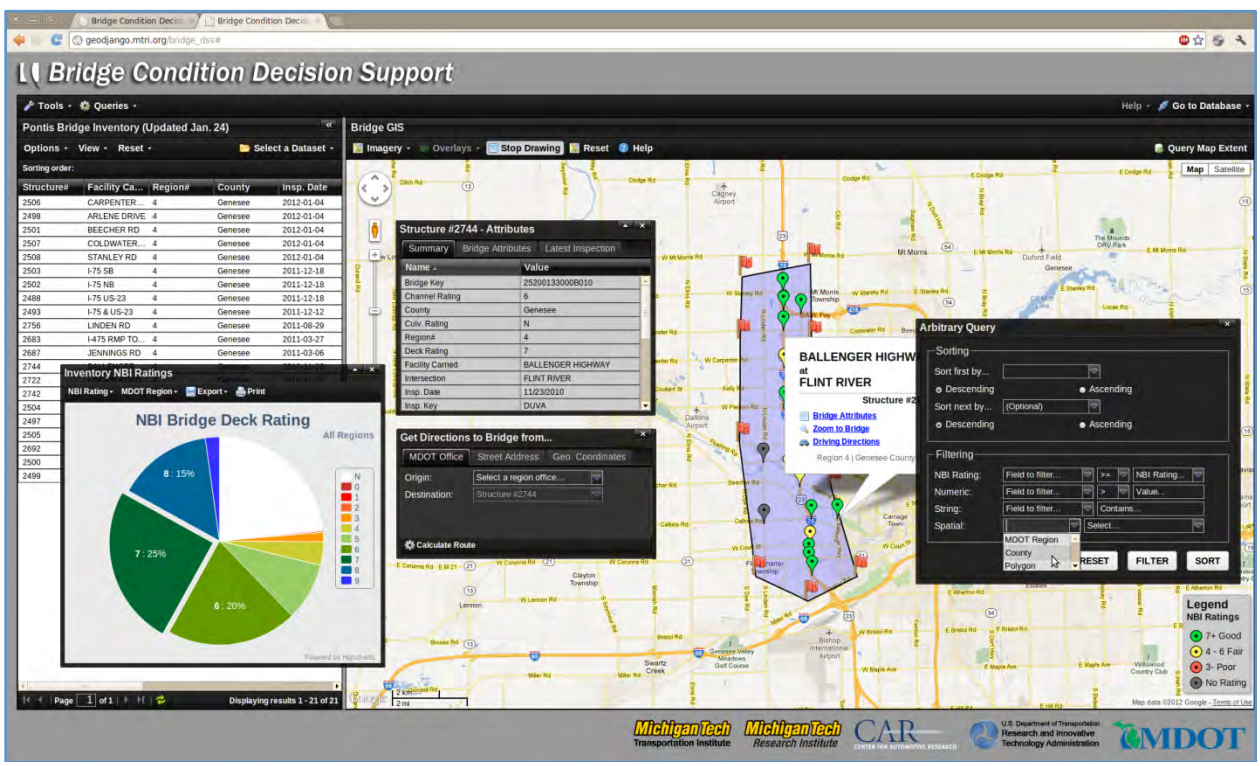

Figure 1: Screenshot of the DSS version as evaluated by the focus group; showcases inventory view of condition information, spatial filtering, arbitrary Pontis query construction, and the directions utility.

Before, during and after lunch, focus group participants were invited to evaluate the DSS themselves. Multiple instances of the DSS were started on laptop computers so that participants could interact with the application. Afterwards, the team presented the focus group participants with a number of questions intended to drive discussion about the DSS version they evaluated.

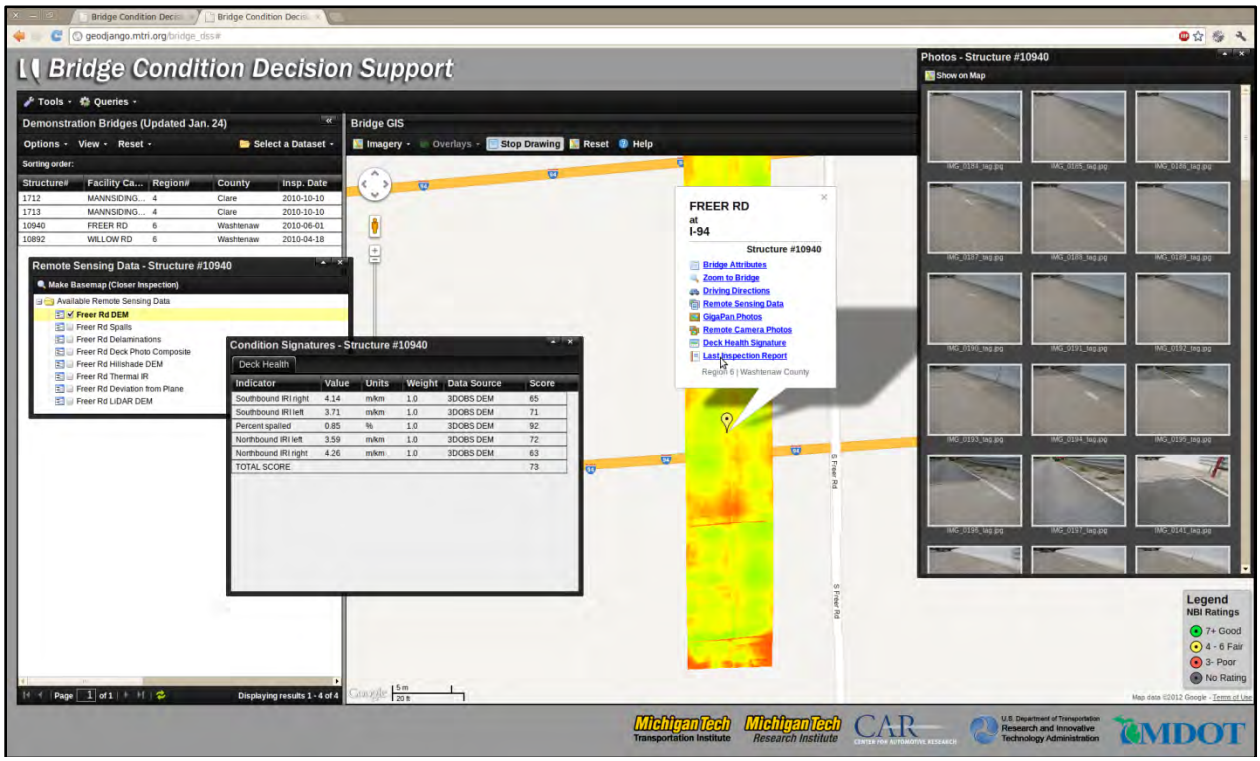

Figure 2: Screenshot of the DSS version as evaluated by the focus group; showcasing the bridge photo inventory, remote sensing overlays, and metrics that are available per bridge.

Beckie Curtis and Rich Kathrens from MDOT were instrumental in the discussion about bridge inventory information visualization and access. In fact, during the lunch hour, Rich Kathrens gave a brief, informal presentation of an early version of an improved Michigan Bridge Reporting System (MBRS) that has some of the features the DSS currently has and some that MDOT would like to see developed. The primary feature requests and improvements that were identified and which are planned to be implemented by project's end are:

- Require login credentials to access the DSS so as to protect MDOT bridge inventory data.

- Remove the count of 'N' ratings from the National Bridge Inventory (NBI) rating distributions.
- Extend the ability to chart the distribution of NBI ratings to filtered subsets of the bridge inventory (e.g., for a specific county, for a spatially-filtered subset).
- Display the date of the last Transportation Management System (TMS) export on the pie chart.
- Charting of historical bridge condition information, namely bridge deterioration curves.
- View more than 30 bridges (current per-page limit), in fact, view the entire inventory or filtered set on the map.
- Order bridge attribute names by structure inventory and appraisal (SIA) number, which is also the NBI item number.

By the end of the month, an evaluation by the TAC is planned. These are some of the improvements to the DSS planned before April is over:

- A secure login has already been implemented.
- More remote sensing overlays will be available, including Light Detecting and Ranging (LiDAR) DEMs, derived DEM products such as deviation-from-a-plane, high-resolution photo composites, and thermal infrared imagery.
- The BVRCS photo inventory points have already been improved with more intuitive positioning.

Appendix D.1 – Bridge Inspection Report: Poor Selection – Mannsiding North Bound

Bridge Safety Inspection Report

S09-18033

Facility	Federal Structure ID	Inspector Name	Agency / Consultant	Inspection Date
MANNSIDING RD	18118033000S090	RUEGSEGGERP		10/11/2010

Feature	Latitude	Longitude	Struc Num	Insp Freq	Insp Key
US-127 NB	435722.67	844633.84	1713	24	YIDK

Location	Length	Width	Year Built	Year Recon	Br Type		Scour Eval	No.Pins
2.3 MI S OF M-61	130.8999	31.170	1966		5	32	N	

LEGEND

9	New
7-8	Good
5-6	Fair
3-4	Poor
2 or Less	Critical

06 08 10

NBI INSPECTION

Deck

1. Surface SIA-58A	5	5	5		Concrete. Light scaling throughout. Deck surface sounded and 176 sq ft or 4.4% of delamination found. Concrete patched areas map cracked with adjacent open cracks. (2010), Concrete. Deck surface sounded and 176 sq ft or 4.4% of delamination found. Concrete patched areas map cracked with adjacent open cracks. (2008), Conc. between 2% - 10% of deck crked with conc. patched areas. 06(2006).
2. Expansion Jts	8	8	7		Strip seals. Debris filled. Rails rusting in scattered locations.(2010), Newer strip seals. Minor debris.(2008), Newer strip seals. Minor debris. 06(2006).
3. Other Joints	6	5	4		HPR at end joints. Adhesion failure along both, 100% at west. Chips in adjacent concrete. Minor evidence of leakage observed from underneath west joint, est. 5%.(2010), HPR at end jts. Minor chips and adhesion failure.(2008), HPR at end jts. Minor chips and adhesion failure. 06(2006).
4. Railings	7	7	7		Concrete open parapet with single aluminum tube, CSC applied and retrofitted with thrie beam SBGR. Few cracks, small chips, and incipient spalls. Several rust stained areas along both. Minor weathering on SBGR panels.(2010), Conc parapet with 1 tube aluminum with thrie BM. retro fit. Vert & Long. crks. CSS applied.(2008), Conc parapet with 1 tube aluminum with thrie BM. retro fit. Vert & Long. crks. CSS applied. 06(2006).
5. Sidewalks or curbs	N	N	N		
6. Deck SIA-58	4	4	4		Deck surface sounded and 176 sq ft or 4.4% of delamination found. Concrete patches are map cracked. Deck underside sounded during detailed soffit inspection, 623 sq ft or 15% distress. False decked by crews over traffic. Deterioration of the combined area of the top and bottom surface of the deck 10%.(2010), Deck surface sounded and 176 sq ft or 4.4% of delamination found. Concrete patched areas map cracked. Span 2W has several large areas of wet leaching map crked areas in sofit. Many trans. and diag. crks. on surface. Many long. and trans. crks. in soffit most of them leaching. Deck underside sounded during detailed soffit inspection, 623 sq ft or 15% distress. False decked by crews over traffic. Deterioration of the combined area of the top and bottom surface of the deck 10%.(2008), Span 2W has several large areas of wet leaching map crked areas in sofit. Many trans. and diag. crks. on surface. Many long. and trans. crks. in sofit most of them leaching. apprx. 200ft sq spalled or delam. on surface. Newer concrete patches on surface. Diag. leaching corner crks. at the NE. See general notes. 06(2006).
7. Drainage					Minor debris along brush blocks.(2010), No problems noted. (2008), No problems noted. 06(2006).

Superstructure

8. Stringer SIA-59	6	6	6		PCI beams. CSC applied to fascias and beam ends at piers. Several minor scrapes and chips on beam 6S over right lane from HLH's. Couple chips have occured since application of CSC. Several beam ends at piers exhibit cracks, small spalls, and/or incipeint spalls, mainly adjacent to sole plates.(2010), PCI beams. Minor chips from HLH on BM 6 S. no steel exposed. Several Bm ends over Prs W/tight Crks & Incip spalls. CSS applied to bm. ends at piers and fascias. (2008), Minor chips from HLH on BM 6 S. no steel exposed. Several Bm ends over Prs W/tight Crks & Incip spalls. CSS applied to bm. ends at piers and fascias. 06(2006).
9. Paint SIA-59A	N	N	N		
10. Section Loss	N	N	N		
11. Bearings	6	4	4		Elasomeric bearing pads. Steel plates have moderate corrosion. Some minor Crks & deformations on Elast Brgs over Prs. 06. Bolster at P2w. delaminated / fractured under beam 3s. in span 3w. causing loss of bearing area. Rating lowered due to loss of bearing support. Noted area marked with paint.(2010), Elasomeric bearing pads. Steel plates have moderate corrosion. Some minor Crks & deformations on Elast Brgs over Prs. 06. Bolster at P2w. delaminated / fractured under beam 3s. in span 3w. causing loss of bearing area. Rating lowered due to loss of bearing support. Noted area marked with paint.(2008), Neopreme pads. Steel plates have moderate corrosion. Some minor Crks & deformations on Elast Brgs over Prs. 06(2006).

Substructure

12. Abutments SIA-60	7	7	7		CSC applied. Couple vertical cracks in both. Crack under beam 4S and moderately leaching crack at north end of west abut. 1/16" open vertical crack in center of east abut. Delam. on east abut. at const. joint marked with paint.(2010), Both have vertical cracks with some leaching, also an incipent spall at const. joint. E. abut. CSS applied.(2008), Both have vertical cracks with some leaching, also an incipent spall at const. joint. E. abut. CSS applied. 06(2006).
13. Piers SIA-60	7	4	4		CSC applied. Horizontal rust stained crack on west face of pier 1W. Bolster at P2w. delaminated / fractured under beam 3s. in span 3w. causing approx. 50% loss of bearing capacity. Rating lowered due to condition of bolster.(2010), Piers have conc. repairs and CSS applied. Bolster at P2w. delaminated / fractured under beam 3s. in span 3w. causing approx. 50% loss of bearing capacity. Rating lowered due to condition of bolster.(2008), Piers have conc. repairs and CSS applied. 06(2006).

Bridge Safety Inspection Report

Facility	Federal Structure ID	Inspector Name	Agency / Consultant	Inspection Date
MANNSIDING RD	18118033000S090	RUEGSEGGERP		10/11/2010

Feature	Latitude	Longitude	Struc Num	Insp Freq	Insp Key
US-127 NB	435722.67	844633.84	1713	24	YIDK

Location	Length	Width	Year Built	Year Recon	Br Type		Scour Eval	No.Pins
2.3 MI S OF M-61	130.8999	31.170	1966		5	32	N	

LEGEND

9	New
7-8	Good
5-6	Fair
3-4	Poor
2 or Less	Critical

NBI INSPECTION

	06	08	10		
14. Slope Protection	6	6	6		Concrete block & grout. Minor cracks and settlement in both slopes. (2010), Conc block & grout. Minor Crks and settlement in both slopes. (2008), Conc block & grout. Minor Crks and settlement in both slopes. 06(2006).

Approach

15. Approach Pavt	9	8	8		Concrete approaches. Several small chips adjacent to reference lines. Couple H/L cracks.(2010), Concrete approaches. No problems noted. (2008), Newer conc. No problems noted. 06(2006).
16. Approach Shldrs Swalk	N	N	6		Concrete C&G at all quads. Settled 1/2-1" at all quads. Bit wedged at NE. (2010), Narrow Bit & Conc curb. (2008), Narrow Bit & Conc curb. (2006).
17. Approach Slopes					Vegetated. No problems noted.(2010), Vegetated. (2008), Well veg. 06(2006).
18. Utilities					
19. Channel SIA-61	N	N	N		
20. Drainage Culverts					No problems noted. (2010), No problems noted.(2008), No problems noted. 06 (2006).

MISCELLANEOUS

Guard Rail

	06	10	10	
36A	1	1	1	1
36B	1	1	1	1
36C	1	1	1	1
36D	1	1	1	1

Crit Feat Insp(SIA-92)

		Freq	Date
92A	Frac Crit		
92B	Und. Watr		
92C	Spl.Insp		

71	Watr Adeq	
72	Appr Align	6
Temp Supp		
Hi Ld Hit (M)		1
Special Insp Euip.		

General Notes

CPM - Deck patch w/ full depth repairs, Substructure repair, Reseal end joints. 08. Note. Photos and description of bolster at P2w. sent to Lansing for analysis. 08 Structure has been scoped for repars 2012 JN106307Inspected 10-11-10

Form 1717A- 01/2002

Michigan Department of Transportation

Structure Inventory and Appraisal

Code in red ink

Control Section: S09-18033

MDOT Bridge ID: 18 1180330000000S09

NBI Bridge ID	Struct Num	Region	TSC	County	City Resp	City Location	7- Facility Carried	User Name
18118033000S090	1713	04	4A	18		0	MANNSIDING RD	RUEGSEGGERP

6- Feature Intersected	9- Location	Latitude	Longitude	Owner	Maint Resp
US-127 NB	2.3 MI S OF M-61	43° 57' 22.67"	84° 46' 33.84"	1	1

Bridge History, Type, Materials

27- Year Built	1966	
106- Year Reconstructed		
202- Year Painted		
203- Year Overlay		
43- Main Span Bridge Type	5	32
44- Appr Span Bridge Type	_	
77- Steel Type	0	
78- Paint Type	0	
79- Rail Type	6	
80- Post Type	2	
107- Deck Type	1	
108A- Wearing Surface	1	
108B- Membrane	0	
108C- Deck Protection	0	

Structure Dimensions

34- Skew	14
35- Struct Flared	0
45- Num Main Spans	3
46- Num Appr Spans	0
48- Max Span Length	61.0
49- Structure Length	130.9
50A- Width Left Curb/SW	1.3
50B- Width Right Curb/SW	1.3
33- Median	0
51- Width Curb to Curb	25.9
52-Width Out to Out	31.2
112- NBIS Length	Y

Inspection Data

90- Inspection Date	10/11/2010	
91- Inspection Freq	24	
92A- Frac Crit Req/Freq	N	
93A- Frac Crit Insp Date		
92B- Und Water Req/Freq	N	
93B- Und Water Insp Date		
92C- Oth Spec Insp Req/Freq	N	
93C- Oth Spep Insp Date		
176A- Und Water Insp Method	0	
58- Deck Rating	4	
58A- Deck Surface Rtg	5	
59- Superstructure Rating	6	
59A- Paint Rating	N	
60- Substructure Rating	4	
61- Channel Rating	N	
62- Culvert Rating	N	

Navigation Data

38- Navigation Control	N
39- Vertical Clearance	0.0
40- Horizontal Clearance	0.0
111- Pier Protection	
116- Lift Brdg Vert Clear	0.0

Route Carried By Structure (ON Record)

5A- Record Type	1	
5B- Route Signing	4	
5C- Level of Service	1	
5D- Route Number	01840	
5E- Direction Suffix	0	
10L- Best 10ft Unclr- Lt	0	0
10R- Best 10ft Uncl- Rt	99	99
PR Number		
Control Section		
11- Mile Point		
12- Base Highway Network	0	
13- LRS Route-Subroute	0000010481	00
19- Detour Length	10	
20- Toll Facility	3	
26- Functional Class	07	
28A- Lanes On	2	
29- ADT	1000	
30- Year of ADT	1996	
32- Appr Roadway Width	33.8	
32A/B- Ap Pvt Type/Width	4	33.8
42A- Service Type On	1	
47L- Left Horizontal Clear	0.0	
47R- Right Horizontal Clear	28.9	
53- Min Vert Clr Ov Deck	99	99
100- STRAHNET	0	
102- Traffic Direct	2	
109- Truck %	3	
110- Truck Network	0	
114- Future ADT	1500	
115- Year Future ADT	2010	
Freeway	0	

Structure Appraisal

36A- Bridge Railing	1
36B- Rail Transition	1
36C- Approach Rail	1
36D- Rail Termination	1
67- Structure Evaluation	4
68- Deck Geometry	5
69- Underclearance	5
71- Waterway Adequacy	N
72- Approach Alignment	6
103- Temporary Structure	_
113- Scour Criticality	N

Miscellaneous

37- Historical Significance	5
98A- Border Bridge State	
98B- Border Bridge %	
101- Parallel Structure	N
EPA ID	
Stay in Place Forms	

Print Date 5/12/2011 11:56:13

Route Under Structure (UNDER Record)

5A- Record Type	2	
5B- Route Signing	2	
5C- Level of Service	1	
5D- Route Number	00127	
5E- Direction Suffix	0	
10L- Best 10ft Uncl- Lt		
10R- Best 10ft Uncl- Rt	14	6
PR Number		
Control Section	18033	
11- Mile Point	10.510	
12- Base Highway Network	1	
13- LRS Route-Subroute	0000010408	03
19- Detour Length	8	
20- Toll Facility	3	
26- Functional Class	02	
28B- Lanes Under	2	
29- ADT	6,069	
30- Year of ADT	2007	
42B- Service Type Under	1	
47L- Left Horizontal Clear	0.0	
47R- Right Horizontal Clear	44.9	
54A- Left Feature	H	
54B- Left Underclearance	0	0
Left Signed Underclearance	0	0
54C- Right Feature	H	
54D- Right Underclearance	14	4
Right Signed Underclearance	14	3
Under Clearance Year	2010	
55A- Reference Feature	H	
55B- Right Horiz Clearance	10.8	
56- Left Horiz Clearance	21.0	
100- STRAHNET	0	
101- Traffic Direction	1	
109- Truck %	8	
110- Truck Network	1	
114- Future ADT	11,106	
115- Year Future ADT	2018	
Freeway	0	

Proposed Improvements

75- Type of Work		_
76- Length of Improvement		
94- Bridge Cost		
95- Roadway Cost		
96- Total Cost		
97- Year of Cost Estimate		

Load Rating and Posting

31- Design Load	2	
41- Open, Posted, Closed	A	
63- Oper Rtg Method	2	
64F- Fed Operating Rtg	72.7	
64M- Mich Oper Rtg	9	104
65- Inv Rtg Method	2	
66- Inventory Load	24.5	
70- Posting	5	
141- Posted Loading		
195- Analysis ID	5066	
193- Overload Class	A	

BRIDGE INSPECTION REPORT

S09-18033

Facility Carried	Federal Structure ID	Inspector Name	Agency Consultant	Inspection Date
MANNSIDING RD	18118033000S090	RUEGSEGGERP		10/11/2010

Feature Intersected	Latitude	Longitude	Struc Num	Region	Insp Freq	Insp Key
US-127 NB	435722.67	844633.84	1713	4- Bay	24	XHCJ

Location	Length	Width	Year Built	Year Recon	Br Type		Scour Eval	No Pins
2.3 MI S OF M-61	39.8983	9.50062	1966		5	32	N	

CORE ELEMENTS INSPECTION English Units

Element Number	Element Name	Total Quantity	State 1 Old	State 1 New	State 2 Old	State 2 New	State 3 Old	State 3 New	State 4 Old	State 4 New	State 5 Old	State 5 New
12 / 3	Conc Dk Black Bars	4080	0		0		4080		0		0	
400 / 3	Strip Seal Exp Joint	66	66		0		0		0		0	
401 / 3	Pourable Joint Seal	66	0		33		33		0		0	
109 / 3	Prestr Con Girder/Bm	784	718		66		0		0		0	
331 / 3	Concrete Bridge Rail	262	236		23		3		0		0	
310 / 3	Elastomeric Bearing	36	15		20		1		0		0	
205 / 3	Reinf Conc Column	6	6		0		0		0		0	
215 / 3	Reinf Conc Abut	66	59		7		0		0		0	
234 / 3	Reinf Conc Pier Cap	66	64		0		0		2		0	
358 / 3	Dk Cr SmF Conc/Latex	1	0		1		0		0		0	
359 / 3	Deck Bott Surf Sm F	1	0		0		1		0		0	
367 / 3	Conc Surf Coat SmFlg	1	1		0		0		0		0	
378 / 3	False Decking Sm Flg	1	1		0		0		0		0	

CREW RECOMMENDATIONS

Deck Patching	M	Seal deck. 06. Deck patch w/ full depth repair
Approach Pavement		
Joint Repair	M	Reseal end jts. 06. 08Clean strip seals. 10
Railing Repair		
Detailed Inspection		-1
Zone Paint		
Substructure Repair	H	Bolster at P2w. Bolster at P2w. delaminated /
Slope Repair		
Brush Cut		
Other Crew Work	L	Sweep deck. 10Scoped for repairs JN106307

CONTRACT RECOMMENDATIONS

Bridge Replacement		-1
Superstructure Replacement		-1
Deck Replacement		
Overlay		
Widen		
Paint		
Zone Paint		
Pin and Hanger		
Substructure Repair		
Other Contract Work		

Appendix D.2 – Bridge Inspection Report: Fair Selection – Willow Road

Bridge Safety Inspection Report

Facility	Federal Structure ID	Inspector Name	Agency / Consultant	Inspection Date
WILLOW RD	81181076000S020	ZOLNIEREKK	MDOT INSPECTOR	04/19/2010

Feature	Latitude	Longitude	Struc Num	Insp Freq	Insp Key
US-23	420647.34	834056.33	10892	24	SOBS

Location	Length	Width	Year Built	Year Recon	Br Type		Scour Eval	No.Pins
2.1 MI N OF MONROE COL	208.9895	30.839	1962		5	32	N	

LEGEND

9	New
7-8	Good
5-6	Fair
3-4	Poor
2 or Less	Critical

06 08 10

NBI INSPECTION

Deck

1. Surface SIA-58A	5	5	6		Open transverse cracks and areas of delam throughout. Diagonal cracking near the reference lines. Several concrete patches in all spans. (2010), Transverse cracks at a spacing of 3 to 5 feet. There is 64 SFT of bit patched spalls in span 2. The north shoulder ins span 2 is approximately 85% busted up with areas of shallow spalls. There are spallsand STS along all of the joints, some are bit patched. diagonal corners cracks in all quads. Approximatly 30 sft bit fille dpatches in span 3w. (2008), Transverse cracks at a spacing of 3 to 5 feet. There is 64 SFT of bit patched spalls in span 2. The north shoulder ins span 2 is approximately 85% busted up with areas of shallow spalls. There are spalls along all of the joints, most are bit patched. diagonal corners cracks in all quads. Few random shallow spalls in spans 2 and 3.(2006).
2. Expansion Jts	2	2	3		The joints have been concrete patched, no sealer applied. All joints are leaking.(2010), Joints 2,3,4 are completely missing and bit patched with a few open areas of spalling. All of the joints are leaking and are shored up from the underside of the deck.(2008), Joints 2,3,4 are completely missing and bit patched with a few open areas of spalling. All of the joints are leaking and are shored up from the underside of the deck.(2006).
3. Other Joints	3	3	4		Pourable end joints with small spalls and leaking.(2010), Joints 1 and 5 are heavily bit patched. The concrete end headers are breaking up and bit patched. West reference line is approximatly 60% spalled.(2008), Joints 1 and 5 are heavily bit patched. The concrete end headers are breaking up and bit patched.(2006).
4. Railings	5	5	5		Vertical leaching cracks and leaching map cracking in both rails.(2010), Vertical leaching cracks and leaching map cracking in both rails.(2008), vertical cracks typical. 4 SFT map cracked area in the north rail at the west end. 6 LFT map cracked areas on the north rail in span 2. The outside face o the the north brush-block is 100% tight map cracked with some areas of leaching.(2006).
5. Sidewalks or curbs	N	N	N		
6. Deck SIA-58	5	5	5		Bottom: Leaching diagonal and transverse cracking. Leaching longitudinal cracks, wet areas and delam, heaviest in the outside bays. Top: Open transverse cracks and areas of delam throughout. Diagonal cracking near the reference lines. Several concrete patches in all spans. Heavy leaching and stalactite. on the north deck fascia.(2010), Diagonal leaching cracks and spall bays 1 and 5 at the west abutment. Some diagonal leaching cracks bay 1 at east abutment. Leaching map cracks both fascias full length with spalling and spall to steel at the joints.(2008), Diagonal leaching cracks and spall bays 1 and 5 at the west abutment. Some diagonal leaching cracks bay 1 at east abutment. Leaching map cracks both fascias full length with spalling and spall to steel at the joints.(2006).
7. Drainage					Catch basins in all quads.(2010), Catch basins in all quads.(2008), Catch basins in each approach quad shoulder. The northwest catch basin is full of debris.(2006).

Superstructure

8. Stringer SIA-59	6	6	6		Concrete beam ends have cracks and spalls in the bottom flange typical at the piers. High Load Hit with small spalls in span 2 beam 6 over the right lane of traffic, no re-bar is exposed. High Load Hit scraps on beams 1,2,4,5,6 over the right lane. Vertical cracks in the beam webs in span 1 at the north abutment: on the north face of beams 1,2,6 and the south face of beam 6. Span 3 beam 1at pier 2 south face. The concrete diaphragm in span 4, bay 6 has a large spall to steel in the bottom.(2010), Concrete beam ends have cracks and spalls in the bottom flange typical at the piers. High Load Hit with small spalls in span 2 beam 6 over the right lane of traffic, no re-bar is exposed. High Load Hit scraps on beams 1,2,4,5,6 over the right lane. Vertical cracks in the beam webs in span 1 at the north abutment: on the north face of beams 1,2,6 and the south face of beam 6. Span 3 beam 1at pier 2 south face. The concrete diaphragm in span 4, bay 6 has a large spall to steel in the bottom.(2008), Concrete beam ends have cracks and spalls in the bottom flange typical at the piers. High Load Hit with small spalls in span 2 beam 6 over the right lane of traffic, no re-bar is exposed. High Load Hit scraps on beams 1,2,4,5,6 over the right lane. Vertical cracks in the beam webs in span 1 at the north abutment: on the north face of beams 1,2,6 and the south face of beam 6. Span 3 beam 1at pier 2 south face. The concrete diaphragm in span 4, bay 6 has a large spall to steel in the bottom.(2006).
9. Paint SIA-59A	N	N	N		
10. Section Loss	N	N	N		
11. Bearings	6	6	6		Elastomeric pads are splitting at fascias at Piers. Steel bearings are corroding at piers, flake rust at abutments.(2010), Elastomeric pads are splitting at fascias at Piers. Steel bearings are corroding at piers, flake rust at abutments.(2008), Elastomeric pads are splitting at fascias at Piers. Steel bearings are corroding at piers, flake rust at abutments.(2006).

Substructure

Bridge Safety Inspection Report

Facility	Federal Structure ID	Inspector Name	Agency / Consultant	Inspection Date
WILLOW RD	81181076000S020	ZOLNIEREKK	MDOT INSPECTOR	04/19/2010

Feature	Latitude	Longitude	Struc Num	Insp Freq	Insp Key
US-23	420647.34	834056.33	10892	24	SOBS

Location	Length	Width	Year Built	Year Recon	Br Type		Scour Eval	No.Pins
2.1 MI N OF MONROE COL	208.9895	30.839	1962		5	32	N	

LEGEND

9	New
7-8	Good
5-6	Fair
3-4	Poor
2 or Less	Critical

06 08 10

NBI INSPECTION

12. Abutments SIA-60	5	6	6		Tight leaching vertical cracks in both abutments. 6 sft area of delam and cracking under beam 4s in the east abutment.(2010), Leaching vertical cracks in both abutments. 6 sft area of delam and cracking under beam 4s in the east abutment.(2008), Few vertical cracks. East abutment has 4 SFT delaminated / spall area (teacup) under beam 4 with crack extending under bearing. West abutment has 5 SFT delaminated area (t-cup) under beam 2 west, the crack extends under the bearing.(2006).
13. Piers SIA-60	6	6	6		Piers have open cracks, delam and spalling in caps and columns.(2010), Piers have open cracks, delam and spalling in caps and columns.(2008), Pier 1 has a vertical corner cracks on the top of column 2, some cracking in bays 1 and 2. Pier 2 has cracks and small spalls with some exposed re-bar on the south end cap, vertical corner cracks on columns 1,2,3 with some rust staining. Pier 3 has cracks and incipient spalls on the top of column 1 and 2 with some rust staining, horizontal crack in the bottom of cap in bay 1.(2006).
14. Slope Protection	8	7	7		Concrete pad. There is some vegetation growing through the concrete pad.(2010), Concrete pads.(2008), Concrete pad. There is some vegetation growing through the concrete pad.(2006).

Approach

15. Approach Pavt	6	6	6		Bit with chip seal covering. Potholes and raveling in the west reference line.(2010), Bit with chip seal covering. Potholes and raveling in the west reference line.(2008), Bit to the bridge. There are some longitudinal cracks and the bit us busting up at both of the reference lines the full length with some areas of open spalls (2006).
16. Approach Shldrs Swalk	7	7	6		Bit shoulders with concrete curb and gutter pans.(2010), Bit shoulders with concrete curb and gutter pans.(2008), Bit shoulders with concrete curb and gutter pans.(2006).
17. Approach Slopes					Grass and brush.(2010), Brush and weeds.(2008), Grass and brush covered.(2006).
18. Utilities					Conduits in the railings. telephone utilities in both north quads.(2010), conduits in the railings. telephone utilities in both north quads.(2008), Cell tower to the northeast of the bridge. 2- 4" utility conduit running through the north bridge railing. There is a phone box in the northwest and the northeast approach slopes (2006).
19. Channel SIA-61	N	N	N		
20. Drainage Culverts					

MISCELLANEOUS

Guard Rail

	06	10	10	
36A	1	1	1	1
36B	0	0	0	0
36C	0	0	0	0
36D	0	0	0	0

Crit Feat Insp(SIA-92)

		Freq	Date
92A	Frac Crit		
92B	Und. Watr		
92C	Spl.Insp		

71	Watr Adeq	
72	Appr Align	7
Temp Supp		0
Hi Ld Hit (M)		1
Special Insp Euip.		9

General Notes

Southbound posted 14

Form 1717A- 01/2002

Michigan Department of Transportation

Structure Inventory and Appraisal

Code in red ink

Control Section: S02-81076

MDOT Bridge ID: 81 1810760000000S02

NBI Bridge ID	Struct Num	Region	TSC	County	City Resp	City Location	7- Facility Carried	User Name
81181076000S020	10892	06	6B	81		0	WILLOW RD	ZOLNIEREKK

6- Feature Intersected	9- Location	Latitude	Longitude	Owner	Maint Resp
US-23	2.1 MI N OF MONROE COL	42° 06' 47.34"	83° 40' 56.33"	1	1

Bridge History, Type, Materials

27- Year Built	1962	
106- Year Reconstructed		
202- Year Painted		
203- Year Overlay		
43- Main Span Bridge Type	5	32
44- Appr Span Bridge Type	_	
77- Steel Type	0	
78- Paint Type	0	
79- Rail Type	8	
80- Post Type	0	
107- Deck Type	1	
108A- Wearing Surface	1	
108B- Membrane	0	
108C- Deck Protection	0	

Structure Dimensions

34- Skew	0
35- Struct Flared	0
45- Num Main Spans	4
46- Num Appr Spans	0
48- Max Span Length	70.9
49- Structure Length	209.0
50A- Width Left Curb/SW	0.0
50B- Width Right Curb/SW	0.0
33- Median	0
51- Width Curb to Curb	28.5
52-Width Out to Out	30.8
112- NBIS Length	Y

Inspection Data

90- Inspection Date	04/19/2010	
91- Inspection Freq	24	
92A- Frac Crit Req/Freq	N	
93A- Frac Crit Insp Date		
92B- Und Water Req/Freq	N	
93B- Und Water Insp Date		
92C- Oth Spec Insp Req/Freq	N	
93C- Oth Spep Insp Date		
176A- Und Water Insp Method		
58- Deck Rating	5	
58A- Deck Surface Rtg	6	
59- Superstructure Rating	6	
59A- Paint Rating	N	
60- Substructure Rating	6	
61- Channel Rating	N	
62- Culvert Rating	N	

Navigation Data

38- Navigation Control	N
39- Vertical Clearance	0.0
40- Horizontal Clearance	0.0
111- Pier Protection	
116- Lift Brdg Vert Clear	

Route Carried By Structure (ON Record)

5A- Record Type	1	
5B- Route Signing	4	
5C- Level of Service	0	
5D- Route Number	00000	
5E- Direction Suffix	0	
10L- Best 10ft Unclr- Lt	0	0
10R- Best 10ft Uncl- Rt	99	99
PR Number		
Control Section		
11- Mile Point		
12- Base Highway Network	0	
13- LRS Route-Subroute	0000014312	00
19- Detour Length	3	
20- Toll Facility	3	
26- Functional Class	09	
28A- Lanes On	2	
29- ADT	2220	
30- Year of ADT	1997	
32- Appr Roadway Width	29.9	
32A/B- Ap Pvt Type/Width	4	29.9
42A- Service Type On	1	
47L- Left Horizontal Clear	0.0	
47R- Right Horizontal Clear	28.5	
53- Min Vert Clr Ov Deck	99	99
100- STRAHNET	0	
102- Traffic Direct	2	
109- Truck %	3	
110- Truck Network	0	
114- Future ADT	80	
115- Year Future ADT		
Freeway	0	

Structure Appraisal

36A- Bridge Railing	1
36B- Rail Transition	0
36C- Approach Rail	0
36D- Rail Termination	0
67- Structure Evaluation	6
68- Deck Geometry	4
69- Underclearance	5
71- Waterway Adequacy	N
72- Approach Alignment	7
103- Temporary Structure	_
113- Scour Criticality	N

Miscellaneous

37- Historical Significance	5
98A- Border Bridge State	
98B- Border Bridge %	
101- Parallel Structure	N
EPA ID	
Stay in Place Forms	

Print Date 5/11/2011 12:35:06

Route Under Structure (UNDER Record)

5A- Record Type	2	
5B- Route Signing	2	
5C- Level of Service	1	
5D- Route Number	00023	
5E- Direction Suffix	0	
10L- Best 10ft Uncl- Lt	14	6
10R- Best 10ft Uncl- Rt	14	8
PR Number		
Control Section	81076	
11- Mile Point	2.171	
12- Base Highway Network	1	
13- LRS Route-Subroute	0000014312	02
19- Detour Length	3	
20- Toll Facility	3	
26- Functional Class	02	
28B- Lanes Under	4	
29- ADT	41,226	
30- Year of ADT	2007	
42B- Service Type Under	1	
47L- Left Horizontal Clear	67.3	
47R- Right Horizontal Clear	67.3	
54A- Left Feature	H	
54B- Left Underclearance	14	6
Left Signed Underclearance	14	5
54C- Right Feature	H	
54D- Right Underclearance	14	8
Right Signed Underclearance	14	6
Under Clearance Year	2009	
55A- Reference Feature	H	
55B- Right Horiz Clearance	9.8	
56- Left Horiz Clearance	33.5	
100- STRAHNET	2	
101- Traffic Direction	2	
109- Truck %	14	
110- Truck Network	1	
114- Future ADT	48,352	
115- Year Future ADT	2018	
Freeway	0	

Proposed Improvements

75- Type of Work		_
76- Length of Improvement		
94- Bridge Cost		
95- Roadway Cost		
96- Total Cost		
97- Year of Cost Estimate		

Load Rating and Posting

31- Design Load	5	
41- Open, Posted, Closed	A	
63- Oper Rtg Method	2	
64F- Fed Operating Rtg	9.9000015258789	
64M- Mich Oper Rtg	9	159
65- Inv Rtg Method	2	
66- Inventory Load	55.5	
70- Posting	5	
141- Posted Loading		
195- Analysis ID	5315	
193- Overload Class	A	

BRIDGE INSPECTION REPORT

S02-81076

Facility Carried	Federal Structure ID	Inspector Name	Agency Consultant	Inspection Date
WILLOW RD	81181076000S020	ZOLNIEREKK	MDOT INSPECTOR	04/19/2010

Feature Intersected	Latitude	Longitude	Struc Num	Region	Insp Freq	Insp Key
US-23	420647.34	834056.33	10892	6- University	24	RNAR

Location	Length	Width	Year Built	Year Recon	Br Type		Scour Eval	No Pins
2.1 MI N OF MONROE COL	63.70000	9.39999	1962		5	32	N	

CORE ELEMENTS INSPECTION English Units

Element Number	Element Name	Total Quantity	State 1 Old	State 1 New	State 2 Old	State 2 New	State 3 Old	State 3 New	State 4 Old	State 4 New	State 5 Old	State 5 New
12 / 3	Conc Dk Black Bars	6448	0		6448		0		0		0	
401 / 3	Pourable Joint Seal	62	0		0		62		0		0	
405 / 3	Miscellaneous Exp Jt	492	0		0		492		0		0	
109 / 3	Prestr Con Girder/Bm	1250	1225		25		0		0		0	
331 / 3	Concrete Bridge Rail	417	357		60		0		0		0	
310 / 3	Elastomeric Bearing	36	28		8		0		0		0	
313 / 3	Fixed Bearing	12	0		12		0		0		0	
205 / 3	Reinf Conc Column	9	6		2		1		0		0	
215 / 3	Reinf Conc Abut	62	54		4		4		0		0	
234 / 3	Reinf Conc Pier Cap	92	60		25		7		0		0	
358 / 3	Dk Cr SmF Conc/Latex	1	1		0		0		0		0	
359 / 3	Deck Bott Surf Sm F	1	0		0		1		0		0	
362 / 3	Traf Impact SmFlag	1	0		1		0		0		0	
379 / 3	Deck Fascia Sm Flag	1	0		1		0		0		0	

CREW RECOMMENDATIONS

Deck Patching		
Approach Pavement		
Joint Repair		
Railing Repair		
Detailed Inspection		
Zone Paint		
Substructure Repair	H	Repair spall at the east abutment under beam
Slope Repair		
Brush Cut		
Other Crew Work	H	Scale fascias over traffic.

CONTRACT RECOMMENDATIONS

Bridge Replacement		
Superstructure Replacement	M	
Deck Replacement		
Overlay		
Widen		
Paint		
Zone Paint		
Pin and Hanger		
Substructure Repair		
Other Contract Work		

Appendix D.3 – Bridge Inspection Report: Satisfactory Selection – Freer Road

Bridge Safety Inspection Report

Facility	Federal Structure ID	Inspector Name	Agency / Consultant	Inspection Date
FREER RD	81181104000S050	ZOLNIEREKK	MDOT INSPECTOR	06/02/2010

Feature	Latitude	Longitude	Struc Num	Insp Freq	Insp Key
I-94	421744.7	840019.92	10940	24	UTVQ

Location	Length	Width	Year Built	Year Recon	Br Type		Scour Eval	No.Pins
1.0 MI E OF M-52	208.9895	32.808	1960		5	32	N	

LEGEND

9	New
7-8	Good
5-6	Fair
3-4	Poor
2 or Less	Critical

06 08 10

NBI INSPECTION

Deck

1. Surface SIA-58A	6	6	6		Several areas of concrete patching. Few tight transverse and diagonal cracks. Span 2S minor spall with 2 sft of delam surrounding it. (2010), Several areas of concrete patching. Few tight transverse and diagonal cracks. Approx center of span 2S minor spall with 2 sft of delam surrounding it. Surface is worn to the aggregate. (2008), Several areas of concrete patching. Few tight transverse and diagonal cracks.(2006).
2. Expansion Jts	8	8	7		Joints 2,3,4, 5 and 6s are strip-seals with tight cracking in the surrounding concrete.(2010), Joints 2,3,4, 5 and 6 are strip-seals. All of the joints are filled with some debris.(2008), Joints 1,2,3,4&5 are strip-seals, new in 2004. all of the joints are filled with some debris.(2006).
3. Other Joints	8	8	7		Joints 1 and 7s are pourable joints just to the outside of the strip-seals at each end of the bridge with areas of adhesion failure.(2010), Joints 1 and 7 are pourable joints just to the outside of the strip-seals at each end of the bridge. Minor adhesion failure. (2008), There are pourable joints just to the outside of the strip-seals at each end of the bridge.(2006).
4. Railings	7	7	7		Concrete with a twelve inch top. Few tight leaching vertical cracks typical. Coated with concrete surface coating. (2010), Concrete with a twelve inch top. Few tight leaching vertical cracks typical. Coated with CSC. (2008), Concrete jersey with a twelve inch top. Few tight vertical cracks typical.(2006).
5. Sidewalks or curbs	N	N	N		
6. Deck SIA-58	6	6	6		Surface: Several areas of concrete patching. Few tight transverse and diagonal cracks. Span 2S minor spall with 2 sft of delam surrounding it. Surface is worn to the aggregate. Bottom: Random and transverse leaching cracks. There is some leaching, delam, and 1 STS along the center line construction joint. 2 SFT STS in span 1s, bay 5w. The west fascia beam has two incipient spalls and minor leaching. The deck fascias have spalling and cracking near the joint endings.(2010), The west fascia beam has two incipient spalls and minor leaching. The east fascia beam is cracked and spalled at the north abutment and at pier 2S has minor leaching.(2008), There is some leaching along the center line construction joint. Two SFT incipient spall in span one, bay five. The west fascia beam has two incipient spalls. The east fascia beam is cracked and spalled at the north abutment. (2006).
7. Drainage					Catch basins in all approach quads.(2010), Catch basins in all approach quads.(2008), There is some leaching along the center line construction joint. Two SFT incipient spall in span one, bay five. The west fascia beam has two incipient spalls. (2006).

Superstructure

8. Stringer SIA-59	6	7	7		PCIC beams. There are cracks and shallow spalls on most of the beam end locations on the bottom flanges, a few of them have been repaired. Beam ends are coated with concrete surface coating. Concrete diaphragms.(2010), PCIC beams. There are some cracks and shallow spalls at some of the beam end locations on the bottom flanges, a few of them have been repaired. Beam ends are coated with CSC. (2008), PCIC beams. There are some cracks and shallow spalls at some of the beam end locations on the bottom flanges, a few of them have been repaired.(2006).
9. Paint SIA-59A	N	N	N		Concrete surface sealer was applied to the bridge railing, substructure, diaphragms and beam ends at the piers and abutments in 2004. The concrete surface sealer is flaking off because it was applied over debris.(2006).
10. Section Loss	N	N	N		
11. Bearings	6	6	6		Elastomeric bearing pads are split and cracked. The sole plates have moderate rust. The elastomeric pads are walking out from under the beams ends in some locations.(2010), Elastomeric bearing pads are split and cracked. The sole plates are heavily corroded. The elastomeric pads are walking out from under the beams ends in some locations. At South abutment BM1W elastomeric pad is too small. (2008), Elastomeric bearing pads are split and cracked. The sole plates are heavily corroded. The elastomeric pads are walking out from under the beams ends in some locations.(2006).

Substructure

12. Abutments SIA-60	7	7	7		Few vertical cracks typical. North abutment: some areas of concrete patches. South abutment: approx 1 sft delam under beam 6W. (2010), Few vertical cracks typical. North abutment: some areas of concrete patches. South abutment: approx 1 sft delam under beam 6W. (2008), Few vertical cracks typical. The north abutment has some areas of concrete patches.(2006).
13. Piers SIA-60	7	7	7		All of the piers have several areas of concrete patches with tight random cracking. Concrete surface coating is peeling. (2010), All of the piers have several areas of concrete patches. CSC is peeling. (2008), All of the piers have several areas of concrete patches. (2006).
14. Slope Protection	7	7	7		Grouted sandstone. Some vegetation is growing thru.(2010), Grouted sandstone. Some vegetation is growing thru.(2008), Grouted sandstone. Some vegetation is growing thru.(2006).

Bridge Safety Inspection Report

Facility	Federal Structure ID	Inspector Name	Agency / Consultant	Inspection Date
FREER RD	81181104000S050	ZOLNIEREKK	MDOT INSPECTOR	06/02/2010

Feature	Latitude	Longitude	Struc Num	Insp Freq	Insp Key
I-94	421744.7	840019.92	10940	24	UTVQ

Location	Length	Width	Year Built	Year Recon	Br Type		Scour Eval	No.Pins
1.0 MI E OF M-52	208.9895	32.808	1960		5	32	N	

LEGEND

9	New
7-8	Good
5-6	Fair
3-4	Poor
2 or Less	Critical

06 08 10

NBI INSPECTION

Approach

15. Approach Pavt	8 8 6	The approach pavement is a mix of HMA and concrete. South approach: chip seal, patched areas, open random cracking. North approach: chip seal with open random and transverse cracks.(2010), The approach pavement is a mix of HMA and concrete. South approach: chip seal, patched areas, cracking. North approach: chip seal.(2008), The approach pavement is a mix of HMA and new concrete in 2004. The HMA in both approaches is heavily map cracked with some HMA patches and chip sealed over at the east end. (2006).
16. Approach Shldrs Swalk	6 6 7	Bit with concrete curb and gutter. Tight transverse cracks in the bit.(2010), Bit with concrete curb and gutter, (2008), Bit with concrete curb and gutter,(2006).
17. Approach Slopes		Grass and weeds.(2010), Grass covered.(2008), Grass covered with one tree in the southwest approach quad.(2006).
18. Utilities		No utilities are visible in the immediate area.(2010), No utilities are visible in the immediate area.(2008), No utilities are visible in the immediate area.(2006).
19. Channel SIA-61	N N N	
20. Drainage Culverts		

MISCELLANEOUS

Guard Rail

	06	10	10	
36A	1	1	1	1
36B	1	1	1	1
36C	1	1	1	1
36D	1	1	1	1

Crit Feat Insp(SIA-92)

		Freq	Date
92A	Frac Crit		
92B	Und. Watr		
92C	Spl.Insp		

71 Watr Adeq	
72 Appr Align	6
Temp Supp	0
Hi Ld Hit (M)	0
Special Insp Euip.	9

General Notes

Form 1717A- 01/2002

Michigan Department of Transportation

Structure Inventory and Appraisal

Code in red ink

Control Section: S05-81104

MDOT Bridge ID: 81 1811040000000S05

NBI Bridge ID	Struct Num	Region	TSC	County	City Resp	City Location	7- Facility Carried	User Name
81181104000S050	10940	06	6B	81		0	FREER RD	ZOLNIEREKK

6- Feature Intersected	9- Location	Latitude	Longitude	Owner	Maint Resp
I-94	1.0 MI E OF M-52	42° 17' 44.70"	84° 00' 19.92"	1	1

Bridge History, Type, Materials

27- Year Built	1960	
106- Year Reconstructed		
202- Year Painted		
203- Year Overlay		
43- Main Span Bridge Type	5	32
44- Appr Span Bridge Type	_	
77- Steel Type	0	
78- Paint Type	0	
79- Rail Type	8	
80- Post Type	0	
107- Deck Type	1	
108A- Wearing Surface	1	
108B- Membrane	0	
108C- Deck Protection	0	

Structure Dimensions

34- Skew	4
35- Struct Flared	0
45- Num Main Spans	4
46- Num Appr Spans	0
48- Max Span Length	70.9
49- Structure Length	209.0
50A- Width Left Curb/SW	0.0
50B- Width Right Curb/SW	0.0
33- Median	0
51- Width Curb to Curb	28.5
52-Width Out to Out	32.8
112- NBIS Length	Y

Inspection Data

90- Inspection Date	06/02/2010	
91- Inspection Freq	24	
92A- Frac Crit Req/Freq	N	
93A- Frac Crit Insp Date		
92B- Und Water Req/Freq	N	
93B- Und Water Insp Date		
92C- Oth Spec Insp Req/Freq	N	
93C- Oth Spep Insp Date		
176A- Und Water Insp Method		
58- Deck Rating	6	
58A- Deck Surface Rtg	6	
59- Superstructure Rating	7	
59A- Paint Rating	N	
60- Substructure Rating	7	
61- Channel Rating	N	
62- Culvert Rating	N	

Navigation Data

38- Navigation Control	N
39- Vertical Clearance	0.0
40- Horizontal Clearance	0.0
111- Pier Protection	
116- Lift Brdg Vert Clear	

Route Carried By Structure (ON Record)

5A- Record Type	1	
5B- Route Signing	4	
5C- Level of Service	0	
5D- Route Number	00000	
5E- Direction Suffix	0	
10L- Best 10ft Unclr- Lt	0	0
10R- Best 10ft Uncl- Rt	99	99
PR Number		
Control Section		
11- Mile Point		
12- Base Highway Network	0	
13- LRS Route-Subroute	0000014265	00
19- Detour Length	4	
20- Toll Facility	3	
26- Functional Class	09	
28A- Lanes On	2	
29- ADT	150	
30- Year of ADT	1997	
32- Appr Roadway Width	29.9	
32A/B- Ap Pvt Type/Width	4	29.9
42A- Service Type On	1	
47L- Left Horizontal Clear	0.0	
47R- Right Horizontal Clear	30.2	
53- Min Vert Clr Ov Deck	99	99
100- STRAHNET	0	
102- Traffic Direct	2	
109- Truck %	3	
110- Truck Network	0	
114- Future ADT	60	
115- Year Future ADT		
Freeway	0	

Structure Appraisal

36A- Bridge Railing	1
36B- Rail Transition	1
36C- Approach Rail	1
36D- Rail Termination	1
67- Structure Evaluation	7
68- Deck Geometry	6
69- Underclearance	4
71- Waterway Adequacy	N
72- Approach Alignment	6
103- Temporary Structure	_
113- Scour Criticality	N

Miscellaneous

37- Historical Significance	5
98A- Border Bridge State	
98B- Border Bridge %	
101- Parallel Structure	N
EPA ID	
Stay in Place Forms	

Print Date 5/11/2011 12:41:05

Route Under Structure (UNDER Record)

5A- Record Type	2	
5B- Route Signing	1	
5C- Level of Service	1	
5D- Route Number	00094	
5E- Direction Suffix	0	
10L- Best 10ft Uncl- Lt	16	3
10R- Best 10ft Uncl- Rt	16	0
PR Number		
Control Section	81104	
11- Mile Point	6.633	
12- Base Highway Network	1	
13- LRS Route-Subroute	0000014261	09
19- Detour Length	4	
20- Toll Facility	3	
26- Functional Class	01	
28B- Lanes Under	4	
29- ADT	52,222	
30- Year of ADT	2007	
42B- Service Type Under	1	
47L- Left Horizontal Clear	67.3	
47R- Right Horizontal Clear	67.3	
54A- Left Feature	H	
54B- Left Underclearance	16	3
Left Signed Underclearance	0	0
54C- Right Feature	H	
54D- Right Underclearance	16	0
Right Signed Underclearance	0	0
Under Clearance Year	2009	
55A- Reference Feature	H	
55B- Right Horiz Clearance	10.5	
56- Left Horiz Clearance	24.6	
100- STRAHNET	1	
101- Traffic Direction	2	
109- Truck %	26	
110- Truck Network	1	
114- Future ADT	49,964	
115- Year Future ADT	2018	
Freeway	0	

Proposed Improvements

75- Type of Work		_
76- Length of Improvement		
94- Bridge Cost		
95- Roadway Cost		
96- Total Cost		
97- Year of Cost Estimate		

Load Rating and Posting

31- Design Load	2	
41- Open, Posted, Closed	A	
63- Oper Rtg Method	2	
64F- Fed Operating Rtg	0.900001525878	
64M- Mich Oper Rtg	9	111
65- Inv Rtg Method	2	
66- Inventory Load	3.599998474121	
70- Posting	5	
141- Posted Loading		
195- Analysis ID	5326	
193- Overload Class	A	

BRIDGE INSPECTION REPORT

S05-81104

Facility Carried	Federal Structure ID	Inspector Name	Agency Consultant	Inspection Date
FREER RD	81181104000S050	ZOLNIEREKK	MDOT INSPECTOR	06/02/2010

Feature Intersected	Latitude	Longitude	Struc Num	Region	Insp Freq	Insp Key
I-94	421744.7	840019.92	10940	6- University	24	TSUP

Location	Length	Width	Year Built	Year Recon	Br Type		Scour Eval	No Pins
1.0 MI E OF M-52	63.70000	10	1960		5	32	N	

CORE ELEMENTS INSPECTION English Units

Element Number	Element Name	Total Quantity	State 1 Old	State 1 New	State 2 Old	State 2 New	State 3 Old	State 3 New	State 4 Old	State 4 New	State 5 Old	State 5 New
12 / 3	Conc Dk Black Bars	6878	0		6878		0		0		0	
400 / 3	Strip Seal Exp Joint	165	165		0		0		0		0	
401 / 3	Pourable Joint Seal	66	0		66		0		0		0	
109 / 3	Prestr Con Girder/Bm	1253	1205		48		0		0		0	
331 / 3	Concrete Bridge Rail	417	397		20		0		0		0	
310 / 3	Elastomeric Bearing	48	32		16		0		0		0	
205 / 3	Reinf Conc Column	9	9		0		0		0		0	
215 / 3	Reinf Conc Abut	66	58		8		0		0		0	
234 / 3	Reinf Conc Pier Cap	102	98		4		0		0		0	
359 / 3	Deck Bott Surf Sm F	1	0		1		0		0		0	
367 / 3	Conc Surf Coat SmFlg	1	0		1		0		0		0	
379 / 3	Deck Fascia Sm Flag	1	1		0		0		0		0	

CREW RECOMMENDATIONS

Deck Patching	L	2 sft patch in center of span 2 S.
Approach Pavement		
Joint Repair		
Railing Repair		
Detailed Inspection		
Zone Paint		
Substructure Repair		
Slope Repair		
Brush Cut		
Other Crew Work	H	Scale span 2S bay 3W, span 3S bay 3W, and

CONTRACT RECOMMENDATIONS

Bridge Replacement		
Superstructure Replacement		
Deck Replacement		
Overlay	M	Epoxy overlay
Widen		
Paint		
Zone Paint		
Pin and Hanger		
Substructure Repair		
Other Contract Work		

Appendix D.4 – Bridge Inspection Report: Supplemental Selection – Mannsiding South Bound

Bridge Safety Inspection Report

S08-18033

Facility	Federal Structure ID	Inspector Name	Agency / Consultant	Inspection Date
MANNSIDING RD	18118033000S080	RUEGSEGGERP		10/11/2010

Feature	Latitude	Longitude	Struc Num	Insp Freq	Insp Key
US-127 SB	435721.88	844638	1712	24	RHTF

Location	Length	Width	Year Built	Year Recon	Br Type		Scour Eval	No.Pins
2.3 MI S OF M-61	129.8999	31.170	1966		5	32	N	

LEGEND

9	New
7-8	Good
5-6	Fair
3-4	Poor
2 or Less	Critical

06 08 10

NBI INSPECTION

Deck

1. Surface SIA-58A	7 7 7	A couple of unsealed cracks in conc. surface. Light shallow scaling. (2010), A couple of unsealed crks. in conc. surface. Light shallow scaling.(2008), A couple of unsealed crks. in conc. surface. 06(2006).
2. Expansion Jts	8 8 8	Strip seals. Debris in glands. H/L cracks in adjacent concrete.(2010), Newer strip seals. Minor debris. (2008), Newer strip seals. Minor debris. 06(2006).
3. Other Joints	5 5 4	HPR at end joints. Minor spalling. Adhesion faillure along both. Leaking less than 5%.(2010), HPR at end jts. Minor spalling. Leaking less than 5%.(2008), HPR at end jts. Minor spallin. Leaking less than 5%. 06(2006).
4. Railings	7 7 7	Concrete open parapet with single aluminum tube. CSC applied and retrofitted with thrie beam SBGR. Minor spalls and cracks, some small rust stains. Few shallow spalls in S. brush block. Minor scrapes and weathering on SBGR panels.(2010), Conc parapet W/1 tube Alum. New thrie BM retro carried across bridge. N rail over traffic is new due to Bm replacement because of HLH. Minor spalls, with some small rust stains. Shallow spalls in S. brush block. Protective coating applied.(2008), Conc parapet W/1 tube Alum. New thrie BM retro carried across bridge. N rail over traffic is new due to Bm replacement because of HLH. Minor spalls, with some small rust stains. 06 (2006).
5. Sidewalks or curbs	N 7 N	
6. Deck SIA-58	7 7 7	Minor cracking in deck underside. CSC applied to fascias. Few cracks in deck fascias reflecting through coating, some exhibit rust stains. Minor cracking and shallow scaling in deck surface. (2010), Minor cracking in deck underside. CSS applied to fascias. Few cracks in deck fascias reflecting through coating. Minor cracking and shallow scaling in deck surface. (2008), Some leaching on fascias. fascia is 10-15% map cracked both N & S. Same. Most Crks on S fascia are rust stained. CSS applied to fascias. 06(2006).
7. Drainage		No problems noted.(2010), No problems noted.(2008), No problems noted. 06(2006).

Superstructure

8. Stringer SIA-59	6 6 6	PCI beams. CSC applied to fascias and beam ends at piers. Cracks, small spalls, and incipient spalls on beam ends adjacent to sole plates. HLH chips/scrapes on beams 5&6S over right lane span 2W. Beam 5S has been patched, patch has chips from new HLH hit. Beam 6S was replaced in 2000.(2010), PCI beams. S. fascia beam has a small spall on bottom in W. span at W. pier brg. N fascia Bm has been replaced due to HLH 2000. Small repaired area Bm 5S. Minor HLH spall with no exposed steel on BM 6S. Typical cracking on most BM ends over piers. CSS applied at bm. ends at piers and fascias.(2008), S. fascia beam has a small spall on bottom in W. span at W. pier brg. N fascia Bm has been replaced due to HLH 2000. Small repaired area Bm 5S. S. fascia beam has a small spall on bottom in W. span at W. pier brg. Minor HLH spall with no exposed steel on BM 6S. Minor hairline crks on most BM ends over piers. CSS applied at bm. ends at piers and fascias. 06(2006).
9. Paint SIA-59A	N N N	
10. Section Loss	N N N	
11. Bearings	6 6 6	Minor corrosion on steel plates .Minor cracking & deformations on Elast bearings over piers.(2010), Minor corrosion on steel plates .Minor Crking & deformations on Elast Brgs over Prs. (2008), Minor corrosion on steel plates .Minor Crking & deformations on Elast Brgs over Prs. 06(2006).

Substructure

12. Abutments SIA-60	7 7 7	CSC applied. Couple vertical cracks in both.(2010), Few vert. crks. in both abutments. CSS applied.(2008), Few vert. crks. in both abutments. CSS applied. 06(2006).
13. Piers SIA-60	7 7 7	CSC applied. Bolster on Pier 2W is cracked/delaminated near beam 2S.(2010), Conc. repairs made. CSS. applied. (2008), Conc. repairs made. CSS. applied. 06(2006).
14. Slope Protection	6 6 6	Concrete block & grout. Minor cracks, spalls, missing, and scaling blocks. Minor settlment. 2 missing blocks on top of E. slope. Void under blocks at south end of west slope.(2010), Conc block & grout. Minor Crks, spalls with light settlment. 2 missing blocks on top of E. slope.(2008), Conc block & grout. Minor Crks, spalls with light settlment. 2 missing blocks on top of E. slope. 06(2006).

Approach

15. Approach Pavt	9 8 8	Concrete. H/L cracks in both. Minor chips/scaling and reference lines.(2010), Concrete. No problems noted. (2008), New conc. No problems noted. 06(2006).

Bridge Safety Inspection Report

Facility	Federal Structure ID	Inspector Name	Agency / Consultant	Inspection Date
MANNSIDING RD	18118033000S080	RUEGSEGGERP		10/11/2010

Feature	Latitude	Longitude	Struc Num	Insp Freq	Insp Key
US-127 SB	435721.88	844638	1712	24	RHTF

Location	Length	Width	Year Built	Year Recon	Br Type		Scour Eval	No.Pins
2.3 MI S OF M-61	129.8999	31.170	1966		5	32	N	

LEGEND

9	New
7-8	Good
5-6	Fair
3-4	Poor
2 or Less	Critical

06 08 10

NBI INSPECTION

16. Approach Shldrs Swalk	N N N	Narrow Conc curb. (2008), Narrow Conc curb. 06(2006).
17. Approach Slopes		Vegetated. No problems noted.(2010), Well vegetated. (2008), Well veg. 06(2006).
18. Utilities		
19. Channel SIA-61	N N N	
20. Drainage Culverts		Minor dirt and debris at NE. and SE. (2010), Minor dirt and debris at NE. and SE. (2008), Minor dirt and debris at NE. and SE. 06(2006).

MISCELLANEOUS

Guard Rail

	06	10	10	
36A	1	1	1	1
36B	1	1	1	1
36C	1	1	1	1
36D	1	1	1	1

Crit Feat Insp(SIA-92)

		Freq	Date
92A	Frac Crit		
92B	Und. Watr		
92C	Spl.Insp		

71	Watr Adeq	
72	Appr Align	6
	Temp Supp	
	Hi Ld Hit (M)	
	Special Insp Euip.	

General Notes

CSM Crk. seal. Reseal end jts. 06. Healer sealer. 08

Form 1717A- 01/2002

Michigan Department of Transportation

Structure Inventory and Appraisal

Code in red ink

Control Section: S08-18033

MDOT Bridge ID: 18 1180330000000S08

NBI Bridge ID	Struct Num	Region	TSC	County	City Resp	City Location	7- Facility Carried	User Name
18118033000S080	1712	04	4A	18		0	MANNSIDING RD	RUEGSEGGERP

6- Feature Intersected	9- Location	Latitude	Longitude	Owner	Maint Resp
US-127 SB	2.3 MI S OF M-61	43° 57' 21.88"	84° 46' 38.00"	1	1

Bridge History, Type, Materials

27- Year Built	1966	
106- Year Reconstructed		
202- Year Painted		
203- Year Overlay		
43- Main Span Bridge Type	5	32
44- Appr Span Bridge Type	_	
77- Steel Type	0	
78- Paint Type	0	
79- Rail Type	6	
80- Post Type	2	
107- Deck Type	1	
108A- Wearing Surface	1	
108B- Membrane	0	
108C- Deck Protection	0	

Structure Dimensions

34- Skew	14
35- Struct Flared	0
45- Num Main Spans	3
46- Num Appr Spans	0
48- Max Span Length	61.0
49- Structure Length	129.9
50A- Width Left Curb/SW	1.3
50B- Width Right Curb/SW	1.3
33- Median	0
51- Width Curb to Curb	25.9
52-Width Out to Out	31.2
112- NBIS Length	Y

Inspection Data

90- Inspection Date	10/11/2010	
91- Inspection Freq	24	
92A- Frac Crit Req/Freq	N	
93A- Frac Crit Insp Date		
92B- Und Water Req/Freq	N	
93B- Und Water Insp Date		
92C- Oth Spec Insp Req/Freq	N	
93C- Oth Spep Insp Date		
176A- Und Water Insp Method	0	
58- Deck Rating	7	
58A- Deck Surface Rtg	7	
59- Superstructure Rating	6	
59A- Paint Rating	N	
60- Substructure Rating	7	
61- Channel Rating	N	
62- Culvert Rating	N	

Navigation Data

38- Navigation Control	N
39- Vertical Clearance	0.0
40- Horizontal Clearance	0.0
111- Pier Protection	
116- Lift Brdg Vert Clear	0.0

Route Carried By Structure (ON Record)

5A- Record Type	1	
5B- Route Signing	4	
5C- Level of Service	1	
5D- Route Number	01840	
5E- Direction Suffix	0	
10L- Best 10ft Unclr- Lt	0	0
10R- Best 10ft Uncl- Rt	99	99
PR Number		
Control Section		
11- Mile Point		
12- Base Highway Network	0	
13- LRS Route-Subroute	0000010481	00
19- Detour Length	10	
20- Toll Facility	3	
26- Functional Class	07	
28A- Lanes On	2	
29- ADT	1000	
30- Year of ADT	1996	
32- Appr Roadway Width	33.8	
32A/B- Ap Pvt Type/Width	4	33.8
42A- Service Type On	1	
47L- Left Horizontal Clear	0.0	
47R- Right Horizontal Clear	28.9	
53- Min Vert Clr Ov Deck	99	99
100- STRAHNET	0	
102- Traffic Direct	2	
109- Truck %	3	
110- Truck Network	0	
114- Future ADT	1500	
115- Year Future ADT	2010	
Freeway	0	

Structure Appraisal

36A- Bridge Railing	1
36B- Rail Transition	1
36C- Approach Rail	1
36D- Rail Termination	1
67- Structure Evaluation	6
68- Deck Geometry	5
69- Underclearance	5
71- Waterway Adequacy	N
72- Approach Alignment	6
103- Temporary Structure	_
113- Scour Criticality	N

Miscellaneous

37- Historical Significance	5
98A- Border Bridge State	
98B- Border Bridge %	
101- Parallel Structure	N
EPA ID	
Stay in Place Forms	

Print Date 6/27/2011 08:15:56

Route Under Structure (UNDER Record)

5A- Record Type	2	
5B- Route Signing	2	
5C- Level of Service	1	
5D- Route Number	00127	
5E- Direction Suffix	0	
10L- Best 10ft Uncl- Lt		
10R- Best 10ft Uncl- Rt	14	5
PR Number		
Control Section	18033	
11- Mile Point	10.500	
12- Base Highway Network	1	
13- LRS Route-Subroute	0000010410	08
19- Detour Length	8	
20- Toll Facility	3	
26- Functional Class	02	
28B- Lanes Under	2	
29- ADT	6,069	
30- Year of ADT	2007	
42B- Service Type Under	1	
47L- Left Horizontal Clear	56.4	
47R- Right Horizontal Clear	0.0	
54A- Left Feature	H	
54B- Left Underclearance	0	0
Left Signed Underclearance	0	0
54C- Right Feature	H	
54D- Right Underclearance	14	5
Right Signed Underclearance	14	5
Under Clearance Year	2010	
55A- Reference Feature	H	
55B- Right Horiz Clearance	10.8	
56- Left Horiz Clearance	21.3	
100- STRAHNET	0	
101- Traffic Direction	1	
109- Truck %	8	
110- Truck Network	1	
114- Future ADT	11,106	
115- Year Future ADT	2018	
Freeway	0	

Proposed Improvements

75- Type of Work		_
76- Length of Improvement		
94- Bridge Cost		
95- Roadway Cost		
96- Total Cost		
97- Year of Cost Estimate		

Load Rating and Posting

31- Design Load	2	
41- Open, Posted, Closed	A	
63- Oper Rtg Method	2	
64F- Fed Operating Rtg	77.3	
64M- Mich Oper Rtg	9	110
65- Inv Rtg Method	2	
66- Inventory Load	28.2	
70- Posting	5	
141- Posted Loading		
195- Analysis ID	5065	
193- Overload Class	A	

BRIDGE INSPECTION REPORT

S08-18033

06/27/2011

Facility Carried	Federal Structure ID	Inspector Name	Agency Consultant	Inspection Date
MANNSIDING RD	18118033000S080	RUEGSEGGERP		10/11/2010

Feature Intersected	Latitude	Longitude	Struc Num	Region	Insp Freq	Insp Key
US-127 SB	435721.88	844638	1712	4- Bay	24	QGSE

Location	Length	Width	Year Built	Year Recon	Br Type		Scour Eval	No Pins
2.3 MI S OF M-61	39.5935	9.50062	1966		5	32	N	

CORE ELEMENTS INSPECTION English Units

Element Number	Element Name	Total Quantity	State 1 Old	State 1 New	State 2 Old	State 2 New	State 3 Old	State 3 New	State 4 Old	State 4 New	State 5 Old	State 5 New
12 / 3	Conc Dk Black Bars	4047	4047		0		0		0		0	
400 / 3	Strip Seal Exp Joint	66	66		0		0		0		0	
401 / 3	Pourable Joint Seal	66	0		66		0		0		0	
109 / 3	Prestr Con Girder/Bm	781	768		13		0		0		0	
331 / 3	Concrete Bridge Rail	259	120		139		0		0		0	
310 / 3	Elastomeric Bearing	36	8		28		0		0		0	
205 / 3	Reinf Conc Column	6	6		0		0		0		0	
215 / 3	Reinf Conc Abut	66	66		0		0		0		0	
234 / 3	Reinf Conc Pier Cap	66	66		0		0		0		0	
358 / 3	Dk Cr SmF Conc/Latex	1	1		0		0		0		0	
362 / 3	Traf Impact SmFlag	1	1		0		0		0		0	
367 / 3	Conc Surf Coat SmFlg	1	1		0		0		0		0	
379 / 3	Deck Fascia Sm Flag	1	1		0		0		0		0	

CREW RECOMMENDATIONS

Deck Patching	M	Crk. seal. 06. 08 Healer seal(10)
Approach Pavement		
Joint Repair	M	End jts. 06. 08 Clean strip seals 10
Railing Repair		
Detailed Inspection		-1
Zone Paint		
Substructure Repair	H	Fix bolster pier 2W
Slope Repair		-1
Brush Cut		
Other Crew Work		

CONTRACT RECOMMENDATIONS

Bridge Replacement		-1
Superstructure Replacement		-1
Deck Replacement		
Overlay		
Widen		
Paint		
Zone Paint		
Pin and Hanger		
Substructure Repair		
Other Contract Work		

Appendix E – Thermal Infrared Imagery Data

Freer Rd. Bridge

Cell No.	Delaminated area (ft^2)				Correspondence (%)		
	Thermal IR	Sounding	Overlapped	Total	Thermal IR	Sounding	Total
I22							
I21							
I20							
I19	0.0004						
I18							
I17							
I16		0.0002		0.0002			
I15							
I14							
I13							
H22							
H21							
H20							
H19	0.7397			0.7398			
H18							
H17							
H16							
H15							
H14							
H13							
H12	0.8109	2.0397	0.5703	2.2802	70.33	27.96	25.01
H11		1.6224		1.6224			
H10	1.2190	0.7457	0.1755	1.7886	14.40	23.53	9.81
H9	0.2615	1.3253		1.5869	0.00	0.00	0.00
H8							
H7							
H6							
H5							
H4							
H3							
G22							
G21							
G20							
G19							
G18							
G17							
G16							
G15							
G14							
G13							
G12							
G11							
G10	1.0382	1.0656	0.3218	1.7828	31.00	30.20	18.05
G9		0.9935		0.9935			
G8							

Cell No.	Delaminated area (ft^2)				Correspondence (%)		
	Thermal IR	Sounding	Overlapped	Total	Thermal IR	Sounding	Total
G7							
G6							
G5							
G4	0.6377	0.7071	0.4301	0.9145			
G3	0.8910	2.3334	0.5263	2.6982	59.07	22.56	19.51
G2							
G1							
F22							
F21							
F20	1.7844	8.6876	1.6707	8.8001	93.63	19.23	18.99
F19	1.3173	6.8428	1.3173	6.8425	100.00	19.25	19.25
F18	1.3389	3.5024	0.8777	3.9635	65.55	25.06	22.14
F17	1.4808	4.9854	1.2754	5.1908	86.13	25.58	24.57
F16	0.3270	2.3277		2.6547	0.00	0.00	0.00
F15	0.3145	4.1930	0.2678	4.2395	85.15	6.39	6.32
F14							
F13	0.0027			0.0000			
F12							
F11							
F10	0.3524			0.3524			
F9	0.0598						
F8							
F7							
F6							
F5							
F4							
F3	0.4718			0.4718			
F2							
F1							
E22							
E21							
E20							
E19							
E18	0.0220			0.0220			
E17	0.0941	0.3513	0.0877	0.3575	93.20	24.96	24.53
E16	0.5920	0.2638		0.8558			
E15	0.2580	1.5101	0.2015	1.5665	78.10	13.34	12.86
E14							
E13	4.8715	7.4574	3.5404	8.7877	72.68	47.47	40.29
E12							
E11	0.5623	1.4853	0.1419	1.9057	25.24	9.55	7.45
E10	5.0552	6.6901	1.6515	10.0929	32.67	24.69	16.36
E9	0.1500	2.4421	0.0417	2.5503	27.80	1.71	1.64
E8	0.6240	1.9586		2.5825			
E7	0.6945			0.6947			

Cell No.	Delaminated area (ft^2)				Correspondence (%)		
	Thermal IR	Sounding	Overlapped	Total	Thermal IR	Sounding	Total
E6	0.1014			0.1014			
E5	1.4720	4.1312	1.0352	4.5681	70.33	25.06	22.66
E4		3.7551		3.7551			
E3	0.0804	10.9211		11.0015			
E2		1.7106		1.7106			
E1							
D22							
D21		0.1188		0.1188			
D20							
D19							
D18							
D17							
D16							
D15							
D14							
D13							
D12							
D11	0.0536			0.0536			
D10	0.0492	0.0058		0.0550			
D9							
D8	1.1033			1.1033			
D7	0.4162			0.4161			
D6							
D5							
D4		3.8114		3.8114			
D3		1.0385		1.0385			
D2		4.7718		4.7718			
D1		3.9982		3.9982			
C22							
C21		0.6857		0.6857			
C20							
C19							
C18							
C17							
C16							
C15							
C14							
C13							
C12							
C11							
C10							
C9							
C8							
C7							
C6							

Cell No.	Delaminated area (ft^2)				Correspondence (%)		
	Thermal IR	Sounding	Overlapped	Total	Thermal IR	Sounding	Total
C5							
C4							
C3							
C2							
C1							
B13							
B12							
B11							
B10							
B9							
B8							
B7							
B6							
B5							
B4							
B3							
B2							
B1							
A4							
A3							
A2							
A1							
Total	29.2477	98.4787	14.1328	116.7844	48.32	13.89	12.09

Delaminated area outside the grid line 3.2573

Willow Rd. Bridge

Cell No.	Delaminated area (ft^2)				Correspondence (%)		
	Thermal IR	Sounding	Overlapped	Total	Thermal IR	Sounding	Total
V6				0			
V5	0.1362			0.1362			
V4		0.93		0.93			
V3		0.3538		0.3538			
V2	1.1607			1.1607			
V1		0.0192		0.0192			
U6				0			
U5	0.0337			0.0337			
U4		0.0257		0.0257			
U3		0.057		0.057			
U2	1.2566	3.2968		4.5534			
U1	0.7588	3.2576	0.1519	3.8633	20.02	4.66	3.93
T6				0			
T5				0			
T4		0.0585		0.0585			
T3				0			
T2	0.0006			0.0006			
T1	0.51	0.0097		0.5197			
S6		0.0084		0.0084			
S5				0			
S4	3.039	0.0295		3.0685			
S3	2.1049			2.1049			
S2	0.0045	0.0127		0.0172			
S1		0.0156		0.0156			
R6		3.265		3.265			
R5	1.5136	1.2344	0.8328	1.9146	55.02	67.47	43.50
R4	1.3233	1.9699		3.2932	0.00	0.00	0.00
R3	11.0645	2.848	0.0433	13.8692	0.39	1.52	0.31
R2	1.0017	0.4856	0.0003	1.487	0.03	0.06	0.02
R1		0.2684		0.2684			
Q7				0			
Q6		2.189		2.189			
Q5	1.5264	2.8825	0.6681	3.74	43.77	23.18	17.86
Q4	0.3939	2.678	0.1028	2.9672	26.10	3.84	3.46
Q3	2.1736			2.1736			
Q2	1.9915	3.3349	1.1046	4.2208	55.47	33.12	26.17
Q1		1.5883		1.5883			
P7		0.0113		0.0113			
P6				0			
P5				0			
P4	0.4526	0.0428		0.4954			
P3	4.1714	3.6666		7.838			
P2	3.2912	1.4898		4.781			
P1				0			
O7		1.6723		1.6723			

Cell No.	Delaminated area (ft^2)				Correspondence (%)		
	Thermal IR	Sounding	Overlapped	Total	Thermal IR	Sounding	Total
O6	1.1165	0		1.1165			
O5	1.606	0		1.606			
O4	5.1327	4.3911	1.4976	8.0262	29.18	34.11	18.66
O3	5.3707	7.4144	1.5015	11.2828	27.96	20.25	13.31
O2	0.0792	0		0.0792			
O1		0.006		0.006			
N7		0.7425		0.7425			
N6	5.9642	0.9899		6.9541			
N5	1.6984	0		1.6984			
N4	1.3262	2.5504	0.4583	3.4184	34.56	17.97	13.41
N3	0.5275	0.5809	0.0207	1.0878	3.92	3.56	1.90
N2	4.7165	2.2696	0.4893	6.4964	10.37	21.56	7.53
M7		0		0			
M6	0.0204	0		0.0204			
M5	16.3657	0		16.365			
M4	2.7955	1.353	0.0717	4.0768	2.56	5.30	1.76
M3	0.0227	0.7091	0.0168	0.7152	74.01	2.37	2.35
M2	1.0874	4.3327	0.4283	4.991	39.39	9.89	8.58
L7		1.5152		1.5152			
L6		0		0			
L5	0.0531	1.301		1.3541			
L4	0.0144	1.5485	0.0021	1.561	14.58	0.14	0.13
L3	1.4549	3.0811	0.0782	4.4579	5.37	2.54	1.75
L2	0.8876	5.5094	0.4062	5.9906	45.76	7.37	6.78
K7	2.0531	1.5936		3.6467			
K6	0.3941	0		0.3941			
K5	0.1825	0.0454		0.2279			
K4	4.2986	0		4.2986			
K3	0.0756	0.3498	0.0756	0.3497	100.00	21.61	21.62
K2	0.1121	0.8934	0.1119	0.8934	99.82	12.53	12.53
J8		0		0			
J7	0.6742	2.8721		3.5463	0.00	0.00	0.00
J6		0		0			
J5	0.121	0.0566		0.1776			
J4	6.1105	1.6518		7.7623	0.00	0.00	0.00
J3		0		0			
J2		0		0			
I8		0		0			
I7	1.6193	0.3388		1.9581	0.00	0.00	0.00
I6	0.6013	0.6522	0.1256	1.1276	20.89	19.26	11.14
I5	0.1617	1.6504	0.0052	1.8071	3.22	0.32	0.29
I4	0.9799	2.6085	0.3766	3.2116	38.43	14.44	11.73
I3	1.4058	0		1.4058			
I2		0		0			
H8		0		0			

Cell No.	Delaminated area (ft^2)				Correspondence (%)		
	Thermal IR	Sounding	Overlapped	Total	Thermal IR	Sounding	Total
H7	1.3669	3.5331	0.1233	4.7767	9.02	3.49	2.58
H6	3.9983	2.7079	0.0477	6.6585	1.19	1.76	0.72
H5	0.1675	1.183		1.3505	0.00	0.00	0.00
H4	2.4216	5.5525	0.0974	7.8764	4.02	1.75	1.24
H3	1.0425	1.2038	0.0158	2.2306	1.52	1.31	0.71
H2		0		0			
G8		0.0303		0.0303			
G7	4.9148	5.4019	2.3336	7.983	47.48	43.20	29.23
G6	1.9741	0.2586	0.0023	2.2303	0.12	0.89	0.10
G5	1.1839	0.6026	0.4256	1.3608	35.95	70.63	31.28
G4	4.434	5.7178	3.242	6.9084	73.12	56.70	46.93
G3	1.004	4.3975	0.7552	4.6457	75.22	17.17	16.26
G2		0		0			
F8		0		0			
F7	0.0328	0		0.0328			
F6	3.8064	1.7298	0.4597	5.0755	12.08	26.58	9.06
F5	1.7719	0.8682	0.123	2.5172	6.94	14.17	4.89
F4	0.9883	1.1259	0.6743	1.4383	68.23	59.89	46.88
F3	1.8429	0.8459	0.4725	2.216	25.64	55.86	21.32
E8		0.0062		0.0062			
E7	0.0534	0		0.0534			
E6	2.0779	0.8209		2.8988			
E5	0.0411	0.1636		0.2047			
E4	0.7891	0		0.7891			
E3	0.189	0		0.189			
D8		0		0			
D7	0.3198	0		0.3198			
D6	1.3247	0.8318	0.1459	2.0106	11.01	17.54	7.26
D5		0.0195		0.0195			
D4	3.6249	0		3.6249			
D3	0.5299	0.0163		0.5462			
C8	1.1019	0		1.1019			
C7	0.0454	0		0.0454			
C6		0.0828		0.0828			
C5	0.13	0		0.13			
C4	2.1617	0		2.1617			
C3		0		0			
B9		0.1174		0.1174			
B8	0.3322	0.9364		1.2686			
B7	0.0686	0		0.0686			
B6		0.0123		0.0123			
B5	0.0005	0.9542		0.9547			
B4	7.1077	0		7.1077			
B3		0		0			
A9		0		0			

Cell No.	Delaminated area (ft^2)				Correspondence (%)		
	Thermal IR	Sounding	Overlapped	Total	Thermal IR	Sounding	Total
A8		0		0			
A7		0		0			
A6		0		0			
A5		0		0			
A4	0.044	0		0.044			
A3		0		0			
Total	157.8297	127.8289	17.4877	299.8847	11.08	10.96	5.83

Delaminated area outside the grid line 31.71384

Mannsiding Rd. Bridge

Cell No.	Delaminated area (ft^2)				Correspondence (%)		
	Thermal IR	Sounding	Overlapped	Total	Thermal IR	Sounding	Total
A1							
A2							
A3							
A4							
A5							
A6							
A7							
A8							
B1							
B2							
B3							
B4	1.0296			1.03			
B5							
B6							
B7							
B8							
C2							
C3							
C4	1.0044			1.00			
C5	2.6585			2.66			
C6							
C7							
C8							
C9							
D2							
D3		2.7832		2.78			
D4		1.3343		1.33			
D5	3.6493			3.65			
D6	0.0014			0.00			
D7							
D8							
D9							
D10							
E3	0.1651	0.2507	0.0055	0.41	3.33	2.19	1.34
E4	2.6975	6.238	0.5725	8.36	21.22	9.18	6.85
E5	1.707	0.1536	0.0042	1.86	0.25	2.73	0.23
E6	2.4473			2.45	0.00		0.00
E7							
E8							
E9							
E10							
F4							
F5	0.3414	8.0088	0.3215	8.03	94.17	4.01	4.00
F6	0.9598	10.9628	0.7557	11.17	78.74	6.89	6.77

Cell No.	Delaminated area (ft^2)				Correspondence (%)		
	Thermal IR	Sounding	Overlapped	Total	Thermal IR	Sounding	Total
F7	1.5862	8.6017	0.5696	9.62	35.91	6.62	5.92
F8							
F9							
F10							
F11							
G4							
G5		5.8969		5.90		0.00	0.00
G6	0.9524	16.0474	0.9524	16.05	100.00	5.93	5.93
G7	2.2819	6.3223	1.5338	7.07	67.22	24.26	21.69
G8	2.1753	3.2285	1.0718	4.33	49.27	33.20	24.74
G9							
G10							
G11							
G12							
H5							
H6	14.8967	3.2383	0.3374	17.80	2.26	10.42	1.90
H7	4.6945	1.5688	0.0188	6.24	0.40	1.20	0.30
H8	6.2095	8.7542	3.69	11.27	59.43	42.15	32.73
H9							
H10							
H11							
H12							
H13							
I6	1.5878	1.0618	0.0296	2.62	1.86	2.79	1.13
I7	10.4492	8.4951	1.1524	17.79	11.03	13.57	6.48
I8	0.1018	3.4414		3.54	0.00	0.00	0.00
I9	3.4151	9.0902	1.7134	10.79	50.17	18.85	15.88
I10	3.2082			3.21	0.00		0.00
I11							
I12							
I13							
J6							
J7	5.2891			5.29			
J8	16.4208			16.42			
J9	0.6836			0.68			
J10	6.3865	6.6552	2.0359	11.01	31.88	30.59	18.50
J11	1.1077	0.5635	0.0376	1.63	3.39	6.67	2.30
J12							
J13							
J14							
K7							
K8	9.4515	2.857	2.3462	9.96	24.82	82.12	23.55
K9	5.2866	2.4108	0.4238	7.27	8.02	17.58	5.83
K10	6.045	9.3342	3.8545	11.52	63.76	41.29	33.45

Cell No.	Delaminated area (ft^2)				Correspondence (%)		
	Thermal IR	Sounding	Overlapped	Total	Thermal IR	Sounding	Total
K11	3.3068			3.31			
K12	1.2084			1.21			
K13							
K14							
K15							
L8							
L9							
L10							
L11	0.455			0.46			
L12	5.0713			5.07			
L13	0.7771			0.78			
L14							
L15							
M9							
M10				0.00			
M11	0.0032			0.00			
M12	0.7299			0.73			
M13	2.2349			2.23			
M14							
M15							
M16							
N9							
N10							
N11							
N12	0.2392			0.24			
N13	2.5549			2.55			
N14	0.6551			0.66			
N15							
N16							
N17							
O10							
O11							
O12							
O13							
O14							
O15							
O16							
O17							
P11							
P12							
P13							
P14							
P15							
P16							
P17							
Total	136.1265	127.2987	21.43	242.00	21.68	16.83	8.85

Appendix F.1 – Economic Evaluation: First Interview with MDOT Stakeholders

FIRST ROUND INTERVIEW WITH MDOT STAKEHOLDERS

Interview dates: August 31 and September 2, 2011

Interviewees:
Amy Trahey, Great Lakes Engineering Group
Rich Kathrens, MDOT
Dave Juntunen, MDOT
Steve Cook, MDOT
Jason DeRuyver. MDOT

Purpose: 1) To quantify the costs of traditional bridge inspection methods, such as time and labor requirements, equipment needs, cost of special bridge inspections, and develop an estimate of the overall annual budget for bridge inspection programs in Michigan; 2) to measure the benefits of new bridge inspection technologies, as well as incentives or barriers to their implementation (we will schedule a separate interview on this topic after field demonstration data becomes available in October); 3) to obtain results that will be in the white paper "Economic Valuation of Commercial Remote Sensing and Spatial Information for Bridge Health Monitoring."

General Questions about MDOT Bridge Inspection Program

1. *How many people are on the bridge inspection team at MDOT? How many years of experience does a typical bridge inspector have? What are the qualifications for bridge inspection?*

   The type of inspection drives the need for and number of inspectors. For MDOT, there are always two inspectors in each inspecting team. Local agencies vary and a lot time there is only one inspector.

   There are seven regions that have 2-3 dedicated bridge inspectors per region, making a total of 21-24 inspectors in MDOT. There is also an 8th group of inspectors based in Lansing that are called in when bridge inspections require special services. They are responsible for following bridges:

   - Fracture Critical Bridges
   - Complex Large Deck and Large Superstructure
   - Underwater Fatigue Sensitive and Removable

   Qualifications: Potential inspectors must be engineers plus undergo two weeks training. After obtaining 5 years of inspection experience, inspectors can become an inspection team leader. Also the Federal Highway Administration (FHWA) has guidelines for bridge inspector's qualifications.

2. *Of the 4,397 state-owned bridges, how many of them require specialized inspection services by private consultants? What are the determining factors for hiring a private consultant (e.g., special equipment, expertise, in-house staff shortage etc.)?*

For routine bridge inspections, almost 100% are done by MDOT inspectors. By contrast, about 90% of local bridges are contracted out to consultants. For scoping inspections, about half are done in-house and the other half by consultants. There are about 260 total scoping inspections done by MDOT each year. MODT also owns about 200 under water bridges that often require consultants help in inspection. Almost 100% of underwater bridge inspections are hired out.

Most scoping in the University Region is hired out, with an average cost of about $10,000 per bridge.

3. *What is the percentage of state-owned bridges that are inspected at least once every 24 months? What factors cause this to be less than 100%?*

   On-time inspection rate at MDOT is 99.8%. Only a few bridges may be delayed due to their special conditions. Meantime, special needs bridges may be inspected more frequently, at less than 24-month intervals. Annually inspected bridges include:

   - Removable Bridges
   - Fracture Sensitive Bridges
   - Special Needs Bridges
   - Complex and/or Large Bridges
   - Underwater Fatigue Sensitive Bridges

4. *What is the breakdown of bridgework funding at MDOT (e.g., capital scheduled maintenance, capital preventive maintenance, bridge rehabilitation, and bridge replacement)? How much is provided by federal and state governments, respectively?*

   Michigan's annual budget for bridge operations is $185 million. This increased from $28 million due to the gas tax increase.

   - $163 million is distributed to DOT regions for replacements (48%), rehabilitations (32%), and preventive maintenance (20%).
   - $16 million is allocated to the Big Bridge Program.
   - $3 million is allocated to special needs, such as emergency maintenance.
   - $3 million is allocated to Michigan's emerging technology program for trial applications of new materials and methods.

   U.S. Federal Highway Bridge Program (HBP) funds make up $110 million of Michigan's bridge operations budget, about 60% of total. Other federal programs, such as interstate maintenance, surface transportation, and national highway system funds, are also used to fund bridge preservation projects.

   Funds are distributed across state regions based on their proportion of statewide bridge inventory in each work category. For each region, the inventory of bridges in each work category (i.e., prevention, rehabilitation, and replacement) is computed. The work

categories have significantly different costs. The average cost of a bridge preventive maintenance project is $450,000. Replacing a bridge deck will cost $1.7 million for a 5-lane deck. The average cost of bridge replacement is $2.2 million. In 2009, Michigan will execute 118 preventive maintenance projects, 87 rehabilitation projects, and 51 replacement projects.

5. *Over the next ten years, how important are each of the followings to MDOT's bridge inspection program?*

    - *Funding limitations for bridge inspection programs*
      Funding is always an issue, but as long as the inspection is completed on-time, the cost will be reimbursed from the Federal Government. In that sense, funding is not an issue.

    - *Not enough qualified bridge inspectors*
      It's not an issue since MDOT has a lot engineers with potential to become bridge inspectors after training. But on the other hand, some specific regions (e.g. metro region) may have a hard time to fill a vacancy.

    - *Applying new technologies*
      New technologies are the future, and they are a potential solution to many challenges. If a new technology saves time, saves money long term, helps makes bridge inspectors safer, or interrupts traffic less, then it could be a good and attractive investment.

      New technologies will have more impact on bridge construction and management than on bridge inspection itself. Examples of new tools:

        - Optimize bridge data management system
        - Hand held tablets
        - Uploading photos when on-site
        - Online system that can track real-time maintenance records
        - Consolidating/streamlining various paper files
        - Fit in MDOT overall IT strategies

    - *Increasing maintenance and improvements costs*

    - *Optimizing bridge inspection and repair programs*

    - *Meeting federal regulations and inspection guidelines*
      This is a critical component of bridge inspection policy. We have to comply with Federal requirements.

Costs of Current Inspection Techniques

6. *What are the annual budgets for in-house and contract service of bridge inspections at MDOT?*

The annual budget for in-house and contract service is about $1.5 – $2.1 million, which includes inspection, the bridge asset management program, and contract services. (Metro and University Regions spend about 1.5 million on scoping each year.)

7. *What are the current inspection techniques and related equipment requirements for a typical bridge? Is there any way to examine the inspection accuracy of these techniques?*

   The accuracy of current methods used in the bridge inspection process is reliant on the skills of the bridge inspector. Interpreting the results from the inspection methods is subjective, so it takes a keen sense to accomplish the inspection process with a good degree of accuracy.

8. *On average, what is the percent share of annual hours a bridge inspector spends on preparation for inspection, conducting field inspection, data entry and reporting, training, and other activities (such as providing local support)?*

   Preparation for inspection requires about 20% of total inspection time.
   The actual field inspection requires about 70% of the total inspection time.
   Data entry requires the remaining 10% of bridge inspection time.

   As made clear above, three activities account for 90% of an inspector's hours. The remaining 10% are spent on other activities, such as training and supporting local programs.

   MDOT bridge inspectors are required to accept 24 hours training every five years.

   Preparation for inspection takes about15 minutes a bridge.
   Field inspection takes about 90 to 120 minutes a bridge.
   Data entry takes about 30 minutes a bridge.

   Normally we can do about 4-5 bridges a day. There are no field inspections from December to March, but we undertake other activities such as maintenance.

9. *When conducting a field inspection, which element-level inspection requires most of the inspector's time (including inspection and equipment set-up and break-down hours): the deck, superstructure, substructure, or approach?*

   It depends on a bridge's condition and type. For steal-beam bridges, the superstructure takes most time, followed by decks, substructure, and approach.
   A typical 3-5 span bridge will require 4-6 hours inspection time. The deck, superstructure, and substructure will each take about 30% of the total inspection time. The remaining 10% of time is spent on approaches.

   Hours spent on element-level inspection:

   a. The Deck – 1.5 hrs.
   b. Superstructure – 1.5 hrs.

c. Substructure – 1.5 hrs.
d. Approach - .5 hrs.

Completing all the component steps in deck inspection takes a lot of time.

10. *How difficult is it to close traffic lanes when conducting field inspections? How often do closures take place? What is the average expense of deploying traffic lane closures?*

    The cost to set up of traffic closures ranges from $2,000 to $30,000, depending on how many levels of magnitude. The typical cost range is between $2,000 and $3,000. The set-up time usually only requires 15 – 20 minutes. Switch the closure to another lane will also take about 15 minutes. We usually do not close traffic unless we have to. There are other restrictions too, such as hours, for traffic control. Usually lane closures occur from 10:00 am to 2:00 pm for inspection purpose.

    Traffic closures never happen during routine inspections. After routine inspection, 5-7% of the bridges will require in-depth inspections, which then require traffic control. We spent about one million contract dollars on in-depth inspections in the Metro Region.

11. *How much time did it take your team to complete inspections for following bridges? Did you need special access equipment? If so, how much time did it take to set up? Did the inspections require traffic control?*

    - *Freer Road over I-94*
      30 minutes for preparation
      90 to 120 minutes for inspection
      30 minutes for data entry

    - *Willow Road over US-23*
      15 minutes for preparation
      One to two hour for inspection
      30 minutes for data entry

    - *Mannsiding Road over US-127*
      30 minutes for preparation
      Two to Three hours for inspection
      30 minutes for data entry

      Usually it takes about 4 – 6 hrs. per bridge; Contractors try to have it done within two hours

Benefits and Limitations of New Technologies

12. *We will conduct a second-round interview on this topic later. But based on what you have observed from the BCAURS field demonstration, how much potential do you see for using remote sensing technologies for bridge condition assessment?*

Thermal IR seems promising. It can allow us to get deck bottom delamination data without closing traffic. Kansas and the University of Missouri may be using these applications already. 3D photos are also useful. They are useful in creating a reliable record that can be compared with damages caused by accidents.
GPS tagging is not very promising because it takes too much time to do it.

13. *One last question: what technical capabilities would the remote sensing technologies have to have to supplement or even replace current bridge inspection techniques?*

    Remote Sensing has great potential, as long as it is easy to use, easy to deploy, and easy to interpret the data/results. If it meets all these criteria then we will go for it. It's our goal to use less money to do more things, and using technologies definitely will help us achieve this goal. On top of that, remote sensing will not only support the bridge management system (MBI and PONTIS), but also TMS.

    If remote sensing inspection could get the results currently obtained through scoping, and if it's cost effective, then the new technology will be a great value to us.

Appendix F.2 – Economic Evaluation: Second Interview with MDOT Stakeholders

SECOND ROUND INTERVIEW WITH MDOT STAKEHOLDERS

Interview date: March 1, 2012

Interviewees:
Amy Trahey, Great Lakes Engineering Group
Rebecca Curtis, MDOT
Rich Kathrens, MDOT
Jason DeRuyver. MDOT

Purposes: (1) to assess the benefits of new bridge inspection technologies, as well as incentives and barriers to their implementation; and (2) to assess the benefits of the decision support system (DSS) to MDOT's bridge management program.

1. *In your view, what are the most valuable technical capabilities of the remote sensing technologies demonstrated in this project in general?*
    - *Reducing assessment subjectivity by quantifying inspection results*
    - *More useful comparisons across bridges*
    - *Early detection of bridge structural health problems (need to see evidence)*
    - *Useful information for optimizing bridge inspection and maintenance decisions*
    - *Other*

We would like to see new technologies employed to improve upon current practices and being able to provide more quantified inspection results. For example, thermal infrared (ThIR) is attractive since it can detect underside defects and determine delamination and spall areas and locations. RADAR has similar capacity but only if it could do the work more quickly and were less intrusive. Using remote sensing technologies also makes it possible to conduct multiple runs in order to get consistent measurements. To get better and more complete inspection results, a combination use of ThIR and 3D Optical Bridge-Evaluation System (3DOBS) could be a good choice. We also hope that in the future these technologies will be easy to use and require minimum training.

In terms of reducing assessment subjectivity by quantifying inspection results, it seems to be less so with bridge inspection practices (comparing to pavement condition assessment). Current inspection results are more likely influenced by DOT regions, instead of individual inspectors.

Having an inspector stay out of traffic and keeping traffic flowing are the two most important concerns while collecting data on a bridge. We are not disappointed with the quality of the results produced by current chain drag method, but the dangerous process of acquisition is a concern. In this dangerous and time-consuming process, bridge inspectors manually mark a grid pattern on the bridge with duct tape to position themselves for correct acquisition of data. Avoiding lane closures has significant social value. Cost savings are also significant when it is not necessary to compensate the crews needed to close traffic. It would be a major improvement if technologies could collect data at near-highway speeds.

We would like to see further evidence of remote sensing technologies being used for early detection of bridge structural health problems. Scoping is where DOT makes decisions on bridge investments. If remote sensing technologies can provide scoping level results, including useful visual results, they will be of great value.

2. *How promising are each of the following remote sensing technologies for adding additional value to the existing bridge inspection and bridge scoping practices?*
    - *3D Optical Bridge-Evaluation System (3DOBS)*
    - *Bridge Viewer Remote Camera System (BVRCS)/ GIGAPAN System (GigaPan)*
    - *Thermal Infrared (ThIR)*
    - *Digital Image Correlation (DIC)*
    - *Light Detecting and Ranging (LiDAR)*
    - *Ultra Wide Band Imaging RADAR System (UWBIRS)*

If 3DOBS could go faster (e.g., more than 40 MPH), it will be very appealing. Using 3DOBS under the bridge to create point cloud is also very useful.

ThIR was not negatively affected by the epoxy overlay. The air gap between the epoxy overlay and the concrete is usually where the delamination occurs.

Currently we do not have good measurements to support the decisions of fixing a spall with subsurface features or defects. It would be nice to measure the depth of the spall, because we cannot get it from chain drag. Such results will affect preventive decision making.

3D Radar is one of the best tools that can accomplish the needs for assessing in-depth defects, as suggested by many vendors at 2012 TRB Exhibit. This could be part of a long term bridge monitoring solution.

In summary, we would like new technologies to help us making difficult decisions easier. We also expect to adopt some efficient but less expensive new technologies for bridge inspectors first.

3. *What are the major challenges to the implementation of these new technologies?*
    - *Cost of equipment*
    - *Operational cost (labor, equipment, road user cost etc.)*
    - *Data processing time and cost*
    - *Additional training for bridge inspector to use the new technologies*
    - *Other*

Cost is certainly a limiting factor, and new technologies should also make data easier to read, as hiring consultants to analyze data is expensive. Data storage and security are also important. MDOT would very much like to collect image data and would like to hold the data ourselves since it is a long term investment.

4. *Are any of the remote sensing technologies especially valuable applied to certain types of bridges (e.g., functionally obsolete or structurally deficient bridges)? Might these*

technologies provide better and more comprehensive inspection and scoping results, and therefore help actionable bridge maintenance decisions?

The size of a bridge would affect our decision whether or not to use these technologies for inspection and scoping. Large bridges (i.e., with 100,000 square feet or more deck surface) will benefit from using remote sensing technologies (such as ThIR), since it will save time, reduce bridge inspector's risk, and improve mobility.

It would be nice to add ThIR camera to the truck and maybe the 3DOBS as well in addition to normal inspection techniques. With this equipment installed, the inspector could simply drive over the bridge and add the data to the regular inspection process.

5. *For these technologies (e.g., 3D RADAR and LiDAR), what deployment option do you prefer: purchase and operate hardware in house or purchase services from vendors? Does it vary by cost of the technology? How so?*

It depends on many factors, such as the timeframe to get inspection work done. If it is an emergency task, it is likely that the inspection will be done in house. It will come down to timing and available resources; if we have the time and budget available, we may hire a consultant to do the work.

It is clear that the size of DOT inspection teams will not get any bigger. Therefore, it is unlikely that we will create a new division to fulfill the new functions and responsibilities of using remote sensing technologies. Instead, MDOT is more likely to keep many small staff groups that have multiple skill sets and expertise. However, things may change if in particular these new technologies become widespread and are available at a relatively low cost, require minimum training, and can be used frequently.

6. *Do you prefer equipment that is handheld or mounted on a vehicle and used at near-highway speed?*

It depends on the purpose and the types of technologies. If it is the bottom of a bridge, handheld equipment is useful. A thermal IR handheld unit would be really beneficial. Bridge inspectors can use it while standing on the shoulder of the road.

7. *In your view, how effective is the current bridge inspection and reporting system? What is the most important value of the proposed Decision Support System (DSS)?*

To fully capture all condition defects on the bridges, there is a movement to toward using the PONTIS inspection system. AASHTO also released element level bridge inspection manual in 2011, which is quantity-based (e.g., concrete elements – deck, substructure, and even the columns) and includes many new elements, such as coding system for bridge painting. This system requires transferring routine inspection into detailed, precise, repeatable, quantitative-based results. Other features such as assigning an amount to a value, merging with NBI and creating a correlation, and linking condition to location (like a "CAD" model) are always of great value.

The important values of DSS include: keeping all information on a specific structure or network of structures in one place, making data more accessible, producing pie charts and trend lines, and conveying the information to the management and the public in an effective and efficient manner. If the proposed DSS could have an improved filtering function, it would be better.

8. *What features that you've seen today do you think would help your bridge management & assessment work more efficient?*

That is hard to answer. We know there is a lot potential for DSS, but we would like have more choices to customize our view and perform queries.

9. *Do you anticipate any challenges to the implementation of DSS?*

Data security is important. Constantly meeting the needs of different users is also a challenge, since each user wants to use it in a different way and often has individual reasons for selecting bridges, for example. Developing consistent standards for data items, bridge indicators, performance measures, analytical outputs of remote sensing technologies (e.g., mapping scheme), and other definitions are very important. Many of these efforts often require coordination among federal and state agencies. In addition, the provision of the DSS costs money.

10. *How useful would it be to be able to access the DSS and existing bridge condition data sources (MBIS, MBRS) in the field, such as through tablet devices?*

It is very useful in the field as well as in a meeting room when we need the data and information. One valuable feature of the DSS is that possible to access it from anywhere.

Appendix G – Economic Evaluation: Costs of Remote Sensing Technologies

COSTS OF REMOTE SENSING TECHNOLOGIES

Table C1: Itemized Cost for Thermal Infrared (ThIR)

Cost Category	Cost Elements	Research Stage Cost Measurement	CONOPS Cost Estimates
Equipment	FLIR SC640 Thermal IR Camera (307,200 pixels)	$40,000	FLIR A-40 - $25,000
	FLIR i7 Thermal IR Camera (handheld, 14,400 pixels)	$2,000	FLUKE Ti10 (19,200 pixels) - $4,000
	Cart with fabricated hitch (height=6.2ft)	$100	
	GPS installed on the cart	$100	
	Laptop computer	$800	$800
Software	ThermaCAM software (professional edition)	$7,000	Thermacam Researcher - $5,000
IT	Space for one-bridge files - raw and processed data (GB)	1GB for collected images in the field and 3GB for data process	<1GB (less data due to a bigger field of view and less number of images)
Labor	# of persons to do the survey	2 persons	One person
	Set-up time	60 minutes	
	Running (3 span, 2-lane bridge)	90 minutes	30 Minutes
	Break-up	20 minutes	
	Total time	2.5 hours	30 Minutes
Road user costs	Traffic disruption	ThIR camera mounted on a cart; one direction of traffic lanes closed each	ThIR camera mounted on a vehicle that is driven at a lower speed
Post-processing time	To quantify surface condition by creating delamination map and calculating percentage of delamination etc.	40 hours	8 hours
Proposed applications	Quantifying surface conditions		

Table C2: Itemized Cost for 3D Optical Bridge-Evaluation System (3DOBS)

Cost Category	Cost Elements	Research Stage Cost Measurement	CONOPS Cost Estimates
	Nikon D5000 DSLR Camera (including default kit lens)	$700	$700
	or CANON EOS 7D, including 28-135 mm lens	$1,700	$1,700
	Camera Triggering Device	$20	$20
	Camera Truck Mount	$100	$100
	Laptop/Hardware setups	$820	$820
Equipment	GPS	$100	$100
Software	AgiSoft PhotoScan	$3,500 for professional edition	$3,500 for professional edition
IT	Space for one-bridge files - raw and processed data (GB)	0.05 GB for DEM, 0.12 GB for all files after spall detection algrithm is run	0.05 GB for DEM, 0.12 GB for all files after spall detection algrithm is run
	# of persons to do the survey	2 persons	One person
	Set-up time	30 minutes	
	Running	30 minutes	30 minutes
	Break-up	30 minutes	
Labor	Total time	1.5 hour	30 minutes
Road user costs	Traffic disruption	The vehicle was driven at a speed of less than 5 mph	Camera mounted on a vehicle that is driven at a lower speed
Post-processing time	Creating Digital Elevation Models and calculating the size and volume of spalls in ArcGIS (e.g. 5 mm by 5 mm horizontal and 2 mm by 2 mm vertical spalled areas)	>12 hours	12 hours
Proposed applications	Surface roughness, % Spalled, and volume measurements		

Table C3: Itemized Cost for Bridge Viewer Remote Camera System (BVRCS)

Cost Category	Cost Elements	Research Stage Cost Measurement	CONOPS Cost Estimates
	Two Canon PowerShot SX110 IS Cameras	$500	$500
	Garmin GPSMAP 76CSx GPS Unit	$100	$100
	Laptop	$800	$800
Equipment	Breeze Systems PSRemote Camera Control Software	$190	$190
Software	GeoSpatial Experts GPS-Photo Link Software	$350	$350
IT	Space for one-bridge files - raw and processed data (GB)	2.0 GB	< 2.0 GB
	# of persons to do the survey	2 persons	One person
	Set-up time	30 minutes	
	Running	30 minutes	30 minutes
	Break-up	30 minutes	
Labor	Total time	1.5 hour	30 minutes
Road user costs	Traffic disruption	The vehicle was driven at a speed of less than 5 mph	Camera mounted on a vehicle that is driven at a lower speed
Post-processing time	Location-tagged, GIS and Google Earth-compatible files	1.0 hour	1.0 hour
Proposed applications	Photo inventory of bridge deck or the underside of a bridge that can be used in DSS		

Table C4: Itemized Cost for GIGAPAN System (GigaPan)

Cost Category	Cost Elements	Research Stage Cost Measurement	CONOPS Cost Estimates
	GigaPan EPIC robotic camera mount	$299	$299
	PowerShot SX110 IS	$250	$250
Equipment	Camera Tripod	$100	$100
Software	GigaPan Stitch	Included with every EPIC purchase	Included with every EPIC purchase
IT	Space for one-bridge files - raw and processed data (GB)	7 - 12 GB	7 - 12 GB
	# of persons to do the survey	One	One
	Set-up time	10 minutes	10 minutes
	Running	20 - 240 minutes	240 minutes
	Break-up	10 minutes	10 minutes
Labor	Total time	4 - 5 hours	4 hours
Road user costs	Traffic disruption	None	One shoulder closed
Post-processing time	Loading and stitching together the images (1,000 or more 7 to 12+ megapixel images)	4-to-6 hours	4 hours
Proposed applications	Inventory a bridge's visual conditions		

Table C5: Itemized Cost for Digital Image Correlation (DIC)

Cost Category	Cost Elements	Research Stage Cost Measurement	CONOPS Cost Estimates
	Canon DSLR Camera (e.g. EOS-7D)	$2,000	$2,000
	Camera Lens, EF 70-200 mm f/2.8L	$400	$400
	Camera Tripod	$100	$100
	Spray paint (water-based) pattern/distinct markers	$15	$15
Equipment	Scaffolding system	$1,000	$1,000
	Image processing software algorithms such as MATLAB	$1,990 for single user	$1,990 for single user
Software	Correlated Solutions Vic-2D	$12,000	$12,000
IT	Space for one-bridge files - raw and processed data (GB)	32	32
	# of persons to do the survey (including truck driver)	2-3 persons	2-3 persons
	Set-up time	30 minutes	30 minutes
	Running	1 - 1.5 hours	1.5 hours
	Break-up	30 minutes	30 minutes
Labor	Total hours	2 - 2.5 hours	2.5 hours
Road user costs	Traffic disruption	One shoulder closed	One shoulder and one lane closed
Post-processing time	Calculating displacement measurements etc.	2-4 Hours (Per Bridge Set)	2-4 Hours (Per Bridge Set)
Proposed applications	Structural health & global response		

Table C6: Itemized Cost for Light Detecting and Ranging (LiDAR)

Cost Category	Cost Elements	Research Stage Cost Measurement	CONOPS Cost Estimates
Equipment	Leica ScanStation C10 (MDOT) - with built-in user interface	$125,000	Mobile LIDAR System (e.g., Optech Lynx) that includes 2-4 scanners, cameras, antennae, positioning system, and data processing software) - from $500,000 to $750,000 depending on system configuration.
	or RIEGL LMS-Z210ii (MTU)		
	or RIEGL VZ-4000	$150,000	
	Tri-Max Tripods	6-8 ($400 each)	
Software	Certainty 3D TopoDOT + MicroStation	$3,995 plus $2,995 annual maintenance fee	
	or Applied Imagery - Quick Terrain Modeler	$995	
IT	Space for one-bridge files - raw and processed data (GB)	One bridge deck: raw - 5 GB; processed - 0.13 GB	Same as research stage or less
Labor	# of persons to do the survey	2 persons	2 persons
	Initial set-up time	30 minutes	30 minutes
	Running	30-45 minutes for each scan; 12 - 20 scans needed for a bridge	30 - 60 minutes
	Final break-up	30 minutes	30 minutes
	Total hours	7 - 11 hours	0.5 - 1.0 hour
Road user costs	Traffic disruption	One shoulder closed	Vehicle speed at 55 mph for data collection
Post-processing time	To extract data and create density images, e.g., XYZ location, elevation data, RGB values => % spalled, location and volume of spalls	Two weeks or more	2-3 days
Proposed applications	Surface roughness and global metrics		

Table C7: Itemized Cost for Ultra Wide Band Imaging Radar System (UWBIRS) and GPR

Cost Category	Cost Elements	Research Stage Cost Measurement	CONOPS Cost Estimates - Commercial GPR Systems
Equipment	AKELA RF Vector Signal Generator Measurement Unit (AVMU)	$15,000	GSSI SIR-20 with horn antennas - $60,000 or 3D-RADAR - top end package (includes software)-$250,000
	Wideband exponential taper horns	$2,000	
	Laptop computer	$800	
	Portable generator	$400	
	Supporting structure	$2,000	
	special radar cable	$700	
Software			RADAN - $4,000
IT	Space for one-bridge files - raw and processed data (GB)	0.24 MB	0.2 MB
Labor	# of persons to do the survey	2-3 persons	One person
	Set-up time	2 hours	30 minutes or less
	Running time for a bridge	10 hours or more	15 to 30 minutes
	Break-up	45 minutes	30 minutes or less
	Total hours	12 hours or more	2-4 hours
Road user costs	Traffic disruption	One direction of traffic lanes closed	Vehicle speed at 60 mph for data collection
Post-processing time	To create delamination images and quantify bridge conditions	8 hours	8 hours
Proposed applications	Quantify location and size of likely delaminations; subsurface defects.		

Table C8: Cost of Remote Sensing Instrument and Service Fee – Results from Vendor's Interviews

Company	Product Name/Service Type	Description	Costs	Notes
3D-RADAR	GeoScope MK IV and VX-Series	High speed 2D & 3D GPR (2D can travel up to 60 mph; 6.0 to 11 ft. antenna).	Top end package costs about $250k (equipment and software)	Data collection is not limited to daylight; data processing can be done while data acquisition proceeds.
	3dr-Examiner (software)	GPR data processing, visualization, and reporting.		
IDS	STREAM-Em	Vehicle towed radar solution for extensive 3D mapping; travel speed less than 8 mph; 3 ft. antenna.	$100K	
MALA Geoscience USA Inc.	MALA RoadCart	Portable or vehicle mounted.	$18K for one channel, $45K for two channels, $70K for 4 channels; Antenna costs $2k - $7k; using Dean Goodman software (GPR slice)	
GSSI	BridgeScan or RoadScan	Vehicle mounted at 30 mph.	$55K for 4 channels	
	BridgeScan or RoadScan	Pushed by hand	$22K	
	Software - RADAN		$3k	
Infrasense, Inc.	Bridge inspection using GPR	Using GSSI SIR-20 with horn antennas and RADAN; vehicle-mounted and can travel at 60 mph; 15 minutes on site plus 8 hours analysis.	$1,300 for a typical two-span freeway bridge	Costs do not include travel and traffic control.
	Bridge inspection using Thermal IR	Using FLIR A-40 and Thermacam Research; vehicle-mounted and can travel at 5 mph; 15 minutes on site plus 8 hours analysis.	$1,300 for a typical two-span freeway bridge	Costs do not include travel and traffic control.

Appendix H – Technical Evaluation Score Spreadsheet

Performance Rating of Commercial Remote Sensing Technologies

Location	Challenges	Indicator	Desired Measurement Sensitivity	Rating Based, in Part, on Theoretical Sensitivity for Measurement Technologies									
				UWBIRS	3DOBS	Multispectral Satellite Imagery	Giga-Pan	Terrestrial LiDAR	Thermal IR	Digital Image Correlation	SAR Speckle	InSAR	BVRCS
Deck Surface	Expansion Joint	Tom/Missing Seal		-	12	0	N/A	10	13	-	0	-	12
		Armored Plated Damage		-	11	-	N/A	10	N/A	-	-	-	13
		Cracks within 2 Feet	0.8 mm to 4.8 mm (1/32" to 3/16") width	-	11	0	N/A	10	N/A	-	0	-	13
		Spalls within 2 Feet	6.0 mm to 25.0 mm (1/4" to 1") depth	-	12	0	N/A	10	12	-	0	-	13
		Chemical Leaching on Bottom		-	-	N/A	13	N/A	-	-	-	-	N/A
	Map Cracking	Surface Cracks	0.8 mm to 4.8 mm (1/32" to 3/16") width	-	11	0	N/A	10	0	-	0	-	13
	Scaling	Depression in Surface	6.0 mm to 25.0 mm (1/4" to 1") depth	-	12	0	N/A	10	11	-	9	-	13
	Spalling	Depression with Parallel Fracture	6.0 mm to 25.0 mm (1/4" to 1") depth	-	12	0	N/A	10	11	-	9	-	13
	Delamination	Surface Cracks	0.8 mm to 4.8 mm (1/32" to 3/16") width	-	11	0	N/A	10	0	-	N/A	-	13
Deck Subsurface	Expansion Joint	Material in Joint		-	-	-	N/A	-	-	-	-	-	N/A
	Delamination	Moisture in Cracks	Change in moisture content	9	-	-	-	-	12	-	-	-	-
		Internal Horizontal Crack	Approximately 0.1 mm (0.004") level	0	-	-	-	-	-	-	-	-	-
		Hollow Sound		-	-	-	-	-	N/A	-	-	-	-
		Fracture Planes / Open Spaces	Change in return signal	10	-	-	N/A	-	12	-	N/A	-	-
	Scaling	Depression in Surface (eg. Interior of voided sections)	6.0 mm to 25.0 mm (1/4" to 1") depth	10	-	-	-	-	0	-	-	-	-
	Spalling	Depression with Parallel Fracture (eg. Interior of voided sections)	6.0 mm to 25.0 mm (1/4" to 1") depth	10	-	-	-	-	0	-	-	-	-
	Corrosion	Corrosion Rate (Resistivity)	5 to 20 kΩ-cm	N/A	-	-	-	-	N/A	-	-	-	-
	Rebar Corrosion	Change in Cross-Sectional Area	Amplitude of signal from rebar	10	-	-	-	-	-	-	N/A	-	-
	Chloride Ingress	Chloride Content through the Depth	0.4 to 1.0 % chloride by mass of cement	10	-	-	-	-	N/A	-	N/A	-	-
Girder Surface	Steel Structural Cracking	Surface Cracks	< 0.1 mm (.004"), hairline	-	0	N/A	12	0	0	-	N/A	-	N/A
	Concrete Structural Cracking	Surface Cracks	.1 mm (.004")	-	0	N/A	12	0	13	-	N/A	-	-
	Steel Section Loss	Change in Cross-Sectional Area	Percent thickness of web or flange	-	0	-	-	10	N/A	-	N/A	-	-
	Paint	Paint Condition	Amount of missing paint (X %)	-	-	N/A	-	-	N/A	-	-	-	N/A
	Concrete Section Loss	Change in Cross-Sectional Area	Percent volume per foot	-	0	-	-	10	N/A	-	N/A	-	-
Girder Subsurface	Internal Concrete Structural Cracks	Internal Cracks (e.g. Box Beam)	Approx 0.8 mm (1/32")	9	-	-	-	-	N/A	-	N/A	-	-
		Fracture Planes / Open Spaces	Change in return signal	9	-	-	-	-	13.5	-	-	-	-
	Concrete Section Loss	Change in Cross-Sectional Area	Percent volume per foot	-	-	-	-	-	N/A	-	N/A	-	-
	Prestress Strand Breakage	Change in Cross-Sectional Area	Wire 2 mm or strand 9.5 mm diameter	9	-	-	-	-	N/A	-	N/A	-	-
	Corrosion	Corrosion Rate (Resistivity)	5 to 20 kΩ-cm	N/A	-	-	-	-	N/A	-	-	-	-
	Rebar Corrosion	Change in Cross-Sectional Area	Amplitude of signal from rebar	9	-	-	-	-	-	-	N/A	-	-
	Chloride Ingress	Chloride Content through the Depth	0.4 to 1.0 % Chloride by mass of cement	9	-	-	-	-	N/A	-	N/A	-	-
Global Metrics	Bridge Length	Change in Bridge Length	Accuracy to 30 mm (0.1ft) (smaller)	-	11	-	-	-	-	N/A	N/A	N/A	N/A
	Bridge Settlement	Vertical Movement of Bridge	Approximately 6 mm to 12 mm	-	N/A	-	-	N/A	-	N/A	N/A	0	N/A
	Bridge Movement	Transverse Directions	Approximately 6 mm to 12 mm	-	N/A	-	-	N/A	-	N/A	N/A	N/A	N/A
	Surface Roughness	Surface Roughness	Change over time	-	12	0	N/A	10	-	-	10	N/A	12
	Vibration or Live Load Deflection	Vibration or Live Load Deflection	.5 -20 Hz; L/800 deflection	-	-	-	N/A	-	-	12	N/A	N/A	-

Methodology

A	Is requirement met?	2	Resolution is specifically within the current capabilities of the technology Full range of measurements are met or better Other requirements directly measured
		1	Lower limit of resolution/requirements is not within capabilities, but upper limit is Technology can measure somewhere between the range or within 25 % of upper limit Some requirements are only indirectly measured
		0	Upper limit of resolution not met within 25 % Current capabilities do not allow direct measurement at any necessary resolution
		N/A	Not practical or appropriate for the given technology, or not investigated in this study.
B	Availability of instrument	2	Technology is currently commercially available and used for similar application(s) Technologies components are immediately available for use as manufacturer intends (e.g. no commercial DIC or 3D Photogrammetry platform, but digital cameras are widely available for the same purpose)
		1	Technology is available only for research purposes; Components are available commercially but they may have not been applied to this purpose and are not specifically designed for the application
		0	A complete system has not been demonstrated in research The technology is only theoretically available and would have to be built from very fundamental components
C	Cost of measurement	2	Low capital cost Moderate capital cost with reuse (low operational cost)
		1	Moderate capital cost Low capital cost with high operational cost (e.g. dedicated equipment that can't quickly be reused)
		0	High capital cost Moderate capital cost with high operational cost
D	Pre-collection preparation	2	Absolutely no preparation of the structure No/minimal calibration of the instrument are required
		1	The structure requires moderate preparation The instrument requires moderate calibration
		0	Both the structure and/or instrument require extensive preparation
E	Complexity of analysis	2	Analysis consists of either pattern recognition by user (Bridge inspector can easily understand the output) Automated "turn-key" processing by a computer (Software commercially available)
		1	Analysis consists of detailed measurements made by a human user from raw data Processing by an algorithm that must be tuned or trained for each dataset More than one algorithm is needed
		0	Analysis consists of very complex calculations and measurements made by a human user from raw data Processing by an algorithm that either i) requires extensive human supervision ii) a large amount of time per bridge (more than a day) iii) requires multiple algorithms chained together WITH human-in-the-loop I/O
F	Ease of data collection	2	Instrument is used in a straightforward manner as intended by manufacturer AND requires little more from the operator than supervision (i.e. "push the start button and start collecting") Easily accessible structure components
		1	Instrument is used in a custom fashion (may have been modified for this purpose) Requires input from operator Requires real-time verification (QA/QC) of results Environmentally dependent Considerable time window for data collection Physical challenges
		0	Instrument is used in a custom fashion AND requires EITHER input from the operator OR real-time verification (QA/QC) of results Hidden components Team needed
G	Stand-off distance rating	2	No part of the platform is touching the earth
		1	Part of the platform is on the earth or bridge (i.e. on a ground-based vehicle or some other grounded mount) AND the instrument is NOT in contact with the structure
		0	Instrument is in direct contact with structure; technique is not traditional remote sensing
H	Traffic Disruption	2	Absolutely no lane closure(s)
		1	Minor/ short term lane closure with limited effect on traffic
		0	Major/ long term lane closure with limited effect on traffic

UWBIRS

Deck Subsurface

		Moisture in Cracks	Internal Horizontal Crack	Fracture Planes / Open Spaces	Scaling	Spalling	Corrosion	Chloride Ingress	Rebar Corrosion
A	**Is requirement met?**	1	0	1	1	1	N/A	1	1
B	**Availability of instrument**	2	2	2	2	2	N/A	2	2
C	**Cost of measurement**	1	1	1	1	1	N/A	1	1
D	**Pre-collection preparation**	1	2	2	2	2	N/A	2	2
E	**Complexity of analysis**	1	1	1	1	1	N/A	1	1
F	**Ease of data collection**	1	1	1	1	1	N/A	1	1
G	**Stand-off distance rating**	1	1	1	1	1	N/A	1	1
H	**Traffic Disruption**	1	1	1	1	1	N/A	1	1
		9	**0**	**10**	**10**	**10**	**N/A**	**10**	**10**

Girder Subsurface

Internal Cracks (e.g. Box Beam)	Fracture Planes / Open Spaces	Prestress Strand Breakage	Corrosion	Rebar Corrosion	Chloride Ingress
1	1	1	N/A	1	1
2	2	2	N/A	2	2
0	0	0	N/A	0	0
2	2	2	N/A	2	2
1	1	1	N/A	1	1
1	1	1	N/A	1	1
1	1	1	N/A	1	1
1	1	1	N/A	1	1
9	**9**	**9**	**N/A**	**9**	**9**

	A	B
Weights:	**1**	**1**

Deck Subsurface - Delamination - Moisture in Cracks			
	Change in moisture content		
1	A	Is requirement met?	"It was possible to determine moisture distributions, as well as to estimate the moisture content." (Maierhofer, 2001); requirements appear to be loose enough to accommodate the complicating environmental factors. No evidence of moisture content detected during investigation.
2	B	Availability of instrument	Multiple commercial GPR already available and in use
1	C	Cost of measurement	Higher cost for capital equipment, maintenance, downtime, and expense of processing expertise and time
1	D	Pre-collection preparation	Maierhofer and Leipold (2001) required calibration curves in order to calculate the moisture content
1	E	Complexity of analysis	Generating a model of moisture in concrete and comparing it with field measurements to estimate moisture content
1	F	Ease of data collection	This measurement is depended on environmental factors such as snow and rain; presence of water on concrete deck
1	G	Stand-off distance rating	For all commercial GPR implementations, standoff is close
1	H	Traffic Disruption	GPR should be able to be done from a vehicle moving with traffic (Shuchman, 2005). Investigated system was not possible from a moving platform.
9			

Deck Subsurface - Delamination - Internal Horizontal Crack			
	Approximately 0.1 mm (0.004") level		
0	A	Is requirement met?	Method is likely not sensitive to features that occupy so small a part of the range bin; sensitivity is dependent on how homogeneous the subsurface is
2	B	Availability of instrument	Multiple commercial GPR already available and in use
1	C	Cost of measurement	Higher cost for capital equipment, maintenance, downtime, and expense of processing expertise and time
2	D	Pre-collection preparation	Just need to scan the surface
1	E	Complexity of analysis	Radar responses need to be migrated
1	F	Ease of data collection	Amounts to driving over the bridge. Investigated system required lengthy collection process.
1	G	Stand-off distance rating	For all GPR implementations, standoff is close
1	H	Traffic Disruption	GPR should be able to be done from a vehicle moving with traffic (Shuchman, 2005). Investigated system was not possible from a moving platform.
0			

Deck Subsurface - Delamination - Fracture Planes / Open Spaces			
	Change in return signal		
1	A	Is requirement met?	Multiple studies have done mapping of delaminations with amplitude returns; GPR is accurate, on average, to 10 mm (Hugenschmidt, 2006); asphalt thickness measured to within 2.1 mm accuracy (Shuchman, Subotic, et al. 2005)
2	B	Availability of instrument	Multiple commercial GPR already available and in use
1	C	Cost of measurement	Higher cost for capital equipment, maintenance, downtime, and expense of processing expertise and time
2	D	Pre-collection preparation	Just need to scan the surface
1	E	Complexity of analysis	Radar responses need to be migrated
1	F	Ease of data collection	Amounts to driving over the bridge. Investigated system required lengthy collection process.
1	G	Stand-off distance rating	For all GPR implementations, standoff is close
1	H	Traffic Disruption	GPR should be able to be done from a vehicle moving with traffic (Shuchman, 2005). Investigated system was not possible from a moving platform.
10			

Deck Subsurface - Scaling - Depression in Surface (eg. Interior of voided sections)			
	6.0 mm to 25.0 mm (1/4" to 1") depth		
1	A	Is requirement met?	Thinner depressions cannot be detected; lower limit of sensitivity appears to be 10 mm thick
2	B	Availability of instrument	Multiple commercial GPR already available and in use
1	C	Cost of measurement	Higher cost for capital equipment, maintenance, downtime, and expense of processing expertise and time
2	D	Pre-collection preparation	Just need to scan the surface
1	E	Complexity of analysis	Radar responses need to be migrated; these are deck bottom features being detected by measuring from the top of the concrete deck
1	F	Ease of data collection	Amounts to driving over the bridge. Investigated system required lengthy collection process.
1	G	Stand-off distance rating	For all GPR implementations, standoff is close
1	H	Traffic Disruption	GPR should be able to be done from a vehicle moving with traffic (Shuchman, 2005). Investigated system was not possible from a moving platform.
10			

Deck Subsurface - Spalling - Depression with Parallel Fracture (eg. Interior of voided sections) 6.0 mm to 25.0 mm (1/4" to 1") depth			
1	A	Is requirement met?	Thinner depressions cannot be detected; lower limit of sensitivity appears to be 10 mm thick
2	B	Availability of instrument	Multiple commercial GPR already available and in use
1	C	Cost of measurement	Higher cost for capital equipment, maintenance, downtime, and expense of processing expertise and time
2	D	Pre-collection preparation	Just need to scan the surface
1	E	Complexity of analysis	Radar responses need to be migrated; these are deck bottom features being detected by measuring from the top of the concrete deck
1	F	Ease of data collection	Amounts to driving over the bridge. Investigated system required lengthy collection process.
1	G	Stand-off distance rating	For all GPR implementations, standoff is close
1	H	Traffic Disruption	GPR should be able to be done from a vehicle moving with traffic (Shuchman, 2005). Investigated system was not possible from a moving platform.
10			

Deck Subsurface - Corrosion - Corrosion Rate (Resistivity) 5 to 20 kΩ-cm			
N/A	A	Is requirement met?	No evidence in literature that GPR can be used to directly measure resistivity; may affect dielectrics, but nothing in available literature about that
2	B	Availability of instrument	Multiple commercial GPR already available and in use
1	C	Cost of measurement	Higher cost for capital equipment, maintenance, downtime, and expense of processing expertise and time
2	D	Pre-collection preparation	Just need to scan the surface
1	E	Complexity of analysis	Dielectric properties would have to be calculated from radar response
1	F	Ease of data collection	Amounts to driving over the bridge. Investigated system required lengthy collection process.
1	G	Stand-off distance rating	For all GPR implementations, standoff is close
1	H	Traffic Disruption	GPR should be able to be done from a vehicle moving with traffic (Shuchman, 2005). Investigated system was not possible from a moving platform.
N/A			

Deck Subsurface - Rebar Corrosion - Change in Cross-Sectional Area Amplitude of signal from rebar			
2	A	Is requirement met?	Frequent reference to technique in literature; notably Dwayne (2010), Scott (2001), and Barrile (2005)
2	B	Availability of instrument	Multiple commercial GPR already available and in use
1	C	Cost of measurement	Higher cost for capital equipment, maintenance, downtime, and expense of processing expertise and time
2	D	Pre-collection preparation	Just need to scan the surface
1	E	Complexity of analysis	GPR responses must be migrated, particularly for rebar location
1	F	Ease of data collection	Amounts to driving over the bridge. Investigated system required lengthy collection process.
1	G	Stand-off distance rating	For all GPR implementations, standoff is close
1	H	Traffic Disruption	GPR should be able to be done from a vehicle moving with traffic (Shuchman, 2005). Investigated system was not possible from a moving platform.
11			

Deck Subsurface - Chloride Ingress - Chloride Content through the Depth			
	0.4 to 1.0 % chloride by mass of cement		
1	A	Is requirement met?	Literature indicates that chloride content attenuates radar signals, but no documented attempt to quantify chloride content
2	B	Availability of instrument	Multiple commercial GPR already available and in use
1	C	Cost of measurement	Higher cost for capital equipment, maintenance, downtime, and expense of processing expertise and time
2	D	Pre-collection preparation	Just need to scan the surface
1	E	Complexity of analysis	Dielectric properties would have to be calculated from radar response
1	F	Ease of data collection	Amounts to driving over the bridge. Investigated system required lengthy collection process.
1	G	Stand-off distance rating	For all GPR implementations, standoff is close
1	H	Traffic Disruption	GPR should be able to be done from a vehicle moving with traffic (Shuchman, 2005). Investigated system was not possible from a moving platform.
10			

Girder Subsurface - Internal Concrete Structural Cracks - Internal Cracks (e.g. Box Beam)			
	Approx 0.8 mm (1/32")		
0	A	Is requirement met?	GPR is not sensitive enough for this fine of a feature
2	B	Availability of instrument	Multiple commercial GPR already available and in use
0	C	Cost of measurement	Imaging the girders below the deck would be challenging and time-consuming in addition to already substantial capital and operational costs
2	D	Pre-collection preparation	Just need to scan the surface
1	E	Complexity of analysis	Radar responses need to be migrated
1	F	Ease of data collection	Numerous, difficult places to reach
1	G	Stand-off distance rating	For all GPR implementations, standoff is close
1	H	Traffic Disruption	In this case, GPR might interfere with traffic as it is deployed--somehow--on the sides, bottom, and top of bridge from, conceivably, a platform on the bridge deck
0			

Girder Subsurface - Internal Concrete Structural Cracks - Fracture Planes / Open Spaces			
	Change in return signal		
1	A	Is requirement met?	Multiple studies have done mapping of delaminations with amplitude returns; GPR is accurate, on average, to 10 mm (Hugenschmidt, 2006); asphalt thickness measured to within 2.1 mm accuracy (Shuchman, Subotic, et al. 2005)
2	B	Availability of instrument	Multiple commercial GPR already available and in use
1	C	Cost of measurement	Higher cost for capital equipment, maintenance, downtime, and expense of processing expertise and time
2	D	Pre-collection preparation	Just need to scan the surface
1	E	Complexity of analysis	Radar responses need to be migrated
1	F	Ease of data collection	Amounts to driving over the bridge. Investigated system required lengthy collection process.
1	G	Stand-off distance rating	For all GPR implementations, standoff is close
1	H	Traffic Disruption	GPR should be able to be done from a vehicle moving with traffic (Shuchman, 2005). Investigated system was not possible from a moving platform.
10			

Girder Subsurface - Prestress Strand Breakage - Change in Cross-Sectional Area			
	Wire 2 mm or strand 9.5 mm diameter		
1	A	Is requirement met?	"Measurement errors on diameter, have been carried out by radar technology, supported by electromagnetic method, showed a range of error within 3 mm at the 86% significance level." (Barrile, 2005) - that for 13, 25, and 38 mm strands
2	B	Availability of instrument	Multiple commercial GPR already available and in use
0	C	Cost of measurement	Imaging the girders below the deck would be challenging and time-consuming in addition to already substantial capital and operational costs
2	D	Pre-collection preparation	Just need to scan the surface
1	E	Complexity of analysis	Radar responses need to be migrated; otherwise, some modeling is being used to estimate strand thickness
1	F	Ease of data collection	Numerous, difficult places to reach
1	G	Stand-off distance rating	For all GPR implementations, standoff is close
1	H	Traffic Disruption	In this case, GPR might interfere with traffic as it is deployed--somehow--on the sides, bottom, and top of bridge from, conceivably, a platform on the bridge deck
9			

Girder Subsurface - Corrosion - Corrosion Rate (Resistivity)			
	5 to 20 kΩ-cm		
N/A	A	Is requirement met?	No evidence in literature that GPR can be used to directly measure resistivity; may affect dielectrics, but nothing in available literature about that
2	B	Availability of instrument	Multiple commercial GPR already available and in use
0	C	Cost of measurement	Imaging the girders below the deck would be challenging and time-consuming in addition to already substantial capital and operational costs
2	D	Pre-collection preparation	Just need to scan the surface
1	E	Complexity of analysis	Dielectric properties would have to be calculated from radar response
1	F	Ease of data collection	Numerous, difficult places to reach
1	G	Stand-off distance rating	For all GPR implementations, standoff is close
1	H	Traffic Disruption	GPR should be able to be done from a vehicle moving with traffic (Shuchman, 2005). Investigated system was not possible from a moving platform.
N/A			

Girder Subsurface - Rebar Corrosion - Change in Cross-Sectional Area			
	Amplitude of signal from rebar		
1	A	Is requirement met?	Frequent reference to technique in literature; notably Dwayne (2010), Scott (2001), and Barrile (2005) for concrete bridge decks; no application to girders
2	B	Availability of instrument	Multiple commercial GPR already available and in use
0	C	Cost of measurement	High operational costs on top of higher cost for capital equipment, maintenance, downtime, and expense of processing expertise and time
2	D	Pre-collection preparation	Just need to scan the surface
1	E	Complexity of analysis	GPR responses must be migrated, particularly for rebar location
0	F	Ease of data collection	Each girder needs to be scanned by the GPR
1	G	Stand-off distance rating	For all GPR implementations, standoff is close
1	H	Traffic Disruption	Scanning girders (collection geometry) might require lane closure(s) under the bridge
8			

Girder Subsurface - Chloride Ingress - Chloride Content through the Depth			
	0.4 to 1.0 % Chloride by mass of cement		
1	A	Is requirement met?	Lim (2001) showed that radar signal attenuates with increasing chloride content
2	B	Availability of instrument	Multiple commercial GPR already available and in use
0	C	Cost of measurement	Imaging the girders below the deck would be challenging and time-consuming in addition to already substantial capital and operational costs
2	D	Pre-collection preparation	Just need to scan the surface
1	E	Complexity of analysis	Dielectric properties would have to be calculated from radar response
1	F	Ease of data collection	Numerous, difficult places to reach
1	G	Stand-off distance rating	For all GPR implementations, standoff is close
1	H	Traffic Disruption	GPR should be able to be done from a vehicle moving with traffic (Shuchman, 2005). Investigated system was not possible from a moving platform.
9			

3DOBS

		Deck Surface							
		Torn/Missing Seal	Armored Plated Damage	Expansion Joint - Cracks within 2 Feet	Expansion Joint - Spalls within 2 Feet	Map Cracking - Surface Cracks	Scaling - Depression in Surface	Spalling - Depression with Parallel Fracture	Delamination - Surface Cracks
A	Is requirement met?	2	1	1	2	1	2	2	1
B	Availability of instrument	2	2	2	2	2	2	2	2
C	Cost of measurement	2	2	2	2	2	2	2	2
D	Pre-collection preparation	1	1	1	1	1	1	1	1
E	Complexity of analysis	1	1	1	1	1	1	1	1
F	Ease of data collection	2	2	2	2	2	2	2	2
G	Stand-off distance rating	1	1	1	1	1	1	1	1
H	Traffic Disruption	1	1	1	1	1	1	1	1
		12	**11**	**11**	**12**	**11**	**12**	**12**	**11**

			Girder Surface				Global Metrics			
			Steel Structural Cracking	Concrete Structural Cracking	Steel Section Loss	Concrete Section Loss	Change in Bridge Length	Vertical Movement of Bridge	Transverse Directions	Surface Roughness
			0	0	0	0	1	N/A	N/A	2
			2	2	2	2	2	0	0	2
			2	2	2	2	2	0	0	2
			1	1	1	1	1	0	0	1
			1	1	1	1	1	0	0	1
			1	1	1	1	2	0	0	2
	A	**B**	1	1	1	1	1	0	0	1
Weights:	**1**	**1**	1	1	1	1	1	0	0	1
			0	**0**	**0**	**0**	**11**	**N/A**	**N/A**	**12**

Deck Surface - Expansion Joint - Torn/Missing Seal			
2	A	Is requirement met?	Limited studies did not achieve best guess at resolution requirements, but resolution is determined by collection geometry
2	B	Availability of instrument	Common equipment (cameras)
2	C	Cost of measurement	Low cost- long life (without aerial platform)
2	D	Pre-collection preparation	
1	E	Complexity of analysis	Commercial modeling programs generate 3D models automatically. Processing by an algorithm that must be tuned or trained for each dataset
2	F	Ease of data collection	Just a moving collection platform
1	G	Stand-off distance rating	For fine resolution, aerial platforms are probably too high
2	H	Traffic Disruption	High-speed cameras allow imagery to be collected at traffic speeds
14			

Deck Surface - Expansion Joint - Armored Plated Damage			
1	A	Is requirement met?	Limited studies did not achieve best guess at resolution requirements, but resolution is determined by collection geometry
2	B	Availability of instrument	Common equipment (cameras)
2	C	Cost of measurement	Low cost- long life (without aerial platform)
2	D	Pre-collection preparation	
1	E	Complexity of analysis	Commercial modeling programs generate 3D models automatically. Processing by an algorithm that must be tuned or trained for each dataset
2	F	Ease of data collection	Just a moving collection platform
1	G	Stand-off distance rating	For fine resolution, aerial platforms are probably too high
2	H	Traffic Disruption	High-speed cameras allow imagery to be collected at traffic speeds
13			

Deck Surface - Expansion Joint - Cracks within 2 Feet 0.8 mm to 4.8 mm (1/32" to 3/16") width			
1	A	Is requirement met?	Better resolution can be achieved by higher end cameras.
2	B	Availability of instrument	Common equipment (cameras)
2	C	Cost of measurement	Low cost- long life (without aerial platform)
2	D	Pre-collection preparation	
1	E	Complexity of analysis	Commercial modeling programs generate 3D models automatically. Processing by an algorithm that must be tuned or trained for each dataset
2	F	Ease of data collection	Just a moving collection platform
1	G	Stand-off distance rating	For fine resolution, aerial platforms are probably too high
2	H	Traffic Disruption	High-speed cameras allow imagery to be collected at traffic speeds
13			

Deck Surface - Expansion Joint - Spalls within 2 Feet 6.0 mm to 25.0 mm (1/4" to 1") depth			
2	A	Is requirement met?	Limited studies did not achieve best guess at resolution requirements, but resolution is determined by collection geometry
2	B	Availability of instrument	Common equipment (cameras)
2	C	Cost of measurement	Low cost- long life (without aerial platform)
2	D	Pre-collection preparation	
1	E	Complexity of analysis	Commercial modeling programs generate 3D models automatically. Processing by an algorithm that must be tuned or trained for each dataset
2	F	Ease of data collection	Just a moving collection platform. Reference points are required on the bridge deck.
1	G	Stand-off distance rating	For fine resolution, aerial platforms are probably too high
2	H	Traffic Disruption	High-speed cameras allow imagery to be collected at traffic speeds
14			

Deck Surface - Map Cracking - Surface Cracks 0.8 mm to 4.8 mm (1/32" to 3/16") width			
1	A	Is requirement met?	Better resolution can be achieved by higher end cameras.
2	B	Availability of instrument	Common equipment (cameras)
2	C	Cost of measurement	Low cost- long life (without aerial platform)
2	D	Pre-collection preparation	
1	E	Complexity of analysis	Commercial modeling programs generate 3D models automatically. Processing by an algorithm that must be tuned or trained for each dataset
2	F	Ease of data collection	Just a moving collection platform
1	G	Stand-off distance rating	For fine resolution, aerial platforms are probably too high
2	H	Traffic Disruption	High-speed cameras allow imagery to be collected at traffic speeds
13			

Deck Surface - Scaling - Depression in Surface			
	6.0 mm to 25.0 mm (1/4" to 1") depth		
2	A	Is requirement met?	
2	B	Availability of instrument	Common equipment (cameras)
2	C	Cost of measurement	Low cost- long life (without aerial platform)
2	D	Pre-collection preparation	
1	E	Complexity of analysis	Commercial modeling programs generate 3D models automatically. Processing by an algorithm that must be tuned or trained for each dataset
2	F	Ease of data collection	Just a moving collection platform. Reference points are required on the bridge deck.
1	G	Stand-off distance rating	For fine resolution, aerial platforms are probably too high
2	H	Traffic Disruption	High-speed cameras allow imagery to be collected at traffic speeds
14			

Deck Surface - Spalling - Depression with Parallel Fracture			
	6.0 mm to 25.0 mm (1/4" to 1") depth		
2	A	Is requirement met?	
2	B	Availability of instrument	Common equipment (cameras)
2	C	Cost of measurement	Low cost- long life (without aerial platform)
2	D	Pre-collection preparation	
1	E	Complexity of analysis	Commercial modeling programs generate 3D models automatically. Processing by an algorithm that must be tuned or trained for each dataset
2	F	Ease of data collection	Just a moving collection platform. Reference points are required on the bridge deck.
1	G	Stand-off distance rating	For fine resolution, aerial platforms are probably too high
2	H	Traffic Disruption	High-speed cameras allow imagery to be collected at traffic speeds
14			

Deck Surface - Delamination - Surface Cracks			
	0.8 mm to 4.8 mm (1/32" to 3/16") width		
1	A	Is requirement met?	Better resolution can be achieved by higher end cameras.
2	B	Availability of instrument	Common equipment (cameras)
2	C	Cost of measurement	Low cost- long life (without aerial platform)
2	D	Pre-collection preparation	
1	E	Complexity of analysis	Commercial modeling programs generate 3D models automatically. Processing by an algorithm that must be tuned or trained for each dataset
2	F	Ease of data collection	Just a moving collection platform
1	G	Stand-off distance rating	For fine resolution, aerial platforms are probably too high
2	H	Traffic Disruption	High-speed cameras allow imagery to be collected at traffic speeds
13			

Girder Surface - Steel Structural Cracking - Surface Cracks			
	< 0.1 mm (.004"), hairline		
1	A	Is requirement met?	Better resolution can be achieved by higher end cameras.
2	B	Availability of instrument	Common equipment (cameras)
2	C	Cost of measurement	
1	D	Pre-collection preparation	Need more lighting under the bridge.
1	E	Complexity of analysis	Commercial modeling programs generate 3D models automatically. Processing by an algorithm that must be tuned or trained for each dataset
1	F	Ease of data collection	Requires multiple passes for fine resolution of a cumulatively large surface area
1	G	Stand-off distance rating	For fine resolution, aerial platforms are probably too high
1	H	Traffic Disruption	Possible lane closure(s) for a short period of time
10			

Girder Surface - Concrete Structural Cracking - Surface Cracks			
	.1 mm (.004")		
1	A	Is requirement met?	Better resolution can be achieved by higher end cameras.
2	B	Availability of instrument	Common equipment (cameras)
2	C	Cost of measurement	
1	D	Pre-collection preparation	Need more lighting under the bridge.
1	E	Complexity of analysis	Commercial modeling programs generate 3D models automatically. Processing by an algorithm that must be tuned or trained for each dataset
1	F	Ease of data collection	Requires multiple passes for fine resolution of a cumulatively large surface area
1	G	Stand-off distance rating	For fine resolution, aerial platforms are probably too high
1	H	Traffic Disruption	Possible lane closure(s) for a short period of time
10			

Girder Surface - Steel Section Loss - Change in Cross-Sectional Area			
	Percent thickness of web or flange		
1	A	Is requirement met?	Better resolution can be achieved by higher end cameras.
2	B	Availability of instrument	Common equipment (cameras)
2	C	Cost of measurement	
1	D	Pre-collection preparation	Need more lighting under the bridge.
1	E	Complexity of analysis	Commercial modeling programs generate 3D models automatically. Processing by an algorithm that must be tuned or trained for each dataset
1	F	Ease of data collection	Requires multiple passes for fine resolution of a cumulatively large surface area
1	G	Stand-off distance rating	For fine resolution, aerial platforms are probably too high
1	H	Traffic Disruption	Possible lane closure(s) for a short period of time
10			

Girder Surface - Concrete Section Loss - Change in Cross-Sectional Area			
	Percent volume per foot		
1	A	Is requirement met?	Better resolution can be achieved by higher end cameras.
2	B	Availability of instrument	Common equipment (cameras)
2	C	Cost of measurement	
1	D	Pre-collection preparation	Need more lighting under the bridge.
1	E	Complexity of analysis	Commercial modeling programs generate 3D models automatically. Processing by an algorithm that must be tuned or trained for each dataset
1	F	Ease of data collection	Requires multiple passes for fine resolution of a cumulatively large surface area
1	G	Stand-off distance rating	For fine resolution, aerial platforms are probably too high
1	H	Traffic Disruption	Possible lane closure(s) for a short period of time
10			

Global Metrics - Bridge Length - Change in Bridge Length			
	Accuracy to 30 mm (0.1ft) (smaller)		
1	A	Is requirement met?	Uncertainty of resolution
2	B	Availability of instrument	Common equipment (cameras)
2	C	Cost of measurement	Low cost- long life (without aerial platform)
2	D	Pre-collection preparation	Reference points required for improved spatial accuracy
1	E	Complexity of analysis	Commercial modeling programs generate 3D models automatically. Processing by an algorithm that must be tuned or trained for each dataset
2	F	Ease of data collection	Just a moving collection platform. Reference points are required on the bridge deck.
1	G	Stand-off distance rating	For fine resolution, aerial platforms are probably too high
2	H	Traffic Disruption	High-speed cameras allow imagery to be collected at traffic speeds
13			

Global Metrics - Bridge Settlement - Vertical Movement of Bridge			
	Approximately 6 mm to 12 mm		
N/A	A	Is requirement met?	Aerial platform is needed for this application.
	B	Availability of instrument	
	C	Cost of measurement	
	D	Pre-collection preparation	
	E	Complexity of analysis	
	F	Ease of data collection	
	G	Stand-off distance rating	
	H	Traffic Disruption	
N/A			

Global Metrics - Bridge Movement - Transverse Directions			
	Approximately 6 mm to 12 mm		
N/A	A	Is requirement met?	Aerial platform is needed for this application.
	B	Availability of instrument	
	C	Cost of measurement	
	D	Pre-collection preparation	
	E	Complexity of analysis	
	F	Ease of data collection	
	G	Stand-off distance rating	
	H	Traffic Disruption	
N/A			

Global Metrics - Surface Roughness - Surface Roughness			
	Change over time		
2	A	Is requirement met?	Can measure change over time with repeat visits; sub-milimetre resolution possible at 5-6 ft standoff (Dobson, 2010)*
2	B	Availability of instrument	Common equipment (cameras)
2	C	Cost of measurement	Must be done on the bridge with a vehicle (no flights)
2	D	Pre-collection preparation	
1	E	Complexity of analysis	Multiple 3D models will have to be compared at different time scales. Processing by an algorithm that must be tuned or trained for each dataset
2	F	Ease of data collection	Repeat collections consisting of driving over a bridge
1	G	Stand-off distance rating	Vehicle is on the bridge; standoff just several feet
2	H	Traffic Disruption	High-speed cameras allow imagery to be collected at traffic speeds
14			

Multispectral Satellite Imagery

		Deck Surface							
		Torn/Missing Seal	Expansion Joint - Cracks within 2 Feet	Expansion Joint - Spalls within 2 Feet	Chemical Leaching on Bottom	Map Cracking - Surface Cracks	Scaling - Depression in Surface	Spalling - Depression with Parallel Fracture	Delamination - Surface Cracks
A	Is requirement met?	0	0	0	N/A	0	0	0	0
B	Availability of instrument	1	1	1	2	1	1	1	1
C	Cost of measurement	1	1	1	1	1	1	1	1
D	Pre-collection preparation	1	1	1	1	1	1	1	1
E	Complexity of analysis	1	1	1	2	1	1	1	1
F	Ease of data collection	1	1	1	1	1	1	1	1
G	Stand-off distance rating	1	1	1	1	1	1	1	1
H	Traffic Disruption	1	1	1	1	1	1	1	1
		0	**0**	**0**	**N/A**	**0**	**0**	**0**	**0**

	Girder Surface			Global Metrics
	Steel Structural Cracking	Concrete Structural Cracking	Paint Condition	Surface Roughness
A	N/A	N/A	N/A	0
B	1	1	2	2
C	1	1	1	1
D	1	1	1	1
E	1	1	1	1
F	1	1	1	1
G	1	1	1	1
H	1	1	1	1
	N/A	**N/A**	**N/A**	**0**

	A	B
Weights:	**1**	**1**

Deck Surface - Expansion Joint - Torn/Missing Seal			
0	A	Is requirement met?	Likely possible but no studies have been conducted
1	B	Availability of instrument	Equipment is commercially available but not used for this application
1	C	Cost of measurement	Moderate capital cost- long life (without aerial platform)
1	D	Pre-collection preparation	White calibration of the spectroradiometer; possibly clean-up of the target surface
1	E	Complexity of analysis	Detection automation from characteristic peaks, for example
1	F	Ease of data collection	Surface must be visible; unobstructed by snow/ice
1	G	Stand-off distance rating	Usually hand held
1	H	Traffic Disruption	May have to close some lanes for a short time
0			

Deck Surface - Expansion Joint - Cracks within 2 Feet			
	0.8 mm to 4.8 mm (1/32" to 3/16") width		
0	A	Is requirement met?	Likely possible but no studies have been conducted
1	B	Availability of instrument	Equipment is commercially available but not used for this application
1	C	Cost of measurement	Moderate capital cost- long life (without aerial platform)
1	D	Pre-collection preparation	White calibration of the spectroradiometer; possibly clean-up of the target surface
1	E	Complexity of analysis	Detection automation from characteristic peaks, for example
1	F	Ease of data collection	Surface must be visible; unobstructed by snow/ice; may need to be artificially illuminated
1	G	Stand-off distance rating	Usually hand held
1	H	Traffic Disruption	May have to close some lanes for a short time
0			

Deck Surface - Expansion Joint - Spalls within 2 Feet			
	6.0 mm to 25.0 mm (1/4" to 1") depth		
0	A	Is requirement met?	Likely possible but no studies have been conducted
1	B	Availability of instrument	Equipment is commercially available but not used for this application
1	C	Cost of measurement	Moderate capital cost- long life (without aerial platform)
1	D	Pre-collection preparation	White calibration of the spectroradiometer; possibly clean-up of the target surface
1	E	Complexity of analysis	Detection automation from characteristic peaks, for example
1	F	Ease of data collection	Surface must be visible; unobstructed by snow/ice; may need to be artificially illuminated
1	G	Stand-off distance rating	Usually hand held
1	H	Traffic Disruption	May have to close some lanes for a short time
0			

Deck Surface - Expansion Joint - Chemical Leaching on Bottom			
N/A	A	Is requirement met?	Studies have been conducted on determining chemical leaching (Kanada, Ishikawa, et al.)
2	B	Availability of instrument	Equipment is commercially available and has frequently been used for this applicatio
1	C	Cost of measurement	Moderate capital cost- long life (without aerial platform)
1	D	Pre-collection preparation	White calibration of the spectroradiometer; possibly clean-up of the target surface
2	E	Complexity of analysis	Characteristic peaks directly indicate chloride, carbonation, sulfate attack
1	F	Ease of data collection	Surface must be visible; unobstructed by snow/ice; may need to be artificially illuminated
1	G	Stand-off distance rating	Studies have been done at 0.5 to 2.4 meters
1	H	Traffic Disruption	May have to close some lanes for a short time
N/A			

Deck Surface - Map Cracking - Surface Cracks			
	0.8 mm to 4.8 mm (1/32" to 3/16") width		
0	A	Is requirement met?	Likely possible but no studies have been conducted
1	B	Availability of instrument	Equipment is commercially available but not used for this application
1	C	Cost of measurement	Moderate capital cost- long life (without aerial platform)
1	D	Pre-collection preparation	White calibration of the spectroradiometer; possibly clean-up of the target surface
1	E	Complexity of analysis	Detection automation from characteristic peaks, for example
1	F	Ease of data collection	Surface must be visible; unobstructed by snow/ice; may need to be artificially illuminated
1	G	Stand-off distance rating	Usually hand held
1	H	Traffic Disruption	May have to close some lanes for a short time
0			

Deck Surface - Scaling - Depression in Surface 6.0 mm to 25.0 mm (1/4" to 1") depth			
0	A	Is requirement met?	Likely possible but no studies have been conducted
1	B	Availability of instrument	Equipment is commercially available but not used for this application
1	C	Cost of measurement	Moderate capital cost- long life (without aerial platform)
1	D	Pre-collection preparation	White calibration of the spectroradiometer; possibly clean-up of the target surface
1	E	Complexity of analysis	Detection automation from characteristic peaks, for example
1	F	Ease of data collection	Surface must be visible; unobstructed by snow/ice; may need to be artificially illuminated
1	G	Stand-off distance rating	Usually hand held
1	H	Traffic Disruption	May have to close some lanes for a short time
0			

Deck Surface - Spalling - Depression with Parallel Fracture 6.0 mm to 25.0 mm (1/4" to 1") depth			
0	A	Is requirement met?	Likely possible; TARUT study did generalized road condition sufficiency rating (Brooks, Shuchman, et al. 2007)
1	B	Availability of instrument	Equipment is commercially available but not used for this application
1	C	Cost of measurement	Moderate capital cost- long life (without aerial platform)
1	D	Pre-collection preparation	White calibration of the spectroradiometer; possibly clean-up of the target surface
1	E	Complexity of analysis	Detection automation from characteristic peaks, for example
1	F	Ease of data collection	Surface must be visible; unobstructed by snow/ice; may need to be artificially illuminated
1	G	Stand-off distance rating	Usually hand held
1	H	Traffic Disruption	May have to close some lanes for a short time
0			

Deck Surface - Delamination - Surface Cracks 0.8 mm to 4.8 mm (1/32" to 3/16") width			
0	A	Is requirement met?	Likely possible but no studies have been conducted
1	B	Availability of instrument	Equipment is commercially available but not used for this application
1	C	Cost of measurement	Moderate capital cost- long life (without aerial platform)
1	D	Pre-collection preparation	White calibration of the spectroradiometer; possibly clean-up of the target surface
1	E	Complexity of analysis	Detection automation from characteristic peaks, for example
1	F	Ease of data collection	Surface must be visible; unobstructed by snow/ice; may need to be artificially illuminated
1	G	Stand-off distance rating	Usually hand held
1	H	Traffic Disruption	May have to close some lanes for a short time
0			

Girder Surface - Steel Structural Cracking - Surface Cracks < 0.1 mm (.004"), hairline			
N/A	A	Is requirement met?	Likely possible but no studies have been conducted
1	B	Availability of instrument	Equipment is commercially available but not used for this application
1	C	Cost of measurement	Moderate capital cost- long life (without aerial platform)
1	D	Pre-collection preparation	White calibration of the spectroradiometer; possibly clean-up of the target surface
1	E	Complexity of analysis	Detection automation from characteristic peaks, for example
1	F	Ease of data collection	Surface must be visible; unobstructed by snow/ice; may need to be artificially illuminated
1	G	Stand-off distance rating	Usually hand held
1	H	Traffic Disruption	May have to close some lanes for a short time
N/A			

Girder Surface - Concrete Structural Cracking - Surface Cracks			
.1 mm (.004")			
N/A	A	Is requirement met?	Likely possible but no studies have been conducted
1	B	Availability of instrument	Equipment is commercially available but not used for this application
1	C	Cost of measurement	Moderate capital cost- long life (without aerial platform)
1	D	Pre-collection preparation	White calibration of the spectroradiometer; possibly clean-up of the target surface
1	E	Complexity of analysis	Detection automation from characteristic peaks, for example
1	F	Ease of data collection	Surface must be visible; unobstructed by snow/ice; may need to be artificially illuminated
1	G	Stand-off distance rating	Usually hand held
1	H	Traffic Disruption	May have to close some lanes for a short time
N/A			

Girder Surface - Paint Condition			
Amount of missing paint (X %)			
N/A	A	Is requirement met?	Likely possible but no studies have been conducted
2	B	Availability of instrument	Equipment is commercially available and has been used for this application before
1	C	Cost of measurement	Moderate capital cost- long life (without aerial platform)
1	D	Pre-collection preparation	White calibration of the spectroradiometer; possibly clean-up of the target surface
1	E	Complexity of analysis	Detection automation from characteristic peaks, for example
1	F	Ease of data collection	Surface must be visible; unobstructed by snow/ice; may need to be artificially illuminated
1	G	Stand-off distance rating	Usually hand held
1	H	Traffic Disruption	May have to close some lanes for a short time
N/A			

Global Metrics - Surface Roughness			
Change over time			
0	A	Is requirement met?	Likely possible; TARUT study did generalized road condition sufficiency rating (Brooks, Shuchman, et al. 2007)
2	B	Availability of instrument	Equipment is commercially available and has been used for similar applications
1	C	Cost of measurement	Moderate capital cost- long life (without aerial platform)
1	D	Pre-collection preparation	White calibration of the spectroradiometer; possibly clean-up of the target surface
1	E	Complexity of analysis	Detection automation from characteristic peaks, for example
1	F	Ease of data collection	Surface must be visible; unobstructed by snow/ice; may need to be artificially illuminated
1	G	Stand-off distance rating	Usually hand held
1	H	Traffic Disruption	May have to close some lanes for a short time
0			

Giga-Pan

		Deck Surface							
		Torn/Missing Seal	Armored Plated Damage	Expansion Joint - Cracks within 2 Feet	Expansion Joint - Spalls within 2 Feet	Map Cracking - Surface Cracks	Scaling - Depression in Surface	Spalling - Depression with Parallel Fracture	Delamination - Surface Cracks
A	Is requirement met?	N/A	N/A	N/A	N/A	N/A	N/A	N/A	N/A
B	Availability of instrument	2	2	2	2	2	2	2	2
C	Cost of measurement	1	1	1	1	1	1	1	1
D	Pre-collection preparation	2	2	2	2	2	2	2	2
E	Complexity of analysis	2	2	2	2	2	2	2	2
F	Ease of data collection	1	1	1	1	1	1	1	1
G	Stand-off distance rating	1	1	1	1	1	1	1	1
H	Traffic Disruption	1	1	1	1	1	1	1	1
		N/A	**N/A**	**N/A**	**N/A**	**N/A**	**N/A**	**N/A**	**N/A**

		Deck Subsurface			Girder Surface		Global Metrics
		Chemical Leaching on Bottom	Material in Joint	Fracture Planes / Open Spaces	Steel Structural Cracking	Concrete Structural Cracking	Surface Roughness	Vibration or Live Load Deflection
A	Is requirement met?	2	N/A	N/A	1	1	N/A	N/A
B	Availability of instrument	2	2	2	2	2	2	2
C	Cost of measurement	2	1	1	2	2	1	1
D	Pre-collection preparation	1	2	2	1	1	2	2
E	Complexity of analysis	2	2	2	2	2	2	2
F	Ease of data collection	1	1	1	1	1	1	1
G	Stand-off distance rating	1	1	1	1	1	1	1
H	Traffic Disruption	2	1	1	2	2	1	1
		13	**N/A**	**N/A**	**12**	**12**	**N/A**	**N/A**

	A	B
Weights:	**1**	**1**

Deck Surface - Expansion Joint - Torn/Missing Seal			
N/A	A	Is requirement met?	Resolution is achieved with this technology but it has never been demonstrated before; may be too fine
2	B	Availability of instrument	Commercial systems available (see Trilion Optical Test Systems, Trilion.com)
1	C	Cost of measurement	High capital cost (lasers) but could be re-used
2	D	Pre-collection preparation	
2	E	Complexity of analysis	Well-understood algorithms; no user-interventions (MTRI, 2010)
1	F	Ease of data collection	Depending on the technique, field collection may be easy or difficult
1	G	Stand-off distance rating	On bridge, non-contact
1	H	Traffic Disruption	On bridge
N/A			

Deck Surface - Expansion Joint - Armored Plated Damage			
N/A	A	Is requirement met?	Resolution is achieved with this technology but it has never been demonstrated before; may be too fine
2	B	Availability of instrument	Commercial systems available (see Trilion Optical Test Systems, Trilion.com)
1	C	Cost of measurement	High capital cost (lasers) but could be re-used
2	D	Pre-collection preparation	
2	E	Complexity of analysis	Well-understood algorithms; no user-interventions (MTRI, 2010)
1	F	Ease of data collection	Depending on the technique, field collection may be easy or difficult
1	G	Stand-off distance rating	On bridge, non-contact
1	H	Traffic Disruption	On bridge
N/A			

Deck Surface - Expansion Joint - Cracks within 2 Feet 0.8 mm to 4.8 mm (1/32" to 3/16") width			
N/A	A	Is requirement met?	Hatta (2005) resolved sub-mm surface cracks indicative of delamination
2	B	Availability of instrument	Commercial systems available (see Trilion Optical Test Systems, Trilion.com)
1	C	Cost of measurement	Commercial software (license) was used in Hatta (2005); most studies used digital SLR cameras (moderate capital cost); equipment can be re-used immediately for other bridges
2	D	Pre-collection preparation	
2	E	Complexity of analysis	Well-understood algorithms; no user-interventions (MTRI, 2010)
1	F	Ease of data collection	Depending on the technique, field collection may be easy or difficult
1	G	Stand-off distance rating	On bridge, non-contact
1	H	Traffic Disruption	On bridge
N/A			

Deck Surface - Expansion Joint - Spalls within 2 Feet 6.0 mm to 25.0 mm (1/4" to 1") depth			
N/A	A	Is requirement met?	Sub-mm depths resolved (Krajewski, 2006)
2	B	Availability of instrument	Commercial systems available (see Trilion Optical Test Systems, Trilion.com)
1	C	Cost of measurement	Commercial software (license) was used in Hatta (2005); most studies used digital SLR cameras (moderate capital cost); equipment can be re-used immediately for other bridges
2	D	Pre-collection preparation	
2	E	Complexity of analysis	Well-understood algorithms; no user-interventions (MTRI, 2010)
1	F	Ease of data collection	Depending on the technique, field collection may be easy or difficult
1	G	Stand-off distance rating	On bridge, non-contact
1	H	Traffic Disruption	On bridge
N/A			

Deck Surface - Map Cracking - Surface Cracks 0.8 mm to 4.8 mm (1/32" to 3/16") width			
N/A	A	Is requirement met?	Hatta (2005) resolved sub-mm surface cracks indicative of delamination
2	B	Availability of instrument	Commercial systems available (see Trilion Optical Test Systems, Trilion.com)
1	C	Cost of measurement	Commercial software (license) was used in Hatta (2005); most studies used digital SLR cameras (moderate capital cost); equipment can be re-used immediately for other bridges
2	D	Pre-collection preparation	
2	E	Complexity of analysis	Well-understood algorithms; no user-interventions (MTRI, 2010)
1	F	Ease of data collection	Depending on the technique, field collection may be easy or difficult
1	G	Stand-off distance rating	On bridge, non-contact
1	H	Traffic Disruption	On bridge
N/A			

Deck Surface - Scaling - Depression in Surface			
6.0 mm to 25.0 mm (1/4" to 1") depth			
N/A	A	Is requirement met?	Sub-mm depths resolved (Krajewski, 2006)
2	B	Availability of instrument	Commercial systems available (see Trilion Optical Test Systems, Trilion.com)
1	C	Cost of measurement	Commercial software (license) was used in Hatta (2005); most studies used digital SLR cameras (moderate capital cost); equipment can be re-used immediately for other bridges
2	D	Pre-collection preparation	
2	E	Complexity of analysis	Well-understood algorithms; no user-interventions (MTRI, 2010)
1	F	Ease of data collection	Depending on the technique, field collection may be easy or difficult
1	G	Stand-off distance rating	On bridge, non-contact
1	H	Traffic Disruption	On bridge
N/A			

Deck Surface - Spalling - Depression with Parallel Fracture			
6.0 mm to 25.0 mm (1/4" to 1") depth			
N/A	A	Is requirement met?	Sub-mm depths resolved (Krajewski, 2006)
2	B	Availability of instrument	Commercial systems available (see Trilion Optical Test Systems, Trilion.com)
1	C	Cost of measurement	Commercial software (license) was used in Hatta (2005); most studies used digital SLR cameras (moderate capital cost); equipment can be re-used immediately for other bridges
2	D	Pre-collection preparation	
2	E	Complexity of analysis	Well-understood algorithms; no user-interventions (MTRI, 2010)
1	F	Ease of data collection	Depending on the technique, field collection may be easy or difficult
1	G	Stand-off distance rating	On bridge, non-contact
1	H	Traffic Disruption	On bridge
N/A			

Deck Surface - Delamination - Surface Cracks			
0.8 mm to 4.8 mm (1/32" to 3/16") width			
N/A	A	Is requirement met?	Sub-mm depths resolved (Krajewski, 2006)
2	B	Availability of instrument	Commercial systems available (see Trilion Optical Test Systems, Trilion.com)
1	C	Cost of measurement	Commercial software (license) was used in Hatta (2005); most studies used digital SLR cameras (moderate capital cost); equipment can be re-used immediately for other bridges
2	D	Pre-collection preparation	
2	E	Complexity of analysis	Well-understood algorithms; no user-interventions (MTRI, 2010)
1	F	Ease of data collection	Depending on the technique, field collection may be easy or difficult
1	G	Stand-off distance rating	On bridge, non-contact
1	H	Traffic Disruption	On bridge
N/A			

Deck Subsurface - Expansion Joint - Material in Joint			
N/A	A	Is requirement met?	Sub-mm resolution achieved in other applications
2	B	Availability of instrument	Commercial systems available (see Trilion Optical Test Systems, Trilion.com)
1	C	Cost of measurement	Commercial software (license) was used in Hatta (2005); most studies used digital SLR cameras (moderate capital cost); equipment can be re-used immediately for other bridges
2	D	Pre-collection preparation	
2	E	Complexity of analysis	Well-understood algorithms; no user-interventions (MTRI, 2010)
1	F	Ease of data collection	Depending on the technique, field collection may be easy or difficult
1	G	Stand-off distance rating	On bridge, non-contact
1	H	Traffic Disruption	On bridge
N/A			

Deck Subsurface - Delamination - Fracture Planes / Open Spaces			
N/A	A	Is requirement met?	Only capable of detecting delaminations at depths 0.7 mm or less
2	B	Availability of instrument	Commercial systems available (see Trilion Optical Test Systems, Trilion.com)
1	C	Cost of measurement	Commercial software (license) was used in Hatta (2005); most studies used digital SLR cameras (moderate capital cost); equipment can be re-used immediately for other bridges
2	D	Pre-collection preparation	
2	E	Complexity of analysis	Well-understood algorithms; no user-interventions (MTRI, 2010)
1	F	Ease of data collection	Depending on the technique, field collection may be easy or difficult
1	G	Stand-off distance rating	On bridge, non-contact
1	H	Traffic Disruption	On bridge
N/A			

Girder Surface - Steel Structural Cracking - Surface Cracks			
< 0.1 mm (.004"), hairline			
1	A	Is requirement met?	Sub-mm depths resolved (Krajewski, 2006)
2	B	Availability of instrument	Commercial systems available (see Trilion Optical Test Systems, Trilion.com)
2	C	Cost of measurement	Commercial software (license) was used in Hatta (2005); most studies used digital SLR cameras (moderate capital cost); equipment can be re-used immediately for other bridges
1	D	Pre-collection preparation	
2	E	Complexity of analysis	Well-understood algorithms; no user-interventions (MTRI, 2010)
1	F	Ease of data collection	Depending on the technique, field collection may be easy or difficult
1	G	Stand-off distance rating	On bridge, non-contact
2	H	Traffic Disruption	On bridge
12			

Girder Surface - Concrete Structural Cracking - Surface Cracks			
.1 mm (.004")			
1	A	Is requirement met?	Sub-mm depths resolved (Krajewski, 2006)
2	B	Availability of instrument	Commercial systems available (see Trilion Optical Test Systems, Trilion.com)
2	C	Cost of measurement	Commercial software (license) was used in Hatta (2005); most studies used digital SLR cameras (moderate capital cost); equipment can be re-used immediately for other bridges
1	D	Pre-collection preparation	
2	E	Complexity of analysis	Well-understood algorithms; no user-interventions (MTRI, 2010)
1	F	Ease of data collection	Depending on the technique, field collection may be easy or difficult
1	G	Stand-off distance rating	On bridge, non-contact
2	H	Traffic Disruption	On bridge
12			

Global Metrics - Surface Roughness			
Change over time			
N/A	A	Is requirement met?	Spatial resolution (in 3 dimensions) is there; optical speckle produced by surface roughness
2	B	Availability of instrument	Commercial systems available (see Trilion Optical Test Systems, Trilion.com)
1	C	Cost of measurement	Commercial software (license) was used in Hatta (2005); most studies used digital SLR cameras (moderate capital cost); equipment can be re-used immediately for other bridges
2	D	Pre-collection preparation	
2	E	Complexity of analysis	Well-understood algorithms; no user-interventions (MTRI, 2010)
1	F	Ease of data collection	Depending on the technique, field collection may be easy or difficult
1	G	Stand-off distance rating	On bridge, non-contact
1	H	Traffic Disruption	On bridge
N/A			

Global Metrics - Vibration or Live Load Deflection .5 -20 Hz; L/800 deflection			
N/A	A	Is requirement met?	Frequency response achieved by high speed cameras (achievement not difficult for video cameras by their FPS); amplitudes of displacement are likely within the capabilities of this technique
2	B	Availability of instrument	Commercial systems available (see Trilion Optical Test Systems, Trilion.com)
1	C	Cost of measurement	Commercial software (license) was used in Hatta (2005); most studies used digital SLR cameras (moderate capital cost); equipment can be re-used immediately for other bridges
2	D	Pre-collection preparation	
2	E	Complexity of analysis	Well-understood algorithms; no user-interventions (MTRI, 2010)
1	F	Ease of data collection	Depending on the technique, field collection may be easy or difficult
1	G	Stand-off distance rating	On bridge, non-contact
1	H	Traffic Disruption	On bridge
N/A			

Terrestrial LiDAR

		Deck Surface							
		Torn/Missing Seal	Armored Plated Damage	Expansion Joint - Cracks within 2 Feet	Expansion Joint - Spalls within 2 Feet	Chemical Leaching on Bottom	Map Cracking - Surface Cracks	Scaling - Depression in Surface	Spalling - Depression with Parallel Fracture
A	Is requirement met?	1	1	1	1	N/A	1	1	1
B	Availability of instrument	2	2	2	2	0	2	2	2
C	Cost of measurement	1	1	1	1	0	1	1	1
D	Pre-collection preparation	1	1	1	1	0	1	1	1
E	Complexity of analysis	1	1	1	1	0	1	1	1
F	Ease of data collection	2	2	2	2	0	2	2	2
G	Stand-off distance rating	1	1	1	1	0	1	1	1
H	Traffic Disruption	1	1	1	1	0	1	1	1
		10	**10**	**10**	**10**	**N/A**	**10**	**10**	**10**

			Girder Surface					Global Metrics	
			Delamination - Surface Cracks	Steel Structural Cracking	Concrete Structural Cracking	Steel Section Loss	Concrete Section Loss	Vertical Movement of Bridge	Transverse Directions	Surface Roughness
			1	0	0	1	1	N/A	N/A	1
			2	2	2	2	2	2	0	2
			1	1	1	1	1	1	0	1
			1	1	1	1	1	1	0	1
			1	1	1	1	1	1	0	1
			2	2	2	1	1	1	0	2
	A	B	1	1	1	1	1	1	0	1
Weights:	1	1	1	2	2	2	2	2	0	1
			10	**0**	**0**	**10**	**10**	**N/A**	**N/A**	**10**

Deck Surface - Expansion Joint - Torn/Missing Seal			
1	A	Is requirement met?	> 1 mm x 1 mm grid spacing with TLS (Laefer, et al. 2010); Range falloff prevents an accurate measurement across the entire bridge deck; traffic disruptions would be necessary in order to collect more samples to scan evenly. (Hoensheid, 2012)
2	B	Availability of instrument	Commercial LiDAR is ubiquitous
1	C	Cost of measurement	High capital cost; may be some not-insignificant operational costs associated with deployment and data acquisition
1	D	Pre-collection preparation	No preparation of bridge required. Terrestrial LiDAR may need reference points.
1	E	Complexity of analysis	Coordinate transformation required; commercial software available for automated processing but subdivision of point clouds and curvature computation are additional steps necessary for damage identification and 3D modeling (Teza, et al. 2009)
2	F	Ease of data collection	May take up to a day to collect but operation is straightforward scanning (Lubowiecka, et al. 2009)
1	G	Stand-off distance rating	Instrument must be deployed on or near bridge but is non-contact
1	H	Traffic Disruption	Might require lane closure(s) to image some parts of the structure, but likely not this part. Multiple collects would increase disruption, but improve quality (see comment above in A).
10			

Deck Surface - Expansion Joint - Armored Plated Damage			
1	A	Is requirement met?	> 1 mm x 1 mm grid spacing with TLS (Laefer, et al. 2010); Range falloff prevents an accurate measurement across the entire bridge deck; traffic disruptions would be necessary in order to collect more samples to scan evenly. (Hoensheid, 2012)
2	B	Availability of instrument	Commercial LiDAR is ubiquitous
1	C	Cost of measurement	High capital cost; may be some not-insignificant operational costs associated with deployment and data acquisition
1	D	Pre-collection preparation	No preparation of bridge required. Terrestrial LiDAR may need reference points.
1	E	Complexity of analysis	Coordinate transformation required; commercial software available for automated processing but subdivision of point clouds and curvature computation are additional steps necessary for damage identification and 3D modeling (Teza, et al. 2009)
2	F	Ease of data collection	May take up to a day to collect but operation is straightforward scanning (Lubowiecka, et al. 2009)
1	G	Stand-off distance rating	Instrument must be deployed on or near bridge but is non-contact
1	H	Traffic Disruption	Might require lane closure(s) to image some parts of the structure, but likely not this part. Multiple collects would increase disruption, but improve quality (see comment above in A).
10			

Deck Surface - Expansion Joint - Cracks within 2 Feet 0.8 mm to 4.8 mm (1/32" to 3/16") width			
1	A	Is requirement met?	> 1 mm x 1 mm grid spacing with TLS (Laefer, et al. 2010); Range falloff prevents an accurate measurement across the entire bridge deck; traffic disruptions would be necessary in order to collect more samples to scan evenly. (Hoensheid, 2012)
2	B	Availability of instrument	Commercial LiDAR is ubiquitous
1	C	Cost of measurement	High capital cost; may be some not-insignificant operational costs associated with deployment and data acquisition
1	D	Pre-collection preparation	No preparation of bridge required. Terrestrial LiDAR may need reference points.
1	E	Complexity of analysis	Coordinate transformation required; commercial software available for automated processing but subdivision of point clouds and curvature computation are additional steps necessary for damage identification and 3D modeling (Teza, et al. 2009)
2	F	Ease of data collection	May take up to a day to collect but operation is straightforward scanning (Lubowiecka, et al. 2009)
1	G	Stand-off distance rating	Instrument must be deployed on or near bridge but is non-contact
1	H	Traffic Disruption	Might require lane closure(s) to image some parts of the structure, but likely not this part. Multiple collects would increase disruption, but improve quality (see comment above in A).
10			

Deck Surface - Expansion Joint - Spalls within 2 Feet 6.0 mm to 25.0 mm (1/4" to 1") depth			
1	A	Is requirement met?	> 1 mm x 1 mm grid spacing with TLS (Laefer, et al. 2010); Range falloff prevents an accurate measurement across the entire bridge deck; traffic disruptions would be necessary in order to collect more samples to scan evenly. (Hoensheid, 2012)
2	B	Availability of instrument	Commercial LiDAR is ubiquitous
1	C	Cost of measurement	High capital cost; may be some not-insignificant operational costs associated with deployment and data acquisition
1	D	Pre-collection preparation	No preparation of bridge required. Terrestrial LiDAR may need reference points.
1	E	Complexity of analysis	Coordinate transformation required; commercial software available for automated processing but subdivision of point clouds and curvature computation are additional steps necessary for damage identification and 3D modeling (Teza, et al. 2009)
2	F	Ease of data collection	May take up to a day to collect but operation is straightforward scanning (Lubowiecka, et al. 2009)
1	G	Stand-off distance rating	Instrument must be deployed on or near bridge but is non-contact
1	H	Traffic Disruption	Might require lane closure(s) to image some parts of the structure, but likely not this part. Multiple collects would increase disruption, but improve quality (see comment above in A).
10			

Deck Surface - Expansion Joint - Chemical Leaching on Bottom			
N/A	A	Is requirement met?	No reference to chemical leaching detection with LiDAR in the available literature and it was not investigated in this study.
	B	Availability of instrument	
	C	Cost of measurement	
	D	Pre-collection preparation	
	E	Complexity of analysis	
	F	Ease of data collection	
	G	Stand-off distance rating	
	H	Traffic Disruption	
N/A			

Deck Surface - Map Cracking - Surface Cracks 0.8 mm to 4.8 mm (1/32" to 3/16") width			
1	A	Is requirement met?	1 mm x 1 mm grid spacing; LiDAR tends to overestimate crack widths (Laefer et al., 2010); confirm w/ Dean and Hoensheid; Range falloff prevents an accurate measurement across the entire bridge deck; traffic disruptions would be necessary in order to collect more samples to scan evenly. (Hoensheid, 2012)
2	B	Availability of instrument	Commercial LiDAR is ubiquitous
1	C	Cost of measurement	High capital cost; may be some not-insignificant operational costs associated with deployment and data acquisition
1	D	Pre-collection preparation	No preparation of bridge required. Terrestrial LiDAR may need reference points.
1	E	Complexity of analysis	Coordinate transformation required; commercial software available for automated processing but subdivision of point clouds and curvature computation are additional steps necessary for damage identification and 3D modeling (Teza, et al. 2009)
2	F	Ease of data collection	May take up to a day to collect but operation is straightforward scanning (Lubowiecka, et al. 2009)
1	G	Stand-off distance rating	Instrument must be deployed on or near bridge but is non-contact
1	H	Traffic Disruption	Might require lane closure(s) to image some parts of the structure, but likely not this part. Multiple collects would increase disruption, but improve quality (see comment above in A).
10			

Deck Surface - Scaling - Depression in Surface 6.0 mm to 25.0 mm (1/4" to 1") depth			
1	A	Is requirement met?	> 1 mm x 1 mm grid spacing with TLS (Laefer, et al. 2010); Range falloff prevents an accurate measurement across the entire bridge deck; traffic disruptions would be necessary in order to collect more samples to scan evenly. (Hoensheid, 2012)
2	B	Availability of instrument	Commercial LiDAR is ubiquitous
1	C	Cost of measurement	High capital cost; may be some not-insignificant operational costs associated with deployment and data acquisition
1	D	Pre-collection preparation	No preparation of bridge required. Terrestrial LiDAR may need reference points.
1	E	Complexity of analysis	Coordinate transformation required; commercial software available for automated processing but subdivision of point clouds and curvature computation are additional steps necessary for damage identification and 3D modeling (Teza, et al. 2009)
2	F	Ease of data collection	May take up to a day to collect but operation is straightforward scanning (Lubowiecka, et al. 2009)
1	G	Stand-off distance rating	Instrument must be deployed on or near bridge but is non-contact
1	H	Traffic Disruption	Might require lane closure(s) to image some parts of the structure, but likely not this part. Multiple collects would increase disruption, but improve quality (see comment above in A).
10			

Deck Surface - Spalling - Depression with Parallel Fracture 6.0 mm to 25.0 mm (1/4" to 1") depth			
1	A	Is requirement met?	> 1 mm x 1 mm grid spacing with TLS (Laefer, et al. 2010); Range falloff prevents an accurate measurement across the entire bridge deck; traffic disruptions would be necessary in order to collect more samples to scan evenly. (Hoensheid, 2012)
2	B	Availability of instrument	Commercial LiDAR is ubiquitous
1	C	Cost of measurement	High capital cost; may be some not-insignificant operational costs associated with deployment and data acquisition
1	D	Pre-collection preparation	No preparation of bridge required. Terrestrial LiDAR may need reference points.
1	E	Complexity of analysis	Coordinate transformation required; commercial software available for automated processing but subdivision of point clouds and curvature computation are additional steps necessary for damage identification and 3D modeling (Teza, et al. 2009)
2	F	Ease of data collection	May take up to a day to collect but operation is straightforward scanning (Lubowiecka, et al. 2009)
1	G	Stand-off distance rating	Instrument must be deployed on or near bridge but is non-contact
1	H	Traffic Disruption	Might require lane closure(s) to image some parts of the structure, but likely not this part. Multiple collects would increase disruption, but improve quality (see comment above in A).
10			

Deck Surface - Delamination - Surface Cracks 0.8 mm to 4.8 mm (1/32" to 3/16") width			
1	A	Is requirement met?	> 1 mm x 1 mm grid spacing with TLS (Laefer, et al. 2010); Range falloff prevents an accurate measurement across the entire bridge deck; traffic disruptions would be necessary in order to collect more samples to scan evenly. (Hoensheid, 2012)
2	B	Availability of instrument	Commercial LiDAR is ubiquitous
1	C	Cost of measurement	High capital cost; may be some not-insignificant operational costs associated with deployment and data acquisition
1	D	Pre-collection preparation	No preparation of bridge required. Terrestrial LiDAR may need reference points.
1	E	Complexity of analysis	Coordinate transformation required; commercial software available for automated processing but subdivision of point clouds and curvature computation are additional steps necessary for damage identification and 3D modeling (Teza, et al. 2009)
2	F	Ease of data collection	May take up to a day to collect but operation is straightforward scanning (Lubowiecka, et al. 2009)
1	G	Stand-off distance rating	Instrument must be deployed on or near bridge but is non-contact
1	H	Traffic Disruption	Might require lane closure(s) to image some parts of the structure, but likely not this part. Multiple collects would increase disruption, but improve quality (see comment above in A).
10			

Girder Surface - Steel Structural Cracking - Surface Cracks < 0.1 mm (.004"), hairline			
0	A	Is requirement met?	1 mm x 1 mm grid spacing; LiDAR tends to overestimate crack widths (Laefer et al., 2010). Can this level of accuracy be detected in a LiDAR system?
2	B	Availability of instrument	Commercial LiDAR is ubiquitous
1	C	Cost of measurement	High capital cost; may be some not-insignificant operational costs associated with deployment and data acquisition
1	D	Pre-collection preparation	No preparation of bridge required. Terrestrial LiDAR may need reference points.
1	E	Complexity of analysis	Coordinate transformation required; commercial software available for automated processing but subdivision of point clouds and curvature computation are additional steps necessary for damage identification and 3D modeling (Teza, et al. 2009)
2	F	Ease of data collection	May take up to a day to collect but operation is straightforward scanning (Lubowiecka, et al. 2009)
1	G	Stand-off distance rating	Instrument must be deployed on or near bridge but is non-contact
2	H	Traffic Disruption	Could be done from off of the bridge (side-looking TLS)
0			

Girder Surface - Concrete Structural Cracking - Surface Cracks .1 mm (.004")			
0	A	Is requirement met?	1 mm x 1 mm grid spacing; LiDAR tends to overestimate crack widths (Laefer et al., 2010). Can this level of accuracy be detected in a LiDAR system?
2	B	Availability of instrument	Commercial LiDAR is ubiquitous
1	C	Cost of measurement	High capital cost; may be some not-insignificant operational costs associated with deployment and data acquisition
1	D	Pre-collection preparation	No preparation of bridge required. Terrestrial LiDAR may need reference points.
1	E	Complexity of analysis	Coordinate transformation required; commercial software available for automated processing but subdivision of point clouds and curvature computation are additional steps necessary for damage identification and 3D modeling (Teza, et al. 2009)
2	F	Ease of data collection	May take up to a day to collect but operation is straightforward scanning (Lubowiecka, et al. 2009)
1	G	Stand-off distance rating	Instrument must be deployed on or near bridge but is non-contact
2	H	Traffic Disruption	Could be done from off of the bridge (side-looking TLS)
0			

Girder Surface - Steel Section Loss - Change in Cross-Sectional Area Percent thickness of web or flange			
1	A	Is requirement met?	Hauser and Chen (2009) have asserted resolution of LiDAR for section loss is down to 0.5 mm. Can this requirement be met accuarately?
2	B	Availability of instrument	Commercial LiDAR is ubiquitous
1	C	Cost of measurement	High capital cost; may be some not-insignificant operational costs associated with deployment and data acquisition
1	D	Pre-collection preparation	No preparation of bridge required
1	E	Complexity of analysis	Coordinate transformation required; commercial software available for automated processing but subdivision of point clouds and curvature computation are additional steps necessary for damage identification and 3D modeling (Teza, et al. 2009)
1	F	Ease of data collection	May take up to a day to collect but operation is straightforward scanning (Lubowiecka, et al. 2009). Would require complex mounting aparatus.
1	G	Stand-off distance rating	Instrument must be deployed on or near bridge but is non-contact
2	H	Traffic Disruption	Could be done from off of the bridge (side-looking TLS), but generally some minor disruption would be necessary for interior beams.
10			

Girder Surface - Concrete Section Loss - Change in Cross-Sectional Area Percent volume per foot			
1	A	Is requirement met?	Hauser and Chen (2009) have asserted resolution of LiDAR for section loss is down to 0.5 mm. Can this requirement be met accuarately?
2	B	Availability of instrument	Commercial LiDAR is ubiquitous
1	C	Cost of measurement	High capital cost; may be some not-insignificant operational costs associated with deployment and data acquisition
1	D	Pre-collection preparation	No preparation of bridge required
1	E	Complexity of analysis	Coordinate transformation required; commercial software available for automated processing but subdivision of point clouds and curvature computation are additional steps necessary for damage identification and 3D modeling (Teza, et al. 2009)
1	F	Ease of data collection	May take up to a day to collect but operation is straightforward scanning (Lubowiecka, et al. 2009). Would require complex mounting aparatus.
1	G	Stand-off distance rating	Instrument must be deployed on or near bridge but is non-contact
2	H	Traffic Disruption	Could be done from off of the bridge (side-looking TLS), but generally some minor disruption would be necessary for interior beams.
10			

Global Metrics - Bridge Settlement - Vertical Movement of Bridge			
	Approximately 6 mm to 12 mm		
N/A	A	Is requirement met?	> 1 x 1 cm grid spacing with TLS (Laefer, et al. 2010)
2	B	Availability of instrument	Commercial LiDAR is ubiquitous
1	C	Cost of measurement	High capital cost; may be some not-insignificant operational costs associated with deployment and data acquisition
1	D	Pre-collection preparation	No preparation of bridge required. Terrestrial LiDAR may need reference points.
1	E	Complexity of analysis	Coordinate transformation required, but additional processing described for other applications may not be necessary for simple comparison of coordinate spaces
1	F	Ease of data collection	May take up to a day to collect but operation is straightforward scanning (Lubowiecka, et al. 2009). It would be very difficult to maintaining global positioning across scans through time.
1	G	Stand-off distance rating	Instrument must be deployed on or near bridge but is non-contact
2	H	Traffic Disruption	Would have to be done from off the bridge
N/A			

Global Metrics - Bridge Movement - Transverse Directions			
	Approximately 6 mm to 12 mm		
N/A	A	Is requirement met?	> 1 x 1 cm grid spacing with TLS (Laefer, et al. 2010). Technology not practical for this application.
	B	Availability of instrument	
	C	Cost of measurement	
	D	Pre-collection preparation	
	E	Complexity of analysis	
	F	Ease of data collection	
	G	Stand-off distance rating	
	H	Traffic Disruption	
N/A			

Global Metrics - Surface Roughness			
	Change over time		
1	A	Is requirement met?	> 1 mm x 1 mm grid spacing with TLS (Laefer, et al. 2010); Range falloff prevents an accurate measurement across the entire bridge deck; traffic disruptions would be necessary in order to collect more samples to scan evenly. (Hoensheid, 2012)
2	B	Availability of instrument	Commercial LiDAR is ubiquitous
1	C	Cost of measurement	High capital cost; may be some not-insignificant operational costs associated with deployment and data acquisition
1	D	Pre-collection preparation	No preparation of bridge required. Terrestrial LiDAR may need reference points.
1	E	Complexity of analysis	Coordinate transformation required, but additional processing described for other applications may not be necessary for simple comparison of coordinate spaces
2	F	Ease of data collection	May take up to a day to collect but operation is straightforward scanning (Lubowiecka, et al. 2009)
1	G	Stand-off distance rating	Instrument must be deployed on or near bridge but is non-contact
1	H	Traffic Disruption	Might require lane closure(s) to image some parts of the structure, but likely not this part. Multiple collects would increase disruption, but improve quality (see comment above in A).
10			

Thermal IR

Deck Surface

		Torn/Missing Seal	Armored Plated Damage	Expansion Joint - Cracks within 2 Feet	Expansion Joint - Spalls within 2 Feet	Map Cracking - Surface Cracks	Scaling - Depression in Surface	Spalling - Depression with Parallel Fracture	Delamination - Surface Cracks
A	Is requirement met?	1	N/A	N/A	1	0	1	1	0
B	Availability of instrument	2	2	2	2	2	2	2	2
C	Cost of measurement	2	2	2	2	2	2	2	2
D	Pre-collection preparation	2	2	2	2	2	1	1	2
E	Complexity of analysis	2	1	1	2	1	2	2	1
F	Ease of data collection	1	1	1	1	1	1	1	1
G	Stand-off distance rating	1	1	1	1	1	1	1	1
H	Traffic Disruption	2	1	1	1	1	1	1	1
		13	**N/A**	**N/A**	**12**	**0**	**11**	**11**	**0**

Deck Subsurface

Moisture in Cracks	Hollow Sound	Fracture Planes / Open Spaces	Scaling	Spalling	Corrosion	Chloride Ingress
2	N/A	2	0	0	N/A	N/A
2	0	2	2	2	0	0
2	0	2	2	2	0	0
1	0	1	1	1	0	0
2	0	2	2	2	0	0
1	0	1	1	1	0	0
1	0	1	1	1	0	0
1	0	1	1	1	0	0
12	**N/A**	**12**	**0**	**0**	**N/A**	**N/A**

	A	B
Weights:	**1**	**1**

Girder Surface

Steel Structural Cracking	Concrete Structural Cracking	Steel Section Loss	Paint Condition	Concrete Section Loss
0	1	N/A	N/A	N/A
2	2	0	0	0
2	2	0	0	0
2	2	0	0	0
2	2	0	0	0
1	1	0	0	0
1	1	0	0	0
2	2	0	0	0
0	**13**	**N/A**	**N/A**	**N/A**

Girder Subsurface

Internal Concrete Structural Cracks	Fracture Planes / Open Spaces	Concrete Section Loss	Prestress Strand Breakage	Corrosion Rate (Resistivity)	Chloride Ingress
N/A	1.5	N/A	N/A	N/A	N/A
2	2	0	0	0	0
2	2	0	0	0	0
2	2	0	0	0	0
2	2	0	0	0	0
1	1	0	0	0	0
1	1	0	0	0	0
2	2	0	0	0	0
N/A	**13.5**	**N/A**	**N/A**	**N/A**	**N/A**

Deck Surface - Expansion Joint - Torn/Missing Seal			
1	A	Is requirement met?	Potential to pick up different materials. Other technologies are perhaps better suited for this application
2	B	Availability of instrument	Equipment is commercially available.
2	C	Cost of measurement	Can be used for multi bridge inspection. Higher end cameras are required for highway speed data collection which would decrease rating.
2	D	Pre-collection preparation	No preparation of the structure or instrument is required
2	E	Complexity of analysis	Analysis can be done in the field by visual IR images
1	F	Ease of data collection	Environmentally dependent (data collection is most effective between 10am and 3pm), it requires separate camera to identify the presence of other materials on the surface.
1	G	Stand-off distance rating	Standoff is close, Ground based vehicle
2	H	Traffic Disruption	Other research indicates that data collection cannot be done at speed. Rapid data collection will eliminate lane closure. Data collection by standing on the shoulder, No vehicle requirement
13			

Deck Surface - Expansion Joint - Armored Plated Damage			
N/A	A	Is requirement met?	Potential to pick up different materials. Other technologies are perhaps better suited for this application
2	B	Availability of instrument	Equipment is commercially available.
2	C	Cost of measurement	Can be used for multi bridge inspection. Higher end cameras are required for highway speed data collection which would decrease rating.
2	D	Pre-collection preparation	No preparation of the structure or instrument is required
1	E	Complexity of analysis	Analysis can be done in the field by visual IR images
1	F	Ease of data collection	Environmentally dependent (data collection is most effective between 10am and 3pm), it requires separate camera to identify the presence of other materials on the surface.
1	G	Stand-off distance rating	Standoff is close, Ground based vehicle
1	H	Traffic Disruption	Other research indicates that data collection cannot be done at speed. Rapid data collection will eliminate lane closure.
N/A			

Deck Surface - Expansion Joint - Cracks within 2 Feet 0.8 mm to 4.8 mm (1/32" to 3/16") width			
N/A	A	Is requirement met?	Environment and presence of foreign body on the surface can effect measurement, Size of the crack needs to be determined.
2	B	Availability of instrument	Equipment is commercially available.
2	C	Cost of measurement	Can be used for multi bridge inspection. Higher end cameras are required for highway speed data collection which would decrease rating.
2	D	Pre-collection preparation	No preparation of the structure or instrument is required
1	E	Complexity of analysis	Analysis can be done in the field by visual IR images
1	F	Ease of data collection	Environmentally dependent (data collection is most effective between 10am and 3pm), it requires separate camera to identify the presence of other materials on the surface.
1	G	Stand-off distance rating	Standoff is close, Ground based vehicle
1	H	Traffic Disruption	Rapid data collection will eliminate lane closure.
N/A			

Deck Surface - Expansion Joint - Spalls within 2 Feet 6.0 mm to 25.0 mm (1/4" to 1") depth			**Volume?**
1	A	Is requirement met?	Other technologies are perhaps better suited for this application. Can we measure a volume? Maximum depth within the specimen = 76 mm (Washer G., 2010)
2	B	Availability of instrument	Equipment is commercially available.
2	C	Cost of measurement	Can be used for multi bridge inspection. Higher end cameras are required for highway speed data collection which would decrease rating.
2	D	Pre-collection preparation	No preparation of the structure or instrument is required
2	E	Complexity of analysis	Analysis can be done in the field by visual IR images
1	F	Ease of data collection	Environmentally dependent (data collection is most effective between 10am and 3pm), it requires separate camera to identify the presence of other materials on the surface.
1	G	Stand-off distance rating	Standoff is close, Ground based vehicle
1	H	Traffic Disruption	Rapid data collection will eliminate lane closure. Data collection by standing on the shoulder, No vehicle requirement
12			

Deck Surface - Map Cracking - Surface Cracks 0.8 mm to 4.8 mm (1/32" to 3/16") width			
0	A	Is requirement met?	Not applicable based on current technologies resolution. Environment and presence of foreign body on the surface can effect measurement
2	B	Availability of instrument	Equipment is commercially available.
2	C	Cost of measurement	Can be used for multi bridge inspection. Higher end cameras are required for highway speed data collection which would decrease rating.
2	D	Pre-collection preparation	No preparation of the structure or instrument is required
1	E	Complexity of analysis	It may require more analyzes due to the presence of other materials on the surface.
1	F	Ease of data collection	Environmentally dependent (data collection is most effective between 10am and 3pm), it requires separate camera to identify the presence of other materials on the surface.
1	G	Stand-off distance rating	Standoff is close, Ground based vehicle
1	H	Traffic Disruption	Rapid data collection will eliminate lane closure.
0			

Deck Surface - Scaling - Depression in Surface 6.0 mm to 25.0 mm (1/4" to 1") depth			
1	A	Is requirement met?	Other technologies are perhaps better suited for this application. Can we measure volume of scaling with this technique? Maximum depth within the specimen = 76 mm (Washer G., 2010) Environment and presence of foreign body on the surface can effect measurement.
2	B	Availability of instrument	Equipment is commercially available.
2	C	Cost of measurement	Can be used for multi bridge inspection. Higher end cameras are required for highway speed data collection which would decrease rating.
1	D	Pre-collection preparation	No preparation of the structure or instrument is required. Reference points are required when collecting data at speed.
2	E	Complexity of analysis	It may require more analyzes due to the presence of other materials on the surface.
1	F	Ease of data collection	Environmentally dependent (data collection is most effective between 10am and 3pm), it requires separate camera to identify the presence of other materials on the surface.
1	G	Stand-off distance rating	Standoff is close, Ground based vehicle
1	H	Traffic Disruption	Minor traffic disruption is necessary for full bridge collect. Rapid data collection will eliminate lane closure.
11			

Deck Surface - Spalling - Depression with Parallel Fracture 6.0 mm to 25.0 mm (1/4" to 1") depth			
1	A	Is requirement met?	Maximum depth = 76 mm (Washer G., 2010), Environment and presence of foreign body on the surface can effect measurement
2	B	Availability of instrument	Equipment is commercially available.
2	C	Cost of measurement	Can be used for multi bridge inspection. Higher end cameras are required for highway speed data collection which would decrease rating.
1	D	Pre-collection preparation	No preparation of the structure or instrument is required. Reference points are required when collecting data at speed.
2	E	Complexity of analysis	It may require more analyzes due to the presence of other materials on the surface.
1	F	Ease of data collection	Environmentally dependent (data collection is most effective between 10am and 3pm), it requires separate camera to identify the presence of other materials on the surface.
1	G	Stand-off distance rating	Standoff is close, Ground based vehicle
1	H	Traffic Disruption	Minor traffic disruption is necessary for full bridge collect. Rapid data collection will eliminate lane closure.
11			

Deck Surface - Delamination - Surface Cracks 0.8 mm to 4.8 mm (1/32" to 3/16") width			
0	A	Is requirement met?	Not applicable based on current technologies resolution. Environment and presence of foreign body on the surface can effect measurement
2	B	Availability of instrument	Equipment is commercially available.
2	C	Cost of measurement	Can be used for multi bridge inspection. Higher end cameras are required for highway speed data collection which would decrease rating.
2	D	Pre-collection preparation	No preparation of the structure or instrument is required. Reference points are required when collecting data at speed.
1	E	Complexity of analysis	It may require more analyzes due to the presence of other materials on the surface.
1	F	Ease of data collection	Environmentally dependent (data collection is most effective between 10am and 3pm), it requires separate camera to identify the presence of other materials on the surface.
1	G	Stand-off distance rating	Standoff is close, Ground based vehicle
1	H	Traffic Disruption	Rapid data collection will eliminate lane closure.
0			

Deck Subsurface - Delamination - Moisture in Cracks Change in moisture content			
2	A	Is requirement met?	Depth of penetration? Maximum depth = 76 mm (Washer G., 2010), Based on different emissivity of different material.
2	B	Availability of instrument	Equipment is commercially available.
2	C	Cost of measurement	Can be used for multi bridge inspection. Higher end cameras are required for highway speed data collection which would decrease rating.
1	D	Pre-collection preparation	No preparation of the structure or instrument is required. Reference points are required when collecting data at speed.
2	E	Complexity of analysis	It may require more analyzes due to the presence of other materials on the surface.
1	F	Ease of data collection	Environmentally dependent (data collection is most effective between 10am and 3pm), it requires separate camera to identify the presence of other materials on the surface.
1	G	Stand-off distance rating	Standoff is close, Ground based vehicle
1	H	Traffic Disruption	Rapid data collection will eliminate lane closure.
12			

Deck Subsurface - Delamination - Hollow Sound			
N/A	A	Is requirement met?	Not applicable for sounding.
	B	Availability of instrument	
	C	Cost of measurement	
	D	Pre-collection preparation	
	E	Complexity of analysis	
	F	Ease of data collection	
	G	Stand-off distance rating	
	H	Traffic Disruption	
N/A			

Deck Subsurface - Delamination - Fracture Planes / Open Spaces			
	Change in return signal		
2	A	Is requirement met?	Maximum depth = 76 mm (Washer G., 2010)
2	B	Availability of instrument	Equipment is commercially available.
2	C	Cost of measurement	Can be used for multi bridge inspection. Higher end cameras are required for highway speed data collection which would decrease rating.
1	D	Pre-collection preparation	No preparation of the structure or instrument is required
2	E	Complexity of analysis	It may require more analyzes due to the presence of other materials on the surface.
1	F	Ease of data collection	Environmentally dependent (data collection is most effective between 10am and 3pm), it requires separate camera to identify the presence of other materials on the surface.
1	G	Stand-off distance rating	Standoff is close, Ground based vehicle
1	H	Traffic Disruption	Rapid data collection will eliminate lane closure.
12			

Deck Subsurface - Scaling - Depression in Surface (eg. Interior of voided sections)			
	6.0 mm to 25.0 mm (1/4" to 1") depth		
0	A	Is requirement met?	Limitations on detecting internal defects deeper than 3 inches.
2	B	Availability of instrument	Equipment is commercially available.
2	C	Cost of measurement	Can be used for multi bridge inspection. Higher end cameras are required for highway speed data collection which would decrease rating.
1	D	Pre-collection preparation	No preparation of the structure or instrument is required
2	E	Complexity of analysis	It may require more analyzes due to the presence of other materials on the surface. Analysis can be done in the field by visual IR images
1	F	Ease of data collection	Environmentally dependent (data collection is most effective between 10am and 3pm), it requires separate camera to identify the presence of other materials on the surface.
1	G	Stand-off distance rating	Standoff is close, Ground based vehicle
1	H	Traffic Disruption	Rapid data collection will eliminate lane closure.
0			

Deck Subsurface - Spalling - Depression with Parallel Fracture (eg. Interior of voided sections)			
	6.0 mm to 25.0 mm (1/4" to 1") depth		
0	A	Is requirement met?	Limitations on detecting internal defects deeper than 3 inches.
2	B	Availability of instrument	Equipment is commercially available.
2	C	Cost of measurement	Can be used for multi bridge inspection. Higher end cameras are required for highway speed data collection which would decrease rating.
1	D	Pre-collection preparation	No preparation of the structure or instrument is required
2	E	Complexity of analysis	It may require more analyzes due to the presence of other materials on the surface. Analysis can be done in the field by visual IR images
1	F	Ease of data collection	Environmentally dependent (data collection is most effective between 10am and 3pm), it requires separate camera to identify the presence of other materials on the surface.
1	G	Stand-off distance rating	Standoff is close, Ground based vehicle
1	H	Traffic Disruption	Rapid data collection will eliminate lane closure.
0			

Deck Subsurface - Corrosion - Corrosion Rate (Resistivity)			
	5 to 20 kΩ-cm		
N/A	A	Is requirement met?	Correlation not investigated in this study.
	B	Availability of instrument	
	C	Cost of measurement	
	D	Pre-collection preparation	
	E	Complexity of analysis	
	F	Ease of data collection	
	G	Stand-off distance rating	
	H	Traffic Disruption	
N/A			

Deck Subsurface - Chloride Ingress - Chloride Content through the Depth			
	0.4 to 1.0 % chloride by mass of cement		
N/A	A	Is requirement met?	Correlation not investigated in this study.
	B	Availability of instrument	
	C	Cost of measurement	
	D	Pre-collection preparation	
	E	Complexity of analysis	
	F	Ease of data collection	
	G	Stand-off distance rating	
	H	Traffic Disruption	
N/A			

Girder Surface - Steel Structural Cracking - Surface Cracks			
	< 0.1 mm (.004"), hairline		
0	A	Is requirement met?	BridgeGuard report shows that IR can detect scratches on the surface.
2	B	Availability of instrument	Equipment is commercially available.
2	C	Cost of measurement	Can be used for multi bridge inspection. Higher end cameras are required for highway speed data collection which would decrease rating.
2	D	Pre-collection preparation	No preparation of the structure or instrument is required
2	E	Complexity of analysis	Analysis can be done in the field by visual IR images
1	F	Ease of data collection	Environmentally dependent (data collection is most effective between 10am and 3pm), it requires separate camera to identify the presence of other materials on the surface.
1	G	Stand-off distance rating	Standoff is close, Ground based vehicle
2	H	Traffic Disruption	Data collection from shoulders. No vehicle required.
0			

Girder Surface - Concrete Structural Cracking - Surface Cracks			
	.1 mm (.004")		
1	A	Is requirement met?	Size of the crack? Larger cracks are detectable. Other technologies are more applicable.
2	B	Availability of instrument	Equipment is commercially available.
2	C	Cost of measurement	Can be used for multi bridge inspection. Higher end cameras are required for highway speed data collection which would decrease rating.
2	D	Pre-collection preparation	No preparation of the structure or instrument is required
2	E	Complexity of analysis	Analysis can be done in the field by visual IR images
1	F	Ease of data collection	IR Camera needs to be used under the bridge, Environmentally dependent (data collection is most effective between 10am and 3pm), it requires separate camera to identify the presence of other materials on the surface.
1	G	Stand-off distance rating	Standoff is close, Ground based vehicle
2	H	Traffic Disruption	Data collection from shoulders. No vehicle required.
13			

Girder Surface - Steel Section Loss - Change in Cross-Sectional Area			
	Percent thickness of web or flange		
N/A	A	Is requirement met?	Correlation not investigated in this study.
	B	Availability of instrument	
	C	Cost of measurement	
	D	Pre-collection preparation	
	E	Complexity of analysis	
	F	Ease of data collection	
	G	Stand-off distance rating	
	H	Traffic Disruption	
N/A			

Girder Surface - Paint Condition			
	Amount of missing paint (X %)		
N/A	A	Is requirement met?	Correlation not investigated in this study.
	B	Availability of instrument	
	C	Cost of measurement	
	D	Pre-collection preparation	
	E	Complexity of analysis	
	F	Ease of data collection	
	G	Stand-off distance rating	
	H	Traffic Disruption	
N/A			

Girder Surface - Concrete Section Loss - Change in Cross-Sectional Area			
	Percent volume per foot		
N/A	A	Is requirement met?	Can we see a volume? Environment and presence of foreign body on the surface can effect measurement. Percent volume cannot be measured with this technology, however spalls are observable in thermal IR image.
	B	Availability of instrument	
	C	Cost of measurement	
	D	Pre-collection preparation	
	E	Complexity of analysis	
	F	Ease of data collection	
	G	Stand-off distance rating	
	H	Traffic Disruption	
N/A			

Girder Subsurface - Internal Concrete Structural Cracks - Internal Cracks (e.g. Box Beam)			
	Approx 0.8 mm (1/32")		
N/A	A	Is requirement met?	Environment and presence of foreign body on the surface can effect measurement
2	B	Availability of instrument	Equipment is commercially available.
2	C	Cost of measurement	Can be used for multi bridge inspection. Higher end cameras are required for highway speed data collection which would decrease rating.
2	D	Pre-collection preparation	No preparation of the structure or instrument is required
2	E	Complexity of analysis	It may require further analyzes on data.
1	F	Ease of data collection	IR Camera needs to be used under the bridge, Environmentally dependent (data collection is most effective between 10am and 3pm), it requires separate camera to identify the presence of other materials on the surface.
1	G	Stand-off distance rating	Standoff is close
2	H	Traffic Disruption	Minor traffic disruption underneath the bridge. Data collection from shoulders. No vehicle required.
N/A			

Girder Subsurface - Internal Concrete Structural Cracks - Fracture Planes / Open Spaces			
	Change in return signal		
1.5	A	Is requirement met?	Maximum depth = 76 mm (Washer G., 2010)
2	B	Availability of instrument	Equipment is commercially available.
2	C	Cost of measurement	Can be used for multi bridge inspection. Higher end cameras are required for highway speed data collection which would decrease rating.
2	D	Pre-collection preparation	No preparation of the structure or instrument is required
2	E	Complexity of analysis	It may require more analyzes due to the presence of other materials on the surface.
1	F	Ease of data collection	Environmentally dependent (data collection is most effective between 10am and 3pm), it requires separate camera to identify the presence of other materials on the surface.
1	G	Stand-off distance rating	Standoff is close, Ground based vehicle
2	H	Traffic Disruption	Rapid data collection will eliminate lane closure.
13.5			

Girder Subsurface - Concrete Section Loss - Change in Cross-Sectional Area			
	Percent volume per foot		
N/A	A	Is requirement met?	Not likely to pick up section loss within box girder. Maximum depth = 76 mm (Washer G., 2010) Percent volume cannot be measured with this technology, however spalls are observable in thermal IR image.
	B	Availability of instrument	
	C	Cost of measurement	
	D	Pre-collection preparation	
	E	Complexity of analysis	
	F	Ease of data collection	
	G	Stand-off distance rating	
	H	Traffic Disruption	
N/A			

Girder Subsurface - Prestress Strand Breakage - Change in Cross-Sectional Area			
	Wire 2 mm or strand 9.5 mm diameter		
N/A	A	Is requirement met?	Not likely to see strand broken unless the gap has formed between the two sections of strands. Maximum depth = 76 mm (Washer G., 2010)
	B	Availability of instrument	
	C	Cost of measurement	
	D	Pre-collection preparation	
	E	Complexity of analysis	
	F	Ease of data collection	
	G	Stand-off distance rating	
	H	Traffic Disruption	
N/A			

Girder Subsurface - Corrosion - Corrosion Rate (Resistivity)			
	5 to 20 kΩ-cm		
N/A	A	Is requirement met?	Correlation not investigated in this study.
	B	Availability of instrument	
	C	Cost of measurement	
	D	Pre-collection preparation	
	E	Complexity of analysis	
	F	Ease of data collection	
	G	Stand-off distance rating	
	H	Traffic Disruption	
N/A			

Girder Subsurface - Chloride Ingress - Chloride Content through the Depth			
	0.4 to 1.0 % Chloride by mass of cement		
N/A	A	Is requirement met?	Correlation not investigated in this study.
	B	Availability of instrument	
	C	Cost of measurement	
	D	Pre-collection preparation	
	E	Complexity of analysis	
	F	Ease of data collection	
	G	Stand-off distance rating	
	H	Traffic Disruption	
N/A			

Digital Image Correlation

		Global Metrics			
		Change in Bridge Length	Vertical Movement of Bridge	Transverse Directions	Vibration or Live Load De
A	Is requirement met?	N/A	N/A	N/A	2
B	Availability of instrument	1	1	1	2
C	Cost of measurement	1.5	0	0	1.5
D	Pre-collection preparation	1.5	1	1	1.5
E	Complexity of analysis	1	1	1	1
F	Ease of data collection	1	1	1	1
G	Stand-off distance rating	1	1	1	1
H	Traffic Disruption	2	2	2	2
		N/A	**N/A**	**N/A**	**12**

	A	B
Weights:	**1**	**1**

Global Metrics - Bridge Length - Change in Bridge Length

Accuracy to 30 mm (0.1ft) (smaller)

N/A	A	Is requirement met?	Resolution is certainly within capabilities of technology; one experiment indicated 0.1" can be achieved (MTRI, 2010);**Not as practical for this application/Long-term measurements not investigated in this study**
1	B	Availability of instrument	Long-term deployments have never been done; pixel coregistration after months seems unlikely
1.5	C	Cost of measurement	Equipment must be dedicated to bridge (to ensure accurate pixel coregistration); Has the potential to have a low capital cost with moderate operational cost
1.5	D	Pre-collection preparation	Could potentially be done with no preparation
1	E	Complexity of analysis	Automated analysis by MATLAB/analysis package algorithm with additional post-processing; Processing initialization must be changed with each dataset
1	F	Ease of data collection	Stringent requirements on camera position, protection for long-term deployment
1	G	Stand-off distance rating	Must be far enough to image larger portion of bridge
2	H	Traffic Disruption	No lane closure(s) needed as system is not even on the bridge
N/A			

Global Metrics - Bridge Settlement - Vertical Movement of Bridge

Approximately 6 mm to 12 mm

N/A	A	Is requirement met?	Spatial resolution requirements met; temporal resolution requires long-term deployments;**Not as practical for this application/Long-term measurements not investigated in this study**
1	B	Availability of instrument	Long-term deployments have never been done; pixel coregistration after months seems unlikely
0	C	Cost of measurement	Equipment must be dedicated to bridge (to ensure accurate pixel coregistration)
1	D	Pre-collection preparation	Could potentially be done with no preparation
1	E	Complexity of analysis	Automated analysis by MATLAB/analysis package algorithm with additional post-processing; Processing initialization must be changed with each dataset
1	F	Ease of data collection	Stringent requirements on camera position, protection for long-term deployment
1	G	Stand-off distance rating	Must be far enough to image larger portion of bridge
2	H	Traffic Disruption	No lane closure(s) needed as system is not even on the bridge
N/A			

Global Metrics - Bridge Movement - Transverse Directions			
	Approximately 6 mm to 12 mm		
N/A	A	Is requirement met?	Spatial resolution requirements met; temporal resolution requires long-term deployments; **Not as practical for this application/Long-term measurements not investigated in this study**
1	B	Availability of instrument	Long-term deployments have never been done; pixel coregistration after months seems unlikely
0	C	Cost of measurement	Equipment must be dedicated to bridge (to ensure accurate pixel coregistration)
1	D	Pre-collection preparation	Could potentially be done with no preparation
1	E	Complexity of analysis	Automated analysis by MATLAB/analysis package algorithm with additional post-processing; Processing initialization must be changed with each dataset
1	F	Ease of data collection	Stringent requirements on camera position, protection for long-term deployment
1	G	Stand-off distance rating	Must be far enough to image larger portion of bridge
2	H	Traffic Disruption	No lane closure(s) needed as system is not even on the bridge
N/A			

Global Metrics - Vibration or Live Load Deflection			
	.5 -20 Hz; L/800 deflection		
2	A	Is requirement met?	Sub-millimeter (Lee and Shinozuka, 2006); frequency response of technique needed from literature
2	B	Availability of instrument	Common equipment (cameras)
1.5	C	Cost of measurement	Multiple measurements and/or multiple cameras required; Has the potential to have low capital cost with moderate operation cost
1.5	D	Pre-collection preparation	Could potentially be done with no preparation
1	E	Complexity of analysis	Automated analysis by MATLAB/analysis package algorithm with additional post-processing; Processing initialization must be changed with each dataset
1	F	Ease of data collection	Multiple measurements on one bridge may be required
1	G	Stand-off distance rating	Must be far enough to image larger portion of bridge
2	H	Traffic Disruption	No lane closure(s) needed as system is not even on the bridge
12			

SAR Speckle

		Deck Surface						
		Torn/Missing Seal	Expansion Joint - Cracks within 2 Feet	Expansion Joint - Spalls within 2 Feet	Map Cracking - Surface Cracks	Scaling - Depression in Surface	Spalling - Depression with Parallel Fracture	Delamination - Surface Cracks
A	Is requirement met?	0	0	0	0	1	1	N/A
B	Availability of instrument	2	2	2	2	2	2	2
C	Cost of measurement	1	1	1	1	1	1	1
D	Pre-collection preparation	1	1	1	1	1	1	1
E	Complexity of analysis	1	1	1	1	1	1	1
F	Ease of data collection	1	1	1	1	1	1	1
G	Stand-off distance rating	1	1	1	1	1	1	1
H	Traffic Disruption	1	1	1	1	1	1	1
		0	**0**	**0**	**0**	**9**	**9**	**N/A**

Girder Surface					Girder Subsurface						
Steel Structural Cracking	Concrete Structural Cracking	Steel Section Loss	Paint Condition	Concrete Section Loss	Internal Concrete Structural Cracks	Concrete Section Loss	Prestress Strand Breakage	Rebar Corrosion	Chloride Ingress	Change in Bridge Length	Vertical Movement of Bridge
N/A	N/A	N/A	N/A	N/A	N/A	N/A	N/A	N/A	N/A	N/A	N/A
2	2	2	2	2	2	2	2	2	2	2	2
1	1	1	1	1	1	1	0	1	1	1	1
1	1	1	1	1	2	1	2	2	2	1	1
1	1	1	1	1	1	1	1	1	1	1	1
1	1	1	1	1	1	1	1	2	1	1	1
1	1	2	2	2	1	2	1	1	1	2	2
1	1	2	2	2	1	2	1	2	2	2	2
N/A	**N/A**	**N/A**	**N/A**	**N/A**	**N/A**	**N/A**	**N/A**	**N/A**	**N/A**	**N/A**	**N/A**

Global Metrics			Deck Subsurface							
Transverse Directions	Surface Roughness	Vibration or Live Load Deflection	Material in Joint	Moisture in Cracks	Internal Horizontal Crack	Fracture Planes / Open Spaces	Scaling	Spalling	Rebar Corrosion	Chloride Ingress
N/A	1	N/A	N/A	N/A	N/A	N/A	N/A	N/A	N/A	N/A
2	1	2	2	2	2	2	2	2	2	2
1	0	1	1	1	1	1	1	1	1	1
1	2	1	1	2	2	2	1	1	2	2
1	0	1	1	1	1	1	1	1	1	1
1	2	1	1	1	2	2	1	1	2	2
2	2	2	1	1	1	1	1	1	1	1
2	2	2	1	2	2	2	1	1	2	2
N/A	**10**	**N/A**	**N/A**	**N/A**	**N/A**	**N/A**	**N/A**	**N/A**	**N/A**	**N/A**

Deck Surface - Expansion Joint - Torn/Missing Seal			
0	A	Is requirement met?	The challenge presented is being sensitive to this feature when it is smaller than the size of the range bins; 8-10 cm range resolution highest with another (AKELE) radar system (MTRI, 2010)
2	B	Availability of instrument	Commercial-grade instruments are available (e.g. IBIS-S, Olson, 2010)
1	C	Cost of measurement	Moderately high capital cost (compare to GPR)
1	D	Pre-collection preparation	May need to install reflectors on the bridge; may need to visit bridge ahead of time to plan collection geometry
1	E	Complexity of analysis	Some sort of transform or migration is probably needed; frequent references to complex post-processing in literature
1	F	Ease of data collection	Complex operation, as intended by manufacturer, that needs be supervised by operator
1	G	Stand-off distance rating	Non-contact; could be performed at great distances, but geometry of collection restricts standoff distance
1	H	Traffic Disruption	To image expansion joints (on top of bridge deck) the instrument would have to be on the bridge
0			

Deck Surface - Expansion Joint - Cracks within 2 Feet 0.8 mm to 4.8 mm (1/32" to 3/16") width			
0	A	Is requirement met?	The challenge presented is being sensitive to this feature when it is smaller than the size of the range bins; 8-10 cm range resolution highest with another (AKELE) radar system (MTRI, 2010)
2	B	Availability of instrument	Commercial-grade instruments are available (e.g. IBIS-S, Olson, 2010)
1	C	Cost of measurement	Moderately high capital cost (compare to GPR)
1	D	Pre-collection preparation	May need to install reflectors on the bridge; may need to visit bridge ahead of time to plan collection geometry
1	E	Complexity of analysis	Some sort of transform or migration is probably needed; frequent references to complex post-processing in literature
1	F	Ease of data collection	Complex operation, as intended by manufacturer, that needs be supervised by operator
1	G	Stand-off distance rating	Non-contact; could be performed at great distances, but geometry of collection restricts standoff distance
1	H	Traffic Disruption	To image expansion joints (on top of bridge deck) the instrument would have to be on the bridge
0			

Deck Surface - Expansion Joint - Spalls within 2 Feet 6.0 mm to 25.0 mm (1/4" to 1") depth			
0	A	Is requirement met?	The challenge presented is being sensitive to this feature when it is smaller than the size of the range bins; 8-10 cm range resolution highest with another (AKELE) radar system (MTRI, 2010)
2	B	Availability of instrument	Commercial-grade instruments are available (e.g. IBIS-S, Olson, 2010)
1	C	Cost of measurement	Moderately high capital cost (compare to GPR)
1	D	Pre-collection preparation	May need to install reflectors on the bridge; may need to visit bridge ahead of time to plan collection geometry
1	E	Complexity of analysis	Some sort of transform or migration is probably needed; frequent references to complex post-processing in literature
1	F	Ease of data collection	Complex operation, as intended by manufacturer, that needs be supervised by operator
1	G	Stand-off distance rating	Non-contact; could be performed at great distances, but geometry of collection restricts standoff distance
1	H	Traffic Disruption	To image expansion joints (on top of bridge deck) the instrument would have to be on the bridge
0			

Deck Surface - Map Cracking - Surface Cracks 0.8 mm to 4.8 mm (1/32" to 3/16") width			
0	A	Is requirement met?	Extent of map cracking is larger than a range bin so it is possible that map-cracked concrete can be distinguished from intact deck surface(?); this might change the reflectivity
2	B	Availability of instrument	Commercial-grade instruments are available (e.g. IBIS-S, Olson, 2010)
1	C	Cost of measurement	Moderately high capital cost (compare to GPR)
1	D	Pre-collection preparation	May need to install reflectors on the bridge; may need to visit bridge ahead of time to plan collection geometry
1	E	Complexity of analysis	Some sort of transform or migration is probably needed; frequent references to complex post-processing in literature
1	F	Ease of data collection	Complex operation, as intended by manufacturer, that needs be supervised by operator
1	G	Stand-off distance rating	Non-contact; could be performed at great distances, but geometry of collection restricts standoff distance
1	H	Traffic Disruption	To image deck surface (from the top of bridge deck) the instrument would have to be on the bridge
0			

Deck Surface - Scaling - Depression in Surface 6.0 mm to 25.0 mm (1/4" to 1") depth			
1	A	Is requirement met?	The challenge presented is being sensitive to this feature when it is smaller than the size of the range bins; 8-10 cm range resolution highest with another (AKELE) radar system (MTRI, 2010); detecting this feature might be easy, but estimating the depth will be difficult
2	B	Availability of instrument	Commercial-grade instruments are available (e.g. IBIS-S, Olson, 2010)
1	C	Cost of measurement	Moderately high capital cost (compare to GPR)
1	D	Pre-collection preparation	May need to install reflectors on the bridge; may need to visit bridge ahead of time to plan collection geometry
1	E	Complexity of analysis	Some sort of transform or migration is probably needed; frequent references to complex post-processing in literature
1	F	Ease of data collection	Complex operation, as intended by manufacturer, that needs be supervised by operator
1	G	Stand-off distance rating	Non-contact; could be performed at great distances, but geometry of collection restricts standoff distance
1	H	Traffic Disruption	To image deck surface (from the top of bridge deck) the instrument would have to be on the bridge
9			

Deck Surface - Spalling - Depression with Parallel Fracture 6.0 mm to 25.0 mm (1/4" to 1") depth			
1	A	Is requirement met?	The challenge presented is being sensitive to this feature when it is smaller than the size of the range bins; 8-10 cm range resolution highest with another (AKELE) radar system (MTRI, 2010); detecting this feature might be easy, but estimating the depth will be difficult
2	B	Availability of instrument	Commercial-grade instruments are available (e.g. IBIS-S, Olson, 2010)
1	C	Cost of measurement	Moderately high capital cost (compare to GPR)
1	D	Pre-collection preparation	May need to install reflectors on the bridge; may need to visit bridge ahead of time to plan collection geometry
1	E	Complexity of analysis	Some sort of transform or migration is probably needed; frequent references to complex post-processing in literature
1	F	Ease of data collection	Complex operation, as intended by manufacturer, that needs be supervised by operator
1	G	Stand-off distance rating	Non-contact; could be performed at great distances, but geometry of collection restricts standoff distance
1	H	Traffic Disruption	To image deck surface (from the top of bridge deck) the instrument would have to be on the bridge
9			

Deck Surface - Delamination - Surface Cracks 0.8 mm to 4.8 mm (1/32" to 3/16") width			
N/A	A	Is requirement met?	Individual cracks at this scale are probably not detectable even at high range resolution
2	B	Availability of instrument	Commercial-grade instruments are available (e.g. IBIS-S, Olson, 2010)
1	C	Cost of measurement	Moderately high capital cost (compare to GPR)
1	D	Pre-collection preparation	May need to install reflectors on the bridge; may need to visit bridge ahead of time to plan collection geometry
1	E	Complexity of analysis	Some sort of transform or migration is probably needed; frequent references to complex post-processing in literature
1	F	Ease of data collection	Complex operation, as intended by manufacturer, that needs be supervised by operator
1	G	Stand-off distance rating	Non-contact; could be performed at great distances, but geometry of collection restricts standoff distance
1	H	Traffic Disruption	To image deck surface (from the top of bridge deck) the instrument would have to be on the bridge
N/A			

Deck Subsurface - Expansion Joint - Material in Joint			
N/A	A	Is requirement met?	The challenge presented is being sensitive to this feature when it is smaller than the size of the range bins; 8-10 cm range resolution highest with another (AKELE) radar system (MTRI, 2010)
2	B	Availability of instrument	Commercial-grade instruments are available (e.g. IBIS-S, Olson, 2010)
1	C	Cost of measurement	Moderately high capital cost (compare to GPR)
1	D	Pre-collection preparation	May need to install reflectors on the bridge; may need to visit bridge ahead of time to plan collection geometry
1	E	Complexity of analysis	Some sort of transform or migration is probably needed; frequent references to complex post-processing in literature
1	F	Ease of data collection	Complex operation, as intended by manufacturer, that needs be supervised by operator
1	G	Stand-off distance rating	Non-contact; could be performed at great distances, but geometry of collection restricts standoff distance
1	H	Traffic Disruption	To image expansion joints (on top of bridge deck) the instrument would have to be on the bridge
N/A			

Deck Subsurface - Delamination - Moisture in Cracks Change in moisture content			
N/A	A	Is requirement met?	"It was possible to determine moisture distributions, as well as to estimate the moisture content." (Maierhofer, 2001); requirements appear to be loose enough to accommodate the complicating environmental factors; is this a proxy for permeability? How is it tied to chloride ingress?
2	B	Availability of instrument	Multiple commercial GPR already available and in use
1	C	Cost of measurement	Higher cost for capital equipment, maintenance, downtime, and expense of processing expertise and time
2	D	Pre-collection preparation	
1	E	Complexity of analysis	Generating a model of moisture in concrete and comparing it with field measurements to estimate moisture content
1	F	Ease of data collection	This measurement is depended on environmental factors such as snow and rain; presence of water on concrete deck
1	G	Stand-off distance rating	For all commercial GPR implementations, standoff is close
2	H	Traffic Disruption	GPR should be able to be done from a vehicle moving with traffic (Shuchman, 2005)
N/A			

Deck Subsurface - Delamination - Internal Horizontal Crack			
	Approximately 0.1 mm (0.004") level		
N/A	A	Is requirement met?	Method is likely not sensitive to features that occupy so small a part of the range bin; sensitivity is dependent on how homogeneous the subsurface is
2	B	Availability of instrument	Multiple commercial GPR already available and in use
1	C	Cost of measurement	Higher cost for capital equipment, maintenance, downtime, and expense of processing expertise and time
2	D	Pre-collection preparation	
1	E	Complexity of analysis	Radar responses need to be migrated
2	F	Ease of data collection	Amounts to driving over the bridge
1	G	Stand-off distance rating	For all GPR implementations, standoff is close
2	H	Traffic Disruption	GPR should be able to be done from a vehicle moving with traffic (Shuchman, 2005)
N/A			

Deck Subsurface - Delamination - Fracture Planes / Open Spaces			
	Change in return signal		
N/A	A	Is requirement met?	Multiple studies have done mapping of delaminations with amplitude returns; GPR is sensitive down to 10 mm thickness (Hugenschmidt, 2006); asphalt thickness measured to within 2.1 mm accuracy (Shuchman, Subotic, et al. 2005)
2	B	Availability of instrument	Multiple commercial GPR already available and in use
1	C	Cost of measurement	Higher cost for capital equipment, maintenance, downtime, and expense of processing expertise and time
2	D	Pre-collection preparation	
1	E	Complexity of analysis	Radar responses need to be migrated
2	F	Ease of data collection	Amounts to driving over the bridge
1	G	Stand-off distance rating	For all GPR implementations, standoff is close
2	H	Traffic Disruption	GPR should be able to be done from a vehicle moving with traffic (Shuchman, 2005)
N/A			

Deck Subsurface - Scaling - Depression in Surface (eg. Interior of voided sections)			
	6.0 mm to 25.0 mm (1/4" to 1") depth		
N/A	A	Is requirement met?	The challenge presented is being sensitive to this feature when it is smaller than the size of the range bins; 8-10 cm range resolution highest with another (AKELE) radar system (MTRI, 2010); detecting this feature might be easy, but estimating the depth will be difficult
2	B	Availability of instrument	Commercial-grade instruments are available (e.g. IBIS-S, Olson, 2010)
1	C	Cost of measurement	Moderately high capital cost (compare to GPR)
1	D	Pre-collection preparation	May need to install reflectors on the bridge; may need to visit bridge ahead of time to plan collection geometry
1	E	Complexity of analysis	Some sort of transform or migration is probably needed; frequent references to complex post-processing in literature
1	F	Ease of data collection	Complex operation, as intended by manufacturer, that needs be supervised by operator
1	G	Stand-off distance rating	Non-contact; could be performed at great distances, but geometry of collection restricts standoff distance
1	H	Traffic Disruption	To image deck surface (from the top of bridge deck) the instrument would have to be on the bridge
N/A			

Deck Subsurface - Spalling - Depression with Parallel Fracture (eg. Interior of voided sections) 6.0 mm to 25.0 mm (1/4" to 1") depth			
N/A	A	Is requirement met?	The challenge presented is being sensitive to this feature when it is smaller than the size of the range bins; 8-10 cm range resolution highest with another (AKELE) radar system (MTRI, 2010); detecting this feature might be easy, but estimating the depth will be difficult
2	B	Availability of instrument	Commercial-grade instruments are available (e.g. IBIS-S, Olson, 2010)
1	C	Cost of measurement	Moderately high capital cost (compare to GPR)
1	D	Pre-collection preparation	May need to install reflectors on the bridge; may need to visit bridge ahead of time to plan collection geometry
1	E	Complexity of analysis	Some sort of transform or migration is probably needed; frequent references to complex post-processing in literature
1	F	Ease of data collection	Complex operation, as intended by manufacturer, that needs be supervised by operator
1	G	Stand-off distance rating	Non-contact; could be performed at great distances, but geometry of collection restricts standoff distance
1	H	Traffic Disruption	To image deck surface (from the top of bridge deck) the instrument would have to be on the bridge
N/A			

Deck Subsurface - Rebar Corrosion - Change in Cross-Sectional Area Amplitude of signal from rebar			
N/A	A	Is requirement met?	Frequent reference to technique in literature; notably Dwayne (2010), Scott (2001), and Barrile (2005)
2	B	Availability of instrument	Multiple commercial GPR already available and in use
1	C	Cost of measurement	Higher cost for capital equipment, maintenance, downtime, and expense of processing expertise and time
2	D	Pre-collection preparation	
1	E	Complexity of analysis	GPR responses must be migrated, particularly for rebar location
2	F	Ease of data collection	Amounts to driving over the bridge
1	G	Stand-off distance rating	For all GPR implementations, standoff is close
2	H	Traffic Disruption	GPR should be able to be done from a vehicle moving with traffic (Shuchman, 2005)
N/A			

Deck Subsurface - Chloride Ingress - Chloride Content through the Depth 0.4 to 1.0 % chloride by mass of cement			
N/A	A	Is requirement met?	Literature indicates that chloride content attenuates radar signals, but no documented attempt to quantify chloride content
2	B	Availability of instrument	Multiple commercial GPR already available and in use
1	C	Cost of measurement	Higher cost for capital equipment, maintenance, downtime, and expense of processing expertise and time
2	D	Pre-collection preparation	
1	E	Complexity of analysis	Dielectric properties would have to be calculated from radar response
2	F	Ease of data collection	Amounts to driving over the bridge
1	G	Stand-off distance rating	For all GPR implementations, standoff is close
2	H	Traffic Disruption	GPR should be able to be done from a vehicle moving with traffic (Shuchman, 2005)
N/A			

Girder Surface - Steel Structural Cracking - Surface Cracks < 0.1 mm (.004"), hairline			
N/A	A	Is requirement met?	Individual cracks at this scale are probably not detectable even at high range resolution
2	B	Availability of instrument	Commercial-grade instruments are available (e.g. IBIS-S, Olson, 2010)
1	C	Cost of measurement	Moderately high capital cost (compare to GPR)
1	D	Pre-collection preparation	May need to install reflectors on the bridge; may need to visit bridge ahead of time to plan collection geometry
1	E	Complexity of analysis	Some sort of transform or migration is probably needed; frequent references to complex post-processing in literature
1	F	Ease of data collection	Complex operation, as intended by manufacturer, that needs be supervised by operator
1	G	Stand-off distance rating	Non-contact; could be performed at great distances, but geometry of collection restricts standoff distance
1	H	Traffic Disruption	To image deck surface (from the top of bridge deck) the instrument would have to be on the bridge
N/A			

Girder Surface - Concrete Structural Cracking - Surface Cracks .1 mm (.004")			
N/A	A	Is requirement met?	Individual cracks at this scale are probably not detectable even at high range resolution
2	B	Availability of instrument	Commercial-grade instruments are available (e.g. IBIS-S, Olson, 2010)
1	C	Cost of measurement	Moderately high capital cost (compare to GPR)
1	D	Pre-collection preparation	May need to install reflectors on the bridge; may need to visit bridge ahead of time to plan collection geometry
1	E	Complexity of analysis	Some sort of transform or migration is probably needed; frequent references to complex post-processing in literature
1	F	Ease of data collection	Complex operation, as intended by manufacturer, that needs be supervised by operator
1	G	Stand-off distance rating	Non-contact; could be performed at great distances, but geometry of collection restricts standoff distance
1	H	Traffic Disruption	To image deck surface (from the top of bridge deck) the instrument would have to be on the bridge
N/A			

Girder Surface - Steel Section Loss - Change in Cross-Sectional Area Percent thickness of web or flange			
N/A	A	Is requirement met?	Might be a measurable bulk effect; not clear with no specified metric for the requirement whether or not the technique would be sensitive enough
2	B	Availability of instrument	Commercial-grade instruments are available (e.g. IBIS-S, Olson, 2010)
1	C	Cost of measurement	Moderately high capital cost (compare to GPR)
1	D	Pre-collection preparation	May need to install reflectors on the bridge; may need to visit bridge ahead of time to plan collection geometry
1	E	Complexity of analysis	Some sort of transform or migration is probably needed; frequent references to complex post-processing in literature
1	F	Ease of data collection	Complex operation, as intended by manufacturer, that needs be supervised by operator
2	G	Stand-off distance rating	Non-contact; able to be deployed up to 2 km distance (Pieraccini, 2008)
2	H	Traffic Disruption	Collection geometry does not require measurements to be taken on the bridge
N/A			

Girder Surface - Paint Condition			
	Amount of missing paint (X %)		
N/A	A	Is requirement met?	Might be possible, but no reference to this application of microwave backscatter/speckle in the literature
2	B	Availability of instrument	Commercial-grade instruments are available (e.g. IBIS-S, Olson, 2010)
1	C	Cost of measurement	Moderately high capital cost (compare to GPR)
1	D	Pre-collection preparation	May need to install reflectors on the bridge; may need to visit bridge ahead of time to plan collection geometry
1	E	Complexity of analysis	Some sort of transform or migration is probably needed; frequent references to complex post-processing in literature
1	F	Ease of data collection	Complex operation, as intended by manufacturer, that needs be supervised by operator
2	G	Stand-off distance rating	Non-contact; able to be deployed up to 2 km distance (Pieraccini, 2008)
2	H	Traffic Disruption	Collection geometry does not require measurements to be taken on the bridge
N/A			

Girder Surface - Concrete Section Loss - Change in Cross-Sectional Area			
	Percent volume per foot		
N/A	A	Is requirement met?	Might be a measurable bulk effect; not clear with no specified metric for the requirement whether or not the technique would be sensitive enough
2	B	Availability of instrument	Commercial-grade instruments are available (e.g. IBIS-S, Olson, 2010)
1	C	Cost of measurement	Moderately high capital cost (compare to GPR)
1	D	Pre-collection preparation	May need to install reflectors on the bridge; may need to visit bridge ahead of time to plan collection geometry
1	E	Complexity of analysis	Some sort of transform or migration is probably needed; frequent references to complex post-processing in literature
1	F	Ease of data collection	Complex operation, as intended by manufacturer, that needs be supervised by operator
2	G	Stand-off distance rating	Non-contact; able to be deployed up to 2 km distance (Pieraccini, 2008)
2	H	Traffic Disruption	Collection geometry does not require measurements to be taken on the bridge
N/A			

Girder Subsurface - Internal Concrete Structural Cracks - Internal Cracks (e.g. Box Beam)			
	Approx 0.8 mm (1/32")		
N/A	A	Is requirement met?	Technique is likely not sensitive enough for this fine of a feature
2	B	Availability of instrument	Multiple commercial GPR already available and in use
1	C	Cost of measurement	Higher cost for capital equipment, maintenance, downtime, and expense of processing expertise and time
2	D	Pre-collection preparation	
1	E	Complexity of analysis	Radar responses need to be migrated
1	F	Ease of data collection	Numerous, difficult places to reach
1	G	Stand-off distance rating	For all GPR implementations, standoff is close
1	H	Traffic Disruption	In this case, GPR might interfere with traffic as it is deployed--somehow--on the sides, bottom, and top of bridge from, conceivably, a platform on the bridge deck
N/A			

Girder Subsurface - Concrete Section Loss - Change in Cross-Sectional Area			
	Percent volume per foot		
N/A	A	Is requirement met?	Might be a measurable bulk effect; not clear with no specified metric for the requirement whether or not the technique would be sensitive enough
2	B	Availability of instrument	Commercial-grade instruments are available (e.g. IBIS-S, Olson, 2010)
1	C	Cost of measurement	Moderately high capital cost (compare to GPR)
1	D	Pre-collection preparation	May need to install reflectors on the bridge; may need to visit bridge ahead of time to plan collection geometry
1	E	Complexity of analysis	Some sort of transform or migration is probably needed; frequent references to complex post-processing in literature
1	F	Ease of data collection	Complex operation, as intended by manufacturer, that needs be supervised by operator
2	G	Stand-off distance rating	Non-contact; able to be deployed up to 2 km distance (Pieraccini, 2008)
2	H	Traffic Disruption	Collection geometry does not require measurements to be taken on the bridge
N/A			

Girder Subsurface - Prestress Strand Breakage - Change in Cross-Sectional Area			
	Wire 2 mm or strand 9.5 mm diameter		
N/A	A	Is requirement met?	"Measurement errors on diameter, have been carried out by radar technology, supported by electromagnetic method, showed a range of error within 3 mm at the 86% significance level." (Barrile, 2005) - that for 13, 25, and 38 mm strands
2	B	Availability of instrument	Multiple commercial GPR already available and in use
0	C	Cost of measurement	Imaging the girders below the deck would be challenging and time-consuming in addition to already substantial capital and operational costs
2	D	Pre-collection preparation	
1	E	Complexity of analysis	Radar responses need to be migrated; otherwise, some modeling is being used to estimate strand thickness
1	F	Ease of data collection	Numerous, difficult places to reach
1	G	Stand-off distance rating	For all GPR implementations, standoff is close
1	H	Traffic Disruption	In this case, GPR might interfere with traffic as it is deployed--somehow--on the sides, bottom, and top of bridge from, conceivably, a platform on the bridge deck
N/A			

Girder Subsurface - Rebar Corrosion - Change in Cross-Sectional Area			
	Amplitude of signal from rebar		
N/A	A	Is requirement met?	Frequent reference to technique in literature; notably Dwayne (2010), Scott (2001), and Barrile (2005)
2	B	Availability of instrument	Multiple commercial GPR already available and in use; more generalized radar system likely needed but these are also commercially available
1	C	Cost of measurement	Higher cost for capital equipment, maintenance, downtime, and expense of processing expertise and time
2	D	Pre-collection preparation	
1	E	Complexity of analysis	GPR responses must be migrated, particularly for rebar location
2	F	Ease of data collection	Amounts to driving under the bridge and scanning the girders at traffic speeds
1	G	Stand-off distance rating	For all GPR implementations, standoff is close
2	H	Traffic Disruption	GPR should be able to be done from a vehicle moving with traffic (Shuchman, 2005)
N/A			

Girder Subsurface - Chloride Ingress - Chloride Content through the Depth			
0.4 to 1.0 % Chloride by mass of cement			
N/A	A	Is requirement met?	Lim (2001) showed that radar signal attenuates with increasing chloride content
2	B	Availability of instrument	Multiple commercial GPR already available and in use
1	C	Cost of measurement	Higher cost for capital equipment, maintenance, downtime, and expense of processing expertise and time
2	D	Pre-collection preparation	
1	E	Complexity of analysis	Dielectric properties would have to be calculated from radar response
1	F	Ease of data collection	Numerous, difficult places to reach
1	G	Stand-off distance rating	For all GPR implementations, standoff is close
2	H	Traffic Disruption	GPR should be able to be done from a vehicle moving with traffic (Shuchman, 2005)
N/A			

Global Metrics - Bridge Length - Change in Bridge Length			
Accuracy to 30 mm (0.1ft) (smaller)			
N/A	A	Is requirement met?	SAR imaging could provide the measurement, but likely won't meet the resolution required
2	B	Availability of instrument	Commercial-grade instruments are available (e.g. IBIS-S, Olson, 2010)
1	C	Cost of measurement	Moderately high capital cost (compare to GPR)
1	D	Pre-collection preparation	May need to install reflectors on the bridge; may need to visit bridge ahead of time to plan collection geometry
1	E	Complexity of analysis	Some sort of transform or migration is probably needed; frequent references to complex post-processing in literature
1	F	Ease of data collection	Complex operation, as intended by manufacturer, that needs be supervised by operator
2	G	Stand-off distance rating	Non-contact; able to be deployed up to 2 km distance (Pieraccini, 2008)
2	H	Traffic Disruption	Collection geometry does not require measurements to be taken on the bridge
N/A			

Global Metrics - Bridge Settlement - Vertical Movement of Bridge			
Approximately 6 mm to 12 mm			
N/A	A	Is requirement met?	SAR imaging could provide the measurement, but likely won't meet the resolution required
2	B	Availability of instrument	Commercial-grade instruments are available (e.g. IBIS-S, Olson, 2010)
1	C	Cost of measurement	Moderately high capital cost (compare to GPR)
1	D	Pre-collection preparation	May need to install reflectors on the bridge; may need to visit bridge ahead of time to plan collection geometry
1	E	Complexity of analysis	Some sort of transform or migration is probably needed; frequent references to complex post-processing in literature
1	F	Ease of data collection	Complex operation, as intended by manufacturer, that needs be supervised by operator
2	G	Stand-off distance rating	Non-contact; able to be deployed up to 2 km distance (Pieraccini, 2008)
2	H	Traffic Disruption	Collection geometry does not require measurements to be taken on the bridge
N/A			

Global Metrics - Bridge Movement - Transverse Directions			
	Approximately 6 mm to 12 mm		
N/A	A	Is requirement met?	SAR imaging could provide the measurement, but likely won't meet the resolution required
2	B	Availability of instrument	Commercial-grade instruments are available (e.g. IBIS-S, Olson, 2010)
1	C	Cost of measurement	Moderately high capital cost (compare to GPR)
1	D	Pre-collection preparation	May need to install reflectors on the bridge; may need to visit bridge ahead of time to plan collection geometry
1	E	Complexity of analysis	Some sort of transform or migration is probably needed; frequent references to complex post-processing in literature
1	F	Ease of data collection	Complex operation, as intended by manufacturer, that needs be supervised by operator
2	G	Stand-off distance rating	Non-contact; able to be deployed up to 2 km distance (Pieraccini, 2008)
2	H	Traffic Disruption	Collection geometry does not require measurements to be taken on the bridge
N/A			

Global Metrics - Surface Roughness			
	Change over time		
1	A	Is requirement met?	*"By associating the actual roughness, measured in situ, with the contrast (as measured by the SAR), one can establish a calibration curve, by which one can make roughness measurements remotely."* (Shuchman, Subotic, 2005)
1	B	Availability of instrument	Commercial-grade instruments are available (e.g. IBIS-S, Olson, 2010)
0	C	Cost of measurement	Moderately high capital cost (compare to GPR)
2	D	Pre-collection preparation	May need to install reflectors on the bridge; may need to visit bridge ahead of time to plan collection geometry
0	E	Complexity of analysis	Some sort of transform or migration is probably needed; frequent references to complex post-processing in literature
2	F	Ease of data collection	Complex operation, as intended by manufacturer, that needs be supervised by operator
2	G	Stand-off distance rating	Non-contact; able to be deployed up to 2 km distance (Pieraccini, 2008)
2	H	Traffic Disruption	Collection geometry does not require measurements to be taken on the bridge
10			

Global Metrics - Vibration or Live Load Deflection			
	.5 -20 Hz; L/800 deflection		
N/A	A	Is requirement met?	Frequency resolution of ~0.02 Hz (Gentile, 2009); displacement resolution of 0.1 mm (Pieraccini, 2009)
2	B	Availability of instrument	Commercial-grade instruments are available (e.g. IBIS-S, Olson, 2010)
1	C	Cost of measurement	Moderately high capital cost (compare to GPR)
1	D	Pre-collection preparation	May need to install reflectors on the bridge; may need to visit bridge ahead of time to plan collection geometry
1	E	Complexity of analysis	Some sort of transform or migration is probably needed; frequent references to complex post-processing in literature
1	F	Ease of data collection	Complex operation, as intended by manufacturer, that needs be supervised by operator
2	G	Stand-off distance rating	Non-contact; able to be deployed up to 2 km distance (Pieraccini, 2008) for larger bridges (based on the spreading of the beam width)
2	H	Traffic Disruption	Collection geometry does not require measurements to be taken on the bridge
N/A			

InSAR

		Global Metrics				
		Change in Bridge Length	Vertical Movement of Bridge	Transverse Directions	Surface Roughness	Vibration or Live Load Deflection
A	Is requirement met?	N/A	0	N/A	N/A	N/A
B	Availability of instrument	2	2	2	2	2
C	Cost of measurement	1	1	1	1	1
D	Pre-collection preparation	2	2	2	2	2
E	Complexity of analysis	0	0	0	0	0
F	Ease of data collection	2	2	2	2	2
G	Stand-off distance rating	2	2	2	2	1
H	Traffic Disruption	2	2	2	2	2
		N/A	**0**	**N/A**	**N/A**	**N/A**

	A	B
Weights:	**1**	**1**

Global Metrics - Bridge Length - Change in Bridge Length

Accuracy to 30 mm (0.1ft) (smaller)

N/A	A	Is requirement met?	Technique capable of detecting changes in height (based on phase differences) on the order of the wavelength and at X-band, 10 GHz the wavelength is 30 mm; Shinozuka et al. (2000) detected 10 cm change in building height
2	B	Availability of instrument	RADARSAT and Intermap are just two commercial InSAR services
1	C	Cost of measurement	Imagery would probably have to be purchased on a per-bridge basis for practical purposes and change detection requires multiple images of the same bridge separated in time
2	D	Pre-collection preparation	Corner reflectors might be installed but they are not required
0	E	Complexity of analysis	Artifacts are a common problem that need to be removed; bridges over water exhibit multiple reflections; much preprocessing is needed to transform InSAR data into a world coordinate system (Soergel, 2008)
2	F	Ease of data collection	Instrument simply flies over and images the structure
2	G	Stand-off distance rating	High-altitude aerial flights or satellite passes
2	H	Traffic Disruption	Instrument does not interfere with traffic whatsoever
N/A			

Global Metrics - Bridge Settlement - Vertical Movement of Bridge

Approximately 6 mm to 12 mm

0	A	Is requirement met?	Technique capable of detecting changes in height (based on phase differences) on the order of the wavelength and at X-band, 10 GHz the wavelength is 30 mm; Shinozuka et al. (2000) detected 10 cm change in building height
2	B	Availability of instrument	RADARSAT and Intermap are just two commercial InSAR services
1	C	Cost of measurement	Imagery would probably have to be purchased on a per-bridge basis for practical purposes and change detection requires multiple images of the same bridge separated in time
2	D	Pre-collection preparation	Corner reflectors might be installed but they are not required
0	E	Complexity of analysis	Artifacts are a common problem that need to be removed; bridges over water exhibit multiple reflections; much preprocessing is needed to transform InSAR data into a world coordinate system (Soergel, 2008)
2	F	Ease of data collection	Instrument simply flies over and images the structure
2	G	Stand-off distance rating	High-altitude aerial flights or satellite passes
2	H	Traffic Disruption	Instrument does not interfere with traffic whatsoever
0			

Global Metrics - Bridge Movement - Transverse Directions Approximately 6 mm to 12 mm			
N/A	A	Is requirement met?	Technique capable of detecting changes in height (based on phase differences) on the order of the wavelength and at X-band, 10 GHz the wavelength is 30 mm; Shinozuka et al. (2000) detected 10 cm change in building height
2	B	Availability of instrument	RADARSAT and Intermap are just two commercial InSAR services
1	C	Cost of measurement	Imagery would probably have to be purchased on a per-bridge basis for practical purposes and change detection requires multiple images of the same bridge separated in time
2	D	Pre-collection preparation	Corner reflectors might be installed but they are not required
0	E	Complexity of analysis	Artifacts are a common problem that need to be removed; bridges over water exhibit multiple reflections; much preprocessing is needed to transform InSAR data into a world coordinate system (Soergel, 2008)
2	F	Ease of data collection	Instrument simply flies over and images the structure
2	G	Stand-off distance rating	High-altitude aerial flights or satellite passes
2	H	Traffic Disruption	Instrument does not interfere with traffic whatsoever
N/A			

Global Metrics - Surface Roughness Change over time			
N/A	A	Is requirement met?	"...Surface roughness and moisture estimates [can be recovered] from the ratios of measured InSAR coherence." (Hajnsek, 2005); without strict definition of the requirement (without metrics) this technique fully satisfies the need to detect a change in surface roughness (but likely won't quantify surface roughness)
2	B	Availability of instrument	RADARSAT and Intermap are just two commercial InSAR services
1	C	Cost of measurement	Imagery would probably have to be purchased on a per-bridge basis for practical purposes and change detection requires multiple images of the same bridge separated in time
2	D	Pre-collection preparation	Corner reflectors might be installed but they are not required
0	E	Complexity of analysis	Artifacts are a common problem that need to be removed; bridges over water exhibit multiple reflections; much preprocessing is needed to transform InSAR data into a world coordinate system (Soergel, 2008)
2	F	Ease of data collection	Instrument simply flies over and images the structure
2	G	Stand-off distance rating	High-altitude aerial flights or satellite passes
2	H	Traffic Disruption	Instrument does not interfere with traffic whatsoever
N/A			

Global Metrics - Vibration or Live Load Deflection .5 -20 Hz; L/800 deflection			
N/A	A	Is requirement met?	Don't know frequency response; literature shows sub-mm resolution possible (Pieraccini, 2000)
2	B	Availability of instrument	RADARSAT and Intermap are just two commercial InSAR services
1	C	Cost of measurement	Imagery would probably have to be purchased on a per-bridge basis for practical purposes and change detection requires multiple images of the same bridge separated in time
2	D	Pre-collection preparation	Corner reflectors might be installed but they are not required
0	E	Complexity of analysis	Artifacts are a common problem that need to be removed; bridges over water exhibit multiple reflections; much preprocessing is needed to transform InSAR data into a world coordinate system (Soergel, 2008)
2	F	Ease of data collection	Instrument simply flies over and images the structure
1	G	Stand-off distance rating	For the resolution requirements, this cannot be done from spaceborne or high-altitude aerial platforms
2	H	Traffic Disruption	Instrument does not interfere with traffic whatsoever
N/A			

BVRCS

		Deck Surface							
		Torn/Missing Seal	Armored Plated Damage	Expansion Joint - Cracks within 2 Feet	Expansion Joint - Spalls within 2 Feet	Map Cracking - Surface Cracks	Scaling - Depression in Surface	Spalling - Depression with Parallel Fracture	Delamination - Surface Cracks
A	Is requirement met?	1	2	2	2	2	2	2	2
B	Availability of instrument	2	2	2	2	2	2	2	2
C	Cost of measurement	2	2	2	2	2	2	2	2
D	Pre-collection preparation	2	2	2	2	2	2	2	2
E	Complexity of analysis	1	1	1	1	1	1	1	1
F	Ease of data collection	2	2	2	2	2	2	2	2
G	Stand-off distance rating	1	1	1	1	1	1	1	1
H	Traffic Disruption	1	1	1	1	1	1	1	1
		12	**13**	**13**	**13**	**13**	**13**	**13**	**13**

	Girder Surface	Global Metrics			
	Steel Structural Cracking	Change in Bridge Length	Vertical Movement of Bridge	Transverse Directions	Surface Roughness
	N/A	N/A	N/A	N/A	1
	2	2	2	2	2
	2	2	0	0	2
	1	1	1	2	2
	2	2	1	1	1
	2	2	2	0	2
	1	2	2	2	1
	2	2	2	2	1
	N/A	**N/A**	**N/A**	**N/A**	**12**

	A	B
Weights:	**1**	**1**

Other Additional Notes:

N/A This technique is not recommended for "Chemical Leaching on Bottom" as many bridges in an inventory won't have car access underneath.

N/A This technique is not recommended for "Material in Joints" because the material may be obscured from view, particularly oblique view

N/A This technique is not recommended for "Paint Condition" because it does not provide a synoptic view of the structure(?)

Deck Surface - Expansion Joint - Torn/Missing Seal			
1	A	Is requirement met?	Limited studies, but should be possible depending on camera resolution and hardware setup
2	B	Availability of instrument	Commercial systems are currently available
2	C	Cost of measurement	Potential for low cost research system- long life, but commercial systems can cost up to xxx
2	D	Pre-collection preparation	Minor preparation for low cost and commercial systems
1	E	Complexity of analysis	Turn-key system with visual analysis if using commercial system
2	F	Ease of data collection	Collection platform is vehicle based
1	G	Stand-off distance rating	Close to structure on vehicle platform
1	H	Traffic Disruption	No lane closure or traffic disruption likely
12			

Deck Surface - Expansion Joint - Armored Plated Damage			
2	A	Is requirement met?	Limited studies, but should be possible depending on camera resolution and hardware setup
2	B	Availability of instrument	Commercial systems are currently available
2	C	Cost of measurement	Potential for low cost research system- long life, but commercial systems can cost up to xxx
2	D	Pre-collection preparation	Minor preparation for low cost and commercial systems
1	E	Complexity of analysis	Turn-key system with visual analysis if using commercial system
2	F	Ease of data collection	Collection platform is vehicle based
1	G	Stand-off distance rating	Close to structure on vehicle platform
1	H	Traffic Disruption	No lane closure or traffic disruption likely
13			

Deck Surface - Expansion Joint - Cracks within 2 Feet 0.8 mm to 4.8 mm (1/32" to 3/16") width			
2	A	Is requirement met?	Limited studies, but should be possible depending on camera resolution and hardware setup
2	B	Availability of instrument	Commercial systems are currently available
2	C	Cost of measurement	Potential for low cost research system- long life, but commercial systems can cost up to xxx
2	D	Pre-collection preparation	Minor preparation for low cost and commercial systems
1	E	Complexity of analysis	Turn-key system with visual analysis if using commercial system
2	F	Ease of data collection	Collection platform is vehicle based
1	G	Stand-off distance rating	Close to structure on vehicle platform
1	H	Traffic Disruption	No lane closure or traffic disruption likely
13			

Deck Surface - Expansion Joint - Spalls within 2 Feet 6.0 mm to 25.0 mm (1/4" to 1") depth			
2	A	Is requirement met?	Limited studies, but should be possible depending on camera resolution and hardware setup
2	B	Availability of instrument	Commercial systems are currently available
2	C	Cost of measurement	Potential for low cost research system- long life, but commercial systems can cost up to xxx
2	D	Pre-collection preparation	Minor preparation for low cost and commercial systems
1	E	Complexity of analysis	Turn-key system with visual analysis if using commercial system
2	F	Ease of data collection	Collection platform is vehicle based
1	G	Stand-off distance rating	Close to structure on vehicle platform
1	H	Traffic Disruption	No lane closure or traffic disruption likely
13			

Deck Surface - Map Cracking - Surface Cracks 0.8 mm to 4.8 mm (1/32" to 3/16") width			
2	A	Is requirement met?	Limited studies, but should be possible depending on camera resolution and hardware setup
2	B	Availability of instrument	Commercial systems are currently available
2	C	Cost of measurement	Potential for low cost research system- long life, but commercial systems can cost up to xxx
2	D	Pre-collection preparation	Minor preparation for low cost and commercial systems
1	E	Complexity of analysis	Turn-key system with visual analysis if using commercial system
2	F	Ease of data collection	Collection platform is vehicle based
1	G	Stand-off distance rating	Close to structure on vehicle platform
1	H	Traffic Disruption	No lane closure or traffic disruption likely
13			

Deck Surface - Scaling - Depression in Surface 6.0 mm to 25.0 mm (1/4" to 1") depth			
2	A	Is requirement met?	Limited studies, but should be possible depending on camera resolution and hardware setup
2	B	Availability of instrument	Commercial systems are currently available
2	C	Cost of measurement	Potential for low cost research system- long life, but commercial systems can cost up to xxx
2	D	Pre-collection preparation	Minor preparation for low cost and commercial systems
1	E	Complexity of analysis	Turn-key system with visual analysis if using commercial system
2	F	Ease of data collection	Collection platform is vehicle based
1	G	Stand-off distance rating	Close to structure on vehicle platform
1	H	Traffic Disruption	No lane closure or traffic disruption likely
13			

Deck Surface - Spalling - Depression with Parallel Fracture 0.4 to 1.0 % chloride by mass of cement			
2	A	Is requirement met?	Limited studies, but should be possible depending on camera resolution and hardware setup
2	B	Availability of instrument	Commercial systems are currently available
2	C	Cost of measurement	Potential for low cost research system- long life, but commercial systems can cost up to xxx
2	D	Pre-collection preparation	Minor preparation for low cost and commercial systems
1	E	Complexity of analysis	Turn-key system with visual analysis if using commercial system
2	F	Ease of data collection	Collection platform is vehicle based
1	G	Stand-off distance rating	Close to structure on vehicle platform
1	H	Traffic Disruption	No lane closure or traffic disruption likely
13			

Deck Surface - Delamination - Surface Cracks 0.8 mm to 4.8 mm (1/32" to 3/16") width			
2	A	Is requirement met?	Limited studies, but should be possible depending on camera resolution and hardware setup
2	B	Availability of instrument	Commercial systems are currently available
2	C	Cost of measurement	Potential for low cost research system- long life, but commercial systems can cost up to xxx
2	D	Pre-collection preparation	Minor preparation for low cost and commercial systems
1	E	Complexity of analysis	Turn-key system with visual analysis if using commercial system
2	F	Ease of data collection	Collection platform is vehicle based
1	G	Stand-off distance rating	Close to structure on vehicle platform
1	H	Traffic Disruption	No lane closure or traffic disruption likely
13			

Girder Surface - Steel Structural Cracking - Surface Cracks < 0.1 mm (.004"), hairline			
N/A	A	Is requirement met?	Limited studies, but should be possible depending on camera resolution and hardware setup
2	B	Availability of instrument	Commercial systems are currently available
2	C	Cost of measurement	Potential for low cost research system- long life, but commercial systems can cost up to xxx
1	D	Pre-collection preparation	Minor preparation for low cost and commercial systems
2	E	Complexity of analysis	Turn-key system with visual analysis if using commercial system
2	F	Ease of data collection	Collection platform is vehicle based
1	G	Stand-off distance rating	Close to structure on vehicle platform
2	H	Traffic Disruption	No lane closure or traffic disruption likely
N/A			

Global Metrics - Bridge Length - Change in Bridge Length			
	Accuracy to 30 mm (0.1ft) (smaller)		
N/A	A	Is requirement met?	Systems not designed to or capable of measuring bridge length
2	B	Availability of instrument	Commercial systems are currently available
2	C	Cost of measurement	Potential for low cost research system- long life, but commercial systems can cost up to xxx
1	D	Pre-collection preparation	Minor preparation for low cost and commercial systems
2	E	Complexity of analysis	Turn-key system with visual analysis if using commercial system
2	F	Ease of data collection	Collection platform is vehicle based
2	G	Stand-off distance rating	Close to structure on vehicle platform
2	H	Traffic Disruption	No lane closure or traffic disruption likely
N/A			

Global Metrics - Bridge Settlement - Vertical Movement of Bridge			
	Approximately 6 mm to 12 mm		
N/A	A	Is requirement met?	Systems not designed to or capable of measuring bridge length
2	B	Availability of instrument	Commercial systems are currently available
0	C	Cost of measurement	Potential for low cost research system- long life, but commercial systems can cost up to xxx
1	D	Pre-collection preparation	Minor preparation for low cost and commercial systems
1	E	Complexity of analysis	Turn-key system with visual analysis if using commercial system
2	F	Ease of data collection	Collection platform is vehicle based
2	G	Stand-off distance rating	Close to structure on vehicle platform
2	H	Traffic Disruption	No lane closure or traffic disruption likely
N/A			

Global Metrics - Bridge Movement - Transverse Directions			
	Approximately 6 mm to 12 mm		
N/A	A	Is requirement met?	Systems not designed to or capable of measuring bridge length
2	B	Availability of instrument	Commercial systems are currently available
0	C	Cost of measurement	Potential for low cost research system- long life, but commercial systems can cost up to xxx
2	D	Pre-collection preparation	Minor preparation for low cost and commercial systems
1	E	Complexity of analysis	Turn-key system with visual analysis if using commercial system
0	F	Ease of data collection	Collection platform is vehicle based
2	G	Stand-off distance rating	Close to structure on vehicle platform
2	H	Traffic Disruption	No lane closure or traffic disruption likely
N/A			

Global Metrics - Surface Roughness			
	Change over time		
1	A	Is requirement met?	Likely surface roughness and change could be assessed visually
2	B	Availability of instrument	Commercial systems are currently available
2	C	Cost of measurement	Potential for low cost research system- long life, but commercial systems can cost up to xxx
2	D	Pre-collection preparation	Minor preparation for low cost and commercial systems
1	E	Complexity of analysis	Turn-key system with visual analysis if using commercial system
2	F	Ease of data collection	Collection platform is vehicle based
1	G	Stand-off distance rating	Close to structure on vehicle platform
1	H	Traffic Disruption	No lane closure or traffic disruption likely
12			